MycoKeys 110: 1–33 (2024)
DOI: 10.3897/mycokeys.110.132628

Research Article

Morpho-phylogenetic evidence reveals novel species and new records of *Nigrograna* (Nigrograna ceae) associated with medicinal plants in Southwestern China

Hong-Zhi Du[1,2,3,4*], Yu-Hang Lu[1,3,4*], Ratchadawan Cheewangkoon[3,4], Jian-Kui Liu[1,3]

1 *School of Life Science and Technology, Center for Informational Biology, University of Electronic Science and Technology of China, Chengdu 611731, Sichuan Province, China*
2 *School of Pharmacy, Guizhou University of Traditional Chinese Medicine, Guiyang 550025, Guizhou Province, China*
3 *Department of Entomology and Plant Pathology, Faculty of Agriculture, Chiang Mai University, Chiang Mai 50200, Thailand*
4 *Innovative Agriculture Research Centre, Faculty of Agriculture, Chiang Mai University, Chiang Mai 50200, Thailand*

Corresponding authors: Jian-Kui Liu (liujiankui@uestc.edu.cn); Ratchadawan Cheewangkoon (ratchadawan.c@cmu.ac.th)

Abstract

During a survey of saprobic fungal niches in Southwestern China, eighteen ascomycetous collections of *Nigrograna* (Nigrograna ceae, Pleosporales, Dothideomycetes) were found on dead branches of medicinal plants. These taxa were characterized and identified based on morphological and culture characteristics, and phylogenetic analyses of a combined the internal transcribed spacer region of rDNA (ITS), nuclear large subunit rDNA (28S, LSU), RNA polymerase second-largest subunit (*rpb2*), nuclear small subunit rDNA (18S, SSU), and translation elongation factor 1-alpha (*tef1-α*) sequence dataset also confirmed their placement. As a result, four novel species, namely *Nigrograna camelliae*, *N. guttulata*, *N. longiorostiolata* and *N. neriicola* were described. Additionally, four new host records of *N. acericola*, *N. magnoliae*, *N. oleae* and *N. thymi* were introduced. Furthermore, this study addresses the taxonomic status of *N. trachycarpi*, proposing its synonymy under *N. oleae*. Detailed illustrations, descriptions and informative notes for each newly identified taxon and novel host record are provided in this study.

Key words: 4 new taxa, Dothideomycetes, multi-locus, phylogeny, sexual morph, taxonomy

Academic editor: Chitrabhanu Bhunjun
Received: 20 July 2024
Accepted: 23 September 2024
Published: 23 October 2024

Citation: Du H-Z, Lu Y-H, Cheewangkoon R, Liu J-K (2024) Morpho-phylogenetic evidence reveals novel species and new records of *Nigrograna* (Nigrograna ceae) associated with medicinal plants in Southwestern China. MycoKeys 110: 1–33. https://doi.org/10.3897/mycokeys.110.132628

Introduction

The utilization of medicinal plants is integral to disease prevention and treatment in human life (Nalawade et al. 2003; Cole et al. 2007; Schmidt 2017; Rahman et al. 2019). These plants harbor diverse biological compounds that hold potential for drug development due to their rich reservoir of bioactive ingredients (Samy and Gopalakrishnakone 2007; Ali et al. 2021; Atanasov et al. 2021). Southwestern China, recognized as one of the primary regions for traditional Chinese herbal medicine, boasts remarkable diversity in medicinal plant species. This diversity is largely driven by the region's unique karst landforms, which

* These authors contributed equally to this work.

promote species differentiation and abundance (Huang et al. 2012; Taylor et al. 2014; Lu et al. 2018; Guo et al. 2020; Shan et al. 2022). Recent studies in Southwest China have revealed novel micro-fungi species associated with medicinal plants, including pathogens (Abtahi and Nourani 2017), saprobes (Du et al. 2022a; Sun et al. 2023; Wu et al. 2024) and endophytes (Helaly et al. 2018; Keshri et al. 2021; Du et al. 2022b), highlighting the potential of these plants as reservoirs for discovering fungal diversity.

Nigrograna ceae (Pleosporales, Dothideomycetes) was established by Jaklitsch and Voglmayr (2016) based on morpho-molecular evidence, with *Nigrograna* as the type genus. The divergence of Nigrograna ceae is established at approximately 79 (44–124) Mya in crown age and 131 (86–180) Mya in stem age (Liu et al. 2017). Initially, the genus *Nigrograna* was proposed by de Gruyter et al. (2012) to accommodate *Pyrenochaeta mackinnonii* (a pathogenic species in humans isolated from a mycetoma patient), which was later synonymized as *Nigrograna mackinnonii*. However, phylogenetic studies revealed that *N. mackinnon*ii was closely related to *Biatriospora marina*, the type species of the monotypic genus *Biatriospora* (Ahmed et al. 2014), leading to the reclassification of *N. mackinnonii* as *Biatriospora mackinnonii* (Ahmed et al. 2014). Jaklitsch and Voglmayr (2016) subsequently proposed the family Nigrograna ceae, describing three new taxa that differed significantly from *Biatriospora* in morphology and ecology. Hongsanan et al. (2020) further revised the taxonomic status of *Biatriospora* and *Nigrograna*, suggesting that both genera should be retained. To date, there are 37 species epithets of *Nigrograna* listed in Index Fungorum (http://www.indexfungorum.org/Names/Names.asp; accessed 7 September 2024).

Most members of *Nigrograna* have cryptic morphological characters, leading Jaklitsch and Voglmayr (2016) to classify them as cryptic species. The sexual morphs of *Nigrograna* are characterized by having globose to subglobose ascomata with ostiole, multi-layered peridium, clavate and fissitunicate asci, fusoid to narrowly ellipsoid, straight or curved, septate, and smooth or verruculose ascospores (Jaklitsch and Voglmayr 2016; Zhang et al. 2020; Lu et al. 2022). In contrast, the asexual morphs are defined by globose to subglobose or pyriform pycnidia, filiform and branched conidiophores, hyaline, phialidic and discrete conidiogenous cells, sub-hyaline, aseptate and ellipsoidal conidia (de Gruyter et al. 2012; Jaklitsch and Voglmayr 2016; Lu et al. 2022). The life modes of *Nigrograna* species are diverse, ranging from endophytic and saprobic to pathogenic (in human) (Kolařík 2018; Zhao et al. 2018; Lu et al. 2022; Li et al. 2023). These species have been reported from various hosts in terrestrial, marine, and freshwater habitats (Hyde et al. 2017; Tibpromma et al. 2017; Dayarathne et al. 2020; Lu et al. 2022; Bundhun et al. 2023; Hu et al. 2023; Li et al. 2023; Senanayake et al. 2023; Shu et al. 2023), underscoring the broad ecological diversity of this genus. In recent years, an increasing number of new species and records of *Nigrograna* have been reported from various hosts in China. Most of these species have been identified as saprotrophic fungi from terrestrial habitats (Tibpromma et al. 2017; Boonmee et al. 2021; de Silva et al. 2022; Lu et al. 2022; Hu et al. 2023; Li et al. 2023; Liu et al. 2024; Ren et al. 2024; Xu et al. 2024). However, reports of *Nigrograna* occurring on medicinal plants are

limited. Given the ecological and economic importance of these plants, it is essential to explore the taxonomy and phylogeny of *Nigrograna* species associated with medicinal flora. Such investigations will deepen our understanding of fungal diversity in these specialized niches and may reveal new insights into the potential applications of these fungi.

This study focuses on elucidating the diversity of Nigrogranaceae in Southwestern China, identifying eight species associated with medicinal plants. We aim to describe these novel findings and contribute to the understanding of fungal diversity in this region. Through a combination of morphological comparisons and multi-locus phylogenetic analyses, we introduce four new species and four new host records, supported by both morphological and phylogenetic evidence.

Materials and methods

Collection and examination of specimens

Specimens in this study were collected from medicinal plants of nine families (Apocynaceae, Berberidaceae, Buxaceae, Celastraceae, Eucommiaceae, Fabaceae, Primulaceae, Rutaceae and Theaceae) in Southwest China during 2021 and 2023, viz., (1) Guizhou Province (26°30'43"N–26°32'18"N, 106°39'32"E–106°41'48"E, elevation 1,127–1,155 m); (2) Sichuan Province (29°29'1"N–31°8'4"N, 103°2'23"E–104°14'19"E, elevation 504–1,200 m); (3) Yunnan Province (21°55'53"N–25°14'27"N, 101°23'19"E–102°44'28"E, elevation 505–1,922 m). The sampling information (date, host, place, GPS, etc.) was recorded. Samples were packaged in envelopes and brought to the laboratory following the method described by Senanayake et al. (2020). Morphological observations were made using a Motic SMZ (Stereoscopic Zoom Microscope) 168 Series dissecting microscope (Motic, Xiamen, China) for fungal structures on a natural substrate. Fruiting bodies were collected using a syringe needle and transferred to a drop of tap water on a clean slide. The features were examined and photographed using a Nikon ECLIPSE Ni-U compound microscope fitted with a Nikon DS-Ri2 digital camera. Measurements were made with the Tarosoft Image Frame Work v. 0.9.7 software following the procedures outlined by Liu et al. (2010), and images used for photo plates were processed with Adobe Photoshop CC 2018 software (Adobe Systems, San Jose, CA, USA). Single spore isolations were made on potato dextrose agar (PDA, Oxoid) or water agar (WA, Oxoid) and later transferred onto new PDA plates following the methods described in Senanayake et al. (2020). Incubation and cultural growth were observed at 25 °C in dark and pure cultures were obtained.

Herbarium specimens were deposited in the Herbarium of Cryptogams, Kunming Institute of Botany Academia Sinica (HKAS), Kunming, China, and the herbarium of University of Electronic Science and Technology (HUEST), Chengdu, China. The pure cultures obtained in this study were deposited in the China General Microbiological Culture Collection Center (CGMCC) in Beijing, China and the University of Electronic Science and Technology Culture Collection (UESTCC), Chengdu, China. Names of the new taxa were registered in MycoBank (http://www.mycobank.org/).

DNA extraction, PCR amplification and sequencing

Isolates were grown in PDA medium at 25 °C in dark for three weeks to one month. Fungal mycelia were scraped off and transferred to 1.5 mL microcentrifuge tubes using a sterilized lancet for genomic DNA extraction. Fungal DNA was extracted from mycelia (about 50–100 mg) using the Trelief TM Plant Genomic DNA Kit (TsingKe Co., Beijing, China). Five different gene regions were amplified by Polymerase Chain Reaction (PCR). The internal transcribed spacer region of rDNA (ITS), nuclear large subunit rDNA (28S, LSU), nuclear small subunit rDNA (18S, SSU), RNA polymerase second-largest subunit (*rpb2*) and translation elongation factor 1-alpha (*tef1-α*) were selected for the study. The primers used were LR0R/LR5 for LSU (Vilgalys and Hester 1990), NS1/NS4 for SSU (White et al. 1990), ITS5/ITS4 for ITS (White et al. 1990), fRPB2-5F and fRPB2-7cR for *rpb2* (Liu et al. 1999) and TEF1-983F/TEF1-2218R for *tef1-α* (Rehner and Buckley 2005). Amplifications were performed in a 25 µL reaction volume containing 9.5 µL of ddH_2O, 12.5 µL of 2× Taq PCR Master Mix with blue dye (Sangon Biotech, Shanghai, China), 1 µL of DNA template and 1 µL of each primer. The amplification condition for ITS, LSU, SSU, and *tef1-α* consisted of initial denaturation at 94 °C for 3 min, followed by 40 cycles of 45 s at 94 °C, 50 s at 55 °C and 1 min at 72 °C, and a final extension period of 10 min at 72 °C. The amplification condition for the *rpb2* gene consisted of initial denaturation at 95 °C for 5 min; followed by 37 cycles of 15 s at 95 °C, 50 s at 56 °C and 2 min at 72 °C, and a final extension period of 10 min at 72 °C. The PCR product purification and sequencing were performed at Beijing Tsingke Biotechnology (Chengdu) Co., Ltd., Chengdu, China.

Phylogenetic analyses

In this study, the taxa included in the phylogenetic analyses were selected and obtained from previous studies and GenBank (Table 1), with a total of 67 taxa. *Occultibambusa pustula* (MFLUCC 11-0502) and *O. bambusae* (MFLUCC 13-0855) (Occultibambusaceae, Pleosporales) were selected as outgroup taxa. Single-locus alignments were made in MAFFT v. 7 (http://mafft.cbrc.jp/alignment/server/) (Katoh and Standley 2013) and checked visually using AliView (Larsson 2014). The alignments were trimmed using trimAl v 1.2 (Capella-Gutierrez et al. 2009). Five single-locus alignments were combined using SequenceMatrix 1.7.8 (Vaidya et al. 2011). Maximum likelihood (ML) and Bayesian inference (BI) analyses were employed to assess phylogenetic relationships as detailed in Dissanayake et al. (2020).

ML analyses were performed with RAxML-HPC v.8 on XSEDE (8.2.12) (Stamatakis 2006; Stamatakis et al. 2008) through the CIPRES Science Gateway V. 3.3 (https://www.phylo.org/portal2/login!input.action) (Miller et al. 2010). The tree search included 1,000 non-parametric bootstrap replicates; the best scoring tree was selected among suboptimal trees from each run by comparing likelihood scores under the GTRGAMMA substitution model. The resulting replicates were plotted onto the best scoring tree obtained previously. ML bootstrap values equal to or greater than 75% were marked near each node.

BI was performed in MrBayes 3.2.6 (Ronquist et al. 2012). The program MrModeltest 2 v. 2.3 (Nylander 2008) was used to determine the best nucleotide

substitution model for each data partition. The evolutionary model of SYM+I+G substitution model was selected for ITS, HKY+G substitution model was selected for SSU, and GTR+I+G substitution model was selected for LSU, *rpb2* and *tef1-α*. Posterior probabilities (PP) (Rannala and Yang 1996) were determined by Markov chain Monte Carlo sampling (MCMC). Six simultaneous Markov chains were run for 10 million generations, and trees were sampled every 1,000 th generation. The first 25% of saved trees, representing the burn-in phase of the analysis, were discarded. The remaining trees were used for calculating posterior probabilities in the majority rule consensus tree (Larget and Simon 1999). PP values equal to or greater than 0.95 were marked near each node.

Phylogenetic trees were printed with Fig Tree v. 1.4.4 (http://tree.bio.ed.ac.uk/software/figtree/) and the layout was created in Adobe Illustrator CS6 software (Adobe Systems, USA). The new sequences generated in this study were deposited in GenBank (Table 1).

Table 1. Taxa used in the phylogenetic analyses and the corresponding GenBank accession numbers.

Taxa names	Strain/Specimen number	GenBank accession numbers					References
		ITS	LSU	*rpb2*	SSU	*tef1-α*	
Nigrograna acericola	CGMCC 3.24957 T	OR253153	OR253312	N/A	N/A	OR263572	Li et al. (2023)
Nigrograna acericola	**UESTCC 23.0208**	**PP812425**	**PP812460**	**PP838917**	**PP812443**	**PP838935**	**In this study**
Nigrograna acericola	**UESTCC 23.0191**	**PP812426**	**PP812461**	**PP838918**	**PP812444**	**PP838936**	**In this study**
Nigrograna antibiotica	CCF 4378 T	JX570932	KF925327	N/A	KF925328	JX570934	Kolařík (2018)
Nigrograna antibiotica	CCF 4498	LT221894	LT221895	N/A	N/A	N/A	Kolařík (2018)
Nigrograna aquatica	MFLUCC 17-2318 T	MT627705	MN913705	N/A	N/A	N/A	Dong et al. (2020)
Nigrograna asexualis	ZHKUCC 22-0214 T	OP450965	OP450971	OP432241	OP450979	OP432245	Lu et al. (2022)
Nigrograna camelliae	**CGMCC 3.25625 T**	**PP812431**	**PP812466**	**PP838923**	**PP812449**	**PP838939**	**In this study**
Nigrograna camelliae	**UESTCC 23.0197**	**PP812432**	**PP812468**	**PP838924**	**PP812450**	**PP838940**	**In this study**
Nigrograna cangshanensis	MFLUCC 15-0253 T	KY511063	KY511064	N/A	KY511065	N/A	Tibpromma et al. (2017)
Nigrograna carollii	CCF 4484 T	LN626657	LN626682	LN626662	LN626674	LN626668	Kolařík (2018)
Nigrograna chromolaenae	MFLUCC 17-1437 T	MT214379	MT214473	N/A	N/A	MT235801	Mapook et al. (2020)
Nigrograna coffeae	ZHKUCC 22-0210 T	OP450967	OP450973	OP432243	OP450981	OP432247	Lu et al. (2022)
Nigrograna coffeae	ZHKUCC 22-0211	OP450968	OP450974	OP432244	OP450982	OP432248	Lu et al. (2022)
Nigrograna fuscidula	CBS 141556 T	KX650550	N/A	N/A	N/A	KX650525	Jaklitsch and Voglmayr (2016)
Nigrograna fuscidula	CBS 141476	KX650547	N/A	KX650576	KX650509	KX650522	Jaklitsch and Voglmayr (2016)
Nigrograna guizhouensis	CGMCC 3.25501 T	OR680498	OR680565	OR842915	OR680867	OR858897	Zhang et al. (2024)
Nigrograna guizhouensis	ZY22.020	OR680499	OR680566	OR842916	OR680868	OR858898	Zhang et al. (2024)
Nigrograna guttulata	**CGMCC 3.25689 T**	**PP812433**	**PP812469**	**PP838925**	**PP812451**	**PP838941**	**In this study**
Nigrograna guttulata	**UESTCC 23.0295**	**PP812434**	**PP812470**	**PP838926**	**PP812452**	**PP838942**	**In this study**
Nigrograna heveae	ZHKUCC 22-0284 T	OP584490	OP584488	OP750374	OP584492	OP750372	Hyde et al. (2023)
Nigrograna hydei	GZCC 19-0050 T	MN387225	MN387227	N/A	N/A	MN389249	Zhang et al. (2020)
Nigrograna impatientis	GZCC 19-0042 T	MN387226	MN387228	N/A	N/A	MN389250	Zhang et al. (2020)
Nigrograna italica	MFLU 23-0139 T	OR538590	OR538591	OR531365	N/A	OR531366	Bundhun et al. (2023)
Nigrograna jinghongensis	KUMUCC 21-0035 T	MZ493303	MZ493317	MZ508421	MZ493289	MZ508412	Boonmee et al. (2021)
Nigrograna jinghongensis	KUMUCC 21-0036	MZ493304	MZ493318	MZ508422	MZ493290	MZ508413	Boonmee et al. (2021)
Nigrograna kunmingensis	ZHKUCC 22-0242 T	OP456214	OP456379	N/A	OP456382	OP471608	Liu et al. (2024)
Nigrograna kunmingensis	ZHKUCC 22-0243	OP484334	OP456380	N/A	OP456383	OP471609	Liu et al. (2024)
Nigrograna lincangensis	ZHKUCC 23-0798 T	OR853099	OR922323	OR966280	OR941079	OR966282	Xu et al. (2024)
Nigrograna lincangensis	ZHKUCC 23-0799	OR853100	OR922324	OR966281	OR941080	OR966283	Xu et al. (2024)

Taxa names	Strain/Specimen number	GenBank accession numbers					References
		ITS	LSU	*rpb2*	SSU	*tef1-α*	
Nigrograna locuta-pollinis	CGMCC 3.18784 T	MF939601	MF939583	MF939610	N/A	MF939613	Zhao et al. (2018)
Nigrograna longiorostiolata	**CGMCC 3.25626 T**	**PP812421**	**PP812458**	**PP838913**	**PP812439**	**PP838945**	**In this study**
Nigrograna longiorostiolata	**UESTCC 23.0200**	**PP812422**	**PP812457**	**PP838914**	**PP812440**	**PP838946**	**In this study**
Nigrograna mackinnonii	CBS 674.75 T	KF015654	KF015612	KF015703	GQ387552	KF407986	de Gruyter et al. (2012)
Nigrograna magnoliae	MFLUCC 20-0020 T	MT159628	MT159622	MT159611	MT159634	MT159605	Wanasinghe et al. (2020)
Nigrograna magnoliae	MFLUCC 20-0021	MT159629	MT159623	MT159612	MT159635	MT159606	Wanasinghe et al. (2020)
Nigrograna magnoliae	**UESTCC 23.0203**	**PP812419**	**PP812454**	**PP838929**	**PP812437**	**PP838943**	**In this study**
Nigrograna magnoliae	**CGMCC 3.25627**	**PP812420**	**PP812453**	**PP838927**	**PP812435**	**PP838931**	**In this study**
Nigrograna magnoliae	**UESTCC 23.0190**	**PP812417**	**PP812456**	**PP838930**	**PP812438**	**PP838944**	**In this study**
Nigrograna magnoliae	**UESTCC 23.0206**	**PP812418**	**PP812455**	**PP838928**	**PP812436**	**PP838932**	**In this study**
Nigrograna mycophila	CBS 141478 T	KX650553	N/A	N/A	N/A	KX650526	Jaklitsch and Voglmayr (2016)
Nigrograna mycophila	CBS 141483	KX650555	N/A	KX650577	KX650510	KX650528	Jaklitsch and Voglmayr (2016)
Nigrograna neriicola	**CGMCC 3.25624 T**	**PP812430**	**PP812467**	**PP838921**	**PP812447**	**PP838937**	**In this study**
Nigrograna neriicola	**UESTCC 23.0195**	**PP812429**	**PP812465**	**PP838922**	**PP812448**	**PP838938**	**In this study**
Nigrograna norvegica	CBS 141485 T	KX650556	N/A	KX650578	KX650511	N/A	Jaklitsch and Voglmayr (2016)
Nigrograna obliqua	CBS 141477 T	KX650560	N/A	KX650580	N/A	KX650531	Jaklitsch and Voglmayr (2016)
Nigrograna obliqua	CBS 141475	KX650558	N/A	KX650579	KX650512	KX650530	Jaklitsch and Voglmayr (2016)
Nigrograna oleae	CGMCC 3.24423 T	OR253080	OR253232	N/A	N/A	OR262140	Li et al. (2023)
***Nigrograna oleae* (*N. trachycarpi*)**	**GMB0499**	**OR120437**	**N/A**	**N/A**	**N/A**	**OR150024**	Hu et al. (2023); **In this study**
***Nigrograna oleae* (*N. trachycarpi*)**	**GMB0505**	**OR120440**	**N/A**	**N/A**	**N/A**	**OR150025**	Hu et al. (2023); **In this study**
Nigrograna oleae	**UESTCC 23.0209**	**PP812424**	**PP812463**	**PP838915**	**PP812441**	**PP838933**	**In this study**
Nigrograna oleae	**UESTCC 23.0193**	**PP812423**	**PP812459**	**PP838916**	**PP812442**	**PP838934**	**In this study**
Nigrograna peruviensis	CCF 4485 T	LN626658	LN626683	LN626665	LN626677	LN626671	Kolařík (2018)
Nigrograna puerensis	ZHKUCC 22-0212 T	OP450969	OP450975	N/A	OP450983	OP432249	Lu et al. (2022)
Nigrograna rhizophorae	MFLUCC 18-0397 T	MN047085	N/A	MN431489	N/A	MN077064	Dayarathne et al. (2020)
Nigrograna rubescens	CHEM 2344 T	OQ400924	OQ400934	OQ413082	N/A	OQ413077	Mack et al. (2024)
Nigrograna samueliana	NFCCI 4383 T	MK358817	MK358812	MK330939	MK358810	MK330937	Dayarathne et al. (2020)
Nigrograna schinifolii	GMB0498 T	OR120434	N/A	N/A	N/A	OR150022	Hu et al. (2023)
Nigrograna schinifolii	GMB0504	OR120441	N/A	N/A	N/A	OR150023	Hu et al. (2023)
Nigrograna sichuanensis	CGMCC 3.24424 T	OR253096	OR253248	N/A	N/A	OR251058	Li et al. (2023)
Nigrograna thailandica	MFLUCC 17-2663	MK762709	MK762716	N/A	MK762704	N/A	Senanayake et al. (2023)
Nigrograna thymi	MFLUCC 14-1096 T	KY775576	KY775573	N/A	KY775574	KY775578	Hyde et al. (2017)
Nigrograna thymi	**UESTCC 23.0210**	**PP812428**	**PP812464**	**PP838919**	**PP812445**	**N/A**	**In this study**
Nigrograna thymi	**UESTCC 23.0194**	**PP812427**	**PP812462**	**PP838920**	**PP812446**	**N/A**	**In this study**
Nigrograna verniciae	CGMCC 3.24425	OR253116	OR253275	N/A	N/A	OR251168	Li et al. (2023)
Nigrograna wuhanensis	ZHKUCC 22-0329 T	OP941389	OP941390	N/A	OQ061465	OP947079	Shu et al. (2023)
Nigrograna yasuniana	YU 101026 T	HQ108005	LN626684	LN626664	LN626676	LN626670	Kolařík (2018)
Occultibambusa bambusae	MFLUCC 13-0855 T	KU940123	KU863112	KU940170	N/A	KU940193	Dai et al. (2017)
Occultibambusa pustula	MFLUCC 11-0502 T	KU940126	KU863115	N/A	N/A	N/A	Dai et al. (2017)

*** Remarks:** The superscript T denotes ex-type isolates. "N/A" denotes sequence is unavailable. The newly generated sequences, new species and synonymized isolates are indicated in black bold font. **Abbreviations: CBS:** CBS–KNAW Fungal Biodiversity Centre, Utrecht, The Netherlands; **CCF:** Culture Collection of Fungi, Charles University, Prague, Czech Republic; **CGMCC:** China General Microbiological Culture Collection Center, Institute of Microbiology, Chinese Academy of Sciences, Beijing, China; **GMB:** Herbaria of Guizhou Medical University, Guiyang, China; **GZCC:** Guizhou Culture Collection, Guizhou, China; **KUMUCC:** Kunming Medical University Culture Collection, Kunming, China; **MFLUCC:** Mae Fah Luang University Culture Collection, Chiang Rai, Thailand; **NFCCI:** National Fungal Culture Collection of India, India; **UESTCC:** University of Electronic Science and Technology Culture Collection, Chengdu, China; **YU:** Yale University Herbarium, Connecticut, America; **ZHKUCC:** Zhongkai University of Agriculture and Engineering Culture Collection, Guangzhou, China; **Personal collections**: **ZY** and **CHEM:** These numbers are assigned by the author and have no annotations.

Phylogenetic results

In this study, five loci, ITS, LSU, *rpb2*, SSU, and *tef1-α*, were used to determine the phylogenetic placement of the new collections. The concatenated matrix was comprised of 69 taxa with a total of 4,236 bp characters (ITS: 1–473 bp; LSU: 474–1,306 bp; *rpb2*: 1,307–2,331 bp; SSU: 2,332–3,335 bp; *tef1-α*: 3,336–4,236 bp) including gaps. Single-locus analyses were carried out to compare the topologies and clade stabilities, respectively. The results showed that ML and BI were similar in topology without significant conflicts. The best RAxML tree with a final likelihood value of -20,464.246121 is presented in Fig. 1. RAxML analysis yielded 1,200 distinct alignment patterns and 26.42% of undetermined characters or gaps. Estimated base frequencies were as follows: A = 0.247595, C = 0.247214, G = 0.264771, T = 0.240420, with substitution rates AC = 1.651782, AG = 5.572876, AT = 1.491922, CG = 1.179397, CT = 11.546850, GT = 1.000000; gamma distribution shape parameter alpha = 0.139617. Tree-Length = 1.453662. The final average standard deviation of split frequencies at the end of total MCMC generations for BI analysis was 0.009978 (the critical value for the topological convergence diagnostic is below 0.01).

Representatives of all the species of *Nigrograna* were including in our phylogenetic analysis (Fig. 1). Four strains (CGMCC 3.25627, UESTCC 23.0203, UESTCC 23.0190 and UESTCC 23.0206) were nested with *N. magnoliae* (ex-type strain MFLUCC 20-0020 and MFLUCC 20-0021), and strains, UESTCC 23.0208 and UESTCC 23.0191, UESTCC 23.0210 and UESTCC 23.0194, clustered with *N. acericola* (ex-type strain, CGMCC 3.24957) and *N. thymi* (ex-type strain, MFLUCC 14-1096), respectively. *Nigrograna trachycarpi* (GMB0499 and GMB0505) was synonymized under *N. oleae*, these two strains of *N. trachycarpi* and our two isolates (UESTCC 23.0209 and UESTCC 23.0193) grouped with ex-type strain of *N. oleae* (CGMCC 3.24423) with maximum support (100% MLBS/1.00 BIPP).

Nigrograna camelliae (CGMCC 3.25625 and UESTCC 23.0197) and *N. guttulata* (CGMCC 3.25689 and UESTCC 23.0295) were sister to *N. coffeae* (ex-type strain ZHKUCC 22-0210 and ZHKUCC 22-0211) and *N. peruviensis* (ex-type strain CCF 4485), respectively. They formed two distinct clades with 100% MLBS/1.00 BIPP and 63% MLBS/0.98 BIPP, respectively. *Nigrograna neriicola* (CGMCC 3.25624 and UESTCC 23.0195) was sister to *N. schinifolii* (ex-type strain GMB0498 and GMB0504) and formed a strongly supported monophyletic lineage (96% MLBS/1.00 BIPP). *Nigrograna longiorostiolata* (CGMCC 3.25626 and UESTCC 23.0200) formed a distinct lineage with high bootstrap support (100% MLBS/1.00 BIPP).

Taxonomy

***Nigrograna magnoliae* Wanas, PLoS One, 15(7): 10 (2020)**
MycoBank No: 557331
Fig. 2

Description. ***Saprobic*** on dead branches of *Buxus sinica* (Buxaceae). **Sexual morph:** ***Ascomata*** 204–326 µm wide, 140–220 µm high ($\bar{x}$ = 248 × 187 µm, n = 20), solitary or gregarious, scattered, immersed to semi-immersed, with only ostiolar necks visible on the host surface, trigonoid, uniloculate, perithecioid, globose to subglobose, brown to dark brown, with an ostiole. ***Ostiole*** central or eccentric,

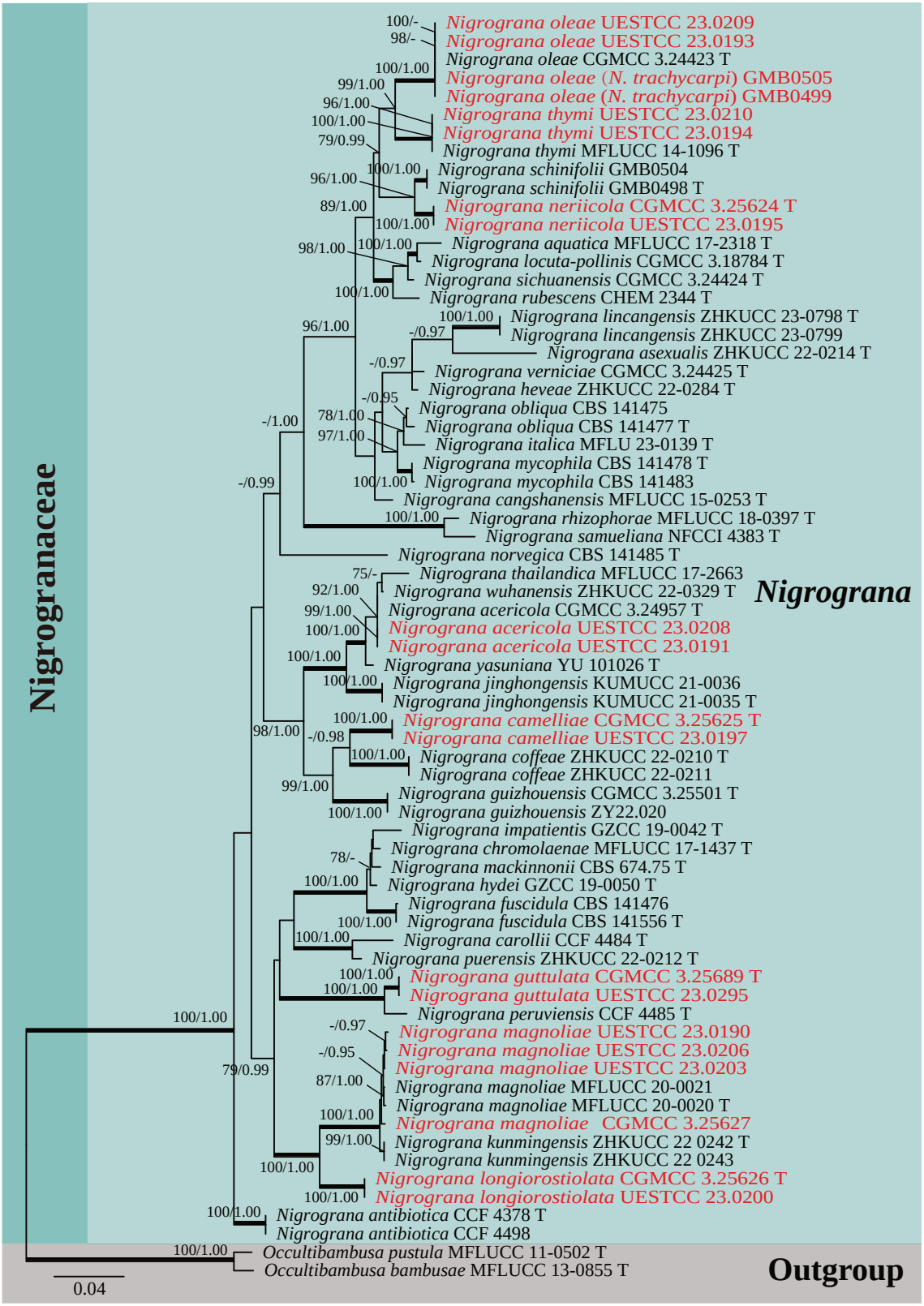

Figure 1. Phylogenetic tree constructed from maximum likelihood (RAxML) analyses of a combined ITS, LSU, *rpb2*, SSU, and *tef1-a* sequence data for selected genera within the family Nigrograniaceae (Pleosporales, Dothideomycetes). Branches support for Maximum likelihood (MLBS) equal to or greater than 75% and Bayesian inference posterior probabilities (BIPP) equal to or greater than 0.95 are marked above or below nodes as MLBS/BIPP. The abbreviation T indicates the ex-type strain. Species names and culture collections in red are newly collected taxa and synonymized isolates. The tree was rooted with *Occultibambusa pustula* (MFLUCC 11-0502) and *O. bambusae* (MFLUCC 13-0855).

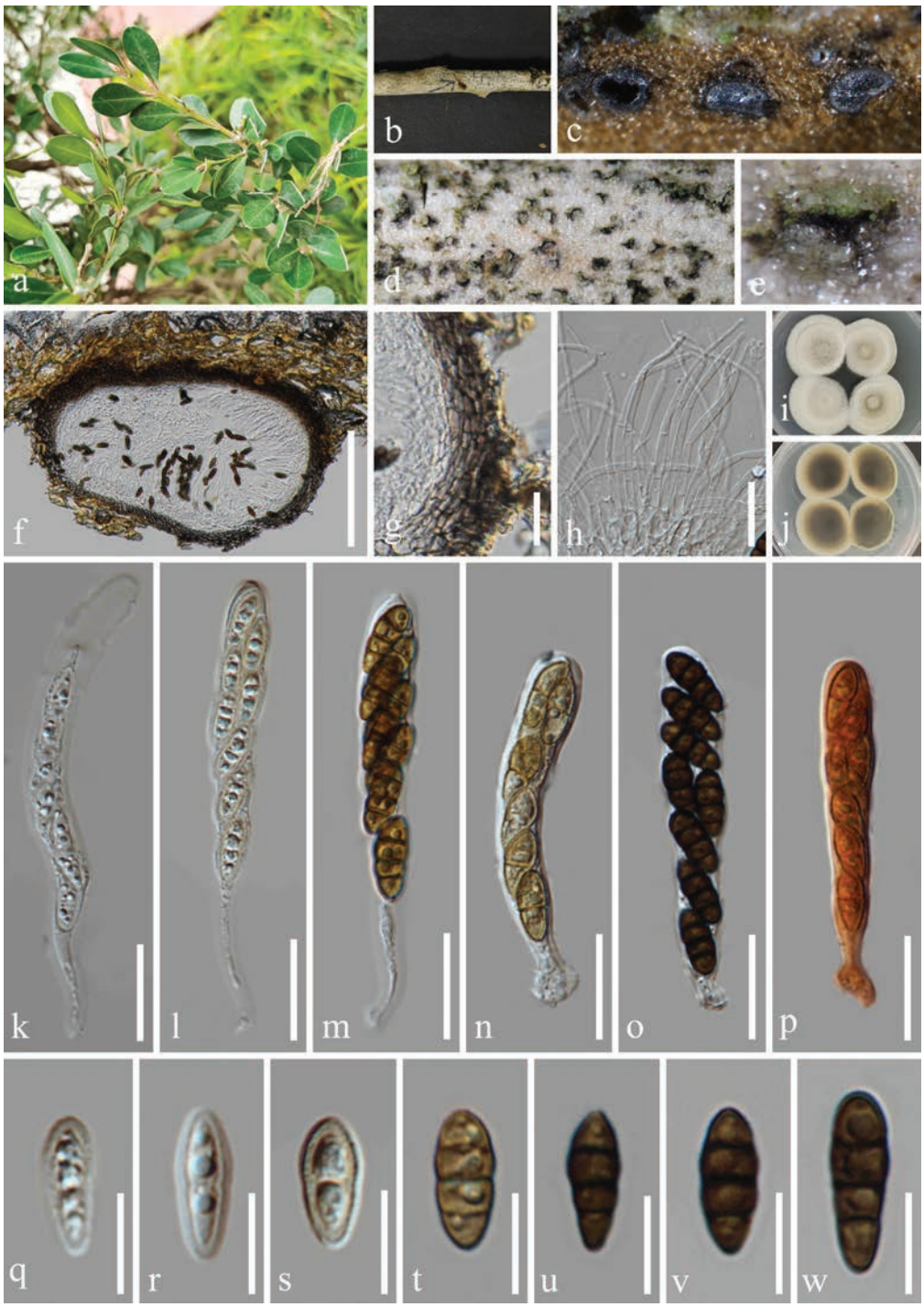

Figure 2. *Nigrograna magnoliae* (HUEST 23.0203, new host record) **a** host *Buxus sinica* **b** branch of *Buxus sinica* **c–e** appearance of ascomata on host surface **f** vertical section through ascoma **g** peridium **h** hamathecium **i, j** colonies on PDA, above (**i**) and below (**j**) **k–o** asci **p** asci in Congo red **q–w** ascospores. Scale bars: 100 µm (**f**); 20 µm (**g, h**, **k–p**); 10 µm (**q–w**).

brittle. ***Peridium*** 15–23 µm ($\bar{x}$ = 18 µm, n = 20) composed of angular cells, consisting 4–5 layers, brown to dark brown thick-walled cells of outer layer, hyaline to subhyaline thin-walled cells of inner layer. ***Hamathecium*** 1–3 µm ($\bar{x}$ = 2 µm, n = 20) wide, composed of numerous, filamentous, hyaline, aseptate or separate, rarely branched, smooth-walled pseudoparaphyses. ***Asci*** 57–103 × 8–11 µm ($\bar{x}$ = 72.5 × 10 µm, n = 30), 8-spored, bitunicate, fissitunicate, clavate to long cylindric-clavate, short cylindrical pedicellate with a swollen base, apically rounded, with a minute

ocular chamber. ***Ascospores*** 13–19 × 4.5–6 µm ($\bar{x}$ = 14.5 × 5 µm, n = 50), 1–2-seriate, partially overlapping, fusoid to ellipsoid, tapering towards the blunt ends, or blunt at both ends, guttulate, smooth-walled, olivaceous to yellowish-brown when young, 1-septate; deeply constricted at septa, becoming 3-septate, brown to dark brown when mature, without appendages. **Asexual morph:** Undetermined.

Culture characteristics. Ascospores germinated on PDA within 24 h, and germ tubes produced from basal cell. Colonies growing on PDA reached 32–33 mm in diameter after three weeks at 25 °C in dark, white in the whole colony from above, and slightly raised in the center, circular, flat, edge entire, margin well-defined; in reverse, grayish black in the center, off-white at the margin, the color gradually lightens from center to edge, no pigmentation on PDA.

Material examined. China • Yunnan Province, Kunming City, Panlong District, Kunming Botanical Garden. 25°8'27"N, 102°44'24"E, elevation 1,922 m, on dead branches of medicinal plant *Buxus sinica* (Rehder & E. H. Wilson) M. Cheng (Buxaceae), 11 November 2022, H.Z. Du, S735 (HUEST 23.0203), living culture UESTCC 23.0203; • ibid., Sichuan Province, Chengdu City, High-tech West District, Yaobo Park, 30°43'57"N, 103°56'21"E, elevation 504 m, on dead branches of medicinal plant *Eucommia ulmoides* Oliv. (Eucommiaceae), 11 August 2021, H.Z. Du, S347 (HUEST 23.0206), living culture UESTCC 23.0206; • ibid., Guizhou Province, Guiyang City, Nanming District, Guiyang Medicinal Botanical Garden, 26°32'18"N, 106°41'48"E, elevation 1,127 m, on dead branches of medicinal plant *Mahonia bealei* (Fort.) Carr. (Berberidaceae), 12 October 2021, H.Z. Du, S370 (HUEST 23.0207), living culture CGMCC 3.25627 = UESTCC 23.0207; • ibid., Guizhou Province, Guiyang City, Huaxi District, 26°30'43"N, 106°39'32"E, elevation 1,155 m, on dead branches of medicinal plant *Camellia sinensis* (L.) O. Ktze. (Theaceae), 2 February 2023, Y.X. Yu, GY33 (HUEST 23.0190), living culture UESTCC 23.0190.

Notes. *Nigrograna magnoliae* was introduced by Wanasinghe et al. (2020) with both asexual and sexual morphs reported in China. The host distribution of this species is presented in Table 2. Our collections are identical to *N. magnoliae* based on morphology and phylogeny. Therefore, we reported it as new host records from medicinal plants of *Buxus sinica*, *Camellia sinensis*, *Eucommia ulmoides* and *Mahonia bealei* in China.

Table 2. The host distribution of *Nigrograna magnoliae*.

Host distribution	Collecting sites	References
Magnolia denudate (Magnoliaceae)	China (Yunnan Province)	Wanasinghe et al. (2020)
Submerged wood from aquatic habitats	Thailand (Chiang Rai Province)	Zhang et al. (2020)
Decaying twigs of unidentified host	China (Guizhou Province)	Zhang et al. (2020)
Acer truncatum (Aceraceae)	China (Sichuan Province)	Li et al. (2023)
Juglans regia (Juglandaceae)	China (Sichuan Province)	Li et al. (2023)
Olea europaea (Oleaceae)	China (Sichuan Province)	Li et al. (2023)
Michelia alba (Magnoliaceae)	China (Guizhou Province)	Chethana et al. (2023)
Rosa sp. (Rosaceae)	China (Sichuan Province)	Chethana et al. (2023)
Fruiting bodies of *Shearia* sp. (Dothioraceae)	China (Guizhou Province)	Chethana et al. (2023)
Magnolia grandiflora (Magnoliaceae)	Thailand (Chiang Mai Province)	https://www.ncbi.nlm.nih.gov/nuccore/MN081891.1
Castanopsis indica (Fagaceae)	China (Yunnan Province)	Ren et al. (2024)
Buxus sinica (Buxaceae)	China (Yunnan Province)	In this study
Eucommia ulmoides (Eucommiaceae)	China (Sichuan Province)	In this study
Mahonia bealei (Berberidaceae)	China (Guizhou Province)	In this study
Camellia sinensis (Theaceae)	China (Guizhou Province)	In this study

***Nigrograna longiorostiolata* H.Z. Du & Jian K. Liu, sp. nov.**
MycoBank No: 854177
Fig. 3

Etymology. The epithet '*longiorostiolata*' refers to the longer-ostiolate of ascomata.

Holotype. HKAS 131311

Description. ***Saprobic*** on dead branches of *Citrus medica* (Rutaceae). **Sexual morph:** ***Ascomata*** 222–293 µm wide, 144–486 µm high ($\bar{x}$ = 264 × 303 µm, n = 20), solitary, scattered, immersed, visible as black dots on the host surface, uniloculate, globose to subglobose, sometimes obpyriform with a long ostiole. ***Ostioles*** 175–302 µm long, 83–128 µm wide ($\bar{x}$ = 263 × 102 µm, n = 20) central or eccentric, longer, with a crest-like apex, filled with hyaline or slightly brown periphyses. ***Peridium*** 17–32 µm ($\bar{x}$ = 23.5 µm, n = 20) composed of *textura prismatica* cells, consisting 3–4 layers, brown to dark brown of outer layer, hyaline to subhyaline of inner layer. ***Hamathecium*** 1–2 µm ($\bar{x}$ = 1.5 µm, n = 20) wide, composed of numerous, filiform, hyaline, aseptate or separate, rarely branched, guttulate, smooth-walled pseudoparaphyses. ***Asci*** 40–70 × 6–9 µm ($\bar{x}$ = 53 × 8 µm, n = 30), 5–8-spored, bitunicate, fissitunicate, clavate, short cylindrical pedicellate with a swollen base, apically rounded, with a minute ocular chamber. ***Ascospores*** 10–13 × 4–6 µm ($\bar{x}$ = 12 × 5 µm, n = 50), 1–2-seriate, partially overlapping, fusoid to ellipsoid, tapering towards the blunt ends, or blunt at both ends, guttulate, olivaceous to yellowish-brown when young, aseptate or 1-septate; deeply constricted at septa, becoming 3-septate, brown to dark brown when mature, without appendages. **Asexual morph:** Undetermined.

Culture characteristics. Ascospores germinated on PDA within 24 h, and germ tubes produced from basal cell. Colonies growing on PDA reached 17–18 mm in diameter after three weeks at 25 °C in dark, white in the whole colony from above, circular, edge entire, margin well-defined; in reverse, off-white to grayish brown, no pigmentation on PDA.

Material examined. China • Yunnan Province, Xishuangbanna Dai Autonomous Prefecture, Mengla County, Xishuangbanna Tropical Botanical Garden Chinese Academy of Sciences. 21°56'1"N, 101°25'33"E, elevation 505 m, on dead branches of medicinal plant *Citrus medica* L. (Rutaceae), 10 November 2022, H.Z. Du, S655 (HKAS 131311, holotype; HUEST 23.0200, isotype); ex-holotype living culture CGMCC 3.25626; ex-isotype living culture UESTCC 23.0200.

Notes. *Nigrograna longiorostiolata* shares similar morphology with *N. magnoliae* (holotype, MFLU 20–0092) and *N. kunmingensis* (holotype, ZHKU 22-0141) in having immersed, globose to subglobose ascomata, bitunicate and clavate asci, fusoid to ellipsoid, 3-septate mature ascospores. However, the ascomata size of *N. longiorostiolata* (222–293 × 144–486 µm) is larger than *N. magnoliae* (200–300 × 100–150 µm) (Wanasinghe et al. 2020) and smaller than *N. kunmingensis* (300–500 × 390–450 µm) (Liu et al. 2024). The phylogenetic result (Fig. 1) showed that *N. longiorostiolata* (CGMCC 3.25626 and UESTCC 23.0200) can be recognized as a distinct phylogenetic species with high bootstrap support (100% MLBS/1.00 BIPP). Additionally, *N. longiorostiolata* (ex-type strain, CGMCC 3.25626) can be distinguished from *N. magnoliae* (ex-type strain, MFLUCC 20-0020) by 26/471 bp (5.5%, 2 gaps) in ITS, 14/831 bp (1.7%, without gaps) in LSU, 30/855 bp (3.5%, 3 gaps) in *tef1-α* and 96/1042

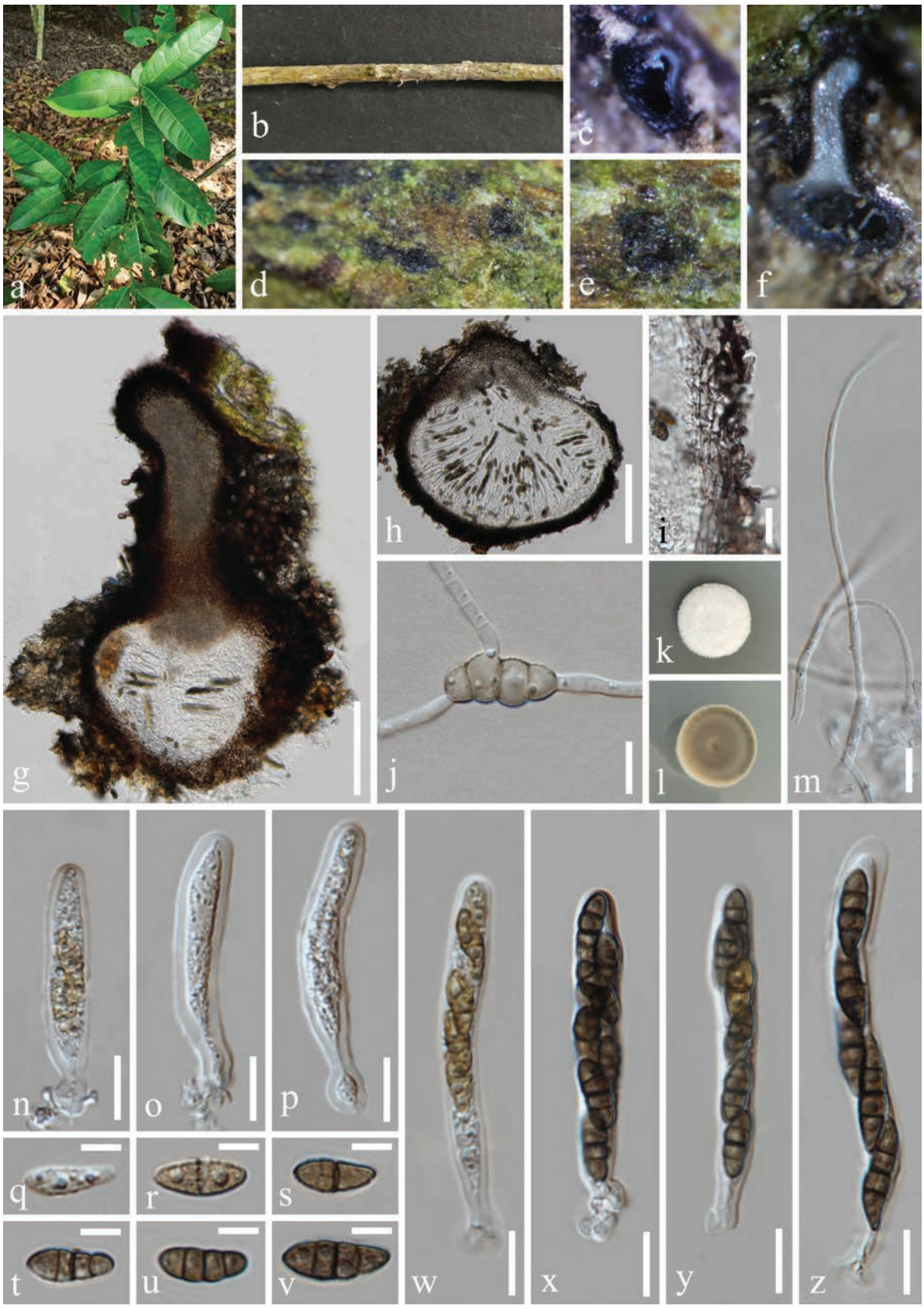

Figure 3. *Nigrograna longiorostiolata* (HKAS 131311, holotype) **a** host *Citrus medica* **b** branch of *Citrus medica* **c–f** appearance of ascomata on host surface **g, h** vertical section through ascoma **i** peridium **j** germinated ascospore **k, l** colony on PDA, above (**k**) and below (**l**) **m** hamathecium **n–p, w–z** asci **q–v** ascospores. Scale bars: 100 µm (**g, h**); 10 µm (**i, j, m–p, w–z**); 5 µm (**q–v**).

bp (9.2%, without gaps) in *rpb2* differences, and differs from *N. kunmingensis* (ex-type strain, ZHKUCC 22-0242) with 70/823 bp (8.5%, 21 gaps) of ITS, 14/844 bp (1.7%, without gaps) of LSU and 30/855 bp (3.5%, 3 gaps) of *tef1-α* differences. Therefore, *N. longiorostiolata* associated with *Citrus medica* is a phylogenetically distinct specie and introduced as a new species.

***Nigrograna acericola* W.L. Li & Jian K. Liu, Mycosphere, 14(1): 1496–1500 (2023)**

MycoBank No: 849155

Fig. 4

Description. ***Saprobic*** on dead branches of *Gymnosporia acuminata* (Celastraceae). **Sexual morph:** ***Ascomata*** 524–647 × 341–475 µm ($\bar{x}$ = 586 × 424 µm, n = 20), solitary, scattered, immersed, ostiolar necks visible on the host surface or erumpent, subglobose to ellipsoid, coriaceous, brown to dark brown, with an ostiole. ***Ostioles*** 86–138 µm long, 64–119 µm wide ($\bar{x}$ = 113 × 96 µm, n = 20), mostly central, some eccentric, with a crest-like apex, central, filled with hyaline periphyses. ***Peridium*** 15–58 µm ($\bar{x}$ = 40 µm, n = 20) µm wide, composed of 4–5 layers of flattened, brown to dark brown, thin-walled cells of ***textura angularis***, the inner layer is dense, the outer layer sparse. ***Hamathecium*** 1.5–3 µm ($\bar{x}$ = 2 µm, n = 20) wide, composed of numerous, filamentous, hyaline, unbranched pseudoparaphyses. ***Asci*** 70–87 × 12–14 µm ($\bar{x}$ = 77 × 13 µm, n = 30), 8-spored, bitunicate, fissitunicate, cylindrical to clavate, short pedicellate, apically rounded, with a minute ocular chamber. ***Ascospores*** 16–19 × 5–7 µm ($\bar{x}$ = 17 × 6 µm, n = 50), 1–2-seriate, biseriate or partially overlapping, fusoid to ellipsoid, with obtuse ends, tapering towards the ends, guttulate, smooth-walled, 1-septate, subhyaline to yellowish-brown when young; becoming 3-septate, slightly constricted at the middle septum, brown to dark brown when mature, without appendages. **Asexual morph:** Undetermined.

Culture characteristics. Ascospores germinated on PDA within 24 h, and germ tubes produced from basal cell. Colonies growing on PDA reached 38–40 mm in diameter after three weeks at 25 °C in dark, white in the whole colony from above, circular, edge entire, margin well-defined; in reverse, light brown in the center, olive gray at the margin, no pigmentation on PDA.

Material examined. China • Yunnan Province, Xishuangbanna Dai Autonomous Prefecture, Mengla County, Xishuangbanna Tropical Botanical Garden Chinese Academy of Sciences. 21°55'54"N, 101°15'16"E, elevation 511 m, on dead branches of medicinal plant *Gymnosporia acuminata* Hook. f. (Celastraceae), 10 November 2022, H.Z. Du, D03 (HUEST 23.0208), living culture UESTCC 23.0208; *ibid*., Sichuan Province, Zigong City, Rong County, 29°29'1"N, 104°14'19"E, elevation 850 m, on dead branches of medicinal plant *Camellia sinensis* (L.) O. Ktze. (Theaceae), 3 November 2022, Y. H. Lu & Y. Xiao, CS11(HUEST 23.0191), living culture UESTCC 23.0191.

Notes. *Nigrograna acericola* was introduced by Li et al. (2023) from *Acer truncatum* (Aceraceae) in China. Our collections are identical to *N. acericola* based on morphology and phylogeny. We reported it as new host records from *Camellia sinensis* and *Gymnosporia acuminata* in China.

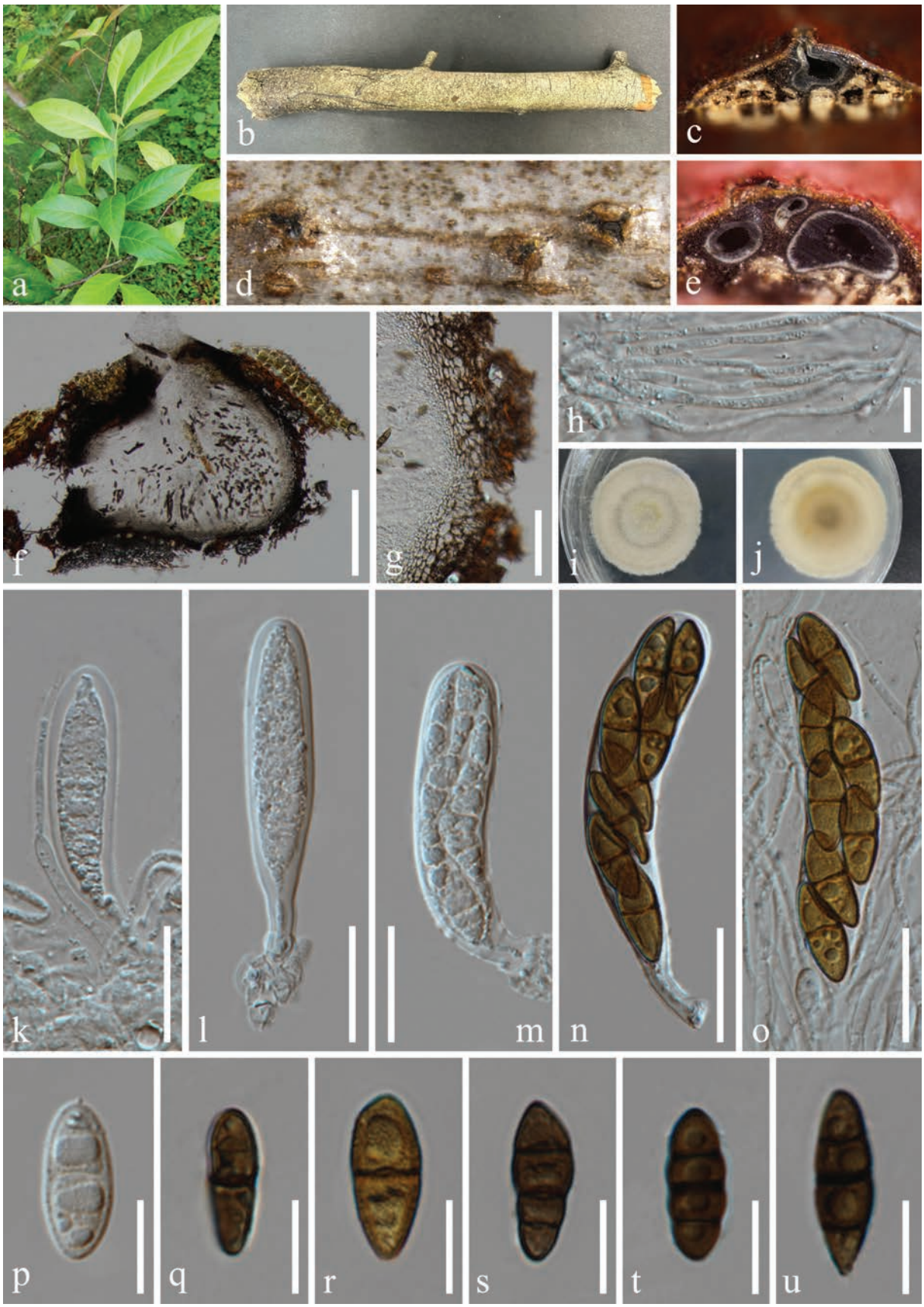

Figure 4. *Nigrograna acericola* (HUEST 23.0208, new host record) **a** host *Gymnosporia acuminata* **b** branch of *Gymnosporia acuminata* **c–e** appearance of ascomata on host surface **f** vertical section through ascoma **g** peridium **h** hamathecium **i, j** colony on PDA, above (**i**) and below (**j**) **k–o** asci. **p–u** ascospores. Scale bars: 200 µm (**f**); 50 µm (**g**); 10 µm (**h, p–u**); 20 µm (**k–o**).

Nigrograna camelliae **Y.H. Lu, H.Z. Du & Jian K. Liu, sp. nov.**
MycoBank No: 854178
Fig. 5

Etymology. The epithet '*camelliae*' refers to the host genus *Camelliae* from which the fungus was originally isolated.

Holotype. HKAS 131310

Description. ***Saprobic*** on dead branches of *Camellia sinensis* (Theaceae). **Sexual morph:** ***Ascomata*** 137–270 µm wide, 208–324 µm high ($\bar{x}$ = 212 × 265 µm, n = 20), solitary, scattered, immersed, black spots on the host substrate, globose to subglobose, sometimes obpyriform, ostiolate, hairs of ascomata 2–3 µm wide, slightly brown, septate. ***Ostioles*** 65–138 µm long, 32–60 µm wide ($\bar{x}$ = 100 × 45 µm, n = 20) mostly central, some eccentric, with a crest-like apex. ***Peridium*** 19–30 µm ($\bar{x}$ = 23 µm, n = 20) wide, composed of 2–3 layers, comprising reddish brown to dark brown pigmented cells. ***Hamathecium*** 2–3 µm ($\bar{x}$ = 2.5 µm, n = 20) wide, composed of numerous, filiform, hyaline, aseptate or separate, filamentous, smooth-walled pseudoparaphyses. ***Asci*** 70–108 × 9–11 µm ($\bar{x}$ = 80 × 10 µm, n = 30), 8-spored, bitunicate, fissitunicate, clavate to cylindric-clavate, short stalked, some with a swollen base, apically rounded, with a small ocular chamber. ***Ascospores*** 13–16 × 4–6 µm ($\bar{x}$ = 15 × 5 µm, n = 50), overlapping uni- to bi-seriately arranged, fusoid to ellipsoid, tapering towards the blunt ends, or blunt at both ends, straight or slightly curved, 1-septate, constricted, with obviously guttulate, hyaline to slightly brown when immature, pale brown to brown when mature, without appendages. **Asexual morph:** Undetermined.

Culture characteristics. Ascospores germinated on PDA within 24 h, and germ tubes produced from basal cell. Colonies growing on PDA reached 35–36 mm in diameter after three weeks at 25 °C in dark, white in the whole colony and slightly bright yellow in the center from above, circular, edge entire, margin well-defined; in reverse, yellowish brown in the center, slightly brown at the margin and presented an outer ring, no pigmentation on PDA.

Material examined. China • Sichuan Province, Yaan City, Mingshan County, Mengding Mountain. 30°4'32"N, 103°2'23"E, elevation 1,200 m, on dead branches of medicinal plant *Camellia sinensis* (L.) O. Ktze. (Theaceae), 16 July 2023, Y. H. Lu & X. D. Liang, MD03A (HKAS 131310, holotype; HUEST 23.0197, isotype); ex-holotype living culture CGMCC 3.25625; ex-isotype living culture UESTCC 23.0197.

Notes. *Nigrograna camelliae* is phylogenetically close to *N. coffeae* and represents as a distinct lineage (Fig. 1). Additionally, the nucleotide base pair comparison between *N. camelliae* (ex-type strain, CGMCC 3.25625) and *N. coffeae* (ex-type strain, ZHKUCC 22-0210) revealed 15/514 bp (2.9%, 1 gap) of ITS, 11/698 bp (1.6%, without gaps) of LSU, 74/739 bp (10.0% without gaps) of *rpb2* and 28/914 bp (3.1%, without gaps) of *tef1-α* differences. Furthermore, *N. camelliae* morphologically resembles *N. coffeae* in having immersed ascomata, clavate and short pedicellate asci, pale brown to brown and septate ascospores with obviously guttulate (Lu et al. 2022). However, *N. camelliae* differs from *N. coffeae* in having ascomata with hairs and ostioles, solitary or scattered in the substrate. Additionally, they can be distinguished in having larger ascomata (208–324 × 137–270 µm vs. 140–200 × 90–140 µm) and asci (70–108 × 9–11 µm vs. 50–70 × 7–11 µm). Therefore, *N. camelliae* is introduced as a new species with the justification of phylogenetic and morphological evidence.

Figure 5. *Nigrograna camelliae* (HKAS 131310, holotype) **a** host *Camellia sinensis* **b** branch of *Camellia sinensis* **c–e** appearance of ascomata on host surface **f, g** vertical section through ascoma **h** peridium **i** hairs on ascomata **j–m, w, x** asci **n–s** ascospores **t** germinated ascospore **u, v** colony on PDA, above (**u**) and below (**v**). Scale bars: 100 μm (**f, g**); 20 μm (**h–m, w, x**); 5 μm (**n–s**); 10 μm (**t**).

***Nigrograna oleae* W.L. Li & Jian K. Liu, Mycosphere, 14(1): 1503–1505 (2023)**
MycoBank No: 849157
Fig. 6

= *Nigrograna trachycarpi*, MycoKeys 100: 141 (2023).

Description. ***Saprobic*** on dead branches of *Ardisia crenata* (Primulaceae). **Sexual morph:** ***Ascomata*** 190–334 µm wide, 303–406 µm high ($\bar{x}$ = 233 × 370 µm, n = 20), solitary or gregarious, scattered, immersed, often lying parallelly or obliquely to the bark or host surface, with a cylindrical ostiolar neck, coriaceous, obpyriform, brown to dark brown. ***Ostioles*** central or eccentric, filled with hyaline periphyses. ***Peridium*** 16.5–25 µm ($\bar{x}$ = 21 µm, n = 20) wide, consisting 4–6 layers of brown-walled cells of ***textura angularis***. ***Hamathecium*** 1–2 µm ($\bar{x}$ = 1.5 µm, n = 20) wide, aseptate or separate, composed of numerous, filiform, smooth-walled pseudoparaphyses. ***Asci*** 62–127 × 9–12 µm ($\bar{x}$ = 82 × 10 µm, n = 30), 8-spored, bitunicate, fissitunicate, clavate to long cylindric-clavate, with a short pedicel, apically rounded, with a smaller ocular chamber. ***Ascospores*** 14–17 × 4–6 µm ($\bar{x}$ = 15 × 5 µm, n = 50), 1–2-seriate, fusoid to ellipsoid, apical cell mostly obtuse, straight or slightly curved, guttulate, smooth-walled, 3-septate, constricted at the septa, pale brown to yellow-brown when young, brown to chocolate-brown at maturation, without appendages. **Asexual morph:** Undetermined.

Culture characteristics. Ascospores germinated on PDA within 24 h, and germ tubes produced from basal cell. Colonies growing on PDA reached 22–23 mm in diameter after three weeks at 25 °C in dark. Colonies from above, circular, margin entire, dense, surface smooth, velvety appearance, white in the center, presented a pale greenish furrowed ring, white to cream at the margin; in reverse, brown in the central point, brown-gray in the middle, white to pale brownish at the edge, no pigmentation on PDA.

Material examined. China • Yunnan Province, Xishuangbanna Dai Autonomous Prefecture, Mengla County, Xishuangbanna Tropical Botanical Garden Chinese Academy of Sciences. 21°55'49"N, 101°15'19"E, elevation 516 m, on dead branches of medicinal plant *Ardisia crenata* Sims (Primulaceae), 10 November 2022, H.Z. Du, D01 (HUEST 23.0209), living culture UESTCC 23.0209; • ibid., Sichuan Province, Chengdu City, Pujiang County, 30°11'42"N, 103°22'21"E, elevation 630 m, on dead branches of *Camellia sinensis* (L.) O. Ktze. (Theaceae), 5 October 2022, Y.H. Lu & Y. Xiao, A11 (HUEST 23.0193), living culture UESTCC 23.0193.

Notes. *Nigrograna oleae* was introduced by Li et al. (2023) from *Olea europaea* and *N. trachycarpi* was described by Hu et al. (2023) from *Trachycarpus* sp. in China. In this study, multi-locus phylogeny indicated that our two isolates clustered together with *N. oleae* (ex-type strain, CGMCC 3.24423) and *N. trachycarpi* (ex-type strain, GMB0499) by strong support (100% MLBS/1.00 BIPP) (Fig. 1). In addition, the nucleotide base pair comparison of ex-type strain between *N. oleae* (CGMCC 3.24423) and *N. trachycarpi* (GMB0499) was identical by 421/421 bp (100%) of ITS, and 466/466 bp (100%) of *tef1-α*. Additionally, our newly collected specimens share similar morphology with *N. oleae* and *N. trachycarpi*. Therefore, we identify our collections as *N. oleae* and propose the synonymy of *N. trachycarpi* under *N. oleae* based on morphology and phylogeny. The new host records for *N. oleae* from medicinal plants *Ardisia crenata* and *Camellia sinensis* are reported in this study.

Figure 6. *Nigrograna oleae* (HUEST 23.0209, new host record) **a** host *Ardisia crenata* **b** branch of *Ardisia crenata* **c–f** appearance of ascomata on host surface **g, h** vertical section through ascoma **i** peridium **j–l** asci **m–q** ascospores **r, s** colony on PDA, above (**r**) and below (**s**). Scale bars: 100 μm (**g, h**); 20 μm (**i–l**); 10 μm (**m–q**).

***Nigrograna thymi* Mapook, Camporesi & K.D. Hyde, Fungal Diversity, 87: 68–70 (2017)**
MycoBank No: 552958
Fig. 7

Description. ***Saprobic*** on dead branches of *Huangtcia renifolia* (Fabaceae). **Sexual morph:** ***Ascomata*** 292–359 µm wide, 166–278 µm high ($\bar{x}$ = 327 × 218 µm, n = 20), solitary or scattered, immersed or semi-immersed to slightly erumpent through host tissue, coriaceous, globose to subglobose, brown to dark brown, hairs of ascomata 2–3 µm wide, brown, septate, branched. ***Ostiole*** inconspicuous, without papillate. ***Peridium*** 15–44 µm ($\bar{x}$ = 29.5 µm, n = 20) wide, 5–6 layers, comprising dark brown cells of ***textura angularis***. ***Hamathecium*** comprising 1–3 µm ($\bar{x}$ = 2 µm, n = 20) wide, cylindrical to filiform, septate, branched, smooth-walled pseudoparaphyses. ***Asci*** 43–86 × 7–9 µm ($\bar{x}$ = 66 × 8 µm, n = 30), 8-spored, bitunicate, cylindrical to broadly filiform, with small ocular chamber. ***Ascospores*** 11–15 × 4–6 µm ($\bar{x}$ = 13 × 4.5 µm, n = 50), 1–2-seriate, overlapping, broadly fusiform to inequilateral, widest at the middle cell, guttulate, smooth-walled, aseptate or 1-septate, hyaline when immature, becoming 3-septate, slightly constricted at the septum, pale brown to brown at maturity, without appendages. **Asexual morph:** Undetermined.

Culture characteristics. Ascospores germinated on PDA within 24 h, and germ tubes produced from basal cell. Colonies growing on PDA reached 20 mm in diameter after three weeks at 25 °C in dark. Colonies from above, white in the whole colony and raised in the center, circular, edge entire, margin well-defined; in reverse, grayish-green in the center, white to pale green ring at the margin, no pigmentation on PDA.

Material examined. China • Yunnan Province, Xishuangbanna Dai Autonomous Prefecture, Mengla County, Xishuangbanna Tropical Botanical Garden Chinese Academy of Sciences. 21°55'50"N, 101°15'29"E, elevation 515 m, on dead branches of medicinal plant *Huangtcia renifolia* (L.) H. Ohashi & K. Ohashi (Fabaceae), 10 November 2022, H.Z. Du, D02 (HUEST 23.0210), living culture UESTCC 23.0210; • ibid., Sichuan Province, Leshan City, Emeishan County, 29°36'10"N, 103°21'54"E, elevation 1,100 m, on dead branches of *Camellia sinensis* (L.) O. Ktze. (Theaceae), 18 July 2023, Y.H. Lu & X.D. Liang, EM03 (HUEST 23.0194), living culture UESTCC 23.0194.

Notes. *Nigrograna thymi* was introduced by Hyde et al. (2017) from *Thymus oenipontanus* in Italy. Our collections are identical to *N. thymi* based on morphology and phylogeny (Fig. 1). We reported it as new host records from medicinal plants *Huangtcia renifolia* and *Camellia sinensis* in China.

***Nigrograna neriicola* Y.H. Lu, H.Z. Du & Jian K. Liu, sp. nov.**
MycoBank No: 854179
Fig. 8

Etymology. The epithet '*neriicola*' refers to the host genus *Nerium* from which the fungus was originally isolated.

Holotype. HKAS 131313.

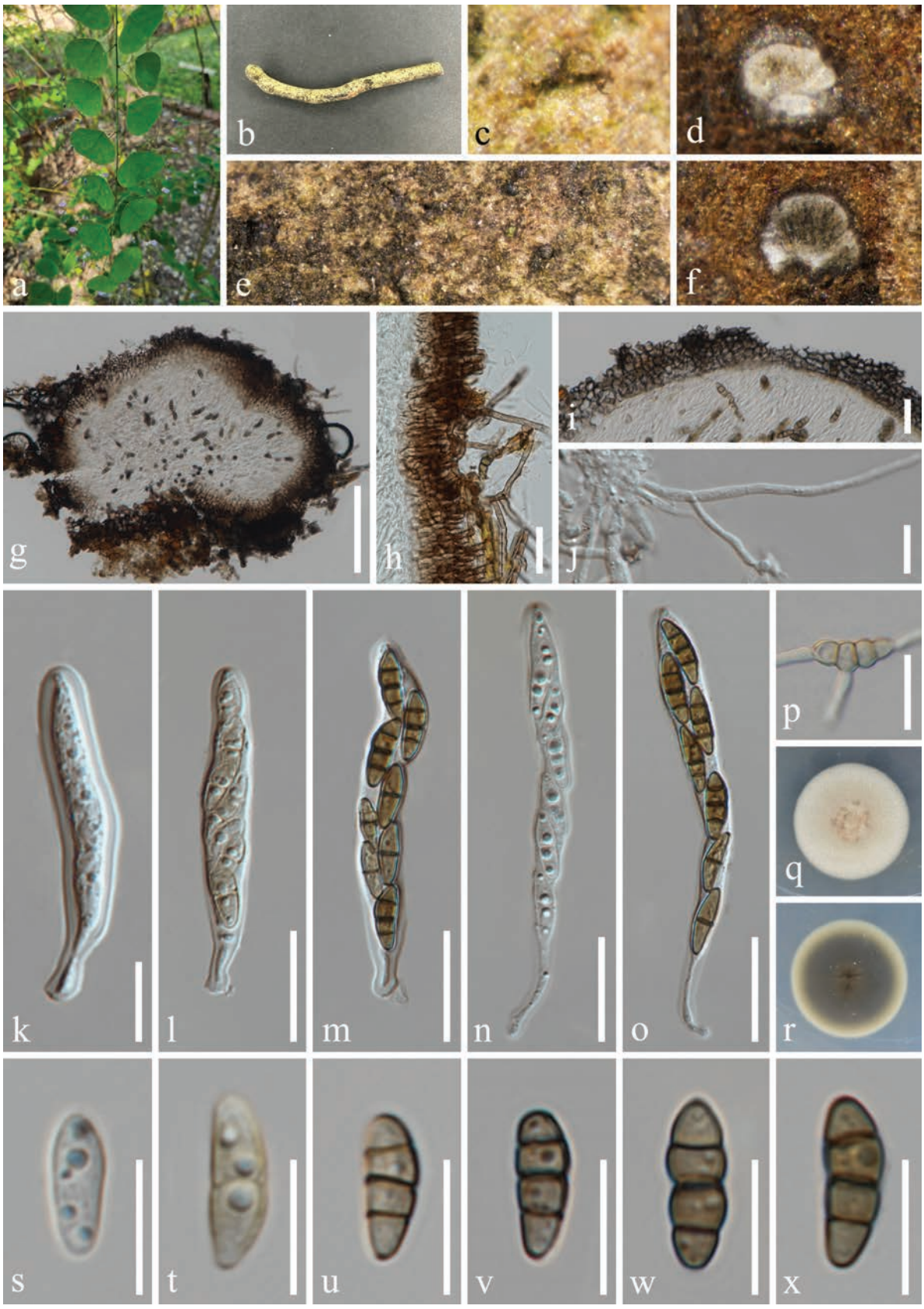

Figure 7. *Nigrograna thymi* (HUEST 23.0210, new host record) **a** host *Huangtcia renifolia* **b** branch of *Huangtcia renifolia* **c–f** appearance of ascomata on host surface **g** vertical section through ascoma **h** hairs on ascomata **i** peridium **j** hamathecium **k–o** asci **p** germinated ascospore **q, r** colony on PDA, above (**q**) and below (**r**) **s–x** ascospores. Scale bars: 100 µm (**g**); 20 µm (**h, i, l–p**); 10 µm (**j, k, s–x**).

Description. ***Saprobic*** on dead branches of *Nerium oleander* (Apocynaceae). **Sexual morph:** ***Ascomata*** 138–231 µm wide, 156–251 µm high ($\bar{x}$ = 182 × 202 µm, n = 20), mostly gregarious, sometimes solitary, scattered, immersed to semi-immersed, appearing as black irregular protrusions and cracks, globose to subglobose, sometimes obpyriform, dark brown to black, with an ostiole. ***Ostioles*** 32–54 µm long, 14–34 µm wide ($\bar{x}$ = 45 × 25 µm, n = 20) mostly central, some eccentric, with a crest-like apex. ***Peridium*** 16–61 µm ($\bar{x}$ = 32 µm, n = 20) wide, multi-layered, reticulate structure, comprising dark brown to reddish brown pigmented cells of ***textura angularis***. ***Hamathecium*** 1–2.5 µm wide ($\bar{x}$ = 2 µm, n = 20), composed of numerous, filiform, hyaline, aseptate or separate, rarely branched, filamentous, smooth-walled pseudoparaphyses. ***Asci*** 35–80 × 7–10 µm ($\bar{x}$ = 56 × 8.5 µm, n = 30), 8-spored, bitunicate, fissitunicate, clavate to cylindric-clavate, short stalked, some with club-shape pedicel, apically rounded with a small ocular chamber. ***Ascospores*** 12–21(–31) × 3.5–5 µm ($\bar{x}$ = 16 × 4 µm, n = 50), uni- to bi-seriately arranged, partially overlapping, fusoid to ellipsoid, tapering towards the blunt ends, or blunt at both ends, straight or slightly curved, guttulate, smooth-walled, 1-septate, subhyaline to slightly brown when young; becoming 3-septate, yellowish-brown to dark brown when mature, deeply constricted at septa, without appendages. **Asexual morph:** Undetermined.

Culture characteristics. Ascospores germinated on PDA within 24 h, and germ tubes produced from basal cell. Colonies growing on PDA reached 33–35 mm in diameter after one month at 25 °C in dark, slightly brown in the whole colony and raised in the central point from above, circular, edge entire, margin well-defined, aerial mycelia dense; in reverse, black-brown in the center, slightly brown ring at the margin, no pigmentation on PDA.

Material examined. China • Yunnan Province, Xishuangbanna Dai Autonomous Prefecture, Mengla County, Xishuangbanna Tropical Botanical Garden Chinese Academy of Sciences. 21°55'52"N, 101°15'29"E, elevation 505 m, on dead branches of medicinal plant *Nerium oleander* L. (Apocynaceae), 10 November 2022, H.Z. Du, D04 (HKAS 131313, holotype); ex-holotype living culture CGMCC 3.25624; • ibid., Sichuan Province, Chengdu City, Pujiang County. 30°11'40"N, 103°22'25"E, elevation 600 m, on dead branches of *Camellia sinensis* (L.) O. Ktze. (Theaceae), 5 October 2022, Y.H. Lu & Y. Xiao, M03 (HUEST 23.0195, paratype); ex-paratype living culture UESTCC 23.0195.

Notes. *Nigrograna neriicola* (CGMCC 3.25624 and UESTCC 23.0195) has close phylogenetic relationships with *N. schinifolii* (GMB0498 and GMB0504) but formed a distinct lineage (Fig. 1). Morphologically, the ascomata of *N. neriicola* differs from *N. schinifolii* in having black irregular protrusions and cracks, mostly gregarious, and ascospores that are slightly larger than *N. schinifolii* (12–21 × 3.5–5 µm vs. 10–14 × 2.8–4 µm) (Hu et al. 2023). Additionally, the nucleotide base pair comparison between *N. neriicola* (ex-type strain, CGMCC 3.25624) and *N. schinifolii* (ex-type strain, GMB0498) revealed no significant differences by 375/377 bp (99.5%, 1 gap) of ITS and 507/511 bp (99.2%, without gaps) of *tef1-α*. However, for *tef1-α* gene, the length of the two *N. schinifolii* strains (GMB0498 and GMB0504) is only 511 bp. The problem of low similarity occurred after the blastn search without a corresponding sequence in the same genus for alignment. Therefore, *N. neriicola* is introduced as a new species with the morpho-molecular data analysis.

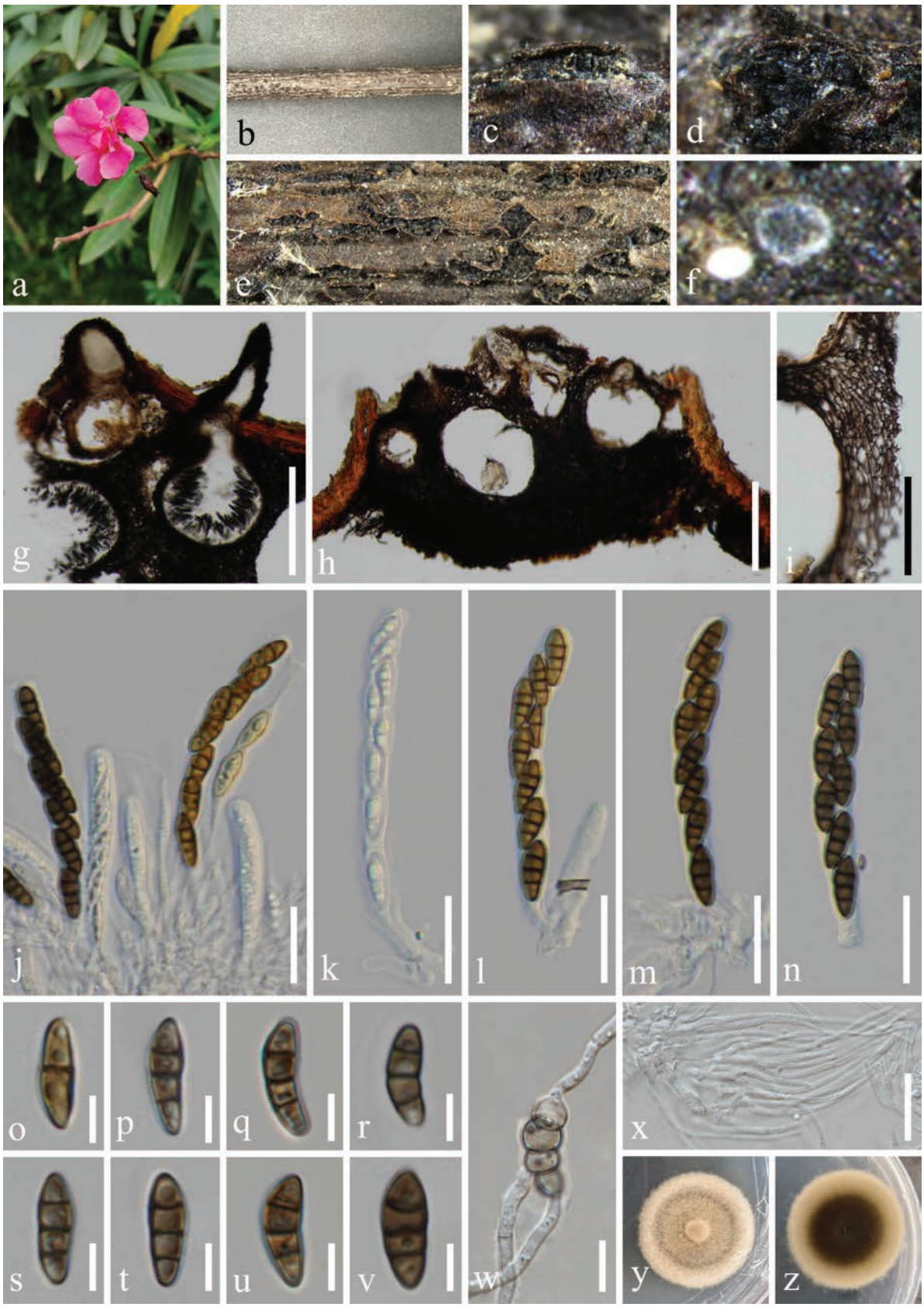

Figure 8. *Nigrograna neriicola* (HKAS 131313, holotype) **a** host *Nerium oleander* **b** branch of *Nerium oleander* **c–f** appearance of ascomata on host surface **g, h** vertical section through ascoma **i** peridium **j–n** asci **o–v** ascospores **w** germinated ascospore **x** hamathecium **y, z** colony on PDA, above (**y**) and below (**z**). Scale bars: 200 µm (**g, h**); 100 µm (**i**); 20 µm (**j–n, x**); 5 µm (**o–v**); 10 µm (**w**).

***Nigrograna guttulata* Y.H. Lu, H.Z. Du & Jian K. Liu, sp. nov.**
MycoBank No: 854180
Fig. 9

Etymology. The epithet '*guttulata*' refers to the guttulate ascospores.

Holotype. HKAS 131992.

Description. ***Saprobic*** on dead branches of *Camellia sinensis* (Theaceae). **Sexual morph:** ***Ascomata*** 182–283 µm wide, 106–276 µm high ($\bar{x}$ = 241 × 183 µm, n = 20), solitary, immersed, ostiolar necks visible on the host surface or erumpent, triangular, globose to subglobose, sometimes obpyriform, coriaceous, ostiolate, dark brown to black. ***Ostioles*** 35–61 µm long, 15–30 µm wide ($\bar{x}$ = 47 × 22 µm, n = 20) mostly central, some eccentric, filled with hyaline periphyses. ***Peridium*** 15–37 µm ($\bar{x}$ = 25 µm, n = 20) wide, multi-layered, reticulate structure, comprising dark brown to reddish brown pigmented cells of ***textura angularis***. ***Hamathecium*** 1–2.5 µm wide ($\bar{x}$ = 2 µm, n = 20), composed of numerous, filiform, hyaline, aseptate or separate, some branched, filamentous, smooth-walled pseudoparaphyses. ***Asci*** 35–70 × 7–12 µm ($\bar{x}$ = 48 × 8.5 µm, n = 30), 8-spored, bitunicate, fissitunicate, clavate to cylindric-clavate, short stalked, some with club-shape pedicel, apically rounded, with small ocular chamber. ***Ascospores*** 10–13 × 3–5 µm ($\bar{x}$ = 12 × 4 µm, n = 50), 1–2-seriate, overlapping, fusoid to ellipsoid, tapering towards the blunt ends, or blunt at both ends, straight or slightly curved, guttulate, smooth-walled, subhyaline to slightly brown when young, 1-septate; yellowish-brown to dark brown when mature, becoming 3-septate, deeply constricted at septa, without appendages. **Asexual morph:** Undetermined.

Culture characteristics. Ascospores germinated on PDA within 24 h, and germ tubes produced from basal cell. Colonies growing on PDA reached 35–38 mm in diameter after one month at 25 °C in dark. Colonies from above, white in the whole colony and raised in the central point, circular, margin well-defined, aerial mycelia dense; in reverse, grayish green in the center, white ring at the margin, no pigmentation on PDA.

Material examined. China • Guizhou Province, Guiyang City, Huaxi District, 26°30'40"N, 106°39'30"E, elevation 1,155 m, on dead branches of medicinal plant *Camellia sinensis* (Linnaeus) Kuntze (Theaceae), 2 February 2023, Y.X. Yu & Y.H. Lu, GY15 (HKAS 131992, holotype; HUEST 23.0295, isotype), ex-holotype living culture CGMCC 3.25689; ex-isotype living culture UESTCC 23.0295.

Notes. *Nigrograna peruviensis* was reported by Kolařík et al. (2017) as an endophytic fungus (*Biatriospora peruviensis*) and was synonymized under the genus *Nigrograna* by Kolařík (2018), but with a lack of detailed morphological structures. In this study, our isolates of *N. guttulata* (CGMCC 3.25689 and UESTCC 23.0295) have a close phylogenetic relationship with *N. peruviensis* (Kolařík et al. 2017; Kolařík 2018) based on ITS, LSU, *rpb2*, SSU, and *tef1-α* sequence data, and formed a distinct lineage with absolute bootstrap support (100% MLBS/1.00 BIPP) (Fig. 1). Additionally, *N. guttulata* (ex-type strain, CGMCC 3.25689) can be distinguished from *N. peruviensis* (ex-type strain, CCF 4485) by 8/462 bp (1.7%, 3 gaps) in ITS, 24/1020 bp (2.4%, without gaps) in LSU and 10/618 bp (1.6%, without gaps) in *rpb2* differences. Therefore, the establishment of the new species *N. guttulata* is justified by the phylogenetic evidence.

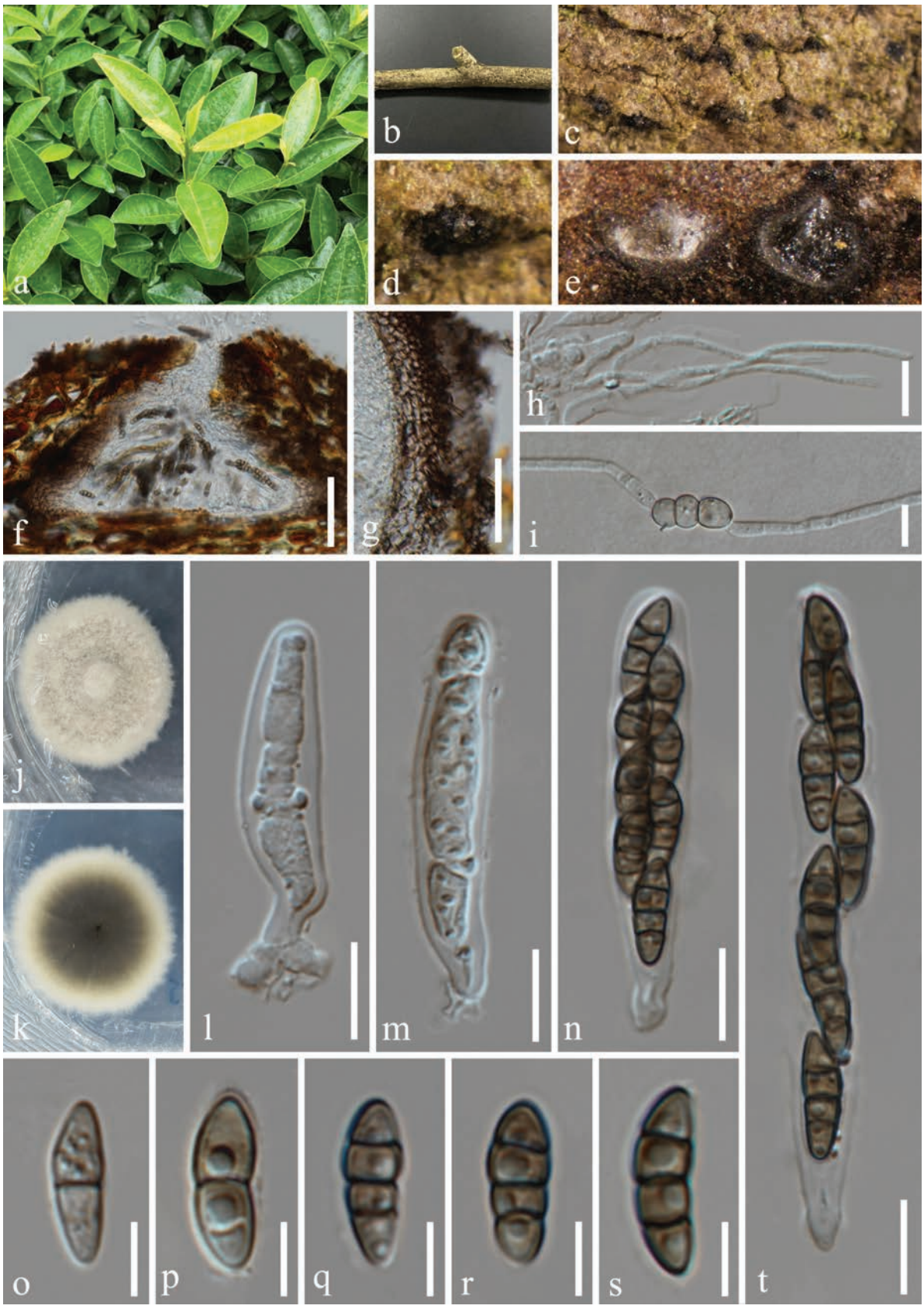

Figure 9. *Nigrograna guttulata* (HKAS 131992, holotype) **a** host *Camellia sinensis* **b** branch of *Camellia sinensis* **c–e** appearance of ascomata on host surface **f** vertical section through ascoma **g** peridium **h** hamathecium **i** germinated ascospore **j, k** colony on PDA, above (**j**) and below (**k**) **l–n, t** asci **o–s** ascospores. Scale bars: 50 µm (**f**); 40 µm (**g**); 10 µm (**h, i, l–n, t**); 5 µm (**o–s**).

Discussion

In this study, eighteen isolates of *Nigrograna* (Nigrograna ceae, Pleosporales, Dothideomycetes) were obtained from medicinal plants in Southwest China (Guizhou, Sichuan and Yunnan Provinces). Based on morphological and culture characteristics, and phylogenetic analyses of combined ITS, LSU, *rpb2*, SSU, and *tef1-α* sequence data, four novel species were identified, namely *Nigrograna camelliae*, *N. guttulata*, *N. longiorostiolata* and *N. neriicola*, Additionally, our known species, namely *N. acericola*, *N. magnoliae*, *N. oleae* and *N. thymi*, were reported from medical plants as new host records. These isolates were associated with terrestrial habitat and collected from medicinal plants in nine plant families, including Apocynaceae, Berberidaceae, Buxaceae, Celastraceae, Eucommiaceae, Fabaceae, Primulaceae, Rutaceae, and Theaceae.

Species within the genus *Nigrograna* exhibit considerable morphological similarity, often complicating species delimitation based solely on morphological traits (Jaklitsch and Voglmayr 2016; Zhang et al. 2020; Lu et al. 2022; Li et al. 2023). As such, molecular data play a critical role in species identification. For example, Jaklitsch and Voglmayr (2016) demonstrated that morphologically similar species, such as *N. coffeae* and *N. camelliae*, can be distinguished phylogenetically. These species sequence divergence across multiple loci, including (15/514 bp, 2.9%, 1 gap), LSU (11/698 bp, 1.6%, without gaps), *rpb2* (74/739 bp, 10.0%, without gaps) and *tef1-α* (28/914 bp, 3.1%, without gaps), highlighting the importance of molecular analysis for accurate taxonomic placement. *Nigrograna* is a worldwide distributed genus, with species reported from Asia (Dayarathne et al. 2020; Mapook et al. 2020; Zhang et al. 2020; Lu et al. 2022; Li et al. 2023), the Americas, and Europe (Jaklitsch and Voglmayr 2016; Hyde et al. 2017; Kolařík et al. 2017; Tibpromma et al. 2017; Kolařík 2018; Zhao et al. 2018; Dayarathne et al. 2020; Wanasinghe et al. 2020). While certain species, such as *N. carollii*, *N. peruviensis* and *N. yasuniana*, have been reported as endophytes on various hosts (Kolařík et al. 2017), the majority of known species are saprotrophs on the bark or corticated twigs and branches of various hardwoods (Jaklitsch and Voglmayr 2016; Mapook et al. 2020; Zhang et al. 2020; Lu et al. 2022; Hu et al. 2023; Li et al. 2023). Reports of *Nigrograna* species on flowers, fruits, leaves, or herbaceous plants are rare, indicating a preference for woody hosts. Consistent with these findings, the isolates in this study were primarily recovered from the branches of medicinal woody plants, such as *Eucommia ulmoides* (Eucommiaceae), *Gymnosporia acuminata* (Celastraceae), and *Mahonia bealei* (Berberidaceae).

It is noteworthy that *Nigrograna magnoliae* was isolated from the bark of *Eucommia ulmoides*, which is a primary medicinal component of the plant. The quality of medicinal plants is closely tied to their clinical efficacy, and the presence of fungal species such as *N. magnoliae* raises important questions about the potential impact of fungal colonization on the medicinal properties of their hosts (Balekundri and Mannur 2020; Rasool et al. 2020; Ali et al. 2021). This finding warrants further investigation to assess whether *N. magnoliae* could affect the quality or bioactive compounds of *E. ulmoides*. In addition to their ecological diversity, certain species within *Nigrograna* have been found to produce bioactive secondary metabolites. For instance, *Nigrograna rubescens* has been reported to produce naphthoquinone compounds, which are known for their broad spectrum

of biological activities (Naysmith et al. 2017; Mack et al. 2024). These metabolites share structural similarities with those found in *N. antibiotica*, which also produces bioactive compounds (Stodůlková et al. 2014). Such findings suggest that members of *Nigrograna* have significant potential for biotechnological applications, particularly in drug discovery. Understanding the relationships between *Nigrograna* species and their medicinal plant hosts, as well as the impact of fungal colonization on the quality of these plants, remains a critical area of research.

In conclusion, this study highlights the diversity of *Nigrograna* species associated with medicinal plants in Southwest China and underscores the importance of integrating morphological and molecular data for accurate species identification. Given the potential ecological and economic implications of *Nigrograna* colonization on medicinal plants, continued research is essential. Detailed taxonomic and ecological studies of *Nigrograna* from medicinal plants will provide valuable insights into the species diversity, host specificity, and potential biotechnological applications of this genus. Ongoing efforts to collect and analyze fresh isolates will further enhance our understanding of the genus and its broader ecological and medicinal significance.

Acknowledgments

Hong-Zhi Du is grateful to Dr. Shaun Pennycook for corrections on the Latin names of the novel taxa. Ning-Guo Liu and Chuan-Gen Lin are thanked for their valuable suggestions on taxonomic identification. Hong-Zhi Du thanks Yong-Xiu Yu, Xiang-Dong Liang and Yue Xiao for their help with sample collections.

Additional information

Conflict of interest

The authors have declared that no competing interests exist.

Ethical statement

No ethical statement was reported.

Funding

This study was supported by the Science and Technology Fundamental Resources Investigation Program (Grant No. 2021FY100906).

Author contributions

Conceptualization: HZD, JKL. Data curation: HZD, YHL, RC. Formal analysis: HZD, YHL, JKL. Funding acquisition: JKL. Investigation: HZD, YHL. Methodology: HZD. Project administration: HZD, JKL, RC. Supervision: JKL, RC. Writing – original draft: HZD. Writing – review & editing: HZD, JKL. All authors have read and agreed to the published version of the manuscript.

Author ORCIDs

Hong-Zhi Du https://orcid.org/0000-0003-0350-4530
Yu-Hang Lu https://orcid.org/0009-0005-9819-3182
Ratchadawan Cheewangkoon https://orcid.org/0000-0001-8576-3696
Jian-Kui Liu https://orcid.org/0000-0002-9232-228X

Data availability

All of the data that support the findings of this study are available in the main text.

References

Abtahi F, Nourani SL (2017) The most important fungal diseases associated with some useful medicinal plants. In: Ghorbanpour M, Varma A (Eds) Medicinal Plants and Environmental Challenges. Springer, Cham, 279–293. https://doi.org/10.1007/978-3-319-68717-9_16

Ahmed SA, van de Sande WW, Stevens DA, Fahal A, van Diepeningen AD, Menken SB, de Hoog GS (2014) Revision of agents of black-grain eumycetoma in the order Pleosporales. Persoonia 33(1): 141–154. https://doi.org/10.3767/003158514X684744

Ali SI, Sheikh WM, Rather MA, Venkatesalu V, Muzamil Bashir S, Nabi SU (2021) Medicinal plants: Treasure for antiviral drug discovery. Phytotherapy Research 35(7): 3447–3483. https://doi.org/10.1002/ptr.7039

Atanasov AG, Zotchev SB, Dirsch VM, Orhan IE, Banach M, Rollinger JM, Barreca D, Weckwerth W, Bauer R, Bayer EA, Majeed M, Bishayee A, Bochkov V, Bonn GK, Braidy N, Bucar F, Cifuentes A, D'Onofrio G, Bodkin M, Diederich M, Dinkova-Kostova AT, Efferth T, El Bairi K, Arkells N, Fan TP, Fiebich BL, Freissmuth M, Georgiev MI, Gibbons S, Godfrey KM, Gruber CW, Heer J, Huber LA, Ibanez E, Kijjoa A, Kiss AK, Lu A, Macias FA, Miller MJS, Mocan A, Müller R, Nicoletti F, Perry G, Pittalà V, Rastrelli L, Ristow M, Russo GL, Silva AS, Schuster D, Sheridan H, Skalicka-Woźniak K, Skaltsounis L, Sobarzo-Sánchez E, Bredt DS, Stuppner H, Sureda A, Tzvetkov NT, Vacca RA, Aggarwal BB, Battino M, Giampieri F, Wink M, Wolfender JL, Xiao J, Yeung AWK, Lizard G, Popp MA, Heinrich M, Berindan-Neagoe I, Stadler M, Daglia M, Verpoorte R, Supuran CT (2021) Natural products in drug discovery: Advances and opportunities. Nature Reviews. Drug Discovery 20(3): 200–216. https://doi.org/10.1038/s41573-020-00114-z

Balekundri A, Mannur V (2020) Quality control of the traditional herbs and herbal products: A review. Future Journal of Pharmaceutical Sciences 6(1): 67. https://doi.org/10.1186/s43094-020-00091-5

Boonmee S, Wanasinghe DN, Calabon MS, Huanraluek N, Chandrasiri SKU, Jones GEB, Rossi W, Leonardi M, Singh SK, Rana S, Singh PN, Maurya DK, Lagashetti AC, Choudhary D, Dai YC, Zhao CL, Mu YH, Yuan HS, He SH, Phookamsak R, Jiang HB, Martín MP, Dueñas M, Telleria MT, Kałucka IL, Jagodziński AM, Liimatainen K, Pereira DS, Phillips AJL, Suwannarach N, Kumla J, Khuna S, Lumyong S, Potter TB, Shivas RG, Sparks AH, Vaghefi N, Abdel-Wahab MA, Abdel-Aziz FA, Li GJ, Lin WF, Singh U, Bhatt RP, Lee HB, Nguyen TTT, Kirk PM, Dutta AK, Acharya K, Sarma VV, Niranjan M, Rajeshkumar KC, Ashtekar N, Lad S, Wijayawardene NN, Bhat DJ, Xu RJ, Wijesinghe SN, Shen HW, Luo ZL, Zhang JY, Sysouphanthong P, Thongklang N, Bao DF, Aluthmuhandiram JVS, Abdollahzadeh J, Javadi A, Dovana F, Usman M, Khalid AN, Dissanayake AJ, Telagathoti A, Probst M, Peintner U, Garrido-Benavent I, Bóna L, Merényi Z, Boros L, Zoltán B, Stielow JB, Jiang N, Tian CM, Shams E, Dehghanizadeh F, Pordel A, Javan-Nikkhah M, Denchev TT, Denchev CM, Kemler M, Begerow D, Deng CY, Harrower E, Bozorov T, Kholmuradova T, Gafforov Y, Abdurazakov A, Xu JC, Mortimer PE, Ren GC, Jeewon R, Maharachchikumbura SSN, Phukhamsakda C, Mapook A, Hyde KD (2021) Fungal diversity notes 1387–1511: Taxonomic and phylogenetic contributions on genera and species of fungal taxa. Fungal Diversity 111(1): 1–335. https://doi.org/10.1007/s13225-021-00489-3

Bundhun D, Jayawardena RS, Camporesi E (2023) Introducing *Nigrograna italica* sp. nov. (Nigrogranaceae) from *Corylus avellana* and *Valsaria tectonae* sp. nov. (Valsariaceae) from *Tectona grandis*. Phytotaxa 618(2): 103–119. https://doi.org/10.11646/phytotaxa.618.2.1

Capella-Gutierrez S, Silla-Martinez JM, Gabaldon T (2009) TrimAl: A tool for automated alignment trimming in large-scale phylogenetic analyses. Bioinformatics (Oxford, England) 25(15): 1972–1973. https://doi.org/10.1093/bioinformatics/btp348

Chethana KWT, Rathnayaka AR, Samarakoon BC, Wu N, Wijesinghe SN, Yasanthika WAE, Sysouphanthong P, Thiyagaraja V, Armand A, Lestari AS, Madagammana AD, Ediriweera AN, Prematunga C, Li CJ-Y, Tennakoon DS, Gomdola D, Marasinghe DS, Bundhun D, Pem D, Ren G, Zhao H, Su HL, Win H, Li H, Lu L, Calabon MS, Samarakoon MC, Chaiwan N, Huanraluek N, Samaradiwakara NP, Kularathnage ND, Abeywickrama PD, Perera RH, Tang SM, Du T-Y, Punyaboon W, Ma X, Yang YH, Tun ZL, Bhunjun CS, Manawasinghe IS, Senanayake IC, Liu JK, Tibpromma S, Wadduwage KS, Wijayalath WHDN, Raspé O, Bulgakov TS, Camporesi E, Promputtha I, Hyde KD (2023) AJOM new records and collections of fungi: 151–200. Asian Journal of Mycology 6(2): 89–243. https://doi.org/10.5943/ajom/6/2/7

Cole I, Saxena P, Murch S (2007) Medicinal biotechnology in the genus *Scutellaria.* In Vitro Cellular & Developmental Biology. Plant 43(4): 318–327. https://doi.org/10.1007/s11627-007-9055-4

Dai DQ, Phookamsak R, Wijayawardene NN, Li WJ, Bhat DJ, Xu JC, Taylor JE, Hyde KD, Chukeatirote E (2017) Bambusicolous fungi. Fungal Diversity 82(1): 1–105. https://doi.org/10.1007/s13225-016-0367-8

Dayarathne MC, Jones EBG, Maharachchikumbura SSN, Devadatha B, Sarma V, Khongphinitbunjong K, Chomnunti P, Hyde KD (2020) Morpho-molecular characterization of microfungi associated with marine based habitats. Mycosphere 11(1): 1–188. https://doi.org/10.5943/mycosphere/11/1/1

de Gruyter J, Woudenberg JH, Aveskamp MM, Verkley GJ, Groenewald JZ, Crous PW (2012) Redisposition of phoma-like anamorphs in Pleosporales. Studies in Mycology 75: 1–36. https://doi.org/10.3114/sim0004

de Silva NI, Hyde KD, Lumyong S, Phillips AJL, Bhat DJ, Maharachchikumbura SSN, Thambugala KM, Tennakoon DS, Suwannarach N, Karunarathna SC (2022) Morphology, phylogeny, host association and geography of fungi associated with plants of Annonaceae, Apocynaceae and Magnoliaceae. Mycosphere 13(1): 955–1076. https://doi.org/10.5943/mycosphere/13/1/12

Dissanayake AJ, Bhunjun CS, Maharachchikumbura SSN, Liu JK (2020) Applied aspects of methods to infer phylogenetic relationships amongst fungi. Mycosphere 11(1): 2652–2676. https://doi.org/10.5943/mycosphere/11/1/18

Dong W, Wang B, Hyde KD, McKenzie EHC, Raja HA, Tanaka K, Abdel-Wahab MA, Abdel-Aziz FA, Doilom M, Phookamsak R, Hongsanan S, Wanasinghe DN, Yu XD, Wang GN, Yang H, Yang J, Thambugala KM, Tian Q, Luo ZL, Yang JB, Miller AN, Fournier J, Boonmee S, Hu DM, Nalumpang S, Zhang H (2020) Freshwater Dothideomycetes. Fungal Diversity 105(1): 319–575. https://doi.org/10.1007/s13225-020-00463-5

Du TY, Karunarathna SC, Zhang X, Dai DQ, Gao Y, Mapook A, Tibpromma S (2022a) Morphology and multigene phylogeny revealed *Peroneutypa aquilariae* sp. nov. (Diatrypaceae, Xylariales) from *Aquilaria sinensis* in Yunnan Province, China. Studies in Fungi 7(1): 1–11. https://doi.org/10.48130/SIF-2022-0018

Du TY, Karunarathna SC, Zhang X, Dai DQ, Mapook A, Suwannarach N, Xu JC, Stephenson SL, Elgorban AM, Al-Rejaie S, Tibpromma S (2022b) Endophytic fungi associated with *Aquilaria sinensis* (Agarwood) from China show antagonism against bacterial and fungal pathogens. Journal of Fungi (Basel, Switzerland) 8(11): 1197. https://doi.org/10.3390/jof8111197

Guo B, Luo W, Zang W (2020) Spatial-temporal shifts of ecological vulnerability of Karst Mountain ecosystem-impacts of global change and anthropogenic interference.

The Science of the Total Environment 741: 140256. https://doi.org/10.1016/j.scitotenv.2020.140256

Helaly SE, Thongbai B, Stadler M (2018) Diversity of biologically active secondary metabolites from endophytic and saprotrophic fungi of the ascomycete order Xylariales. Natural Product Reports 35(9): 992–1014. https://doi.org/10.1039/C8NP00010G

Hongsanan S, Hyde KD, Phookamsak R, Wanasinghe DN, McKenzie EHC, Sarma VV, Boonmee S, Lücking R, Bhat DJ, Liu NG, Tennakoon DS, Pem D, Karunarathna A, Jiang SH, Jones EBG, Phillips AJL, Manawasinghe IS, Tibpromma S, Jayasiri SC, Sandamali DS, Jayawardena RS, Wijayawardene NN, Ekanayaka AH, Jeewon R, Lu YZ, Dissanayake AJ, Zeng XY, Luo ZL, Tian Q, Phukhamsakda C, Thambugala KM, Dai DQ, Chethana KWT, Samarakoon MC, Ertz D, Bao DF, Doilom M, Liu JK, PérezOrtega S, Suija A, Senwanna C, Wijesinghe SN, Konta S, Niranjan M, Zhang SN, Ariyawansa HA, Jiang HB, Zhang JF, Norphanphoun C, de Silva NI, Thiyagaraja V, Zhang H, Bezerra JDP, Miranda-González R, Aptroot A, Kashiwadani H, Harishchandra D, Sérusiaux E, Aluthmuhandiram JVS, Abeywickrama PD, Devadatha B, Wu HX, Moon KH, Gueidan C, Schumm F, Bundhun D, Mapook A, Monkai J, Chomnunti P, Suetrong S, Chaiwan N, Dayarathne MC, Yang J, Rathnayaka AR, Bhunjun CS, Xu JC, Zheng JS, Liu G, Feng Y, Xie N (2020) Refined families of Dothideomycetes: Dothideomycetidae and Pleosporomycetidae. Mycosphere 11(1): 1553–2107. https://doi.org/10.5943/mycosphere/11/1/13

Hu HM, He MH, Wu YP, Long SH, Zhang X, Liu LL, Shen XC, Wijayawardene NN, Meng ZB, Long QD, Kang JC, Li QR (2023) Taxonomic and phylogenetic characterisations of six species of Pleosporales (in Didymosphaeriaceae, Roussoellaceae and Nigrograna ceae) from China. MycoKeys 100: 123–151. https://doi.org/10.3897/mycokeys.100.109423

Huang LQ, Xiao PG, Wang YY (2012) Investigation on resources of rare and endangered medicinal plants in China. Shanghai Scientific and Technical Publishers, Shanghai, 284 pp.

Hyde KD, Norphanphoun C, Abreu VP, Bazzicalupo A, Thilini Chethana KW, Clericuzio M, Dayarathne MC, Dissanayake AJ, Ekanayaka AH, He MQ, Hongsanan S, Huang SK, Jayasiri SC, Jayawardena RS, Karunarathna A, Konta S, Kušan I, Lee H, Li J, Lin CG, Liu NG, Lu YZ, Luo ZL, Manawasinghe IS, Mapook A, Perera RH, Phookamsak R, Phukhamsakda C, Siedlecki I, Soares AM, Tennakoon DS, Tian Q, Tibpromma S, Wanasinghe DN, Xiao YP, Yang J, Zeng XY, Abdel-Aziz FA, Li WJ, Senanayake IC, Shang QJ, Daranagama DA, de Silva NI, Thambugala KM, Abdel-Wahab MA, Bahkali AH, Berbee ML, Boonmee S, Bhat DJ, Bulgakov TS, Buyck B, Camporesi E, Castañeda-Ruiz RF, Chomnunti P, Doilom M, Dovana F, Gibertoni TB, Jadan M, Jeewon R, Jones EBG, Kang JC, Karunarathna SC, Lim YW, Liu JK, Liu ZY, Plautz Jr HL, Lumyong S, Maharachchikumbura SSN, Matočec N, McKenzie EHC, Mešić A, Miller D, Pawłowska J, Pereira OL, Promputtha I, Romero AI, Ryvarden L, Su HY, Suetrong S, Tkalčec Z, Vizzini A, Wen TC, Wisitrassameewong K, Wrzosek M, Xu JC, Zhao Q, Zhao RL, Mortimer PE (2017) Fungal diversity notes 603–708: Taxonomic and phylogenetic notes on genera and species. Fungal Diversity 87(1): 1–235. https://doi.org/10.1007/s13225-017-0391-3

Hyde KD, Norphanphoun C, Ma J, Yang HD, Zhang JY, Du TY, Gao Y, Gomes de Farias AR, Gui H, He SC, He YK, Li CJY, Liu XF, Lu L, Su HL, Tang X, Tian XG, Wang SY, Wei DP, Xu RF, Xu RJ, Yang Q, Yang YY, Zhang F, Zhang Q, Bahkali AH, Boonmee S, Chethana KWT, Jayawardena RS, Lu YZ, Karunarathna SC, Tibpromma S, Wang Y, Zhao Q (2023) Mycosphere notes 387–412 – novel species of fungal taxa from around the world. Mycosphere 14(1): 663–744. https://doi.org/10.5943/mycosphere/14/1/8

Jaklitsch WM, Voglmayr H (2016) Hidden diversity in *Thyridaria* and a new circumscription of the Thyridariaceae. Studies in Mycology 85(1): 35–64. https://doi.org/10.1016/j.simyco.2016.09.002

Katoh K, Standley DM (2013) MAFFT multiple sequence alignment software version 7: Improvements in performance and usability. Molecular Biology and Evolution 30(4): 772–780. https://doi.org/10.1093/molbev/mst010

Keshri P, Rai N, Verma A, Kamble S, Barik S, Mishra P, Singh S, Salvi P, Gautam V (2021) Biological potential of bioactive metabolites derived from fungal endophytes associated with medicinal plants. Mycological Progress 20(5): 577–594. https://doi.org/10.1007/s11557-021-01695-8

Kolařík M (2018) New taxonomic combinations in endophytic representatives of the genus *Nigrograna*. Czech Mycology 70(2): 123–126. https://doi.org/10.33585/cmy.70202

Kolařík M, Spakowicz DJ, Gazis R, Shaw J, Kubátová A, Nováková A, Chudíčková M, Forcina GC, Kang KW, Kelnarová I, Skaltsas D, Portero CE, Strobel SA, Narváez-Trujillo A (2017) *Biatriospora* (Ascomycota: Pleosporales) is an ecologically diverse genus including facultative marine fungi and endophytes with biotechnological potential. Plant Systematics and Evolution 303(1): 35–50. https://doi.org/10.1007/s00606-016-1350-2

Larget B, Simon DL (1999) Markov chain Monte Carlo algorithms for the Bayesian analysis of phylogenetic trees. Molecular Biology and Evolution 16(6): 750–759. https://doi.org/10.1093/oxfordjournals.molbev.a026160

Larsson A (2014) AliView: A fast and lightweight alignment viewer and editor for large datasets. Bioinformatics (Oxford, England) 30(22): 3276–3278. https://doi.org/10.1093/bioinformatics/btu531

Li WL, Liang RR, Dissanayake AJ, Liu JK (2023) Mycosphere Notes 413–448: Dothideomycetes associated with woody oil plants in China. Mycosphere 14(1): 1436–1529. https://doi.org/10.5943/mycosphere/14/1/16

Liu YJ, Whelen S, Hall BD (1999) Phylogenetic relationships among Ascomycetes: Evidence from an RNA polymerse II subunit. Molecular Biology and Evolution 16(12): 1799–1808. https://doi.org/10.1093/oxfordjournals.molbev.a026092

Liu JK, Chomnunti P, Cai L, Phookamsak R, Chukeatirote R, Jones EBG, Moslem M, Hyde KD (2010) Phylogeny and morphology of *Neodeightonia palmicola* sp. nov. from palms. Sydowia 62(2): 261–276. https://www.zobodat.at/pdf/Sydowia_062_0261-0276.pdf

Liu JK, Hyde KD, Jeewon R, Phillips AJ, Maharachchikumbura SS, Ryberg M, Liu ZY, Zhao Q (2017) Ranking higher taxa using divergence times: A case study in Dothideomycetes. Fungal Diversity 84(1): 75–99. https://doi.org/10.1007/s13225-017-0385-1

Liu SL, Wang XW, Li GJ, Deng CY, Rossi W, Leonardi M, Liimatainen K, Kekki T, Niskanen T, Smith ME, Ammirati J, Bojantchev D, Abdel-Wahab MA, Zhang M, Tian E, Lu YZ, Zhang JY, Ma J, Dutta AK, Acharya K, Du TY, Xu J, Kim JS, Lim YW, Gerlach A, Zeng NK, Han YX, Razaghi P, Raza M, Cai L, Calabon MS, Jones EBG, Saha R, Kumar TKA, Krishnapriya K, Thomas A, Kaliyaperumal M, Kezo K, Gunaseelan S, Singh SK, Singh PN, Lagashetti AC, Pawar KS, Jiang S, Zhang C, Zhang H, Qing Y, Bau T, Peng XC, Wen TC, Ramirez NA, Niveiro N, Li MX, Yang ZL, Wu G, Tarafder E, Tennakoon DS, Kuo CH, da Silva TM, Souza-Motta CM, Bezerra JDP, He G, Ji XH, Suwannarach N, Kumla J, Lumyong S, Wannathes N, Rana S, Hyde KD, Zhou LW (2024) Fungal diversity notes 1717–1817: Taxonomic and phylogenetic contributions on genera and species of fungal taxa. Fungal Diversity 124(1): 1–216. https://doi.org/10.1007/s13225-023-00529-0

Lu LM, Mao LF, Yang T, Ye JF, Liu B, Li HL, Sun M, Miller JT, Mathews S, Hu HH, Niu YT, Peng DX, Chen YH, Smith SA, Chen M, Xiang KL, Le CT, Dang VC, Lu AM, Soltis PS, Soltis DE, Li JH, Chen ZD (2018) Evolutionary history of the angiosperm flora of China. Nature 554(7691): 234–238. https://doi.org/10.1038/nature25485

Lu L, Karunarathna SC, Dai DQ, Jayawardena RS, Suwannarach N, Tibpromma S (2022) Three new species of *Nigrograna* (Dothideomycetes, Pleosporales) associated with

Arabica coffee from Yunnan Province, China. MycoKeys 94: 51–71. https://doi.org/10.3897/mycokeys.94.95751

Mack JN, Sproule A, Shields SW, Seifert KA, Smith M, Overy DP (2024) Two novel Pleosporales species isolated from the bark of *Acer saccharum.* Fungal Systematics and Evolution 13(1): 1–14. https://doi.org/10.3114/fuse.2024.13.01

Mapook A, Hyde KD, Hyde KD, Hyde KD, McKenzie EHC, Jones EBG, Bhat DJ, Jeewon R, Stadler M, Samarakoon MC, Malaithong M, Tanunchai B, Buscot F, Wubet T, Purahong WJFD (2020) Taxonomic and phylogenetic contributions to fungi associated with the invasive weed *Chromolaena odorata* (Siam weed). Fungal Diversity 101(1): 1–175. https://doi.org/10.1007/s13225-020-00444-8

Miller MA, Pfeiffer W, Schwartz T (2010) Creating the CIPRES science gateway for inference of large phylogenetic trees. Proceedings of the Gateway Computing Environments Workshop (GCE) 14: 1–8. https://doi.org/10.1109/GCE.2010.5676129

Nalawade S, Sagare A, Lee CY, Kao CL, Tsay HS (2003) Studies on tissue culture of Chinese medicinal plant resources in Taiwan and their sustainable utilization. Botanical Bulletin-Academia Sinica Taipei 44(2): 79–98. https://ejournal.sinica.edu.tw/bbas/content/2003/2/bot442-01.pdf

Naysmith BJ, Hume PA, Sperry J, Brimble MA (2017) Pyranonaphthoquinones - isolation, biology and synthesis: An update. Natural Product Reports 34(1): 25–61. https://doi.org/10.1039/C6NP00080K

Nylander J (2008) MrModeltest 2 v. 2.3 (Program for selecting DNA substitution models using PAUP*). Evolutionary Biology Centre, Uppsala, Sweden. https://mybiosoftware.com/mrmodeltest-2-3-program-selecting-dna-substitution-models-paup.html

Rahman IU, Afzal A, Iqbal Z, Ijaz F, Ali N, Shah M, Ullah S, Bussmann RW (2019) Historical perspectives of ethnobotany. Clinics in Dermatology 37(4): 382–388. https://doi.org/10.1016/j.clindermatol.2018.03.018

Rannala B, Yang Z (1996) Probability distribution of molecular evolutionary trees: A new method of phylogenetic inference. Journal of Molecular Evolution 43(3): 304–311. https://doi.org/10.1007/BF02338839

Rasool A, Bhat KM, Sheikh AA, Jan A, Hassan S (2020) Medicinal plants: Role, distribution and future. Journal of Pharmacognosy and Phytochemistry 9: 2111–2114. https://doi.org/10.15171/jhp.2018.01

Rehner SA, Buckley E (2005) A *Beauveria* phylogeny inferred from nuclear ITS and EF1-*α* sequences: Evidence for cryptic diversification and links to *Cordyceps* teleomorphs. Mycologia 97(1): 84–98. https://doi.org/10.3852/mycologia.97.1.84

Ren GC, Jayasiri SC, Tibpromma S, De Farias ARG, Chethana KWT, Faraj KH, Wanasinghe DN, Xu JC, Hyde KD, Gui H (2024) Saprobic ascomycetes associated with woody litter from the Greater Mekong Subregion (Southwestern China and Northern Thailand). Mycosphere 15(1): 954–1082.

Ronquist F, Teslenko M, van der Mark P, Ayres DL, Darling A, Hohna S, Larget B, Liu L, Suchard MA, Huelsenbeck JP (2012) MrBayes 3.2: Efficient Bayesian phylogenetic inference and model choice across a large model space. Systematic Biology 61(3): 539–542. https://doi.org/10.1093/sysbio/sys029

Samy RP, Gopalakrishnakone P (2007) Current status of herbal and their future perspectives. Nature Precedings, 1–13. https://doi.org/10.1038/npre.2007.1176.1

Schmidt BM (2017) Ethnobotany: a phytochemical perspective. Ethnobotany, 1–109. https://doi.org/10.1002/9781118961933.ch1

Senanayake IC, Rathnayaka AR, Sandamali DS, Calabon MS, Gentekaki E, Lee HB, Hurdeal VG, Pem D, Dissanayake LS, Wijesinghe SN, Bundhun D, Nguyen TT, Goonasekara ID,

Abeywickrama PD, Bhunjun CS, Jayawardena RS, Wanasinghe DN, Jeewon R, Bhat DJ, Xiang MM (2020) Morphological approaches in studying fungi: Collection, examination, isolation, sporulation and preservation. Mycosphere 11(1): 2678–2754. https://doi.org/10.5943/mycosphere/11/1/20

Senanayake IC, Rossi W, Leonardi M, Weir A, McHugh M, Rajeshkumar KC, Verma RK, Karunarathna SC, Tibpromma S, Ashtekar N, Ashtamoorthy SK, Raveendran S, Kour G, Singh A, De la Peña-Lastra S, Mateos A, Kolařík M, Antonín V, Ševčíková H, Esteve-Raventós F, Larsson E, Pancorbo F, Moreno G, Altés A, Turégano Y, Du TY, Lu L, Li QR, Kang JC, Gunaseelan S, Kezo K, Kaliyaperumal M, Fu J, Samarakoon MC, Gafforov Y, Teshaboeva S, Kunjan PC, Chamaparambath A, Flakus A, Etayo J, Rodriguez-Flakus P, Zhurbenko MP, de Silva NI, Tennakoon DS, Latha KPD, Manimohan P, Raj KNA, Calabon MS, Ahmadpour A, Heidarian Z, Alavi Z, Alavi F, Ghosta Y, Azizi R, Luo M, Zhao MP, Kularathnage ND, Hua L, Yang YH, Liao CF, Zhao HJ, Lestari AS, Jayasiri SC, Yu FM, Lei L, Liu JW, Karimi O, Tang SM, Sun YR, Wang Y, Zeng M, Htet ZH, Linaldeddu BT, Alves A, Phillips AJL, Bregant C, Montecchio L, De Kesel A, Hustad VP, Miller AN, Fedosova AG, Kučera V, Raza M, Hussain M, Chen YP, Thiyagaraja V, Gomdola D, Rathnayaka AR, Dissanayake AJ, Suwannarach N, Hongsanan S, Maharachchikumbura SSN, Dissanayake LS, Wijayawardene NN, Phookamsak R, Lumyong S, Jones EBG, Yapa N, Wanasinghe DN, Xie N, Doilom M, Manawasinghe IS, Liu JK, Zhao Q, Xu B, Hyde KD, Song J (2023) Fungal diversity notes 1611–1716: Taxonomic and phylogenetic contributions on fungal genera and species emphasis in south China. Fungal Diversity 122(1): 161–403. https://doi.org/10.1007/s13225-023-00523-6

Shan ZJ, Ye JF, Hao DC, Xiao PG, Chen ZD, Lu AM (2022) Distribution patterns and industry planning of commonly used traditional Chinese medicinal plants in China. Plant Diversity 44(3): 255–261. https://doi.org/10.1016/j.pld.2021.11.003

Shu YX, Cheng R, Huang J, Li K, Zhao S, Zhao H, Dong W, Dong Z, Doilom M, Xu B (2023) Introducing *Nigrograna wuhanensis* sp. nov. (Nigrograna ceae, Pleosporales) from *Camellia japonica* in China. Warasan Khana Witthayasat Maha Witthayalai Chiang Mai 50(3): 1–11. https://doi.org/10.12982/CMJS.2023.025

Stamatakis A (2006) RAxML-VI-HPC: Maximum likelihood-based phylogenetic analyses with thousands of taxa and mixed models. Bioinformatics (Oxford, England) 22(21): 2688–2690. https://doi.org/10.1093/bioinformatics/btl446

Stamatakis A, Hoover P, Rougemont J (2008) A rapid bootstrap algorithm for the RAxML web servers. Systematic Biology 57(5): 758–771. https://doi.org/10.1080/10635150802429642

Stodůlková E, Man P, Kuzma M, Černý J, Císařová I, Kubátová A, Chudíčková M, Kolařík M, Flieger M (2014) A highly diverse spectrum of naphthoquinone derivatives produced by the endophytic fungus *Biatriospora* sp. CCF 4378. Folia Microbiologica 60(3): 259–267. https://doi.org/10.1007/s12223-014-0366-7

Sun YR, Jayawardena RS, Sun JE, Wang Y (2023) Pestalotioid species associated with medicinal plants in Southwest China and Thailand. Microbiology Spectrum 11(1): e0398722. https://doi.org/10.1128/spectrum.03987-22

Taylor DL, Hollingsworth T, McFarland J, Lennon N, Nusbaum C, Ruess R (2014) A first comprehensive census of fungi in soil reveals both hyperdiversity and fine-scale niche partitioning. Ecological Monographs 84(1): 3–20. https://doi.org/10.1890/12-1693.1

Tibpromma S, Hyde KD, Jeewon R, Maharachchikumbura SSN, Liu JK, Bhat DJ, Jones EBG, McKenzie EHC, Camporesi E, Bulgakov TS, Doilom M, de Azevedo Santiago

ALCM, Das K, Manimohan P, Gibertoni TB, Lim YW, Ekanayaka AH, Thongbai B, Lee HB, Yang JB, Kirk PM, Sysouphanthong P, Singh SK, Boonmee S, Dong W, Raj KNA, Latha KPD, Phookamsak R, Phukhamsakda C, Konta S, Jayasiri SC, Norphanphoun C, Tennakoon DS, Li J, Dayarathne MC, Perera RH, Xiao Y, Wanasinghe DN, Senanayake IC, Goonasekara ID, de Silva NI, Mapook A, Jayawardena RS, Dissanayake AJ, Manawasinghe IS, Chethana KWT, Luo ZL, Hapuarachchi KK, Baghela A, Soares AM, Vizzini A, Meiras-Ottoni A, Mešić A, Dutta AK, de Souza CAF, Richter C, Lin CG, Chakrabarty D, Daranagama DA, Lima DX, Chakraborty D, Ercole E, Wu F, Simonini G, Vasquez G, da Silva GA, Plautz HL, Ariyawansa HA, Lee H, Kušan I, Song J, Sun J, Karmakar J, Hu K, Semwal KC, Thambugala KM, Voigt K, Acharya K, Rajeshkumar KC, Ryvarden L, Jadan M, Hosen MI, Mikšík M, Samarakoon MC, Wijayawardene NN, Kim NK, Matočec N, Singh PN, Tian Q, Bhatt RP, de Oliveira RJV, Tulloss RE, Aamir S, Kaewchai S, Marathe SD, Khan S, Hongsanan S, Adhikari S, Mehmood T, Bandyopadhyay TK, Svetasheva TY, Nguyen TTT, Antonín V, Li WJ, Wang Y, Indoliya Y, Tkalčec Z, Elgorban AM, Bahkali AH, Tang AMC, Su HY, Zhang H, Promputtha I, Luangsa-ard J, Xu JC, Yang J, Kang JC, Stadler M, Mortimer PE, Chomnunti P, Zhao Q, Phillips AJL, Nontachaiyapoom S, Wen TC, Karunarathna SC (2017) Fungal diversity notes 491–602: Taxonomic and phylogenetic contributions to fungal taxa. Fungal Diversity 83(1): 1–261. https://doi.org/10.1007/s13225-017-0378-0

Vaidya G, Lohman DJ, Meier R (2011) SequenceMatrix concatenation software for the fast assembly of multi gene datasets with character set and codon information. Cladistics 27(2): 171–180. https://doi.org/10.1111/j.1096-0031.2010.00329.x

Vilgalys R, Hester M (1990) Rapid genetic identification and mapping of enzymatically amplified ribosomal DNA from several *Cryptococcus* species. Journal of Bacteriology 172(8): 4238–4246. https://doi.org/10.1128/jb.172.8.4238-4246.1990

Wanasinghe DN, Wijayawardene NN, Xu JC, Cheewangkoon R, Mortimer PE (2020) Taxonomic novelties in *Magnolia*-associated pleosporalean fungi in the Kunming Botanical Gardens (Yunnan, China). PLoS ONE 15(7): e0235855. https://doi.org/10.1371/journal.pone.0235855

White TJ, Bruns T, Lee S, Taylor J (1990) Amplification and direct sequencing of fungal ribosomal RNA genes for phylogenetics. PCR protocols: a guide to methods and applications 18(1): 315–322. https://doi.org/10.1016/B978-0-12-372180-8.50042-1

Wu N, Thilini Chethana KW, Liu JK (2024) *Velutinus*, a novel genus in Patellariopsidaceae from medicinal plants in Sichuan Province, China. Phytotaxa 638(2): 165–174. https://doi.org/10.11646/phytotaxa.638.2.5

Xu RF, Karunarathna SC, Phukhamsakda C, Dai DQ, Elgorban AM, Suwannarach N, Kumla J, Wang XY, Tibpromma S (2024) Four new species of Dothideomycetes (Ascomycota) from Pará Rubber (*Hevea brasiliensis*) in Yunnan Province, China. MycoKeys 103: 71–95. https://doi.org/10.3897/mycokeys.103.117580

Zhang JF, Liu JK, Thambugala KM, Yang J, Meng ZH, Liu ZY (2020) Two new species and a new record of *Nigrograna* (Nigrograniaceae, Pleosporales) from China and Thailand. Mycological Progress 19(11): 1365–1375. https://doi.org/10.1007/s11557-020-01633-0

Zhang ZY, Pan H, Tao G, Li X, Han YF, Feng Y, Tong SQ, Ding CY (2024) Culturable Mycobiota from Guizhou Wildlife Park in China. Mycosphere 15(1): 654–763.

Zhao YZ, Zhang ZF, Cai L, Peng WJ, Liu F (2018) Four new filamentous fungal species from newly-collected and hive-stored bee pollen. Mycosphere 9(6): 1089–1116. https://doi.org/10.5943/mycosphere/9/6/3

MycoKeys

MycoKeys 110: 35–66 (2024)
DOI: 10.3897/mycokeys.110.133450

Research Article

Additions to the genus *Kirschsteiniothelia* (Dothideomycetes); Three novel species and a new host record, based on morphology and phylogeny

Xia Tang[1,2,3], Rajesh Jeewon[4], Ruvishika S. Jayawardena[2,3], Deecksha Gomdola[2,3], Yong-Zhong Lu[5], Rong-Ju Xu[2,3], Abdulwahed Fahad Alrefaei[6], Fatimah Alotibi[7], Kevin D. Hyde[2,3,7], Ji-Chuan Kang[1]

1 *Engineering and Research Center for Southwest Biopharmaceutical Resource of National Education Ministry of China, Guizhou University, Guiyang, 550025, Guizhou Province, China*
2 *Center of Excellence in Fungal Research, Mae Fah Luang University, Chiang Rai, 57100, Thailand*
3 *School of Science, Mae Fah Luang University, Chiang Rai, 57100, Thailand*
4 *Department of Health Sciences, Faculty of Medicine and Health Sciences, University of Mauritius, Reduit, Mauritius*
5 *School of Food and Pharmaceutical Engineering, Guizhou Institute of Technology, Guiyang, Guizhou Province 550003, China*
6 *Department of Zoology, College of Science, King Saud University, P.O. Box 2455, Riyadh 11451, Saudi Arabia*
7 *Department of Botany and Microbiology, College of Science, King Saud University, P.O. Box 22452, 11495 Riyadh, Saudi Arabia*

Corresponding authors: Ji-Chuan Kang (jckang@gzu.edu.cn); Kevin D. Hyde (kdhyde3@gmail.com)

This article is part of:
Exploring the Hidden Fungal Diversity: Biodiversity, Taxonomy, and Phylogeny of Saprobic Fungi
Edited by Samantha C. Karunarathna, Danushka Sandaruwan Tennakoon, Ajay Kumar Gautam

Academic editor:
Danushka Sandaruwan Tennakoon
Received: 30 July 2024
Accepted: 1 October 2024
Published: 28 October 2024

Citation: Tang X, Jeewon R, Jayawardena RS, Gomdola D, Lu Y-Z, Xu R-J, Alrefaei AF, Alotibi F, Hyde KD, Kang J-C (2024) Additions to the genus *Kirschsteiniothelia* (Dothideomycetes); Three novel species and a new host record, based on morphology and phylogeny. MycoKeys 110: 35–66. https://doi.org/10.3897/mycokeys.110.133450

Abstract

During a survey of microfungi associated with forest plants, four specimens related to *Kirschsteiniothelia* were collected from decaying wood in Guizhou, Hainan and Yunnan Provinces, China. *Kirschsteiniothelia* species have sexual and asexual forms. They are commonly found as saprophytes on decaying wood and have been reported as disease-causing pathogens in humans as well. In this study, we introduce three novel *Kirschsteiniothelia* species (*K. bulbosapicalis*, *K. dendryphioides* and *K. longirostrata*) and describe a new host record for *K. atra*, based on morphology and multi-gene phylogenetic analyses of a concatenated ITS, LSU and SSU rDNA sequence data. These taxa produced a dendryphiopsis- or sporidesmium-like asexual morph and detailed descriptions and micromorphological illustrations are provided. Furthermore, we provide a checklist for the accepted *Kirschsteiniothelia* species, including detailed host information, habitat preferences, molecular data, existing morphological type, country of origin and corresponding references.

Key words: Checklist, diversity, Dothideomycetes, Kirschsteiniotheliales, one new host record, taxonomy, three new taxa

Introduction

Kirschsteiniothelia was introduced by Hawksworth (1985) and typified by *K. aethiops*, based on morphological observation, linking it to its asexual genus, *Dendryphiopsis* S. Hughes. Later, the type species was reclassified with its asexual morph, *K. atra* (Hyde et al 2011; Wijayawardene et al. 2014). The connection between the sexual morphs of *Kirschsteiniothelia atra* (characterised by cylindrical-clavate, bitunicate, 8-spored or rarely 4-spored asci and ellipsoidal verruculose or smooth ascospores with 1–2 septa, lacking a distinct gelatinous sheath) and the asexual morphs (characterised by macronematous, mononematous and

branched conidiophores, monotretic, terminal or intercalary, cylindrical, doliiform conidiogenous cells and acrogenous, solitary, cylindrical, oblong, septate conidia with obtuse ends) were previously established by Hughes (1978). This connection was confirmed from cultures obtained from fragments of the ascomata, based on morphological examination. Schoch et al. (2006) further confirmed the connection between the sexual and asexual morphs of *Kirschsteiniothelia*, based on both morphology and phylogenetic analysis of SSU, LSU, *tef1-α* and *rpb2*. Boonmee et al. (2012) established a novel family, Kirschsteiniotheliaceae, based on the connection between the sexual and asexual morph of *Kirschsteiniothelia* and multiple gene (LSU, SSU and ITS) phylogeny. Wijayawardene et al. (2014) suggested the use of *Kirschsteiniothelia* as the updated genus to accommodate *Dendryphiopsis* species. As a result, *Dendryphiopsis atra* was re-assigned to *Kirschsteiniothelia* and synonymised with *K. atra*, based on morphological and phylogenetic analyses. In the meantime, Wijayawardene et al. (2014) suggested using *K. atra* to replace *K. aethiops* as the type species of *Kirschsteiniothelia*. This recommendation was supported by later studies (Rossman et al. 2015; Su et al. 2016; Bao et al. 2018; Yang et al. 2023; Jin et al. 2024; Sruthi et al. 2024; Tian et al. 2024). Sruthi et al. (2024) legitimately placed five species from *Dendryphiopsis* under *Kirschsteiniothelia*, namely, *K. arbuscula*, *K. binsarensis*, *K. biseptata*, *K. fascicularis* and *K. goaensis*. *Kirschsteiniothelia* usually exhibits both sexual and asexual morphs (Hawksworth 1985; Boonmee et al. 2012; Hyde et al. 2013; Sun et al. 2021; Xu et al. 2023). The sexual morph of *Kirschsteiniothelia* is characterised by superficial, erumpent, papillate, brown or black and hemi-spherical or subglobose ascomata and cylindrical or clavate, bitunicate, pedicellate asci that are usually 8-spored comprising an ocular apical chamber. The ascospores are ellipsoidal, usually asymmetrical, verruculose or smooth and olivaceous to dark brown, comprising 1–2 septa, with a mucilaginous sheath being occasionally present (Chen et al. 2006; Hyde et al. 2018; Meng et al. 2024). Furthermore, ascospores occasionally display longitudinal or sinuate furrows that are visible from the face view (Hawksworth 1985; Boonmee et al. 2012; Hyde et al. 2013; Mehrabi et al. 2017; Yang et al. 2023).

The asexual morph is further categorised into two types, namely the dendryphiopsis- and sporidesmium-like morphs. The dendryphiopsis-like morph was described by Hughes (1978), who found that the ascomatal fragments of *Kirschsteiniothelia aethiops* (≡ *Amphisphaeria incrustans*) exhibited agar sporulation and morphological traits similar to those of *Dendryphiopsis atra*. This was later supported by Hawksworth (1985). Subsequently, Boonmee et al. (2012) supported the connection between the sexual morph of *Kirschsteiniothelia* and the asexual dendryphiopsis-like morph, based on morphological and phylogenetic analyses. The dendryphiopsis-like morph is characterised by macronematous, septate, cylindrical conidiophores that are irregularly or subscorpioidly branched at the apex. Their conidiogenous cells are mono- to polytretic, integrated, terminal or lateral, doliiform or lageniform. Moreover, the conidia are holoblastic, acrogenous, obclavate, rostrate, obovoid to broadly obovoid, solitary or branched in acropetal chains, exhibiting rounded ends. Taxa exhibiting the dendryphiopsis-like characteristics are *K. atra*, *K. arbuscula*, *K. binsarensis*, *K. biseptata*, *K. dendryphioides*, *K. ebriosa*, *K. emarceis*, *K. fascicularis*, *K. goaensis*, *K. inthanonensis*, *K. lignicola*, *K. longisporum*, *K. nabanheensis*, *K. ramus*, *K. recessa*, *K. saprophytica*, *K. septemseptatum*, *K. shimlaensis*, *K. vinigena* and *K. zizyphifolii* (Hughes 1978; Boonmee et al. 2012; de Farias et al. 2024; Tian et al. 2024; this study).

The sporidesmium-like asexual morph was described by Su et al. (2016), based on morphological and phylogenetic evidence. Despite having different morphological characteristics from other *Kirschsteiniothelia* species, the sporidesmium-like morphs fits into the generic concept of *Kirschsteiniothelia* as they display similar morphologies including unbranched, slender conidiophores that are straight or slightly curved, multi-septate and brown to pale brown, usually truncate at the base and rounded at the apex, producing small conidia. The sporidesmium-like morph is depicted by macronematous, mononematous, unbranched, multi-septate, cylindrical conidiophores, holoblastic, integrated, terminal, determinate, percurrent, cylindrical and caliciform conidiogenous cells and acrogenous, multi-septate, obclavate to obspathulate, rostrate and fusiform conidia that are swollen at the tips or middle of the beak, with or without a conspicuous, gelatinous, hyaline sheath around the tip or middle of the beak. The presence of the sporidesmium-like asexual morph of *Kirschsteiniothelia* was further supported by subsequent research (Sun et al. 2021; Jayawardena et al. 2022; Xu et al. 2023; Yang et al. 2023). Species exhibiting the sporidesmium-like features are *K. acutispora*, *K. agumbensis*, *K. aquatica*, *K. bulbosapicalis*, *K. cangshanensis*, *K. crustacea*, *K. dujuanhuensis*, *K. dushanensis*, *K. extensum*, *K. fluminicola*, *K. guangdongensis*, *K. longirostrata*, *K. pini*, *K. puerensis*, *K. rostrata*, *K. sichuanensis*, *K. spatiosum*, *K. submersa*, *K. tectonae*, *K. thailandica* and *K. xishuangbannaensis* (Su et al. 2016; Jayawardena et al. 2022; Xu et al. 2023; Yang et al. 2023; Jin et al. 2024; Sruthi et al. 2024; this study).

Although *Kirschsteiniothelia* comprises numerous species, there are likely to be more undescribed species in this genus as predicted by Bhunjun et al. (2022). Most species have been reported as saprobes inhabiting terrestrial and freshwater environments in tropical and subtropical regions. However, *K. ebriosa* and *K. vinigena* have been identified from cork taint of sparkling wine (Bao et al. 2018; Rodríguez-Andrade et al. 2020; Sun et al. 2021; Jayawardena et al. 2022). Moreover, a report indicates the presence of an unidentified *Kirschsteiniothelia* species that is pathogenic to humans, causing infection superimposed on pre-existing non-infectious bursitis of the ankle. This identification was based on the examination of the strain's cultural colony and ITS gene fragment (Nishi et al. 2018). To date, there are 59 species of *Kirschsteiniothelia*, amongst which 18 have been reported only in their sexual morph, 32 reported in their asexual morph and six species documented in both morphs (Boonmee et al. 2012; Su et al. 2016; Sun et al. 2021; Xu et al. 2023; Zhang et al. 2023; de Farias et al. 2024; Sruthi et al. 2024; this study). Amongst the two asexual morphs that have been described so far, only the dendryphiopsis-like morph is linked to the sexual morph, while the sporidesmium-like state has not been associated with the sexual morph (Hawksworth 1985; Wang et al. 2004; Mulenko et al. 2008; Boonmee et al. 2012; Su et al. 2016; Sun et al. 2021; Xu et al.2023; de Farias et al. 2024).

In this study, we aimed to isolate microfungi from unidentified decaying wood collected in Hainan and Yunnan Provinces, China, as well as from *Edgeworthia chrysantha*, collected in Guizhou Province, China. This study has the following objectives: 1) to describe novel species associated with decaying wood through comprehensive morphological examinations and phylogenetic analyses of ITS, LSU and SSU rDNA sequence data; 2) to provide a checklist that includes host information, habitat preferences, availability of molecular data, morphological characteristics and country of origin.

Materials and methods

Sample collection, isolation and morphological studies

Decaying wood materials of *Edgeworthia chrysantha* and unidentified plants were collected from Zunyi City in Guizhou Province, Jianfengling National Forest Park, situated at the confluence of Ledong Li Autonomous County and Dongfang City in Hainan Province and Lushui City in Yunnan Province, China. These specimens were initially stored in Ziploc bags and observed using a stereomicroscope (Motic SMZ-171). The collection, observation and isolation were conducted following the methods outlined in Senanayake et al. (2020) and Tang et al. (2022). The observed features were measured using Tarosoft (R) Image Frame Work (version IFW 0.97) and photoplates were constructed using Adobe Photoshop 2019 (Adobe Systems, USA).

Specimens were deposited at the herbaria of the Kunming Institute of Botany, Chinese Academy of Sciences (HKAS), located in Kunming, China and the Guizhou Academy of Agriculture Sciences (GZAAS), situated in Guiyang, China. In addition, ex-type living cultures were preserved at the Kunming Institute of Botany Culture Collection (KUMCC) and the Guizhou Culture Collection (GZCC). Faces of Fungi and Fungal name numbers were obtained following the guidelines in Jayasiri et al. (2015), Wang et al. (2023) and Fungal names (2024). Species identification and establishment were determined following the guidelines outlined by Jeewon and Hyde (2016), Maharachchikumbura et al. (2021) and Pem et al. (2021).

DNA extraction, PCR amplification and sequencing

Freshly scraped mycelia from the pure cultures obtained by single spore isolation were transferred to 1.5 ml microcentrifuge tubes and stored in the refrigerator at -20 °C. Genomic DNA extraction was carried out using DNA extraction kits provided by Sangon Biotech (Shanghai) Co. Ltd., China. Polymerase Chain Reaction (PCR) was employed for DNA template amplification, using the following primer pairs: ITS5/ITS4 for ITS, NS1/NS4 for SSU (White et al. 1990) and LR0R/LR5 for LSU (Vilgalys and Hester 1990; Cubeta et al. 1991). Further details regarding DNA extraction, PCR amplification, sequencing and phylogenetic analyses are given in Tang et al. (2022, 2023).

In PCR amplification, the total volume of the PCR mixture was 50 µl, comprising the DNA template (2 µl), forward primer (2 µl), reverse primer (2 µl), 2 × Taq PCR Master Mix (25 µl) and 19 µl of double-distilled water. The PCR profiles consisted of 35 cycles, with annealing temperatures set at 52 °C for 1 minute and extension for 90 seconds at 72 °C for ITS, LSU and SSU loci. PCR products were verified on 1% agarose gel prior to submission to Sangon Biotech (Shanghai) Co., Ltd., China, for sequencing.

Phylogenetic analyses

Sequences obtained were subjected to a BLAST search in the NCBI database (https://blast.ncbi.nlm.nih.gov/Blast.cgi). Forward and reverse sequences were assembled using the Contig Express version 3.0.0 application. The ITS, LSU and SSU sequence data of *Kirschsteiniothelia* species were retrieved and downloaded from GenBank (Table 1). Individual sequences were aligned using

Table 1. Taxa used in this study and their respective GenBank accession numbers.

Taxon	Strain number	ITS	LSU	SSU
Kirschsteiniothelia acutispora	MFLU 21-0127^{T}	OP120780	ON980758	ON980754
K. atra	CBS 109.53	–	AY016361	AY016344
K. atra	MFLUCC 15-0424	KU500571	KU500578	KU500585
K. atra	MFLUCC 16-1104	MH182583	MH182589	MH182615
K. atra	S-783	MH182586	MH182595	MH182617
K. atra	GZCC 23-0731	PQ248940	PQ248936	PQ248932
K. atra	DEN^{T}	MG602687	–	–
K. aquatica	MFLUCC 16-1685^{T}	MH182587	MH182594	MH182618
K. arasbaranica	IRAN 2509C	KX621986	KX621987	KX621988
K. arasbaranica	IRAN 2508C^{T}	KX621983	KX621984	KX621985
K. agumbensis	NFCCI 5714^{T}	PP029048	–	PP029049
K. bulbosapicalis	GZCC 23-0732^{T}	PQ248937	PQ248933	PQ248929
K. cangshanensis	GZCC19-0515	–	MW133829	MW134609
K. cangshanensis	MFLUCC 16-1350^{T}	MH182584	MH182592	–
K. chiangmaiensis	MFLU 23-0358^{T}	OR575473	OR575474	OR575475
K. crustacea	MFLU 21-0129^{T}	MW851849	MW851854	
K. dendryphioides	KUNCC 10431^{T}	OP626354	PQ248935	PQ248931
K. dendryphioides	KUNCC 10499	PQ248938	–	–
K. dujuanhuensis	KUNCC 22-12671	OQ874971	OQ732682	
K. dushanensis	GZCC 19-0415^{T}	OP377845	MW133830	MW134610
K. ebriosa	CBS H–23379^{T}	–	LT985885	–
K. emarceis	MFLU 10-0037^{T}	NR_138375	NG_059454	–
K. esperanzae	T. Raymundo 6581^{T}	OQ877253	OQ880482	–
K. extensum	MFLU 21-0130^{T}	MW851850	MW851855	–
K. fluminicola	MFLUCC 16-1263^{T}	MH182582	MH182588	–
K. guangdongensis	ZHKUCC 22-0233^{T}	OR164946	OR164974	–
K. inthanonensis	MFLUCC 23-0277^{T}	OR762773	OR762781	OR764784
K. laojunensis	KUN-L 88727^{T}	PP081651	PP081658	–
K. lignicola	MFLUCC 10-0036^{T}	HQ441567	HQ441568	HQ441569
K. longirostrata	GZCC 23-0733^{T}	PQ248939	PQ248934	PQ248930
K. longisporum	UESTCC 24.0190^{T}	PQ038266	PQ038273	PQ046108
K. nabanheensis	HJAUP C2006	OQ023274	OQ023275	OQ023037
K. nabanheensis	HJAUP C2004^{T}	OQ023197	OQ023273	OQ023038
K. phoenicis	MFLU 18-0153	NR_158532	NG_064508	–
K. phoenicis	MFLUCC 18-0216^{T}	MG859978	MG860484	MG859979
K. pini	UESTCC 24.0131^{T}	PP835321	PP835315	PP835318
K. puerensis	ZHKUCC 21-0271^{T}	OP450977	OP451017	OP451020
K. puerensis	ZHKUCC 22-0272	OP450978	OP451018	OP451021
K. ramus	GZCC 23-0596^{T}	OR098711	OR091333	–
K. rostrata	MFLUCC15-0619	KY697280	KY697276	NG_063633
K. rostrata	MFLU 15-1154	NR_156318	NG_059790	KY697278
K. rostrata	MFLUCC 16-1124	–	MH182590	–
K. saprophytica	MFLUCC 23-0276	OR762775	OR762782	–
K. saprophytica	MFLUCC 23-0275^{T}	OR762774	OR762783	–

Taxon	Strain number	ITS	LSU	SSU
K. septemseptatum	MFLU 21-0126^{T}	OP120779	ON980757	ON980752
K. sichuanensis	UESTCC 24.0127^{T}	PP785368	PP784322	–
Kirschsteiniothelia sp.	KUNCC 23-13755	OR589301	–	–
Kirschsteiniothelia sp.	KUNCC 23-14559	OR589302	–	–
Kirschsteiniothelia sp.	KUNCC 23-13756	OR589303	–	–
Kirschsteiniothelia sp.	E38	MN912317	MN912273	–
Kirschsteiniothelia sp.	CSN602	MT813880	–	–
Kirschsteiniothelia sp.	CSN604	MT813881	–	–
Kirschsteiniothelia sp.	UTHSCSA D122 44	–	ON191450	–
Kirschsteiniothelia sp.	UTHSCSA D122 45	–	ON191449	–
Kirschsteiniothelia sp.	7020611638	–	MZ380317	–
K. spatiosum	MFLU 21-0128^{T}	OP077294	–	ON980753
K. submersa	S-601	MH182585	MH182593	–
K. submersa	S-481	–	MH182591	MH182616
K. submersa	MFLUCC 15-0427^{T}	KU500570	KU500577	KU500584
K. tectonae	MFLUCC 12-0050^{T}	KU144916	KU764707	–
K. tectonae	MFLUCC 13-0470	KU144924	–	–
K. thailandica	MFLUCC 20-0116^{T}	MT985633	MT984443	MT984280
K. thujina	JF13210	KM982716	KM982718	KM982717
K. vinigena	CBS H-23378^{T}	–	NG_075229	–
K. xishuangbannaensis	ZHKUCC 22-0221	OP289563	OP303182	OP289565
K. xishuangbannaensis	ZHKUCC 22-0220^{T}	OP289566	OP303181	OP289564
K. zizyphifolii	MFLUCC 23-0270^{T}	OR762768	OR762776	OR764779
Strigula guangxiensis	HMAS-L0138040	NR146255	MK206256	–
S. nemathora	MPN 72	–	JN887405	JN887389

Notes: Ex-type strains are indicated by "T" in superscript and newly-generated sequences are in red. Abbreviations: **CBS**: Westerdijk Fungal Biodiversity Institute, Utrecht, Netherlands; **CSN**: collection of Chris Spies at ARC-Nietvoorbij, Stellenbosch, South Africa; **GZCC**: Guizhou Culture Collection, Guizhou, China; **HJAUP**: Herbarium of Jiangxi Agricultural University, Plant Pathology; **HMAS-L**: Fungarium of the Institute of Microbiology, Chinese Academy of Sciences; **IRAN**: Iranian Fungal Culture Collection, Iranian Research Institute of Plant Protection, Tehran, Iran; **JF**: Jacques Fournier; **KUNCC:** Kunming Institute of Botany Culture Collection; **KUN-L**: Lichen Herbarium of Kunming Institute of Botany, Chinese Academy of Science, Yunnan, China; **MFLUCC**: Mae Fah Luang University Culture Collection, Chiang Rai, Thailand; **MFLU**: Mae Fah Luang University Herbarium Collection; **NFCCI**: National Fungal Culture Collection of India NFCCI-A National Facility; **ZHKUCC**: Zhongkai University of Agriculture and Engineering Culture Collection, Guangzhou, China. *K.: Kirschsteiniothelia*; *S.: Strigula*; "–": Data not available.

MAFFT version 7 (https://mafft.cbrc.jp/alignment/server/index.html) with the "auto" option (Katoh et al. 2017). The aligned sequences were trimmed using trimAl version 1.2 with the '-gt 0.6' command (Capella-Gutiérrez et al. 2009) and multiple genes were assembled using SequenceMatrix (Vaidya et al. 2011).

The phylogenetic analyses of the concatenated ITS, LSU and SSU sequences were conducted using Maximum Likelihood (ML) and Bayesian Inference (BI). Maximum Likelihood analysis was conducted using the IQ tree web server (http://iqtree.cibiv.univie.ac.at) and BI was carried out in the CIPRES web portal (Miller et al. 2010). The BI was performed using the tool "MrBayes on XSEDE" (Huelsenbeck and Ronquist 2001; Swofford 2002; Stamatakis et al. 2008; Ronquist et al. 2012). Prior to conducting BI, the model of evolution for each gene region was estimated using MrModelTest version 2 (Tang et al. 2023). The aligned Fasta file was converted into a Nexus format for subsequent Bayesian analysis using AliView version 1.27 (Daniel et al. 2010). Phylograms were

visualised using FigTree version 1.4.0 and edited in the Adobe Photoshop 2019 programme (Adobe Systems, USA) and Adobe Illustrator version 51.1052.0.0 (Adobe Inc., San Jose, California, USA).

Results

Phylogenetic analyses

According to the analysis of the concatenated ITS, LSU and SSU rDNA sequence data, all isolates collected in this study cluster within *Kirschsteiniothelia*. The dataset with 67 strains of *Kirschsteiniothelia*, including gaps, comprises 2290 characters (ITS: 1–506 base pairs (bp), LSU: 507–1330 bp and SSU: 1331–2283 bp). The highest-scoring RAxML tree is presented in Fig. 1, with a final ML optimisation likelihood value of -16683.670 (ln). The best-fit model for the BI analysis was GTR+I+G for ITS, LSU and SSU. Bayesian posterior probabilities (PP) from MCMC were analysed, achieving a final average standard deviation of split frequencies of 0.009914.

Taxonomy

***Kirschsteiniothelia atra* (Corda) D. Hawksw., Fungal Diversity 69: 37 (2014)**
Fungal Names number: FN 104401
Facesoffungi number: FoF01738
Fig. 2

≡ *Amphisphaeria aethiops* Sacc., Syll. fung. (Abellini) 1: 722 (1882)
= *Dendryphiopsis atra* (Corda) S. Hughes, Can. J. Bot. 31: 655 (1953)
≡ *Dendryphion atrum* Corda, Icon. fung. (Prague) 4: 33 (1840)
≡ *Kirschsteiniothelia aethiops* (Sacc.) D. Hawksw., J. Linn. Soc., Bot. 91(1–2): 185 (1985)

Description. ***Saprobic*** on decaying wood of *Edgeworthia chrysantha*. ***Sexual morph:*** see Hawksworth (1985). ***Asexual morph: Colonies*** on the natural substrate superficial, effuse, gregarious, dark brown to black, glistening. ***Mycelium*** immersed, composed of branched, septate, thin-walled, smooth, brown hyphae. ***Conidiophores*** 253–396 × 8–15.5 µm ($\bar{x}$ = 334.6 × 11.7 µm, n = 20), macronematous, mononematous, erect, straight or flexuous, cylindrical, septate, smooth, brown to dark brown, becoming paler towards the apex and comprising numerous short branches. ***Conidiogenous cells*** 14.5–29 × 5–10 µm ($\bar{x}$ = 20.6 × 6.8 µm, n = 30), tretic, integrated, sometimes percurrent, terminal, doliiform or lageniform, subhyaline to pale brown, with new cells developing from the apical or subapical part of the subtending cells. ***Conidia*** 32–56.5 × 11–19.5 µm ($\bar{x}$ = 42.3 × 14.5 µm, n = 30), solitary, acrogenous, cylindrical, sometimes clavate, 3–4-septate, constricted and darker at the septa, smooth, brown and rounded at the apex.

Culture characteristics. Conidia germinating on Potato Dextrose Agar (PDA) within 24 h, and producing germ tubes either from the apex or base. Colonies circular, flat, dense, radial sulcate, edge entire, pearl-gray on the surface, dark brown on the reverse and becoming grey-white along the margin.

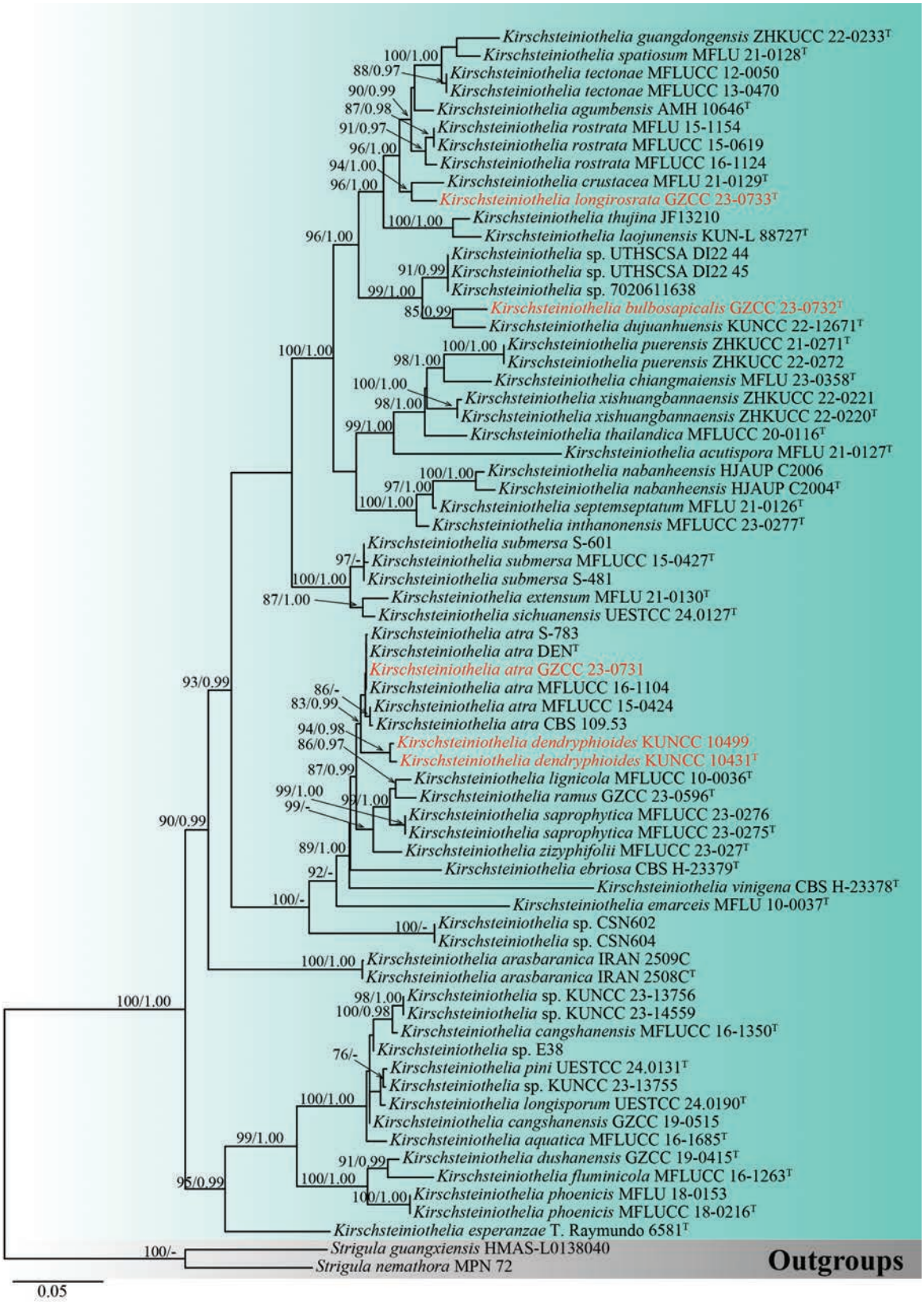

Figure 1. Phylogram of *Kirschsteiniothelia* taxa, based on the RAxML analysis of the combined ITS, LSU and SSU rDNA sequence dataset. Bootstrap support values for Maximum Likelihood (ML) equal to or greater than 75% and Bayesian posterior probabilities (PP) equal to or greater than 0.95 are shown above the nodes. The tree is rooted with *Strigula guangxiensis* (HMAS-L0138040) and *S. nemathora* (MPN 72). Newly-generated strains are denoted in red and type strains are indicated with a superscript "T".

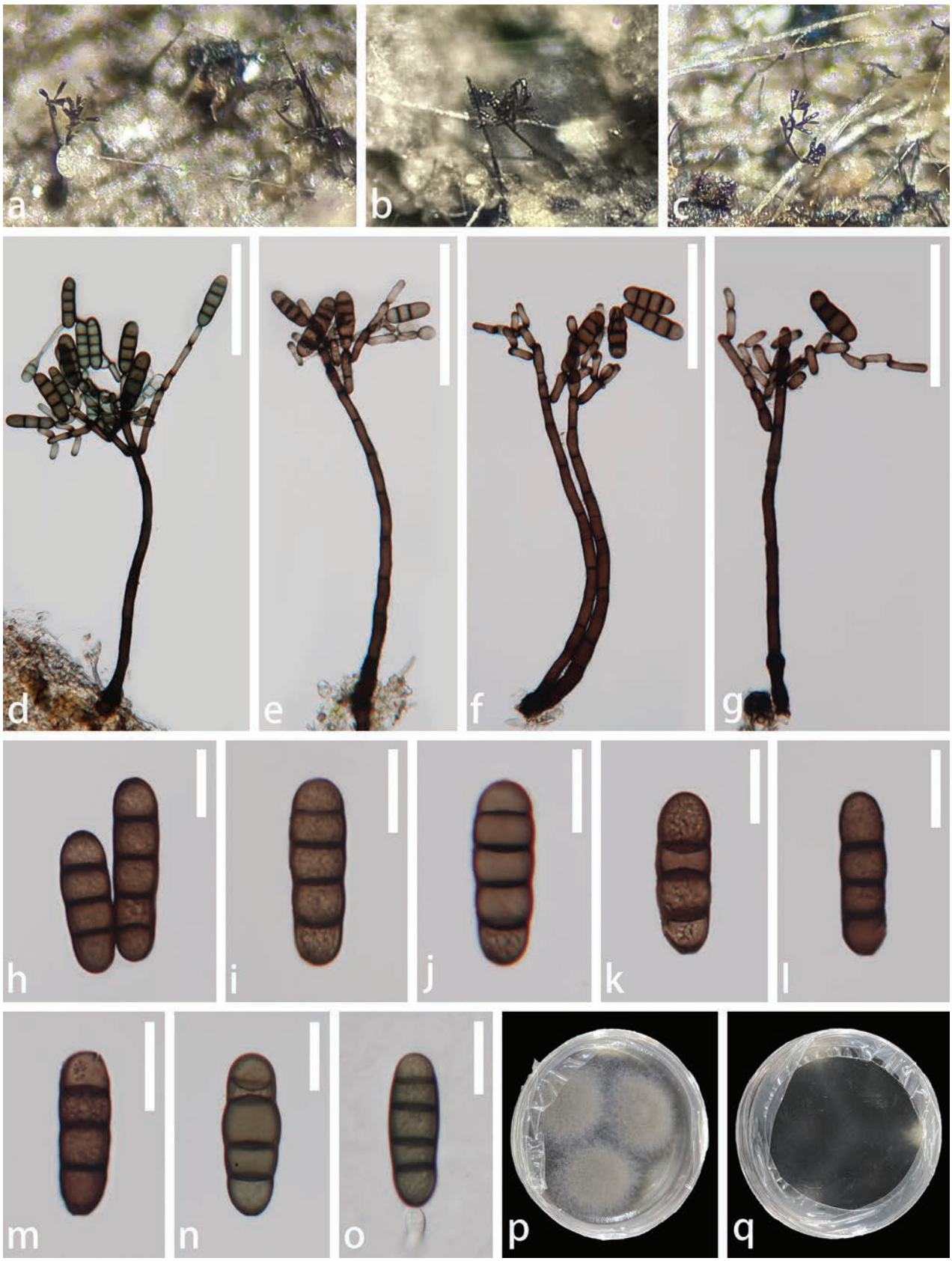

Figure 2. *Kirschsteiniothelia atra* (GZAAS 23-0807, new host record) **a–c** colonies on natural substrate **d–g** conidiophores and conidiogenous cells bearing conidia **h–n** conidia **o** a germinated conidium **p** upper surface view of culture **q** lower surface view of culture. Scale bars: 100 μm (**d–g**); 20 μm (**h–o**).

Material examined. China • Guizhou Province, Zunyi City, Suiyang County, saprobic on decaying branches of *Edgeworthia chrysantha*, 13 February 2023, Xue-Mei Chen, SY12 (GZAAS 23-0807), living culture GZCC 23-0731.

Known distribution (based on molecular data). China (Su et al. 2016; this study).

Known hosts (based on molecular data). *Edgeworthia chrysantha* (This study), Unidentified decaying wood (Su et al. 2016).

Note. Morphologically, our collection matches the characteristics of *Kirschsteiniothelia atra*, including macronematous, mononematous conidiophores with numerous short branches; tretic, doliiform, or lageniform conidiogenous cells that develop new cells from the apical or subapical part of the subtending cells; and cylindrical, occasionally clavate conidia that are 3–4-septate, constricted and darker at the septa, which are rounded at the apex (Su et al. 2016). In the phylogenetic analyses, our collection (GZCC 23-0731) clusters with *Kirschsteiniothelia atra* (CBS 109.53, DEN, MFLUCC 15-0424, MFLUCC 16-1104 and S–783) (Fig. 1). Excluding gaps, no difference was observed in the comparison of nucleotides across the ITS (491 bp), LSU (788 bp) and SSU (844 bp) regions between our collection and *Kirschsteiniothelia atra* (MFLUCC 16-1104). Based on these findings, we identify our isolate as *Kirschsteiniothelia atra*, following the guidelines established by Jeewon and Hyde (2016) and Maharachchikumbura et al. (2021). This is the first time *Kirschsteiniothelia atra* has been reported from *Edgeworthia chrysantha*.

***Kirschsteiniothelia bulbosapicalis* X. Tang, K.D. Hyde, Jayaward. & J.C. Kang, sp. nov.**

Fungal Names number: FN 572044

Facesoffungi number: FoF16485

Fig. 3

Etymology. The specific epithet '*bulbosapicalis*' refers to the bulbous area of the conidia at the apex.

Holotype. GZAAS 23-0808.

Description. ***Saprobic*** on unidentified decaying wood. ***Sexual morph:*** Undetermined. ***Asexual morph: Colonies*** on the natural substrate superficial, effuse, gregarious, hairy, black, glistening. ***Mycelium*** semi-immersed, on the substrate, pale brown to dark brown. ***Conidiophores*** (–47)58–128(–199) µm × 7.5–12.5(–16.5) µm ($\bar{x}$ = 86.7 × 10.6 µm, n = 15), macronematous, mononematous, solitary, straight or slightly flexuous, cylindrical, unbranched, septate, smooth, brown to dark brown, truncate at the apex and wider at the base. ***Conidiogenous cells*** 6–17 µm × 7–10.5 µm ($\bar{x}$ = 10.6 × 8.6 µm, n = 15), monoblastic, holoblastic, terminal, determinate, proliferating, cylindrical, brown to dark brown. ***Conidia*** 118–236.5 µm × 15–27 µm ($\bar{x}$ = 174.8 × 21 µm, n = 30), solitary, acrogenous, cylindrical, ovoid to obclavate, rostrate, smooth, straight or slightly curved, 8–13-septate, slightly constricted at the septa, olivaceous to reddish-brown to dark brown, bulbous at the apex and/or third or fourth cell, truncate at the base, with a spherical hyaline mucilaginous sheath.

Culture characteristics. Conidia germinating on PDA within 24 hours, producing germ tubes from the apex. Colonies displayed a circular morphology with an umbonate elevation, dense growth and a filiform margin. The surface

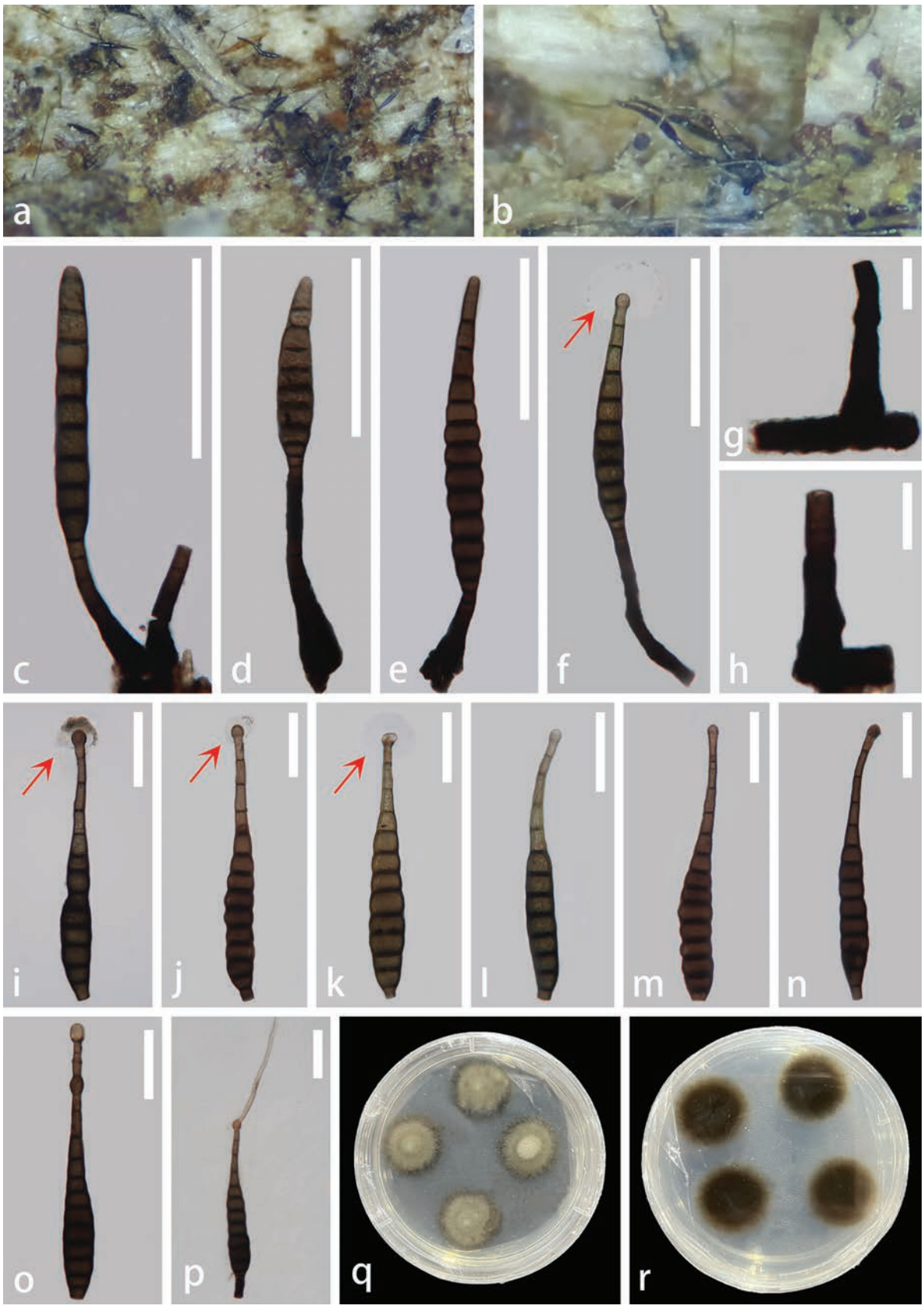

Figure 3. *Kirschsteiniothelia bulbosapicalis* (GZCC 23-0732, holotype) **a, b** colonies natural substrate **c–f** conidiophores, conidiogenous cells bearing conidia (red arrows indicate mucilaginous sheaths) **g, h** conidiophores **i–o** conidia (red arrows indicate mucilaginous sheaths) **p** a germinated conidium **q** upper surface view of culture **r** lower surface view of culture. Scale bars: 100 µm (**c–f**); 20 µm (**g, h**); 50 µm (**i–p**).

appeared greyish-green, occasionally exhibiting paler mycelium in the bulge region. The reverse colonies exhibited a circular shape with a filiform margin, displaying a dark brown colour, becoming olivaceous towards the periphery.

Material examined. China • Hainan Province, Jianfengling National Forest Park, saprobic on unidentified decaying wood, 23 August 2021, Zili Li, JBT04 (GZAAS 23-0808, holotype), ex-type living culture GZCC 23-0732.

Note. *Kirschsteiniothelia bulbosapicalis* exhibits sporidesmium-like characteristics and shares similar morphologies with other *Kirschsteiniothelia* species. However, *K. bulbosapicalis* can be distinguished from other *Kirschsteiniothelia* species in having different sizes of conidiophores, conidiogenous cells and the unique feature of its conidia, which comprises one or two bulbous structures at or near the apex, with a spherical hyaline mucilaginous sheath. Phylogenetically, *K. bulbosapicalis* is sister to *K. dujuanhuensis* (KUNCC 22-12671) with 85% ML and 0.99 PP support (Fig. 1). Similar to our new species, *K. dujuanhuensis* also comprises a spherical hyaline mucilaginous sheath. *Kirschsteiniothelia bulbosapicalis* is characterised by larger conidiophores [(–47)58.5–128(–199) µm × 7.5–12.5(–16.5) µm, L/W ratio = 8.2] compared to *K. dujuanhuensis* [29–74(–119) × 9–11 µm, L/W ratio = 5.1] and larger conidia (118–236.5 µm × 15–27 µm, L/W ratio = 8.3) compared to *K. dujuanhuensis* [(114–)122–155(–170) × 10–13(–16) µm, L/W ratio = 11.5]. In addition, *K. bulbosapicalis* exhibits cylindrical to ovoid or obclavate conidia with 8–13 septa and often consist of bulbous structures at the apex and/or the third or fourth cell, as well as a spherical hyaline mucilaginous sheath. In contrast, *K. dujuanhuensis* typically contains obclavate to subcylindrical conidia that are 6–15 septate.

In addition, the comparison of the nucleotides between the sequences of *K. bulbosapicalis* and *K. dujuanhuensis* showed differences of 9% (47/512 bp) across ITS, 1% (8/812 bp) across LSU and 0.1% (2/1003 bp) across SSU, excluding gaps. Based on these findings, we introduce *K. bulbosapicalis* as a novel species, in accordance with the guidelines established by Jeewon and Hyde (2016) and Maharachchikumbura et al. (2021).

Kirschsteiniothelia dendryphioides **X. Tang, K.D. Hyde, Jayaward. & J.C. Kang, sp. nov.**

Fungal Names number: FN 572046

Facesoffungi number: FoF16486

Figs 4, 5

Etymology. The specific epithet "*dendryphioides*" is derived from the resemblance to the dendryphiopsis-like features.

Holotype. HKAS 136930.

Description. ***Saprobic*** on an unidentified decaying wood. ***Sexual morph:*** Undetermined. ***Asexual morph: Colonies*** on the natural substrate superficial, effuse, scattered, hairy, black, glistening. ***Mycelium*** partly immersed, on the substrate, pale brown to dark brown. ***Conidiophores*** 179–467 × 4.5–8 µm ($\bar{x}$ = 318.2 × 6.1 µm, n = 10), macronematous, mononematous, erect, subscorpioid branched, straight or flexuous, cylindrical, septate, smooth, brown to dark brown, becoming paler towards the apex. ***Conidiogenous cells*** 9–19 × 4–8 µm ($\bar{x}$ = 13.3 × 6.1 µm, n = 30), monotretic, terminal or intercalary, integrated, some-

Figure 4. *Kirschsteiniothelia dendryphioides* (HKAS 136930, holotype) **a, b** colonies on natural substrate **c, d** conidiophores, conidiogenous cells bearing conidia **e–g** conidiogenous cells bearing conidia **h–o** conidia **p** upper surface view of culture **q** lower surface view of culture; Scale bars: 100 μm (**c, d**); 50 μm (**e**); 20 μm (**f–o**).

times percurrent, cylindrical, doliiform, mostly discrete, determinate, smooth, pale brown to brown, both ends appearing darker, with new cells developing from the apical or subapical part of the subtending cells. ***Conidia*** 30–55 × 9–13.5 μm ($\bar{x}$ = 40 × 11.1 μm, n = 30), solitary, acrogenous, cylindrical, oblong

Figure 5. *Kirschsteiniothelia dendryphioides* (HKAS 135651, paratype) **a, b** colonies on natural substrate **c, d** conidiophores, conidiogenous cells bearing conidia **e–g** conidiogenous cells bearing conidia **h–l** conidia **m** upper surface view of culture **n** lower surface view of culture. Scale bars: 100 μm (**c, d**); 20 μm (**e–l**).

and occasionally clavate, smooth, guttulate, 2–4-septate, slightly or deeply constricted and darker at the septa, brown, rounded at the apex and sometimes truncate at the base, exhibiting obtuse ends.

Culture characteristics. Conidia germinating on PDA within 24 hours. Colonies circular, characterised by dense, flat, spreading and fluffy growth, with an entire margin. The surface displayed a dark brown hue, while the reverse colonies exhibited a circular shape with an entire margin, also appearing dark brown.

Material examined. China • Yunnan Province, Lushui City, Sanhe Village, Gaoligong Mountain, saprobic on decaying wood in a freshwater stream, 5 May 2021, Rong-ju Xu, XS17 (HKAS 136930, holotype), ex-type living culture, KUNCC 10431; *ibid.* • saprobic on submerged decaying wood in freshwater habitats, 22 August 2021, Rong-ju Xu, SYC-05 (HKAS 135651, paratype), living culture, KUNCC 10499.

Notes. *Kirschsteiniothelia dendryphioides* exhibits dendryphiopsis-like characteristics and shares similar morphologies with other *Kirschsteiniothelia* species. However, *K. dendryphioides* differs from other species in the size of its conidiophores, conidiogenous cells and conidia. *Kirschsteiniothelia dendryphioides* is distinct from *K. atra* in having larger conidiophores (179–467 × 4.5–8 µm, L/W ratio = 52.2 vs. 148–228 µm × 6–8 µm, L/W ratio = 27), shorter conidiogenous cells (9–19 × 4–8 µm, L/W ratio = 2.2 vs. 25–33 µm × 5–7 µm, L/W ratio = 4.8) and smaller conidia (30–55 × 9–13.5 µm, L/W ratio = 3.6 vs. 54–63 ×14–18 µm, L/W ratio = 3.4).

The establishment of *Kirschsteiniothelia dendryphioides* as a new species is further supported by molecular data. Based on our phylogenetic analyses, *K. dendryphioides* strains (KUNCC 10431 and KUNCC 10499) form a subclade sister to the strains of *Kirschsteiniothelia atra* (CBS 109.53, DEN, MFLUCC 15-0424, MFLUCC 16-1104 and S-783) with 83% ML and 0.99 PP support (Fig. 1). The comparison of the nucleotides between the sequences of *K. dendryphioides* and *K. atra* (MFLUCC 16-1104) shows a difference of 1.9% (9/481 bp) across ITS and 2.4% (11/458 bp) across SSU, but no difference was observed across LSU (777 bp), excluding gaps. Based on these findings, we introduce *Kirschsteiniothelia dendryphioides* as a novel species, following guidelines outlined in Jeewon and Hyde (2016) and Maharachchikumbura et al. (2021). We were unable to compare the nucleotide differences across LSU and SSU of KUNCC 10499 as it lacks sequence data for these loci.

***Kirschsteiniothelia longirostrata* X. Tang, K.D. Hyde, Jayaward. & J.C. Kang, sp. nov.**

Fungal Names number: FN 572045
Facesoffungi number: FoF16487
Fig. 6

Etymology. The specific epithet '*longirostrata*' refers to the conidia containing a long rostrate.

Holotype. GZAAS 23-0809.

Description. ***Saprobic*** on an unidentified submerged decaying wood. ***Sexual morph:*** Undetermined. ***Asexual morph: Colonies*** on the natural substrate superficial, effuse, gregarious, hairy, black, glistening. ***Mycelium*** partly

Figure 6. *Kirschsteiniothelia longirostrata* (GZCC 23-0733, holotype) **a** unidentified submerged wood **b** colonies on natural substrate **c, d** conidiophores, conidiogenous cells **e–g** conidiophores, conidiogenous cells bearing conidia **h–p** conidia (red arrows indicate mucilaginous sheaths) **q** a germinated conidium; **r** Upper surface view of culture **s** lower surface view of culture. Scale bars: 100 μm (**c–g**); 20 μm (**h–q**).

immersed on the substrate, composed of branched, septate, smooth-walled hyphae, pale to dark brown. ***Conidiophores*** 80–252 × 4.5–9.5 µm ($\bar{x}$ = 161.3 × 6.8 µm, n = 20), macronematous, mononematous, solitary, cylindrical, straight, or slightly flexuous, unbranched, percurrent, smooth, guttulate, 4–13-septate, sometimes slightly constricted at the septa, brown to dark brown tapering towards the apex and wider at the base. ***Conidiogenous cells*** 6.5–16 × 5–9 µm ($\bar{x}$ = 13× 7 µm, n = 20), monoblastic, terminal or indeterminate, percurrently proliferating, cylindrical, pale brown to brown. ***Conidia*** 36.5–109(–160) × 8–16 µm ($\bar{x}$ = 71× 12 µm, n = 30), solitary, acrogenous, cylindrical, obpyriform to obclavate, rostrate 15–100(–120) × 2.5–6 µm ($\bar{x}$ = 48 × 4.3 µm, n = 30), smooth, straight or curved, guttulate, 6–18-septate, slightly constricted and darker at the septa, proliferating, pale brown to brown, becoming paler towards the apex, with a truncate base and a mucilaginous sheath surrounding the upper part of the apex.

Culture characteristics. Conidia germinating on PDA within 24 hours, producing germ tubes from the apex. Colonies displayed a circular morphology with dense, flat, spreading and fluffy growth, with an entire margin. The surface exhibited an olivaceous-green hue with a darker edge, while the reverse colonies displayed a circular shape with an entire margin, appearing blackish-green.

Material examined. China • Hainan Province, Jianfengling National Forest Park, saprobic on submerged unidentified decaying wood, 23 August 2021, Zili Li, T10 (GZAAS 23-0809, holotype) ex-type living culture GZCC 23-0733.

Notes. *Kirschsteiniothelia longirostrata* exhibits sporidesmium-like characteristics and shares similar features with other *Kirschsteiniothelia* species. *Kirschsteiniothelia longirostrata* can be distinguished from other *Kirschsteiniothelia* species in having different sizes and shapes of conidiophores, conidiogenous cells and unique features of conidia, such as obpyriform to obclavate, long rostrate, proliferating, with a mucilaginous sheath surrounding the upper part of the apex. Unlike *K. crustacea*, *K. longirostrata* has cylindrical, proliferating conidiogenous cells and obpyriform to obclavate conidia, with longer (15–100(–120) × 2.5–6 µm), guttulate, proliferating rostrate structures and a mucilaginous sheath surrounding the upper part of the apex.

Molecular data further supports the establishment of *Kirschsteiniothelia longirostrata* as a novel taxon. Based on our phylogenetic analyses, *K. longirostrata* is sister to *K. crustacea* (MFLU 21-0129) with 94% ML and 1.00 PP support (Fig.1). The comparison of the nucleotides between the sequences of *K. longirostrata* (GZCC 23-0733) and *K. crustacea* (MFLU 21-0129) shows differences of 8.4% (39/467 bp) across ITS and 0.7% (5/718 bp) across LSU, excluding gaps. However, we were unable to compare the nucleotide differences across SSU as *K. crustacea* lacks sequence data for this locus. Based on these findings, we introduce *Kirschsteiniothelia longirostrata* as a novel species, following guidelines outlined in Jeewon and Hyde (2016) and Maharachchikumbura et al. (2021).

Discussion

During surveys on saprobic fungi associated with woody plants in the subtropical and tropical forests of the Guizhou, Hainan and Yunnan Provinces in China, we discovered three previously undocumented taxa and one known species,

which belong to *Kirschsteiniothelia*. They were found on decaying wood, including some unidentified hosts and *Edgeworthia chrysantha*. All these species have been reported with their asexual morph, either exhibiting the dendryphiopsis-like or sporidesmium-like morphologies.

Our newly-described taxa include two sporidesmium-like species, namely *Kirschsteiniothelia bulbosapicalis* and *K. longirostrata* and one dendryphiopsis-like taxon, *K. dendryphioides*. Both *Kirschsteiniothelia bulbosapicalis* and *K. longirostrata* exhibit distinct characteristics from other species of *Kirschsteiniothelia*. *Kirschsteiniothelia bulbosapicalis* is characterised by acrogenous, cylindrical, ovoid, obclavate, rostrate, straight or slightly curved conidia with 8–13 septa, often bulbous at the apex and/or third or fourth cell, with a spherical hyaline mucilaginous sheath. *Kirschsteiniothelia longirostrata* displays solitary, acrogenous, cylindrical, obpyriform to obclavate, rostrate, smooth, straight or curved and guttulate conidia that are paler towards the apex, consisting of 6–18 septa, slightly constricted and darker at the septa, with a mucilaginous sheath surrounding the tail-like upper part of the apex. *Kirschsteiniothelia longirostrata* has the longest tail amongst all current *Kirschsteiniothelia* species, which proliferates from the apex of the conidium. Our phylogenetic analyses reveal that our new species belong to *Kirschsteiniothelia* with stable support values and, in particular, is closely related to *K. crustacea*.

Kirschsteiniothelia dendryphioides displays solitary, acrogenous, cylindrical, oblong and occasionally clavate, smooth, guttulate, 2–4-septate conidia with slightly or deeply constricted and darker at the septa, rounded at the apex and sometimes truncate at the base, exhibiting obtuse ends. However, *Kirschsteiniothelia dendryphioides* is characterised by larger conidiophores, shorter conidiogenous cells and smaller conidia when compared to *K. atra*. Although they are morphologically similar, there are also sufficient dissimilarities in the DNA sequence data.

The new host record for *Kirschsteiniothelia atra* shows characteristics of solitary, acrogenous, cylindrical, sometimes clavate conidia that are 3–4-septate, constricted and darker at the septa and smooth and rounded at the apex. Based on a comparison of morphological and phylogenetic analyses, no significant differences were observed in the DNA base pairs and the morphological variations fall within the range of intraspecific diversity. Therefore, we identified our new collection (GZCC 23–0731) as the known species *K. atra*. Furthermore, this report extends the known host range of *K. atra* (Table 2).

Whether we can use sporidesmium-like and dendryphiopsis-like morphs to differentiate species is currently obscure. Based on our phylogeny, species with sporidesmium-like and dendryphiopsis-like morphs do constitute distinct clades. There are three dendryphiopsis-like species (*K. inthanonensis*, *K. nabanheensis* and *K. septemseptatum*) that constitute a strongly-supported subclade, but they are nested within sporidesmium-like species. Therefore, segregating species based on this aspect should be dealt with caution. As with other asexual fungi, some species of *Kirschsteiniothelia* occur solely in the sexual morph and, hence, we are unable to compare their morphologies with other asexual species.

Besides establishing three novel *Kirschsteiniothelia* species and a new host record, we provide a checklist of all *Kirschsteiniothelia* taxa (Table 2), which incorporate 41 asexual morph species, amongst which 21 exhibit the sporidesmi-

um-like morph, while 20 display the dendryphiopsis-like features (Hawksworth 1985; Boonmee et al. 2012; Su et al. 2016; Sun et al. 2021; Xu et al. 2023; de Farias et al. 2024; Jin et al. 2024; Tian et al. 2024). This checklist includes data on the host, habitat preferences, reported morphology, country of origin and availability of molecular data for all species of *Kirschsteiniothelia*. The checklist also provides the latest ecological information of species in the genus.

From the checklist (Table 2), we decipher that most *Kirschsteiniothelia* species have been reported from China (23 species), followed by Thailand (14 species), with a few distributed across different countries including Australia, Belgium, Canada, Czechia, France, Germany, Greece, Italy, India, Iran, Mexico, New Zealand, Poland, Russian Federation, Sweden, Switzerland, South Africa, Spain, United Kingdom and USA (Boonmee et al. 2012; Mehrabi et al. 2017; Bao et al. 2018; Rodríguez-Andrade et al. 2020; Jayawardena et al. 2022; Senanayake et al. 2023; Liu et al. 2023b; Yang et al. 2023; de Farias et al. 2024; Louangphan et al. 2024). As noted in Table 2, the proportion of new species of *Kirschsteiniothelia* discovery in China and Thailand reaches 63%, while other countries and regions have only sporadically discovered one or two species. Hence, we presume that *Kirschsteiniothelia* is highly diverse with many potentially more unknown species and other tropical and subtropical regions that should be explored. In addition, most new species in China and Thailand were primarily found in tropical and subtropical regions, with nearly all species growing on decayed wood (Bao et al. 2018; Rodríguez-Andrade et al. 2020; Sun et al. 2021; Jayawardena et al. 2022; Senanayake et al. 2023; Liu et al. 2023b; Yang et al. 2023; de Farias et al. 2024; Louangphan et al. 2024). We speculate that the high proportion of new species discovered in China and Thailand can be attributed to the following reasons: 1) The tropical/subtropical climatic conditions in China and Thailand are suitable for the growth of these species, with optimal temperature and humidity levels that favour spore germination and colony growth; 2) Samples of *Kirschsteiniothelia* are easily observed on natural substrates and easy to collect; 3) They proliferate quite easily and are potentially good decomposers of substrates and they grow well on most common culture media without requiring specific cultivation conditions; 4) There are many mycologists in China and Thailand who are actively involved in fungal taxonomy and are more likely to discover more new species.

Most species of *Kirschsteiniothelia* are saprobes occurring mainly in terrestrial and followed by freshwater habitats, with only a few taxa reported from environments, such as cork stoppers and as a pathogen that infects human beings (Hawksworth 1985; Boonmee et al. 2012; Su et al. 2016; Nishi et al. 2018; Rodríguez-Andrade et al. 2020; Sun et al. 2021; Xu et al. 2023; de Farias et al. 2024). According to our results, species of *Kirschsteiniothelia* are also present in various habitats, albeit in small numbers. That may be because most studies have overlooked these more specific habitats. We recommend that future research should focus on exploring this genus in diverse environments to potentially discover additional species. In addition, most of the newly-discovered species are asexual on decayed wood samples. The latter provides ample organic nutrients which favour the emergence of the asexual morph and allows them to colonise new areas and propagate (Zalamea et al. 2016; Liu et al. 2023a).

Table 2. *Kirschsteiniothelia* species and data related to their host, habitat, country and reported morph.

Taxa	Host	Habitat	Morphological character	Asexual Morph character	Country	Molecular data	References
Kirschsteiniothelia abietina	*Tsuga canadian*	Terrestrial	Sexual	N/A	USA	N/A	Fairman (1905); Wang et al. (2004)
K. acerina	On absorbing mycorrhizal rootlets of *Acer saccharum*	Terrestrial	Sexual	N/A	USA	N/A	Hawksworth (1985)
K. acutispora	Unidentified decaying wood	Terrestrial	Asexual	Sporidesmium-like	Thailand	A	Jayawardena et al. (2022)
K. agumbensis	On decaying wood of *Garcinia* sp.	Terrestrial	Asexual	Sporidesmium-like	India	A	Sruthi et al. (2024)
K. atra	*Abies balsamea*, *Acer negundo*, *Acer* sp., *Agathis australis*, *Alnus glutinosa*, *A. incana*, *Alstonia* sp., *Betula papyrifera*, *Brachyglottis repanda*, *Bursera* sp., *Carpinus betulus*, *Carpinus* sp., *Celtis* sp., *Clematis* sp., *Coprosma australis*, *Corylus avellana*, *Cupressus macrocarpa*, *Cupressus* sp., *Drypetes alba*, *Edgeworthia chrysantha*, *Fraxinus pennsylvanica*, *Fraxinus* sp., *Fuchsia excorticata*, *Hedera helix*, *Juglans* sp., *Knightia excelsa*, *Leptospermum scoparium*, *Lonicera coerulea*, *Machaerocereus* sp., *Macropiper excelsum*, *Nothofagus truncata*, *Phoenix dactylifera*, *Pinus banksiana*, *Populus angustifolia*, *P. balsamifera*, *P. tremuloides*, *Prunus* sp., *Quercus robur*, *Quercus* sp., *Rhopalostylis* sp., *Salix* sp., *Tilia americana*, *Tsuga canadensis*, Unidentified decaying wood	Freshwater, terrestrial	Sexual and Asexual	Dendryphiopsis-like	Australia, Belgium, China, Czech Republic, France, Germany, Mexico, New Zealand, Poland, Russian Federation, Sweden, Unite Kingdom, USA	A	Aptroot (1995, 1997); Cannon et al. (1985); Chlebicki and Chmiel (2006); Conners (1967); Cooke (1985); Eriksson (1992, 2014); Ginns (1986); Hughes (1978); Hyde (1993); Kobayashi (2007); Matsushima (1971, 1975); McKenzie et al. (2000, 2004); Minter et al. (2001); Mulenko et al. (2008); Nattrass (1961); Nordén et al. (1997); Popov et al. (2008); Rao and Varghese (1981); Réblová and Svrcek (1997); Schmid-Heckel (1988); Sieber et al. (1995); Sierra (1984); Su et al. (2016); Sutton (1973); This study; Wang and He (2007); Wang (2010); Wang et al. (2004).
K. aquatica	Unidentified decaying wood	Freshwater	Asexual	Sporidesmium-like	China	A	Bao et al. (2018)
K. arasbaranica	Dead branches of *Quercus petraea*	Terrestrial	Sexual	N/A	Iran	A	Mehrabi et al. (2017)
K. arbuscula	On bark of *Acer*, *Rhus copallinum*, *Carya*, *Magnolia glauca*, and *Acer rubrum*	Terrestrial	Asexual	Dendryphiopsis-like	USA	N/A	Berkeley (1875); Ellis (1976); Pratibha et al. (2010); Sruthi et al. (2024)
K. atkinsonii	*Freycinetia arnotti*	Terrestrial	Sexual	N/A	Greece	N/A	Stevens (1925)
K. binsarensis	On dead twig	Terrestrial	Asexual	Dendryphiopsis-like	India	N/A	Subramanian and Srivastava (1994); Sruthi et al. (2024)
K. biseptata	On dead wood	Terrestrial	Asexual	Dendryphiopsis-like	South Africa	N/A	Morgan-Jones et al. (1983); Sruthi et al. (2024)
K. bulbosapicalis	Unidentified decaying wood	Terrestrial	Asexual	Sporidesmium-like	China	A	This study
K. cangshanensis	Unidentified decaying wood	Freshwater	Asexual	Sporidesmium-like	China	A	Bao et al. (2018)

Taxa	Host	Habitat	Morphological character	Asexual Morph character	Country	Molecular data	References
K. chiangmaiensis	Unidentified decaying wood	Terrestrial	Sexual	N/A	Thailand	A	Louangphan et al. (2024)
K. crustacea	Bamboo	Terrestrial	Asexual	Sporidesmium-like	Thailand	A	Jayawardena et al. (2022)
K. dendryphioides	Unidentified decaying wood	Freshwater	Asexual	Dendryphiopsis-like	China	A	This study
K. dolioloides	*Ramulis decorticatis pineis*	Terrestrial	Sexual	N/A	Switzerland	N/A	Wegelin (1894); Wang et al. (2004)
K. dujuanhuensis	Unidentified submerged wood	Freshwater	Asexual	Sporidesmium-like	China	A	Unpublished
K. dushanensis	Unidentified decaying wood	Freshwater	Asexual	Sporidesmium-like	China	A	Yang et al. (2023)
K. ebriosa	Sparkling wine	N/A	Asexual	Dendryphiopsis-like	Spain	A	Rodríguez-Andrade et al. (2020)
K. emarceis	Unidentified decaying wood	Terrestrial	Sexual and asexual	Dendryphiopsis-like	Thailand	A	Boonmee et al. (2012)
K. esperanzae	Unidentified decaying wood	Terrestrial	Sexual	N/A	Mexico	N/A	Raymundo et al. (2023)
K. extensum	Unidentified decaying wood	Terrestrial	Asexual	Sporidesmium-like	Thailand	A	Jayawardena et al. (2022)
K. fascicularis	On bark of *Liquidambar* sp.	Terrestrial	Asexual	Dendryphiopsis-like	USA	N/A	Berkeley (1875); Hughes (1958); Sruthi et al. (2024)
K. fluminicola	Unidentified decaying wood	Freshwater	Asexual	Sporidesmium-like	China	A	Bao et al. (2018)
K. goaensis	On dead and decaying bark of tree	Terrestrial	Asexual	Dendryphiopsis-like	India	N/A	Pratibha et al. (2010); Sruthi et al. (2024)
K. guangdongensis	Dead branches of unidentified plant	Terrestrial	Asexual	Sporidesmium-like	China	A	Senanayake et al. (2023)
K. inthanonensis	Unidentified decaying wood	Terrestrial	Asexual	Dendryphiopsis-like	Thailand	A	de Farias et al. (2024)
K. laojunensis	Bark of *Abies fabri*	Terrestrial	sexual	N/A	China	A	Meng et al. (2024)
K. lignicola	Unidentified decaying wood	Terrestrial	Sexual and Asexual	Dendryphiopsis-like	Thailand	A	Boonmee et al. (2012)
K. longirostrata	Unidentified submerged decaying wood	Freshwater	Asexual	Sporidesmium-like	China	A	This study
K. longisporum	Dead branches of *Pinus taeda*	Terrestrial	Asexual	Dendryphiopsis-like	China	A	Tian et al. (2024)
K. nabanheensis	Unidentified broadleaf tree	Terrestrial	Asexual	Dendryphiopsis-like	China	A	Liu et al. (2023b)
K. phileura	*Tilia americana*	Terrestrial	Sexual	N/A	USA	N/A	Cooke and Ellis (1876); Saccardo (1882)
K. phoenicis	*Phoenix paludosa*	Marine	Sexual	N/A	Thailand	A	Hyde et al. (2018)
K. pini	On decaying branches of a *Pinus* sp.	Terrestrial	Asexual	Sporidesmium-like	China	A	Jin et al. (2024)
K. populi	*Populus angustifolia*	Terrestrial	Sexual	N/A	USA	N/A	Greene (1901); Wang et al. (2004)

Taxa	Host	Habitat	Morphological character	Asexual Morph character	Country	Molecular data	References
K. proteae	*Protea cynaroides*	N/A	Sexual	N/A	South Africa	N/A	Marincowitz et al. (2008)
K. puerensis	Coffee wood	Terrestrial	Asexual	Sporidesmium-like	China	A	Hyde et al. (2023)
K. ramus	Unidentified decaying wood	Freshwater	Asexual	Dendryphiopsis-like	China	A	Zhang et al. (2023)
K. recessa	Unidentified decaying wood, *Acer rubrum*, *Alnus rubra*, *Pyrus* sp., rotten wood	Terrestrial	Sexual and asexual	Dendryphiopsis-like	Canada, Italy, USA,	N/A	Hawksworth (1985); Barr et al. (1986); Aptroot (1995); Wang et al. (2004)
K. reticulata	Unidentified twigs	Terrestrial	Sexual	N/A	China	N/A	Chen et al. (2006)
K. rostrata	Unidentified decaying wood	Freshwater	Asexual	Sporidesmium-like	China	A	Bao et al. (2018)
K. saprophytica	Unidentified decaying wood	Terrestrial	Sexual and asexual	Dendryphiopsis-like	Thailand	A	de Farias et al. (2024)
K. septemseptatum	Unidentified decaying wood	Terrestrial	Asexual	Dendryphiopsis-like	Thailand	A	Jayawardena et al. (2022)
K. sichuanensis	On decaying branches of an unidentified woody plant	Terrestrial	Asexual	Sporidesmium-like	China	A	Jin et al. (2024)
K. shimlaensis	*Cedrus deodara*	Terrestrial	Asexual	Dendryphiopsis-like	India	N/A	Verma et al. (2021)
K. smilacis	*Smilax* sp.	Terrestrial	Sexual	N/A	China	N/A	Chen et al. (2006)
K. spatiosum	Unidentified decaying wood	Terrestrial	Asexual	Sporidesmium-like	Thailand	A	Jayawardena et al. (2022)
K. striatispora	*Juniperus communis*	Terrestrial	Sexual	N/A	China, Switzerland	N/A	Hawksworth (1985)
K. submersa	Unidentified decaying wood	Freshwater	Asexual	Sporidesmium-like	China	A	Su et al. (2016)
K. tectonae	*Microcos paniculata*, *Tectona grandis*	Terrestrial	Asexual	Sporidesmium-like	Thailand	A	Li et al. (2016); de Farias et al. (2024)
K. thailandica	*Ficus microcarpa*	Terrestrial	Asexual	Sporidesmium-like	Thailand	A	Sun et al. (2021)
K. thujina	*Abies balsamea*, *Thuja occidentalis*	Terrestrial	Sexual	N/A	Canada, USA	A	Saccardo (1882); Hawksworth (1985)
K. umbrinoidea	*Aesculus hippocastanum*	Terrestrial	Sexual	N/A	Italy	N/A	Passerini (1887); Wang et al. (2004)
K. vinigena	Cork stopper, sparkling wine	N/A	Asexual	Dendryphiopsis-like	Spain	A	Rodríguez-Andrade et al. (2020)
K. xera	*Prunus* sp.	Terrestrial	Sexual	N/A	USA	N/A	Fairman (1910); Wang et al. (2004)
K. xishuangbannaensis	*Hevea brasiliensis*	Terrestrial	Asexual	Sporidesmium-like	China	A	Xu et al. (2023)
K. zizyphifolii	*Nayariophyton zizyphifolium*	Terrestrial	Sexual and asexual	Dendryphiopsis-like	Thailand	A	de Farias et al. (2024)

N/A: data not available; **A**: data available.

From a morphological perspective, the sporidesmium-like species are more diverse compared to the dendryphiopsis-like taxa. Interspecies differences are mainly attributed to the number and size of the conidiophores, conidiogenous cells and septa in the conidia. However, relying only on these features for species delineation is challenging and insufficient. Prior to the incorporation of molecular data, the taxonomy of *Kirschsteiniothelia* was challenging, resulting in controversial classifications. This genus was initially accommodated in Pleosporaceae by Hawksworth (1985) and Barr (1987), but later transferred to Pleomassariaceae by Barr (1993), based on morphological data. Based on molecular data, Schoch et al. (2006) suggested that *Kirschsteiniothelia* does not belong to any family within Pleosporales, but would rather be in a new family. Subsequently, Boonmee et al. (2012) introduced Kirschsteiniotheliaceae to accommodate *Kirschsteiniothelia* species, based on morphology and phylogenetic analyses. Hernández-Restrepo et al. (2017) established a novel order, Kirschsteiniotheliales, to accommodate the Kirschsteiniotheliaceae taxa. Subsequent studies have followed this classification, using ITS, LSU and SSU rDNA sequence data in their phylogenies (Sun et al. 2021; Xu et al. 2023; de Farias et al. 2024).

At present, most studies use LSU, ITS and SSU rDNA genes for inferring phylogeny relationships amongst *Kirschsteiniothelia* species. Despite close morphological similarities and overlap amongst species, we noted that there are rather unexpected sequence dissimilarities across the different genes analysed here. We presume that, despite high morphological similarities, these asexual species are characterised by high genetic diversity. This difference in genetic trait presumably enables them to adapt and flourish in different environments, gives them better chances of survival and drives speciation. So far, the ITS, LSU and SSU rDNA genes have most commonly been used to identify species within this genus, but as the number of species increases, we recommend incorporating protein genes like *tub*, *tef1-α* and *rpb2* (Badotti et al. 2017).

Acknowledgements

The author would like to express gratitude to Shaun Pennycook for his valuable suggestions on naming the new fungus. Xia Tang also wishes to thank Mae Fah Luang University for the Thesis Writing Grant and for awarding me a tuition scholarship for my Ph.D. studies at Mae Fah Luang University, Thailand. Rajesh Jeewon thanks the University of Mauritius in Reduit, Mauritius.

Additional information

Conflict of interest

The authors have declared that no competing interests exist.

Ethical statement

No ethical statement was reported.

Funding

This research was supported by grants from the National Natural Science Foundation of China (NSFC Grants Nos. 32170019 & 31670027 & 31460011) and the Open Fund Program of Engineering Research Centre of Southwest Bio-Pharmaceutical Resources,

Ministry of Education, Guizhou University (No. GZUKEY20160702) and the Thailand Research Fund grant "Impact of climate change on fungal diversity and biogeography in the Greater Mekong Sub-region" (RDG6130001). K.D Hyde and Fatimah Al-Otibi were funded by the Distinguished Scientist Fellowship Program (DSFP), King Saud University, Kingdom of Saudi Arabia.

Author contributions

Xia Tang conducted the experiments, analysed the data, and wrote the first draft of the manuscript. Rajesh Jeewon, Yong-Zhong Lu, Ruvishika S. Jayawardena, Kevin D. Hyde and Ji-Chuan Kang planned the experiments. Xia Tang, Deecksha Gomdola and Rong-Ju Xu analysed the data. Xia Tang conducted the experiments. Rajesh Jeewon, Deecksha Gomdola, Yong-Zhong Lu, Ruvishika S. Jayawardena, Fatimah Alotibi, Abdulwahed Fahad Alrefaei, Kevin D. Hyde and Ji-Chuan Kang corrected and revised the manuscript. Kevin D. Hyde and Ji-Chuan Kang funded the experiments. All authors revised and agreed to the published version of the manuscript.

Author ORCIDs

Xia Tang https://orcid.org/0000-0003-2705-604X
Rajesh Jeewon https://orcid.org/0000-0002-8563-957X
Ruvishika S. Jayawardena https://orcid.org/0000-0001-7702-4885
Deecksha Gomdola https://orcid.org/0000-0002-0817-1555
Yong-Zhong Lu https://orcid.org/0000-0002-1033-5782
Rong-Ju Xu https://orcid.org/0000-0002-3968-8442
Abdulwahed Fahad Alrefaei https://orcid.org/0000-0002-3761-6656
Fatimah Alotibi https://orcid.org/0000-0003-3629-5755
Kevin D. Hyde https://orcid.org/0000-0002-2191-0762
Ji-Chuan Kang https://orcid.org/0000-0002-6294-5793

Data availability

All the data that support the findings of this study are available in the main text. DNA sequences generated have been submitted to GenBank.

References

Aptroot A (1995) Redisposition of some species excluded from *Didymosphaeria* (Ascomycotina). Nova Hedwigia 60: 325–379.

Aptroot A (1997) *Corticolous pyrenocarpous* ascomycetes (lichenized and non-lichenized) from the Sonoran Desert (Arizona and Mexico). Nova Hedwigia 64(1–2): 169–176. https://doi.org/10.1127/nova.hedwigia/64/1997/169

Badotti F, de Oliveira FS, Garcia CF, Vaz ABM, Fonseca PLC, Nahum LA, Oliveira G, Góes-Neto A (2017) Effectiveness of ITS and sub-regions as DNA barcode markers for the identification of Basidiomycota (Fungi). BMC Microbiology 17(1): 1–12. https://doi.org/10.1186/s12866-017-0958-x

Bao DF, Luo ZL, Liu JK, Bhat DJ, Sarunya N, Li WL, Su HY, Hyde KD (2018) Lignicolous freshwater fungi in China III: New species and record of *Kirschsteiniothelia* from northwestern Yunnan Province. Mycosphere: Journal of Fungal Biology 9(4): 755–768. https://doi.org/10.5943/mycosphere/9/4/4

Barr ME (1987) Prodomus to class Loculoascomycetes. Publ. by the author, Amherst.

Barr ME (1993) Notes on the Pleomassariaceae. Mycotaxon 49: 129–142. https://doi.org/10.1001/archderm.1993.01680230018001

Barr ME, Rogerson CT, Smith SJ, Haines JH (1986) An annotated catalog of the pyrenomycetes described by Charles H. Bulletin – New York State Museum 459: 1–74. https://doi.org/10.5962/bhl.title.135547

Berkeley MJ (1875) Notices of North American fungi. Grevillea 3: 97–112.

Bhunjun CS, Niskanen T, Suwannarach N, Wannathes N, Chen YJ, McKenzie EH, Maharachchikumbura SSN, Buyck B, Zhao CL, Fan YG, Zhang JY, Dissanayake AJ, Marasinghe DS, Jayawardena RS, Kumla J, Padamsee M, Chen YY, Liimatainen K, Ammirati JF, Phukhamsakda C, Liu JK, Phonrob W, Randrianjohany É, Hongsanan S, Cheewangkoon R, Bundhun D, Khuna S, Yu WJ, Deng LS, Lu YZ, Hyde KD, Lumyong S (2022) The numbers of fungi: Are the most speciose genera truly diverse? Fungal Diversity 114(1): 387–462. https://doi.org/10.1007/s13225-022-00501-4

Boonmee S, Ko TWK, Chukeatirote E, Hyde KD, Chen H, Cai L, McKenzie EHC, Jones EBG, Kodsueb R, Hassan BA (2012) Two new *Kirschsteiniothelia* species with *Dendryphiopsis* anamorphs cluster in Kirschsteiniotheliaceae fam. nov. Mycologia 104(3): 698–714. https://doi.org/10.3852/11-089

Cannon PF, Hawksworth DL, Sherwood-Pike MA (1985) The British Ascomycotina. An Annotated Checklist. Commonwealth Mycological Institute, Kew, Surrey, England, 302.

Capella-Gutiérrez S, Silla-Martínez JM, Gabaldón T (2009) trimAl: A tool for automated alignment trimming in large-scale phylogenetic analyses. Bioinformatics (Oxford, England) 25(15): 1972–1973. https://doi.org/10.1093/bioinformatics/btp348

Chen CY, Wang CL, Huang JW (2006) Two new species of *Kirschsteiniothelia* from Taiwan. Mycotaxon 98: 153–158.

Chlebicki A, Chmiel MA (2006) Microfungi of *Carpinus betulus* from Poland I. Annotated list of microfungi. Acta Mycologica 41(2): 253–278. https://doi.org/10.5586/am.2006.027

Conners IL (1967) An Annotated Index of Plant Diseases in Canada and Fungi Recorded on Plants in Alaska, Canada and Greenland. Publ. Res. Br. Canada Dept Agric 1251: 1–381.

Cooke WB (1985) Fungi of Lassen Volcanic National Park. Cooperative National Park Resources Studies Unit, University of California at Davis, Institute of Ecology 21: 251.

Cooke MC, Ellis JB (1876) New Jersey fungi (cont.). Grevillea 5(34): 49–55.

Cubeta MA, Echandi E, Abernethy T, Vilgalys R (1991) Characterization of anastomosis groups of binucleate *Rhizoctonia* species using restriction analysis of an amplified ribosomal RNA gene. Phytopathology 81(11): 1395–1400. https://doi.org/10.1094/Phyto-81-1395

Daniel GP, Daniel GB, Miguel RJ, Florentino FR, David P (2010) ALTER: Program-oriented conversion of DNA and protein alignments. Nucleic Acids Research 38: W14–W18. https://doi.org/10.1093/nar/gkq321

de Farias ARG, Afshari N, Silva VSH, Louangphan J, Karimi O, Boonmee S (2024) Three novel species and new records of *Kirschsteiniothelia* (Kirschsteiniotheliales) from northern Thailand. MycoKeys 101: 347.

Ellis MB (1976) More dematiaceous hyphomycetes. Commonwealth Mycological Institute, Kew, Surrey. https://doi.org/10.1079/9780851983653.0000

Eriksson OE (1992) The non-lichenized pyrenomycetes of Sweden. Btjtryck, Lund, Sweden 208.

Eriksson OE (2014) Checklist of the non-lichenized ascomycetes of Sweden. Acta Universitatis Upsaliensis 36: 499.

Fairman CE (1905) New or rare Pyrenomycetaceae from western New York. Proceedings of the Rochester Academy of Science 4: 215–224.

Fairman CE (1910) Fungi Lyndonville nses novi vel minus cogniti. Annales Mycologici 8(3): 322–332.

Fungal names (2024) The Fungal names database. https://nmdc.cn/fungalnames/ [Accessed May 24, 2024]

Ginns JH (1986) Compendium of plant disease and decay fungi in Canada 1960–1980. Research Branch, Agriculture Canada 1813: 416. https://doi.org/10.5962/bhl.title.58888

Greene EL (1901) Plantae Bakerianae. Catholic University of America 1(1): 1–53. https://doi.org/10.5962/bhl.title.24815

Hawksworth DL (1985) *Kirschsteiniothelia*, a new genus for the *Microthelia incrustans*-group (Dothideales). Botanical Journal of the Linnean Society 91(1–2): 181–202. https://doi.org/10.1111/j.1095-8339.1985.tb01144.x

Hernández-Restrepo M, Gené J, Castañeda-Ruiz RF, Mena-Portales J, Crous PW, Guarro J (2017) Phylogeny of saprobic microfungi from Southern Europe. Studies in Mycology 86: 53–97. https://doi.org/10.1016/j.simyco.2017.05.002

Huelsenbeck JP, Ronquist F (2001) MRBAYES: Bayesian inference of phylogenetic trees. Bioinformatics (Oxford, England) 17(8): 754–589. https://doi.org/10.1093/bioinformatics/17.8.754

Hughes SJ (1958) Revisiones hyphomycetum aliquot cum appendice de nominibus rejiciendis. Canadian Journal of Botany 36(6): 727–836. https://doi.org/10.1139/b58-067

Hughes SJ (1978) New Zealand Fungi. 25. Miscellaneous species. New Zealand Journal of Botany 16(3): 311–370. https://doi.org/10.1080/0028825X.1978.10425143

Hyde KD (1993) Fungi from palms. II. *Kirschsteiniothelia aethiops* from the date palm, *Phoenix dactylifera*. Sydowia 45: 1–4.

Hyde KD, McKenzie EHC, Koko TW (2011) Towards incorporating anamorphic fungi in a natural classification – checklist and notes for 2010. Mycosphere 2(1): 1–88.

Hyde KD, Jones G, Liu JK, Ariyawansa H, Boehm E, Boonmee S, Braun U, Chomnunti P, Crous PW, Dai DQ, Diederich P, Dissanayake A, Doilom M, Doveri F, Hongsanan S, Jayawardena R, Lawrey JD, Li YM, Liu YX, Lücking R, Monkai J, Muggia L, Nelsen MP, Pang KL, Phookamsak R, Senanayake IC, Shearer CA, Suetrong S, Tanaka K, Thambugala KM, Wijayawardene NN, Wikee S, Wu HX, Zhang Y, Aguirre-Hudson B, Alias SA, Aptroot A, Bahkali AH, Bezerra JL, Bhat DJ, Camporesi E, Chukeatirote E, Gueidan C, Hawksworth DL, Hirayama K, Hoog SD, Kang JC, Knudsen K, Li WJ, Li XH, Liu ZY, Mapook A, McKenzie EHC, Miller AN, Mortimer PE, Phillips AJL, Raja HA, Scheuer C, Schumm F, Taylor JE, Tian Q, Tibpromma S, Wanasinghe DN, Wang Y, Xu JC, Yacharoen S, Yan JY, Zhang M (2013) Families of Dothideomycetes. Fungal Diversity 63(1): 1–313. https://doi.org/10.1007/s13225-013-0263-4

Hyde KD, Chaiwan N, Norphanphoun C, Boonmee S, Camporesi E, Chethana KWT, Dayarathne MC, de Silva NI, Dissanayake AJ, Ekanayaka AH, Hongsanan S, Huang SK, Jayasiri SC, Jayawardena RS, Jiang HB, Karunarathna A, Lin CG, Liu JK, Liu NG, Lu YZ, Luo ZL, Maharachchimbura SSN, Manawasinghe IS, Pem D, Perera RH, Phukhamsakda C, Samarakoon MC, Senwanna C, Shang QJ, Tennakoon DS, Thambugala KM, Tibpromma S, Wanasinghe DN, Xiao YP, Yang J, Zeng XY, Zhang JF, Zhang SN, Bulgakov TS, Bhat DJ, Cheewangkoon R, Goh TK, Jones EBG, Kang JC, Jeewon R, Liu

ZY, Lumyong S, Kuo CH, McKenzie EHC, Wen TC, Yan JY, Zhao Q (2018) Mycosphere notes 169–224. Mycosphere: Journal of Fungal Biology 9(2): 271–430. https://doi.org/10.5943/mycosphere/9/2/8

Hyde KD, Norphanphoun C, Ma J, Yang HD, Zhang JY, Du TY, Gao Y, Gomes de Farias AR, Gui H, He SC, He YK, Li CJY, Liu XF, Lu L, Su HL, Tang X, Tian XG, Wang SY, Wei DP, Xu RF, Xu RJ, Yang Q, Yang YY, Zhang F, Zhang Q, Bahkali AH, Boonmee S, Chethana KWT, Jayawardena RS, Lu YZ, Karunarathna SC, Tibpromma S, Wang Y, Zhao Q (2023) Mycosphere notes 387–412 – novel species of fungal taxa from around the world. Mycosphere: Journal of Fungal Biology 14(1): 663–744. https://doi.org/10.5943/mycosphere/14/1/8

Jayasiri SC, Hyde KD, Ariyawansa HA, Bhat J, Buyck B, Cai L, Dai YC, Abd-Elsalam KA, Ertz D, Hidayat I, Jeewon R, Jones EBG, Bahkali AH, Karunarathna SC, Liu JK, Luangsa-ard JJ, Lumbsch HT, Maharachchikumbura SSN, McKenzie EHC, Moncalvo JM, Ghobad-Nejhad M, Nilsson H, Pang KL, Pereira OL, Phillips AJL, Raspé O, Rollins AW, Romero AI, Etayo J, Selçuk F, Stephenson SL, Suetrong S, Taylor JE, Tsui CKM, Vizzini A, Abdel-Wahab MA, Wen TC, Boonmee S, Dai DQ, Daranagama DA, Dissanayake AJ, Ekanayaka AH, Fryar SC, Hongsanan S, Jayawardena RS, Li WJ, Perera RH, Phookamsak R, de Silva NI, Thambugala KM, Tian Q, Wijayawardene NN, Zhao RL, Zhao Q, Kang JC, Promputtha I (2015) The Faces of Fungi database: Fungal names linked with morphology, phylogeny and human impacts. Fungal Diversity 74(1): 3–18. https://doi.org/10.1007/s13225-015-0351-8

Jayawardena RS, Hyde KD, Wang S, Sun YR, Suwannarach N, Sysouphanthong P, Abdel-Wahab MA, Abdel-Aziz FA, Abeywickrama PD, Abreu VP, Armand A, Aptroot A, Bao DF, Begerow D, Bellanger JM, Bezerra JDP, Bundhun D, Calabon MS, Cao T, Cantillo T, Carvalho JLVR, Chaiwan N, Chen CC, Courtecuisse R, Cui BK, Damm U, Denchev CM, Denchev TT, Deng CY, Devadatha B, de Silva NI, Santos LA, Dubey NK, Dumez S, Ferdinandez HS, Firmino AL, Gafforov Y, Gajanayake AJ, Gomdola D, Gunaseelan S, He SC, Htet ZH, Kaliyaperumal M, Kemler M, Kezo K, Kularathnage ND, Leonardi M, Li JP, Liao CF, Liu S, Loizides M, Luangharn T, Ma J, Madrid H, Mahadevakumar S, Maharachchikumbura SSN, Manamgoda DS, Martín MP, Mekala N, Moreau P-A, Mu YH, Pahoua P, Pem D, Pereira OL, Phonrob W, Phukhamsakda C, Raza M, Ren GC, Rinaldi AC, Rossi W, Samarakoon BC, Samarakoon MC, Sarma VV, Senanayake IC, Singh A, Souza MF, Souza-Motta CM, Spielmann AA, Su WX, Tang X, Tian XG, Thambugala KM, Thongklang N, Tennakoon DS, Wannathes N, Wei DP, Welti S, Wijesinghe SN, Yang HD, Yang YH, Yuan HS, Zhang H, Zhang JY, Balasuriya A, Bhunjun CS, Bulgakov TS, Cai L, Camporesi E, Chomnunti P, Deepika YS, Doilom M, Duan WJ, Han SL, Huanraluek N, Gareth Jones EB, Lakshmidevi N, Li Y, Lumyong S, Luo ZL, Khuna S, Kumla J, Manawasinghe IS, Mapook A, Punyaboon W, Tibpromma S, Lu YZ, Yan JY, Wang Y (2022) Fungal diversity notes 1512–1610: Taxonomic and phylogenetic contributions on genera and species of fungal taxa. Fungal Diversity 117(1): 1–272. https://doi.org/10.1007/s13225-022-00513-0

Jeewon R, Hyde KD (2016) Establishing species boundaries and new taxa among fungi: Recommendations to resolve taxonomic ambiguities. Mycosphere: Journal of Fungal Biology 7(11): 1669–1677. https://doi.org/10.5943/mycosphere/7/11/4

Jin Y, Chen Y, Tian W, Liu JK, Maharachchikumbura SS (2024) Two novel species of *Kirschsteiniothelia* from Sichuan Province, China. Phytotaxa 664(2): 98–110. https://doi.org/10.11646/phytotaxa.664.2.2

Katoh K, Rozewicki J, Yamada KD (2017) MAFFT online service: Multiple sequence alignment, interactive sequence choice and visualization. Briefings in Bioinformatics 20(4): 1160–1166. https://doi.org/10.1093/bib/bbx108

Kobayashi T (2007) Index of fungi inhabiting woody plants in Japan. Host, Distribution and Literature. Index of Fungi Inhabiting Woody Plants in Japan: Host, Distribution and Liter.

Li GJ, Hyde KD, Zhao RL, Hongsanan S, Abdel-Aziz FA, Abdel-Wahab MA, Alvarado P, Alves-Silva G, Ammirati JF, Ariyawansa HA, Baghela A, Bahkali AH, Beug M, Bhat DJ, Bojantchev D, Boonpratuang T, Bulgakov TS, Camporesi E, Boro MC, Ceska O, Chakraborty D, Chen JJ, Chethana KWT, Chomnunti P, Consiglio G, Cui BK, Dai DQ, Dai YC, Daranagama DA, Das K, Dayarathne MC, De Crop E, De Oliveira RJV, de Souza CAF, de Souza JI, Dentinger BTM, Dissanayake AJ, Doilom M, Drechsler-Santos ER, Ghobad-Nejhad M, Gilmore SP, Góes-Neto A, Gorczak M, Haitjema CH, Hapuarachchi KK, Hashimoto A, He MQ, Henske JK, Hirayama K, Iribarren MJ, Jayasiri SC, Jayawardena RS, Jeon SJ, Jerônimo GH, Jesus AL, Jones EBG, Kang JC, Karunarathna SC, Kirk PM, Konta S, Kuhnert E, Langer E, Lee HS, Lee HB, Li WJ, Li XH, Liimatainen K, Lima DX, Lin CG, Liu JK, Liu XZ, Liu ZY, Luangsa-ard JJ, Lücking R, Lumbsch HT, Lumyong S, Leaño EM, Marano AV, Matsumura M, McKenzie EHC, Mongkolsamrit S, Mortimer PE, Nguyen TTT, Niskanen T, Norphanphoun C, O'Malley MA, Parnmen S, Pawłowska J, Perera RH, Phookamsak R, Phukhamsakda C, Pires-Zottarelli CLA, Raspé O, Reck MA, Rocha SCO, de Santiago ALCMA, Senanayake IC, Setti L, Shang QJ, Singh SK, Sir EB, Solomon KV, Song J, Srikitikulchai P, Stadler M, Suetrong S, Takahashi H, Takahashi T, Tanaka K, Tang LP, Thambugala KM, Thanakitpipattana D, Theodorou MK, Thongbai B, Thummarukcharoen T, Tian Q, Tibpromma S, Verbeken A, Vizzini A, Vlasák J, Voigt K, Wanasinghe DN, Wang Y, Weerakoon G, Wen HA, Wen TC, Wijayawardene NN, Wongkanoun S, Wrzosek M, Xiao YP, Xu JC, Yan JY, Yang J, Da Yang S, Hu Y, Zhang JF, Zhao J, Zhou LW, Peršoh D, Phillips AJL, Maharachchikumbura SSN (2016) Fungal diversity notes 253–366: Taxonomic and phylogenetic contributions to fungal taxa. Fungal Diversity 78(1): 1–237. https://doi.org/10.1007/s13225-016-0366-9

Liu L, Yang J, Zhou S, Gu X, Gou J, Wei Q, Zhang M, Liu Z (2023a) Novelties in Microthyriaceae (Microthyriales): Two new asexual genera with three new species from freshwater habitats in Guizhou Province, China. Journal of Fungi (Basel, Switzerland) 9(2): 178. https://doi.org/10.3390/jof9020178

Liu JW, Hu YF, Luo XX, Castañeda-Ruíz RF, Xia JW, Xu ZH, Cui RQ, Shi XG, Zhang LH, Ma J (2023b) Molecular phylogeny and morphology reveal four novel species of *Corynespora* and *Kirschsteiniothelia* (Dothideomycetes, Ascomycota) from China: A Checklist for *Corynespora* Reported Worldwide. Journal of Fungi (Basel, Switzerland) 9(1): 107. https://doi.org/10.3390/jof9010107

Louangphan J, Perera RH, De Farias ARG (2024) A new addition to Kirschsteiniotheliaceae: *Kirschsteiniothelia chiangmaiensis* sp. nov. from Northern Thailand. Phytotaxa 634(1): 49–62. https://doi.org/10.11646/phytotaxa.634.1.4

Maharachchikumbura SSN, Chen Y, Ariyawansa HA, Hyde KD, Haelewaters D, Perera RH, Samarakoon MC, Wanasinghe DN, Bustamante DE, Liu J, Lawrence DP, Cheewangkoon R, Stadler M (2021) Integrative approaches for species delimitation in Ascomycota. Fungal Diversity 109(1): 155–179. https://doi.org/10.1007/s13225-021-00486-6

Marincowitz S, Crous PW, Groenewald JZ, Wingfield MJ (2008) Microfungi occurring on the Proteaceae in the fynbos. CBS Biodiversity Series 7: 1–166.

Matsushima T (1971) Microfungi of the Solomon Islands and Papua-New Guinea. Nippon Printing Pub-lishing Co., Osaka 78.

Matsushima T (1975) Icones Microfungorum a Matsushima Lectorum. Nippon Printing Publishing Co., Osaka.

McKenzie EHC, Buchanan PK, Johnston PR (2000) Checklist of fungi on *Nothofagus* species in New Zealand. New Zealand Journal of Botany 38(4): 635–720. https://doi.org/10.1080/0028825X.2000.9512711

McKenzie EHC, Buchanan PK, Johnston PR (2004) Checklist of fungi on nikau palm (*Rhopalostylis sapida* and *R. baueri* var. *chessemanii*) in New Zealand. New Zealand Journal of Botany 42(2): 335–355. https://doi.org/10.1080/0028825X.2004.9512908

Mehrabi M, Hemmati R, Asgari B (2017) *Kirschsteiniothelia arasbaranica* sp. nov., and an emendation of the Kirschsteiniotheliaceae. Cryptogamie. Mycologie 38(1): 13–25. https://doi.org/10.7872/crym/v38.iss1.2017.13

Meng QF, Thiyagaraja V, Worthy FR, Ertz D, Wang XY, Jayawardena RS, Fu SB, Saichana N (2024) Morphological and phylogenetic appraisal of a new *Kirschsteiniothelia* (Dothideomycetes, Kirschsteiniotheliales) species from Yunnan Province, China. Phytotaxa 661(3): 267–281. https://doi.org/10.11646/phytotaxa.661.3.4

Miller MA, Pfeiffer W, Schwartz T (2010) Creating the CIPRES Science Gateway for inference of large phylogenetic trees. 2010 Gateway Computing Environments Workshop (GCE). Institute of Electrical and Electronics Engineers, New Orleans, LA 1–8. https://doi.org/10.1109/GCE.2010.5676129

Minter DW, Rodriguez Hernandez M, Mena Portales J (2001) Fungi of the Caribbean: an annotated checklist. PDMS Publishing 946.

Morgan-Jones G, Sinclair RC, Eicker A (1983) Notes on Hyphomycetes. XLIV. New and rare Dematiaceous species from the Transvaal. Mycotaxon 17: 301–316.

Mulenko W, Majewski T, Ruszkiewicz-Michalska M (2008) A preliminary checklist of Micromycetes in Poland. W. Szafer Institute of Botany, Polish Academy of Sciences 9: 752.

Nattrass RM (1961) Host lists of Kenya fungi and bacteria. Mycological Papers 81: 1–46.

Nishi M, Okano I, Sawada T, Hara Y, Nakamura K, Inagaki K, Yaguchi T (2018) Chronic *Kirschsteiniothelia* infection superimposed on a pre-existing non-infectious bursitis of the ankle: The first case report of human infection. BMC Infectious Diseases 18(1): 1–5. https://doi.org/10.1186/s12879-018-3152-3

Nordén B, Appelquist T, Barck L, Löhmus M (1997) An ecological field study of wood living pyrenomycetes in a Swedish hardwood forest. Windahlia 22: 57–64.

Passerini G (1887) Diagnosi di funghi nuovi. Nota II. Atti della Reale Accademia dei Lincei. Rendiconti di classe di Scienze Fisiche, Matematiche e Naturale. Ser. 4 3(1): 89–95.

Pem D, Jeewon R, Chethana KWT, Hongsanan S, Doilom M, Suwannarach N, Hyde KD (2021) Species concepts of Dothideomycetes: Classification, phylogenetic inconsistencies and taxonomic standardization. Fungal Diversity 109(1): 283–319. https://doi.org/10.1007/s13225-021-00485-7

Popov ES, Shabunin DA, Melnik VA (2008) Contributions to the studies of mycobiota in Novgorod and Pskov Regions. Mikologiya i Fitopatologiya 42: 137–151.

Pratibha J, Raghukumar S, Bhat DJ (2010) New species of *Dendryphiopsis* and *Stauriella* from Goa, India. Mycotaxon 113(1): 297–303. https://doi.org/10.5248/113.297

Rao V, Varghese KI (1981) Some new or interesting Hyphomycetes from India. Proc. Natl. Acad. Sci. India B 51: 240–243.

Raymundo T, Valenzuela R, Martínez-González CR, García-Jiménez J, Cobos-Villagrán A, Sánchez-Flores M, de la Fuente J, Martínez-Pineda M, Pérez-Valdespino A, Ramírez-Martínez JC, Luna-Vega I (2023) New Ascomycetes from the Mexican Tropical Montane Cloud Forest. Journal of Fungi (Basel, Switzerland) 9(9): 933. https://doi.org/10.3390/jof9090933

Réblová M, Svrcek M (1997) New records of Pyrenomycetes from the Czech Republic I. Czech Mycology 49(3–4): 193–206. https://doi.org/10.33585/cmy.49305

Rodríguez-Andrade E, Stchigel AM, Guarro J, Cano-Lira JF (2020) Fungal Diversity of Deteriorated Sparkling Wine and Cork Stoppers in Catalonia, Spain. Microorganisms 8(1, no. 12): 1–29. https://doi.org/10.3390/microorganisms8010012

Ronquist F, Teslenko M, Van Der Mark P, Ayres DL, Darling A, Höhna S, Larget B, Liu L, Suchard MA, Huelsenbeck JP (2012) MrBayes 3.2: Efficient Bayesian Phylogenetic Inference and model choice across a large model space. Systematic Biology 61(3): 539–542. https://doi.org/10.1093/sysbio/sys029

Rossman AY, Crous PW, Hyde KD, Hawksworth DL, Aptroot A, Bezerra JL, Bhat JD, Boehm E, Braun U, Boonmee S, Camporesi E, Chomnunti P, Dai DQ, D'souza MJ, Dissanayake A, Jones EBG, Groenewald JZ, Hernández-Restrepo M, Hongsanan S, Jaklitsch WM, Jayawardena RS, Jing LW, Kirk PM, Lawrey JD, Mapook A, McKenzie EHC, Monkai J, Phillips AJL, Phookamsak R, Raja HA, Seifert KA, Senanayake I, Slippers B, Suetrong S, Tanaka K, Taylor JE, Thambugala KM, Tian Q, Tibpromma S, Wanasinghe DN, Wijayawardene NN, Wikee S, Woudenberg JHC, Wu HX, Yan JY, Yang T, Zhang Y (2015) Recommended names for pleomorphic genera in Dothideomycetes. IMA Fungus 6(2): 507–523. https://doi.org/10.5598/imafungus.2015.06.02.14

Saccardo PA (1882) Sylloge Pyrenomycetum, Vol. I. Sylloge Fungorum 1: 1–768.

Schmid-Heckel H (1988) Pilze in den Berchtesgadener Alpen. Forschungsberichte Nationalpark Berchtes-gaden 15: 1–136.

Schoch CL, Shoemaker RA, Seifert KA, Hambleton S, Spatafora JW, Crous PW (2006) A multigene phylogeny of the Dothideomycetes using four nuclear loci. Mycologia 98(6): 1041–1052. https://doi.org/10.1080/15572536.2006.11832632

Senanayake IC, Rathnayaka AR, Marasinghe DS, Calabon MS, Gentekaki E, Lee HB, Hurdeal VG, Pem D, Dissanayake LS, Wijesinghe SN, Bundhun D, Nguyen TT, Goonasekara ID, Abeywickrama PD, Bhunjun CS, Jayawardena RS, Wanasinghe DN, Jeewon R, Bhat DJ, Xiang MM (2020) Morphological approaches in studying fungi: Collection, examination, isolation, sporulation and preservation. Mycosphere: Journal of Fungal Biology 11(1): 2678–2754. https://doi.org/10.5943/mycosphere/11/1/20

Senanayake C, Rossi W, Leonardi M, Weir A, McHugh MC, Rajeshkumar K, Verma RK, Karunarathna SC, Tibpromma S, Ashtekar N, Ashtamoorthy SK, Raveendran S, Kour G, Singh A, De la Peña-Lastra S, Mateos A, Kolařík M, Antonín V, Ševčíková H, Esteve-Raventós F, Larsson E, Pancorbo F, Moreno G, Altés A, Turégano Y, Du TY, Lu L, Li QR, Kang JC, Gunaseelan S, Kezo K, Kaliyaperumal M, Fu J, Samarakoon MC, Gafforov Y, Teshaboeva S, Kunjan PC, Chamaparambath A, Flakus A, Etayo J, Rodriguez-Flakus P, Zhurbenko MP, de Silva NI, Tennakoon DS, Latha KPD, Manimohan P, Raj KNA, Calabon MS, Ahmadpour A, Heidarian Z, Alavi Z, Alavi F, Ghosta Y, Azizi R, Luo M, Zhao M-P, Kularathnage ND, Hua L, Yang YH, Liao CF, Zhao H-J, Lestari AS, Jayasiri SC, Yu FM, Lei L, Liu JW, Karimi O, Tang SM, Sun YR, Wang Y, Zeng M, Htet ZH, Linaldeddu BT, Alves A, Phillips AJL, Bregant C, Montecchio L, De Kesel A, Hustad VP, Miller AN, Fedosova AG, Kučera V, Raza M, Hussain M, Chen YP, Thiyagaraja V, Gomdola D, Rathnayaka AR, Dissanayake AJ, Suwannarach N, Hongsanan S, Maharachchikumbura SSN, Dissanayake LS, Wijayawardene NN, Phookamsak R, Lumyong S, Jones EBG, Yapa N, Wanasinghe DN, Xie N, Doilom M, Manawasinghe IS, Liu JK, Zhao Q, Xu B, Hyde KD, Song J (2023) Fungal diversity notes 1611–1716: Taxonomic and phylogenetic contributions on fungal genera and species emphasis in south China. Fungal Diversity 122(1): 161–403. https://doi.org/10.1007/s13225-023-00523-6

Sieber TN, Kowalski T, Holdenrieder O (1995) Fungal assemblages in stem and twig lesions of *Quercus robur* in Switzerland. Mycological Research 99(5): 534–538. https://doi.org/10.1016/S0953-7562(09)80709-0

Sierra AM (1984) Hifomicetes Demaciaceos de Sierra del Rosario, Cuba. Editorial Academica, Havana 181.

Sruthi OP, Rajeshkumar KC, Gowrav SM, Ansil PA, Ashtamoorthy SK (2024) Morphological and phylogenetic evidence for recognition of a new species of *Kirschsteiniothelia*, *K. agumbensis* and validation of five new combinations in Kirschsteiniotheliaceae. Phytotaxa 649(2): 159–181. https://doi.org/10.11646/phytotaxa.649.2.2

Stamatakis A, Hoover P, Rougemont J (2008) A rapid bootstrap algorithm for the RAxML Web servers. Systematic Biology 57(5): 758–771. https://doi.org/10.1080/10635150802429642

Stevens FL (1925) Hawaiian fungi. Bulletin of the Bernice Bishop Museum 19: 1–189. https://doi.org/10.5962/bhl.title.58561

Su HY, Hyde KD, Maharachchikumbura SSN, Ariyawansa HA, Luo ZL, Promputtha I, Tian Q, Lin CG, Shang QJ, Zhao YC, Chai HM, Liu XY, Bahkali AH, Bhat JD, McKenzie EHC, Zhou DQ (2016) The families Distoseptisporaceae fam. nov., Kirschsteiniotheliaceae, Sporormiaceae and Torulaceae, with new species from freshwater in Yunnan Province, China. Fungal Diversity 80(1): 375–409. https://doi.org/10.1007/s13225-016-0362-0

Subramanian CV, Srivastava V (1994) Two new hyphomycetes from Kumaon Himalayas. Proceedings of the Indian National Sciences Academy 60: 167–171.

Sun YR, Jayawardena RS, Hyde KD, Wang Y (2021) *Kirschsteiniothelia thailandica* sp. nov. (Kirschsteiniotheliaceae) from Thailand. Phytotaxa 490(2): 172–182. https://doi.org/10.11646/phytotaxa.490.2.3

Sutton BC (1973) Hyphomycetes from Manitoba and Saskatchewan, Canada. Mycological Papers 132: 1–143.

Swofford DL (2002) PAUP*: Phylogenetic analysis using parsimony (and other methods), version 4.0 b10. MA: Sinauer Associates, Sunderland, UK.

Tang X, Jayawardena RS, Stephenson SL, Kang JC (2022) A new species *Pseudoplagiostoma dipterocarpicola* (Pseudoplagiostomataceae, Diaporthales) found in northern Thailand on members of the Dipterocarpaceae. Phytotaxa 543(4): 233–243. https://doi.org/10.11646/phytotaxa.543.4.3

Tang X, Jeewon R, Lu YZ, Alrefaei AF, Jayawardena RS, Xu RJ, Ma J, Chen XM, Kang JC (2023) Morphophylogenetic evidence reveals four new fungal species within Tetraplosphaeriaceae (Pleosporales, Ascomycota) from tropical and subtropical forest in China. MycoKeys 100: 171–204. https://doi.org/10.3897/mycokeys.100.113141

Tian WH, Jin Y, Liao YC, Faraj TK, Guo XY, Maharachchikumbura SS (2024) New and Interesting Pine-Associated Hyphomycetes from China. Journal of Fungi (Basel, Switzerland) 10(8): 546. https://doi.org/10.3390/jof10080546

Vaidya G, Lohman DJ, Meier R (2011) SequenceMatrix: Concatenation software for the fast assembly of multi-gene datasets with character set and codon information. Cladistics 27(2): 171–180. https://doi.org/10.1111/j.1096-0031.2010.00329.x

Verma RK, Prasher IB, Sushma, Gautam AK, Rajeshkumar KC, Castañeda-Ruiz RF (2021) *Kirschsteiniothelia shimlaensis* sp. nov. from Himachal Pradesh, India. Mycotaxon 136(2): 401–407. https://doi.org/10.5248/136.401

Vilgalys R, Hester M (1990) Rapid genetic identification and mapping of enzymatically amplified ribosomal DNA from several *Cryptococcus* species. Journal of Bacteriology 172(8): 4238–4246. https://doi.org/10.1128/jb.172.8.4238-4246.1990

Wang CJK (2010) Wood-Inhabiting Microfungi (Molds) of New York. Published by the author, Amherst MA, 238.

Wang YZ, He WH (2007) Notes on Amphisphaeria-like species in HMAS, with a new combination: *Phaeodothis hainanensis* (Pleosporales). Mycotaxon 100: 97–104.

Wang YZ, Aptroot A, Hyde KD (2004) Revision of the Ascomycete Genus *Amphisphaeria*. Fungal Diversity Research Series 13: 1–168.

Wang F, Wang K, Cai L, Zhao MJ, Kirk PM, Fan GM, Sun QL, Li B, Wang S, Yu ZF, Han D, Ma J, Wu L, Yao Y (2023) Fungal names: A comprehensive nomenclatural repository and knowledge base for fungal taxonomy. Nucleic Acids Research 51(D1): D708–D716. https://doi.org/10.1093/nar/gkac926

Wegelin H (1894) Beitrag zur Pyrenomycetenflora der Schweiz. Mitteilungen der Thurgaischen Naturforschenden Gesellschaft 11: 1–12. https://doi.org/10.1111/j.1438-8677.1894.tb04545.x

White TJ, Bruns T, Lee SJWT, Taylor J (1990) Amplification and direct sequencing of fungal ribosomal RNA genes for phylogenetics. PCR protocols: a guide to methods and applications 18: 315–322. https://doi.org/10.1016/B978-0-12-372180-8.50042-1

Wijayawardene NN, Crous PW, Kirk PM, Hawksworth DL, Boonmee S, Braun U, Dai DQ, D'souza MJ, Diederich P, Dissanayake A, Doilom M, Hongsanan S, Jones EBG, Groenewald JZ, Jayawardena R, Lawrey JD, Liu J-K, Luecking R, Madrid H, Manamgoda DS, Muggia L, Nelsen MP, Phookamsak R, Suetrong S, Tanaka K, Thambugala KM, Wanasinghe DN, Wikee S, Zhang Y, Aptroot A, Ariyawansa HA, Bahkali AH, Bhat DJ, Gueidan C, Chomnunti P, De Hoog GS, Knudsen K, Li W-J, McKenzie EHC, Miller AN, Phillips AJL, Piatek M, Raja HA, Shivas RS, Slippers B, Taylor JE, Tian Q, Wang Y, Woudenberg JHC, Cai L, Jaklitsch WM, Hyde KD (2014) Naming and outline of Dothideomycetes–2014 including proposals for the protection or suppression of generic names. Fungal Diversity 69(1): 1–55. https://doi.org/10.1007/s13225-014-0309-2

Xu RF, Phukhamsakda C, Dai DQ, Karunarathna SC, Tibpromma S (2023) *Kirschsteiniothelia xishuangbannaensis* sp. *nov*. from pará rubber (*Hevea brasiliensis*) in Yunnan, China. Current Research in Environmental & Applied Mycology 13(1): 34–56. https://doi.org/10.5943/cream/13/1/3

Yang J, Liu LL, Jones EG, Hyde KD, Liu ZY, Bao DF, Liu NG, Li WL, Sheng HW, Yu XD, Liu JK (2023) Freshwater fungi from karst landscapes in China and Thailand. Fungal Diversity 119(1): 1–212. https://doi.org/10.1007/s13225-023-00514-7

Zalamea M, González G, Lodge DJ (2016) Physical, chemical, and biological properties of soil under decaying wood in a tropical wet forest in Puerto Rico. Forests 7(8): 168. https://doi.org/10.3390/f7080168

Zhang YZ, Chen QL, Ma J, Lu YZ, Chen HB, Liu NG (2023) Morphological and multi-gene phylogenetic analyses reveal five new hyphomycetes from freshwater habitats. Frontiers in Microbiology 14: 1253239. https://doi.org/10.3389/fmicb.2023.1253239

MycoKeys 110: 67–92 (2024)
DOI: 10.3897/mycokeys.110.133108

Research Article

Morphological and molecular identification for four new wood-inhabiting species of *Lyomyces* (Basidiomycota) from China

Qi Yuan[1,2], Yunchao Li[2], Yunfei Dai[2], Kunyan Wang[2], Yixuan Wang[3], Changlin Zhao[1,2]

1 *The Key Laboratory of Forest Resources Conservation and Utilization in the Southwest Mountains of China Ministry of Education, Key Laboratory of National Forestry and Grassland Administration on Biodiversity Conservation in Southwest China, Yunnan Provincial Key Laboratory for Conservation and Utilization of In-forest Resource, Southwest Forestry University, Kunming 650224, China*
2 *College of Forestry, Southwest Forestry University, Kunming 650224, China*
3 *Yunnan Yunzhihuang Health Technology Co., LTD, Kunming 650224, China*
Corresponding author: Changlin Zhao (fungi@swfu.edu.cn)

Abstract

Fungi are one of the most diverse groups of organisms on Earth, in which the wood-inhabiting fungi play an important role in forest ecosystem processes and functions. Four new wood-inhabiting fungi, *Lyomyces hengduanensis*, *L. niveomarginatus*, *L. wumengshanensis* and *L. zhaotongensis*, are proposed, based on morphological features and molecular evidence. *Lyomyces hengduanensis* differs in the brittle basidiomata with pruinose hymenial surface, a monomitic hyphal system and ellipsoid basidiospores (3.5–6 × 3–4.5 µm). *Lyomyces niveomarginatus* is distinguished by the subceraceous basidiomata with crackled hymenial surface, a monomitic hyphal system and ellipsoid basidiospores (4.5–7 × 3–4 µm). *Lyomyces wumengshanensis* is distinguished by the grandinioid hymenial surface, a monomitic hyphal system and ellipsoid to broad ellipsoid basidiospores (4–6 × 3–5 µm). *Lyomyces zhaotongensis* is unique in the grandinioid hymenial surface, a monomitic hyphal system and broadly ellipsoid basidiospores measuring as 2.6–3.5 × 2.5–3 µm. Sequences of ITS and nLSU rRNA markers of the studied samples were generated and phylogenetic analyses were performed using the Maximum Likelihood, Maximum Parsimony and Bayesian Inference methods. The phylogram, based on the ITS+nLSU rDNA gene regions, included three genera within the Schizoporaceae viz. *Fasciodontia*, *Lyomyces* and *Xylodon*, in which the four new species were grouped into *Lyomyces*. The phylogenetic tree inferred from the ITS sequences highlighted that *L. hengduanensis* group with *L. zhaotongensis* and then closely grouped with *L. crustosus*, *L. ochraceoalbus*, and *L. vietnamensis*. The new taxon *L. niveomarginatus* was retrieved as a sister to *L. juniperi*. The new species *L. wumengshanensis* was sister to *L. macrosporus*. The new taxon *L. zhaotongensis* grouped with *L. hengduanensis* and then closely grouped with *L. crustosus*, *L. ochraceoalbus* and *L. vietnamensis*.

Key words: Biodiversity, phylogenetic analyses, taxonomy, Yunnan Province

This article is part of:
Exploring the Hidden Fungal Diversity: Biodiversity, Taxonomy, and Phylogeny of Saprobic Fungi
Edited by Samantha C. Karunarathna, Danushka Sandaruwan Tennakoon, Ajay Kumar Gautam

Academic editor:
Samantha C. Karunarathna
Received: 25 July 2024
Accepted: 15 October 2024
Published: 30 October 2024

Citation: Yuan Q, Li Y, Dai Y, Wang K, Wang Y, Zhao C (2024) Morphological and molecular identification for four new wood-inhabiting species of *Lyomyces* (Basidiomycota) from China. MycoKeys 110: 67–92. https://doi.org/10.3897/mycokeys.110.133108

Introduction

Fungi are one of the most diverse groups of organisms on Earth and play an indispensable role in the forest ecosystem processes and functioning (Hyde 2022; Guan et al. 2023; Deng et al. 2024a). The wood-inhabiting fungal family

Schizoporaceae Jülich includes many variations of the fruiting body types within the order Hymenochaetales Oberw. (Larsson et al. 2006; Wu et al. 2022a; Guan et al. 2023; Zhang et al. 2024) and it comprises a number of representative wood-inhabiting fungal taxa, including diverse hymenophoral morphologies as hydnoid, corticioid and polyporoid (Yurchenko and Wu 2016; Riebesehl and Langer 2017; Yurchenko et al. 2017; Cui et al. 2019; Riebesehl et al. 2019; Jiang et al. 2021; Wu et al. 2022a, 2022b; Guan et al. 2023; Deng et al. 2024a, b; Zhang et al. 2024). In addition, taxa of the family Schizoporaceae are widely found in different continents, causing white rot (Langer 1994; Luo et al. 2022; Guan et al. 2023; Zhang et al. 2024).

The genus *Lyomyces* P. Karst. is typified by *L. sambuci* (Pers.) P. Karst. It is characterised by the resupinate-to-effused basidiomata with a smooth-to-odontioid hymenophore, a monomitic hyphal system with generative hyphae bearing clamp connections, the presence of several types of cystidia and with smooth, thin- to slightly thick-walled basidiospores (Karsten 1881; Bernicchia and Gorjón 2010). Based on the MycoBank database (http://www.mycobank.org, accessed on 25 April 2024) and the Index Fungorum (http://www.indexfungorum.org, accessed on 25 April 2024), *Lyomyces* has 55 specific and infraspecific names registered, of which approximately 41 species of *Lyomyces* are currently known (Rabenhorst 1851; Karsten 1881; Karsten 1882; Cunningham 1959; Cunningham 1963; Wu 1990; Hjortstam and Ryvarden 2009; Xiong et al. 2009; Dai 2010; Dai 2011; Yurchenko and Wu 2013; Gafforov et al. 2017; Riebesehl and Langer 2017; Yurchenko et al. 2017; Chen and Zhao 2020; Yurchenko et al. 2020; Luo et al. 2021b; Luo et al. 2021c; Viner et al. 2022; Guan et al. 2023).

On the basis of the frequent inclusion of data from DNA sequences in many phylogenetic studies, the classification of the wood-inhabiting fungi has been updated continuously (Yurchenko et al. 2020). These pioneering research studies into the family Schizoporaceae were just the prelude to the molecular systematics period (Guan et al. 2023; Zhang et al. 2024). The genus *Hyphodontia* s.l. was indicated to be a polyphyletic group, in which the genera *Xylodon* (Pers.) Gray and *Kneiffiella* P. Karst. included the largest number of species (Yurchenko and Wu 2016; Riebesehl and Langer 2017; Riebesehl et al. 2019). Due to the lack of sequences of some wood-inhabiting fungal taxa, it is difficult to clearly distinguish many genera in this family Schizoporaceae using molecular data; therefore, a broad concept of *Hyphodontia* s.l. was accepted (Yurchenko and Wu 2016; Riebesehl and Langer 2017; Wang and Chen 2017; Riebesehl et al. 2019). Based on the nuclear DNA sequence data, six well-distinguished clades as *Hastodontia* clade, *Hyphodontia* clade, *Lagarobasidium* clade, *Kneiffiella-Alutaceodontia* clade, *Xylodon-Lyomyces-Rogersella* clade and *Xylodon-Schizopora-Palifer* clade, were included, based on the phylogenetical studies for *Hyphodontia* s.l., in which the genus *Lyomyces* was nested within the *Xylodon-Lyomyces-Rogersella* clade (Yurchenko and Wu 2013). The research revealed that *Hyphodontia* s.l. was divided into six genera, viz., *Hastodontia* (Parmasto) Hjortstam & Ryvarden, *Hyphodontia* J. Erikss., *Kneiffiella*, *Lagarobasidium* Jülich, *Lyomyces* and *Xylodon*, in which 35 new combinations were proposed, including fourteen *Lyomyces* species (Riebesehl and Langer 2017). On the basis of the sequences of the internal transcribed spacer (ITS) and the nuclear large subunit (nLSU) ribosomal DNA gene, the phylogenetic analysis clarified that the *Lyomyces sambuci* complex divided into four new

species (Yurchenko et al. 2017). Riebesehl et al. (2019) clarified the generic concept and their phylogenetic reconstruction of *Lyomyces* and the species *L. sambuci* was sister to *L. crustosus* (Pers.) P. Karst (Riebesehl et al. 2019). Based on a combination of the morphological and molecular evidence, the fungal diversity of the family Schizoporaceae was analysed, in which six new species were described: *L. fissuratus* C.L. Zhao, *L. fumosus* C.L. Zhao, *L. niveus* C.L. Zhao, *L. ochraceoalbus* C.L. Zhao, *L. albopulverulentus* C.L. Zhao and *L. yunnanensis* (Luo et al. 2021b, 2021c; Guan et al. 2023).

During the investigations of the wood-inhabiting fungi, we collected four new Hymenochaetales taxa from Yunnan Province, China, that could not be assigned to any described species of the order. We present the morphological characteristics and phylogenetic analyses with ITS and nLSU that support the four species in the genus *Lyomyces*.

Materials and methods

Morphology

Fresh basidiomata of the fungi growing on the angiosperm branch were collected from the Honghe, Lincang, Puer, Wenshan and Zhaotong of Yunnan Province, P.R. China after recording important information (Rathnayaka et al. 2024). Specimens were dried in an electric food dehydrator at 40 °C (Hu et al. 2022), then sealed and stored in an envelope bag and deposited in the Herbarium of the Southwest Forestry University (SWFC), Kunming, Yunnan Province, P.R. China. Macromorphological descriptions were based on field notes and photos were captured in the field and lab. Colour terminology follows Petersen (Petersen 1996). Micromorphological data were obtained from the dried specimens when observed under a light microscope following the previous study (Guan et al. 2023). The following abbreviations are used: KOH = 5% potassium hydroxide water solution, CB = Cotton Blue, CB– = acyanophilous, IKI = Melzer's Reagent, IKI– = both inamyloid and indextrinoid, L = mean spore length (arithmetic average for all spores), W = mean spore width (arithmetic average for all spores), Q = variation in the L/W ratios between the specimens studied and n = a/b (number of spores (a) measured from given number (b) of specimens).

Molecular phylogeny

The EZNA HP Fungal DNA Kit (Omega Biotechnologies Co., Ltd., Kunming, China) was used to extract DNA with some modifications from the dried specimens. The nuclear ribosomal ITS region was amplified with primers ITS5 and ITS4 (White et al. 1990). The PCR procedure for ITS was as follows: initial denaturation at 95 °C for 3 min, followed by 35 cycles at 94 °C for 40 s, 58 °C for 45 s and 72 °C for 1 min and a final extension of 72 °C for 10 min. The nuclear nLSU region was amplified with primer pair LR0R and LR7 (Rehner and Samuels 1994). The PCR procedure for nLSU was as follows: initial denaturation at 94 °C for 1 min, followed by 35 cycles at 94 °C for 30 s, 48 °C for 1 min and 72 °C for 1.5 min and a final extension of 72 °C for 10 min. The PCR procedure for ITS and nLSU followed the previous study (Zhao and Wu 2017). All newly-generated sequences were deposited in NCBI GenBank (https://www.ncbi.nlm.nih.gov/genbank/) (Table 1).

Table 1. List of species, specimens, and GenBank accession numbers of sequences used in this study.

Species name	Specimen No.	GenBank accession No.		References
		ITS	nLSU	
Fasciodontia brasiliensis	MSK-F 7245a	MK575201	MK598734	Yurchenko et al. (2020)
F. bugellensis	KAS-FD 10705a	MK575203	MK598735	Yurchenko et al. (2020)
F. bugellensis	MSK-F 7353	MK575205	MK598736	Yurchenko et al. (2020)
F. yunnanensis	CLZhao 6280	MK811275	MZ146327	Luo and Zhao (2021)
F. yunnanensis	CLZhao 6385	MK811277	—	Luo and Zhao (2021)
Hymenochaete ochromarginata	He 47	KU978861	JQ279666	Unpublished
H. rubiginosa	He 458	JQ279580	—	He and Li (2013)
Lyomyces albopulverulentus	CLZhao 21478	OP730712	OP730724	Guan et al. (2023)
L. allantosporus	KAS-GEL4933	KY800401	—	Yurchenko et al. (2017)
L. allantosporus	FR-0249548	KY800397	—	Yurchenko et al. (2017)
L. bambusinus	CLZhao 4831	MN945968	—	Chen and Zhao (2020)
L. bambusinus	CLZhao 4808	MN945970	—	Chen and Zhao (2020)
L. cremeus	CLZhao 4138	MN945974	—	Chen and Zhao (2020)
L. cremeus	CLZhao 8295	MN945972	—	Chen and Zhao (2020)
L. crustosus	TASM:YG G39	MF382993	—	Gafforov et al. (2017)
L. crustosus	UC2022841	KP814310	—	Unpublished
L. densiusculus	Ryvarden 44818	OK273853	—	Viner et al. (2022)
L. elaeidicola	LWZ20180411-20	MT319458	—	Wang et al. (2021)
L. elaeidicola	LWZ20180411-19	MT319457	—	Wang et al. (2021)
L. erastii	TASM:YG 022	MF382992	—	Gafforov et al. (2017)
L. erastii	23cSAMHYP	JX857800	—	Unpublished
L. fimbriatus	Wu910620-7	MK575209	—	Yurchenko et al. (2020)
L. fimbriatus	Wu911204-4	MK575210	—	Yurchenko et al. (2020)
L. fissuratus	CLZhao 4352	MW713742	—	Luo et al. (2021b)
L. fissuratus	CLZhao 4291	MW713738	—	Luo et al. (2021b)
L. fumosus	CLZhao 8188	MW713744	—	Luo et al. (2021b)
L. gatesiae	LWZ20180515-3	MT319447	—	Wang et al. (2021)
L. gatesiae	LWZ20180515-32	MT319448	—	Wang et al. (2021)
L. griseliniae	KHL 12971 (GB)	DQ873651	—	Larsson et al. (2006)
L. hengduanensis	CLZhao 20627	OR793233	PP657611	Present study
L. hengduanensis	CLZhao 25551	OR658999	PP657610	Present study
L. hengduanensis	CLZhao 32713	OR899153	—	Present study
L. hengduanensis	CLZhao 32714	OR899154	—	Present study
L. hengduanensis	CLZhao 32782	OR899155	PP657612	Present study
L. juniperi	FR-0261086	KY081799	—	Riebesehl and Langer (2017)
L. leptocystidiatus	LWZ20170818-1	MT326514	—	Wang et al. (2021)
L. leptocystidiatus	LWZ20170818-2	MT326513	—	Wang et al. (2021)
L. macrosporus	CLZhao 4516	MN945977	—	Chen and Zhao (2020)
L. mascarensis	KAS-GEL4833	KY800399	—	Yurchenko et al. (2020)
L. mascarensis	KAS-GEL4908	KY800400	—	Yurchenko et al. (2020)
L. microfasciculatus	CLZhao 5109	MN954311	—	Chen and Zhao (2020)
L. niveomarginatus	CLZhao 16360	PP537949	PP657607	Present study
L. niveus	CLZhao 6431	MZ262541	MZ262526	Luo et al. (2021b)
L. niveus	CLZhao 6442	MZ262542	MZ262527	Luo et al. (2021b)
L. ochraceoalbus	CLZhao 4385	MZ262535	MZ262521	Luo et al. (2021b)
L. ochraceoalbus	CLZhao 4725	MZ262536	MZ262522	Luo et al. (2021b)
L. ochraceoalbus	MSK7247	KY800403	—	Yurchenko et al. (2017)
L. orientalis	GEL3376	DQ340325	—	Yurchenko et al. (2017)
L. pruni	GEL2327	DQ340312	—	Larsson et al. (2006)
L. pruni	Ryberg 021018 (GB)	DQ873624	—	Larsson et al. (2006)
L. sambuci	KAS-JR7	KY800402	KY795966	Yurchenko et al. (2017)
L. sambuci	83SAMHYP	JX857721	—	Yurchenko et al. (2017)

Species name	Specimen No.	GenBank accession No.		References
		ITS	nLSU	
L. vietnamensis	TNM F9073	JX175044	—	Yurchenko et al. (2017)
L. wuliangshanensis	CLZhao 4108	MN945980	—	Chen and Zhao (2020)
L. wuliangshanensis	CLZhao 4167	MN945979	—	Chen and Zhao (2020)
L. wumengshanensis	CLZhao 29374	OR803021	PP657613	Present study
L. wumengshanensis	CLZhao 31486	OR899208	—	Present study
L. wumengshanensis	CLZhao 32705	OR899209	—	Present study
L. wumengshanensis	CLZhao 32736	OR899210	—	Present study
L. wumengshanensis	CLZhao 32800	OR899211	PP657614	Present study
L. wumengshanensis	CLZhao 32869	OR899212	—	Present study
L. wumengshanensis	CLZhao 32915	OR899213	PP657615	Present study
L. yunnanensis	CLZhao 2463	OP730711	OP730723	Guan et al. (2023)
L. yunnanensis	CLZhao 9375	OP730710	—	Guan et al. (2023)
L. yunnanensis	CLZhao 10041	OP730709	—	Guan et al. (2023)
L. zhaotongensis	CLZhao 32878	PP537950	PP657609	Present study
Xylodon afromontanus	H 7006811	OQ645463	—	Yurchenko et al. (2024)
X. asiaticus	CLZhao 10368	OM959479	—	Zhang et al. (2024)
X. cystidiatus	FR-0249200	MH880195	MH884896	Riebesehl et al. (2019)
X. daweishanensis	CLZhao 18492	OP730719	OP730727	Guan et al. (2023)
X. daweishanensis	CLZhao 18446	OP730717	OP730725	Guan et al. (2023)
X. filicinus	MSK-F 12869	MH880199	NG067836	Riebesehl et al. (2019)
X. fissuratus	CLZhao 7007	OP730713	—	Guan et al. (2023)
X. fissuratus	CLZhao 9407	OP730714	—	Guan et al. (2023)
X. hastifer	K(M) 172400	NR166558	—	Riebesehl and Langer (2017)
X. hyphodontinus	KAS-GEL9222	MH880205	MH884903	Riebesehl et al. (2019)
X. macrosporus	CLZhao 10226	MZ663809	MZ663817	Luo et al. (2021a)
X. puerensis	CLZhao 8142	OP730720	OP730728	Guan et al. (2023)
X. puerensis	CLZhao 8639	OP730721	OP730729	Guan et al. (2023)
X. quercinus	Larsson 11076 (GB)	KT361633	—	Larsson et al. (2004)
X. ramicida	Spirin 7664	NR138013	—	Unpublished
X. subflaviporus	Wu 0809-76	KX857803	—	Chen et al. (2017)
X. tropicus	CLZhao 3351	OL619261	OL619269	Qu et al. (2022)
X. wenshanensis	CLZhao 15729	OM338097	OM338104	Luo et al. (2022)
X. xinpingensis	CLZhao 11224	MW394662	MW394654	Luo et al. (2022)

The sequences were aligned in MAFFT version 7 (Katoh et al. 2019) using the G-INS-i strategy. The alignment was adjusted manually using AliView version 1.27 (Larsson 2014). The sequence alignments were deposited in figshare (DOI: 10.6084/m9.figshare.27166521). Sequences of *Hymenochaete ochromarginata* P.H.B. Talbot and *Hymenochaete rubiginosa* (Dicks.) Lév., retrieved from GenBank, were used as the outgroups in the ITS+nLSU analysis (Fig. 1). The sequence alignments were deposited in figshare (DOI: 10.6084/m9.figshare.27166521). Sequences of *Xylodon quercinus* (Pers.) Gray and *Xylodon ramicida* Spirin & Miettinen, retrieved from GenBank, were used as the outgroups in the ITS analysis (Fig. 2) (Guan et al. 2023; Zhang et al. 2024).

Maximum Parsimony (MP), Maximum Likelihood (ML) and Bayesian Inference (BI) analyses were applied to the combined three datasets following a previous study (Zhao and Wu 2017). All characters were equally weighted and gaps were treated as missing data. Trees were inferred using the heuristic search option with TBR branch swapping and 1,000 random sequence additions. Max-trees were set to 5,000, branches of zero length were collapsed and all parsimonious trees were saved. Clade robustness was assessed using bootstrap

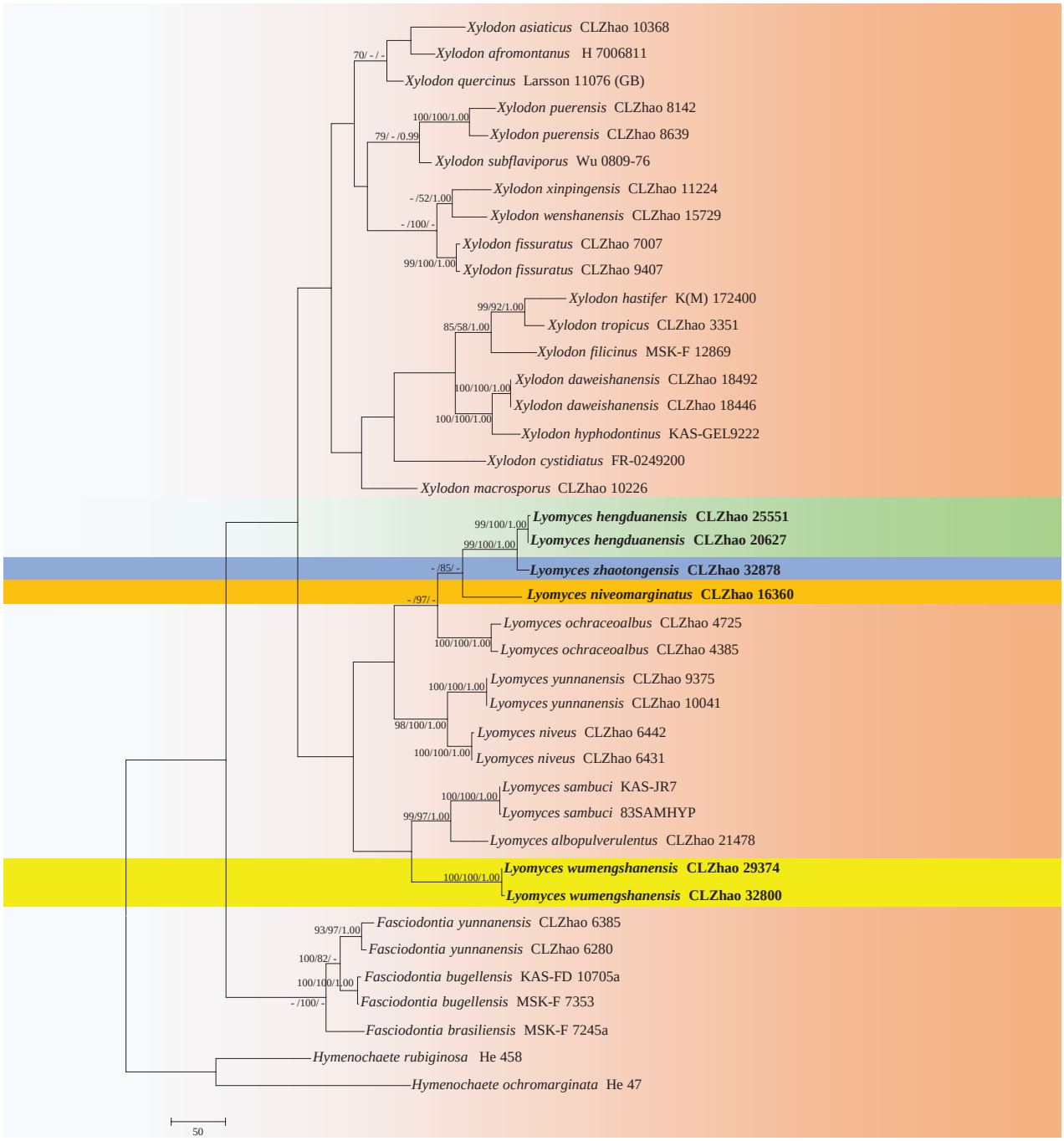

Figure 1. Maximum Parsimony strict consensus tree illustrating the phylogeny of four new species and related species in *Lyomyces* within Schizoporaceae, based on ITS+nLSU sequences. Branches are labelled with Maximum Likelihood bootstrap values ≥ 70%, parsimony bootstrap values ≥ 50% and Bayesian posterior probabilities ≥ 0.95, respectively.

(BT) analysis with 1,000 pseudo-replicates (Felsenstein 1985). Descriptive tree statistics - tree length (TL), composite consistency index (CI), composite retention index (RI), composite rescaled consistency index (RC) and composite homoplasy index (HI) - were calculated for each maximum parsimonious tree generated. The combined dataset was also analysed using Maximum Likelihood (ML) in RAxML-HPC2 through the CIPRES Science Gateway (Miller et al. 2012). Branch support (BS) for the ML analysis was determined by 1000 bootstrap pseudo-replicates.

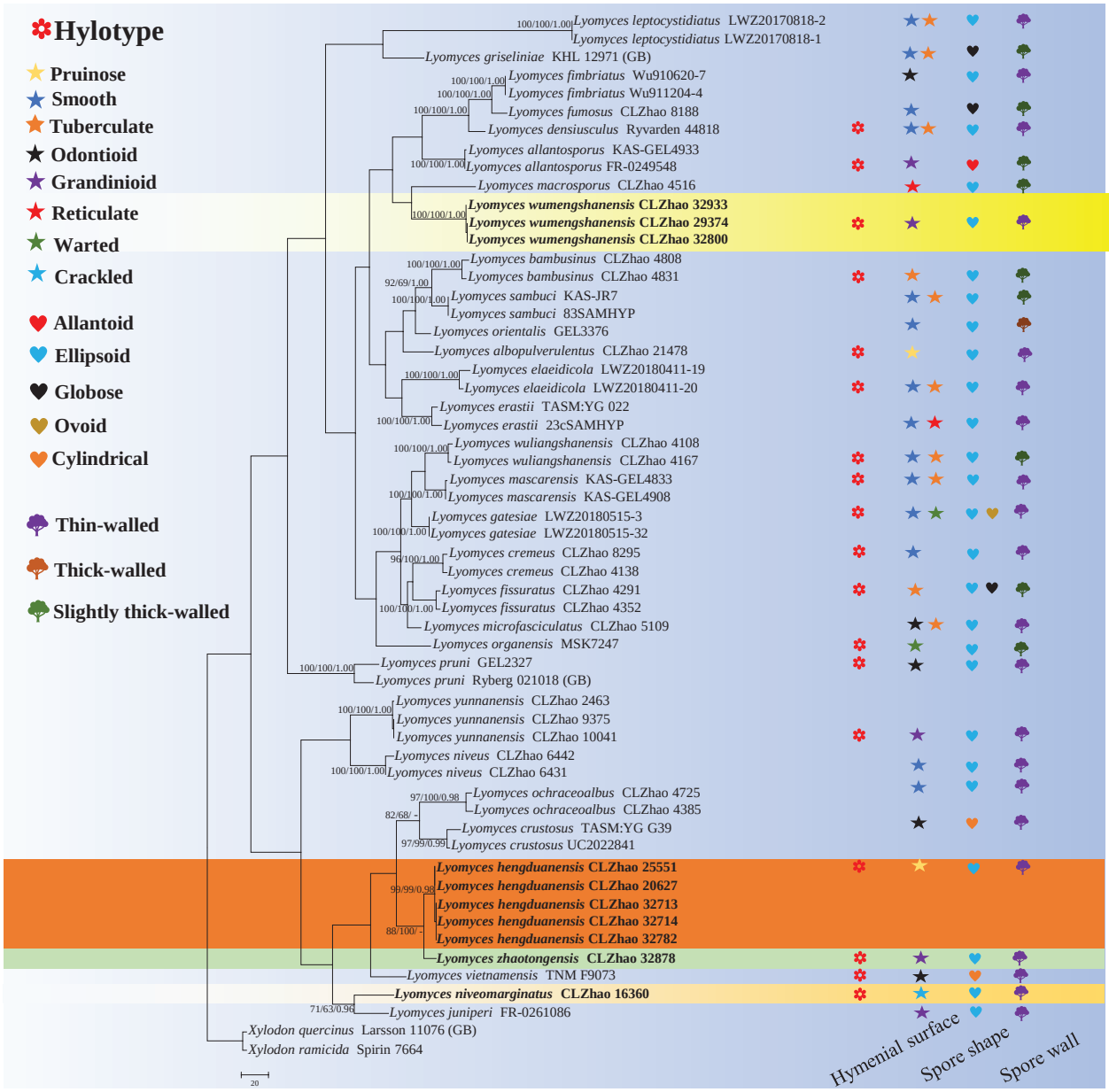

Figure 2. Maximum parsimony strict consensus tree illustrating the phylogeny of the four new species and related species in *Lyomyces*, based on ITS sequences. Branches are labelled with Maximum Likelihood bootstrap values > 70%, parsimony bootstrap values > 50% and Bayesian posterior probabilities > 0.95, respectively.

MrModelTest 2.3 (Nylander 2004) was used to determine the best-fit evolution model for each dataset for Bayesian Inference (BI), which was performed using MrBayes 3.2.7a with a GTR+I+G model of DNA substitution and a gamma distribution rate variation across sites (Ronquist et al. 2012). A total of four Markov chains were run for two runs from random starting trees for 1.905 million generations for ITS+nLSU (Fig. 1) and 2 million generations for ITS (Fig. 2), with trees and parameters sampled every 1,000 generations. The first quarter of all of the generations were discarded as burn-in. A majority rule consensus tree was computed from the remaining trees. Branches were considered as significantly supported if they received a Maximum Likelihood bootstrap support value (BS) of ≥ 70%, a Maximum Parsimony bootstrap support value (BT) of ≥ 70% or a Bayesian Posterior Probability (BPP) of ≥ 0.95.

Results

Molecular phylogeny

The ITS+nLSU dataset (Fig. 1) comprised sequences from 40 fungal specimens representing 29 taxa. The dataset had an aligned length of 2,112 characters, of which 1,298 characters were constant, 254 were variable and parsimony-uninformative and 560 were parsimony-informative. Maximum parsimony analysis yielded one equally parsimonious tree (TL = 2,513, CI = 0.4990, HI = 0.5010, RI = 0.6658 and RC = 0.3322). The best model of nucleotide evolution for the ITS+nLSU dataset estimated and applied in the Bayesian analysis was found to be GTR+I+G. Bayesian analysis and ML analysis resulted in a similar topology as in the MP analysis. The Bayesian analysis had an average standard deviation of split frequencies = 0.009992 (BI) and the effective sample size (ESS) across the two runs is double the average ESS (avg. ESS) = 2078.5. The phylogram, based on the ITS+nLSU rDNA gene regions (Fig. 1), included three genera within Schizoporaceae (Hymenochaetales), which were *Fasciodontia*, *Lyomyces* and *Xylodon*, in which four new species were grouped into the genera *Lyomyces*.

The ITS dataset (Fig. 2) comprised sequences from 57 fungal specimens representing 33 taxa. The dataset had an aligned length of 696 characters, of which 270 characters were constant, 41 were variable and parsimony-uninformative and 385 were parsimony-informative. Maximum parsimony analysis yielded 80 equally parsimonious tree (TL = 1,748, CI = 0.4027, HI = 0.5973, RI = 0.6935 and RC = 0.2793). The best model of nucleotide evolution for the ITS dataset estimated and applied in the Bayesian analysis was found to be GTR+I+G. Bayesian analysis and ML analysis resulted in a similar topology as in the MP analysis. The Bayesian analysis had an average standard deviation of split frequencies = 0.014964 (BI) and the effective sample size (ESS) across the two runs is double the average ESS (avg. ESS) = 1,387.5. The phylogenetic tree (Fig. 2), inferred from the ITS sequences, highlighted that *L. hengduanensis* group with *L. zhaotongensis*; and then closely grouped with *L. crustosus* (Pers.) P. Karst., *L. ochraceoalbus* C.L. Zhao and *L. vietnamensis* (Yurchenko & Sheng H. Wu) Riebesehl & Langer. *Lyomyces niveomarginatus* was retrieved as a sister to *L. juniperi* (Bourdot & Galzin) Riebesehl & Langer. *Lyomyces wumengshanensis* was retrieved as a sister to *L. macrosporus* C.L. Zhao. Moreover, *Lyomyces zhaotongensis* grouped with *L. hengduanensis* and closely clustered with *L. crustosus*, *L. ochraceoalbus* and *L. vietnamensis*.

Taxonomy

***Lyomyces hengduanensis* Q. Yuan & C.L. Zhao, sp. nov.**
MycoBank No: 853724
Figs 3, 4

Type material. *Holotype*. China • Yunnan Province, Lincang, Fengqing County, Yaojie Town, GPS coordinates 24°66'N, 100°19'E, altitude 2060 m, on a fallen branch of angiosperm, leg. C.L. Zhao, 22 October 2022, CLZhao 25551 (SWFC).

Etymology. *Hengduanensis* (Lat.) refers to the type locality "Hengduan Mountain".

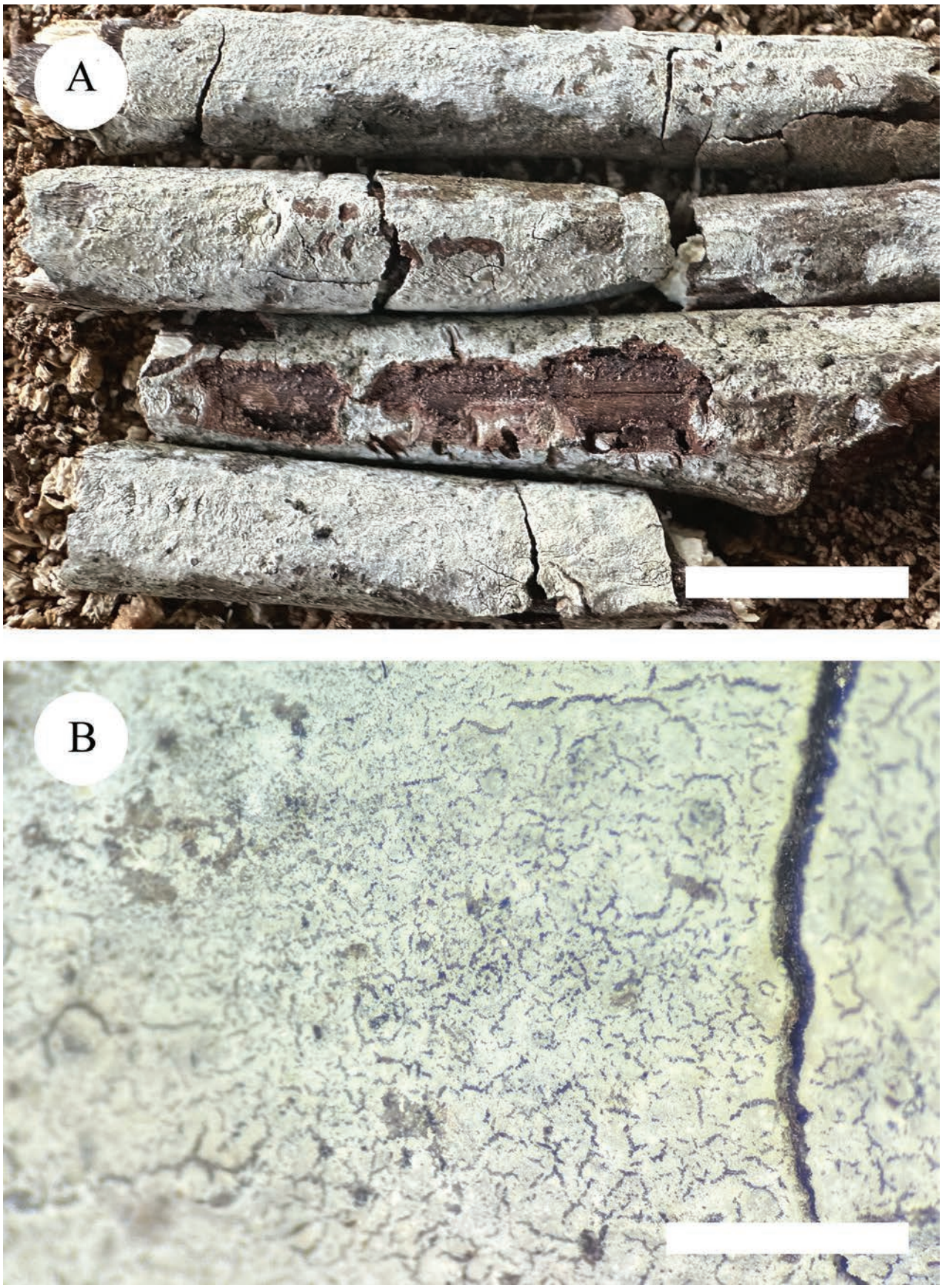

Figure 3. Basidiomata of *Lyomyces hengduanensis* (holotype). Scale bars: 1 cm (**A**); 2 mm (**B**).

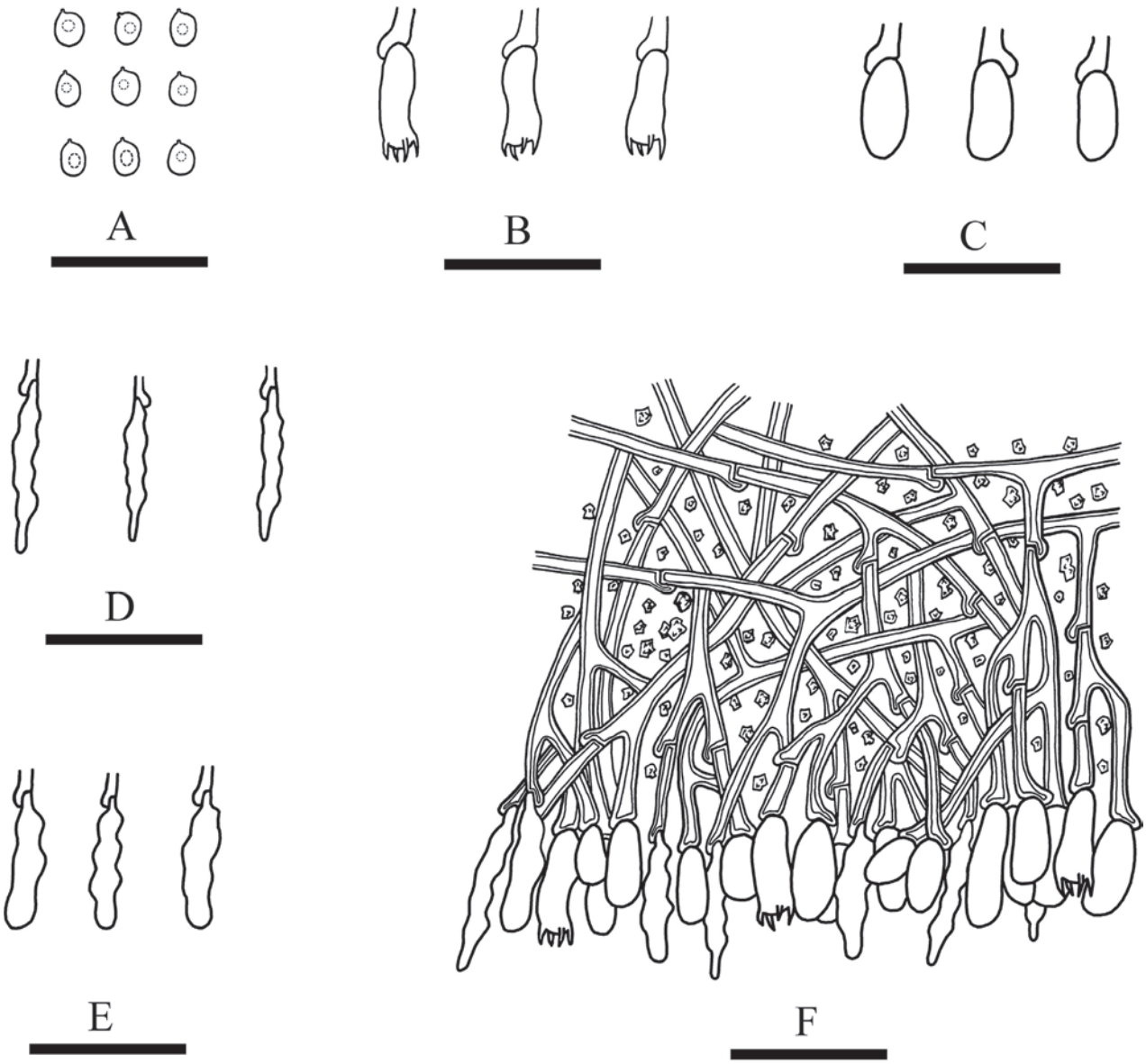

Figure 4. Microscopic structures of *Lyomyces hengduanensis* (holotype): basidiospores (**A**), basidia (**B**), basidioles (**C**), fusoid cystidia (**D**), subclavate cystidia (**E**), a section of hymenium (**F**). Scale bars: 20 μm (**A–F**).

Description. Basidiomata annual, resupinate, adnate, brittle, without odour and taste when fresh and up to 3.5 cm long, 1 cm wide, 100 μm thick. Hymenial surface pruinose, white to cream when fresh, to cream to slightly buff upon drying. Sterile margin white to cream and up to 1 mm wide.

Hyphal system monomitic, generative hyphae with clamp connections, colourless, thick-walled, branched, 2–3 μm in diameter; IKI–, CB–, tissues unchanged in KOH. Numerous crystals present amongst generative hyphae.

Cystidia of two types: (1) fusoid, colourless, thin-walled, smooth, slightly constricted in the middle to somewhat sinuous, 17.5–25 × 3–4 μm; (2) subclavate, colourless, thin-walled, smooth, slightly constricted in the middle to somewhat sinuous, 16–23 × 3–4.5 μm; basidia clavate, with 4 sterigmata and a basal clamp connection, 10.5–14 × 3.5–5 μm.

Basidiospores ellipsoid, colourless, thin-walled, smooth, with one oil drop, CB–, IKI–, 3.5–6 × 3–4.5 µm, L = 4.63 µm, W = 3.65 µm, Q = 1.25–1.28 (n = 90/3).

Additional specimens examined (*paratypes*). China • Yunnan Province, Zhaotong, Qiaojia County, Yaoshan Town, Yaoshan National Nature Reserve, 26°50'N, 102°59'E, altitude 2500 m, on a fallen branch of angiosperm, leg. C.L. Zhao, 22 August 2020, CLZhao 20627 (SWFC) • Zhaotong, Wumeng Mountain National Nature Reserve, GPS coordinates 27°72'N, 103°92'E, altitude 1424 m, on a fallen branch of angiosperm, leg. C.L. Zhao, 29 August 2023, CLZhao 32713, CLZhao 32714, CLZhao 32782 (SWFC).

***Lyomyces niveomarginatus* Q. Yuan & C.L. Zhao, sp. nov.**

MycoBank No: 853725

Figs 5, 6

Type material. *Holotype*. China • Yunnan Province, Wenshan, Wenshan National Nature Reserve, GPS coordinates 23°21'N, 104°10'E, altitude 1950 m, on a fallen branch of angiosperm, leg. C.L. Zhao, 26 July 2019, CLZhao 16360 (SWFC).

Etymology. *Niveomarginatus* (Lat.) refers to the niveous margin of basidiomata.

Description. Basidiomata annual, resupinate, adnate, subceraceous, without odour and taste when fresh and up to 7.5 cm long, 2 cm wide, 150 µm thick. Hymenial surface crackled, white to cream when fresh, to cream to slightly buff upon drying. Sterile margin distinct, whitish and up to 2 mm wide.

Hyphal system monomitic, generative hyphae with clamp connections, colourless, thin-walled, branched, 1.5–3.5 µm in diameter; IKI–, CB–, tissues unchanged in KOH. Numerous crystals present amongst generative hyphae.

Cystidia of two types: (1) fusoid, colourless, thin-walled, smooth, 25–29 × 2–3 µm; (2) clavate, colourless, thin-walled, smooth, 20–25.5 × 4.5–5.5 µm; basidia subclavate, with 4 sterigmata and a basal clamp connection, 23–29 × 2.5–3.5 µm.

Basidiospores ellipsoid, colourless, thin-walled, smooth, with one oil drop, CB–, IKI–, 4.5–7 × (2.5–)3–4 µm, L = 5.51 µm, W = 3.15 µm, Q = 1.75 (n = 30/1).

Additional specimens examined (*paratypes*). China • Yunnan Province, Wenshan, Wenshan National Nature Reserve, GPS coordinates 23°21'N, 104°10'E, altitude 1950 m, on a fallen branch of angiosperm, leg. C.L. Zhao, 7 August 2024, CLZhao 40333, CLZhao 40334 (SWFC).

***Lyomyces wumengshanensis* Q. Yuan & C.L. Zhao, sp. nov.**

MycoBank No: 853726

Figs 7, 8

Type material. *Holotype*. China • Yunnan Province, Zhaotong, Daguan County, Wumeng Mountain National Nature Reserve, GPS coordinates 27°72'N, 103°92'E, altitude 1424 m, on a fallen branch of angiosperm, leg. C.L. Zhao, 3 July 2023, CLZhao 29374 (SWFC).

Etymology. *Wumengshanensis* (Lat.) refers to the type locality "Wumeng Mountain".

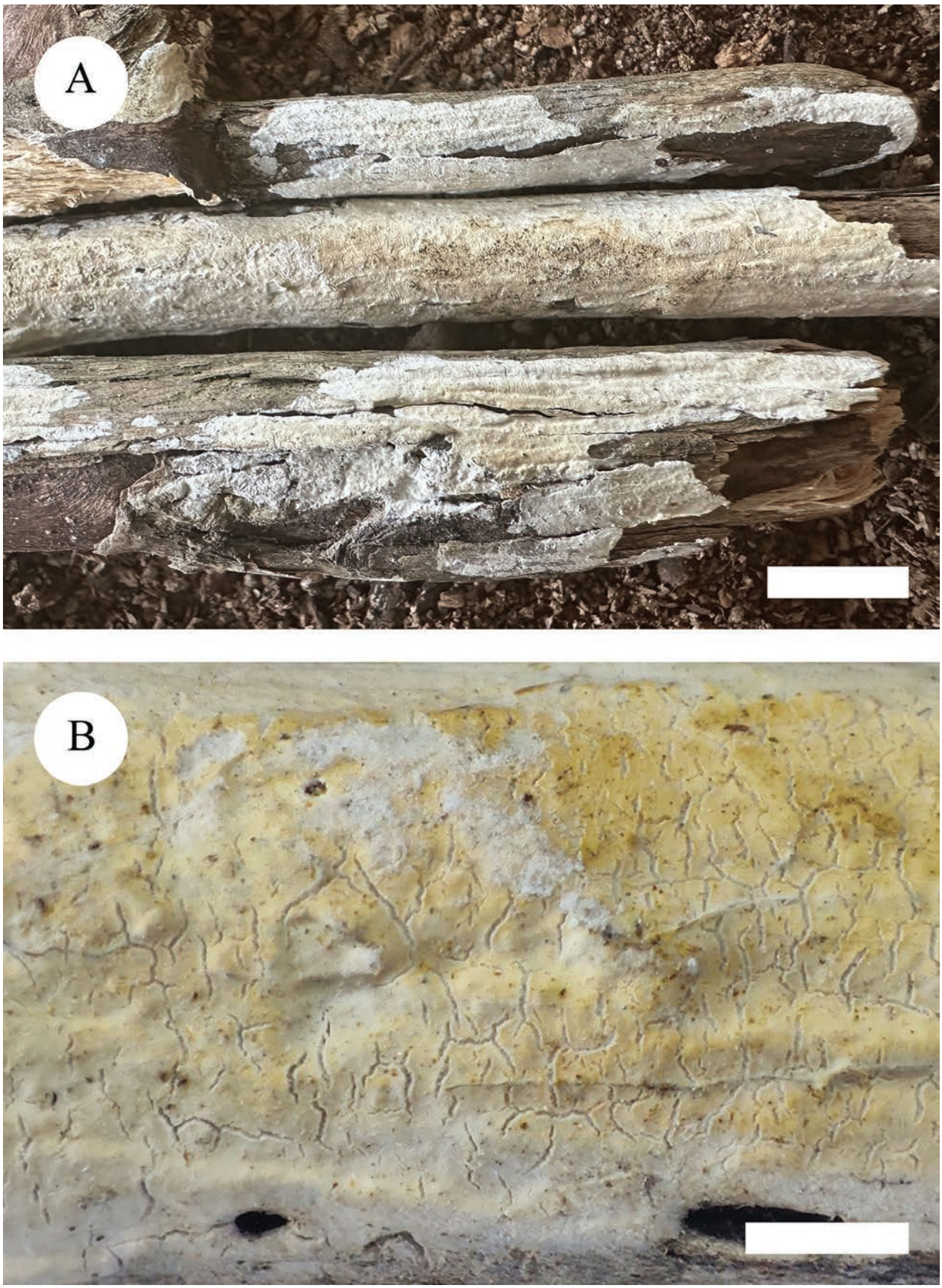

Figure 5. Basidiomata of *Lyomyces niveomarginatus* (holotype). Scale bars: 1 cm (**A**); 2 mm (**B**).

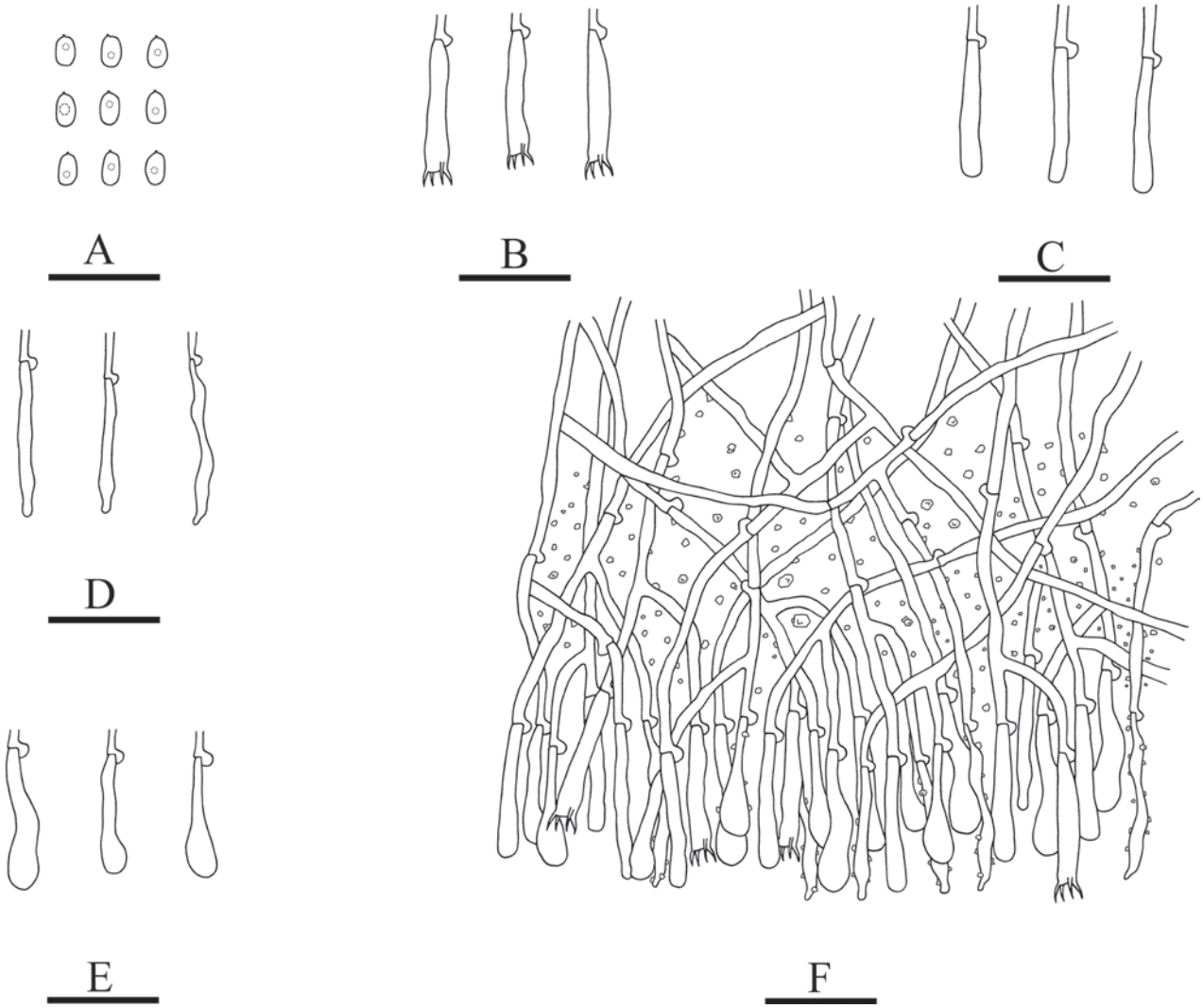

Figure 6. Microscopic structures of *Lyomyces niveomarginatus* (holotype): basidiospores (**A**), basidia (**B**), basidioles (**C**), fusoid cystidia (**D**), clavate cystidia (**E**), a section of hymenium (**F**). Scale bars: 20 μm (**A–F**).

Description. Basidiomata annual, resupinate, adnate, coriaceous when fresh, becoming farinaceous upon drying, without odour and taste when fresh and up to 5 cm long, 2 cm wide, 150 μm thick. Hymenial surface grandinioid, white when fresh, to cream upon drying. Sterile margin white and up to 1 mm wide.

Hyphal system monomitic, generative hyphae with clamp connections, colourless, thick-walled, branched, 3–4 μm in diameter; IKI–, CB–, tissues unchanged in KOH. Numerous crystals present amongst generative hyphae.

Cystidia capitate, colourless, thin-walled, smooth, 24.5–29 × 3–4 μm; basidia subclavate to barrelled, colourless, with 4 sterigmata and a basal clamp connection, 11.5–14 × 5.5–6.5 μm.

Basidiospores ellipsoid to broad ellipsoid, colourless, thin-walled, smooth, with one oil drop, CB–, IKI–, 4–6 × 3–5 μm, L = 5.4 μm, W = 4.2 μm, Q = 1.28–1.32 (n = 120/4).

Additional specimen examined (*paratype*). China • Yunnan Province, Zhaotong, Wumeng Mountain National Nature Reserve, 27°72'N, 103°92'E, altitude 1424 m, on a fallen branch of angiosperm, leg. C.L. Zhao, 29 August 2023, CLZ-

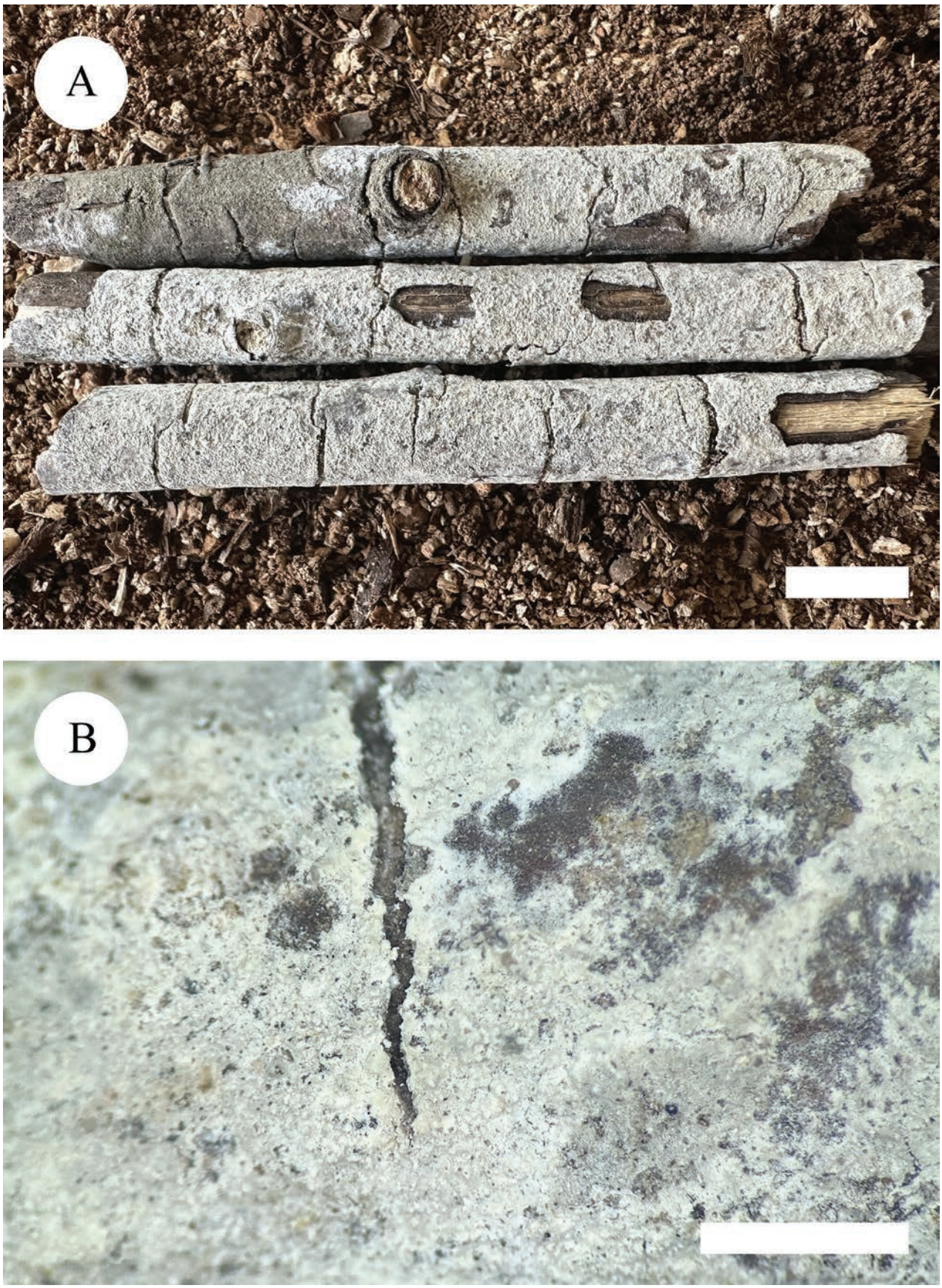

Figure 7. Basidiomata of *Lyomyces wumengshanensis* (holotype). Scale bars: 1 cm (**A**); 2 mm (**B**).

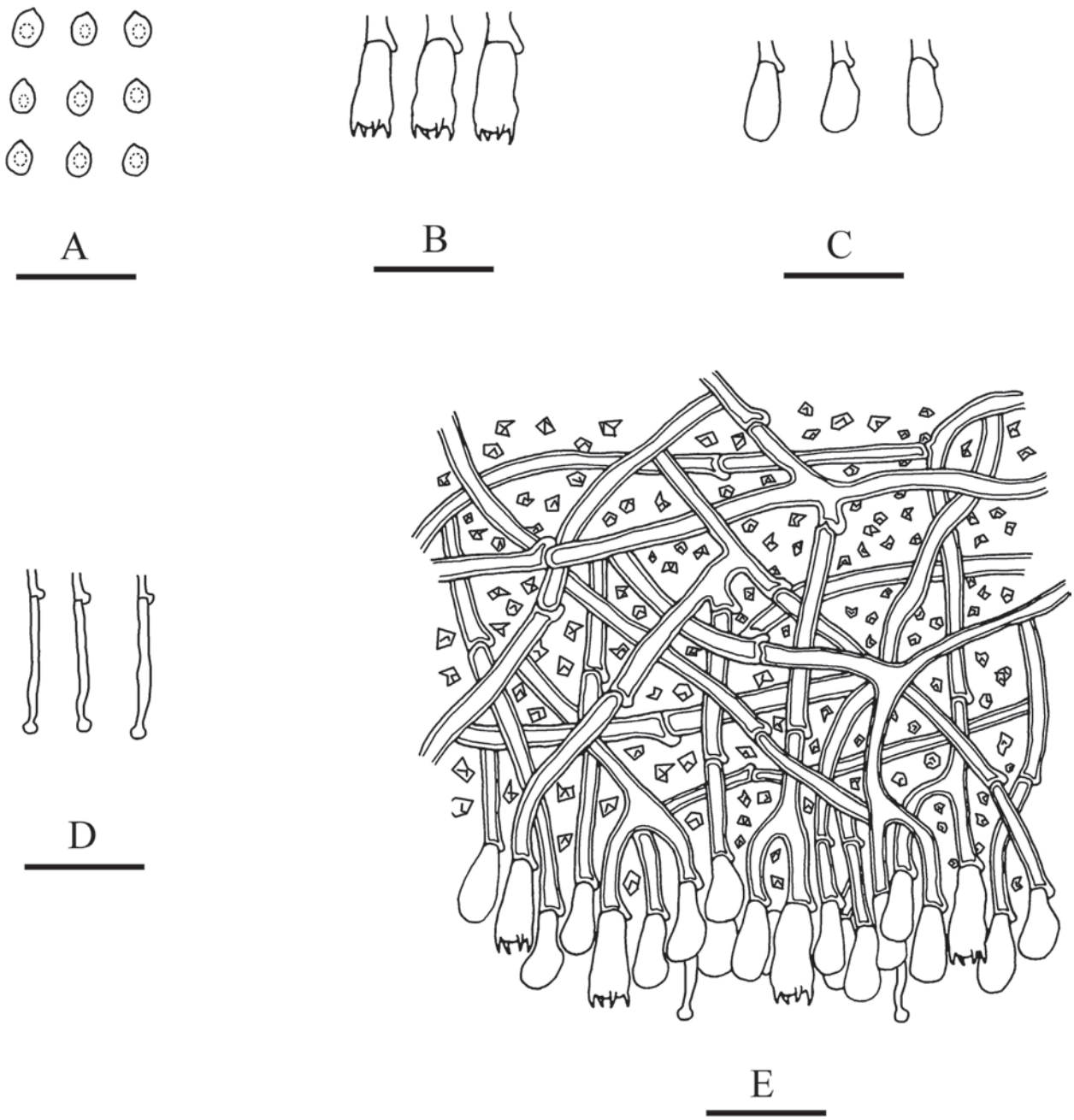

Figure 8. Microscopic structures of *Lyomyces wumengshanensis* (holotype): basidiospores (**A**), basidia (**B**), basidioles (**C**), capitate cystidia (**D**), a section of hymenium (**E**). Scale bars: 10 μm (**A–E**).

hao 31486, CLZhao 32705, CLZhao 32736, CLZhao 32800, CLZhao 32869, CLZhao 32915, CLZhao 32933 (SWFC).

***Lyomyces zhaotongensis* Q. Yuan & C.L. Zhao, sp. nov.**
MycoBank No: 853727
Figs 9, 10

Type material. *Holotype*. China •Yunnan Province, Zhaotong, Wumeng Mountain National Nature Reserve, GPS coordinates 27°77'N, 104°29'E, altitude

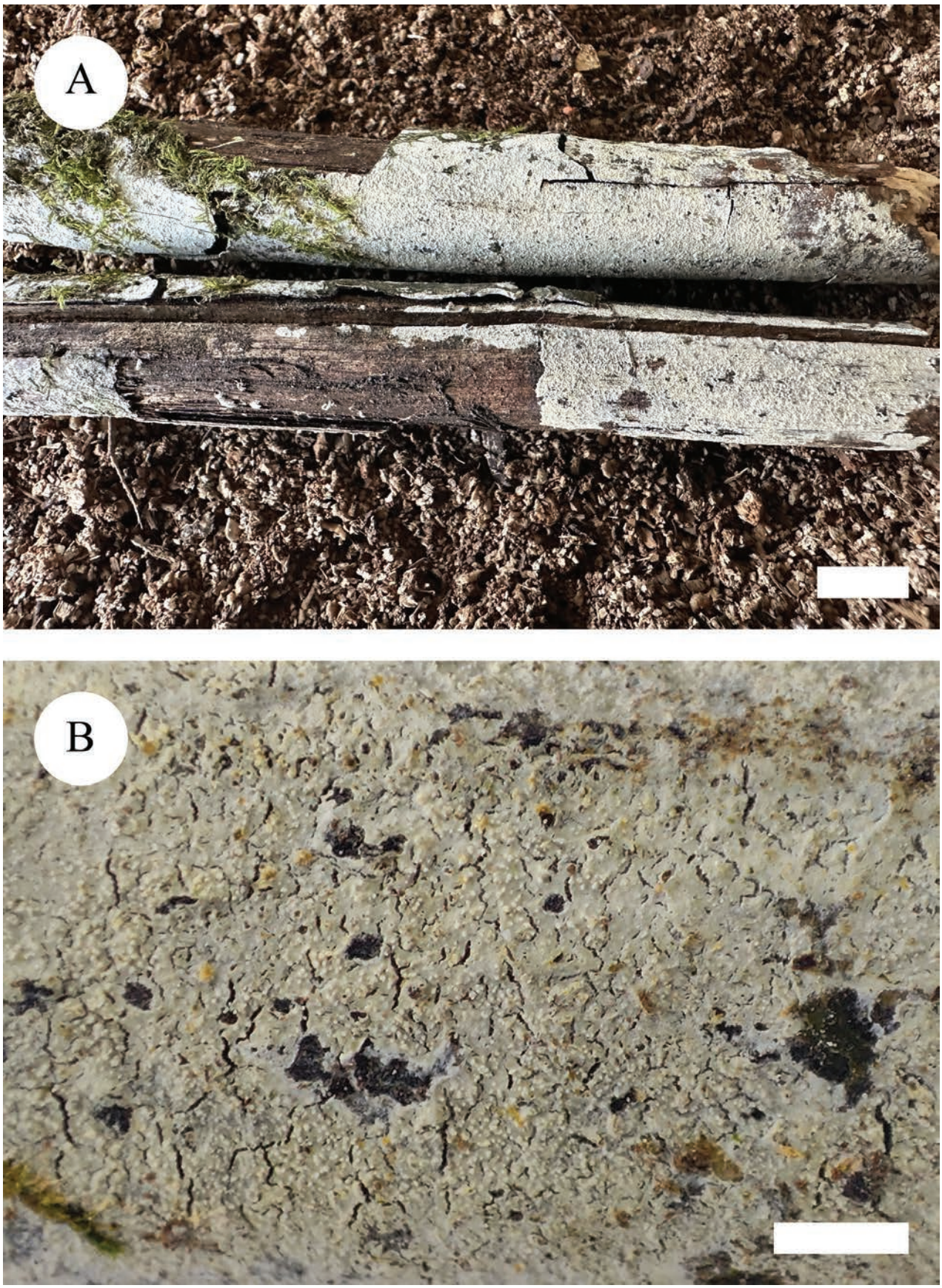

Figure 9. Basidiomata of *Lyomyces zhaotongensis* (holotype). Scale bars: (**A**) 1 cm; (**B**) 2 mm.

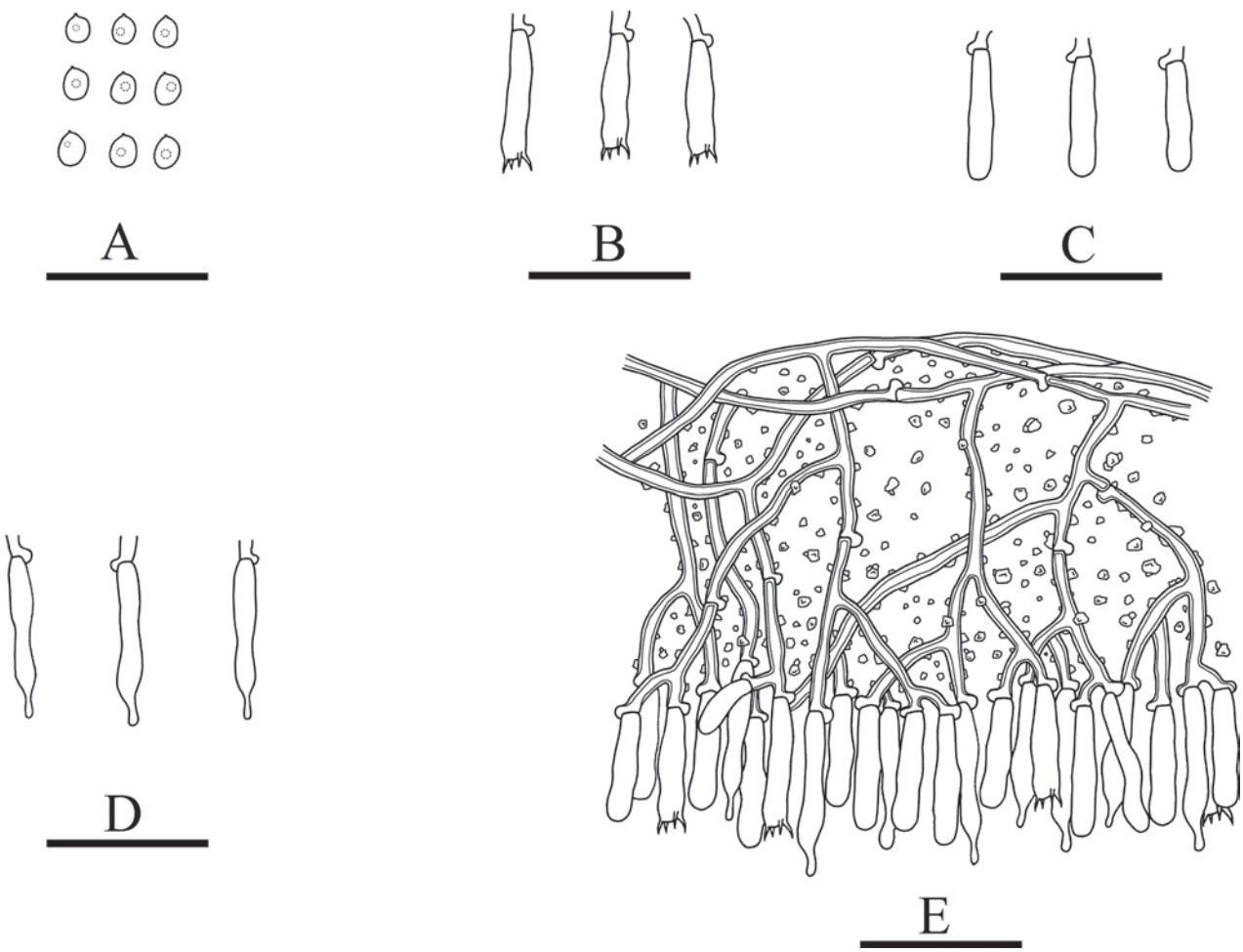

Figure 10. Microscopic structures of *Lyomyces zhaotongensis* (holotype): basidiospores (**A**), basidia (**B**), basidioles (**C**), fusoid cystidia (**D**), a section of hymenium (**E**). Scale bars: 20 μm (**A–E**).

2900 m, on the fallen branch of angiosperm, leg. C.L. Zhao, 29 August 2023, CLZhao 32878 (SWFC).

Etymology. *Zhaotongensis* (Lat.) refers to the type locality "Zhaotong".

Description. Basidiomata annual, resupinate, adnate, farinaceous when fresh, becoming coriaceous upon drying and up to 9.5 cm long, 3 cm wide, 30–80 um thick. Hymenial surface grandinioid, cream when fresh and cream to buff upon drying. Sterile margin white to cream and up to 1 mm wide.

Hyphal system monomitic, generative hyphae with clamp connections, colourless, thick-walled, branched, 1.5–2 μm in diameter; IKI–, CB–, tissues unchanged in KOH. Numerous crystals present amongst generative hyphae.

Cystidia fusoid, colourless, thin-walled, smooth, 16–20.5 × 2.5–3.5 μm. Basidia clavate, with 4 sterigmata and a basal clamp connection, 14–16.5 × 2.5–3.5 μm.

Basidiospores broadly ellipsoid, colourless, thin-walled, smooth, with oil drops, CB–, IKI–, 2.6–3.5 × 2.5–3 μm, L = 2.99 μm, W = 2.75 μm, Q = 1.08 (n = 30/1).

Additional specimen examined (*paratype*). China • Yunnan Province, Zhaotong, Wumeng Mountain National Nature Reserve, GPS coordinates 27°77'N, 104°29'E, altitude 2900 m, on the fallen branch of angiosperm, leg. C.L. Zhao, 10 August 2024, CLZhao 40335 (SWFC).

Discussion

Many recently new wood-inhabiting fungal taxa have been reported in the subtropics and tropics, including in the genus *Lyomyces* (Xiong et al. 2009; Chen et al. 2017; Kan et al. 2017a, b; Riebesehl and Langer 2017; Viner et al. 2018; Chen and Zhao 2020; Luo et al. 2021a, b, c, 2022; Qu and Zhao 2022; Qu et al. 2022; Viner et al. 2022; Guan et al. 2023; Deng et al. 2024a, b; Zhang et al. 2024). Prior to this study, the following sixteen *Lyomyces* species were reported from China as *L. albopulverulentus* C.L. Zhao, *L. albus* (Sheng H. Wu) Riebesehl & Langer, *L. bambusinus*, *L. capitatocystidiatus* (H.X. Xiong, Y.C. Dai & Sheng H. Wu) Riebesehl & Langer, *L. cremeus* C.L. Zhao, *L. fissuratus*, *L. fumosus*, *L. leptocystidiatus* Xue W. Wang & L.W. Zhou, *L. macrosporus* C.L. Zhao & K.Y. Luo, *L. microfasciculatus* (Yurchenko & Sheng H. Wu) Riebesehl & Langer, *L. niveus*, *L. ochraceoalbus*, *L. sambuci*, *L. tenuissimus* (Yurchenko & Sheng H. Wu) Riebesehl & Langer, *L. wuliangshanensis* C.L. Zhao and *L. yunnanensis* C.L. Zhao (Xiong et al. 2009; Yurchenko et al. 2013; Riebesehl and Langer 2017; Chen and Zhao 2020; Luo et al. 2021b, c; Wang et al. 2021). The present study reports four new species in the genus *Lyomyces*, based on a combination of morphological features and molecular evidence.

Phylogenetically, based on the multiple loci in *Hyphodontia* s.l., six genera of *Fasciodontia*, *Hastodontia*, *Hyphodontia*, *Lyomyces*, *Kneiffiella* and *Xylodon*, were divided into four clades in the wood-inhabiting fungal order Hymenochaetales (Wang et al. 2021). In the present study, the phylogram inferred from the ITS+nLSU data, four new species grouped into the genus *Lyomyces* (Fig. 1). Based on ITS topology (Fig. 2), in which *L. hengduanensis* group with *L. zhaotongensis* and then closely grouped with *L. crustosus*, *L. ochraceoalbus* and *L. vietnamensis*. *Lyomyces niveomarginatus* was retrieved as a sister to *L. juniperi*. *L. wumengshanensis* was sister to *L. macrosporus*. Moreover, *L. zhaotongensis* grouped with *L. hengduanensis* and then closely clustered with three species: *L. crustosus*, *L. ochraceoalbus* and *L. vietnamensis*. However, morphologically, *L. zhaotongensis* can be delimited from *L. hengduanensis* by its the grandinioid hymenial surface and longer basidia (14–16.5 × 2.5–3.5 µm); *L. crustosus* can be separated from *L. hengduanensis* by its odontioid hymenial surface and narrow basidiospores (5–7.5 × 2.5–3 µm) (Lentz and McKay 1976); *L. ochraceoalbus* differs in *L. hengduanensis* by having a smooth hymenial surface and lacking a cystidium (Luo et al. 2021c); *L. vietnamensis* differs from *L. hengduanensis* by its aculeate hymenial surface and narrow basidiospores (5.8–6.1 × 2.6–2.9 µm; Yurchenko and Wu (2013)). *L. juniperi* can be delimited from *L. niveomarginatus* by its smooth hymenial surface with some scattered small granules and wider basidia (15–25 × 4–4.5 µm; Hjortstam and Ryvarden (2004)); *L. macrosporus* can be separated from *L. wumengshanensis* by its reticulate hymenial surface and longer basidiospores (6.7–8.9 × 4.4–5.4 µm; Chen and Zhao (2020)); *L. crustosus* can be delimited from *L. zhaotongensis* by its odontioid hymenial surface and longer basidiospores (5–7.5 × 2.5–3 µm; Lentz and McKay (1976)); *L. hengduanensis* can be delimited from *L. zhaotongensis* by its pruinose hymenial surface and shorter basidia (14–16.5 × 2.5–3.5 µm); *L. ochraceoalbus* differs in *L. zhaotongensis* by having smooth hymenial surface and longer basidiospores (4–5 × 2.5–3.5 µm; Luo et al. (2021c)); *L. vietnamensis* can be delimited from *L. zhaotongensis* by its

aculeate hymenial surface and longer basidiospores (5.8–6.1 × 2.6–2.9 µm; Yurchenko and Wu (2013)).

Morphologically, *Lyomyces hengduanensis* resembles four taxa viz. *L. albopulverulentus*, *L. bambusinus*, *L. mascarensis* Riebesehl, Yurch. & Langer and *L. yunnanensis*, by the similar ellipsoid basidiospores. However, *L. albopulverulentus* differs from *L. hengduanensis* by its larger basidia (24.5–28.5 × 7–9 µm) and basidiospores (8–10.5 × 5.5–7 µm; Guan et al. (2023)); *L. bambusinus* can be separated from *L. hengduanensis* by its colliculose to tuberculate hymenial surface and longer basidia (16.5–35 × 3.5–7 µm; Chen and Zhao (2020)); *L. mascarensis* is distinct from *L. hengduanensis* by having indistinctly colliculose hymenial surface and longer basidia (16–17.5 × 3.5–4.5 µm; Yurchenko et al. (2017)); *L. yunnanensis* is distinguished from *L. hengduanensis* by its grandinioid hymenial surface and longer basidia (16.5–27 × 4–5.5 µm; Guan et al. (2023)).

Morphologically, *Lyomyces niveomarginatus* resembles several species viz. *L. albopulverulentus*, *L. cremeus*, *L. macrosporus*, *L. wuliangshanensis* and *L. yunnanensis* by the cream to buff hymenial surface and ellipsoid basidiospores. However, *L. albopulverulentus* differs from *L. niveomarginatus* by its pruinose hymenial surface and wider basidia (24.5–28.5 × 7–9 µm; Guan et al. (2023)); *L. cremeus* can be separated from *L. niveomarginatus* by its smooth hymenial surface and shorter basidia (9–18.5 × 3–6 µm; Chen and Zhao (2020)); *L. macrosporus* differs from *L. niveomarginatus* by its reticulate hymenial surface and wider basidia (23–29 × 2.5–3.5 µm) and wider basidiospores (6.7–8.9 × 4.4–5.4 µm; Chen and Zhao (2020)); *L. wuliangshanensis* can be delimited from *L. niveomarginatus* by its smooth to more or less tuberculate hymenial surface and shorter basidia (12–20 × 3–4.3 µm; Chen and Zhao (2020)); *L. yunnanensis* is distinct from *L. niveomarginatus* by having grandinioid hymenial surface and wider basidia (16.5–27 × 4–5.5 µm; Guan et al. (2023)).

Morphologically, *Lyomyces wumengshanensis* resembles *L. bambusinus*, *L. cremeus*, *L. fumosus*, *L. fissuratus*, *L. wuliangshanensis* and *L. yunnanensis* by having the capitate cystidia. However, *L. bambusinus* is distinct from *L. wumengshanensis* by possessing tapering cystidia (40–65 × 4–5.5 µm) and longer basidia (16.5–35 × 3.5–7 µm; Chen and Zhao (2020)); *L. cremeus* differs from *L. wumengshanensis* by its smooth hymenial surface and possesses tapering cystidia (18–35 × 3–4.5 µm; Chen and Zhao (2020)); *L. fumosus* can be separated from *L. wumengshanensis* by its smooth, smoky grey hymenial surface and narrower basidia (11.5–17.5 × 3–5 µm; Luo et al. (2021b)); *L. fissuratus* can be delimited from *L. wumengshanensis* by its longer and narrower basidia (14.7–23.3 × 2.9–4.8 µm; Luo et al. (2021b)); *L. wuliangshanensis* differs from *L. wumengshanensis* by its smooth to more or less tuberculate hymenial surface and narrower basidia (12–20 × 3–4.3 µm; Chen and Zhao (2020)); *L. yunnanensis* is separated from *L. wumengshanensis* by the longer basidia (16.5–27 × 4–5.5 µm) and possessing fusiform cystidia (18–39 × 4–6 µm; Guan et al. (2023)).

Morphologically, *Lyomyces zhaotongensis* reminds *L. albopulverulentus*, *L. cremeus*, *L. denudatus* Viner, *L. macrosporus* and *L. wuliangshanensis* by having the ellipsoid basidiospores. However, *L. albopulverulentus* can be separated from *L. zhaotongensis* by its pruinose hymenial surface and larger basidia (24.5–28.5 × 7–9 µm) and larger basidiospores (8–10.5 × 5.5–7 µm; Guan et al. (2023)); *L. cremeus* is distinct from *L. zhaotongensis* by its smooth hymenial surface and larger basidiospores (4.5–5.6 × 3.3–4.3 µm; Chen and Zhao

(2020)); *L. denudatus* is separated from *L. zhaotongensis* by the smooth hymenial surface and longer basidiospores (4.8–7 × 2.8–4.2 µm; Viner and Miettinen (2022)); *L. macrosporus* differs from *L. zhaotongensis* due to its reticulate hymenial surface and larger basidia (22.2–38 × 4.5–7 µm) and larger basidiospores (6.7–8.9 × 4.4–5.4 µm; Chen and Zhao (2020)); *L. wuliangshanensis* can be delimited from *L. zhaotongensis* by its smooth to more or less tuberculate hymenial surface and longer basidiospores (3.5–5.3 × 2.8–4 µm; Chen and Zhao (2020)). A morphological comparison amongst four new *Lyomyces* species and seven similar species are presented in Table 2.

The Basidiomycota is a major phylum of the kingdom Fungi (He et al. 2019; Wijayawardene et al. 2020; Yuan et al. 2023; He et al. 2024), in which the wood-inhabiting fungi are an extensively studied group of Basidiomycota (Gilbertson and Ryvarden 1987; Bernicchia and Gorjón 2010; Núñez and Ryvarden 2001; Dai 2012; Ryvarden and Melo 2014; Wu et al. 2022b; Zhao et al. 2023; Dong et al. 2024), but the wood-inhabiting fungal diversity is still not well known in China, especially in subtropical and tropical areas, and many recently-described taxa of this ecologically important group were from China (Zhao et al. 2014; Zhao et al. 2015; Zhao et al. 2016; Bian et al. 2016; Ma and Zhao 2019; Guan et al. 2020; Huang and Zhao 2020; Guan et al. 2023; Ji et al. 2023; Liu et

Table 2. A morphological comparison between four new *Lyomyces* species and seven similar species in the genus *Lyomyces*. The bold are new taxa.

Species name	Hymenial surface	Generative hyphae	Cystidia	Basidia	Basidiospores	References
Lyomyces albopulverulentus	Pruinose/ white	Thick-walled/ frequently branched	Capitate, 37–54 × 5–9 µm	Clavate, 24.5–28.5 × 7–9 µm	Ellipsoid, (7.5–)8–10.5(–11) × (5–)5.5–7 µm	Guan et al. (2023)
Lyomyces bambusinus	Colliculose to tuberculate/ cream to buff	Thick-walled/ branched	Capitate, 35–55 × 4–7 µm; tapering, 40–65 × 4–5.5 µm, cystidioles, 12–17 × 2–3 µm	Clavate, 16.5–35 × 3.5–7 µm	Broadly ellipsoid, (4.5–)4.7–5.9 (–6.2) × (3.4–)3.7–4.6(–4.8) µm	Chen and Zhao (2020)
Lyomyces cremeus	Smooth/ pale cream	Thick-walled/ branched	Capitate, 20–40 × 3–5 µm; tapering, 18–35 × 3–4.5 µm	Clavate, 9–18.5 × 3–6 µm	Ellipsoid, 4.5–5.6(–5.8) × 3.3–4.3(–4.5) µm	Chen and Zhao (2020)
Lyomyces denudatus	Smooth/ cream	Thin-walled to slightly thick-walled	Capitate, (21–)34.9–62 × (3.5–)4–5.5(–7) µm	Suburniform, 15–21.1(–25) × 3.8–5.5 µm	Ellipsoid, (4.1–)4.8–7 × 2.8–4.2(–4.7) µm	Viner and Miettinen (2022)
Lyomyces hengduanensis	Pruinose/ cream to slightly buff	Thick-walled/ branched	Fusoid, 17.5–25 × 3–4 µm; subclavate, 16–23 × 3–4.5 µm	Clavate, 10.5–14 × 3.5–5 µm	Ellipsoid, 3.5–6 × 3–4.5 µm	**Present study**
Lyomyces mascarensis	Smooth / cream or brownish	Thin-walled	Capitate, 17–38 × 3.5–6(–7) µm; submoniliform, 18–22 × 5–5.5 µm; tapering, 25–30 × 3.5–4.5 µm	Subcylindrical with one constriction, 16–17.5(–19) × 3.5–4.5(–6) µm	Ellipsoid or broadly ellipsoid, (4–)4.5–6 × (3–)3.3–4 µm	Yurchenko et al. (2017)
Lyomyces niveomarginatus	Smooth / cream to slightly buff	Thin-walled, branched	Fusoid, 25–29 × 2–3 µm; clavate, 20–25.5 × 4.5–5.5 µm	Subclavate, 23–29 × 2.5–3.5 µm	Ellipsoid, 4.5–7 × (2.5–)3–4 µm	**Present study**
Lyomyces wuliangshanensis	Tuberculate/ cream to buff	Thick-walled/ branched	Capitate, 22–37 × 3–6 µm; tapering, 21–35 × 4–6.5 µm	Clavate, 12–20 × 3–4.3 µm	Ellipsoid, (3.3–)3.5–5.3(–5.5) × 2.8–4(–4.2) µm	Chen and Zhao (2020)
Lyomyces wumengshanensis	Grandinioid/ white to cream	Thick-walled/ branched	Capitate, 24.5–29 × 3–4 µm	Subclavate to barreled, 11.5–14 × 5.5–6.5 µm	Ellipsoid to broad ellipsoid, 4–6 × 3–5 µm	**Present study**
Lyomyces yunnanensis	Grandinioid/ cream to buff	Thick-walled, frequently branched	Tapering, 18–39 × 4–6 µm; capitate, 16–23.5 × 3–5 µm	Clavate, 16.5–27 × 4–5.5 µm	Ellipsoid, (4.5–)5–7 × 3–4.5 µm	Guan et al. (2023)
Lyomyces zhaotongensis	Grandinioid/ cream to buff	Thick-walled/ branched	Fusoid, 16–20.5 × 2.5–3.5 µm	Clavate, 14–16.5 × 2.5–3.5 µm	Broadly ellipsoid, 2.6–3.5 × 2.5–3 µm	**Present study**

al. 2023; Yang et al. 2023; Deng et al. 2024a, b; Yang et al. 2024; Zhang et al. 2024; Zhou et al. 2024). Four new species in the present study are described, based on morphological and molecular phylogenetic analyses, also from the subtropics. This study enriches the wood-inhabiting fungal diversity in China and the world.

Additional information

Conflict of interest

The authors have declared that no competing interests exist.

Ethical statement

No ethical statement was reported.

Funding

The research was supported by the National Natural Science Foundation of China (Project No. 32170004, U2102220), Forestry Innovation Programs of Southwest Forestry University (Grant No: LXXK-2023Z07), the High-level Talents Program of Yunnan Province (YNQR-QNRC-2018-111).

Author contributions

Conceptualization, C.Z.; methodology, C.Z. and Q.Y.; software, C.Z.; validation, C.Z.and Q.Y.; formal analysis, C.Z. and Q.Y.; investigation, C.Z., Q.Y., Y.D. Y.L., K.W. and Y.W.; resources, C.Z.; writing—original draft preparation, C.Z. and Q.Y.; writing—review and editing, C.Z. and Q.Y.; visualization, C.Z. and Q.Y.; supervision, C.Z.; project administration, C.Z.; funding acquisition, C.Z. All authors have read and agreed to the published version of the manuscript.

Author ORCIDs

Qi Yuan https://orcid.org/0000-0002-6732-1656
Yunchao Li https://orcid.org/0009-0007-3500-3761
Yunfei Dai https://orcid.org/0009-0007-7734-4142
Kunyan Wang https://orcid.org/0009-0004-1678-9963
Changlin Zhao https://orcid.org/0000-0002-8668-1075

Data availability

All of the data that support the findings of this study are available in the main text.

References

Bernicchia A, Gorjón SP (2010) Fungi Europaei 12: Corticiaceae s.l. Edizioni Candusso, Alassio, Italy, 1008 pp.

Bian LS, Wu F, Dai YC (2016) Two new species of *Coltricia* (Hymenochaetaceae, Basidiomycota) from Southern China based on evidence from morphology and DNA sequence data. Mycological Progress 15: 27. https://doi.org/10.1007/s11557-016-1173-0

Chen JZ, Zhao CL (2020) Morphological and molecular identification of four new resupinate species of *Lyomyces* (Hymenochaetales) from southern China. Mycokeys 65: 101–118. https://doi.org/10.3897/mycokeys.65.48660

Chen CC, Wu SH, Chen CY (2017) Three new species of *Hyphodontia* s.l. (Basidiomycota) with poroid or raduloid hymenophore. Mycological Progress 16(5): 553–564. https://doi.org/10.1007/s11557-017-1286-0

Cui BK, Li HJ, Ji X, Zhou JL, Song J, Si J, Yang ZL, Dai YC (2019) Species diversity, taxonomy and phylogeny of Polyporaceae (Basidiomycota) in China. Fungal Diversity 97(1): 137–392. https://doi.org/10.1007/s13225-019-00427-4

Cunningham GH (1959) Hydnaceae of New Zealand. Part II. The genus *Odontia*. Transactions of the Royal Society of New Zealand 86: 65–103.

Cunningham GH (1963) The Thelephoraceae of Australia and New Zealand. Bulletin of the New Zealand Department of Scientific and Industrial Research 145: 1–359.

Dai YC (2010) Hymenochaetaceae (Basidiomycota) in China. Fungal Diversity 45(1): 131–343. https://doi.org/10.1007/s13225-010-0066-9

Dai YC (2011) A revised checklist of corticioid and hydnoid fungi in China for 2010. Mycoscience 52(1): 69–79. https://doi.org/10.1007/S10267-010-0068-1

Dai YC (2012) Polypore diversity in China with an annotated checklist of Chinese polypores. Mycoscience 53(1): 49–80. https://doi.org/10.1007/s10267-011-0134-3

Deng YL, Jabeen SN, Zhao CL (2024a) Species diversity and taxonomy of *Vararia* (Russulales, Basidiomycota) with descriptions of six species from Southwestern China. MycoKeys 103: 97–128. https://doi.org/10.3897/mycokeys.103.118980.

Deng YL, Li JF, Zhao CL, Zhao J (2024b) Four new fungal species in forest ecological system from southwestern China. Journal of Fungi 10: 194. https://doi.org/10.3390/jof10030194

Dong JH, Li Q, Yuan Q, Luo YX, Zhang XC, Dai YF, Zhou Q, Liu XF, Deng YL, Zhou HM, Muhammad A, Zhao CL (2024) Species diversity, taxonomy, molecular systematics and divergence time of wood-inhabiting fungi in Yunnan-Guizhou Plateau, Asia. Mycosphere 15: 1110–1293. https://doi.org/10.5943/mycosphere/15/1/10

Felsenstein J (1985) Confidence intervals on phylogenetics: An approach using bootstrap. Evolution. International Journal of Organic Evolution 39(4): 783–791. https://doi.org/10.2307/2408678

Gafforov Y, Riebesehl J, Ordynets A, Langer E, Yarasheva M, Ghobad-Nejhad M, Zhou LW, Wang XW, Gugliotta AM (2017) *Hyphodontia* (Hymenochaetales, Basidiomycota) and similar taxa from Central Asia. Botany 95(11): 1041–1056. https://doi.org/10.1139/cjb-2017-0115

Gilbertson RL, Ryvarden L (1987) North American polypores 1–2. Fungiflora, Oslo, 433 pp.

Guan QX, Zhao TJ, Zhao CL (2020) Morphological characters and phylogenetic analyses reveal two new species of *Peniophorella* from Southern China. Mycological Progress 19: 397–404. https://doi.org/10.1007/s11557-020-01568-6

Guan QX, Huang J, Huang J, Zhao CL (2023) Five new species of Schizoporaceae (Basidiomycota, Hymenochaetales) from East Asia. MycoKeys 96: 25–56. https://doi.org/10.3897/mycokeys.96.99327

He SH, Li HJ (2013) *Pseudochaete latesetosa* and *P. subrigidula* spp. nov. (Hymenochaetales, Basidiomycota) from China based on morphological and molecular characters. Mycological Progress 12(2): 331–339. https://doi.org/10.1007/s11557-012-0838-6

He MQ, Zhao RL, Hyde KD, Begerow D, Kemler M, Yurkov A, McKenzie EHC (2019) Notes, outline and divergence times of Basidiomycota. Fungal Diversity 99: 105–367. https://doi.org/10.1007/s13225-019-00435-4

He MQ, Cao B, Liu F, Boekhout T, Denchev TT, Schoutteten N, Denchev CM, Kemler M, Gorjón SP, Begerow D and Valenzuela R (2024) Phylogenomics, divergence times and notes of orders in Basidiomycota. Fungal diversity 126: 127–406. https://doi.org/10.1007/s13225-024-00535-w

Hjortstam K, Ryvarden L (2004) Some new and noteworthy corticioid fungi (Basidiomycotina, Aphyllophorales) from Japan. Synopsis Fungorum 18: 8–13.

Hjortstam K, Ryvarden L (2009) A checklist of names in *Hyphodontia* sensu stricto-sensu lato and *Schizopora* with new combinations in *Lagarobasidium*, *Lyomyces*, *Kneiffiella*, *Schizopora*, and *Xylodon*. Synopsis Fungorum 26: 33–55.

Hu Y, Karunarathna SC, Li H, Galappaththi MC, Zhao CL, Kakumyan P, Mortimer PE (2022) The impact of drying temperature on basidiospore size. Diversity 14(4): 239. https://doi.org/10.3390/d14040239

Huang RX, Zhao CL (2020) Three new species of *Phlebia* (Polyporales, Basidiomycota) based on the evidence from morphology and DNA sequence data. Mycological Progress 19, 753–767. https://doi.org/10.1007/s11557-020-01591-7

Hyde KD (2022) The numbers of fungi. Fungal Diversity 114(1): 1. https://doi.org/10.1007/s13225-022-00507-y

Ji X, Sun YF, Wu DM, Gao N, Cui BK (2023) An updated phylogenetic assessment and taxonomic revision of *Perenniporia* sensu lato (Polyporales, Basidiomycota). Journal of Fungi 9: 173. https://doi.org/10.3390/jof9020173

Jiang N, Voglmayr H, Bian DR, Piao CG, Wnag SK, Li Y (2021) Morphology and phylogeny of *Gnomoniopsis* (Gnomoniaceae, Diaporthales) from fagaceae leaves in China. Journal of Fungi 7(10): 792. https://doi.org/10.3390/jof7100792

Kan YH, Gafforov Y, Li T, Zhou LW (2017a) *Hyphodontia zhixiangii* sp. nov. (Schizoporaceae, Basidiomycota) from Uzbekistan. Phytotaxa 299(2): 273–279. https://doi.org/10.11646/phytotaxa.299.2.12

Kan YH, Qin WM, Zhou LW (2017b) *Hyphodontia mollissima* sp. nov. (Schizoporaceae, Hymenochaetales) from Hainan, southern China. Mycoscience 58(4): 297–301. https://doi.org/10.1016/j.myc.2017.04.003

Karsten PA (1881) Enumeratio Thelephorearum Fr. et Clavariearum Fr. Fennicarum, systemate novo dispositarum. Revue Mycologique Toulouse 3: 21–23.

Karsten PA (1882) Rysslands, Finlands och den Skandinaviska halföns Hattsvampar. Sednare Delen: Pip-, Tagg-, Hud-, Klubboch Gelésvampar. Bidrag till Kännedom av Finlands Natur och. Folk 37: 1–257.

Katoh K, Rozewicki J, Yamada KD (2019) MAFFT online service: Multiple sequence alignment, interactive sequence choice and visualization. Briefings in Bioinformatics 20(4): 1160–1166. https://doi.org/10.1093/bib/bbx108

Langer E (1994) Die Gattung *Hyphodontia* John Eriksson. Bibliotheca Mycologica, Schweizerbart Science Publishers, Stuttgart, Germany, Vol. 154, 298 pp.

Larsson A (2014) AliView: A fast and lightweight alignment viewer and editor for large data sets. Bioinformatics 30(22): 3276–3278. https://doi.org/10.1093/bioinformatics/btu531

Larsson KH, Larsson E, Kõljalg U (2004) High phylogenetic diversity among corticioid homobasidiomycetes. Mycological Research 108(9): 983–1002. https://doi.org/10.1017/S0953756204000851

Larsson KH, Parmasto E, Fischer M, Langer E, Nakasone KK, Redhead SA (2006) Hymenochaetales: A molecular phylogeny for the hymenochaetoid clade. Mycologia, 98: 926–936. https://doi.org/10.1080/15572536.2006.11832622

Lentz PL, McKay HH (1976) Basidiocarp and culture descriptions of *Hyphoderma* and *Hyphodontia* (Corticiaceae) in the Mississippi Delta Region. Memoirs of the New York Botanical Garden 28: 141–162.

Liu S, Shen LL, Xu TM, Song CG, Gao N, Wu DM, Sun YF, Cui BK (2023) Global diversity, molecular phylogeny and divergence times of the brown-rot fungi within the Polyporales. Mycosphere 14: 1564–1664. https://doi.org/10.5943/mycosphere/14/1/18

Luo KY, Zhao CL (2021) *Fasciodontia yunnanensis* (Schizoporaceae, Hymenochaetales), a new species from southern China. Annales Botanici Fennici 58(4–6): 259–266. https://doi.org/10.5735/085.058.0411

Luo KY, Qu MH, Zhao CL (2021a) Additions to the knowledge of Corticioid *Xylodon* (Schizoporaceae, Hymenochaetales): Introducing three new *Xylodon* species from southern China. Diversity 13(11): 581. https://doi.org/10.3390/d13110581

Luo X, Chen YH, Zhao CL (2021b) *Lyomyces fissuratus* and *L. fumosus* (Schizoporaceae, Hymenochaetales), new species from southern China. Annales Botanici Fennici 4(4–6): 58. https://doi.org/10.5735/085.058.0404

Luo X, Chen YH, Zhao CL (2021c) Morphological and phylogenetic characterization of fungi within Hymenochaetales: Introducing two new species from southern China. Nordic Journal of Botany 12(12): 39. https://doi.org/10.1111/njb.03414

Luo KY, Chen ZY, Zhao CL (2022) Phylogenetic and taxonomic analyses of three new woodinhabiting Fungi of *Xylodon* (Basidiomycota) in a Forest Ecological System. Journal of Fungi (Basel, Switzerland) 8(4): 405. https://doi.org/10.3390/jof8040405

Ma X, Zhao CL (2019) *Crepatura ellipsospora* gen. et sp. nov. in Phanerochaetaceae (Polyporales, Basidiomycota) bearing a tuberculate hymenial surface. Mycological Progress 18: 785–793. https://doi.org/10.1007/s11557-019-01488-0

Miller MA, Pfeiffer W, Schwartz T (2012) The CIPRES Science Gateway: Enabling high-impact science for phylogenetics researchers with limited resources. Association for Computing Machinery 39: 1–8. https://doi.org/10.1145/2335755.2335836

Núñez M, Ryvarden L (2001) East Asian polypores 2. Synopsis Fungorum 14: 165–522.

Nylander JAA (2004) MrModeltest v.2. Program Distributed by the Author; Evolutionary Biology Centre, Uppsala University, Uppsala, Sweden.

Petersen JH (1996) The Danish Mycological Society's colour-chart. Foreningen til Svampekundskabens Fremme, Greve.

Qu MH, Zhao CL (2022) *Xylodon flocculosus* sp. nov. from Yunnan, China. Mycotaxon 137(2): 189–201. https://doi.org/10.5248/137.189

Qu MH, Wang DQ, Zhao CL (2022) A phylogenetic and taxonomic study on *Xylodon* (Hymenochaetales): Focusing on three new *Xylodon* species from southern China. Journal of Fungi 8(1): 35. https://doi.org/10.3390/jof8010035

Rabenhorst GL (1851) Klotzschii herbarium vivum mycologicum sistens fungorum per totam Germaniam crescentium collectionem perfectam. Editio prima. Centuria 8: 1501–1600.

Rathnayaka AR, Tennakoon DS, Jones GE, Wanasinghe DN, Bhat DJ, Priyashantha A HAH, Stephenson SL, Tibpromma S, Karunarathna SC (2024) Significance of precise documentation of hosts and geospatial data of fungal collections, with an emphasis on plant-associated fungi. New Zealand Journal of Botany 1–28. https://doi.org/10.1080/0028825X.2024.2381734

Rehner SA, Samuels GJ (1994) Taxonomy and phylogeny of *Gliocladium* analysed from nuclear large subunit ribosomal DNA sequences. Mycological Research 98(6): 625–634. https://doi.org/10.1016/S0953-7562(09)80409-7

Riebesehl J, Langer E (2017) *Hyphodontia* s.l. (Hymenochaetales, Basidiomycota): 35 new combinations and new keys to currently all 120 species. Mycological Progress 16(6): 637–666. https://doi.org/10.1007/s11557-017-1299-8

Riebesehl J, Yurchenko E, Nakasone KK, Langer E (2019) Phylogenetic and morphological studies in *Xylodon* (Hymenochaetales, Basidiomycota) with the addition of four new species. MycoKeys 47: 97–137. https://doi.org/10.3897/mycokeys.47.31130

Ronquist F, Teslenko M, van der Mark P, Ayres DL, Darling A, Hohna S, Larget B, Liu L, Suchard MA, Huelsenbeck JP (2012) MrBayes 3.2: Efficient Bayesian phylogenetic inference and model choice across a large model space. Systematic Biology 61(3): 539–542. https://doi.org/10.1093/sysbio/sys029

Ryvarden L, Melo I (2014) Poroid fungi of Europe. Synopsis Fungorum 31: 1–455.

Viner I, Miettinen O (2022) *Lyomyces denudatus*, a new species with a disjunct distribution. Lilloa 59: 377–385. https://doi.org/10.30550/j.lil/2022.59.S/2022.09.14

Viner I, Spirin V, Zíbarová L, Larsson KH (2018) Additions to the taxonomy of *Lagarobasidium* and *Xylodon* (Hymenochaetales, Basidiomycota). MycoKeys 41: 65–90. https://doi.org/10.3897/mycokeys.41.28987

Viner I, Bortnikov F, Miettinen O (2022) On six African species of *Lyomyces* and *Xylodon*. Fungal Systematics and Evolution 8: 163–178. https://doi.org/10.3114/fuse.2021.08.13

Wang M, Chen YY (2017) Phylogeny and taxonomy of the genus *Hyphodontia* (Hymenochaetales, Basidiomycota) in China. Phytotaxa 309(1): 45–54. https://doi.org/10.11646/phytotaxa.309.1.4

Wang XW, May TW, Liu SL, Zhou LW (2021) Towards a natural classification of *Hyphodontia* sensu lato and the trait evolution of basidiocarps within Hymenochaetales (Basidiomycota). Journal of Fungi (Basel, Switzerland) 7(6): 478. https://doi.org/10.3390/jof7060478

White TJ, Bruns T, Lee S, Taylor J (1990) Amplification and direct sequencing of fungal ribosomal RNA genes for phylogenetics. In: Innis MA, Gelfand DH, Sninsky JJ, White TJ (Eds) PCR protocols: A Guide to Methods and Applications. Academic Press, San Diego, CA, 315–322. https://doi.org/10.1016/B978-0-12-372180-8.50042-1

Wijayawardene NN, Hyde KD, Al-Ani LKT, Tedersoo L, Haelewaters D, Rajeshkumar KC, et al. (2020) Outline of Fungi and fungus-like taxa. Mycosphere 11(1): 1060–1456. https://doi.org/10.5943/mycosphere/11/1/8

Wu SH (1990) The Corticiaceae (Basidiomycetes) subfamilies Phlebioideae, Phanerochaetoideae and Hyphodermoideae in Taiwan. Acta Botanica Fennica 142: 1–123.

Wu F, Zhou LW, Vlasák J, Dai YC (2022a) Global diversity and systematics of Hymenochaetaceae with poroid hymenophore. Fungal Diversity 113(1): 1–192. https://doi.org/10.1007/s13225-021-00496-4

Wu F, Man XW, Tohtirjap A, Dai YC (2022b) A comparison of polypore fungal and species composition in forest ecosystems of China, North America, and Europe. Forest Ecosystems 9: 100051. https://doi.org/10.1016/j.fecs.2022.100051

Xiong HX, Dai YC, Wu SH (2009) Three new species of *Hyphodontia* from Taiwan. Mycological Progress 8(3): 165–169. https://doi.org/10.1007/s11557-009-0587-3.

Yang Y, Jiang QQ, Li Q, Yang JW, Cha L, Cheng LJ, Yang SQ, Zhao CL (2023) Zhou, H.M. Molecular systematics and taxonomic analyses of three new wood-inhabiting fungi of *Hyphoderma* (Hyphodermataceae,Basidiomycota). Journal of Fungi 9: 1044. https://doi.org/10.3390/jof9111044

Yang Y, Li R, Jiang QQ, Zhou HM, Muhammad A, Wang HJ, Zhao CL (2024) Phylogenetic and taxonomic analyses reveal three new wood-inhabiting fungi (Polyporales, Basidiomycota) in China. Journal of Fungi 10: 55. https://doi.org/10.3390/jof10010055

Yuan Q, Luo KY, Zhang Y, Zhao CL (2023) Morphological characteristics and phylogenetic analyses revealed three new wood-inhabiting fungi (Agaricomycetes, Basidiomycota) in Southern China. Phytotaxa 592: 179–195. https://doi.org/10.11646/phytotaxa.592.3.1

Yurchenko E, Wu SH (2013) Three new species of *Hyphodontia* with peg-like hyphal aggregations. Mycological Progress 13(3): 533–545. https://doi.org/10.1007/s11557-013-0935-1

Yurchenko E, Wu SH (2016) A key to the species of *Hyphodontia* sensu lato. MycoKeys 12: 1–27. https://doi.org/10.3897/mycokeys.12.7568

Yurchenko E, Xiong HX, Wu SH (2013) Four new species of *Hyphodontia* (*Xylodon* ss. Hjortstam & Ryvarden, Basidiomycota) from Taiwan. Nova Hedwigia 96(3–4): 545–558. https://doi.org/10.1127/0029-5035/2013/0092

Yurchenko E, Riebesehl J, Langer E (2017) Clarification of *Lyomyces sambuci* complex with the descriptions of four new species. Mycological Progress 16(9): 865–876. https://doi.org/10.1007/s11557-017-1321-1

Yurchenko E, Riebesehl J, Langer E (2020) *Fasciodontia* gen. nov. (Hymenochaetales, Basidiomycota) and the taxonomic status of *Deviodontia*. Mycological Progress 19(2): 171–184. https://doi.org/10.1007/s11557-019-01554-7

Yurchenko E, Riebesehl J, Viner I, Motato-Vásquez V, Miettinen O (2024) *Xylodon lanatus* complex and other additions to *Xylodon*. Mycological Progress 23: 9. https://doi.org/10.1007/s11557-024-01947-3

Zhang XC, Li YC, Wang YY, Xu Z, Zhao CL, Zhou HM (2024) *Xylodon asiaticus* (Hymenochaetales, Basidiomycota), a new species of corticioid fungus from southern China. Phytotaxa 634: 1–15. https://doi.org/10.11646/phytotaxa.634.1.1

Zhao CL, Wu ZQ (2017) *Ceriporiopsis kunmingensis* sp. nov. (Polyporales, Basidiomycota) evidenced by morphological characters and phylogenetic analysis. Mycological Progress 16: 93–100. https://doi.org/10.1007/s11557-016-1259-8

Zhao CL, He XS, Wanghe KY, Cui BK, Dai YC (2014) *Flammeopellis bambusicola* gen. et. sp. nov. (Polyporales, Basidiomycota) evidenced by morphological characters and phylogenetic analysis. Mycological Progress 13: 771–780. https://doi.org/10.1007/s11557-014-0960-8

Zhao CL, Chen H, Song J, Cui BK (2015) Phylogeny and taxonomy of the genus *Abundisporus* (Polyporales, Basidiomycota). Mycological Progress 14: 38. https://doi.org/10.1007/s11557-015-1062-y

Zhao CL, Wu F, Dai YC (2016) *Leifiporia rhizomorpha* gen. et sp. nov. and *L. eucalypti* comb. nov. in Polyporaceae (Basidiomycota). Mycological Progress 15: 799–809. https://doi.org/10.1007/s11557-016-1210-z

Zhao CL, Qu MH, Huang RX, Karunarathna SC (2023) Multi-Gene Phylogeny and Taxonomy of the Wood-Rotting Fungal Genus *Phlebia* sensu lato (Polyporales, Basidiomycota). Journal of Fungi 9: 320. https://doi.org/10.3390/jof9030320

Zhou Q, Jiang QQ, Yang X, Yang JW, Zhao CL, Zhao J (2024) Phylogenetic and taxonomic analyses of five new wood-inhabiting fungi of *Botryobasidium*, *Coltricia* and *Coltriciella* (Basidiomycota) from China. Journal of Fungi 10: 205. https://doi.org/10.3390/jof10030205

MycoKeys 110: 93–115 (2024)
DOI: 10.3897/mycokeys.110.135538

Research Article

Ophiostomatalean fungi associated with *Polygraphus* bark beetles in the Qinghai-Tibet Plateau, China

Zheng Wang[1], Caixia Liu[2], Xiuyue Song[1], Yingjie Tie[1], Huimin Wang[2], Huixiang Liu[1], Quan Lu[2]

1 *Shandong Research Center for Forestry Harmful Biological Control Engineering and Technology, College of Plant Protection, Shandong Agricultural University, Tai'an 271018, China*

2 *Key Laboratory of Forest Protection of National Forestry and Grassland Administration, Ecology and Nature Conservation Institute, Chinese Academy of Forestry, Beijing 100091, China*

Corresponding author: Quan Lu (luquan@caf.ac.cn)

Abstract

Climate change has exacerbated outbreaks of forest pests worldwide. In recent years, bark beetles have caused significant damage to coniferous forests of the Northern Hemisphere. *Polygraphus* bark beetles are widely distributed secondary pests. Recently, tree mortality caused by these beetles on the Qinghai-Tibet Plateau has been increasing; however, few studies have focused on their fungal associations. In the present study, we explored the diversity of ophiostomatalean fungi associated with these beetles on the north-eastern and southern Qinghai-Tibet Plateau. We isolated 442 ophiostomatalean strains from adult beetles and their fresh galleries, specifically targeting *Polygraphus poligraphus* and *Polygraphus rudis* infesting *Picea crassifolia* and/or *Pinus griffithii*. Based on phylogenetic and morphological features, we assigned the 442 strains to 16 species belonging to *Grosmannia* spp., *Leptographium* spp. and *Ophiostoma* spp. Amongst these, *Ophiostoma maixiuense* and *Ophiostoma bicolor* were the most frequently isolated species, accounting for 20.8% and 18.1% of the total number of ophiostomatalean assemblages, respectively. By comparing their fungal communities, we found that the different patterns of fungal assemblages of bark beetles from the north-eastern and southern Qinghai-Tibet Plateau may be influenced by biogeographic barriers and host tree species. The results of this study enhance our understanding of bark beetle fungal assemblages, especially *Polygraphus*, on the Qinghai–Tibet Plateau, with implications for forest management under changing climate.

Key words: Conifer, forest pest, *Grosmannia*, *Leptographium*, *Ophiostoma*, pine, spruce, symbiosis

Academic editor: Xinlei Fan
Received: 26 August 2024
Accepted: 8 October 2024
Published: 1 November 2024

Citation: Wang Z, Liu C, Song X, Tie Y, Wang H, Liu H, Lu Q (2024) Ophiostomatalean fungi associated with *Polygraphus* bark beetles in the Qinghai-Tibet Plateau, China. MycoKeys 110: 93–115. https://doi.org/10.3897/mycokeys.110.135538

Introduction

Extreme heat and frequent droughts driven by climate change have exacerbated forest pest outbreaks (Biedermann et al. 2019). Recently, bark beetles have inflicted severe damage on coniferous forests across the Northern Hemisphere. In Europe, *Ips typographus* continues to devastate spruce forests, while the frequency of *Ips acuminatus* outbreaks has increased, leading to significant pine tree mortality (Popkin 2021; Papek et al. 2024). A similar trend has been

observed in North America, where elevated temperatures have removed climatic barriers, enabling the northward spread of the aggressive beetles *Dendroctonus frontalis* and *Dendroctonus ponderosae*, which now threaten additional pine forest species and regions (Bentz and Jönsson 2015; Lesk et al. 2017). In China, the Qinghai-Tibet Plateau has not been spared from bark beetle infestations, with species such as *Dendroctonus*, *Ips* and *Polygraphus* causing significant damage (Yin et al. 2016; Wang et al. 2021, 2023). There is growing evidence that fungal symbionts play a crucial role in the ability of bark beetles to respond to climate change and cause tree mortality (Netherer et al. 2021). Despite this, the fungal communities associated with some of these beetles remain poorly understood.

Ophiostomatoid fungi, the most well-known fungal partners of bark beetles, belong to the orders Ophiostomatales (Sordariomycetidae, Sordariomycetes, Ascomycota) and Microascales (Hypocreomycetidae, Sordariomycetes, Ascomycota) (De Beer et al. 2013). Amongst these, the Ophiostomatales is the most diverse group associated with bark beetles, with over 300 species reported across 20 genera (De Beer et al. 2022). The genera *Ophiostoma*, *Leptographium* and *Grosmannia* are particularly notable for their species diversity, close symbiotic relationships with insect vectors and inclusion of species that act as virulent pathogens in host trees. *Ophiostoma* is an ancient genus first described by Sydow and Sydow (1919) and its taxonomy has undergone considerable revision since then. Advances in DNA-based taxonomy and the implementation of the "one fungus, one name" nomenclature have clarified the taxonomic status of this genus. Zipfel et al. (2006) demonstrated that *Ceratocystiopsis* and *Grosmannia* are distinct from *Ophiostoma*, based on multi-gene phylogenies of ribosomal DNA and β-tubulin sequences. Subsequently, *Sporothrix*, which was previously considered part of *Ophiostoma*, was recognised as a separate genus, based on four-gene phylogenies and *sporothrix*-like asexual morphs (De Beer et al. 2016). The taxonomic boundaries between *Grosmannia* and *Leptographium* were historically blurred, but new species in the *Grosmannia penicillata* complex were later described under the genus *Grosmannia* (De Beer and Wingfield 2013; Yin et al. 2020). Today, these two genera are clearly distinguished, based on genome-wide sequence data (de Beer et al. 2022). Additionally, *Heinzbutinia*, *Jamesreidia* and *Masuyamyces* have been recognised as distinct from *Ophiostoma*. The current taxonomic framework for ophiostomatalean fungi, which is considered the most authoritative, defines *Ophiostoma*, *Leptographium* and *Grosmannia* as comprising six complexes and four groups, eight complexes and two groups and two complexes and one group, respectively (De Beer et al. 2022).

Many ophiostomatoid fungi have been shown to play a positive role in the success of conifer bark beetles, mainly by producing beetle semio-chemicals, exhausting tree defences, providing nutrition and promoting environmental adaptation (Raffa et al. 2015). *Grosmannia penicillata* and *Leptographium europhioides* were found to synthesise the beetle aggregation pheromone 2-methyl-3-buten-2-ol and similar functions have been demonstrated in a variety of ophiostomatoid fungi, indicating their ability to regulate beetle mass attacks (Zhao et al. 2015; Kandasamy et al. 2019, 2023). In contrast, *Endoconidiophora polonica* can skilfully degrade the phenolic defence compounds of spruce as a carbon source (Wadke et al. 2016), indirectly providing nutrients for its vector,

I. typographus. Fungal associates of *D. ponderosae*, *Leptographium clavigerum*, have been shown to contribute to host mortality by triggering the pine tree myriad defence responses (Fortier et al. 2024). Interestingly, the expression of high-altitude adaption-related genes in *Ips nitidus* was upregulated after feeding on *Ophiostoma bicolor*, suggesting that fungal symbionts may promote the adaptation of insect vectors to extreme environments (Wang et al. 2023).

The genus *Polygraphus* is a secondary pest; however, in recent years, it has been reported to cause an increase in tree mortality in Eurasian coniferous forests (Yin et al. 1984; Viklund et al. 2019). This genus is widely distributed in China and mainly attacks conifers, with a few species using hardwoods as a host (Yin et al. 1984). Only a few fungal associates of *Polygraphus* have been reported, most of which have been isolated from mites associated with beetles. Yin et al. (2016, 2019, 2020) successively reported seven ophiostomatalean species associated with *Polygraphus poligraphus*, three of which were subsequently isolated from beetle mite associates by Chang et al. (2020). In addition, 11 ophiostomatalean species have been isolated from mites associated with *Polygraphus aterrimus*, *P. poligraphus*, *Polygraphus szemaoensis*, *Polygraphus verrucifrons* and *Polygraphus* sp. in Yunnan and Qinghai Provinces (Chang et al. 2017, 2020). Overall, only 18 species from six genera (*Graphilbum*, *Grosmannia*, *Leptographium*, *Masuyamyces*, *Ophiostoma* and *Sporothrix*) associated with five *Polygraphus* beetles were recorded in the two Provinces (Table 1). Although 16 species of this genus have been recorded (Yin et al. 1984; Huang and Lu 2015), most of their fungal associates remain unknown.

Table 1. Ophiostomatalean fungi isolated from *Polygraphus* beetles and their mite associates reported from China.

Fungal species	Host	Beetle vector	Location	Reference[1]
Graphilbum kesiyae	*Pinus kesiya*	*Polygraphus* sp.; *P. aterrimus*; *P. szemaoensis*	Simao and Ning'er, Yunnan, China	Chang et al. (2017)*
Gra. puerense	*P. kesiya*	*P. szemaoensis*	Ning'er Yunnan, China	Chang et al. (2017)*
Grosmannia crassifolia	*Picea crassifolia*	*P. poligraphus*	Zeku, Qinghai, China	Yin et al. (2020)
G. maixiuense	*P. crassifolia*	*P. poligraphus*	Zeku, Qinghai, China	Yin et al. (2020)
G. xianmiense	*P. crassifolia*	*P. poligraphus*	Zeku and Menyuan, Qinghai, China	Yin et al. (2020); Chang et al. (2020)*
Leptographium breviscapum	*P. crassifolia*	*P. poligraphus*	Zeku, Qinghai, China	Yin et al. (2019); Chang et al. (2020)*
L. conjunctum	*P. kesiya*	*Polygraphus* sp.	Ning'er Yunnan, China	Chang et al. (2017)*
L. xiningense	*P. crassifolia*	*P. poligraphus*	Menyuan, Qinghai, China	Yin et al. (2019)
L. yunnanense	*P. kesiya*	*P. szemaoensis*; *Polygraphus* sp.	Ning'er Yunnan, China	Chang et al. (2017)*
Masuyamyces acarorum	*P. kesiya*	*P. szemaoensis*	Ning'er Yunnan, China	Chang et al. (2017)*
Ophiostoma ainoae	*P. crassifolia*	*P. poligraphus*	Zeku, Qinghai, China	Yin et al. (2016); Chang et al. (2020)*
O. bicolor	*P. crassifolia*	*P. poligraphus*	Zeku, Qinghai, China	Chang et al. (2020)*
O. ips	*P. kesiya*	*P. szemaoensis*; *Polygraphus* sp.	Simao and Ning'er, Yunnan, China	Chang et al. (2017)*
O. nitidum	*P. crassifolia*	*P. poligraphus*	Zeku, Qinghai, China	Chang et al. (2020)*
O. qinghaiense	*P. crassifolia*	*P. poligraphus*	Zeku, Qinghai, China	Yin et al. (2016)
O. quercus	*P. kesiya*; *P. yunnanensis*	*P. verrucifrons*; *P. szemaoensis*	Simao and Ning'er, Yunnan, China	Chang et al. (2017)*
O. shangrilae	*P. crassifolia*	*P. poligraphus*	Zeku, Qinghai, China	Chang et al. (2020)*
Sporothrix nebularis	*P. kesiya*	*Polygraphus* sp.	Ning'er Yunnan, China	Chang et al. (2017)*

[1] *represents the references on fungal isolation from mites associated with *Polygraphus* beetles.

In the present study, a survey of fungi associated with *P. poligraphus* and *Polygraphus rudis* was conducted on the Qinghai-Tibet Plateau between 2019 and 2020. We sought to increase our understanding of the fungal assemblages associated with *Polygraphus* beetles, based on the accurate identification and comparison of fungal associates across geographic ranges, hosts and beetle vectors.

Materials and methods

Sample collection and isolation

Adult beetles of *P. poligraphus* and *P. rudis* and/or their galleries were collected during the emergence period from four sites on the north-eastern and southern Qinghai-Tibet Plateau from 2019 to 2020 (Suppl. material 1: table S1). The branches or trunks of the host tree damaged by the beetles were cut into one-metre-long logs and brought back to the laboratory. After peeling the bark, 15 vigorous adults and/or their fresh galleries were selected for fungal isolation from each *Polygraphus* species at each sampling site. Each adult was separated into approximately 15 tissue pieces and transferred to the surface of 2% water agar. The galleries were surface-disinfected with 1.5% sodium hypochlorite and then placed on the surface of 2% water agar. After incubation in the dark at 25 °C, single hyphal tips were transferred to the surface of 2% malt extract agar (MEA) medium to purify the fungal isolates. All strains were deposited in the culture collection at the Forest Pathology Laboratory of the Chinese Academy of Forestry (CXY). Representative strains were deposited at the China Forestry Culture Collection Center, Beijing, China (CFCC).

Morphological studies

The morphological structure of each pure culture was carefully observed using an Olympus BX43 microscope (Olympus Corporation, Tokyo, Japan) and recorded using a BioHD-A20c colour digital camera (FluoCa Scientific, China, Shanghai). For the holotype of the new species, we measured the lengths and widths of 30 reproductive structures and presented the following format: (minimum–) mean minus standard deviation–mean plus standard deviation (–maximum). 5-mm diameter agar plugs were transferred from the actively growing margin of fungal colonies and placed in the centre of a 90-mm-diameter Petri plate containing 2% MEA to conduct cultural character studies. Five replicates of culture were incubated at temperatures ranging from 5 °C to 40 °C at 5 °C intervals in darkness. The colony diameters were measured daily until the mycelia reached the margins of the Petri dishes. Culture features were observed and recorded daily until the colonies no longer showed any significant changes. All the data from the type specimens were deposited in MycoBank (www.MycoBank.org).

DNA extraction, PCR amplification and sequencing

Actively growing mycelia of each representative strain were collected for DNA extraction using an Invisorb Spin Plant Mini Kit (Tiangen, Beijing, China), following the manufacturer's instructions. The internal transcribed spacer regions 1 and 2 of the nuclear ribosomal DNA operon, including the 5.8S region (ITS), internal transcribed spacer 2, part of the 28S of the rDNA operon (ITS2-LSU), β-tubulin gene

region (*tub2*) and transcription elongation factor 1-α gene region (*tef1-α*) were amplified using the primer pairs of ITS1-F/ITS4 (White et al. 1990; Gardes and Bruns 1993), ITS3/LR3 (Vilgalys and Hester 1990; White et al. 1990), Bt2a/Bt2b (Glass and Donaldson 1995) or T10/Bt2b (O'Donnell and Cigelnik 1997) or EF1F/EF2R (Jacobs et al. 2004), respectively, using 2 × Taq PCR MasterMix (Tiangen, Beijing, China), following the manufacturer's instructions. PCR and sequencing were performed according to protocols described by Wang et al. (2020, 2021).

Phylogenetic analysis

Newly-obtained sequences were identified using a standard nucleotide BLAST search in NCBI and deposited in GenBank. Reference sequences in the phylogenetic analyses were confirmed, based on the BLAST results, relevant literature and sequences downloaded from GenBank. MAFFT v.7 (Katoh et al. 2019) was used to construct the multiple sequence alignment. Molecular Evolutionary Genetic Analyses (MEGA) 7.0 (Kumar et al. 2016) were used to edit and/or splice alignments to generate combined gene datasets.

Maximum Likelihood (ML) analyses were conducted using RAxML-HPC v.8.2.3 (Stamatakis 2014) with 1000 replicates using the GTRGAMMA model. The bootstrap support values of the nodes were estimated using 1,000 bootstrap replicates after retaining the best tree. jModelTest v.2.1.7 (Darriba et al. 2012) was used to determine the best substitution models for conducting Bayesian Inference (BI) analyses in MrBayes v. 3.1.2 (Ronquist and Huelsenbeck 2003). Four Markov Chain Monte Carlo (MCMC) chains were run simultaneously from a random starting tree for 10,000,000 generations. The trees were sampled every 100 generations. Posterior probabilities were calculated, based on the remaining trees after discarding the first 25% of the sampled trees. Phylogenetic trees were edited and polished using FigTree v.1.4.3 (http://tree.bio.ed.ac.uk/software/figtree/) and Adobe Illustrator CS6. The final sequence datasets were submitted to TreeBASE (31618).

Results

Sampling collection and fungal isolation

In the present study, 442 ophiostomatalean strains were isolated from 75 vigorous adult *Polygraphus* species and 180 fresh galleries of *Picea crassifolia* and *Pinus griffithii*. Morphological characterisations and *tub2* or ITS sequence features, based on standard nucleotide BLAST searches at GenBank, were used for preliminary identification. Subsequently, 49 representative strains were selected for detailed morphological and phylogenetic analyses (Table 2).

Phylogenetic analysis

Grosmannia spp. and *Leptographium* spp.

The ITS2-LSU dataset was used to construct phylogenetic inferences for the two genera. The dataset contained 610 characters, including gaps and the best evolutionary model for BI analysis was estimated to be GTR+I+G.

Table 2. Representative strains of ophiostomatalean fungi isolated from *Polygraphus* bark beetles in this study. [1] CFCC: the China Forestry Culture Collection Center; CXY: the culture collection at the Forest Pathology Laboratory of the Chinese Academy of Forestry.

Species	Taxon	Isolate no[1]	Host	Insect vector	Location	GenBank accession no		
						ITS or ITS2-LSU	tub2	tef1-α
Grosmannia								
G. penicillata complex								
G. crassifolia	1	CFCC57904	*Picea crassifolia*	*Polygraphus poligraphus*	Zeku, Qinghai, China	PQ166546	PQ166449	PQ166498
G. maixiuensis	2	CFCC57902	*P. crassifolia*	*P. poligraphus*	Zeku, Qinghai, China	PQ166547	PQ166450	PQ166499
		CFCC57903	*P. crassifolia*	*P. poligraphus*	Zeku, Qinghai, China	-	PQ166451	PQ166500
Grosmannia sp. 1	3	CFCC57905	*P. crassifolia*	*P. rudis*	Zeku, Qinghai, China	PQ166548	PQ166452	PQ166501
		CFCC57906	*P. crassifolia*	*P. rudis*	Zeku, Qinghai, China	-	PQ166453	PQ166502
		CFCC57907	*P. crassifolia*	*P. poligraphus*	Qilian, Qinghai, China	-	PQ166454	PQ166503
		CFCC57908	*P. crassifolia*	*P. poligraphus*	Qilian, Qinghai, China	-	PQ166455	PQ166504
Leptographium								
L. lundbergii complex								
L. griffithii	4	CFCC57893	*Pinus griffithii*	*P. rudis*	Yadong, Tibet, China	PQ166549	PQ166456	PQ166505
		CFCC57894	*P. griffithii*	*P. rudis*	Yadong, Tibet, China	-	PQ166457	PQ166506
		CFCC57895	*P. griffithii*	*P. rudis*	Yadong, Tibet, China	-	PQ166458	PQ166507
L. jilongense	5	CFCC57896	*P. griffithii*	*P. rudis*	Jilong, Tibet, China	PQ166550	PQ166459	PQ166508
L. pseudojilongense	6	CFCC57901	*P. griffithii*	*P. rudis*	Jilong, Tibet, China	PQ166551	PQ166460	PQ166509
		CXY3348	*P. griffithii*	*P. rudis*	Jilong, Tibet, China	-	PQ166461	PQ166510
		CXY3349	*P. griffithii*	*P. rudis*	Jilong, Tibet, China	-	PQ166462	PQ166511
L. yadongense	7	CFCC57897	*P. griffithii*	*P. rudis*	Yadong, Tibet, China	PQ166552	PQ166463	PQ166512
		CFCC57898	*P. griffithii*	*P. rudis*	Yadong, Tibet, China	-	PQ166464	PQ166513
		CFCC57899	*P. griffithii*	*P. rudis*	Yadong, Tibet, China	-	PQ166465	PQ166514
		CFCC57900	*P. griffithii*	*P. rudis*	Yadong, Tibet, China	-	PQ166466	PQ166515
L. olivaceum complex								
L. breviscapum	8	CFCC57890	*P. crassifolia*	*P. poligraphus*	Zeku, Qinghai, China	PQ166553	PQ166467	PQ166516
		CFCC57891	*P. crassifolia*	*P. poligraphus*	Zeku, Qinghai, China	-	PQ166468	PQ166517
		CFCC57892	*P. crassifolia*	*P. poligraphus*	Zeku, Qinghai, China	-	PQ166469	PQ166518
Ophiostoma								
O. clavatum complex								
O. pseudobrevipilosi	9	CFCC57916	*P. griffithii*	*P. rudis*	Yadong, Tibet, China	-	PQ166470	-
		CFCC57917	*P. griffithii*	*P. rudis*	Yadong, Tibet, China	PQ166530	PQ166471	-
		CFCC57918	*P. griffithii*	*P. rudis*	Yadong, Tibet, China	-	PQ166472	-
		CFCC57919	*P. griffithii*	*P. rudis*	Yadong, Tibet, China	-	PQ166473	-
O. stebbingi	10	CFCC57920	*P. griffithii*	*P. rudis*	Jilong, Tibet, China	-	PQ166474	PQ166519
		CFCC57921	*P. griffithii*	*P. rudis*	Jilong, Tibet, China	PQ166531	PQ166475	-
		CFCC57922	*P. griffithii*	*P. rudis*	Jilong, Tibet, China	-	PQ166476	-
Ophiostoma sp. 1	11	CFCC57923	*P. griffithii*	*P. rudis*	Jilong, Tibet, China	PQ166532	PQ166477	PQ166520
		CFCC57924	*P. griffithii*	*P. rudis*	Jilong, Tibet, China	-	PQ166478	-
		CFCC57925	*P. griffithii*	*P. rudis*	Jilong, Tibet, China	-	PQ166479	-
O. ips complex								
O. bicolor	12	CFCC57909	*P. crassifolia*	*P. poligraphus*	Zeku, Qinghai, China	PQ166533	PQ166480	-
		CFCC57910	*P. crassifolia*	*P. poligraphus*	Zeku, Qinghai, China	-	PQ166481	-
		CFCC57911	*P. crassifolia*	*P. poligraphus*	Zeku, Qinghai, China	-	PQ166482	-
		CFCC57912	*P. crassifolia*	*P. poligraphus*	Qilian, Qinghai, China	-	PQ166483	-
O. shigatsense	13	CFCC57913	*P. griffithii*	*P. rudis*	Jilong, Tibet, China	PQ166534	PQ166484	-
		CFCC57914	*P. griffithii*	*P. rudis*	Jilong, Tibet, China	-	PQ166485	-
		CFCC57915	*P. griffithii*	*P. rudis*	Jilong, Tibet, China	-	PQ166486	-

Species	Taxon	Isolate no[1]	Host	Insect vector	Location	GenBank accession no		
						ITS or ITS2-LSU	tub2	tef1-α
Group A								
O. maixiuense	14	CFCC57930	*P. griffithii*	*P. rudis*	Jilong, Tibet, China	PQ166535	PQ166487	-
		CFCC57931	*P. griffithii*	*P. rudis*	Jilong, Tibet, China	PQ166536	PQ166488	-
		CFCC57932	*P. crassifolia*	*P. poligraphus*	Zeku, Qinghai, China	PQ166537	PQ166489	-
		CFCC57933	*P. crassifolia*	*P. poligraphus*	Zeku, Qinghai, China	PQ166538	PQ166490	-
		CFCC57934	*P. griffithii*	*P. rudis*	Yadong, Tibet, China	PQ166539	PQ166491	-
		CFCC57935	*P. griffithii*	*P. rudis*	Yadong, Tibet, China	PQ166540	PQ166492	-
O. pacis	15	CFCC57936	*P. crassifolia*	*P. poligraphus*	Zeku, Qinghai, China	PQ166541	PQ166493	-
O. sanum	16	CFCC57926	*P. crassifolia*	*P. rudis*	Zeku, Qinghai, China	PQ166542	PQ166494	-
		CFCC57927	*P. crassifolia*	*P. rudis*	Zeku, Qinghai, China	PQ166543	PQ166495	-
		CFCC57928	*P. crassifolia*	*P. rudis*	Zeku, Qinghai, China	PQ166544	PQ166496	-
		CFCC57929	*P. crassifolia*	*P. rudis*	Zeku, Qinghai, China	PQ166545	PQ166497	-

The results showed that our eight representative isolates nested into three complexes, namely the *G. penicillata*, *L. lundbergii* and *L. olivaceum* complexes (Fig. 1). Amongst these, the *G. penicillata* complex belongs to *Grosmannia*, whereas the *L. lundbergii* and *L. olivaceum* complexes belong to *Leptographium*. Subsequently, we constructed the phylogenetic inference of *tub2*, *tef1-α* and the concatenated (*tub2*+*tef1-α*) datasets for each complex.

Grosmannia penicillata complex

The *tub2*, *tef1-α* and concatenated (*tub2*+*tef1-α*) datasets were aligned (containing 402, 694 and 1096 characters, including gaps, respectively) and used to construct the phylogenetic inference. The best models of the three datasets for BI analysis were estimated as HKY+I (*tub2* dataset) and GTR+G (*tef1-α* and concatenated datasets). Based on the concatenated tree (Fig. 2), the seven isolates formed three separate well-supported terminal clades, representing two known and one undescribed taxa: *G. crassifolia* (Taxon 1), *G. maixiuensis* (Taxon 2) and *Grosmannia* sp. 1 (Taxon 3). These three species formed a subclade with *G. chlamydata* and *G. nitidi* that was phylogenically consistent, based on the three datasets (Fig. 2, Suppl. material 2: figs S1, S2).

Leptographium lundbergii complex

The *tub2*, *tef1-α* and concatenated (*tub2*+*tef1-α*) datasets were aligned (containing 373, 666 and 1039 characters, including gaps, respectively) and used to construct the phylogenetic inference. The best models of the three datasets for BI analysis were SYM+I, HKY+G and GTR+G. Based on the concatenated tree (Fig. 3), our ten isolates formed four separate well-supported terminal clades, representing three known (Taxon 4: *L. griffithii*; Taxon 5: *L. jilongense*; Taxon 7: *L. yadongense*) and one undescribed (Taxon 6) taxa. Taxa 4, 5 and 6 were sister species and formed a subclade with *L. panxianense*, *L. yunnanensis*, *L. puerense*, *L. wushanense* and *L. conjunctum*, all of which were isolated from *Pinus* trees in southwest China (Fig. 3, Suppl. material 2: figs S3, S4). The four isolated strains were identical in sequence to the two strains isolated from *Ips schmutzenhoferi*, representing *L. yadongense*, which was a phylogenetic sister to *L. sejilanum* (Fig. 3, Suppl. material 2: figs S3, S4).

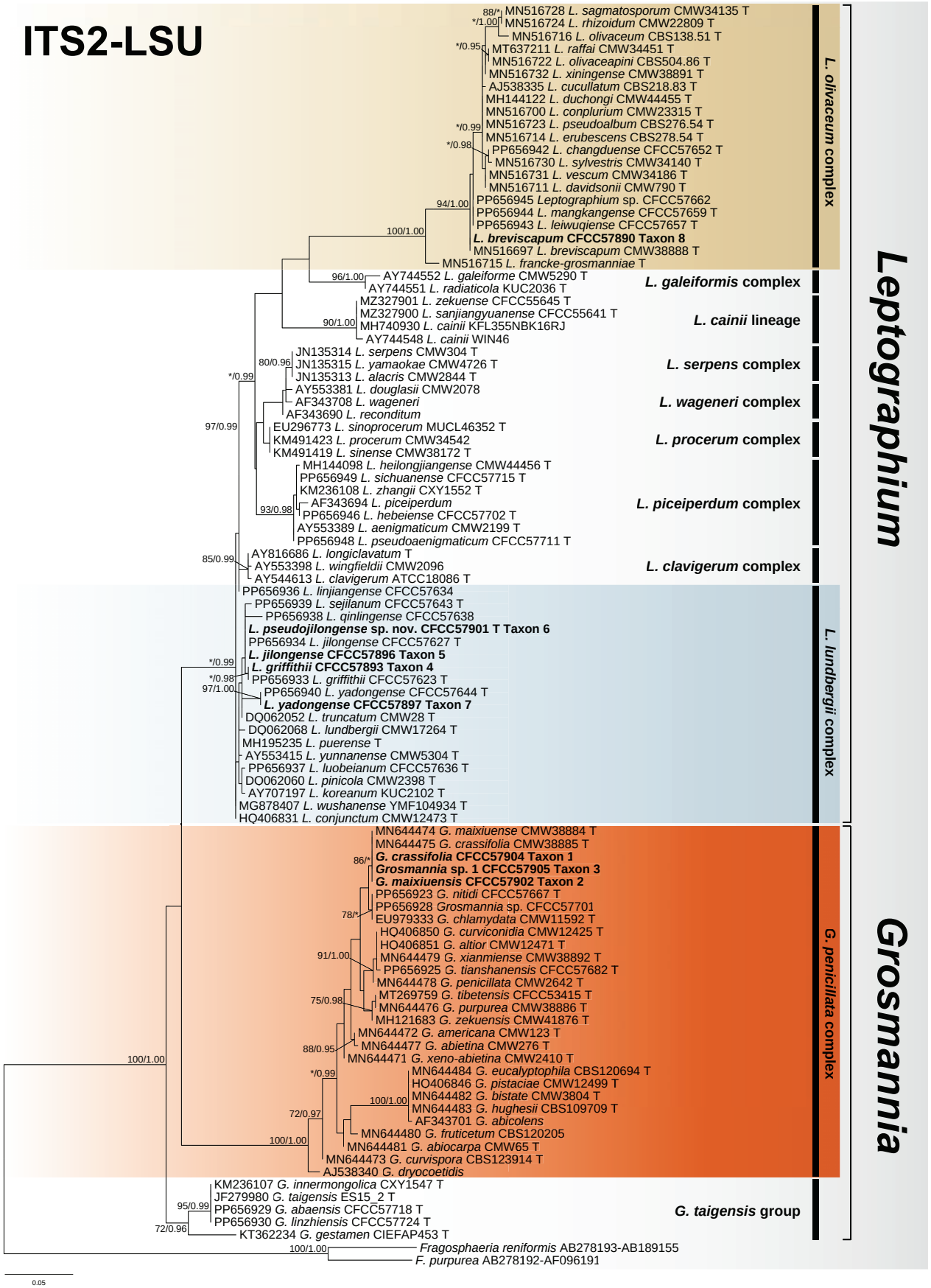

Figure 1. Phylogram of *Grosmannia* spp. and *Leptographium* spp. based on ITS2-LSU sequence data. The ML bootstrap support values ≥ 70% and posterior probability values ≥ 0.9 are recorded at the nodes. T = ex-type isolates.

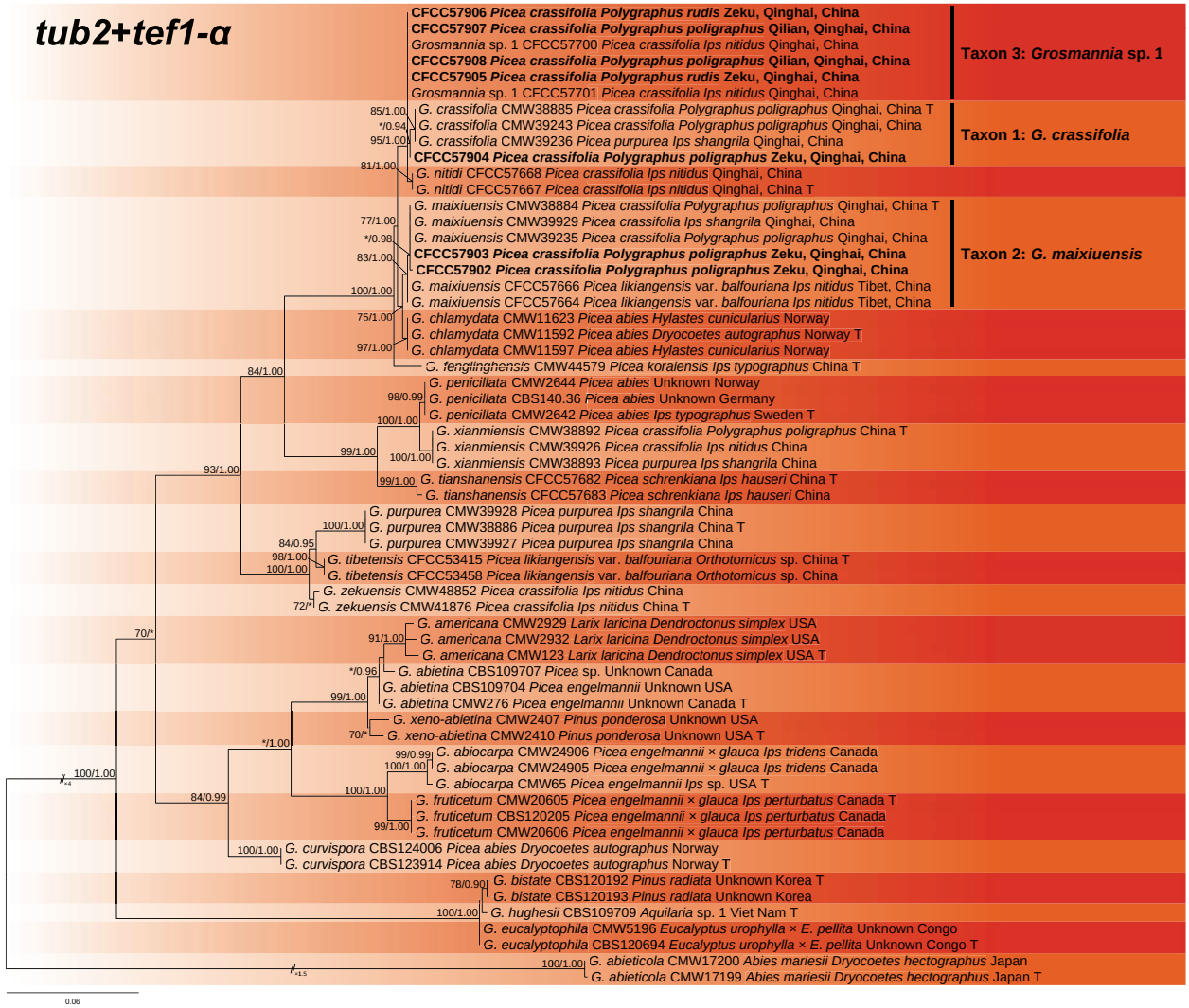

Figure 2. Phylogram of *Grosmannia penicillata* complex (including Taxa 1–3) based on combined (*tub2*+*tef1-α*) sequence data. The ML bootstrap support values ≥ 70% and posterior probability values ≥ 0.9 are recorded at the nodes. T = ex-type isolates.

Leptographium olivaceum complex

The *tub2*, *tef1-α* and concatenated (*tub2*+*tef1-α*) datasets were aligned (containing 278, 677 and 955 characters, including gaps, respectively) and used to construct the phylogenetic inference. The best models of the three datasets for BI analysis were estimated as (*tub2* dataset) and GTR+G (*tef1-α* and concatenated datasets). Based on the concatenated tree (Fig. 4), the three isolates formed a separate, well-supported, terminal clade representing *L. breviscapum* (Taxon 8). The 10 strains of *L. breviscapum* formed a subclade with *L. leiwuqiense*, *L. mangkangense* and *Leptographium* sp. 1, all of which were isolated from *Picea* trees on the Qinghai-Tibet Plateau (Fig. 4, Suppl. material 2: figs S5, S6).

Ophiostoma spp.

An ITS dataset was used to construct a phylogenetic inference for this genus. The dataset contained 743 characters, including gaps and the best evolutionary model for BI analysis was estimated to be GTR+I+G. The results showed

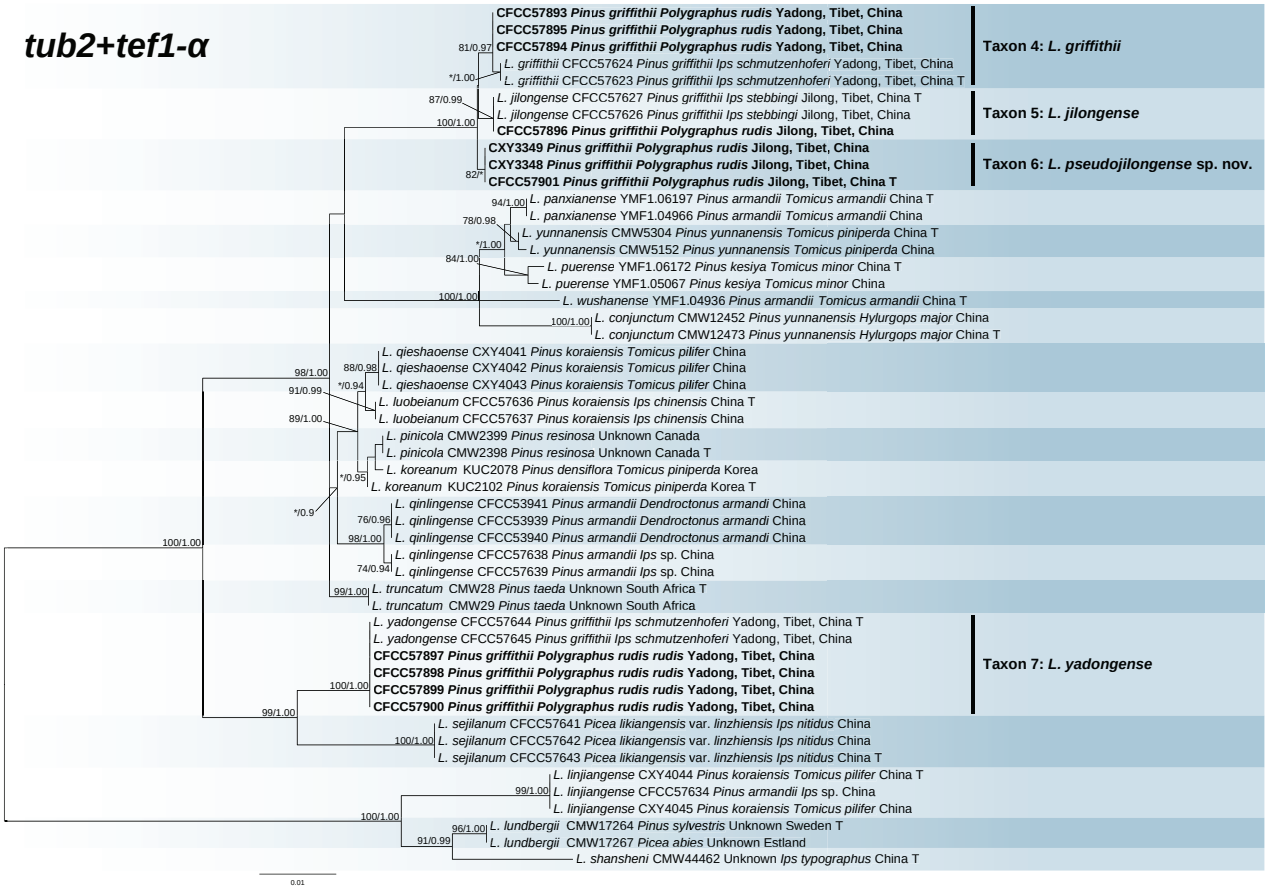

Figure 3. Phylogram of *Leptographium lundbergii* complex (including Taxa 4–7) based on combined (*tub2+tef1-α*) sequence data. The ML bootstrap support values ≥ 70% and posterior probability values ≥ 0.9 are recorded at the nodes. T = ex-type isolates.

that our eight representative isolates nested into two complexes and one Group A, namely the *O. clavatum* complex, *O. ips* complex and Group A (Fig. 5). Subsequently, we constructed the phylogenetic inference of *tub2*, *tef1-α* and/or the concatenated (*tub2+tef1-α* or ITS+*tub2*) datasets for each complex or Group.

Ophiostoma clavatum complex

The *tub2*, *tef1-α* and concatenated (*tub2+tef1-α*) datasets were aligned (containing 438, 594 and 1032 characters, including gaps, respectively) and used to construct the phylogenetic inference. The best models of the three datasets for BI analysis were estimated as HKY+I, GTR+G and GTR+I+G. Based on the concatenated tree (Fig. 6), our ten isolates formed three separate well-supported terminal clades, representing two known (Taxon 9: *O. pseudobrevipilosi*; Taxon 10: *O. stebbingi*) and one undescribed (Taxon 11: *Ophiostoma* sp. 1) taxa. *Ophiostoma pseudobrevipilosi*, *O. stebbingi* and *Ophiostoma* sp. 1 formed the main subclade in this complex with *O. ainoae*, *O. brevipilosi*, *O. pseudobrevipilosi*, *O. schmutzenhoferi*, *O. shangrilae* and *O. yadongense* (Fig. 6, Suppl. material 2: figs S7, S8).

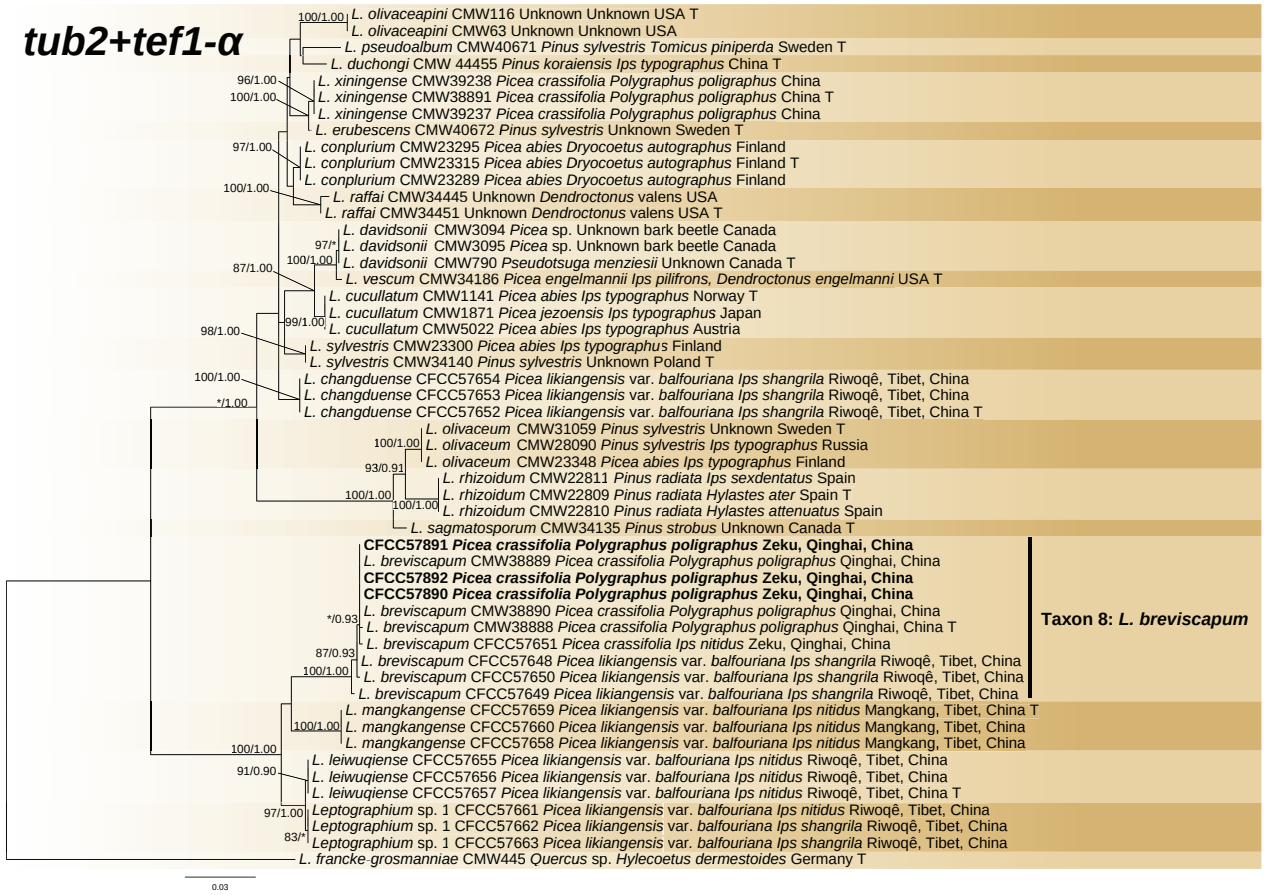

Figure 4. Phylogram of *Leptographium olivaceum* complex (including Taxon 8) based on combined (*tub2*+*tef1-α*) sequence data. The ML bootstrap support values ≥ 70% and posterior probability values ≥ 0.9 are recorded at the nodes. T = ex-type isolates.

Ophiostoma ips complex

The *tub2* dataset was aligned (containing 274 characters including gaps) and used to construct a phylogenetic inference. The best model of the three datasets for BI analysis was estimated to be HKY+I. The seven isolates formed two clades: *O. bicolor* (Taxon12) and *O. shigatsense* (Taxon 13) (Fig. 7).

Group A

The ITS, *tub2* and concatenated (ITS+*tub2*) datasets were aligned (containing 685, 445 and 1130 characters, including gaps) and used to construct the phylogenetic inference. The best models of the three datasets for BI analysis were estimated to be GTR+I+G (ITS dataset) and GTR+G (ITS and concatenated datasets). Based on the concatenated tree (Fig. 8), the 11 isolates formed three separate well-supported terminal clades representing three known taxa (Taxon 14: *O. maixiuense*, Taxon 15: *O. pacis* and Taxon 16: *O. sanum*). *Ophiostoma maixiuense* and *O. sanum* showed intraspecific sequence variation and were phylogenetic sisters to *O. aggregatum* and *O. pacis* (Fig. 8, Suppl. material 2: figs S9, S10).

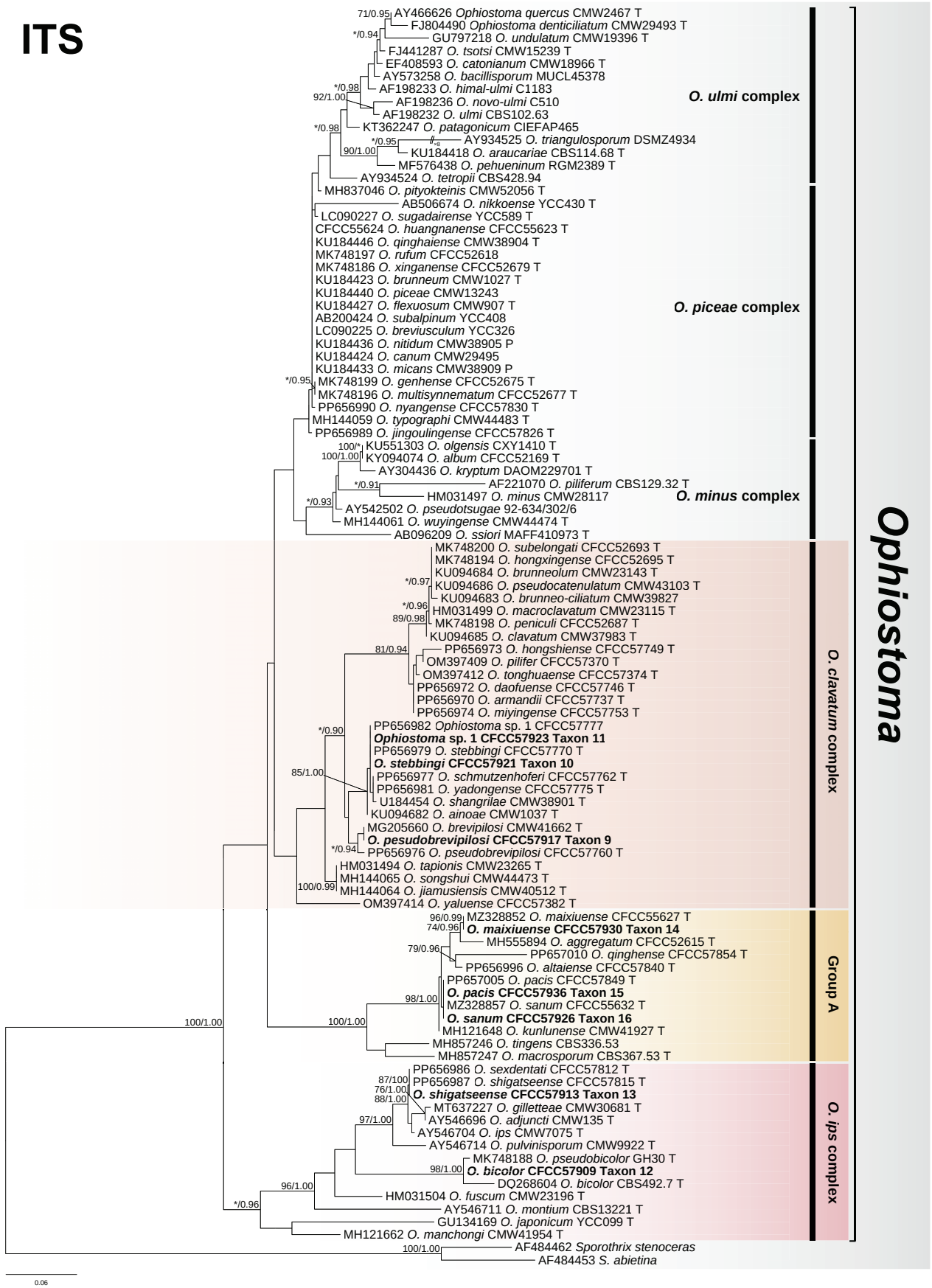

Figure 5. Phylogram of *Ophiostoma* spp. based on ITS sequence data. The ML bootstrap support values ≥ 70% and posterior probability values ≥ 0.9 are recorded at the nodes. T = ex-type isolates.

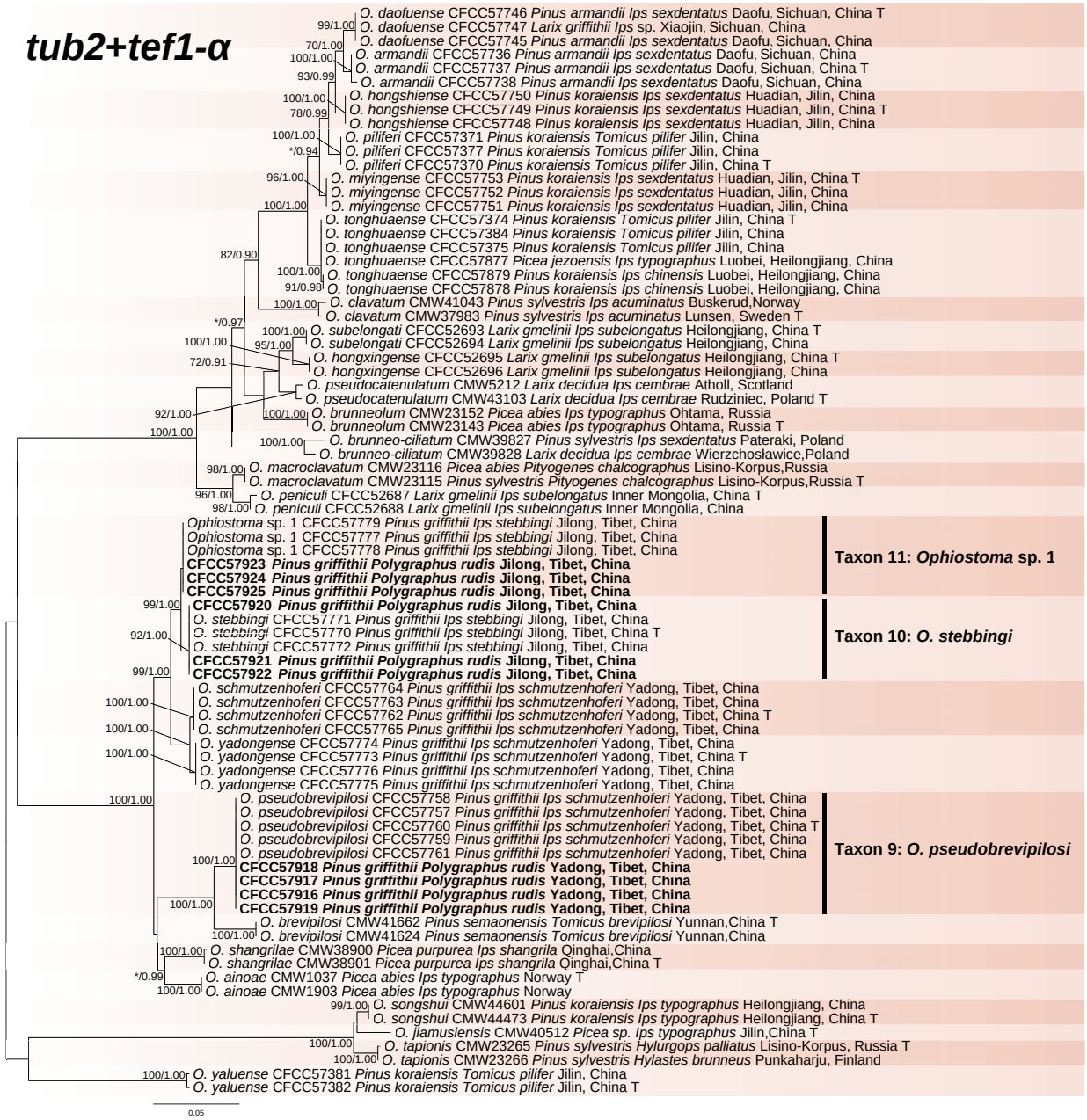

Figure 6. Phylogram of *Ophiostoma clavatum* complex (including Taxa 9–11) based on combined (*tub2*+*tef1-α*) sequence data. The ML bootstrap support values ≥ 70% and posterior probability values ≥ 0.9 are recorded at the nodes. T = ex-type isolates.

Taxonomy

***Leptographium pseudojilongense* Z. Wang & Q. Lu, sp. nov.**
MycoBank No: 855413
Taxon 6, Fig. 9

Etymology. The epithet *pseudojilongense* (Latin) refers to its sister species *L. jilongense*.

Holotype. CXY3312.

Description. Sexual morph: not observed. **Asexual morph:** ***Leptographium***-like. ***Conidiophores*** occurring singly, upright, arising directly from the mycelium,

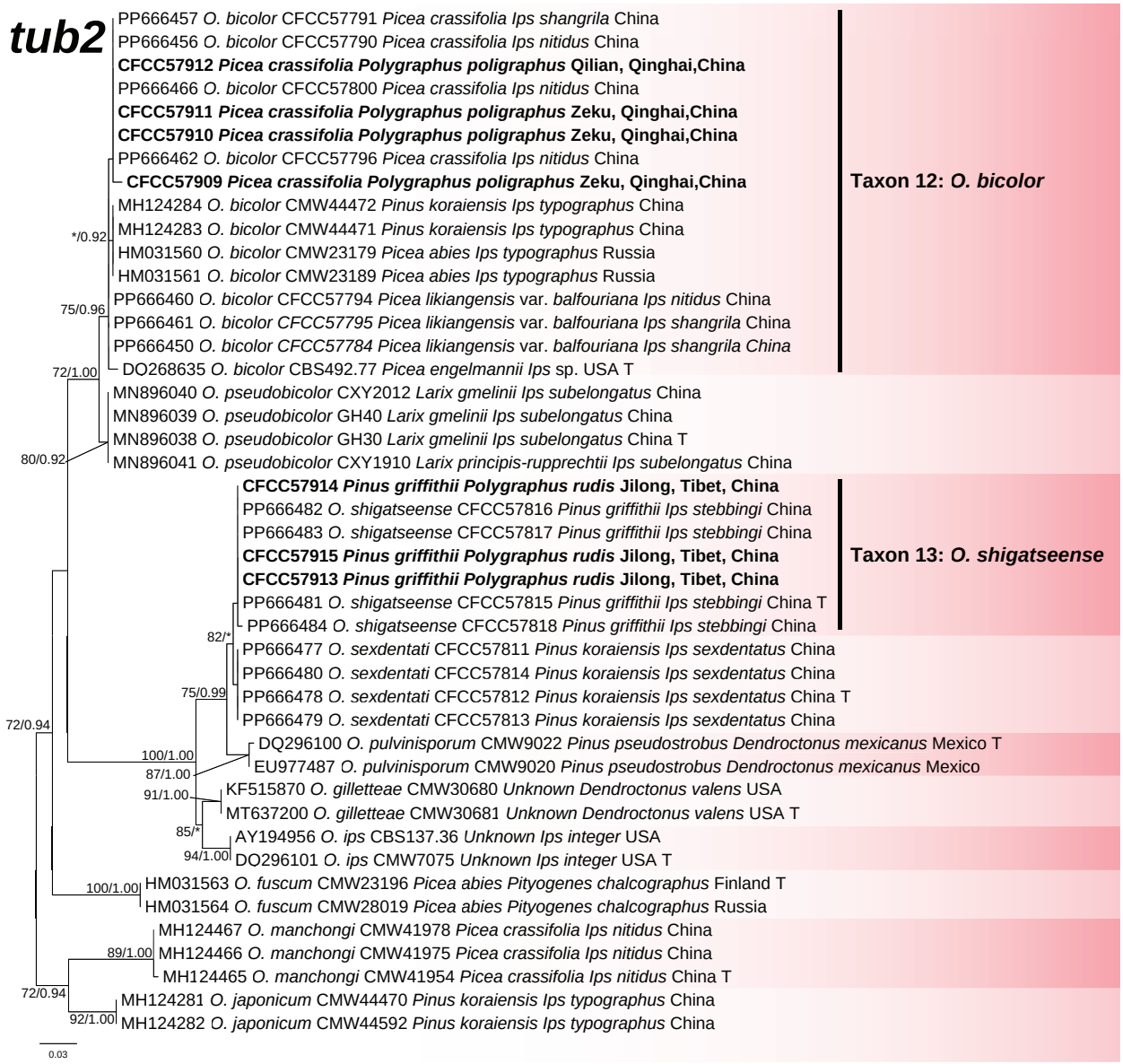

Figure 7. Phylogram of *Ophiostoma ips* complex (including Taxa 12–13) based on *tub2* sequence data. The ML bootstrap support values ≥ 70% and posterior probability values ≥ 0.9 are recorded at the nodes. T = ex-type isolates.

macronematous, mononematous, (247.7–)343.3–484.6(–513.7) µm in length including the conidiogenous apparatus, rhizoid-like structures absent. ***Stipes*** light olivaceous, not constricted, cylindrical, simple, 3–10-septate, (98.8–)103.0–230.0(–301.2) µm in length, (9.0–)11.1–16.9(–18.6) µm wide at base, the basal cell swollen or not, (7.1–)8.5–14.2(–16.6) µm wide below primary branches, apical cell not swollen. ***Conidiogenous apparatus*** (100.8–)180.1–362.1(–417.4) µm in length, excluding the conidial mass, consisting of 1–4 series of branches, the primary branching type B. ***Primary branches*** light olivaceous, cylindrical, (15.4–)19.6–31.8(–35.4) × (6.2–)7.3–10.6(–12.3) µm; ***secondary branches*** light olivaceous, aseptate, (12.4–)13.3–16.7(–18.4) × (6.0–)6.4–9.5(–10.2) µm; ***tertiary branches*** light olivaceous or hyaline, aseptate, (8.0–)8.4–14.0(–16.1) × 5.3–7.6(–8.9) µm. ***Conidiogenous cells*** discrete, 2–3 per branch, smooth or rough, cylindrical, (16.9–)22.2–35.4(–52.6) × (3.9–)4.0–4.8(–5.1) µm. ***Conidia*** hyaline, smooth, aseptate, obovoid, (11.9–)12.9–15.7(–17.9) × (5.5–)6.3–7.8(–8.2) µm.

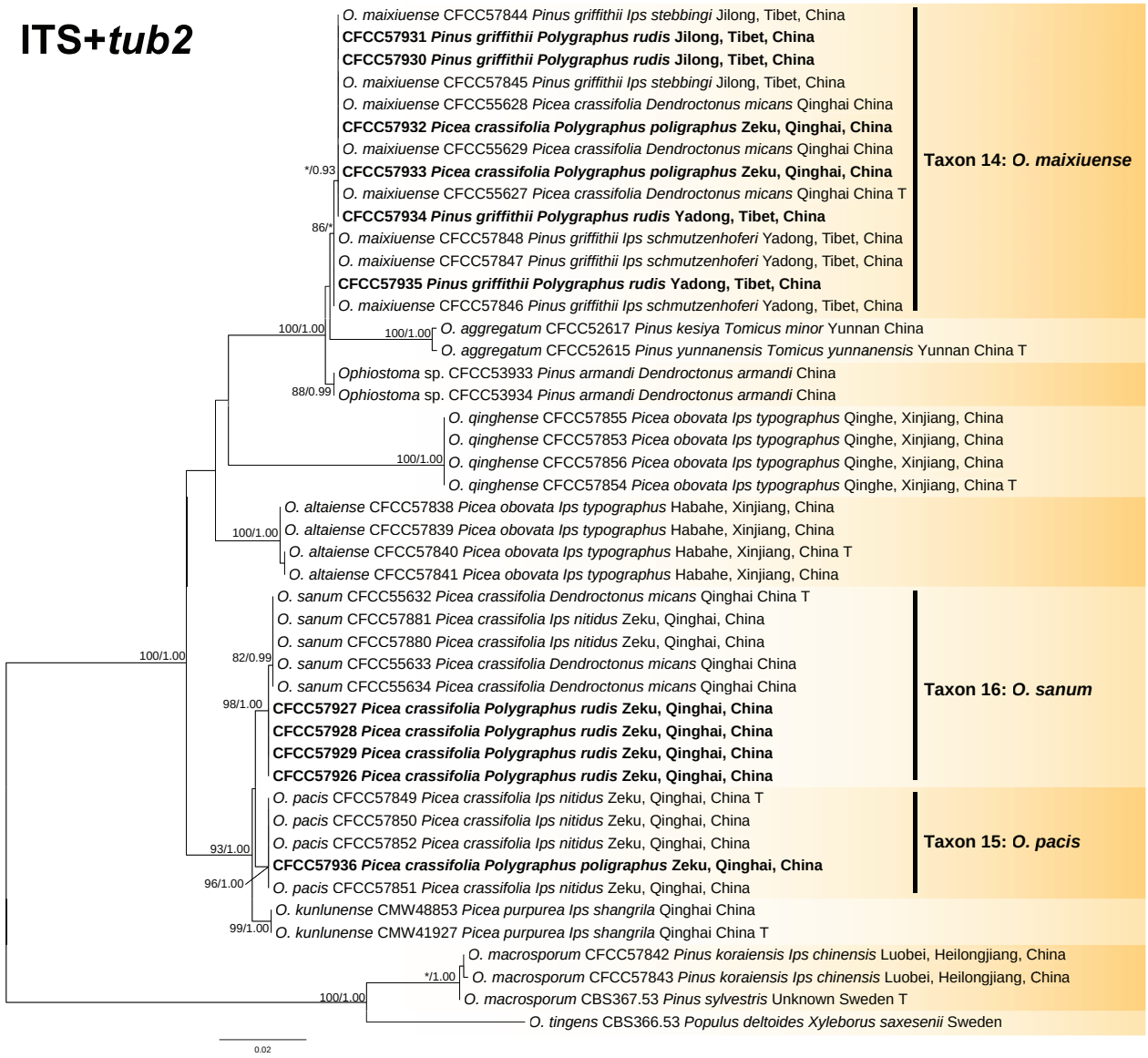

Figure 8. Phylogram of Group A (including Taxa 14–16) based on combined (ITS+*tub2*) sequence data. The ML bootstrap support values ≥ 70% and posterior probability values ≥ 0.9 are recorded at the nodes. T = ex-type isolates.

Culture characters. Colonies on 2% MEA at 25 °C reaching a diameter of 50.1 mm in 4 days, initially hyaline or light white, later becoming light olivaceous from the centre of the colony to the sides, then becoming dark olivaceous, mycelium submerged and superficial with abundant aerial mycelia and the colony margin thinning radially. Optimal temperature for growth was 25 °C, with slow growth observed at 5 °C (45.3 mm in 30 days) and no growth at 35 °C.

Associated insects. *Polygraphus rudis*.

Hosts. *Pinus griffithii*.

Material examined. China • Xizang Autonomous Region, Shigatse City, Jilong County, from *Polygraphus rudis* infesting *Pinus griffithii*, July 2019, Z. Wang and Q. Lu, holotype: CXY3312, ex-type culture CFCC57901, ibid. CXY3348, CXY3349.

Notes. *Leptographium pseudojilongense* was a phylogenetic sister to *L. griffithii* and *L. jilongense* (Fig. 9), both of which were associated with *Pinus griffithii* in Shigatse, Xizang (Wang et al. 2024). *Leptographium pseudojilongense* can be distinguished from *L. griffithii* in the concatenated alignment by 1/373 bp in *tub2*

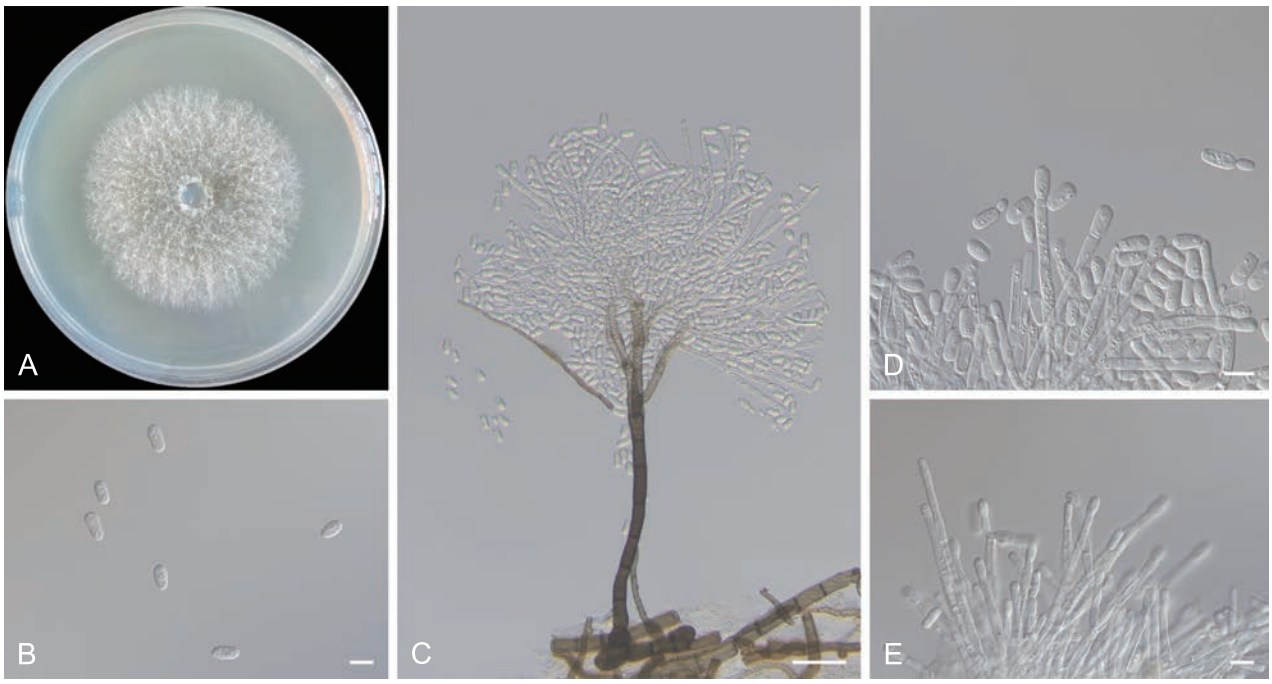

Figure 9. Morphological characteristics of *Leptographium pseudojilongense* sp. nov. (Taxon 9, CXY3312, holotype) **A** four-day-old cultures on 2% MEA **B–E** *Leptographium*-like asexual morph: conidiogenous cells and conidia. Scale bars: 10 μm (**B, D, E**); 40 μm (**C**).

and 3/666 bp in *tef1-α* and from *L. jilongense* in the concatenated alignment by 3/666 bp in *tef1-α*. In terms of morphological characteristics, *L. pseudojilongense* can be distinguished from the other two species by the presence of a *leptographium*-like asexual state, which is absent in the latter two. For culture characteristics, the optimum growth temperature for both was 25 °C, but the former grew slower than the latter two (4 days: 50.1 mm vs. 64.5 and 76.0 mm). At 5 °C, *L. pseudojilongense* was observed growing slowly with 45.3 mm in 30 days, whereas the other two did not grow. Furthermore, *L. pseudojilongense* was isolated from Jilong County, whereas *L. griffithii* and *L. jilongense* were isolated from *Ips schmutzenhoferi* from Yadong County and *Ips stebbingi* from Jilong County, respectively.

Discussion

In total, 442 ophiostomatalean strains representing 16 species were obtained from adult *Polygraphus* beetles and their galleries in *Picea crassifolia* and *Pinus griffithii* on the north-eastern and southern Qinghai-Tibet Plateau. These species were assigned to *Grosmannia* (*G. crassifolia*, *G. maixiuensis* and *Grosmannia* sp. 1 in *G. penicillata* complex), *Leptographium* (*L. griffithii*, *L. jilongense*, *L. pseudojilongense* and *L. yadongense* in *L. lundbergii* complex; *L. breviscapum* in *L. olivaceum* complex) and *Ophiostoma* (*O. pseudobrevipilosi*, *O. stebbingi* and *Ophiostoma* sp. 1 in *O. clavatum* complex; *O. bicolor* and *O. shigatsense* in *O. ips* complex; *O. maixiuense*, *O. pacis* and *O. sanum* in Group A). Amongst them, 12 species were first recorded as associated with *Polygraphus* beetles in China. Yin et al. (2016, 2019, 2020) reported seven ophiostomatalean associates of *P. poligraphus*, but we only collected three of them, which may be because of sample size and sampling time or because the remaining four species are occasional (the previous reports did not count the proportions of each species). To date, three genera (20 species) of

ophiostomatalean fungi have been reported to be associated with *Polygraphus* beetles in China (Yin et al. 2016, 2019, 2020), increasing to six genera (30 species) when the fungi isolated from mites associated with these beetles are included (Chang et al. 2017, 2020), showing an abundance of species diversity (Tables 1, 3).

The dominant species in this study were *O. maixiuense*, *O. bicolor*, *L. yadongense* and *O. pseudobrevipilosi*, representing 20.8%, 18.1%, 17.4% and 13.4% of the ophiostomatalean isolates, respectively, while the other 12 species all had < 10% (Table 3). *Ophiostoma maixiuense* was first reported to be associated with *Dendroctonus micans* infesting *P. crassifolia* on the north-eastern Qinghai-Tibet Plateau (Wang et al. 2021). This species was also obtained from *P. poligraphus* from the same host tree and sampling location. In addition, although several fungal associates of *P. rudis*, *I. schmutzenhoferi* and *I. stebbingi* have been isolated from *P. griffithii* in the Jilong and Yadong Counties on the southern Qinghai-Tibet Plateau, only *O. maixiuense* was shared (Table 3; Wang et al. (2024)). Therefore, this species may be widespread on the Qinghai-Tibet Plateau and its pathogenicity to host trees and association with bark beetles deserve further study. *Ophiostoma bicolor* is frequently associated with bark beetles that harm spruce trees, such as some *Ips* and *Polygraphus* beetles in the Northern Hemisphere (Yamaoka et al. 1997; Kirisits 2004; Alamouti et al. 2007; Chang et al. 2019, 2020; Wang et al. 2021, 2024). It plays multiple roles in the association between beetles and spruce. Solheim (1988) found that it is weakly pathogenic to spruce trees, which may induce the host defence rather than deplete it (Liu et al. 2022). This is not necessarily beneficial during the early stages of insect vector attacks on trees (Mageroy et al. 2020). Conversely, although *O. bicolor* is not attractive to *I. typographus* (Kandasamy et al. 2019; Zhao et al. 2019), *I. nitidus* prefers to feed on *O. bicolor*-colonised substrates and may benefit from their aid in detoxification and improved ecological fitness (Wang et al. 2023). The mechanisms underlying the functional diversity traits in *O. bicolor* and their roles in tree–beetle–fungal interactions need to be further explored.

Table 3. Strains of ophiostomatalean fungi associated with *Polygraphus* in this study.

Taxon	Genus	Species group and complex	Species	Numbers of isolates[1]					Total	Total Percentages
				PrJ	PrY	PrZ	PpZ	PpQ		
1	*Grosmannia*	*G. penicillata*	*G. crassifolia*				8		8	1.81%
2			*G. maixiuensis*				9		9	2.04%
3			*Grosmannia* sp. 1			10		2	12	2.71%
4	*Leptographium*	*L. lundbergii*	*L. griffithii*		14				14	3.17%
5			*L. jilongense*	1					1	0.23%
6			*L. pseudojilongense*	3					3	0.68%
7			*L. yadongense*		77				77	17.42%
8		*L. olivaceum*	*L. breviscapum*				33		33	7.47%
9	*Ophiostoma*	*O. clavatum*	*O. pseudobrevipilosi*		59				59	13.35%
10			*O. stebbingi*	16					16	3.62%
11			*Ophiostoma* sp. 1	18					18	4.07%
12		*O. ips*	*O. bicolor*				20	60	80	18.10%
13			*O. shigatsense*	4					4	0.90%
14		Group A	*O. maixiuense*	28	39		25		92	20.81%
15			*O. pacis*				1		1	0.23%
16			*O. sanum*			15			15	3.39%
Total				70	189	25	96	62	442	100.00%

[1] PrJ = *Polygraphus rudis* from Jilong County; PrY = *P. rudis* from Yadong County; PrZ = *P. rudis* from Zeku County; PpZ = *P. poligraphus* from Zeku County; PpQ = *P. poligraphus* from Qilian County.

Comparisons of the fungal assemblages of bark beetles from the north-eastern and southern Qinghai-Tibet Plateau showed different patterns (30 vs. 12 fungal species), with only *O. maixiuense* being a shared species (Suppl. material 1: tables S2, S3), which may be due to biogeographic barriers and host species. On the north-eastern Qinghai-Tibet Plateau, there are 14, 21 and 14 fungal associates of *Dendroctonus*, *Ips* and *Polygraphus*, respectively (Yin et al. 2016, 2019, 2020; Chang et al. 2020; Wang et al. 2021, 2024). *Ophiostoma ainoae*, *O. bicolor*, *O. nitidum*, *O. sanum* and *O. shangrilae* are shared by these three beetle genera, the latter three of which are currently found only on the Qinghai-Tibet Plateau, whereas the first two are thought to be widely distributed in the coniferous forests of China and are associated with a variety of bark beetles (Chang et al. 2019; Wang et al. 2024). Six fungal associates of *Polygraphus* were shared only with *Ips* and only two were shared with *Dendroctonus* (Suppl. material 1: table S2). This may be because of overlap in the niches of the first two genera of beetles. Furthermore, *Dendroctonus* mainly harms trunks below the DBH (diameter at breast height) of the host tree, which is not the preferred choice for *Polygraphus* and *Ips*. On the southern Qinghai-Tibet Plateau, although the straight-line distance between Jilong and Yadong Counties is not large, the fungal assemblages of bark beetles from the two Counties are divergent, with only one of the 12 species shared (Suppl. material 1: table S3). Interestingly, the fungal associations of different beetles at the two sites were highly coincident. Four of the six fungal associates of *P. rudis* are shared with *I. stebbingi*. Similarly, all four of the *P. rudis*' fungal associates in Yadong County were also isolated from *I. schmutzenhoferi* by Wang et al. (2024). This suggests that the biogeographic barrier caused by the high mountain-and-gorge landform on the southern slopes of the Himalayas creates this fungal assemblage pattern of bark beetles, even though the host species are the same and geographical distances are not far.

Overall, this study deepens our understanding of the composition of ophiostomatoid fungi associated with bark beetles, especially *Polygraphus*, on the Qinghai-Tibet Plateau. The discovery of a large number of new fungal species and new tree-bark beetle-fungal associations has made it an urgent task to reveal their biological functions and ecological features.

Additional information

Conflict of interest

The authors have declared that no competing interests exist.

Ethical statement

No ethical statement was reported.

Funding

This work was supported by the National Natural Science Foundation of China [32301598] and the National Key R&D Program of China [2023YFC2604801-4].

Author contributions

Conceptualization, Zheng Wang, Quan Lu; data curation, Zheng Wang, Caixia Liu, Xiuyue Song, Yingjie Tie; funding acquisition, Zheng Wang; investigation, Zheng Wang, Caixia Liu, Huimin Wang, Quan Lu; project administration, Zheng Wang; resources, Zheng

Wang, Caixia Liu, Xiuyue Song, Yingjie Tie; supervision, Zheng Wang, Huixiang Liu, Quan Lu; writing-original draft, Zheng Wang; writing-review and editing, Zheng Wang, Quan Lu. All authors have read and agreed to the published version of the manuscript.

Author ORCIDs

Zheng Wang https://orcid.org/0000-0003-0207-4321
Quan Lu https://orcid.org/0000-0002-6007-2677

Data availability

All of the data that support the findings of this study are available in the main text or Supplementary Information.

References

Alamouti SM, Kim JJ, Humble LM, Uzunovic A, Breuil C (2007) Ophiostomatoid fungi associated with the northern spruce engraver, *Ips perturbatus*, in western Canada. Antonie van Leeuwenhoek 91(1): 19–34. https://doi.org/10.1007/s10482-006-9092-8

Bentz BJ, Jönsson AM (2015) Modeling bark beetle responses to climate change. In: Vega FE, Hofstetter RW (Eds) Bark Beetles Biology and Ecology of Native and Invasive Species. London: Elsevier, Academic Press, 533–553 pp.

Biedermann PH, Müller J, Grégoire JC, Gruppe A, Hagge J, Hammerbacher A, Hofstetter RW, Kandasamy D, Kolarik M, Kostovcik M, Krokene P, Sallé A, Six DL, Turrini T, Vanderpool D, Wingfield MJ, Bässler C (2019) Bark beetle population dynamics in the Anthropocene: Challenges and solutions. Trends in Ecology & Evolution 34(10): 914–924. https://doi.org/10.1016/j.tree.2019.06.002

Chang R, Duong TA, Taerum SJ, Wingfield MJ, Zhou X, De Beer ZW (2017) Ophiostomatoid fungi associated with conifer-infesting beetles and their phoretic mites in Yunnan, China. MycoKeys 28: 19–64. https://doi.org/10.3897/mycokeys.28.21758

Chang R, Duong TA, Taerum SJ, Wingfield MJ, Zhou X, Yin M, De Beer ZW (2019) Ophiostomatoid fungi associated with the spruce bark beetle *Ips typographus*, including 11 new species from China. Persoonia 42(1): 50–74. https://doi.org/10.3767/persoonia.2019.42.03

Chang R, Duong TA, Taerum SJ, Wingfield MJ, Zhou X, De Beer ZW (2020) Ophiostomatoid fungi associated with mites phoretic on bark beetles in Qinghai, China. IMA Fungus 11(1): 1–18. https://doi.org/10.1186/s43008-020-00037-9

Darriba D, Taboada GL, Doallo R, Posada D (2012) jModelTest 2: More models, new heuristics and parallel computing. Nature Methods 9(8): 772–772. https://doi.org/10.1038/nmeth.2109

De Beer ZW, Wingfield MJ (2013) Emerging lineages in the Ophiostomatales. In: Seifert KA, De Beer ZW, Wingfield MJ (Eds) The Ophiostomatoid fungi: expanding frontiers, CBA biodiversity series. Netherlands: CBS-KNAW Fungal Biodiversity Centre, 21–46 pp.

De Beer ZW, Seifert KA, Wingfield MJ (2013) The ophiostomatoid fungi: their dual position in the Sordariomycetes. In: Seifert KA, De Beer ZW, Wingfield MJ (Eds) The Ophiostomatoid fungi: expanding frontiers, CBA biodiversity series. Netherlands: CBS-KNAW Fungal Biodiversity Centre, 19 pp.

De Beer ZW, Duong TA, Wingfield MJ (2016) The divorce of *Sporothrix* and *Ophiostoma*: Solution to a problematic relationship. Studies in Mycology 83(1): 165–191. https://doi.org/10.1016/j.simyco.2016.07.001

De Beer ZW, Procter M, Wingfield MJ, Marincowitz S, Duong TA (2022) Generic boundaries in the Ophiostomatales reconsidered and revised. Studies in Mycology 101(1): 57–120. https://doi.org/10.3114/sim.2022.101.02

Fortier CE, Musso AE, Evenden ML, Zaharia LI, Cooke JE (2024) Evidence that Ophiostomatoid fungal symbionts of mountain pine beetle do not play a role in overcoming lodgepole pine defenses during mass attack. Molecular Plant-Microbe Interactions 37(5): 445–458. https://doi.org/10.1094/MPMI-06-23-0077-R

Gardes M, Bruns TD (1993) ITS primers with enhanced specificity for basidiomycetes-application to the identification of mycorrhizae and rusts. Molecular Ecology 2(2): 113–118. https://doi.org/10.1111/j.1365-294X.1993.tb00005.x

Glass NL, Donaldson GC (1995) Development of primer sets designed for use with the PCR to amplify conserved genes from filamentous ascomycetes. Applied and Environmental Microbiology 61(4): 1323–1330. https://doi.org/10.1128/aem.61.4.1323-1330.1995

Huang FS, Lu J (2015) The Classification Outline of Scolytidae from China. Shanghai: Tongji University Press, 37–38 pp.

Jacobs K, Bergdahl DR, Wingfield MJ, Halik S, Seifert KA, Bright DE, Wingfield BD (2004) *Leptographium wingfieldii* introduced into North America and found associated with exotic *Tomicus piniperda* and native bark beetles. Mycological Research 108(4): 411–418. https://doi.org/10.1017/S0953756204009748

Kandasamy D, Gershenzon J, Andersson MN, Hammerbacher A (2019) Volatile organic compounds influence the interaction of the Eurasian spruce bark beetle (*Ips typographus*) with its fungal symbionts. The ISME Journal 13(7): 1788–1800. https://doi.org/10.1038/s41396-019-0390-3

Kandasamy D, Zaman R, Nakamura Y, Zhao T, Hartmann H, Andersson MN, Hammerbacher A, Gershenzon J (2023) Conifer-killing bark beetles locate fungal symbionts by detecting volatile fungal metabolites of host tree resin monoterpenes. PLoS Biology 21(2): e3001887. https://doi.org/10.1371/journal.pbio.3001887

Katoh K, Rozewicki J, Yamada KD (2019) MAFFT online service: Multiple sequence alignment, interactive sequence choice and visualization. Briefings in Bioinformatics 20(4): 1160–1166. https://doi.org/10.1093/bib/bbx108

Kirisits T (2004) Fungal associates of European bark beetles with special emphasis on the ophiostomatoid fungi. In: Lieutier F, Day KR, Battisti A, Gregoire JC, Evans HF (Eds) Bark and Wood Boring Insects in Living Trees in Europe. London: Kluwer Academic Publishers, 185–223 pp.

Kumar S, Stecher G, Tamura K (2016) MEGA7: Molecular evolutionary genetics analysis version 7.0 for bigger datasets. Molecular Biology and Evolution 33(7): 1870–1874. https://doi.org/10.1093/molbev/msw054

Lesk C, Coffel E, D'Amato AW, Dodds K, Horton R (2017) Threats to North American forests from southern pine beetle with warming winters. Nature Climate Change 7(10): 713–717. https://doi.org/10.1038/nclimate3375

Liu Y, Zhou Q, Wang Z, Wang H, Zheng G, Zhao J, Lu Q (2022) Pathophysiology and transcriptomic analysis of *Picea koraiensis* inoculated by bark beetle-vectored fungus *Ophiostoma bicolor.* Frontiers in Plant Science 13: 944336. https://doi.org/10.3389/fpls.2022.944336

Mageroy MH, Christiansen E, Långström B, Borg-Karlson AK, Solheim H, Björklund N, Zhao T, Schmidt A, Fossdal CG, Krokene P (2020) Priming of inducible defenses protects Norway spruce against tree-killing bark beetles. Plant, Cell & Environment 43(2): 420–430. https://doi.org/10.1111/pce.13661

Netherer S, Kandasamy D, Jirosová A, Kalinová B, Schebeck M, Schlyter F (2021) Interactions among Norway spruce, the bark beetle *Ips typographus* and its fungal

symbionts in times of drought. Journal of Pest Science 94(3): 591–614. https://doi.org/10.1007/s10340-021-01341-y

O'Donnell K, Cigelnik E (1997) Two divergent intragenomic rDNA ITS2 types within a monophyletic lineage of the fungus *Fusarium* are nonorthologous. Molecular Phylogenetics and Evolution 7(1): 103–116. https://doi.org/10.1006/mpev.1996.0376

Papek E, Ritzer E, Biedermann PH, Cognato AI, Baier P, Hoch G, Kirisits T, Schebeck M (2024) The pine bark beetle *Ips acuminatus*: An ecological perspective on life-history traits promoting outbreaks. Journal of Pest Science 97(3): 1–30. https://doi.org/10.1007/s10340-024-01765-2

Popkin G (2021) Forest fight. Science 374(6572): 1184–1189. https://doi.org/10.1126/science.acx9733

Raffa KF, Gregoire JC, Lindgren BS (2015) Natural history and ecology of bark beetles. In: Vega FE, W HR (Eds) Bark Beetles: Biology and Ecology of Native and Invasive Species. Elsevier, San Diego, 40 pp. https://doi.org/10.1016/B978-0-12-417156-5.00001-0

Ronquist F, Huelsenbeck JP (2003) MrBayes 3: Bayesian phylogenetic inference under mixed models. Bioinformatics 19(12): 1572–1574. https://doi.org/10.1093/bioinformatics/btg180

Solheim H (1988) Pathogenicity of some *Ips typographus*-associated blue-stain fungi to Norway spruce. Medd Nor Inst Skoforsk 40: 1–11.

Stamatakis A (2014) RAxML version 8: A tool for phylogenetic analysis and post-analysis of large phylogenies. Bioinformatics 30(9): 1312–1313. https://doi.org/10.1093/bioinformatics/btu033

Sydow H, and Sydow P (1919) Mycologische Mitteilungen. Annales Mycologici 17: 33e47.

Viklund L, Rahmani R, Bång J, Schroeder M, Hedenström E (2019) Optimizing the attractiveness of pheromone baits used for trap** the four-eyed spruce bark beetle *Polygraphus poligraphus*. Journal of Applied Entomology 143(7): 721–730. https://doi.org/10.1111/jen.12641

Vilgalys R, Hester M (1990) Rapid genetic identification and mapping of enzymatically amplified ribosomal DNA from several *Cryptococcus* species. Journal of Bacteriology 172(8): 4238–4246. https://doi.org/10.1128/jb.172.8.4238-4246.1990

Wadke N, Kandasamy D, Vogel H, Lah L, Wingfield BD, Paetz C, Wright LP, Gershenzon J, Hammerbacher A (2016) The bark-beetle-associated fungus, *Endoconidiophora polonica*, utilizes the phenolic defense compounds of its host as a carbon source. Plant Physiol. 171(2):914–931. https://doi.org/10.1104/pp.15.01916

Wang Z, Liu Y, Wang H, Meng X, Liu X, Decock C, Zhang X, Lu Q (2020) Ophiostomatoid fungi associated with *Ips subelongatus*, including eight new species from northeastern China. IMA Fungus 11(1): 3. https://doi.org/10.1186/s43008-019-0025-3

Wang Z, Zhou Q, Zheng G, Fang J, Han F, Zhang X, Lu Q (2021) Abundance and diversity of ophiostomatoid fungi associated with the Great Spruce Bark Beetle (*Dendroctonus micans*) in the Northeastern Qinghai-Tibet Plateau. Frontiers in Microbiology 12: 721395. https://doi.org/10.3389/fmicb.2021.721395

Wang Z, Liu Y, Wang H, Roy A, Liu H, Han F, Zhang X, Lu Q (2023) Genome and transcriptome of *Ips nitidus* provide insights into high-altitude hypoxia adaptation and symbiosis. iScience 26(10): 107793. https://doi.org/10.1016/j.isci.2023.107793

Wang Z, Liang L, Wang H, Decock C, Lu Q (2024) Ophiostomatoid fungi associated with *Ips* bark beetles in China. PREPRINT (Version 1) [available at Research Square]. https://doi.org/10.21203/rs.3.rs-4896600/v1

White TJ, Bruns T, Lee S, Taylor J (1990) Amplification and direct sequencing of fungal ribosomal RNA genes for phylogenetics. PCR Protocols: A Guide to Methods and Applications 18: 315–322. https://doi.org/10.1016/B978-0-12-372180-8. 50042-1

Yamaoka Y, Wingfield MJ, Takahashi I, Solheim H (1997) Ophiostomatoid fungi associated with the spruce bark beetle *Ips typographus* f. *japonicus* in Japan. Mycological Research 101(10): 1215–1227. https://doi.org/10.1017/S0953756297003924

Yin HF, Huang FS, Li ZL (1984) Economic Insect Fauna of China (Fasc. 29) Coleoptera: Scolytidae. Beijing: Science Press, 82–92 pp.

Yin M, Wingfield MJ, Zhou X, De Beer ZW (2016) Multigene phylogenies and morphological characterization of five new *Ophiostoma* spp. associated with spruce-infesting bark beetles in China. Fungal Biology 120(4): 454–470. https://doi.org/10.1016/j.funbio.2015.12.004

Yin M, Wingfield MJ, Zhou X, Linnakoski R, De Beer ZW (2019) Taxonomy and phylogeny of the *Leptographium olivaceum* complex (Ophiostomatales, Ascomycota), including descriptions of six new species from China and Europe. MycoKeys 60: 93–123. https://doi.org/10.3897/mycokeys.60.39069

Yin M, Wingfield MJ, Zhou X, De Beer ZW (2020) Phylogenetic re-evaluation of the *Grosmannia penicillata* complex (Ascomycota, Ophiostomatales), with the description of five new species from China and USA. Fungal Biology 124(2): 110–124. https://doi.org/10.1016/j.funbio.2019.12.003

Zhao T, Axelsson K, Krokene P, Borg-Karlson AK (2015) Fungal symbionts of the spruce bark beetle synthesize the beetle aggregation pheromone 2-methyl-3-buten-2-ol. Journal of Chemical Ecology 41(9): 848–852. https://doi.org/10.1007/s10886-015-0617-3

Zhao T, Ganji S, Schiebe C, Bohman B, Weinstein P, Krokene P, Borg-Karlson AK, Unelius CR (2019) Convergent evolution of semiochemicals across Kingdoms: Bark beetles and their fungal symbionts. The ISME Journal 13(6): 1535–1545. https://doi.org/10.1038/s41396-019-0370-7

Zipfel RD, De Beer ZW, Jacobs K, Wingfield BD, Wingfield MJ (2006) Multi-gene phylogenies define *Ceratocystiopsis* and *Grosmannia* distinct from *Ophiostoma*. Studies in Mycology 55(1): 75–97. https://doi.org/10.3114/sim.55.1.75

Supplementary material 1

Supplementary tables

Authors: Zheng Wang, Caixia Liu, Xiuyue Song, Yingjie Tie, Huimin Wang, Huixiang Liu, Quan Lu

Data type: rar

Explanation note: **table S1.** List of sampling information of *Polygraphus* bark beetles. **table S2.** Comparisons of fungal assemblages of bark beetles in the north-eastern Qinghai-Tibet Plateau. **table S3.** Comparisons of fungal assemblages of bark beetles in the southern Qinghai-Tibet Plateau.

Link: https://doi.org/10.3897/mycokeys.110.135538.suppl1

Supplementary material 2

Supplementary figures

Authors: Zheng Wang, Caixia Liu, Xiuyue Song, Yingjie Tie, Huimin Wang, Huixiang Liu, Quan Lu

Data type: rar

Explanation note: **figure S1.** Phylogram of *Grosmannia penicillata* complex (including Taxa 1–3) based on *tub2* sequence data. **figure S2.** Phylogram of *Grosmannia penicillata* complex (including Taxa 1–3) based on *tef1-α* sequence data. **figure S3.** Phylogram of *Leptographium lundbergii* complex (including Taxa 4–7) based on *tub2* sequence data. **figure S4.** Phylogram of *Leptographium lundbergii* complex (including Taxa 4–7) based on *tef1-α* sequence data. **figure S5.** Phylogram of *Leptographium olivaceum* complex (including Taxon 8) based on *tub2* sequence data. **figure S6.** Phylogram of *Leptographium olivaceum* complex (including Taxon 8) based on *tef1-α* sequence data. **figure S7.** Phylogram of *Ophiostoma clavatum* complex (including Taxa 9–11) based on *tub2* sequence data. **figure S8.** Phylogram of *Ophiostoma clavatum* complex (including Taxa 9–11) based on *tef1-α* sequence data. **figure S9.** Phylogram of Group A (including Taxa 14–16) based on ITS sequence data. The ML bootstrap support values ≥ 70% and posterior probability values ≥ 0.9 are recorded at the nodes. T = ex-type isolates. **figure S10.** Phylogram of Group A (including Taxa 14–16) based on *tub2* sequence data.

Link: https://doi.org/10.3897/mycokeys.110.135538.suppl2

MycoKeys 110: 117–140 (2024)
DOI: 10.3897/mycokeys.110.130733

Research Article

Distribution patterns of *Calonectria* (Ascomycota, Sordariomycetes, Hypocreales, Nectriaceae) species complexes related to diseased leaves and soil habitats during leaf blight outbreak season in *Eucalyptus* plantations in southern China

WenXia Wu[1], ShuaiFei Chen[1]

1 *Research Institute of Fast-growing Trees (RIFT), Chinese Academy of Forestry (CAF), Zhanjiang, 524022, Guangdong Province, China*
Corresponding author: ShuaiFei Chen (shuaifei.chen@gmail.com)

Abstract

Calonectria leaf blight caused by *Calonectria* species is one of the most important diseases associated with *Eucalyptus* plantations in Asia and South America. This study aimed to clarify the distribution patterns of *Calonectria* species residing in different species complexes associated with diseased trees and soils during leaf blight outbreak season in *Eucalyptus* plantations in southern China. In this study, 482 *Calonectria* isolates obtained from diseased *Eucalyptus* trees and soils under these trees in eight sampling sites in three provinces were identified by DNA sequence analyses of *tef1*, *tub2*, *cmdA*, and *his3* gene regions. Six species residing in three species complexes were identified: *Calonectria pseudoreteaudii* and *C. acaciicola* in the *Calonectria reteaudii* species complex; *C. hongkongensis*, *C. aconidialis*, and *C. chinensis* in *C. kyotensis* species complex; and *C. auriculiformis* in *C. cylindrospora* species complex. The habitats of *Calonectria* in different species complexes differed, *C. reteaudii* species complex inhabits in both diseased trees and soils, *C. kyotensis* species complex only in soils. The Calonectria leaf blight in the sampled regions was caused by species in the *C. reteaudii* species complex but not by the species in the *C. kyotensis* species complex. These findings suggest that the species in the *C. reteaudii* species complex should receive more attention in disease management, as they are the primary cause of the disease in the sampled regions.

Key words: Calonectria leaf blight, *Eucalyptus* disease, forest pathogens, fungal ecology, phylogeny

Academic editor:
Malgorzata Ruszkiewicz-Michalska
Received: 30 June 2024
Accepted: 15 October 2024
Published: 4 November 2024

Citation: Wu WX, Chen SF (2024) Distribution patterns of *Calonectria* (Ascomycota, Sordariomycetes, Hypocreales, Nectriaceae) species complexes related to diseased leaves and soil habitats during leaf blight outbreak season in *Eucalyptus* plantations in southern China. MycoKeys 110: 117–140. https://doi.org/10.3897/mycokeys.110.130733

Introduction

The eucalypts, commonly known as gum trees, include the genera *Angophora*, *Corymbia*, and *Eucalyptus*, with more than 800 species, of which *Eucalyptus* spp. are the most numerous (Thornhill et al. 2019). *Eucalyptus* species are widely cultivated as commercial trees in Southeast Asia, Brazil, China, Australia, India, Europe, and South Africa due to their ability of fast-growing, adaptability, and versatility (Xie and Du 2019). In China, *Eucalyptus* plantations cover an area of approximately 5.46 million hm^2, accounting for approx. 2.5% of the country's total forest area, and provide one-third of the country's timber production (Xie et al. 2017; Xie and Du 2019).

The Eucalyptus leaf blight, caused by *Calonectria* spp., is considered one of the most severe diseases affecting *Eucalyptus* plantations, especially in Asia and South America (Crous 2002; Rodas et al. 2005; Alfenas et al. 2015; Pham et al. 2019, 2022a, 2022b; Wang and Chen 2020; Li et al. 2023a; Liang et al. 2023). The disease initially presents as water-soaked and light gray lesions of the middle and lower leaves. As it rapidly spreads, the lesions progress to light brown color and cover a significant portion of the leaf blade, ultimately leading to defoliation and even the death of the entire tree under highly favorable environmental conditions (Old et al. 2003; Rodas et al. 2005; Wang and Chen 2020; Wu and Chen 2021; Liang et al. 2023).

Severe outbreaks of Calonectria leaf blight have significantly impacted the growth of *Eucalyptus* plantations in southern China, resulting in substantial economic losses (Zhou and Wingfield 2011; Wang and Chen 2020; Wu and Chen 2021; Li et al. 2023a; Liang et al. 2023). The disease was initially observed in an *Eucalyptus* nursery located in Hainan Province in 1985, which resulted in significant mortality among *Eucalyptus* seedlings (Feng and Zheng 1986). In recent years, leaf blight caused by *Calonectria* species has been observed and confirmed in plantation in Fujian, Guangdong, Guangxi, and Hainan Provinces (Chen et al. 2013; Wang and Chen 2020; Wu and Chen 2021; Li et al. 2023b; Liang et al. 2023). The *Calonectria* species that are frequently isolated from diseased *Eucalyptus* trees in China include *C. acaciicola*, *C. pseudoreteaudii*, and *C. queenslandica* (Wang and Chen 2020; Wu and Chen 2021; Li et al. 2023a; Liang et al. 2023).

Calonectria has been detected not only in *Eucalyptus* tissues (mainly from tree leaves, as well as tree shoots and seedling stems) but also in soils under diseased trees and seedlings in China (Li et al. 2017, 2023a; Wang and Chen 2020; Liang et al. 2023). Presently, 26 *Calonectria* species associated with *Eucalyptus* have been identified and reported, including 19 species isolated from diseased leaves, 17 species isolated from soils associated with *Eucalyptus*, and 10 species isolated from both diseased tissues and soils associated with *Eucalyptus* (Lombard et al. 2010c; Li et al. 2017; Liu et al. 2020, 2021; Wu and Chen 2021; Zhang et al. 2022; Liang et al. 2023; Liu and Chen 2023).

Calonectria species have been frequently isolated from diseased *Eucalyptus* trees and soils in their plantations (Liu et al. 2020, 2021; Wu and Chen 2021; Li et al. 2023b; Liu and Chen 2023). However, only two studies were conducted to understand the species diversity and distribution characteristics of *Calonectria*, both from diseased plantation *Eucalyptus* trees and soils under these trees (Wu and Chen 2021; Li et al. 2023b). These studies were conducted solely in one *Eucalyptus* plantation (Wu and Chen 2021), or in a limited number of sampling regions, and there are significant differences in the number of samples between diseased trees and the soil under these trees (Li et al. 2023b). As a result, the distribution patterns of *Calonectria* species associated with diseased *Eucalyptus* trees and soils under these trees are still unclear. The purpose of this study was to comprehensively understand the distribution characteristics of *Calonectria* species related to diseased leaves and soil habitats during leaf blight outbreak season in *Eucalyptus* plantations in southern China. This was achieved by systematically procuring sampled collections of *Calonectria* from eight Calonectria leaf blight outbreak *Eucalyptus* plantations in three provinces in southern China.

Materials and methods

Disease survey, sample collection, and fungal isolation

In September 2021, we conducted several extensive surveys of the disease caused by *Calonectria* species in *E. urophylla* hybrid plantations in Guangdong, Guangxi, and Hainan Provinces in southern China. After the surveys, eight plantations were selected for sampling (Fig. 1). At each of the eight plantations, the trees were one-year-old, and the disease of *Calonectria* leaf blight occurred for about a month. The disease symptoms of Calonectria leaf blight were observed on 60%–80% of trees in each plantation (Fig. 2A, B) typically included leaf spots and blight (Fig. 2C), which resulted in defoliation (Fig. 2D). Depending on the plantation area, a number of diseased trees were selected for diseased leaf sampling. These trees were randomly distributed across each plantation. Three to five fresh symptomatic leaves were collected from each sampled tree. The same number of soil samples was collected under it from the upper 0–20 cm soil profile by removing the thick layer of leaf litter, as described by Liu and Chen (2023). The diseased leaf and soil samples were taken to our laboratory for further study.

To induce *Calonectria* sporulation on leaf samples, one diseased leaf of each sampled tree with typical symptoms of Calonectria leaf blight was selected for incubation in a moist petri dish chamber at room temperature until

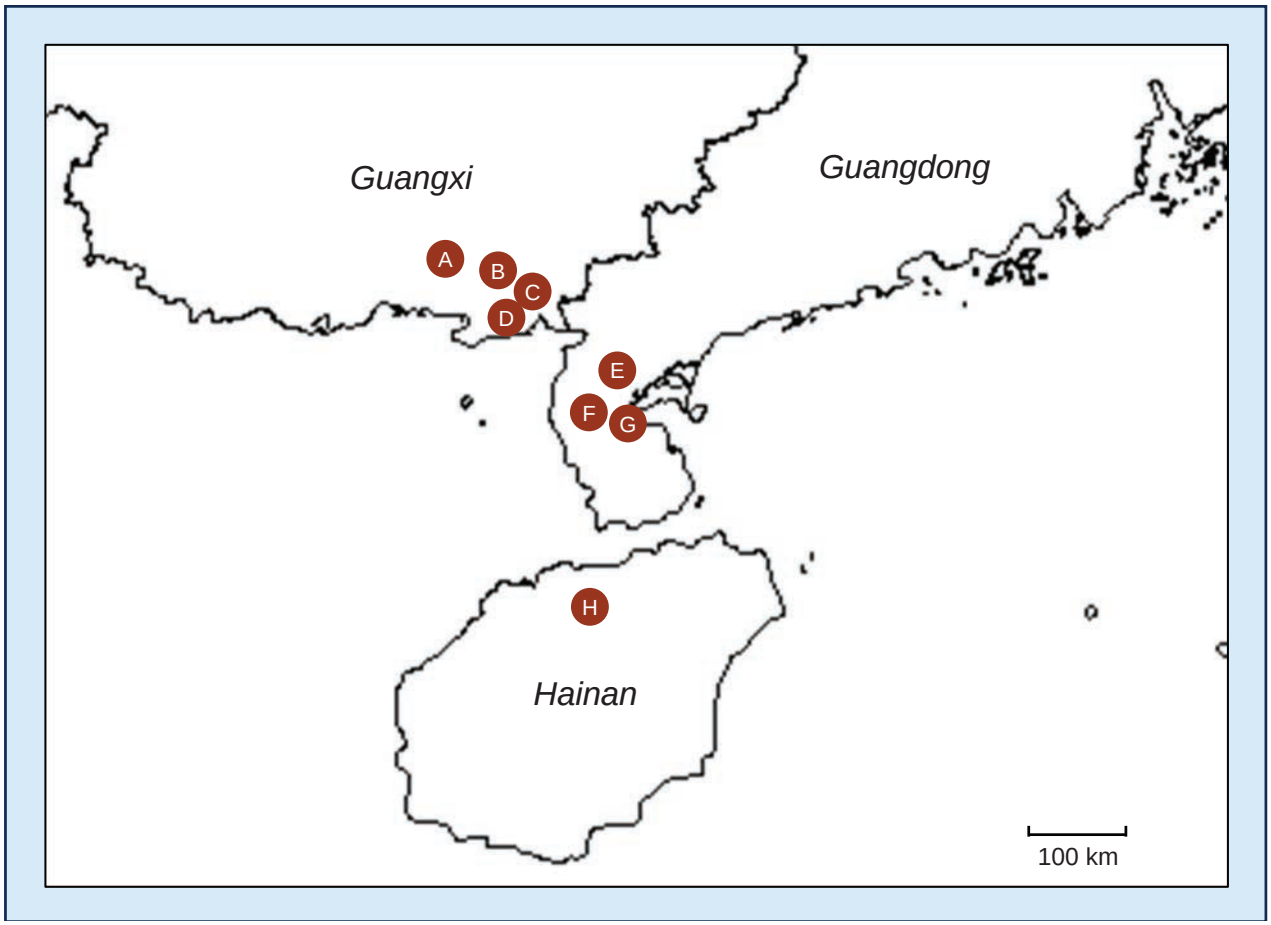

Figure 1. Locations of the eight sampled plantations in the Guangxi (sites **A, B, C, D**), Guangdong (sites **E, F, G**), and Hainan (site **H**) provinces in southern China.

Figure 2. Diseased leaves and soil samples at plantations of a *Eucalyptus urophylla* hybrid in southern China **A, B** leaf spot and blight caused by *Calonectria* species were observed on 60%–80% of the trees in the plantations **C** blighted and dried dead leaves **D** leaves that were dying and drying, resulting in defoliation in the plantation.

the conidiophores were observed. The development of *Calonectria* strains in soil samples was induced by using *Medicago sativa* (alfalfa) seeds, as described by Liu and Chen (2023). The single conidia from conidial masses of *Calonectria* that sporulated from the diseased leaf or soil samples were transferred to 2% (v/v) malt extract agar (MEA) also following Wu and Chen's protocol (2023). One isolate with typical morphological characteristics of the conidiophores

of *Calonectria*, was isolated from each diseased leaf sample or soil sample. Occasionally, two *Calonectria* isolates were isolated from each sample when the isolates with different morphological vesicles were observed. All obtained single conidium cultures were deposited in the Culture Collection (CSF) at the Research Institute of Fast-growing Trees (RIFT), Chinese Academy of Forestry (CAF), Zhanjiang, Guangdong Province, China.

DNA extraction, PCR amplification, and sequencing

The obtained *Calonectria* isolates were cultivated in a 2% MEA medium for a week at room temperature for total genomic DNA extraction. The mycelia were scraped from the cultures. The total genomic DNA of each isolate was extracted using the cetyltrimethylammonium bromide (CTAB) method, as described by van Burik et al. (1998). Four gene regions, namely the translation elongation factor 1-alpha (*tef1*), β-tubulin (*tub2*), calmodulin (*cmdA*), and histone H3 (*his3*), were amplified using the primer pairs and PCR protocols described by Liu et al. (2020). All PCR products were Sanger sequenced in both directions by the same primers used for PCR amplification. The PCR products were sequenced by the Beijing Genomics Institute, Guangzhou, China. All initial sequences were edited using Geneious v.7.1.8 (Kearse et al. 2012). The sequences obtained in this study were deposited in GenBank (http://www.ncbi.nlm.nih.gov).

Phylogenetic analyses

The *tef1* and *tub2* regions were sequenced for all *Calonectria* isolates selected for identification in the current study. All these isolates were preliminarily identified through standard nucleotide BLAST searches in the NCBI database (https://blast.ncbi.nlm.nih.gov/) using the *tef1* and *tub2* sequences. Based on their preliminary identification, representative isolates were selected for sequencing the additional gene regions of *cmdA* and *his3*. Based on the combined genotype of *tef1*, *tub2*, *cmdA*, and *his3* sequences, representative isolates presenting all genotypes obtained in this study were used for molecular identification. Sequences of the isolates from the type specimens of all the published species in the preliminarily identified *Calonectria* species complexes were used for phylogenetic analyses. The sequence datasets were aligned using online MAFFT v. 7 (http://mafft.cbrc.jp/alignment/server/) with the FFT-NS-i strategy (slow; interactive refinement method) (Katoh and Standley 2013). The aligned sequence datasets were manually edited and cut using MEGA v. 7.0 software (Kumar et al. 2016).

The sequence datasets of each gene region and the combination of four gene regions were performed on Maximum likelihood (ML) and Bayesian inference (BI) phylogenetic analyses using CIPRES Science Gateway v. 3.3. For the BI analyses, the most suitable models of the five sequence databases were carried through the jModelTest v. 2.1.5 (Posada 2008). Both ML and BI analyses were completed using online software, RaxML v. 8.2.12 (Stamatakis 2014) and MrBayes. v. 3.2.7 (Ronquist et al. 2012), respectively, as described by Wu and Chen (2023). Phylogenetic trees were viewed via FigTree v 1.4.2 and MEGA v. 7 for BI and ML trees, respectively.

Results

Sample collection and fungal isolation

After a comprehensive collection of samples across eight sites (A–H) in Guangdong, Guangxi, and Hainan Provinces of southern China, a total of 802 samples were collected. These included 401 diseased leaf samples from 401 trees, and 401 soil samples (Table 1, Figs 1, 2). At each sampling site, 39–62 diseased leaf samples, and the same number of soil samples were collected.

Calonectria isolates were obtained from leaf samples from the diseased trees from the eight sampling sites, except for one of the 62 samples from site A and one of the 50 samples from site G. The proportion of diseased leaf samples successfully obtained from *Calonectria* ranged from 98% to 100% for the eight sampling sites (avg. 99.5%). Each isolate was obtained from a single *Calonectria* diseased leaf sample, except for 54 *Calonectria* isolates from 50 such samples at site H. This is because four diseased leaf samples at site H exhibited differing vesicle morphologies, therefore, two isolates were obtained from each of them (Table 1).

A relatively large proportion of *Calonectria* isolates were obtained from the soil samples from the eight sites, except for sites F and G (Guangdong Province). The proportion of soil samples with *Calonectria* ranged from 2% (site G) to 100% (site H) (avg. 51.1%). Each isolate was obtained from a single *Calonectria* soil sample at sites B, E, F, and G, while more than one isolate was obtained from some of the soil samples at the sites A, C, D, and H where isolates with different morphologies of the conidia or vesicles were observed (Table 1).

In total, 642 isolates with typical morphological characteristics of *Calonectria* were obtained. These included 403 isolates from the 401 diseased leaf samples and 239 isolates from the 401 soil samples (Table 1).

Table 1. The number of samples and *Calonectria* spp. obtained from *Eucalyptus* plantations at eight sampling sites.

Site code	Diseased leaf samples						Soil samples									
	Total number of diseased leaf samples	No. of samples which yielded *Calonectria*	Total number of *Calonectria* isolates	No. of *Calonectria* isolates which selected for sequencing	No. of *C. pseudoreteaudii* isolates	No. of *C. acaciicola* isolates	Total number of soil samples	No. of samples obtained *Calonectria*	Total number of *Calonectria* isolates	No. of *Calonectria* isolates which selected for sequencing	No. of *C. pseudoreteaudii* isolates	No. of *C. acaciicola* isolates	No. of *C. hongkongensis* isolates	No. of *C. aconidialis* isolates	No. of *C. chinensis* isolates	No. of *C. auriculiformis* isolates
A	62	61	61	20	20	0	62	47	53	26	20	0	0	6	0	0
B	50	50	50	50	50	0	50	19	19	19	19	0	0	0	0	0
C	50	50	50	20	20	0	50	34	35	21	20	0	0	1	0	0
D	50	50	50	50	50	0	50	30	31	31	29	0	2	0	0	0
E	50	50	50	50	50	0	50	26	26	26	25	0	0	0	0	1
F	39	39	39	20	20	0	39	5	5	5	5	0	0	0	0	0
G	50	49	49	20	20	0	50	1	1	1	1	0	0	0	0	0
H	50	50	54	54	33	21	50	50	69	69	29	21	14	0	5	0
Total	401	399	403	284	263	21	401	212	239	198	148	21	16	7	5	1

Sequencing

Calonectria isolates were obtained from a relatively large proportion of the samples, from both the diseased trees and soils, at sites A, B, C, D, E, and H. All isolates from sites B, D, E, and H were sequenced. Since sites A, and C are relatively near to B, and D, only partial isolates obtained from diseased trees and soils at sites A, and C were sequenced. Since *Calonectria* was obtained from a small proportion of the soil samples at sites F, and G, all the isolates obtained from soils, and partial isolates obtained from diseased trees at the two sites were sequenced (Table 1). In total, 482 isolates were used to sequence the *tef1* and *tub2* gene regions (Table 1, Suppl. material 1). This included 54 isolates that were also identified by Liang et al. (2023) (Suppl. material 1). Based on the combined genotypes of the *tef1* and *tub2* gene sequences, and the sampling source, 169 isolates were selected for further sequencing of the *cmdA* and *his3* gene regions (Suppl. material 1). A total of 18 genotypes were generated based on the sequences of the *tef1*, *tub2*, *cmdA*, and *his3* regions of the 169 isolates that allowed for their identification. The remaining 313 isolates were identified based on *tef1* and *tub2* gene regions exclusively.

Phylogenetic analyses

To analyze their phylogenetic relationships, one or two isolates representing single genotype were selected that resulted in selection of 29 isolates representing 18 genotypes in total (Suppl. material 1). Additionally, the sequences from 90 isolates, including all ex-type isolates of all the *Calonectria* species of their respective species complexes, corresponding to 52 published *Calonectria* species, were retrieved from GenBank (Table 2). These sequences were used in phylogenetic analyses of the four individual gene regions and a combination of them.

The sequenced isolates yielded approximately 500 bp for *tef1*, 560 bp for *tub2*, 680 bp for *cmdA*, and 430 bp for *his3* gene regions. The model for each gene region was selected based on jModeltest v. 2.1.5. The TIM2+I+G, HKY+I+G, TrN+I+G, HKY+I+G, and TIM2+I+G models were selected for *tef1*, *tub2*, *cmdA*, *his3*, and the consolidated dataset, respectively. The topological structures generated from BI analyses were similar to those generated from ML analyses for each dataset. The ML trees displayed bootstrap values from ML and the posterior probabilities from BI are shown in Fig. 3, Suppl. materials 2–5.

The 29 *Calonectria* isolates were clustered into six distinct groups (Groups A–F) based on the phylogenetic analyses of the four gene regions' combination (Fig. 3). Among them, isolates in Group A and Group B belong to the *C. reteaudii* complex. Isolates in Group A were clustered with or closely related to *C. acaciicola*, *C. pseudoreteaudii*, *C. reteaudii*, or *C. guangdongensis* in the *tef1*, *cmdA*, and *his3* trees (Suppl. materials 2, 4, 5), and with *C. acaciicola* in the *tub2* tree (Suppl. material 3). The *tef1*/*tub2*/*cmdA*/*his3* tree confirmed that isolates in Group A were most closely related to *C. acaciicola* (Fig. 3), and thus they were accepted as belonging to this species. Isolates in Group B were clustered with, or most closely related to, *C. pseudoreteaudii* in each of the *tef1*, *tub2*, *cmdA*, *his3*, and *tef1*/*tub2*/*cmdA*/*his3* trees (Fig. 3, Suppl. materials 2–5). Thus, isolates in Group B are referred as *C. pseudoreteaudii*.

Table 2. *Calonectria* spp. isolates from the published studies used for phylogenetic analyses in this study.

Species code [a]	Species	Isolates no. [b, c]	Other collection number [c]	Substrate/host	Area of occurrence	Collector	GenBank accession numbers [d]				References of source of the isolates/sequencing data
							cmdA	*his3*	*tef1*	*tub2*	
B1	*C. acaciicola*	CMW 47173^{T}	CBS 143557	Soil (*Acacia auriculiformis* plantation)	Do Luong, Nghe An, Vietnam	N.Q. Pham and T.Q. Pham	MT335160	MT335399	MT412690	MT412930	Pham et al. 2019; Liu et al. 2020
		CMW 47174	CBS 143558	Soil (*A. auriculiformis* plantation)	Do Luong, Nghe An, Vietnam	N.Q. Pham and T.Q. Pham	MT335161	MT335400	MT412691	MT412931	Pham et al. 2019; Liu et al. 2020
B2	*C. acicola*	CMW 30996^{T}	–	*Phoenix canariensis*	Northland, New Zealand	H. Pearson	MT335162	MT335401	MT412692	MT412932	Gadgil and Dick 2004; Lombard et al. 2010a; Liu et al. 2020
		CBS 114812	CMW 51216	*P. canariensis*	Northland, New Zealand	H. Pearson	MT335163	MT335402	MT412693	MT412933	Gadgil and Dick 2004; Lombard et al. 2010a; Liu et al. 2020
B4	*C. aconidialis*	CMW 35174^{T}	CBS 136086; CERC 1850	Soil (*Eucalyptus* plantation)	Hainan, China	X. Mou and S.F. Chen	MT335165	MT335404	MT412695	OK357463	Lombard et al. 2015a; Liu et al. 2020, 2021
		CMW 35384	CBS 136091; CERC 1886	Soil (*Eucalyptus* plantation)	Hainan, China	X. Mou and S.F. Chen	MT335166	MT335405	MT412696	OK357464	Lombard et al. 2015a; Liu et al. 2020, 2021
B5	*C. aeknauliensis*	CMW 48253^{T}	CBS 143559	Soil (*Eucalyptus* plantation)	Aek Nauli, North Sumatra, Indonesia	M.J. Wingfield	MT335180	MT335419	MT412710	OK357465	Pham et al. 2019; Liu et al. 2020, 2021
		CMW 48254	CBS 143560	Soil (*Eucalyptus* plantation)	Aek Nauli, North Sumatra, Indonesia	M.J. Wingfield	MT335181	MT335420	MT412711	OK357466	Pham et al. 2019; Liu et al. 2020, 2021
B8	*C. asiatica*	CBS 114073^{T}	CMW 23782; CPC 3900	Debris (leaf litter)	Prathet Thai, Thailand	N.L. Hywel-Jones	AY725741	AY725658	AY725705	AY725616	Crous et al. 2004; Lombard et al. 2010a
B9	*C. auriculiformis*	CMW 47178^{T}	CBS 143561	Soil (*A. auriculiformis* plantation)	Hau Loc, Thanh Hoa, Vietnam	N.Q. Pham and T.Q. Pham	MT335190	MT335430	MT412721	MT412944	Pham et al. 2019; Liu et al. 2020
		CMW 47179	CBS 143562	Soil (*A. auriculiformis* plantation)	Hau Loc, Thanh Hoa, Vietnam	N.Q. Pham and T.Q. Pham	MT335191	MT335431	MT412722	MT412945	Pham et al. 2019; Liu et al. 2020
B10	*C. australiensis*	CMW 23669^{T}	CBS 112954; CPC 4714	*Ficus pleurocarpa*	Queensland, Australia	C. Pearce and B. Paulus	MT335192	MT335432	MT412723	MT412946	Crous et al. 2006; Lombard et al. 2010a; Liu et al. 2020
B14	*C. brasiliensis*	CBS 230.51^{T}	IMI 299576	*Eucalyptus* sp.	Ceara state, Brazil	T.R. Ciferri	MT335200	MT335440	MT412731	MT412953	Batista 1951; Crous 2002; Lombard et al. 2010b; Liu et al. 2020
		CMW 32949	CBS 114257; CPC 1944	*Eucalyptus* sp.	Aracruz, Brazil	A.C. Alfenas	MT335201	MT335441	MT412732	MT412954	Lombard et al. 2010a; Liu et al. 2020
B17	*C. brassicicola*	CBS 112841^{T}	CMW 51206; CPC 4552	Soil at *Brassica* sp.	Indonesia	M.J. Wingfield	KX784561	N/A	KX784689	KX784619	Lombard et al. 2016
B19	*C. bumicola*	CMW 48257^{T}	CBS 143575	Soil (*Eucalyptus* plantation)	Aek Nauli, North Sumatra, Indonesia	M.J. Wingfield	MT335205	MT335445	MT412736	OK357467	Pham et al. 2019; Liu et al. 2020, 2021
B20	*C. canadiana*	CMW 23673^{T}	CBS 110817; STE-U 499	*Picea* sp.	Canada	S. Greifenhagen	MT335206	MT335446	MT412737	MT412958	Kang et al. 2001b; Crous 2002; Lechat et al. 2010; Liu et al. 2020
		CERC 8952	–	Soil	Henan, China	S.F. Chen	MT335290	MT335530	MT412821	MT413035	Liu and Chen 2017; Liu et al. 2020
B22	*C. cerciana*	CMW 25309^{T}	CBS 123693	*E. urophylla* × *E. grandis* hybrid cutting	CERC nursery, Guangdong, China	M.J. Wingfield and X.D. Zhou	MT335211	MT335451	MT412742	MT412963	Lombard et al. 2010c; Liu et al. 2020
		CMW 25290	CBS 123695	*E. urophylla* × *E. grandis* hybrid cutting	CERC nursery, Guangdong, China	M.J. Wingfield and X.D. Zhou	MT335212	MT335452	MT412743	MT412964	Lombard et al. 2010c; Liu et al. 2020

Species code [a]	Species	Isolates no. [b, c]	Other collection number [c]	Substrate/host	Area of occurrence	Collector	GenBank accession numbers [d]				References of source of the isolates/sequencing data
							cmdA	*his3*	*tef1*	*tub2*	
B23	*C. chinensis*	CMW 23674[T]	CBS 114827; CPC 4101	Soil	Hong Kong, China	E.C.Y. Liew	MT335220	MT335460	MT412751	MT412972	Crous et al. 2004; Lombard et al. 2010a; Liu et al. 2020
		CMW 30986	CBS 112744; CPC 4104	Soil	Hong Kong, China	E.C.Y. Liew	MT335221	MT335461	MT412752	MT412973	Crous et al. 2004; Lombard et al. 2010a; Liu et al. 2020
B26	*C. cochinchinensis*	CMW 49915[T]	CBS 143567	Soil (*Hevea brasiliensis* plantation)	Duong Minh Chau, Tay Ninh, Vietnam	N.Q. Pham, Q.N. Dang and T.Q. Pham	MT335225	MT335465	MT412756	MT412977	Pham et al. 2019; Liu et al. 2020
		CMW 47186	CBS 143568	Soil (*A. auriculiformis* plantation)	Song May, Dong Nai, Vietnam	N.Q. Pham and T.Q. Pham	MT335226	MT335466	MT412757	MT412978	Pham et al. 2019; Liu et al. 2020
B29	*C. colombiensis*	CMW 23676[T]	CBS 112220; CPC 723	Soil (*E. grandis* trees)	La Selva, Colombia	M.J. Wingfield	MT335228	MT335468	MT412759	MT412980	Crous et al. 2004; Liu et al. 2020
		CMW 30985	CBS 112221; CPC 724	Soil (*E. grandis* trees)	La Selva, Colombia	M.J. Wingfield	MT335229	MT335469	MT412760	MT412981	Crous et al. 2004; Liu et al. 2020
B30	*C. crousiana*	CMW 27249[T]	CBS 127198	*E. grandis*	Fujian, China	M.J. Wingfield	MT335230	MT335470	MT412761	MT412982	Chen et al. 2011; Liu et al. 2020
		CMW 27253	CBS 127199	*E. grandis*	Fujian, China	M.J. Wingfield	MT335231	MT335471	MT412762	MT412983	Chen et al. 2011; Liu et al. 2020
B31	*C. curvispora*	CMW 23693[T]	CBS 116159; CPC 765	Soil	Tamatave, Madagascar	P.W. Crous	MT335232	MT335472	MT412763	OK357468	Victor et al. 1997; Crous 2002; Lombard et al. 2010a, 2015a; Liu et al. 2020, 2021
		CMW 48245	CBS 143565	Soil (*Eucalyptus* plantation)	Aek Nauli, North Sumatra, Indonesia	M.J. Wingfield	MT335233	MT335473	MT412764	N/A [e]	Pham et al. 2019; Liu et al. 2020
B32	*C. cylindrospora*	CBS 119670	CMW 51310; CPC 12766	*Pistacia lentiscus*	Italy	N/A	MT335236	MT335476	MT412767	MT412985	Lombard et al. 2015a, 2015b, 2016; Liu et al. 2020
		CMW 30978	CBS 110666; P90.1479; STE-U 497	*Ilex vomitoria*	Florida, USA	N.E. El-Gholl	MT335237	MT335477	MT412768	MT412986	Crou 2002; Lombard et al. 2010a, 2015b; Liu et al. 2020
B44	*C. hawksworthii*	CBS 111870[T]	CMW 51194; CPC 2405	*Nelumbo nucifera*	Pamplemousses garden, Mauritius	A. Peerally	MT335254	MT335494	MT412785	MT413003	Crous 2002; Liu et al. 2020
		CMW 31393	CBS 136641	*E. urophylla* × *E. grandis*	Guangxi, China	X. Zhou and G. Zhao	MT335247	MT335487	MT412778	MT412996	Lombard et al. 2015a; Liu et al. 2020
B46	*C. heveicola*	CMW 49913[T]	CBS 143570	Soil (*Hevea brasiliensis* plantation)	Bau Bang, Binh Duong, Vietnam	N.Q. Pham, Q.N. Dang and T.Q. Pham	MT335255	MT335495	MT412786	MT413004	Pham et al. 2019; Liu et al. 2020
		CMW 49928	CBS 143571	Soil	Bu Gia Map National Park, Binh Phuoc, Vietnam	N.Q. Pham, Q.N. Dang and T.Q. Pham	MT335280	MT335520	MT412811	MT413025	Pham et al. 2019; Liu et al. 2020
B48	*C. hongkongensis*	CBS 114828[T]	CMW 51217; CPC 4670	Soil	Hong Kong, China	M.J. Wingfield	MT335258	MT335498	MT412789	MT413007	Crous et al. 2004; Liu et al. 2020
		CERC 3570	CMW 47271	Soil (*Eucalyptus* plantation)	Beihai, Guangxi, China	S.F. Chen,J.Q. Li and G.Q. Li	MT335260	MT335500	MT412791	MT413009	Li et al. 2017; Liu et al. 2020
B51	*C. ilicicola*	CMW 30998[T]	CBS 190.50; IMI 299389; STE-U 2482	*Solanum tuberosum*	Bogor, Java, Indonesia	K.B. Boedijn and J. Reitsma	MT335266	MT335506	MT412797	OK357469	Boedijn and Reitsma 1950; Crous 2002; Lombard et al. 2010a; Liu et al. 2020, 2021
B52	*C. indonesiae*	CMW 23683[T]	CBS 112823; CPC 4508	*Syzygium aromaticum*	Warambunga, Indonesia	M.J. Wingfield	MT335267	MT335507	MT412798	MT413015	Crous et al. 2004; Liu et al. 2020
		CBS 112840	CMW 51205; CPC 4554	*S. aromaticum*	Warambunga, Indonesia	M.J. Wingfield	MT335268	MT335508	MT412799	MT413016	Crous et al. 2004; Liu et al. 2020

Species code [a]	Species	Isolates no. [b, c]	Other collection number [c]	Substrate/host	Area of occurrence	Collector	GenBank accession numbers [d]				References of source of the isolates/sequencing data
							cmdA	*his3*	*tef1*	*tub2*	
B54	*C. insularis*	CMW 30991^{T}	CBS 114558; CPC 768	Soil	Tamatave, Madagascar	P.W. Crous	MT335269	MT335509	MT412800	MT413017	Schoch et al. 1999; Lombard et al. 2010a, 2016; Liu et al. 2020
		CMW 30992	CBS 114559; CPC 954	Soil	Conejos, Veracruz, Mexico	M.J. Wingfield	MT335270	MT335510	MT412801	MT413018	Lombard et al. 2010a, 2016; Liu et al. 2020
B55	*C. kyotensis*	CBS 114525^{T}	ATCC 18834; CMW 51824; CPC 2367	*Robinia pseudoacacia*	Japan	T. Terashita	MT335271	MT335511	MT412802	MT413019	Terashita 1968; Crous 2002; Lombard et al. 2016; Liu et al. 2020
		CBS 114550	CMW 51825; CPC 2351	Soil	China	M.J. Wingfield	MT335246	MT335486	MT412777	MT412995	Lombard et al. 2016; Liu et al. 2020
B56	*C. lageniformis*	CBS 111324^{T}	CMW 51177; CPC 1473	Leaf of *Eucalyptus* sp.	Rivière Noire, Mauritius	H. Smith	KX784574	N/A	KX784702	KX784632	Lombard et al. 2016; Marin-Felix et al. 2017
B57	*C. lantauensis*	CERC 3302^{T}	CBS 142888; CMW 47252	Soil	Lidao, Hong Kong, China	M.J. Wingfield and S.F. Chen	MT335272	MT335512	MT412803	OK357470	Li et al. 2017; Liu et al. 2020, 2021
		CERC 3301	CBS 142887; CMW 47251	Soil	Lidao, Hong Kong, China	M.J. Wingfield and S.F. Chen	MT335273	MT335513	MT412804	OK357471	Li et al. 2017; Liu et al. 2020, 2021
B58	*C. lateralis*	CMW 31412^{T}	CBS 136629	Soil (*Eucalyptus* plantation)	Guangxi, China	X. Zhou, G. Zhao and F. Han	MT335274	MT335514	MT412805	MT413020	Lombard et al. 2015a; Liu et al. 2020
B63	*C. lombardiana*	CMW 30602^{T}	CBS 112634; CPC 4233; Lynfield 417	*Xanthorrhoea australis*	Victoria, Australia	T. Baigent	MT335395	MT335635	MT412926	MT413133	Crous 2002; Crous et al. 2006; Lombard et al. 2010c; Liu et al. 2020
B66	*C. malesiana*	CMW 23687^{T}	CBS 112752; CPC 4223	Soil	Northern Sumatra, Indonesia	M.J. Wingfield	MT335286	MT335526	MT412817	MT413031	Crous et al. 2004; Liu et al. 2020
		CBS 112710	CMW 51199; CPC 3899	Leaf litter	Prathet, Thailand	N.L. Hywel-Jones	MT335287	MT335527	MT412818	MT413032	Crous et al. 2004; Liu et al. 2020
B67	*C. maranhensis*	CBS 134811^{T}	LPF142	*Eucalyptus* sp. (leaf)	Açailandia, Maranhao, Brazil	A.C. Alfenas	KM396035	KM396118	KM395861	KM395948	Alfenas et al. 2015
		CBS 134812	LPF143	*Eucalyptus* sp. (leaf)	Açailandia, Maranhao, Brazil	A.C. Alfenas	KM396036	KM396119	KM395862	KM395949	Alfenas et al. 2015
B74	*C. multiseptata*	CMW 23692^{T}	CBS 112682; CPC 1589	*E. grandis*	North Sumatra, Indonesia	M.J. Wingfield	MT335299	MT335539	MT412830	MT413044	Crous et al. 2004; Lombard et al. 2010a; Liu et al. 2020
B80	*C. pacifica*	CMW 16726^{T}	A1568; CBS 109063; IMI 354528; STE-U 2534	*Araucaria heterophylla*	Hawaii, USA	M. Aragaki	MT335311	MT335551	MT412842	OK357472	Kang et al. 2001b; Crous 2002, Crous et al. 2004; Liu et al. 2020, 2021
		CMW 30988	CBS 114038	*Ipomoea aquatica*	Auckland, New Zealand	C.F. Hill	MT335312	MT335552	MT412843	OK357473	Crous 2002; Crous et al. 2004; Lombard et al. 2010a; Liu et al. 2020, 2021
B86	*C. penicilloides*	CMW 23696^{T}	CBS 174.55; STE-U 2388	*Prunus* sp.	Hatizyo Island, Japan	M. Ookubu	MT335338	MT335578	MT412869	MT413081	Tubaki 1958; Crous 2002; Liu et al. 2020
B89	*C. plurilateralis*	CBS 111401^{T}	CMW 51178; CPC 1637	Soil	Ecuador	M.J. Wingfield	MT335340	MT335580	MT412871	MT413083	Lombard et al. 2016; Liu et al. 2020
B90	*C. propaginicola*	CBS 134815^{T}	LPF220	*Eucalyptus* sp. (seeding)	Santana, Pará, Brazil	A.C. Alfenas	KM396040	KM396123	KM395866	KM395953	Alfenas et al. 2015
		CBS 134816	LPF222	*Eucalyptus* sp. (seeding)	Santana, Pará, Brazil	A.C. Alfenas	KM396041	KM396124	KM395867	KM395954	Alfenas et al. 2015

Species code [a]	Species	Isolates no. [b, c]	Other collection number [c]	Substrate/host	Area of occurrence	Collector	GenBank accession numbers [d]				References of source of the isolates/sequencing data
							cmdA	*his3*	*tef1*	*tub2*	
B97	*C. pseudoreteaudii*	CMW 25310^{T}	CBS 123694	*E. urophylla* × *E. grandis*	Guangdong, China	M.J. Wingfield and X.D. Zhou	MT335354	MT335594	MT412885	MT413096	Lombard et al. 2010c; Liu et al. 2020
		CMW 25292	CBS 123696	*E. urophylla* × *E. grandis*	Guangdong, China	M.J. Wingfield and X.D. Zhou	MT335355	MT335595	MT412886	MT413097	Lombard et al. 2010c; Liu et al. 2020
B104	*C. queenslandica*	CMW 30604^{T}	CBS 112146; CPC 3213	*E. urophylla*	Lannercost, Queensland, Australia	B. Brown	MT335367	MT335607	MT412898	MT413108	Kang et al. 2001a; Lombard et al. 2010c; Liu et al. 2020
		CMW 30603	CBS 112155; CPC 3210	*E. pellita*	Lannercost, Queensland, Australia	P.Q Thu and K.M. Old	MT335368	MT335608	MT412899	MT413109	Kang et al. 2001a; Lombard et al. 2010c; Liu et al. 2020
B106	*C. reteaudii*	CMW 30984^{T}	CBS 112144; CPC 3201	*E. camaldulensis*	Chon Thanh, Binh Phuoc, Vietnam	M.J. Dudzinski and P.Q. Thu	MT335370	MT335610	MT412901	MT413111	Kang et al. 2001a; Crous 2002; Crous et al. 2006; Liu et al. 2020
		CMW 16738	CBS 112143; CPC 3200	*Eucalyptus* leaves	Binh Phuoc, Vietnam	M.J. Dudzinski and P.Q. Thu	MT335371	MT335611	MT412902	MT413112	Kang et al. 2001a; Crous 2002; Crous et al. 2006; Liu et al. 2020
B112	*C. sumatrensis*	CMW 23698^{T}	CBS 112829; CPC 4518	Soil	Northern Sumatra, Indonesia	M.J. Wingfield	MT335382	MT335622	MT412913	OK357474	Crous et al. 2004; Liu et al. 2020, 2021
		CMW 30987	CBS 112934; CPC 4516	Soil	Northern Sumatra, Indonesia	M.J. Wingfield	MT335383	MT335623	MT412914	OK357475	Crous et al. 2004; Liu et al. 2020, 2021
B113	*C. syzygiicola*	CBS 112831^{T}	CMW 51204; CPC 4511	*Syzygium aromaticum*	Sumatra, Indonesia	M.J. Wingfield	N/A	N/A	KX784736	KX784663	Lombard et al. 2016
B115	*C. tonkinensis*	CMW 47430^{T}	CBS 143576	Soil (*Eucalyptus* plantation)	Bavi, Hanoi, Vietnam	N.Q. Pham and T.Q. Pham	MT335384	MT335624	MT412915	MT413122	Pham et al. 2019; Liu et al. 2020
B116	*C. uniseptata*	CBS 413.67^{T}	CMW 23678; CPC 2391; IMI 299577	*Paphiopedilum callosum*	Celle, Germany	W. Gerlach	GQ267379	GQ267248	GQ267307	GQ267208	Lombard et al. 2016
B118	*C. variabilis*	CMW 3187^{T}	AR2675; CBS 114677; CPC 2436	*Schefflera morototoni*	Pará, Brazil	F.C. de Albuquerque	MT335392	MT335632	MT412923	MT413130	Crous et al. 1993; Crous 2002; Lombard et al. 2010a, 2016; Liu et al. 2020
		CMW 2914	CBS 112691; CPC 2506	*Theobroma grandiflorum*	Pará, Brazil	F. Carneiro	MT335393	MT335633	MT412924	MT413131	Crous et al. 1993; Crous 2002; Lombard et al. 2010a, 2016; Liu et al. 2020
B120	*C. yunnanensis*	CERC 5339^{T}	CBS 142897; CMW 47644	Soil (*Eucalyptus* plantation)	Yunnan, China	S.F. Chen and J.Q. Li	MT335396	MT335636	MT412927	MT413134	Li et al. 2017; Liu et al. 2020
		CERC 5337	CBS 142895; CMW 47642	Soil (*Eucalyptus* plantation)	Yunnan, China	S.F. Chen and J.Q. Li	MT335397	MT335637	MT412928	MT413135	Li et al. 2017; Liu et al. 2020
B124	*C. singaporensis*	CBS 146715^{T}	MUCL 048320	leaf litter (submerged in a small stream)	South East Asian rainforest, Mac Ritchie Reservoir, Singapore	C. Decock	MW890042	MW890055	MW890086	MW890124	Crous et al. 2021
		CBS 146713	MUCL 048171	leaf litter (submerged in a small stream)	South East Asian rainforest, Mac Ritchie Reservoir, Singapore	C. Decock	MW890040	MW890053	MW890084	MW890123	Crous et al. 2021
B127	*C. borneana*	CMW 50782^{T}	CBS 144553	Soil (*Eucalyptus* plantation)	Sabah, Tawau, Brumas, Malaysia	N.Q. Pham, Marincowitz and M.J. Wingfield	OL635067	OL635043	OL635019	N/A	Pham et al. 2022a
		CMW 50832	CBS 144551	Soil (*Eucalyptus* plantation)	Sabah, Tawau, Brumas, Malaysia	N.Q. Pham, Marincowitz and M.J. Wingfield	OL635065	OL635041	OL635017	N/A	Pham et al. 2022a

Species code [a]	Species	Isolates no. [b, c]	Other collection number [c]	Substrate/host	Area of occurrence	Collector	GenBank accession numbers [d]				References of source of the isolates/sequencing data
							cmdA	*his3*	*tef1*	*tub2*	
B128	*C. ladang*	CMW 50776[T]	CBS 144550	Soil (*Eucalyptus* plantation)	Sabah, Tawau, Brumas, Malaysia	N.Q. Pham, Marincowitz and M.J. Wingfield	OL635075	OL635051	OL635027	N/A	Pham et al. 2022a
		CMW 50775	CBS 144549	Soil (*Eucalyptus* plantation)	Sabah, Tawau, Brumas, Malaysia	N.Q. Pham, Marincowitz and M.J. Wingfield	OL635074	OL635050	OL635026	N/A	Pham et al. 2022a
B129	*C. pseudomalesiana*	CMW 50821[T]	CBS 144563	Soil (*Eucalyptus* plantation)	Sabah, Tawau, Brumas, Malaysia	N.Q. Pham, Marincowitz and M.J. Wingfield	OL635076	OL635052	OL635028	OL635137	Pham et al. 2022a
		CMW 50779	CBS 144668	Soil (*Eucalyptus* plantation)	Sabah, Tawau, Brumas, Malaysia	N.Q. Pham, Marincowitz and M.J. Wingfield	OL635077	OL635053	OL635029	OL635138	Pham et al. 2022a
B130	*C. tanah*	CMW 50777[T]	CBS 144562	Soil (*Eucalyptus* plantation)	Sabah, Tawau, Brumas, Malaysia	N.Q. Pham, Marincowitz and M.J. Wingfield	OL635088	OL635064	OL635040	OL635146	Pham et al. 2022a
		CMW 50771	CBS 144560	Soil (*Eucalyptus* plantation)	Sabah, Tawau, Brumas, Malaysia	N.Q. Pham, Marincowitz and M.J. Wingfield	OL635086	OL635062	OL635038	OL635144	Pham et al. 2022a
B131	*C. cassiae*	ZHKUCC 210011 T	–	*Cassia surattensis*	Guangzhou City, Guangdong, China	Y. X. Zhang, C. T. Chen, Manawas., and M. M. Xiang	ON260790	N/A	MZ516860	MZ516863	Zhang et al. 2022
		ZHKUCC 210012	–	*Cassia surattensis*	Guangzhou City, Guangdong, China	Y. X. Zhang, C. T. Chen, Manawas., and M. M. Xiang	ON260791	N/A	MZ516861	MZ516864	Zhang et al. 2022
B132	*C. guangdongensis*	ZHKUCC 21-0062T	–	*Heliconia metallica*	Guangdong, China	Y. X. Zhang, C. T. Chen, Manawas., and M. M. Xiang	MZ491127	N/A	MZ491149	MZ491171	Zhang et al. 2022
		ZHKUCC 21-0063	–	*Heliconia metallica*	Guangdong, China	Y. X. Zhang, C. T. Chen, Manawas., and M. M. Xiang	MZ491128	N/A	MZ491150	MZ491172	Zhang et al. 2022
	Curvicladiella cignea	CBS 109167T	CPC 1595; MUCL 40269	Decaying leaf	French Guiana	C. Decock	KM231287	KM231461	KM231867	KM232002	Decock and Crous 1998; Crous et al. 2006; Lombard et al. 2015b
		CBS 109168	CPC 1594; MUCL 40268	Decaying seed	French Guiana	C. Decock	KM231286	KM231460	KM231868	KM232003	Decock and Crous 1998; Crous et al. 2006; Lombard et al. 2015b

[a] Codes (B1–B120) of the 120 accepted *Calonectria* species accepted according to Liu et al. (2020).
[b] T: ex-type isolates of the species.
[c] AR: Amy Y. Rossman working collection; ATCC: American Type Culture Collection, Virginia, USA; CBS: Westerdijk Fungal Biodiversity Institute, Utrecht, The Netherlands; CERC: China Eucalypt Research Centre, Zhanjiang, Guangdong Province, China; CMW: Culture collection of the Forestry and Agricultural Biotechnology Institute (FABI), University of Pretoria, Pretoria, South Africa; CPC: Pedro Crous working collection housed at Westerdijk Fungal Biodiversity Institute; IMI: International Mycological Institute, CABI Bioscience, Egham, Bakeham Lane, UK; MUCL: Mycotheque, Laboratoire de Mycologie Systematique st Appliqee, I'Universite, Louvian-la-Neuve, Belgium; STE-U: Department of Plant Pathology, University of Stellenbosch, South Africa; ZHKUCC: Zhongkai University of Agriculture and Engineering Culture Collection; –: no other collection number.
[d] *tef1*: translation elongation factor 1-alpha; *tub2*: β-tubulin; *cmdA*: calmodulin; *his3*: histone H3.
[e] N/A: information is not available.

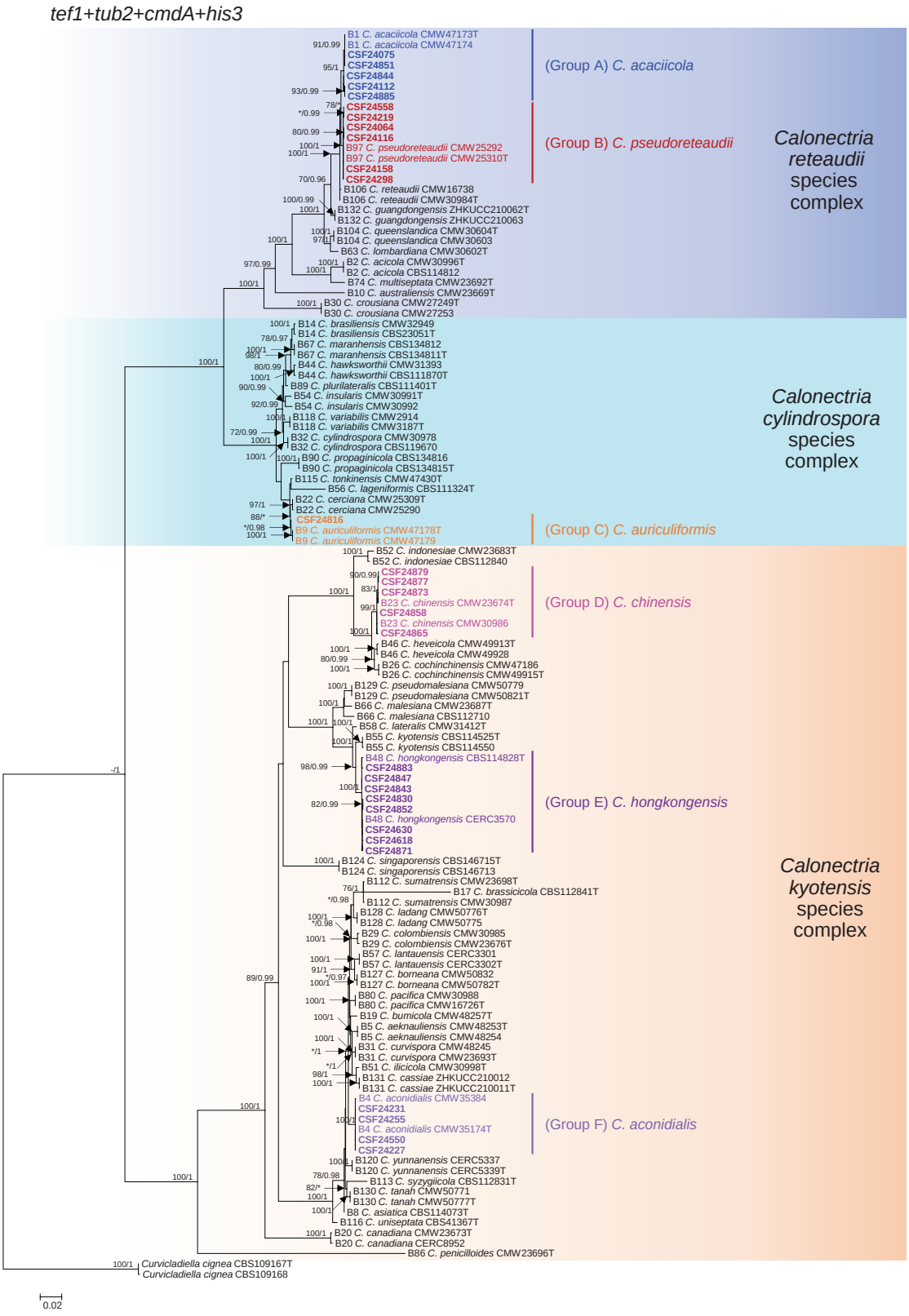

Figure 3. Phylogenetic tree of *Calonectria* species based on maximum likelihood (ML) analyses of a combined DNA dataset of *tef1*, *tub2*, *cmdA*, and *his3* gene sequences. Bootstrap support values ≥ 70% for ML and posterior probability values ≥ 0.95 for Bayesian inference (BI) analyses are presented above the branches as ML/BI. Bootstrap values < 70% or probability values < 0.95 are marked with "*," and absent analysis values are marked with "-". Ex-type isolates are marked with "T." Isolates sequenced in this study are highlighted in bold. The outgroup taxon was *Curvicladiella cignea* (CBS 109167 and CBS 109168).

Isolate CSF24816 (Group C) was grouped in the *C. cylindrospora* species complex (Fig. 3, Suppl. materials 2–5). It was clustered with *C. auriculiformis* in the *tef1* tree, with *C. cerciana* in the *tub2* tree, with *C. cerciana* and *C. tonkinensis* in the *cmdA* tree, and with *C. auriculiformis*, *C. cerciana*, and *C. tonkinensis* in the *his3* tree (Suppl. materials 2–5). It was most closely related to *C. auriculiformis* in the *tef1/tub2/cmdA/his3* tree (Fig. 3), thus the isolate CSF24816 was identified as *C. auriculiformis*.

Isolates in Groups D, E, and F resided in the *C. kyotensis* species complex based on the phylogenetic trees of *tef1*, *tub2*, *cmdA*, *his3*, and *tef1/tub2/cmdA/his3* (Fig. 3, Suppl. materials 2–5). Isolates in Group D, Group E, and Group F were consistently clustered with or most closely related to *C. chinensis*, *C. hongkongensis*, and *C. aconidialis*, respectively (Fig. 3, Suppl. materials 2–5). Therefore, isolates in Group D, Group E, and Group F were identified as *C. chinensis*, *C. hongkongensis* and *C. aconidialis*, respectively.

Calonectria distribution associated with diseased leaves and soil in *Eucalyptus* plantations

The 482 *Calonectria* isolates used for molecular identification in the current study were identified as six species, which resided in three species complexes. The six species were *C. pseudoreteaudii* (411 isolates, 85.27%), *C. acaciicola* (42 isolates, 8.71%), *C. hongkongensis* (16 isolates, 3.32%), *C. aconidialis* (seven isolates, 1.45%), *C. chinensis* (five isolates, 1.04%), and *C. auriculiformis* (one isolate, 0.21%) (Fig. 4).

At each of the eight sampling sites, *C. pseudoreteaudii* was dominant in the samples collected from both the diseased trees and soil under these trees, particularly at sites A–G located on the mainland of China. *Calonectria acaciicola* isolates were obtained from site H in Hainan Province, and this species was also frequently isolated from both diseased trees and soil. The other four *Calonectria* species, *C. hongkongensis*, *C. aconidialis*, *C. chinensis*, and *C. auriculiformis*, were only isolated from samples collected from soils (Table 1, Figs 4, 5).

When considering the species complexes associated with diseased leaves and soils, all *Calonectria* isolates obtained from diseased trees resided in the *C. reteaudii* species complex; and 14.14% of *Calonectria* isolates obtained from soils resided in the *C. kyotensis* species complex. All isolates residing in the *C. kyotensis* species complex were obtained from soils. For the isolates residing in the *C. reteaudii* species complex, 62.69% of the isolates come from diseased trees and 37.31% were from soil samples (Table 1, Fig. 5).

Discussion

In this study, a systematic and comprehensive investigation of Calonectria leaf blight occurring on *Eucalyptus* plantations in a wide geographic range in southern China was conducted. The results of this study clearly showed that the *Calonectria* species in the *C. cylindrospora* species complex was occasionally distributed in *Eucalyptus* plantations. *Calonectria* species in both the *C. reteaudii* species complex and *C. kyotensis* species complex were widely distributed. The distribution patterns of *Calonectria* species in the *C. reteaudii* species complex and *C. kyotensis* species complex were related to diseased leaves and soil habitats during leaf blight outbreak season in *Eucalyptus* plantations in southern China.

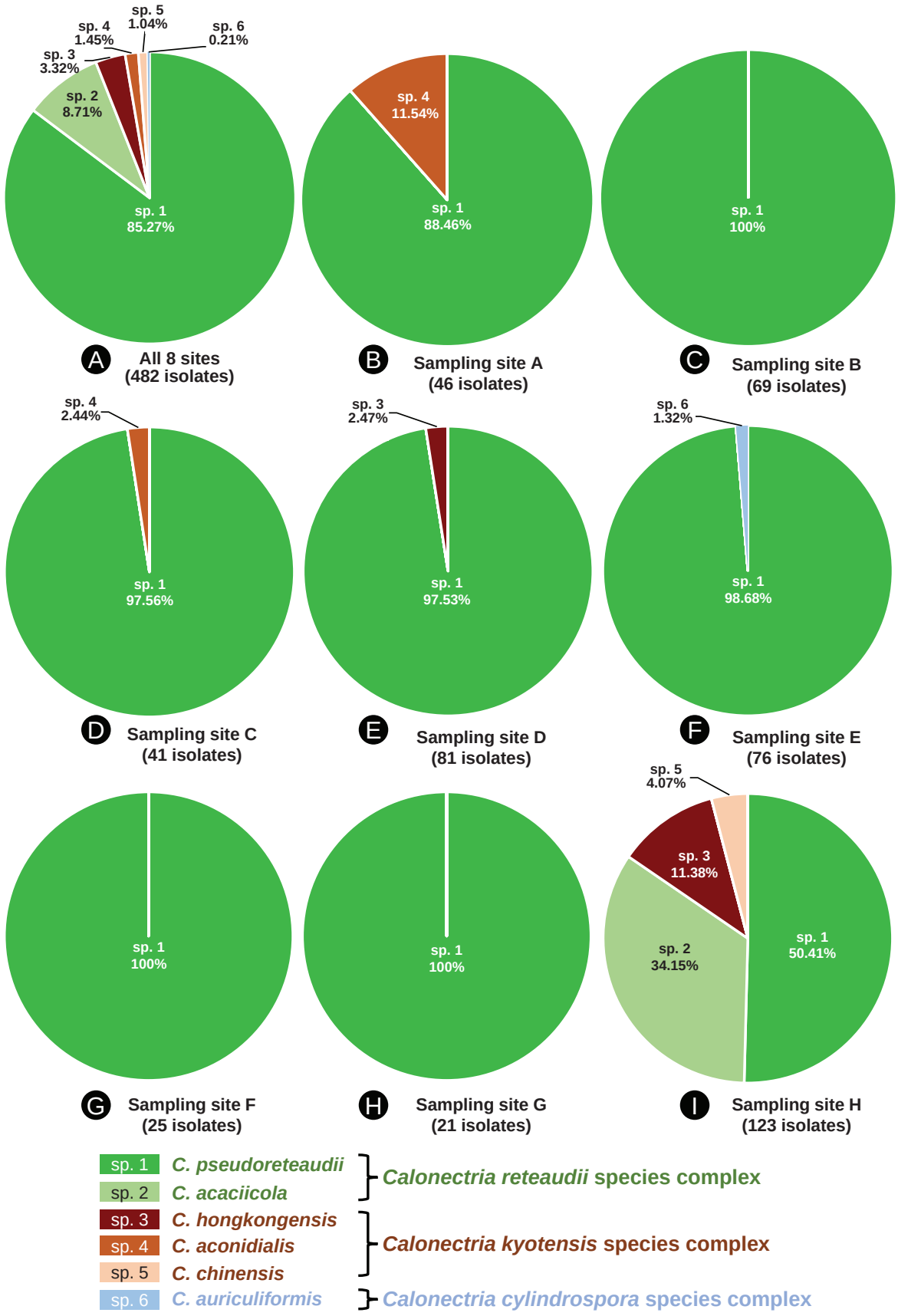

Figure 4. The isolate number and percentage of each *Calonectria* species at the eight sampling sites. "sp. 1, 2, 3, 4, 5, 6" indicate the six *Calonectria* species **A** isolates and species obtained from all eight sites **B-I** isolates and species obtained from a particular site (sites **A–H**).

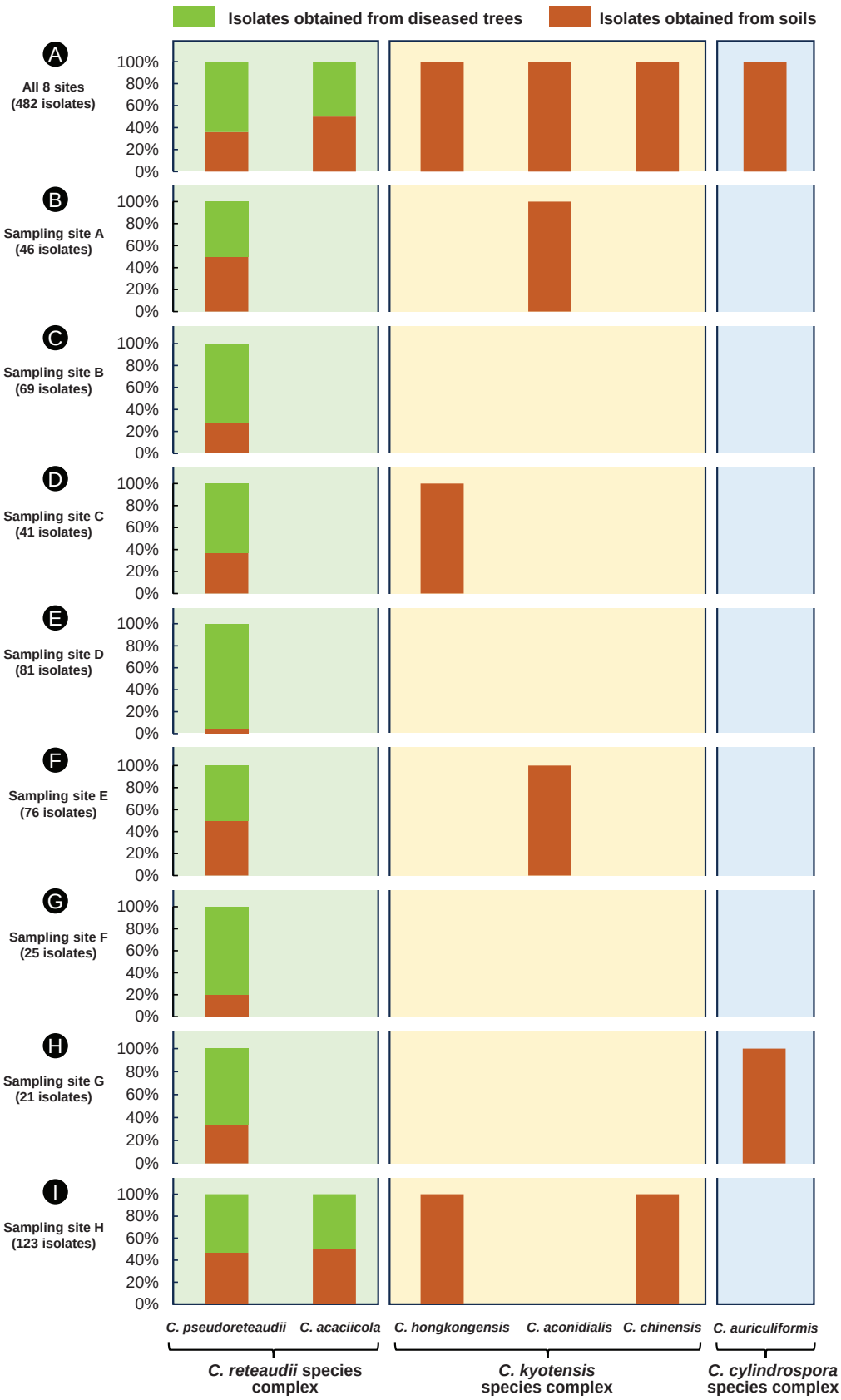

Figure 5. Histogram showing the proportions of each of the six *Calonectria* species reside in three species complexes isolated from diseased leaves and soil at the eight sampling sites. The histograms in green and orange indicated isolates obtained from diseased trees and soils, respectively **A** species obtained from all the eight sites **B–I** species obtained from a particular site (sites **A–H**).

The results of this study showed that all isolates obtained from diseased trees resided in the *C. reteaudii* species complex, which indicated that they are the causal agents of Calonectria leaf blight at the sampled sites in China. Moreover, *C. pseudoreteaudii* was the dominant species of all the eight sampling sites in the three provinces. This was consistent with previous studies in which *C. pseudoreteaudii* was frequently obtained from diseased *Eucalyptus* trees in Guangdong, Guangxi, Fujian, and Hainan Provinces in southern China (Chen et al. 2013; Wang and Chen 2020; Wu and Chen 2021; Li et al. 2023a; Liang et al. 2023). *Calonectria acaciicola* was only isolated from site H in Hainan Province in this and a previous study by Liang et al. (2023). Furthermore, inoculation results from previous studies indicated that both *C. pseudoreteaudii* and *C. acaciicola* were highly virulent to the tested *Eucalyptus* genotypes (Liang et al. 2023). *C. pseudoreteaudii* is one of the main causal agents of Calonectria leaf blight widely observed in southern China, and *C. acaciicola* is causal agent of the disease in Hainan Province in particular.

It is still unclear whether the species in the *C. reteaudii* complex are soil-borne or not. The results of the previous studies consistently indicated that species in the *C. reteaudii* complex can survive in the soils, at least for a certain time (Crous 2002; Liu et al. 2021). Both *C. pseudoreteaudii* and *C. acaciicola* were frequently isolated from soils under the diseased trees in this study. Results of the previous research confirmed that *Calonectria* species in the *C. reteaudii* species complex were frequently isolated from soils under diseased *Eucalyptus* trees in southern China (Wu and Chen 2021; Li et al. 2023b). A recent population study showed that the genetic diversity of the *C. pseudoreteaudii* isolates obtained from diseased leaves was higher than that of the *C. pseudoreteaudii* isolates obtained from the soil in one *Eucalyptus* plantation, and the *C. pseudoreteaudii* isolates in soil may spread from diseased leaves (Wu et al. 2023). The results of the current study highlight that *C. pseudoreteaudii* from the soils in *Eucalyptus* plantations also needs to be carefully monitored for disease management purposes. It is necessary to clarify whether *Calonectria* in the *C. reteaudii* species complex is soil-borne or not and further understand the sources and dispersal pathways of the pathogens from this complex.

Previous studies showed that the species in the *C. kyotensis* complex were widely isolated from soils, both in natural forests and commercial plantations (Liu et al. 2021, 2022; Wu and Chen 2021, 2023; Li et al. 2023b; Liu and Chen 2023), and a relatively small number of isolates were isolated from susceptible *Eucalyptus* leaves (Li et al. 2023a; Liang et al. 2023). The research in this study indicated that all isolates residing in the *C. kyotensis* species complex were obtained from soils but not from diseased trees. Moreover, the results of this study revealed that isolates in the *C. kyotensis* species complex may not be the pathogens causing leaf blight in *Eucalyptus*. Further research is needed to clarify their ecological niche since they were also frequently isolated from diseased leaves (Li et al. 2023b; Liang et al. 2023).

Conclusion

This study clarified the distribution patterns of *Calonectria* species complexes related to the *Calonectria* isolated sources of diseased trees and soils during the disease outbreak season. The results of this study clearly showed that all isolates obtained from diseased leaves resided in the *C. reteaudii* species com-

plex, and species in the *C. reteaudii* species complex were widely distributed in diseased leaves and soils. All the isolates residing in the *C. kyotensis* species complex were obtained from soils. This indicated that species in the *C. kyotensis* species complex are soil inhabitants. These results highlight that *Calonectria* species in the *C. reteaudii* species complex, but not in the *C. kyotensis* species complex, are the causal agents of Calonectria leaf blight in southern China. More attention should be paid to the causal agents of Calonectria leaf blight, especially *C. pseudoreteaudii*, with a wide geographic distribution during the disease outbreak season, for disease management in the future.

Acknowledgements

We thank Mr. QuanChao Wang, Ms. LinFang Liu, Ms. XueYing Liang, and Mr. BingYin Chen for their assistance in collecting samples.

Additional information

Conflict of interest

The authors have declared that no competing interests exist.

Ethical statement

No ethical statement was reported.

Funding

This study was initiated through the bilateral agreement between the Governments of South Africa and China and supported by The National Key R&D Program of China (China-South Africa Forestry Joint Research Centre Project; Project No. 2018YFE0120900), the National Ten-thousand Talents Program (Project No. W03070115), and the Guangdong Top Young Talents Program in China (Project No. 20171172).

Author contributions

Conceptualization: SFC. Formal analysis: WXW. Funding acquisition: SFC. Methodology: SFC, WXW. Project administration: SFC. Resources: SFC, WXW. Software: WXW. Supervision: SFC. Writing - original draft: WXW. Writing - review and editing: SFC, WXW.

Author ORCIDs

WenXia Wu https://orcid.org/0009-0000-1685-9627
ShuaiFei Chen https://orcid.org/0000-0002-3920-9982

Data availability

All of the data that support the findings of this study are available in the main text or Supplementary Information.

References

Alfenas RF, Lombard L, Pereira OL, Alfenas AC, Crous PW (2015) Diversity and potential impact of *Calonectria* species in *Eucalyptus* plantations in Brazil. Studies in Mycology 80: 89–130. https://doi.org/10.1016/j.simyco.2014.11.002

Batista AC (1951) *Cylindrocladium scoparium* Morgan var. *brasiliensis* Batista Ciferri, a new fungus on *Eucalyptus*. Boletim da Secretaria de agricultura, industria e comercio do Estado de Pernambuco 18: 188–191.

Boedijn KB, Reitsma J (1950) Notes on the genus *Cylindrocladium* (Fungi: Mucedineae). Reinwardtia 1: 51–60.

Chen SF, Lombard L, Roux J, Xie YJ, Wingfield MJ, Zhou XD (2011) Novel species of *Calonectria* associated with Eucalyptus leaf blight in Southeast China. Persoonia 26: 1–12. https://doi.org/10.3767/003158511X555236

Chen QZ, Guo WS, Ye XZ, Huang XP, Wu, YZ (2013) Identification of *Calonectria* associated with Eucalyptus leaf blight in Fujian Province. Journal of Fujian College of Forestry 33: 176–182.

Crous PW (2002) Taxonomy and pathology of *Cylindrocladium* (*Calonectria*) and allied genera. American Phytopathological Society Press, St Paul, MN.

Crous PW, Janse BJH, Victor D, Marais GF, Alfenas AC (1993) Characterization of some *Cylindrocladium* species with three–septate conidia using morphology, isozyme banding patterns and DNA polymorphisms. Systematic and Applied Microbiology 16: 266–273. https://doi.org/10.1016/S0723-2020(11)80479-0

Crous PW, Groenewald JZ, Risède JM, Simoneau P, Hywel–Jones NL (2004) *Calonectria* species and their *Cylindrocladium* anamorphs: species with sphaeropedunculate vesicles. Studies in Mycology 50: 415–430.

Crous PW, Groenewald JZ, Risède JM, Simoneau P, Hywel–Jones NL (2006) *Calonectria* species and their *Cylindrocladium* anamorphs: species with clavate vesicles. Studies in Mycology 55: 213–226. https://doi.org/10.3114/sim.55.1.213

Crous PW, Hernández–Restrepo M, Schumacher RK, Cowan DA, Maggs-Kölling G, Marais E, Wingfield MJ, Yilmaz N, Adan OCG, Akulov A, Álvarez Duarte E, Berraf–Tebbal A, Bulgakov TS, Carnegie AJ, Beer ZW, Decock C, Dijksterhuis J, Duong TA, Eichmeier A, Hien LT, Houbraken JAMP, Khanh TN, Liem NV, Lombard L, Lutzoni FM, Miądlikowska JM, Nel WJ, Pascoe IG, Roets F, Roux J, Samson RA, Shen M, Spetik M, Thangavel R, Thanh HM, Thao LD, Nieuwenhuijzen EJ, Zhang JQ, Zhang Y, Zhao LL, Groenewald JZ (2021) New and Interesting Fungi. 4. Fungal Systematics and Evolution 7: 255–343. https://doi.org/10.3114/fuse.2021.07.13

Decock C, Crous PW (1998) *Curvicladium* gen. nov., a new hyphomycete genus from French Guiana. Mycologia 90: 276–281. https://doi.org/10.1080/00275514.1998.12026907

Feng SF, Zheng JH (1986) A new disease occurs on nursery seedlings of *Eucalyptus parvula* in HaiNan Island. Tropical Agricultural Science 1: 59–61. [In Chinese]

Gadgil P, Dick M (2004) *Fungi silvicolae novazelandiae*: 10. New Zealand Journal of Forestry Science 44: 1–7. https://doi.org/10.1186/s40490-014-0030-7

Kang JC, Crous PW, Old KM, Dudzinski MJ (2001a) Non–conspecificity of *Cylindrocladium quinqueseptatum* and *Calonectria quinqueseptata* based on a *β–tubulin* gene phylogeny and morphology. Canadian Journal of Botany 79: 1241–1247. https://doi.org/10.1139/b01-101

Kang JC, Crous PW, Schoch CL (2001b) Species concepts in the *Cylindrocladium floridanum* and *Cy. spathiphylli* complexes (Hypocreaceae) based on multi–allelic sequence data, sexual compatibility and morphology. Systematic and Applied Microbiology 24: 206–217. https://doi.org/10.1078/0723-2020-00026

Katoh K, Standley DM (2013) MAFFT multiple sequence alignment software version 7: improvements in performance and usability. Molecular Biology and Evolution 30: 772–780. https://doi.org/10.1093/molbev/mst010

Kearse M, Moir R, Wilson A, Stones–Havas S, Cheung M, Sturrock S, Buxton S, Cooper A, Markowitz S, Duran C, Thierer T (2012) Geneious Basic: an integrated and extendable desktop software platform for the organization and analysis of sequence data. Bioinformatics 28: 1647–1649. https://doi.org/10.1093/bioinformatics/bts199

Kumar S, Stecher G, Tamura K (2016) MEGA7: molecular evolutionary genetics analysis version 7.0 for bigger datasets. Molecular Biology and Evolution 33: 1870–1874. https://doi.org/10.1093/molbev/msw054

Lechat C, Crous PW, Groenewald JZ (2010) The enigma of *Calonectria* species occurring on leaves of *Ilex aquifolium* in Europe. IMA Fungus 1: 101–108 https://doi.org/10.5598/imafungus.2010.01.02.01

Li JQ, Wingfield MJ, Liu QL, Barnes I, Roux J, Lombard L, Crous PW, Chen SF (2017) *Calonectria* species isolated from *Eucalyptus* plantations and nurseries in South China. IMA Fungus 8: 259–286. https://doi.org/10.5598/imafungus.2017.08.02.04

Li WW, Chen SF, Wingfield MJ, Duong TA (2023a) *Calonectria queenslandica*: Causal agent of *Eucalyptus* leaf blight in Southern China. Plant Disease 107: 730–742. https://doi.org/10.1094/PDIS-01-22-0196-RE

Li WW, Chen SF, Wingfield MJ, Duong TA (2023b) *Calonectria* species associated with diseased leaves and soils in southern China *Eucalyptus* plantations. Phytopathology Research 5: 29. https://doi.org/10.1186/s42483-023-00183-z

Liang XY, Wang QC, Chen SF (2023) Phylogeny, morphology, distribution, and pathogenicity of seven *Calonectria* species from leaf blighted *Eucalyptus* in Hainan Island, China. Plant Disease 107: 2579–2605 https://doi.org/10.1094/PDIS-12-22-2802-RE

Liu QL, Chen SF (2017) Two novel species of *Calonectria* isolated from soil in a natural forest in China. MycoKeys 26: 25–60. https://doi.org/10.3897/mycokeys.26.14688

Liu Y, Chen SF (2023) Diversity and distribution of *Calonectria* species in soils from *Eucalyptus urophylla* × *E. grandis*, *Pinus massoniana*, and *Cunninghamia lanceolata* plantations in four provinces in Southern China. Journal of Fungi 9: 198. https://doi.org/10.3390/jof9020198

Liu QL, Li JQ, Wingfield MJ, Duong TA, Wingfield BD, Crous PW, Chen SF (2020) Reconsideration of species boundaries and proposed DNA barcodes for *Calonectria*. Studies in Mycology 97: 100106. https://doi.org/10.1016/j.simyco.2020.08.001

Liu LL, Wu WX, Chen SF (2021) Species diversity and distribution characteristics of *Calonectria* in five soil layers in a *Eucalyptus* plantation. Journal of Fungi 7: 857. https://doi.org/10.3390/jof7100857

Liu QL, Wingfield MJ, Duong TA, Wingfield BD, Chen SF (2022) Diversity and distribution of *Calonectria* species from plantation and forest soils in Fujian Province, China. Journal of Fungi 8: 811. https://doi.org/10.3390/jof8080811

Lombard L, Crous PW, Wingfield BD, Wingfield MJ (2010a) Phylogeny and systematics of the genus *Calonectria*. Studies in Mycology 66: 31–69. https://doi.org/10.3114/sim.2010.66.03

Lombard L, Crous PW, Wingfield BD, Wingfield MJ (2010b) Multigene phylogeny and mating tests reveal three cryptic species related to *Calonectria pauciramosa*. Studies in Mycology 66: 15–30. https://doi.org/10.3114/sim.2010.66.02

Lombard L, Zhou XD, Crous PW, Wingfield BD, Wingfield MJ (2010c) *Calonectria* species associated with cutting rot of *Eucalyptus*. Persoonia 24: 1–11. https://doi.org/10.3767/003158510X486568

Lombard L, Chen SF, Mou X, Zhou XD, Crous PW, Wingfield MJ (2015a) New species, hyper–diversity and potential importance of *Calonectria* spp. from *Eucalyptus* in South China. Studies in Mycology 80: 151–188. https://doi.org/10.1016/j.simyco.2014.11.003

Lombard L, van der Merwe NA, Groenewald JZ, Crous PW (2015b) Generic concepts in Nectriaceae. Studies in Mycology 80: 189–245. https://doi.org/10.1016/j.simyco.2014.12.002

Lombard L, Wingfield MJ, Alfenas AC, Crous PW (2016) The forgotten *Calonectria* collection: pouring old wine into new bags. Studies in Mycology 85: 159–198. https://doi.org/10.1016/j.simyco.2016.11.004

Marin–Felix Y, Groenewald JZ, Cai L, Chen Q, Marincowitz S, Barnes I, Bensch K, Braun U, Camporesi E, Damm U, de Beer ZW, Dissanayake A, Edwards J, Giraldo A, Hernández-Restrepo M, Hyde KD, Jayawardena RS, Lombard L, Luangsa-ard J, McTaggart AR, Rossman AY, Sandoval-Denis M, Shen M, Shivas RG, Tan YP, van der Linde EJ, Wingfield MJ, Wood AR, Zhang JQ, Zhang Y, Crous PW (2017) Genera of phytopathogenic fungi: GOPHY 1. Studies in Mycology 86: 99–216. https://doi.org/10.1016/j.simyco.2017.04.002

Old KM, Wingfield MJ, Yuan ZQ (2003) A manual of diseases of *Eucalypts* in Southeast Asia. Centre for International Forestry Research, Bogor.

Pham NQ, Barnes I, Chen SF, Liu FF, Dang QN, Pham TQ, Lombard L, Crous PW, Wingfield MJ (2019) Ten new species of *Calonectria* from Indonesia and Vietnam. Mycologia 111: 78–102. https://doi.org/10.1080/00275514.2018.1522179

Pham NQ, Marincowitz S, Chen SF, Rodas C, Wingfield MJ (2022a) Soil–borne *Calonectria* (Hypocreales, Nectriaceae) associated with *Eucalyptus* plantations in Colombia. MycoKeys 94: 17–35. https://doi.org/10.3897/mycokeys.94.96301

Pham NQ, Marincowitz S, Chen SF, Yaparudin Y, Wingfield MJ (2022b) *Calonectria* species, including four novel taxa, associated with *Eucalyptus* in Malaysia. Mycology Progress 21: 181–197. https://doi.org/10.1007/s11557-021-01768-8

Posada D (2008) jModelTest: phylogenetic model averaging. Molecular biology and Evolution 25: 1253–1256. https://doi.org/10.1093/molbev/msn083

Rodas CA, Lombard L, Gryzenhout M, Slippers B, Wingfield MJ (2005) Cylindrocladium blight of *Eucalyptus grandis* in Colombia. Australasian Plant Pathology 34: 143–149. https://doi.org/10.1071/AP05012

Ronquist F, Teslenko M, Van Der Mark P, Ayres D, Darling A, Höhna S, Larget B, Liu L, Suchard M, Huelsenbeck J (2012) MrBayes 3.2: efficient Bayesian phylogenetic inference and model choice across a large model space. Systematic Biology 61: 539–542. https://doi.org/10.1093/sysbio/sys029

Schoch CL, Crous PW, Wingfield BD, Wingfield MJ (1999) The *Cylindrocladium candelabrum* species complex includes four distinct mating populations. Mycologia 91: 286–298. https://doi.org/10.1080/00275514.1999.12061019

Stamatakis A (2014) RAxML version 8: a tool for phylogenetic analysis and post–analysis of large phylogenies. Bioinformatics 30: 1312–1313. https://doi.org/10.1093/bioinformatics/btu033

Terashita T (1968) A new species of *Calonectria* and its conidial state. Transactions of the Mycological Society of Japan 8: 124–129.

Thornhill AH, Crisp M, Külheim CD, Lam KE, Nelson LA, Yeates DK, Miller JT (2019) A dated molecular perspective of eucalypt taxonomy, evolution and diversification. Australian Systematic Botany 32: 29–48. https://doi.org/10.1071/SB18015

Tubaki K (1958) Studies on the Japanese Hyphomycetes. V. Leaf & stem group with a discussion of the classification of Hyphomycetes and their perfect stages. The Journal of the Hattori Botanical Laboratory 20: 142–244.

van Burik JAH, Schreckhise RW, White TC, Bowden RA, Myerson D (1998) Comparison of six extraction techniques for isolation of DNA from filamentous fungi. Medical Mycology 36: 299–303. https://doi.org/10.1046/j.1365-280X.1998.00161.x

Victor D, Crous PW, Janse BJH, Wingfield MJ (1997) Genetic variation in *Cylindrocladium floridanum* and other morphologically similar *Cylindrocladium* species. Systematic and Applied Microbiology 20: 268–285. https://doi.org/10.1016/S0723-2020(97)80074-4

Wang QC, Chen SF (2020) *Calonectria pentaseptata* causes severe leaf disease on cultivated *Eucalyptus* in Leizhou Peninsula of southern China. Plant Disease 104: 493–509. https://doi.org/10.1094/PDIS-05-19-1009-RE

Wu WX, Chen SF (2021) Species diversity, mating strategy and pathogenicity of *Calonectria* species from diseased leaves and soils in the *Eucalyptus* plantation in Southern China. Journal of Fungi 7: 73. https://doi.org/10.3390/jof7020073

Wu WX, Chen SF (2023) Wide distribution and intraspecies diversity in the pathogenicity of *Calonectria* in soil from *Eucalyptus* plantations in southern Guangxi of China. Journal of Fungi 9: 802. https://doi.org/10.3390/jof9080802

Wu WX, Li WW, Liu FF, Chen SF (2023) Evidence of high genetic diversity and differences in the population diversity of the Eucalyptus Leaf Blight pathogen *Calonectria pseudoreteaudii* from diseased leaves and soil in a plantation in Guangxi, China. Microorganisms 11: 2785. https://doi.org/10.3390/microorganisms11112785

Xie YJ, Du AP (2019) *Eucalyptus* in South China. Party School of the CPC Central Committee Press, Beijing. [In Chinese]

Xie YJ, Arnold RJ, Wu ZH, Chen SF, Du AP, Luo JZ (2017) Advances in eucalypt research in China. Frontiers of Agricultural Science & Engineering 4: 380–390. https://doi.org/10.15302/J-FASE-2017171

Zhang Y, Chen C, Chen C, Chen J, Xiang M, Wanasinghe DN, Hsiang T, Hyde KD, Manawasinghe IS (2022) Identification and characterization of *Calonectria* species associated with plant diseases in Southern China. Journal of Fungi 8: 719. https://doi.org/10.3390/jof8070719

Zhou XD, Wingfield MJ (2011) Eucalypt diseases and their management in China. Australasian Plant Pathology 40: 339–345. https://doi.org/10.1007/s13313-011-0053-y

Supplementary material 1

Calonectria isolates obtained from eight *Eucalyptus* plantations in this study

Authors: WenXia Wu, ShuaiFei Chen

Data type: docx

Link: https://doi.org/10.3897/mycokeys.110.130733.suppl1

Supplementary material 2

Phylogenetic tree of *Calonectria* species based on maximum likelihood (ML) analyses of a combined DNA dataset of *tef1* gene sequences

Authors: WenXia Wu, ShuaiFei Chen

Data type: pdf

Link: https://doi.org/10.3897/mycokeys.110.130733.suppl2

Supplementary material 3

Phylogenetic tree of *Calonectria* species based on maximum likelihood (ML) analyses of a combined DNA dataset of *tub2* gene sequences

Authors: WenXia Wu, ShuaiFei Chen

Data type: pdf

Link: https://doi.org/10.3897/mycokeys.110.130733.suppl3

Supplementary material 4

Phylogenetic tree of *Calonectria* species based on maximum likelihood (ML) analyses of a combined DNA dataset of *cmdA* gene sequences

Authors: WenXia Wu, ShuaiFei Chen

Data type: pdf

Link: https://doi.org/10.3897/mycokeys.110.130733.suppl4

Supplementary material 5

Phylogenetic tree of *Calonectria* species based on maximum likelihood (ML) analyses of a combined DNA dataset of *his3* gene sequences

Authors: WenXia Wu, ShuaiFei Chen

Data type: pdf

Link: https://doi.org/10.3897/mycokeys.110.130733.suppl5

MycoKeys 110: 141–158 (2024)
DOI: 10.3897/mycokeys.110.135724

Research Article

Two new *Cordyceps*-like species, *Perennicordyceps zongqii* sp. nov. (Polycephalomycetaceae) and *Purpureocillium zongqii* sp. nov. (Ophiocordycipitaceae), in Hypocreales from karst region of China

Wan-Hao Chen[1,2,3], Dan Li[1,4], Jian-Dong Liang[1,3], Xiu-Xiu Ren[1], Jie-Hong Zhao[1,4], Yan-Feng Han[2]

1 *Center for Mycomedicine Research, Basic Medical School, Guizhou University of Traditional Chinese Medicine, Guiyang 550025, Guizhou, China*
2 *Institute of Fungus Resources, Department of Ecology, College of Life Sciences, Guizhou University, Guiyang 550025, Guizhou, China*
3 *Key Laboratory of Microbio and Infectious Disease Prevention & Control in Guizhou Province, Guiyang 550025, Guizhou, China*
4 *College of Pharmacy, Guizhou University of Traditional Chinese Medicine, Guiyang 550025, Guizhou, China*
Corresponding author: Yan-Feng Han (swallow1128@126.com)

Abstract

Two new *Cordyceps*-like species, *Perennicordyceps zongqii* and *Purpureocillium zongqii*, isolated from a larva and soil, are introduced. Morphological comparisons and phylogenetic analyses based on multigene datasets (ITS, LSU, *RPB2* and *TEF*) support the establishment of the new species. Moreover, new species in the families Polycephalomycetaceae and Ophiocordycipitaceae were introduced into Tiankeng and the valley for the first time. Further attention needs to be paid to the diversity of other *Cordyceps*-like fungi in the special eco-environment of the karst region.

Key words: *Cordyceps*-like species, morphology, Ophiocordycipitaceae, phylogenetic analysis, Polycephalomycetaceae

Academic editor: Marc Stadler
Received: 28 August 2024
Accepted: 21 October 2024
Published: 7 November 2024

Citation: Chen W-H, Li D, Liang J-D, Ren X-X, Zhao J-H, Han Y-F (2024) Two new *Cordyceps*-like species, *Perennicordyceps zongqii* sp. nov. (Polycephalomycetaceae) and *Purpureocillium zongqii* sp. nov. (Ophiocordycipitaceae), in Hypocreales from karst region of China. MycoKeys 110: 141–158. https://doi.org/10.3897/mycokeys.110.135724

Introduction

Cordyceps-like fungi, also known as *Cordyceps* sensu lato, refers to species belonging to Hypocreales, Sordariomycetes and Ascomycota, and contains all the species in the families Cordycipitaceae, Ophiocordycipitaceae and Polycephalomycetaceae, as well as some species in the family Clavicipitaceae (Li et al. 2021; Xiao et al. 2023). Currently, more than 2000 species of *Cordyceps*-like fungi have been reported worldwide, while there are just over 300 species in China (Chen et al. 2021d; Li et al. 2023, http://www.indexfungorum.org/Names/Names.asp, 17 August, 2024). Therefore, more attention needs to be paid to the diversity of *Cordyceps*-like fungi in China.

The karst region, especially in southern China, preserves unique, large-scale, and continuously distributed primitive forests with extremely rich biodiversity. The complex ecological environment and special geographical conditions in the region have become shelters for many unique species (Özkan et al. 2010; Su et al. 2017). Previous studies have shown that the resources of *Cordyceps*-like fungi in karst areas are very abundant (Zhu et al. 2004; Song et al. 2011). In recent years, Yunnan and Guizhou Province have become hot areas for research on *Cordyceps*-like fungi

(Ming et al. 2021; Chen et al. 2021a, b, c, 2022a, b, c, 2023; Qu et al. 2021; Dong et al. 2022; Wang et al. 2022, 2024a; Zhou et al. 2022; Zou et al. 2022; Peng et al. 2023, 2024; Tang et al. 2023a, b, c; Xiao et al. 2023, 2024; Zhang et al. 2023; Dai et al. 2024), and the majority of sampling locations were located in karst forest habitats. However, there are also some special habitats in karst areas, such as Tiankeng and the valley, because of its unique geological landscape, which creates a microclimate distinct from its surrounding area and a unique habitat suitable for biological survival. Unfortunately, the *Cordyceps*-like fungi in these habitats have been neglected.

Chen et al. (2022b, 2023) reported ten new *Cordyceps*-like fungi in the family Cordycipitaceae from Tiankeng and the valley. Two new genera and three new species in the family Clavicipitaceae were introduced from the valley by Chen et al. (2022a). However, *Cordyceps*-like fungi were rarely reported in other families from Tiankeng or the valley. Besides, *Cordyceps*-like fungi was omnipresent in the obtaining nutrients and was abundant in the soil (Chen et al. 2022a, Quesada-Moraga et al. 2007). Unfortunately, few reports exist about the *Cordyceps*-like fungi from the soil of Tiankeng or the valley.

During a survey of *Cordyceps*-like fungi associated with insects and soil from Southwest China, the infected specimen and soil were collected, and strains were isolated. After detailed multiloci phylogenic analysis and morphological observations, two new species were identified as belonging to the family Polycephalomycetaceae and Ophiocordycipitaceae.

Materials and methods

Specimen and soil collection, isolation

The specimen and soil (for the photo descriptions of the sampling site see Suppl. materials 1–5) were collected from Mayao River Valley (26°22'8.3748"N, 107°23'16.96"E), Duyun City, Qiannan Buyei and Miao Autonomous Prefecture and Monkey-Ear Tiankeng (27°5'12.138"N, 107°0'48.42"E), Kaiyang County, Guiyang, Guizhou Province, on 1 May 2022 and 19 July 2023. The samples were placed in an ice box and brought to the laboratory. Specimens were preserved in the refrigerator at 4 °C until further processing. The surface of each arthropod body was rinsed with sterile water, followed by sterilization with 75% ethanol for 3–5 s and rinsing again three times with sterilized water. After drying on sterilized filter paper, a piece of the synnemata, mycelium or sclerotia was cut from the specimen and inoculated on agar plates of potato dextrose agar (PDA) or PDA modified by the addition of 1% w/v peptone containing 0.1 g/l streptomycin and 0.05 g/l tetracycline (Chen et al. 2019). After fungal colonies emerged from the inoculated samples, a piece of mycelium from the colony edge was transferred onto new agar plated and cultured at 25 °C for 14 days under 12 h light/12 h dark conditions (Zou et al. 2010). Then 2 g collected soil were placed into a sterile conical flask containing 20 ml sterile water and thoroughly shaken using a Vortex vibration meter. Next, the suspension was diluted to a concentration of 10^{-3}. Subsequently, 1 ml of the diluted sample was added to a sterile Petri dish and mixed with Sabouraud's dextrose agar (SDA; peptone 10 g/l, dextrose 40 g/l, agar 20 g/l, 3.3 ml of 1% Bengal red aqueous solution) medium containing 50 mg/l penicillin and 50 mg/l streptomycin. After the plates were incubated at 25 °C for 1–2 weeks, single colonies were transferred

from the plates to new PDA plates (Wang et al. 2024b). The holotypes and extypes were deposited at the Institute of Fungus Resources, Guizhou University (formally Herbarium of Guizhou Agricultural College; code, GZAC), Guiyang City, Guizhou, China. MycoBank numbers have been obtained as outlined in MycoBank (http://www.MycoBank.org) (Crous et al. 2004).

Morphological studies

Colony morphology was determined on PDA cultures incubated at 25 °C for 14 days and the growth rate, the presence of octahedral crystals and the colony colours (surface and reverse) were observed. To investigate the microscopic characteristics, a little of the mycelia was picked up from the colony and mounted in lactophenol cotton blue or 20% lactate acid solution and the asexual morphological characteristics (e.g., conidiophores, phialides and conidia) were observed and measured using a Leica DM4 B microscope. Twenty measurements were recorded for hyphae, conidiophores, phialides and conidium.

DNA extraction, PCR and sequencing

DNA extraction was carried out using a fungal genomic DNA extraction kit (DP2033, BioTeke Corporation) according to Liang et al. (2011). The extracted DNA was stored at −20 °C. Polymerase chain reaction (PCR) was used to amplify genetic markers using the following primer pairs: ITS4/ITS5 for the internal transcribed spacer (ITS) region (White et al. 1990), LR0R/LR5 for 28s large subunit ribosomal (LSU) (Vilgalys and Hester 1990), fRPB2-5F/fRPB2-7cR for RNA polymerase II second largest subunit (*RPB2*) (Liu et al. 1999) and 983F/2218R for translation elongation factor 1 alpha (*TEF*) (Castlebury et al. 2004). The thermal cycle of PCR amplification for these phylogenetic markers was set up following the procedure described by Chen et al. (2021c). PCR products were purified and sequenced at Sangon Biotech (Shanghai) Co. by Sanger dideoxy sequencing. All newly generated sequences were deposited in GenBank and accession numbers were obtained. The sequences used in the study were listed in Table 1.

Sequence alignments and phylogenetic analyses

DNASTAR™ Lasergene (v 6.0) was used to edit DNA sequences in this study. The ITS, LSU, *RPB2* and *TEF* sequences were downloaded from GenBank, based on Xiao et al. (2023), Calvillo-Medina et al. (2021), Luangsa-ard et al. (2011), Chen et al. (2024) and others selected based on BLASTn searches in GenBank. ITS sequences and other loci were aligned and edited by MAFFT v.7.037b (Katoh and Standley 2013) and MEGA6 (Tamura et al. 2013). Combined sequences of ITS, LSU, *RPB2* and *TEF* were obtained using SequenceMatrix v.1.7.8 (Vaidya et al. 2011). The model was selected for Bayesian analysis by ModelFinder (Kalyaanamoorthy et al. 2017) in PhyloSuite (v1.2.2) software (Zhang et al. 2020).

The combined dataset of ITS, LSU, *RPB2* and *TEF* sequence data (Suppl. materials 1–5) was analyzed using Bayesian inference (BI) and maximum likelihood (ML) methods. For BI, a Markov chain Monte Carlo (MCMC) algorithm was used to generate phylogenetic trees with Bayesian probabilities for the combined sequence datasets using MrBayes v.3.2 (Ronquist et al. 2012).

Table 1. List of strains and GenBank accession numbers of sequences used in this study.

Species	Strain	Host/ substrate	GenBank Accession Number				Reference
			ITS	LSU	RPB2	TEF	
Perennicordyceps cuboidea	NBRC 103836	Larva of beetle	JN943332	JN941420	AB972955	AB972951	Schoch et al. 2012
Perennicordyceps cuboidea	NBRC 100941	stroma of *Cordyceps stylophora*	JN943329	JN941416	–	–	Schoch et al. 2012
Perennicordyceps cuboidea	NBRC 101740	Larva of beetle	JN943331	JN941417	–	KF049684	Schoch et al. 2012
Perennicordyceps elaphomyceticola	MFLU 21-0264	*Elaphomyces* sp.	OQ172067	OQ172035	OQ459794	OQ459720	Xiao et al. 2023
Perennicordyceps elaphomyceticola	MFLU 21-0263	*Elaphomyces* sp.	OQ172065	OQ172033	OQ459793	OQ459719	Xiao et al. 2023
Perennicordyceps elaphomyceticola	MFLU 21-0262	*Elaphomyces* sp.	OQ172064	OQ172032	OQ459792	OQ459718	Xiao et al. 2023
Perennicordyceps lutea	KUMCC 3004^{T}	*Ophiocordyceps sinensis*	–	OQ474910	–	–	Xiao et al. 2023
Perennicordyceps paracuboidea	NBRC 101742^{T}	Larva of beetle	JN943338	JN941431	KF049669	KF049685	Ban et al. 2015a
Perennicordyceps paracuboidea	NBRC 100942	Larva of beetle	JN943337	JN941430	AB972958	AB972954	Ban et al. 2015a
Perennicordyceps prolifica	NBRC 101750	Larva of *Tanna japonensis*	JN943340	JN941433	AB972957	AB972953	Ban et al. 2009
Perennicordyceps prolifica	NBRC 100744	Larva of *Tanna japonensis*	AB925942	JN941432	AB972956	AB972952	Ban et al. 2009
Perennicordyceps prolifica	TNS-F-18547	Larvae of cicada	KF049660	KF049632	KF049670	KF049687	Kepler et al. 2013
Perennicordyceps ryogamiensis	NBRC 101751	Larva of beetle	JN943343	JN941438	–	KF049688	Schoch et al. 2012
Perennicordyceps ryogamiensis	NBRC 103837	Larva of beetle	JN943346	JN941439	–	–	Schoch et al. 2012
Perennicordyceps ryogamiensis	NBRC 103842	*Cordyceps ryogamiensis*	JN943345	JN941440	–	–	Schoch et al. 2012
Perennicordyceps zongqii	**DY05421^{T}**	**Larva of moth**	**PQ211278**	**PQ211282**	**PQ223677**	**PQ223679**	This study
Perennicordyceps zongqii	**DY05422**	**Larva of moth**	**PQ211279**	**PQ211283**	**PQ223678**	**PQ223680**	This study
Pleurocordyceps parvicapitata	MFLU 21-0270	*Elaphomyces* sp.	OQ172082	OQ172054	OQ459796	OQ459722	Xiao et al. 2019
Pleurocordyceps parvicapitata	MFLU 21-0271^{T}	*Elaphomyces* sp.	OQ172083	OQ172055	OQ459797	OQ459723	Xiao et al. 2023
Pleurocordyceps sinensis	HMAS 43720^{T}	Larvae of *Hepialus armocanus*	NR_119928	NG_042573	–	–	Sun et al. 2019
Pleurocordyceps vitellina	KUMCC 3006^{T}	*Ophiocordyceps nigrella*	OQ172089	OQ172061	OQ459803	OQ459729	Xiao et al. 2023
Pleurocordyceps vitellina	KUMCC 3007	*Ophiocordyceps nigrella*	OQ172090	OQ172062	OQ459804	OQ459730	Xiao et al. 2023
Polycephalomyces formosus	NBRC 109993^{T}	Larvae of Coleoptera	MN586833	MN586842	MN598064	MN598057	Wang et al. 2021
Polycephalomyces albiramus	GACP 21-XS08^{T}	Gryllotalpa	OQ172092	OQ172037	OQ459807	OQ459735	Xiao et al. 2023
Polycephalomyces albiramus	GACPCC 21-XS08	Gryllotalpa	OQ172093	OQ172038	OQ459808	OQ459736	Xiao et al. 2023
Purpureocillium atypicola	CBS 744.73	*Atypus karschi*	GU980041	EF468841	–	EF468786	Perdomo et al. 2013
Purpureocillium jiangxiense	JX17D04	Soil	PP555636	PP555645	–	PP658209	Chen et al. 2024
Purpureocillium jiangxiense	JX13B01^{T}	Soil	PP555637	PP555646	–	PP658210	Chen et al. 2024
Purpureocillium lavendulum	FMR 10376^{T}	Soil	FR734106	–	–	FR775516	Perdomo et al. 2013
Purpureocillium lavendulum	CBS 128678	Human	MH864977	MH876430	–	–	Perdomo et al. 2013
Purpureocillium lilacinum	CBS 284.36^{T}	Soil	FR734101	–	–	FR734156	Perdomo et al. 2013
Purpureocillium lilacinum	FMR 8652	Human	FR734090	FR775473	–	–	Perdomo et al. 2013
Purpureocillium roseum	IOM 325363.1	Human	MT560195	MT560197	–	–	Calvillo-Medina et al. 2021
Purpureocillium roseum	IOM 325363.2	Human	MT560196	MT560198	–	–	Calvillo-Medina et al. 2021
Purpureocillium sodanum	IBRC-M 30175^{T}	Salt crystals	KX668542	–	–	–	Hyde et al. 2016
Purpureocillium takamizusanense	NBRC 100742	*Tanna japonensis*	LC008197	–	–	LC008333	Ban et al. 2015b
Purpureocillium takamizusanense	NBRC 108982	Cicada	LC008204	–	–	LC008338	Ban et al. 2015b
Purpureocillium takamizusanense	NBRC 110232	-	LC008205	–	–	LC008339	Ban et al. 2015b
Purpureocillium zongqii	**TK041^{T}**	**Soil**	**PQ211280**	**PQ211284**	–	**PQ223681**	This study
Purpureocillium zongqii	**TK042**	**Soil**	**PQ211281**	**PQ211285**	–	**PQ223682**	This study
Simplicillium lamellicola	CBS 116.25^{T}	*Agaricus bisporus*	MH854806	AF339552	DQ522462	DQ522356	Luangsa-ard et al. 2011
Simplicillium lanosoniveum	CBS 704.86	*Hemileia vastatrix*	AJ292396	AF339553	DQ522464	DQ522358	Luangsa-ard et al. 2011

Note: New strains or species are in bold type."^{T}" denotes ex-type. Abbreviations for collections: CBS, Centraalbureau voor Schimmelcultures, Utrecht, the Netherlands; TNS-F, the mycological herbarium of the National Museum of Nature and Science, Tsukuba, Ibaraki, Japan; HMAS, Herbarium of Mycology, Chinese Academy of Sciences; IBRC, Iranian Biological Resource Center, Tehran, Iran; NBRC, NITE Biological Resource Center, Sayaka Ban National Institute of Technology and Evaluation, Japan; IOM, Instituto de Oftalmología 'Fundación Conde de Valenciana' IAP Mexico Culture Collection; MFLU, Mae Fah Luang University; GACP, Herbarium of Guizhou University, China; KUMCC, Culture collection of Kunming Institute of Botany, Kunming, China; FMR, Facultad de Medicina, Reus, Tarragona, Spain.

The Bayesian analysis resulted in 20,001 trees after 10,000,000 generations. The first 4,000 trees, representing the burn-in phase of the analysis, were discarded, while the remaining 16,001 trees were used to calculate posterior probabilities in the majority rule consensus tree. After the analysis was finished, each run was examined if it was greater than 200 using the program Tracer v.1.5 (Drummond and Rambaut 2007) to determine burn-in and confirm that both runs had converged. ML analyses were constructed with IQ-TREE (v 2.0) (Trifinopoulos et al. 2016), using an automatic selection of the model according to BIC.

Results

Phylogenetic analyses

The phylogenetic tree (Fig. 1) was generated to determine the relationship among those new strains and its related species. *Simplicillium lanosoniveum* (J.F.H. Beyma) Zare & W. Gams (CBS 704.86) and *S. lamellicola* (F.E.V. Sm.) Zare & W. Gams (CBS 116.25) were used as the outgroups. The concatenated sequences included 40 taxa and consisted of 3,392 (ITS, 616; LSU, 841; *RPB2*, 1,041; and *TEF*, 894) characters with gaps.

The selected model for ML analysis was TN+F+I+G4. The final value of the highest scoring tree was −15,988.941, which was obtained from an ML analysis of the dataset (ITS, LSU, *RPB2* and *TEF*). The parameters of the rate heterogeneity model used to analyze the dataset were estimated using the following frequencies: A = 0.230, C = 0.288, G = 0.278, T = 0.204; substitution rates AC = 1.00000, AG = 2.57904, AT = 1.00000, CG = 1.00000, CT = 5.70221 and GT = 1.00000, as well as the gamma distribution shape parameter α = 0.805. The selected models for BI analysis were GTR+F+I+G4 (ITS, LSU, *RPB2* and *TEF*). The phylogenetic trees (Fig. 1) constructed using ML and BI analyses were largely congruent and strongly supported in most branches. The new strains DY05421 and DY05422 were clustered into an independent clade in the group of the genus *Perennicordyceps* and have a close relationship with *Perennicordyceps cuboidea* (Kobayasi & Shimizu) Matočec & I. Kušan (NBRC 101740, NBRC 103836 and NBRC 100941) and *P. ryogamiensis* (Kobayasi & Shimizu) Matočec & I. Kušan (NBRC 101751, NBRC 103842 and NBRC 103837). Strains TK041, TK042 were clustered into the group of the genus *Purpureocillium* and have a close relationship with *Purpureocillium lilacinum* (Thom) Luangsa-ard, Houbraken, Hywel-Jones & Samson (CBS 284.36).

Taxonomy

Perennicordyceps zongqii **W.H. Chen, Y.F. Han & J.D. Liang, sp. nov.**
MycoBank No: 855564
Fig. 2

Etymology. In honor of Prof. Zongqi Liang, for his support and guidance in arthropod pathogenic fungi research.

Type. China • Guizhou Province, Qiannan Buyei and Miao Autonomous Prefecture, Duyun City, Mayao River Valley (26°22'8.3748"N, 107°23'16.96"E), on a larva of moth (Lepidoptera), on the leaf litter, 1 May 2022, Wanhao Chen, GZAC DY0542 (holotype), ex-type DY05421.

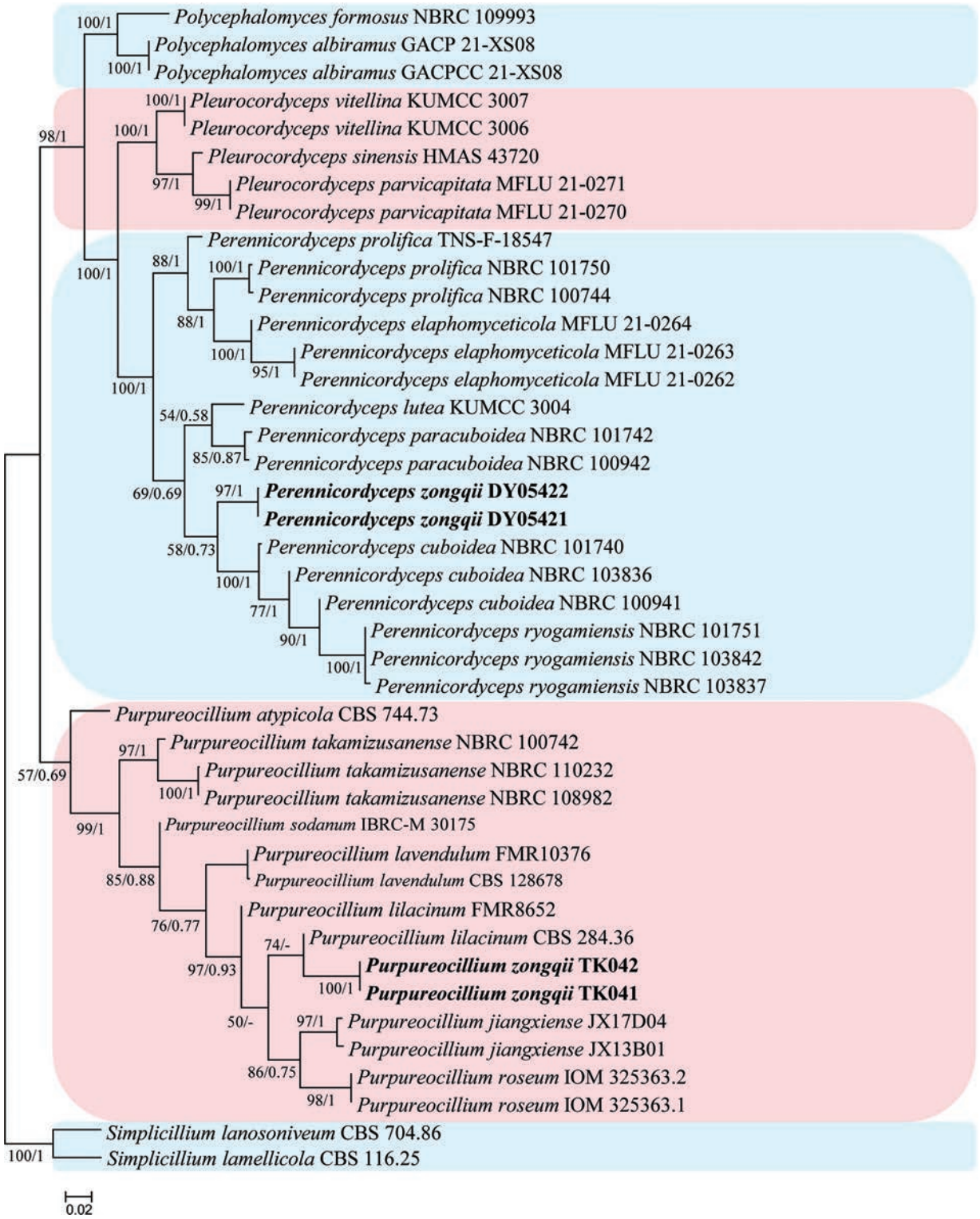

Figure 1. Phylogenetic analysis of the new strains and its related species based on multigene dataset (ITS, LSU, *RPB2* and *TEF*). Statistical support values (≥ 50%/0.5) are shown at the nodes for ML bootstrap support/BI posterior probabilities.

Description. Colonies on PDA, attaining a diameter of 56–59 mm after 14 days at 25 °C, white, consisting of a basal felt, floccose hyphal overgrowth, yellowish in middle; reverse yellow to pale yellowish, light brown to brown in the middle. Hyphae septate, hyaline, yellowish in the middle part of the colony, smooth-walled, 1.1–2.1 µm wide. Conidiophores erect, hyaline, irregular

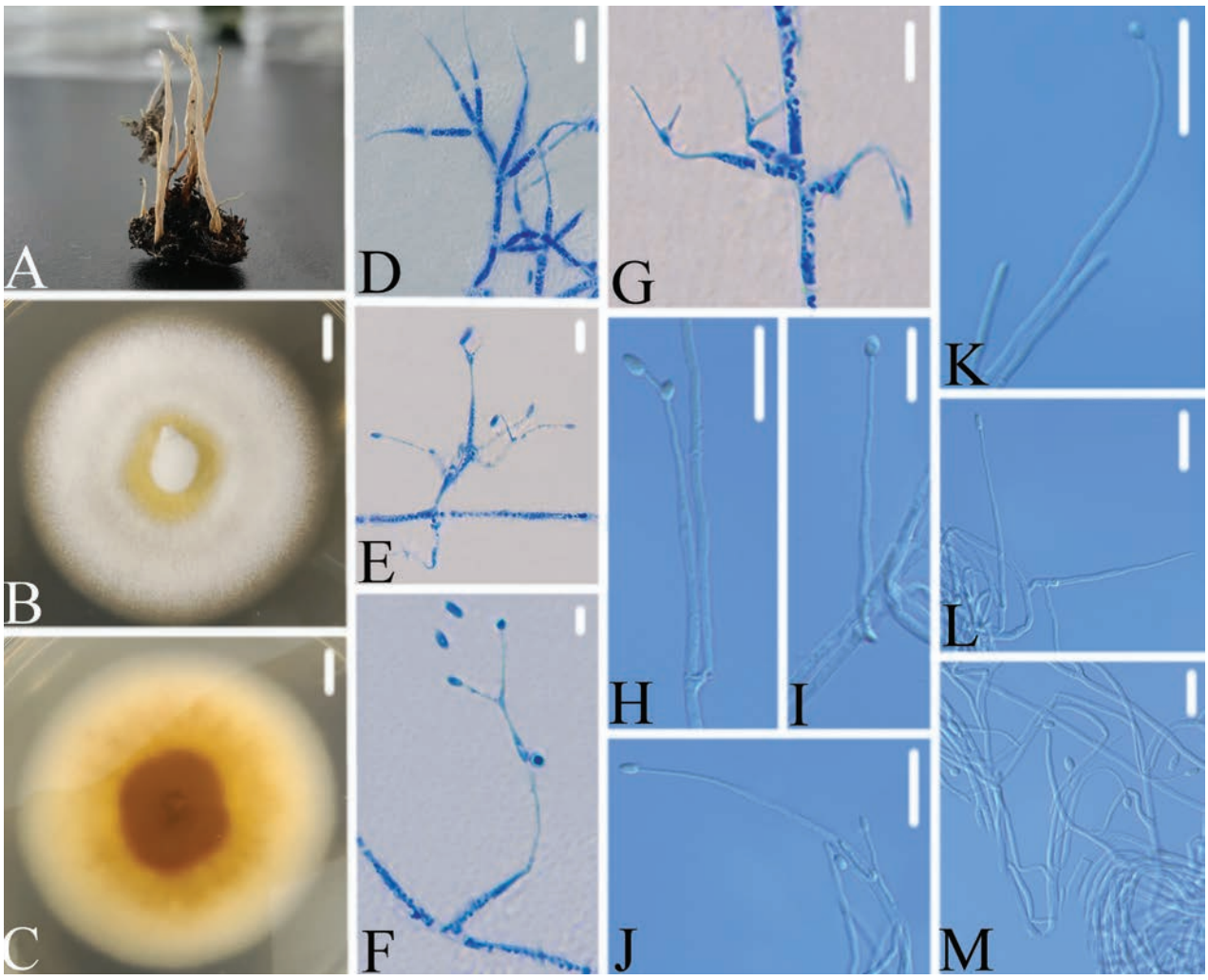

Figure 2. *Perennicordyceps zongqii* **A** infected larva **B**, **C** colony on PDA (**B** obverse, **C** reverse) **D–M** phialides and conidia. Scale bars: 10 mm (**B**, **C**); 10 µm (**D–M**).

branched, with 1–4 phialides. Phialides 29.3–31.1 × 1.5–2.4 µm, hyaline, cylindrical at base, gradually tapering near the apex, holoblastic or branch. Conidia 3.4–4.8 × 2.5–2.7 µm, hyaline, smooth-walled, thin-walled, ellipsoidal to cylindrical, unicellular, acuminate, arranged in chains not observed.

Distribution. Duyun City, Guizhou Province, China.

Host. Larva (Lepidoptera).

Additional strain examined. China • Guizhou Province, Qiannan Buyei and Miao Autonomous Prefecture, Duyun City, Mayao River Valley (26°22'8.3748"N, 107°23'16.96"E). On a larva of moth (Lepidoptera), on the leaf litter, 1 May 2022, Wanhao Chen, DY05422 (living culture).

Notes. Strain DY05421 was easily identified as *Perennicordyceps*, based on the BLASTn result in NCBI. Phylogenetic analyses show that strain DY05421 has close relationships to *P. cuboidea and P. ryogamiensis* (Fig. 1). However, strain DY05421 was easily distinguished from *P. cuboidea* (globose to ellipsoid conidia, 1.3–3.7 × 1.1–2.3 µm; phialide, 18.9–22.2 × 0.8–1.1 µm; substrate, larvae of Coleoptera) by its larger ellipsoidal to cylindrical conidia, larger phialide and the substrate (Ban et al. 2009). Strain DY05421 was easily distinguished from *P. ryogamiensis* (ellipsoid conidia, 2.5–3.9 × 1.0–1.4 µm; phialide, 17.5–55.2 ×

0.8–2.7 µm; substrate, larvae of Coleoptera) by its larger ellipsoidal to cylindrical conidia, smaller phialide and the substrate (Ban et al. 2009). Thus, the morphological characteristics and molecular phylogenetic results support *strain* DY05421 as a new *Perennicordyceps* species and named *Perennicordyceps zongqii*.

Purpureocillium zongqii **W.H. Chen, Y.F. Han & J.D. Liang, sp. nov.**
MycoBank No: 855565
Fig. 3

Etymology. In honor of Prof. Zongqi Liang, for his support and guidance in arthropod pathogenic fungi research.

Type. China • Guizhou Province, Guiyang, Kaiyang County, Monkey-Ear Tiankeng (27°5'12.138"N, 107°0'48.42"E), soil, 19 July 2023, Wanhao Chen, GZAC TK04 (dried holotype), ex-type TK041.

Description. Colonies on PDA, attaining a diameter of 23–25 mm after 14 days at 25 °C, white, consisting of a basal felt, floccose hyphal overgrowth, white; reverse yellowish. Hyphae septate, hyaline, smooth-walled, 1.1–1.9 µm wide. Conidiophores 9.3–12.7 × 2.1–2.4 µm, erect, hyaline, verticillately branched, with 1–4 phialides. Phialides 6.8–11.7 × 2.6–4.0 µm, hyaline, cylindrical at base, gradually tapering near the apex. Conidia 2.7–4.2 × 2.0–2.4 µm, hyaline, smooth-walled, thin-walled, ellipsoidal, unicellular, acuminate, arranged in chains not observed.

Substrate. Soil.

Distribution. Kaiyang County, Guizhou Province, China.

Additional strain examined. China • Guizhou Province, Guiyang, Kaiyang County, Monkey-Ear Tiankeng (27°5'12.138"N, 107°0'48.42"E), soil, 19 July 2023, Wanhao Chen, TK042 (living culture).

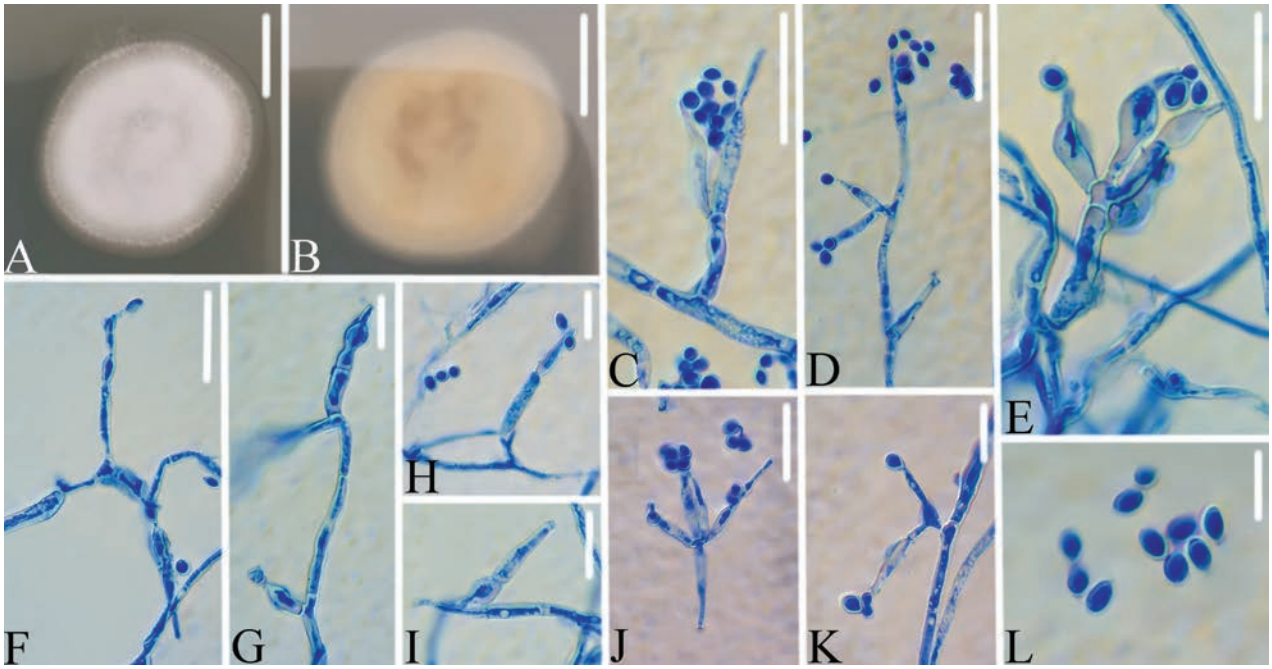

Figure 3. *Purpureocillium zongqii* **A**, **B** colony on PDA (**A** obverse, **B** reverse) **C–J** Phialides and conidia. Scale bars: 10 mm (**A**, **B**); 10 µm (**C–J**).

Notes. *Purpureocillium zongqii* was easily identified as *Purpureocillium*, based on the BLASTn result in NCBI. Phylogenetic analyses show that *P. zongqii* has a close relationship to *P. lilacinum* (Fig. 1). However, *P. zongqii* was easily distinguished from *P. lilacinum* (conidiophores: 4–6 × 3–4 µm; conidia: ellipsoidal to fusiform, 2–3 × 2–4 µm; phialide, 6–9 × 2.5–3 µm; purple colony) (Luangsa-ard et al. 2011) by its larger conidiophores, larger ellipsoidal conidia, larger phialide and white colony. Thus, the morphological characteristics and molecular phylogenetic results support *P. zongqii* as a new species.

Keys of the genus *Perennicordyceps*

1 Parasitic on fungi **2**
– Parasitic on insects **3**
2 Phialides 14.8–64.9 × 1.9–3.1 µm, conidia globose to ellipsoid ..... ***Perennicordyceps lutea***
– Phialides 12–16 × 0.6–1.5 µm, conidia fusiform to ellipsoid to inequilateral shaped ..... ***Perennicordyceps elaphomyceticola***
3 Typical host larva of cicada or moth **4**
– Typical host larva of beetle **5**
4 Typical host larva of cicada, conidia globose, fusiform 1.5–3.5 (2.5) × 1.1–1.8 (1.4) µm ..... ***Perennicordyceps prolifica***
– Typical host larva of moth, conidia ellipsoidal to cylindrical, 3.4–4.8 × 2.5–2.7 µm ..... ***Perennicordyceps zongqii***
5 Conidiophores quasi-verticillate branching **6**
– Conidiophores irregular branching ..... ***Perennicordyceps cuboidea***
6 Conidia ellipsoid, 2.5–3.9 (3.1) × 1.0–1.4 (1.2) µm, mainly *Acremonium*-like phialide ..... ***Perennicordyceps ryogamiensis***
– Conidia aubglobose, fusiform, 1.3–1.9 (1.8) × 1.0–1.9 (1.4) µm, mainly *Hirsutella*-like phialide ..... ***Perennicordyceps paracuboidea***

Keys of the genus *Purpureocillium*

1 Species that grow on spiders and insect forming synnemata of colours purple to lilac **2**
– Species isolated, clinical specimens on human, animals, soil and crystals salt **3**
2 Synnemata lilac coloured, conidia ellipsoid to cylindrical 4.8–5.6 × 1.6–2.4 µm; parasite trapdoor spiders; sexual state *Cordyceps cylindrica* ..... ***Purpureocillium atypicola***
– Synnemata lilac coloured, conidia ellipsoid 2.5–4 × 1.4–1.8 µm; parasite on cadavers of cicada adults; sexual state in *Cordyceps ryogamimontana* ..... ***Purpureocillium takamizusanense***
3 *Acremonium*-like synanamorph absent **4**
– *Acremonium*-like synanamorph present **5**
4 Phialides 8–10 (14) × 2–3 µm, conidia globose, 2–2.5 µm ..... ***Purpureocillium roseum***
– Phialides 6.8–11.7 × 2.6–4.0 µm, conidia ellipsoidal, 2.7–4.2 × 2.0–2.4 µm ..... ***Purpureocillium zongqii***

5 Conidia subglobose with apiculate base or limoniform **6**
– Conidia ellipsoidal to fusiform ..... ***Purpureocillium lilacinum***
6 Conidia 2–3 × 2–2.5 µm ..... ***Purpureocillium lavendulum***
– Conidia 3.5–5.5 × 3–4.5 µm ..... ***Purpureocillium sodanum***

Discussion

The genus *Perennicordyceps* was proposed to accommodate four species of *Polycephalomyces*, *Polycephalomyces prolificus* (Kobayasi) Kepler & Spatafora, *P. cuboideus* (Kobayasi & Shimizu) Kepler & Spatafora, *P. paracuboideus* (S. Ban, Sakane & Nakagiri) Kepler & Spatafora and *P. ryogamiensis* (Kobayasi & Shimizu) Kepler & Spatafora (Matočec et al. 2014). Species in the genus usually known as entomopathogenic fungi with host in the orders Coleoptera and Hemiptera (Matočec et al. 2014). Xiao et al. (2023) reported a new species, *Perennicordyceps lutea* Y.B. Wang, H. Yu & Y.P. Xiao and a new combined species, *P. elaphomyceticola* (W.Y. Chuang, H.A. Ariyaw., J.I. Yang & Stadler) Y.P. Xiao & K.D. Hyde, which were both recorded as fungicolous. In the present study, the new species *P. zongqii* with Lepidoptera larvae was introduced. *Cordyceps*-like fungi have evolved adaptively through nutrient exchange and the ultimate goal is in the search of ideal food (Moonjely et al. 2016; Vidhate et al. 2023). Whether the new species has coevolved with its hosts and has special metabolizing processes is worthy of further research.

The genus *Purpureocillium* was established to accommodate *Paecilomyces lilacinus* Thom (Luangsa-ard et al. 2011). Members of *Purpureocillium* have a global distribution, especially for the type species *P. lilacinum*, which is commonly isolated from soil, decaying vegetation, insects, nematodes and laboratory air (as contaminant) (Luangsa-ard et al. 2011; Perdomo et al. 2013; Quandt et al. 2014; Ban et al. 2015b; Calvillo-Medina et al. 2021). In the present study, the new species *P. zongqii* was isolated from soil in Monkey-Ear Tiankeng. Tiankeng acts as a refugium for biodiversity amid changing global climate and some ancient (*Alsophila spinulosa* (Wall. ex Hook.) R. M. Tryon) and unique plants (cool-adapted plants) were present in Tiankeng (Shui et al. 2015; Bátori et al. 2017; Pu et al. 2019; Shen et al. 2020). Whether the new species is more ancient than others, has coevolved with its environment and has special metabolizing processes is worthy of further research.

The karst region in southwestern China is one of the 36 biodiversity hotspots in the world, nurturing a large number of endemic species (Delgado Baquerizo et al. 2020), especially in the special eco-environment, Tiankeng and the valley. The species that exist in these habitats often have very narrow distribution areas and very small populations, and urgently need to be protected (Wu and Zhang 2020). In the present study, species in the families Polycephalomycetaceae and Ophiocordycipitaceae were introduced in Tiankeng and the valley for the first time. Further attention needs to be paid to the diversity of other *Cordyceps*-like fungi in the special eco-environment of karst region.

Additional information

Conflict of interest

The authors have declared that no competing interests exist.

Ethical statement

No ethical statement was reported.

Funding

This work was funded by National Natural Science Foundation of China (31860002, 81960692), High-level Innovative Talents Training Object in Guizhou Province (Qiankehepingtairencai [2020]6005), Construction Program of Key Laboratory of Guizhou Province (Qiankehepingtairencai-ZDSYS[2023]004), Research Center Project of Guizhou University of Traditional Chinese Medicine (Guizhongyi ZX hezi [2024]021).

Author contributions

Data curation: WHC. Formal analysis: XXR, JDL. Funding acquisition: YFH, JHZ, WHC. Methodology: YFH. Resources: WHC, DL. Writing - original draft: JDL, WHC, XXR, DL. Writing - review and editing: YFH, JHZ.

Author ORCIDs

Wan-Hao Chen https://orcid.org/0000-0001-7240-6841
Jian-Dong Liang https://orcid.org/0000-0002-3939-3900
Yan-Feng Han https://orcid.org/0000-0002-8646-3975

Data availability

All of the data that support the findings of this study are available in the main text or Supplementary Information.

References

Ban S, Sakane T, Toyama K, Nakagiri A (2009) Teleomorph–anamorph relationships and reclassification of *Cordyceps cuboidea* and its allied species. Mycoscience 50(4): 261–272. https://doi.org/10.1007/S10267-008-0480-Y

Ban S, Sakane T, Nakagiri A (2015a) Three new species of *Ophiocordyceps* and overview of anamorph types in the genus and the family Ophiocordyceptaceae. Mycological Progress 14(1): 1017. https://doi.org/10.1007/s11557-014-1017-8

Ban S, Azuma Y, Sato H, Suzuki KI, Nakagiri A (2015b) *Isaria takamizusanensis* is the anamorph of *Cordyceps ryogamimontana*, warranting a new combination, *Purpureocillium takamizusanense* comb. nov. International Journal of Systematic and Evolutionary Microbiology 65(8): 2459–2465. https://doi.org/10.1099/ijs.0.000284

Bátori Z, Vojtkó A, Farkas T, Szabó A, Havadtői K, Vojtkó AE, Tölgyesi C, Cseh V, Erdős L, Maák IE, Keppel G (2017) Large-and small-scale environmental factors drive distributions of cool-adapted plants in karstic microrefugia. Annals of Botany 119(2): 301–309. https://doi.org/10.1093/aob/mcw233

Calvillo-Medina RP, Ponce-Angulo DG, Raymundo T, Müller-Morales CA, Escudero-Leyva E, Campos Guillén J, Bautista-de Lucio VM (2021) *Purpureocillium roseum* sp. nov. A new ocular pathogen for humans and mice resistant to antifungals. Mycoses 64(2): 162–173. https://doi.org/10.1111/myc.13198

Castlebury LA, Rossman AY, Sung GH, Hyten AS, Spatafora JW (2004) Multigene phylogeny reveals new lineage for *Stachybotrys chartarum*, the indoor air fungus. Mycological Research 108(8): 864–872. https://doi.org/10.1017/S0953756204000607

Chen WH, Liu C, Han YF, Liang JD, Tian WY, Liang ZQ (2019) Three novel insect-associated species of *Simplicillium* (Cordycipitaceae, Hypocreales) from Southwest China. MycoKeys 58: 83–102. https://doi.org/10.3897/mycokeys.58.37176

Chen WH, Han YF, Liang JD, Liang ZQ (2021a) Taxonomic and phylogenetic characterizations reveal four new species of *Simplicillium* (Cordycipitaceae, Hypocreales) from Guizhou, China. Scientific Reports 11(1): 1–12. https://doi.org/10.1038/s41598-021-94893-z

Chen WH, Han YF, Liang JD, Tian WY, Liang ZQ (2021b) Multi-gene phylogenetic evidence indicates that *Pleurodesmospora* belongs in Cordycipitaceae (Hypocreales, Hypocreomycetidae) and *Pleurodesmospora lepidopterorum* sp. nov. on pupa from China. MycoKeys 80: 45–55. https://doi.org/10.3897/mycokeys.80.66794

Chen WH, Liang JD, Ren XX, Zhao JH, Han YF, Liang ZQ (2021c) Cryptic diversity of *Isaria*-like species in Guizhou, China. Life (Basel, Switzerland) 11(10): 1093. https://doi.org/10.3390/life11101093

Chen WH, Liang JD, Han YF, Zou X, Zhang YJ, Liang ZQ (2021d) Research overviews of *Cordyceps*: Past, present and future. Junwu Xuebao 40(11): 2894–2905.

Chen WH, Liang JD, Ren XX, Zhao JH, Han YF, Liang ZQ (2022a) Phylogenetic, ecological and morphological characteristics reveal two new spider-associated genera in Clavicipitaceae. MycoKeys 91: 49–66. https://doi.org/10.3897/mycokeys.91.86812

Chen WH, Liang JD, Ren XX, Zhao JH, Han YF, Liang ZQ (2022b) Species diversity of *Cordyceps*-like fungi in the Tiankeng karst region of China. Microbiology Spectrum 10(5): e01975–e22. https://doi.org/10.1128/spectrum.01975-22

Chen WH, Liang JD, Ren XX, Zhao JH, Han YF, Liang ZQ (2022c) Multigene phylogeny, phylogenetic network, and morphological characterizations reveal four new arthropod-associated *Simplicillium* species and their evolutional relationship. Frontiers in Microbiology 13: 950773. https://doi.org/10.3389/fmicb.2022.950773

Chen WH, Liang JD, Ren XX, Zhao JH, Han YF (2023) Two new species of *Samsoniella* (Cordycipitaceae, Hypocreales) from the Mayao River Valley, Guizhou, China. MycoKeys 99: 209–226. https://doi.org/10.3897/mycokeys.99.109961

Chen W, Tang Y, Liu T, Hu H, Ou C, Hu Q, Weng Q (2024) *Purpureocillium jiangxiense* sp. nov.: Entomopathogenic effects on *Ostrinia furnacalis* and *Galleria mellonella.* Microorganisms 12(6): 1041. https://doi.org/10.3390/microorganisms12061041

Crous PW, Gams W, Stalpers JA, Robert V, Stegehuis G (2004) MycoBank: An online initiative to launch mycology into the 21st century. Studies in Mycology 50(1): 19–22.

Dai YD, Chen SQ, Wang YB, Wang Y, Yang ZL, Yu H (2024) Molecular phylogenetics of the *Ophiocordyceps sinensis*-species complex lineage (Ascomycota, Hypocreales), with the discovery of new species and predictions of species distribution. IMA Fungus 15(1): 2. https://doi.org/10.1186/s43008-023-00131-8

Delgado-Baquerizo M, Reich PB, Trivedi C, Eldridge DJ, Abades S, Alfaro DF, Bastida F, Berhe AA, Cutler NA, Gallardo A, García-Velázquez L, Hart SC, Hayes PE, He JZ, Hseu ZY, Hu HW, Kirchmair M, Neuhauser S, Pérez CA, Reed SC, Santos F, Sullivan BW, Trivedi P, Wang JT, Weber-Grullon L, Williams MA, Singh BK (2020) Multiple elements of soil biodiversity drive ecosystem functions across biomes. Nature Ecology & Evolution 4(2): 210–220. https://doi.org/10.1038/s41559-019-1084-y

Dong QY, Wang Y, Wang ZQ, Tang DX, Zhao ZY, Wu HJ, Yu H (2022) Morphology and phylogeny reveal five novel species in the genus *Cordyceps* (Cordycipitaceae, Hypocreales) From Yunnan, China. Frontiers in Microbiology 13: 846909. https://doi.org/10.3389/fmicb.2022.846909

Drummond A, Rambaut A (2007) BEAST: Bayesian evolutionary analysis by sampling trees. BMC Evolutionary Biology 7(1): e214. https://doi.org/10.1186/1471-2148-7-214

Hyde KD, Hongsanan S, Jeewon R, Bhat DJ, McKenzie EHC, Jones EBG, Phookamsak R, Ariyawansa HA, Boonmee S, Zhao Q, Abdel-Aziz FA, Abdel-Wahab MA, Banmai S, Chomnunti P, Cui BK, Daranagama DA, Das K, Dayarathne MC, de Silva NI, Dissanayake AJ, Doilom M, Ekanayaka AH, Gibertoni TB, Góes-Neto A, Huang SK, Jayasiri SC, Jayawardena RS, Konta S, Lee HB, Li WJ, Lin CG, Liu JK, Lu YZ, Luo ZL, Manawasinghe IS, Manimohan P, Mapook A, NiskanenT, Norphanphoun C, Papizadeh M, Perera RH, Phukhamsakda C, Richter C et al. (2016) Fungal diversity notes 367–490: Taxonomic and phylogenetic contributions to fungal taxa. Fungal Diversity 80: 1–270. https://doi.org/10.1007/s13225-016-0373-x

Kalyaanamoorthy S, Minh BQ, Wong TK, Von Haeseler A, Jermiin LS (2017) ModelFinder: Fast model selection for accurate phylogenetic estimates. Nature Methods 14(6): 587–589. https://doi.org/10.1038/nmeth.4285

Katoh K, Standley DM (2013) MAFFT multiple sequence alignment software version 7: Improvements in performance and usability. Molecular Biology and Evolution 30(4): 772–780. https://doi.org/10.1093/molbev/mst010

Kepler R, Ban S, Nakagiri A, Bischoff J, Hywel-Jones N, Owensby CA, Spatafora JW (2013) The phylogenetic placement of hypocrealean insect pathogens in the genus *Polycephalomyces*: An application of One Fungus One Name. Fungal Biology 117(9): 611–622. https://doi.org/10.1016/j.funbio.2013.06.002

Li Y, Song B, Wang K, Deng CY, Wang YH, Yuan Y, Wen HS, Li TH (2021) Current status and protection of threatened *Cordyceps* s. l. species in China. Acta Edulis Fungi 28(2): 113–122.

Li CH, Yang SS, Deng WQ, Lin QY (2023) *Cordyceps* sensu lato and their domestication and cultivation in China. Acta Edulis Fungi 30(5): 113–148.

Liang JD, Han YF, Zhang JW, Du W, Liang ZQ, Li ZZ (2011) Optimal culture conditions for keratinase production by a novel thermophilic *Myceliophthora thermophila* strain GZUIFR-H49-1. Journal of Applied Microbiology 110(4): 871–880. https://doi.org/10.1111/j.1365-2672.2011.04949.x

Liu YJ, Whelen S, Hall BD (1999) Phylogenetic relationships among ascomycetes: Evidence from an RNA polymerase II subunit. Molecular Biology and Evolution 16(12): 1799–1808. https://doi.org/10.1093/oxfordjournals.molbev.a026092

Luangsa-ard J, Houbraken J, van Doorn T, Hong SB, Borman AM, Hywel-Jones NL, Samson RA (2011) *Purpureocillium*, a new genus for the medically important *Paecilomyces lilacinus*. FEMS Microbiology Letters 321(2): 141–149. https://doi.org/10.1111/j.1574-6968.2011.02322.x

Matočec N, Kušan I, Ozimec R (2014) The genus *Polycephalomyces* (Hypocreales) in the frame of monitoring Veternica cave (Croatia) with a new segregate genus *Perennicordyceps*. Ascomycete.Org : Revue Internationale pour la Taxinomie des Ascomycota 6: 125–133.

Ming DQ, Luo LY, He XX, Wang MS, Fang WX, Chen SF, Chen WH, Han YF, Liang ZQ (2021) *Paracremonium lepidopterorum*, a new insect-associated fungus. Phytotaxa 524(2): 85–91. https://doi.org/10.11646/phytotaxa.524.2.2

Moonjely S, Barelli L, Bidochka MJ (2016) Insect pathogenic fungi as endophytes. Advances in Genetics 94: 107–135. https://doi.org/10.1016/bs.adgen.2015.12.004

Özkan K, Gulsoy S, Mert A, Ozturk M, Muys B (2010) Plant distribution-altitude and landform relationships in karstic sinkholes of Mediterranean region of Turkey. Journal of Environmental Biology 31(1): 51–60.

Peng XC, Xiao YP, Zhang Y, Chomnunti P, Tangtrakulwanich K, Wen TC (2023) *Cordyceps poluscapitis* sp. nov., an ant-pathogenic fungus from Guizhou, China. Phytotaxa 599(4): 239–251. https://doi.org/10.11646/phytotaxa.599.4.3

Peng XC, Wen TC, Wei DP, Liao YH, Wang Y, Zhang X, Wang GY, Zhou Y, Tangtrakulwanich K, Liang JD (2024) Two new species and one new combination of *Ophiocordyceps* (Hypocreales, Ophiocordycipitaceae) in Guizhou. MycoKeys 102: 245–266. https://doi.org/10.3897/mycokeys.102.113351

Perdomo H, Cano J, Gené J, García D, Hernández M, Guarro J (2013) Polyphasic analysis of *Purpureocillium lilacinum* isolates from different origins and proposal of the new species *Purpureocillium lavendulum*. Mycologia 105(1): 151–161. https://doi.org/10.3852/11-190

Pu GZ, Lv YN, Dong L, Zhou LW, Huang KC, Zeng DJ, Mo L, Xu GP (2019) Profiling the bacterial diversity in a typical karst Tiankeng of China. Biomolecules 9(5): 187. https://doi.org/10.3390/biom9050187

Qu JJ, Zou X, Cao W, Xu ZS, Liang ZQ (2021) Two new species of *Hirsutella* (Ophiocordycipitaceae, Sordariomycetes) that are parasitic on lepidopteran insects from China. MycoKeys 82: 81–96. https://doi.org/10.3897/mycokeys.82.66927

Quandt CA, Kepler RM, Gams W, Araújo JP, Ban S, Evans HC, Hughes D, Humber R, Hywel-Jones N, Li ZZ, Luangsa-ard JJ, Rehner SA, Sanjuan T, Sato H, Shrestha B, Sung GH, Yao YJ, Zare R, Spatafora JW (2014) Phylogenetic-based nomenclatural proposals for Ophiocordycipitaceae (Hypocreales) with new combinations in *Tolypocladium*. IMA Fungus 5(1): 121–134. https://doi.org/10.5598/imafungus.2014.05.01.12

Quesada-Moraga E, Navas-Cortés JA, Maranhao EA, Ortiz-Urquiza A, Santiago-Álvarez C (2007) Factors affecting the occurrence and distribution of entomopathogenic fungi in natural and cultivated soils. Mycological Research 111(8): 947–966. https://doi.org/10.1016/j.mycres.2007.06.006

Ronquist F, Teslenko M, van der Mark P, Ayres DL, Darling A, Höhna S, Larget B, Liu L, Suchard MA, Huelsenbeck JP (2012) MrBayes 3.2: Efficient Bayesian phylogenetic inference and model choice across a large model space. Systematic Biology 61(3): 539–542. https://doi.org/10.1093/sysbio/sys029

Schoch CL, Seifert KA, Huhndorf S, Robert V, Spouge JL, Levesque CA, Chen W, Bolchacova E, Voigt K, Crous PW, Miller AN, Wingfield MJ, Aime MC, An K-D, Bai F-Y, Barreto RW, Begerow D, Bergeron M-J, Blackwell M, Boekhout T, Bogale M, Boonyuen N, Burgaz AR, Buyck B, Cai L, Cai Q, Cardinali G, Chaverri P, Coppins BJ, Crespo A, Cubas P, Cummings C, Damm U, de Beer ZW, de Hoog GS, Del-Prado R, Dentinger B, Diéguez-Uribeondo J, Divakar PK, Douglas B, Dueñas M, Duong TA, Eberhardt U, Edwards JE, Elshahed MS, Fliegerova K, Furtado M, García MA, Ge Z-W, Griffith GW, Griffiths K, Groenewald JZ, Groenewald M, Grube M, Gryzenhout M, Guo L-D, Hagen F, Hambleton S, Hamelin RC, Hansen K, Harrold P, Heller G, Herrera C, Hirayama K, Hirooka Y, Ho H-M, Hoffmann K, Hofstetter V, Högnabba F, Hollingsworth PM, Hong S-B, Hosaka K, Houbraken J, Hughes K, Huhtinen S, Hyde KD, James T, Johnson EM, Johnson JE, Johnston PR, Jones EBG, Kelly LJ, Kirk PM, Knapp DG, Kõljalg U, Kovács GM, Kurtzman CP, Landvik S, Leavitt SD, Liggenstoffer AS, Liimatainen K, Lombard L, Luangsa-ard JJ, Lumbsch HT, Maganti H, Maharachchikumbura SSN, Martin MP, May TW, McTaggart AR, Methven AS, Meyer W, Moncalvo J-M, Mongkolsamrit S, Nagy LG, Nilsson RH, Niskanen T, Nyilasi I, Okada G, Okane I, Olariaga I, Otte J, Papp T, Park D, Petkovits T, Pino-Bodas R, Quaedvlieg W, Raja HA, Redecker D, Rintoul TL, Ruibal C, Sarmiento-Ramírez JM, Schmitt I, Schüßler A, Shearer C, Sotome K, Stefani FOP, Stenroos S, Stielow B, Stockinger H, Suetrong S, Suh S-O, Sung G-H, Suzuki M, Tanaka K, Tedersoo L, Telleria MT, Tretter E, Untereiner WA, Urbina H, Vágvölgyi C, Vialle A, Vu TD, Walther G, Wang Q-M, Wang Y, Weir BS, Weiß M, White MM, Xu J, Yahr R, Yang ZL,

Yurkov A, Zamora J-C, Zhang N, Zhuang W-Y, Schindel D (2012) Nuclear ribosomal internal transcribed spacer (ITS) region as a universal DNA barcode marker for Fungi. Proceedings of the National Academy of Sciences of the United States of America 109(16): 6241–6246. https://doi.org/10.1073/pnas.1117018109

Shen LN, Hou MF, Xu WB, Huang YF, Liang SC, Zhang YH, Jiang ZC, Chen WH (2020) Research on flora of seed plants in Dashiwei Karst Tiankeng group of Leye. Guangxi Guihaia 40: 751–764.

Shui W, Chen YP, Wang YW, Su ZA, Zhang S (2015) Origination, study progress and prospect of karst tiankeng research in China. Acta Geographica Sinica 70: 431–446.

Song B, Wu XL, Li TH (2011) Species of *Cordyceps*-like fungi from Guangxi, China. Guizhou Science 29(1): 47–51.

Su Y, Tang Q, Mo F, Xue Y (2017) Karst tiankengs as refugia for indigenous tree flora amidst a degraded landscape in southwestern China. Scientific Reports 7(1): 1–10. https://doi.org/10.1038/s41598-017-04592-x

Sun JZ, Liu XZ, McKenzie EH, Jeewon R, Liu JK, Zhang XL, Zhao Q, Hyde KD (2019) Fungicolous fungi: Terminology, diversity, distribution, evolution, and species checklist. Fungal Diversity 95(1): 1–94. https://doi.org/10.1007/s13225-019-00422-9

Tamura K, Stecher G, Peterson D, Filipski A, Kumar S (2013) MEGA6: Molecular evolutionary genetics analysis version 6.0. Molecular Biology and Evolution 30(12): 2725–2729. https://doi.org/10.1093/molbev/mst197

Tang D, Xu Z, Wang Y, Wang Y, Tran NL, Yu H (2023a) Multigene phylogeny and morphology reveal two novel zombie-ant fungi in *Ophiocordyceps* (Ophiocordycipitaceae, Hypocreales). Mycological Progress 22(4): 22. https://doi.org/10.1007/s11557-023-01874-9

Tang D, Zhao J, Lu Y, Wang Z, Sun T, Liu Z, Yu H (2023b) Morphology, phylogeny and host specificity of two new *Ophiocordyceps* species belonging to the "zombie-ant fungi" clade (Ophiocordycipitaceae, Hypocreales). MycoKeys 99: 269–296. https://doi.org/10.3897/mycokeys.99.107565

Tang D, Huang O, Zou W, Wang Y, Wang Y, Dong Q, Sun T, Yang G, Yu H (2023c) Six new species of zombie-ant fungi from Yunnan in China. IMA Fungus 14(1): 9. https://doi.org/10.1186/s43008-023-00114-9

Trifinopoulos J, Nguyen LT, von Haeseler A, Minh BQ (2016) W-IQ-TREE: A fast online phylogenetic tool for maximum likelihood analysis. Nucleic Acids Research 44(W1): W232–W235. https://doi.org/10.1093/nar/gkw256

Vaidya G, Lohman DJ, Meier R (2011) SequenceMatrix: Concatenation software for the fast assembly of multi-gene datasets with character set and codon information. Cladistics 27(2): 171–180. https://doi.org/10.1111/j.1096-0031.2010.00329.x

Vidhate RP, Dawkar VV, Punekar SA, Giri AP (2023) Genomic determinants of entomopathogenic fungi and their involvement in pathogenesis. Microbial Ecology 85(1): 49–60. https://doi.org/10.1007/s00248-021-01936-z

Vilgalys R, Hester M (1990) Rapid genetic identification and mapping of enzymatically amplified ribosomal DNA from several *Cryptococcus* species. Journal of Bacteriology 172(8): 4238–4246. https://doi.org/10.1128/jb.172.8.4238-4246.1990

Wang YH, Sayaka B, Wang WJ, Li Y, Wang K, Kirk PM, Bushley KE, Dong CH, Hawksworth DL, Yao YJ (2021) *Pleurocordyceps* gen. nov. for a clade of fungi previously included in *Polycephalomyces* based on molecular phylogeny and morphology. Journal of Systematics and Evolution 59(5): 1065–1080. https://doi.org/10.1111/jse.12705

Wang Z, Wang Y, Dong Q, Fan Q, Dao VM, Yu H (2022) Morphological and phylogenetic characterization reveals five new species of *Samsoniella* (Cordycipitaceae, Hypocreales). Journal of Fungi (Basel, Switzerland) 8(7): 747. https://doi.org/10.3390/jof8070747

Wang Y, Wang ZQ, Luo R, Souvanhnachit S, Thanarut C, Dao VM, Yu H (2024a) Species diversity and major host/substrate associations of the genus *Akanthomyces* (Hypocreales, Cordycipitaceae). MycoKeys 101: 113–141. https://doi.org/10.3897/mycokeys.101.109751

Wang HY, Li X, Dong CB, Zhang YW, Chen WH, Liang JD, Han YF (2024b) Two new species of Sordariomycetes (Chaetomiaceae and Nectriaceae) from China. MycoKeys 102: 301–315. https://doi.org/10.3897/mycokeys.102.114480

White TJ, Bruns T, Lee S, Taylor J (1990) Amplification and direct sequencing of fungal ribosomal RNA genes for phylogenetics. In: Innis MA, Gelfand DH, Sninsky JJ, White TJ (Eds) PCR protocols: a guide to methods and applications. Academic Press, New York, 315–322. https://doi.org/10.1016/B978-0-12-372180-8.50042-1

Wu J, Zhang CH (2020) Research status and prospect of karst Tiankengs in Guizhou Province. Carsologica Sinica 39(1): 119–126.

Xiao YP, Hongsanan S, Hyde KD, Brooks S, Xie N, Long FY, Wen TC (2019) Two new entomopathogenic species of *Ophiocordyceps* in Thailand. MycoKeys 47: 53–74. https://doi.org/10.3897/mycokeys.47.29898

Xiao YP, Wang YB, Hyde KD, Eleni G, Sun JZ, Yang Y, Meng J, Yu H, Wen TC (2023) Polycephalomycetaceae, a new family of clavicipitoid fungi segregates from Ophiocordycipitaceae. Fungal Diversity 120(1): 1–76. https://doi.org/10.1007/s13225-023-00517-4

Xiao YP, Yang Y, Jayawardena RS, Gentekaki E, Peng XC, Luo ZL, Lu YZ (2024) Four novel *Pleurocordyceps* (Polycephalomycetaceae) species from China. Frontiers in Microbiology 14: 1256967. https://doi.org/10.3389/fmicb.2023.1256967

Zhang D, Gao F, Jakovlic I, Zou H, Zhang J, Li WX, Wang GT (2020) PhyloSuite: An integrated and scalable desktop platform for streamlined molecular sequence data management and evolutionary phylogenetics studies. Molecular Ecology Resources 20(1): 348–355. https://doi.org/10.1111/1755-0998.13096

Zhang Y, Wen T, Xiao Y, Yang Y, Peng X (2023) A new species of *Papiliomyces* (Clavicipiteae, Hypocreales) from China. Biodiversity Data Journal 11: e86868. https://doi.org/10.3897/BDJ.11.e86868

Zhou YM, Zhi JR, Qu JJ, Zou X (2022) Estimated divergence times of *Lecanicillium* in the family Cordycipitaceae provide insights into the attribution of *Lecanicillium.* Frontiers in Microbiology 13: 859886. https://doi.org/10.3389/fmicb.2022.859886

Zhu GS, Liu ZY, Wu XL, Liu YX (2004) The research of *Cordyceps* in the karst area of Yunnan, Guizhou and Guangxi Provinces in China. Guizhou Science 1: 27–30.

Zou X, Liu AY, Liang ZQ, Han YF, Yang M (2010) *Hirsutella liboensis*, a new entomopathogenic species affecting Cossidae (Lepidoptera) in China. Mycotaxon 111(1): 39–44. https://doi.org/10.5248/111.39

Zou W, Tang D, Xu Z, Huang O, Wang Y, Tran NL, Yu H (2022) Multigene phylogeny and morphology reveal *Ophiocordyceps hydrangea* sp. nov. and *Ophiocordyceps bidoupensis* sp. nov. (Ophiocordycipitaceae). MycoKeys 92: 109–130. https://doi.org/10.3897/mycokeys.92.86160

Supplementary material 1

Alignment dataset 1

Authors: Wan-Hao Chen, Dan Li, Jian-Dong Liang, Xiu-Xiu Ren, Jie-Hong Zhao, Yan-Feng Han
Data type: fas

Link: https://doi.org/10.3897/mycokeys.110.135724.suppl1

Supplementary material 2

Alignment dataset 2

Authors: Wan-Hao Chen, Dan Li, Jian-Dong Liang, Xiu-Xiu Ren, Jie-Hong Zhao, Yan-Feng Han
Data type: fas

Link: https://doi.org/10.3897/mycokeys.110.135724.suppl2

Supplementary material 3

Alignment dataset 3

Authors: Wan-Hao Chen, Dan Li, Jian-Dong Liang, Xiu-Xiu Ren, Jie-Hong Zhao, Yan-Feng Han
Data type: fas

Link: https://doi.org/10.3897/mycokeys.110.135724.suppl3

Supplementary material 4

Alignment dataset 4

Authors: Wan-Hao Chen, Dan Li, Jian-Dong Liang, Xiu-Xiu Ren, Jie-Hong Zhao, Yan-Feng Han
Data type: fas

Link: https://doi.org/10.3897/mycokeys.110.135724.suppl4

Supplementary material 5

Alignment dataset 5

Authors: Wan-Hao Chen, Dan Li, Jian-Dong Liang, Xiu-Xiu Ren, Jie-Hong Zhao, Yan-Feng Han
Data type: nxs

Link: https://doi.org/10.3897/mycokeys.110.135724.suppl5

MycoKeys 110: 159–183 (2024)
DOI: 10.3897/mycokeys.110.131741

Research Article

Phylogenetic analysis shows that *Pyrenula* (Pyrenulaceae) diversity is larger than expected: three new species and one new record discovered in China

Mingzhu Dou[1], Jiechen Li[1], Yongshun Hu[1], André Aptroot[2], Zefeng Jia[1]

1 *College of Agriculture and Life Sciences, Liaocheng University, Liaocheng 252059, China*
2 *Laboratório de Botânica, Liquenologia, Instituto de Biociências, Universidade Federal de Mato Grosso do Sul, Avenida Costa e Silva s/n, Bairro Universitário, CEP 79070-900, Campo Grande, Mato Grosso do Sul, Brazil*

Corresponding authors: Mingzhu Dou (kadmz@163.com); Zefeng Jia (zfjia2008@163.com)

Abstract

The lichenised fungal genus *Pyrenula* is a very common crustose lichen element in tropical to subtropical forests, but little research has been done on this genus in China. We carried out an integrative taxonomic study on *Pyrenula* in China using morphological, anatomical, chemical characters, and molecular data (ITS, nuLSU, mtSSU). Three new species with muriform ascospores containing red oil when over-mature were found: *Pyrenula submacularis* **sp. nov.**, *P. yunguiensis* **sp. nov.** and *P. rufotetraspora* **sp. nov.** Molecular data and TLC results of *P. macularis* and *P. breutelii* are for the first time reported and show that they are not synonyms. This is the first report of *P. breutelii* in China. Contrary to the previous reports of this genus, we found lichen substances in all the five species in this study, seemingly terpenoids. A key for the *Pyrenula* species reported in China is provided.

Key words: Chemical substances, diversity, morphology, new taxa, phylogeny

Academic editor: Gerhard Rambold
Received: 10 July 2024
Accepted: 23 October 2024
Published: 12 November 2024

Citation: Dou M, Li J, Hu Y, Aptroot A, Jia Z (2024) Phylogenetic analysis shows that *Pyrenula* (Pyrenulaceae) diversity is larger than expected: three new species and one new record discovered in China. MycoKeys 110: 159–183. https://doi.org/10.3897/mycokeys.110.131741

Introduction

The lichen genus *Pyrenula* Ach. (Pyrenulaceae) was first established by Acharius, with *Pyrenula nitida* (Weigel) Ach. as the type species (Acharius 1814). *Pyrenula* grows on bark mainly in tropical and subtropical forests (Aptroot 2012; Mendonça et al. 2016). The genus is characterised by perithecioid ascomata, with or without pseudocyphellae, with or without lichexanthone or anthraquinones, with distoseptate, transversely septate or (sub)muriform ascospores. UV-reaction of thallus, presence of hamathecium inspersion and the shape of the ascospore lumina (especially whether there is an endospore between the end lumina and the wall) are also important characters (Aptroot 2012; Mendonça et al. 2016).

Based on integrative taxonomic studies applying molecular, morphological, anatomical, and chemical characters, including the long-overlooked characters inspersion and iodine reaction of the hamathecium, we reported three new species of *Pyrenula* (*P. inspersa*, *P. thailandicoides* and *P. apiculata*), which have 3-septate ascospores with red or orange oil when over-mature (Dou et al. 2024). The presence of red or orange oily granules, which occur in over-mature ascospores

of some *Pyrenula* species, was first recognised by Harris (Harris 1989). He pointed out the significance of the degradation stage of spores for the taxonomy of *Pyrenula*. Aptroot et al. described the degradation process in detail: in a few species, the old spores assume a reddish tinge, the wall becomes red-brown and the remains of the lumina develop into red or orange granules (Aptroot et al. 2013). Now, a total of eleven species with red or orange oil in over-mature ascospores are known, of which seven have transversely distoseptate ascospores, viz. *P. concastroma* R.C. Harris, *P. bahiana* Malme, *P. sexlocularis* (Nyl.) Müll. Arg., *P. thailandica* Aptroot, *P. inspersa* M.Z. Dou & Z.F. Jia, *P. thailandicoides* M.Z. Dou & Z.F. Jia and *P. apiculata* M.Z. Dou & Z.F. Jia; four have (sub)muriform ascospores, viz. *P. endocrocea* Aptroot, *P. seminuda* (Müll. Arg.) Sipman & Aptroot, *P. breutelii* (Müll. Arg.) Aptroot and *P. macularis* (Zahlbr.) R.C. Harris.

In the world key of *Pyrenula* species, Aptroot accepted 169 species out of the ca. 745 named taxa in the genus (Aptroot 2012). Since then, many new species of *Pyrenula* have been described and the genus now comprises ca. 245 species (Aptroot 2012, 2021; Aptroot et al. 2012, 2013, 2018; Mendonça et al. 2016; Ingle et al. 2018; Miranda-González et al. 2022; Mishra et al. 2022; Soto-Medina et al. 2023; Lücking et al. 2023; Sipman, 2023; Dou et al. 2024), of which 46 species have so far been found in China (Aptroot and Seaward 1999; Aptroot 2003; Fu et al. 2018, 2019; Wang et al. 2018; Wei 2020; Xie et al. 2021; Dou et al. 2024; Li et al. 2024).

Here, we add three new species of *Pyrenula* with muriform ascospores with red oil when over-mature. In addition, we found that *P. macularis* is not synonymous with *P. breutelii* (Aptroot 2012). These classification results are strongly supported by molecular phylogeny. Few species of *Pyrenula* have been established based on phylogenetic result previously.

Materials and methods

Morphological and chemical analyses

The specimens were collected in the provinces Hunan, Fujian, Guizhou and Guangdong of China and are preserved in the Fungarium of the College of Life Sciences, Liaocheng University, China (LCUF). Morphological characters of thalli and apothecia were examined in the usual way and photographed under an Olympus SZX16 dissecting microscope with an Axio Imager. The anatomical characters were observed and measured under an Olympus BX53 compound microscope with an Olympus DP74 Imager. The lichen secondary metabolites were studied by thin-layer chromatography using solvent C (Orange et al. 2010).

DNA extraction, PCR sequencing and phylogenetic analysis

The genomic DNA of ascomata was extracted using the Hi-DNA-secure Plant Kit (Tiangen, Beijing, China) according to the manufacturer's protocol. The mtSSU, ITS and nuLSU regions were amplified using the primer pair mrSSU1/3R (Zoller et al. 1999), ITS1F/ITS4 (White et al. 1990; Gardes and Bruns 1993) and AL2R/LR6 (Vilgalys and Hester 1990; Mangold et al. 2008). PCR reactions were carried out in 25 µL reaction system containing 1 µL each primer solution (10 µM), 0.5 µL genomic DNA, 10 µL ddH2O, and 12.5 µL 2×Taq PCR MasterMix®. Thermocycling conditions for mtSSU comprised initial denaturation at 94 °C (3 min);

35 denaturation cycles at 94 °C (30 s), annealing at 52 °C (30 s), extension at 72 °C (1.5 min), and a final extension at 72 °C for 10 min. The PCR amplification progress for nuLSU followed Dou et al. (Dou et al. 2018). Thermocycling conditions for ITS comprised initial denaturation at 94 °C (3 min); 35 denaturation cycles at 94 °C (30 s), annealing at 52 °C (30 s), extension at 72 °C (1.5 min), and a final extension at 72 °C for 10 min. The target products of PCR were affirmed by electrophoresis on 1% agarose gels and sequenced by TsingkeBiotechnology Co.,Ltd. (Tsingtao). The newly-generated sequences were submitted to GenBank (https://www.ncbi.nlm.nih.gov/, accessed on 31 December 2025; Table 1).

The sequences of mtSSU, ITS and nuLSU were combined, and the alignment included 118 ITS sequences, 94 LSU sequences and 76 SSU sequences, representing 127 taxa. The sequences of 5 taxa were newly generated (Table 1) and the sequences of 122 taxa were downloaded in GenBank (Suppl. material 1) (Lutzoni et al. 2001; Geiser et al. 2006; Weerakoon et al. 2012; Gueidan et al. 2016). *Endocarpon pusillum* and *Cyphellophora europaea* were chosen as outgroup, based on previous studies (Gueidan et al. 2016). All *Pyrenula* taxa that could be found in GenBank were included in our data matrix.

The alignment of sequences for each marker (mtSSU, ITS and nuLSU) was undertaken independently by applying MAFFT 7 (Katoh and Standley 2013). We used the "maskSegment" function in the R package AlignmentFilter (Zhang et al. 2023) to mask ambiguously-aligned or overly-divergent segments (stringency-controlling parameter prob set to 0.05) and then used the "degap" function to remove sites with more than 50% gaps. The congruence of the two datasets was tested using a 70% reciprocal bootstrap criterion (Mason-Gamer and Kellogg 1996): the three matrices (mtSSU, ITS and nuLSU) were analysed separately with RaxML v.8.2.12 (Stamatakis 2014) using 100 bootstrap pseudoreplicates and implementing a GTRGAMMA model on the CIPRES Web Portal (http://www.phylo.org). The resulting trees were compared and any hard conflicts detected were eliminated by pruning sequences or taxa out of the datasets. The three single-locus alignments were concatenated in PhyloSuite v.1.2.2 (Zhang et al. 2020). The concatenated data matrix comprised 2440 characters (726 for mtSSU, 730 for ITS and 984 fornuLSU). For BI (Bayesian Inference) analysis, PartitionFinder 2 (Lanfear et al. 2017) was used to determine the best-fit model for each partition. The dataset was partitioned into gene groups, with the

Table 1. Information for the sequences used in this study. Newly generated sequences are shown in bold.

Species name	Specimen No.	Locality	GenBank accession number		
			ITS	nuLSU	mtSSU
P. submacularis M.Z. Dou & Z.F. Jia	FJ211750	China Fujian	**PP692372**	**PP692480**	**—**
P. submacularis M.Z. Dou & Z.F. Jia	FJ220211	China Fujian	**PP692377**	**PP692481**	**—**
P. yunguiensis M.Z. Dou & Z.F. Jia	GZ18096	China Guizhou	**PP692374**	**PP692478**	**—**
P. yunguiensis M.Z. Dou & Z.F. Jia	GZ18128	China Guizhou	**PP692373**	**PP692479**	**—**
P. yunguiensis M.Z. Dou & Z.F. Jia	YN221461	China Yunnan	**PP692378**	**PP692477**	**—**
P. rufotetraspora M.Z. Dou & Z.F. Jia	GZ18377	China Guizhou	**PP692371**	**PP692474**	**—**
P. macularis (Zahlbr.) R.C. Harris	HNX18016	China Hunan	**PP692368**	**—**	**—**
P. macularis (Zahlbr.) R.C. Harris	HNX18017	China Hunan	**PP692369**	**—**	**—**
P. macularis (Zahlbr.) R.C. Harris	HNX18018	China Hunan	**PP692370**	**PP692473**	**PP659691**
P. breutelii (Müll. Arg.) Aptroot	GD19285	China Guangdong	**PP692375**	**PP692475**	**—**
P. breutelii (Müll. Arg.) Aptroot	GD19286	China Guangdong	**PP692376**	**PP692476**	**PP659692**

GTR+I+G, SYM+I+G and GTR+I+G substitution models applied to mtSSU gene, ITS gene and nuLSU gene, respectively. BI analysis was performed with MrBayes 3.2.7 (Ronquist et al. 2012). Two runs of four chains were carried out for 10,000,000 generations and trees were sampled every 1000 generations. The first 25% of the convergence runs were discarded as burn-in. Construction of the ML (Maximum Likelihood) tree was undertaken by applying RAxML v.8.2.12 (Stamatakis 2014), using 100 bootstrap pseudoreplicates and a GTRGAMMA model on the CIPRES Web Portal (http://www.phylo.org). ML bootstrap values (BS) ≥ 70% and Bayesian posterior probabilities (PP) ≥ 0.95 were considered as significantly supported. The alignments were deposited in TreeBase (http://purl.org/phylo/treebase/phylows/study/TB2:S31341).

Results

Phylogenetic analyses

The dataset includes 118 ITS sequences, 76 mtSSU sequences and 94 nuLSU sequences, of which 11 ITS sequences, 2 mtSSU sequences, and 9 LSU sequences are newly generated in this study. The BI and ML (Suppl. material 2) trees showed similar topologies, so only the BI tree is provided here as Fig. 1. Compared with the dataset of Gueidan et al. (2016), our phylogenetic analysis includes eleven additional species (the three new species, *Pyrenula macularis*, *P. breutelii*, *P. sanguinea*, *P. nitidella*, *P. cf. acutalis*, *P. punctella*, *P. cf. leucostoma* and *P. occidentalis*). Our phylogenetic result confirms the presence of two main well-supported monophyletic groups coinciding with the presence/absence of pseudocyphellae as shown in Weerakoon et al. (2012) and Gueidan et al. (2016). Our phylogenetic results also confirm the delimitation problems of several taxa, for example, *P. quassiicola*, *P. mamillana* and *P. rubrostigma*, which is consistent with Gueidan et al. (2016).

The phylogenetic tree revealed five monophyletic lineages corresponding to five different species: *Pyrenula submacularis* M.Z. Dou & Z.F. Jia, sp. nov., *P. yunguiensis* M.Z. Dou & Z.F. Jia, sp. nov., *P. rufotetraspora* M.Z. Dou & Z.F. Jia, sp. nov., *P. macularis* (Zahlbr.) R.C. Harris and *P. breutelii* (Müll. Arg.) Aptroot. The clades of the five species were all strongly supported. The support values [posterior probability (PP)/bootstrap value (BS)] of the two specimens of *P. submacularis* was 1/100, the three specimens of *P. yunguiensis* 0.99/98, the two specimens of *P. breutelii* 0.96/83, the three specimens of *P. macularis* 1/100. Although *P. rufotetraspora* clustered with *P. submacularis* with high support (1/92), *P. yunguiensis* clustered with *P. pyrenuloides* (0.99/-), and *P. breutelii* clustered with *P. thelomorpha* (1/100), they can be distinguished easily in anatomical characters. *P. macularis* and *P. breutelii* are far apart on the phylogenetic tree. These five species all belong to Group 1.

Chemistry

Before the report (Dou et al. 2024), TLC results had not been described in detail in the literature of *Pyrenula*. They were either not mentioned or interpreted as nothing detected. However, our TLC results show several spots, indicating that there are multiple lichen substances in species of *Pyrenula* (Suppl. materials 3, 4). The weak visibility in short-wave UV (plate A) and the reddish color after charring (plate B) suggest that most spots concern terpenoids.

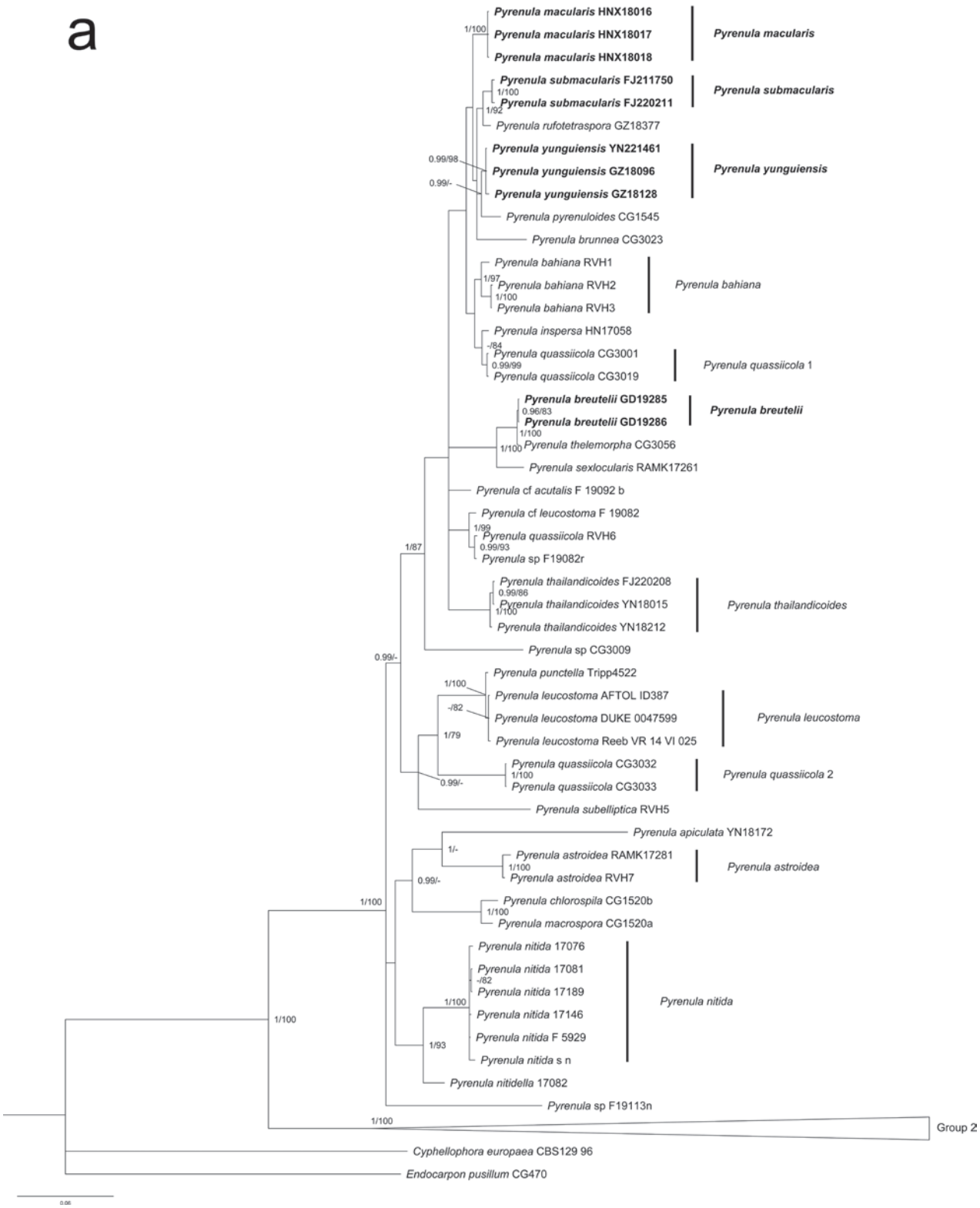

Figure 1. Phylogeny of the genus *Pyrenula* based on a three-gene dataset (mtSSU, ITS and nuLSU) **a** overview of the entire tree and details of Group 1 **b** details of Group 2. Most likely tree obtained using MrBayes. Support values are reported above the branches [posterior probability (PP)/bootstrap value (BS)]. Only significant values (higher than 95% PP and higher than 70% BS) are shown. *Cyphellophora europaea* and *Endocarpon pusillum* are the out-group taxa.

Figure 1. Continued.

Additional solvents and an experienced chemist will be needed to identify them further. On plate C the terpenoid spots are more intensely colored. A comparison between the *Pyrenula* species represented on the plate C suggests that all have the same series of red color that are green under daylight on the plate B. Reddish spots with yellow rim in class 7 in Suppl. material 3 are probably terpenoids from treebark; they are strongest in samples without lichen. In some samples some of the spots are different from those of the other species.

The TLC experiments of less closely related species were also carried out (Suppl. materials 5, 6). The species in Suppl. materials 5, 6 belong to ten genera (*Pyrenula*, *Phyllobaeis*, *Coenogonium*, *Ocellularia*, *Allographa*, *Graphis*, *Platythecium*, *Phyrrospora*, *Malmidea*, *Thelotrema*) and eight families (Pyrenulaceae, Baeomycetaceae, Coenogoniaceae, Diploschistaceae, Graphidaceae, Lecanoraceae, Malmideaceae, Thelotremataceae). The *Pyrenula* sp. in Suppl. material 5 is a record in China not yet published and included in the Group 2 of phylogenetic tree. This *Pyrenula* species did not produce the chemical substances that were red after charring under 365 nm ultraviolet light and green under daylight. The two white spots of this *Pyrenula* species at Rf 2 on the plate C in Suppl. material 5 might represent the same chemical substances as the two white spots of *P. macularis* (no. nr. 5 and 6) on the plate C in Suppl. material 4. Although the species of *Allographa* (no. nr. 2, 7, 11, 12, 13 of Suppl. material 5) showed red spots after charring under 365 nm ultraviolet light at Rf 5, the spots were yellow under daylight, not green. None of the other species in Suppl. materials 5, 6 produces the same chemical substance as the five species of *Pyrenula* reported here. Given that phylogenetic approach and that chemical characters are underestimated and limited to few specimens and areas, we predict that our findings only represent the tip of the iceberg in this genus.

Taxonomy

Pyrenula submacularis **M.Z. Dou & Z.F. Jia, sp. nov.**
MycoBank No: 853430
Fig. 2

Etymology. The specific epithet submacularis refers to the similarity to *Pyrenula macularis*.

Holotype. China • Fujian Province, Wuyi Mountain, Tongmu Village Reserve, Wuyi Mountain National Park, Science and Technology Building, 27°44'31"N, 117°40'44"E, alt. 700 m, on bark, 24 October 2021, Y.F. Zhao (LCUF FJ211750, holotype; GenBank PP692372 for ITS, and PP692480 for nuLSU).

Diagnosis. The new species can be distinguished from the most similar species *Pyrenula macularis* Aptroot by bigger ascospores with more locules and different lichen substances.

Description. Thallus corticolous, crustose, olive-green in the field and khaki after drying, surface dull, corticate with pseudocyphellae, UV-. Apothecia emergent, dispersed, low conical, 1.0–2.0 mm diam., the sides often partly covered by the thallus, with crystals, wall completely carbonized when mature and even falls apart. Ostioles apical, white. Hamathecium not inspersed, IKI+ blue and occasionally red. Ascospores 8 per ascus, uniseriate or subbiseriate, elliptical, with rounded ends, 40–65 × 16–21(–28) µm, hyaline to brown, muriform, with c. 7–9 × 2–7 locules, lumina rounded, old spores containing globules of red oily substance.

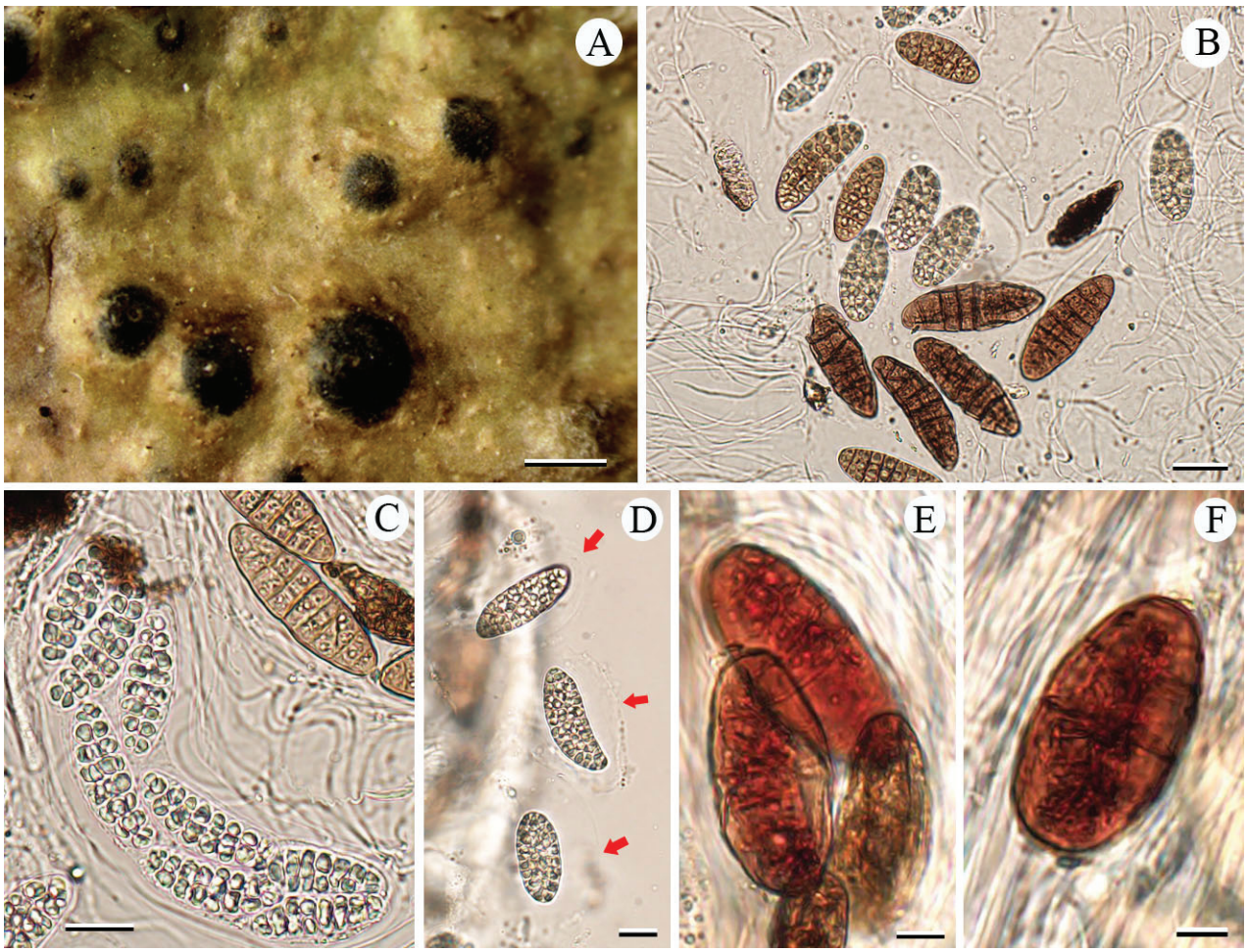

Figure 2. *Pyrenula submacularis* sp. nov. (holotype, LCUF FJ211750) **A** thallus with ascomata and pseudocyphellae **B** ascospores at different developmental stages **C** ascus, with 8 ascospores **D** red arrows show gelatinous halo **E, F** over-mature ascospores with orange-oil. Scale bars: 1 mm (**A**); 30 µm (**B**); 20 µm (**C, D**); 10 µm (**E, F**).

Chemistry. Thallus UV-. TLC with solvent C showed unidentified black spots at Rf two, three, four, five and six under 254 nm ultraviolet light; unidentified green spot at Rf four and brick red spots at Rf five after charring under daylight; unidentified red spots at Rf three and four, and one unidentified fluorescent spot at Rf five after charring under 365 nm ultraviolet light (Suppl. material 3).

Habitat and distribution. The new species is currently only known from the subtropical regions of southern China on bark.

Additional specimens examined. China • Fujian Province, Longyan City, Dongxiao National Forest Park, Frog Stone, 24°58'07"N, 117°01'14"E, alt. 679 m, on bark, 12 July 2022, Z.G. Ma (LCUF FJ220211; GenBank PP692377 for ITS, and PP692481 for nuLSU).

Notes. This new species is similar to *Pyrenula seminuda*, *P. endocrocea*, *P. breutelii* and *P. macularis* in having (sub)muriform ascospores with red or orange oil when over-mature. This new species differs from *P. seminuda* by bigger and muriform ascospores with more locules, the latter 22–40 × 10–17 µm and submuriform with 6 × 1–2 locules, most transverse locules being single and few with an oblique or longitudinal division (Aptroot et al. 2013). *P. endocrocea* differs from this new species by medulla with a soft layer of copious orange

anthraquinone crystals reacting UV+ red and KOH+ crimson, and smaller ascospores, (30–)32–44(–50) × 13–16(–19) µm (Aptroot et al. 2012). This new species (*P. submacularis*) differs from *P. breutelii* in lichen substances (Suppl. material 3) and by bigger ascospores and more locules, the latter 25–35 × 12–13 µm and 8 × 3–4 locules (Müller 1885). *P. submacularis* (no. nr. 5 and nr. 6 in Suppl. material 3) has two more black spots at Rf two and three under 254 nm ultraviolet light than *P. breutelii* (no. nr. 15 and nr. 16 in Suppl. material 3). And the new species has one more spot with fluorescence at Rf five after charring under 365 nm ultraviolet light than *P. breutelii* (Suppl. materials 3, 4). This new species (*P. submacularis*) can be distinguished from the most similar species *P. macularis* by different lichen substances and bigger ascospores and more locules, the latter 34–45 × 14–16 µm and 8 × 1–3 locules (Zahlbruckner 1930). *P. macularis* (no. nr. 5 and nr. 6 in Suppl. material 4) has two more black spots at Rf two under 254 nm ultraviolet light than *P. submacularis* (no. nr. 8 and nr. 10 in Suppl. material 4). And the new species has one more spot with fluorescence at Rf five after charring under 365 nm ultraviolet light than *P. macularis* (Suppl. materials 3, 4).

Pyrenula yunguiensis **M.Z. Dou & Z.F. Jia, sp. nov.**
MycoBank No: 853431
Fig. 3

Etymology. The specific epithet yunguiensis refers to the place where the specimen was collected.

Holotype. China • Guizhou Province, Duyun City, Doupeng Mountain Reserve, Mayao River Street, 26°22'32"N, 107°22'11"E, alt. 1107 m, on bark, 17 March 2018, F.Y. Liu (LCUF GZ18096, holotype; GenBank PP692374 for ITS, and PP692478 for nuLSU).

Diagnosis. The new species can be distinguished from the most similar species *P. submacularis* by bigger ascospores and different lichen substances.

Description. Thallus corticolous, crustose, olive-green in the field and khaki after drying, surface dull, corticate with pseudocyphellae, UV-. Apothecia emergent, dispersed, low conical, 0.5–2.0 mm diam., the sides often partly covered by the thallus, with crystals. Excipulum carbonized when mature and falls apart when over-mature. Ostioles apical, white. Hamathecium not inspersed, IKI+ red and occasional blue, the colour relating to development stage. Ascospores 8 per ascus, uniseriate, fusiform, with pointed or blunt ends, 50–70(–80) × 17–22(–26) µm, hyaline to brown, muriform, with c. 8 × 2–4 locules, lumina rounded, old spores containing globules of red oily substance.

Chemistry. Thallus UV-. TLC with solvent C showed unidentified black spots at Rf four and six under 254 nm ultraviolet light; unidentified green spot at Rf four on charred plate under daylight; unidentified red spots at Rf three, four and five on charred plate under 365 nm ultraviolet light (Suppl. material 3).

Habitat and distribution. The new species is currently only known from the subtropical regions of southern China on bark.

Additional specimens examined. China • Guizhou Province, Duyun City, Doupeng Mountain Reserve, Old Post Street, 26°22'35"N, 107°21'52"E, alt.

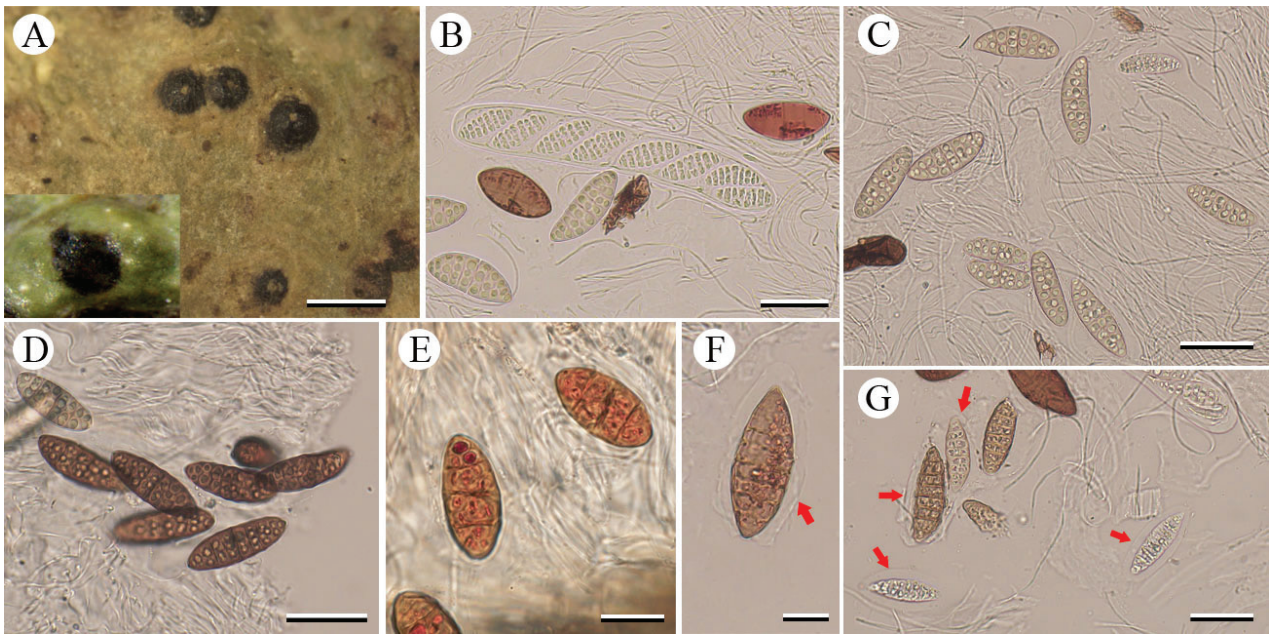

Figure 3. *Pyrenula yunguiensis* sp. nov. (holotype, LCUF GZ18096) **A** thallus with ascomata and pseudocyphellae **B** ascus, with 8 ascospores **C–G** ascospores at different developmental stages **E, F** over-mature ascospores with red-oil **F, G** red arrows show gelatinous halo. Scale bars: 1 mm (**A**); 50 µm (**B–D**); 20 µm (**E, F**); 40 µm (**G**).

1154 m, on bark, 17 March 2018, X.H. Wu (LCUF GZ18128; GenBank PP692373 for ITS and PP692479 for nuLSU). China • Yunnan Province, Jingdong County, Taizhong Town, Aishanting, 24°32'11"N, 101°01'53"E, alt. 2625 m, on bark, 16 August 2022, T. Jia (LCUF YN221461; GenBank PP692378 for ITS, and PP692477 for nuLSU).

Notes. This new species is similar to *Pyrenula seminuda*, *P. endocrocea*, *P. breutelii*, *P. macularis* and *P. submacularis* in having (sub)muriform ascospores with red or orange oil when over-mature. This new species differs from *P. seminuda* by bigger and muriform ascospores with more locules, the latter 22–40 × 10–17 µm and submuriform with 6 × 1–2 locules, most transverse locules being single and few with an oblique or longitudinal division (Aptroot et al. 2013). *P. endocrocea* differs from this new species by medulla with a soft layer of copious orange anthraquinone crystals reacting UV+ red and KOH+ crimson, and smaller ascospores, (30–)32–44(–50) × 13–16(–19) µm (Aptroot et al. 2012). This new species differs from *P. breutelii* by bigger ascospores, the latter 25–35 × 12–13 µm (Müller 1885). This new species can be distinguished from *P. macularis* by bigger ascospores, the latter 34–45 × 14–16 µm and 8 × 1–3 locules (Zahlbruckner 1930). This new species can be distinguished from the most similar species *P. submacularis* by different lichen substances, bigger ascospores and less locules, the latter 40–65 × 16–21(–28) µm and 7–9 × 2–7 locules. *P. submacularis* (no. nr. 5 and nr. 6 in Suppl. material 3; no. nr. 8 and nr. 10 in Suppl. material 4) has one more spot with fluorescence at Rf five after charring under 365 nm ultraviolet light than *P. yunguiensis* (no. nr. 8 and nr. 11 in Suppl. material 3; no. nr. 12 and nr. 14 in Suppl. material 4). Although *P. yunguiensis* clustered with *P. pyrenuloides* with high support (0.99/-), they can be distinguished easily in anatomical characters. *P. pyrenuloides* has no red or orange oil in over-mature ascospores and more locules (8–10 rows of up to ca. 10 each) (Harris 1989).

***Pyrenula rufotetraspora* M.Z. Dou & Z.F. Jia, sp. nov.**
MycoBank No: 853432
Fig. 4

Etymology. The specific epithet rufo refers to the red oil in over-mature ascospores and tetraspora means that there are four spores in each ascus.

Holotype. China • Guizhou Province, Libo County, Xiaoqikong Scenic Area, Laya Waterfall, 25°15'10"N, 107°44'06"E, alt. 425 m, on bark, 24 October 2018, Z.F. Jia (LCUF GZ18377, holotype; GenBank PP692371 for ITS, and PP692474 for nuLSU).

Diagnosis. This new species can be distinguished from the most similar species *Pyrenula yunguiensis* by fewer ascospores per ascus, bigger ascospores, more locules and different lichen substances.

Description. Thallus corticolous, crustose, olive-green in the field and khaki after drying, surface dull, corticate with pseudocyphellae, UV-. Apothecia emergent, dispersed, conical, 0.6–1.2 mm diam., the sides often partly covered by the thallus, with crystals. Excipulum completely carbonized when mature and falls apart when over-mature. Ostioles apical, white or brown. Hamathecium not inspersed, IKI+ red. Ascospores 4 per ascus, uniseriate, fusiform, with pointed or blunt ends, 70–100(–106) × (17–)21–27(–41) µm, hyaline to brown, muriform, with c. 10–12 × 3–14 locules, lumina rounded, old spores containing globules of red oily substance.

Chemistry. Thallus UV-. TLC with solvent C showed one unidentified black spot at the dividing line of Rf three and four under 254 nm ultraviolet light; unidentified red substances at Rf four under 365 nm ultraviolet light (Suppl. material 3).

Habitat and distribution. The new species is currently only known from the subtropical regions of southern China on bark.

Notes. This new species is similar to *Pyrenula seminuda*, *P. endocrocea*, *P. breutelii*, *P. macularis*, *P. submacularis* and *P. yunguiensis* in having (sub) muriform ascospores with red or orange oil when over-mature. This new species differs from *P. seminuda* by bigger and muriform ascospores with more locules, the latter 22–40 × 10–17 µm and submuriform with 6 × 1–2 locules, most transverse locules being single and few with an oblique or longitudinal division (Aptroot et al. 2013). *P. endocrocea* differs from this new species by medulla with a soft layer of copious orange anthraquinone crystals reacting UV+ red and KOH+ crimson, and smaller ascospores, (30–)32–44(–50) × 13–16(–19) µm (Aptroot et al. 2012). This new species can be distinguished from *P. breutelii*, *P. macularis*, *P. submacularis* and *P. yunguiensis* by different lichen substances (Suppl. materials 3, 4), bigger ascospores, more locules and fewer ascospores per ascus. There are 8 ascospores in per ascus in *P. breutelii*, *P. macularis*, *P. submacularis* and *P. yunguiensis*, 4 in the new species. *P. rufotetraspora* showed a black spot at the dividing line of Rf three and four under 254 nm ultraviolet light (no. nr. 13 on Suppl. material 3), which was not red on charred plate under 365 nm ultraviolet light. This black spot did not exist in *P. breutelii*, *P. macularis*, *P. submacularis* and *P. yunguiensis* and located at Rf four under 254 nm ultraviolet light on Suppl. material 4 (no. nr. 16). The difference of locations of this spot on Suppl. materials 3, 4 might be caused by edge effect. *P. submacularis* is sister to *P. rufotetraspora* with high support (1/92), but the latter has fewer ascospores in ascus (4) and obviously bigger ascospores.

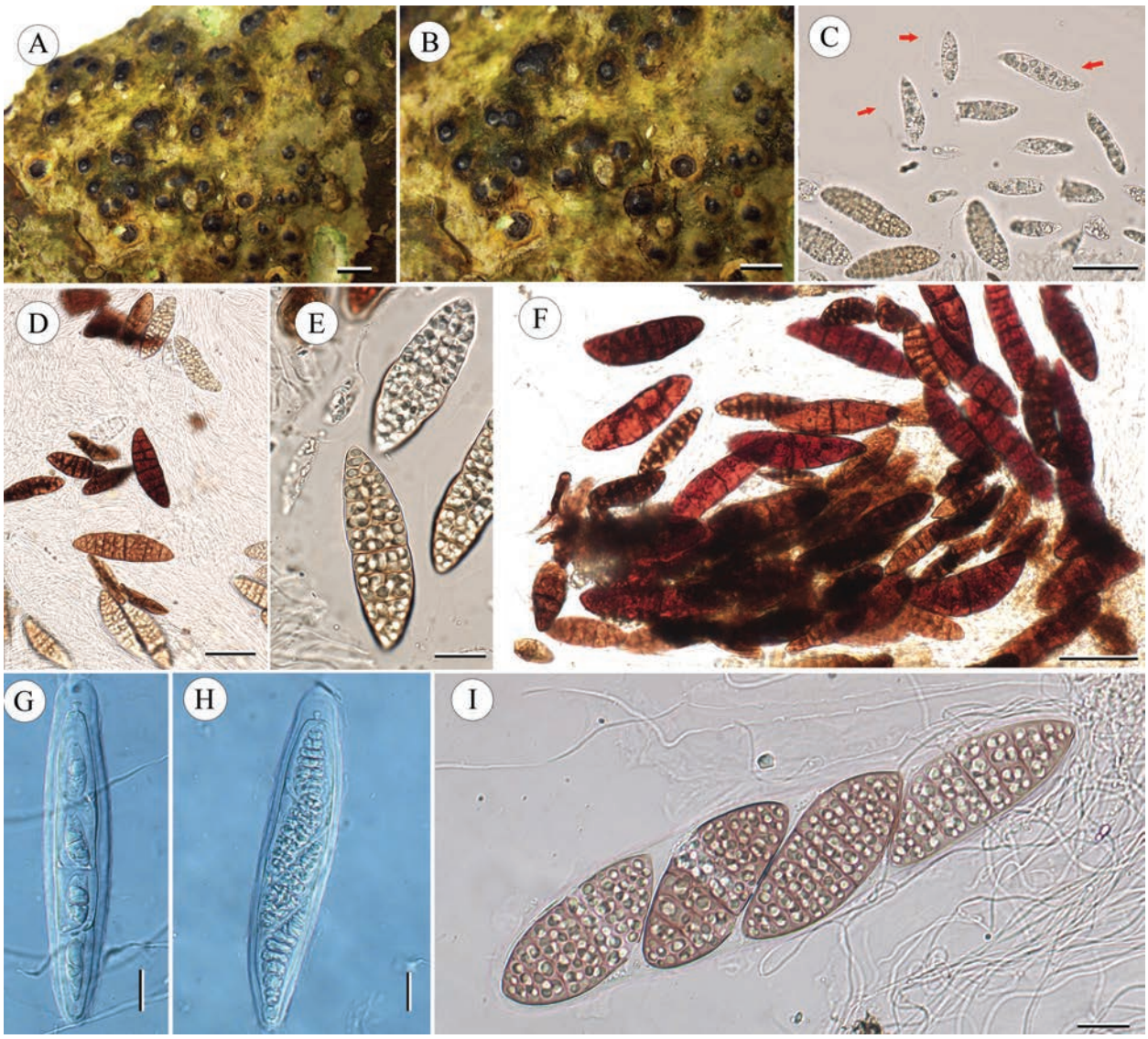

Figure 4. *Pyrenula rufotetraspora* sp. nov. (holotype, LCUF GZ18377) **A, B** thallus with ascomata **C–F** ascospores at different developmental stages, red arrows in **C** show gelatinous halo around immature ascospores **G–I** ascus, with 4 ascospores. Scale bars: 2 mm (**A, B**); 50 µm (**C, D**); 20 µm (**E**); 50 µm (**F**); 20 µm (**G, H**); 25 µm (**I**).

***Pyrenula breutelii* (Müll. Arg.) Aptroot**
MycoBank No: 563102
Fig. 5

Basionym. *Anthracothecium breutelii* Müll. Arg., *Flora* 68: 339 (1885).

Holotype. St Thomas, *Breutel*, ex hb. Hampe 1877 (G).

Description. Thallus corticolous, crustose, olive-green in the field and khaki after drying, surface dull, corticate with abundant pseudocyphellae, UV-. Apothecia perithecioid, dispersed, aggregated occasionally when crowded, low conical, 0.3–0.5 mm diam., the sides often partly covered by the thallus, with crystals. Excipulum carbonized when mature and falls apart when over-mature. Ostioles apical, white. Hamathecium not inspersed, IKI+ red. Ascospores 8 per ascus, subbiseriate, fusiform, with pointed or blunt ends, (23–)25–37(–41) × (10–)12–15(–18) µm, hyaline to brown, muriform, with c. 8 × 1–4 locules, lumina rounded, old spores containing globules of red oily substance.

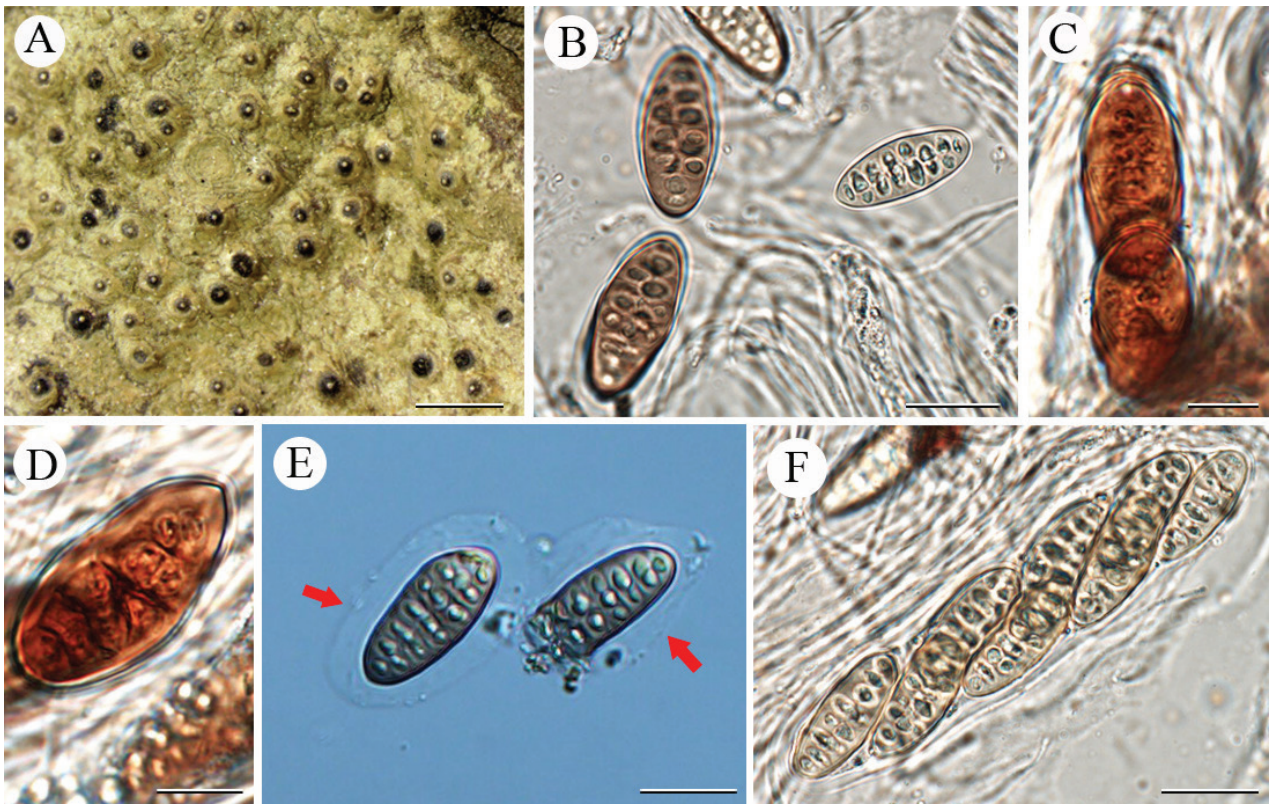

Figure 5. *Pyrenula breutelii* (LCUF GD19285) **A** thallus with ascomata and pseudocyphellae **B** hyaline immature ascospores and brown mature ascospores **C, D** over-mature ascospores with red oil **E** red arrows show gelatinous halo **F** ascus, with 8 ascospores. Scale bars: 1 mm (**A**); 20 µm (**B**); 10 µm (**C, D**); 20 µm (**E, F**).

Chemistry. Thallus UV-. TLC with solvent C showed unidentified black spots at Rf four and five under 254 nm ultraviolet light on fresh plate; unidentified green spot at Rf four on charred plate under daylight; unidentified red spots at Rf three, four and five, unidentified red and black spots at Rf five on charred plate under 365 nm ultraviolet light (Suppl. material 3).

Additional specimens examined. China • Guangdong Province, Guangzhou City, South China Botanical Garden, Chinese Academy of Sciences, Australian Garden, Energy Road, 23°10'44"N, 113°21'20"E, alt. 26 m, on bark, 20 January 2019, Z.T. Yao (LCUF GD19285; GenBank PP692375 for ITS and PP692475 for LSU). China • Guangdong Province, Guangzhou City, South China Botanical Garden, Chinese Academy of Sciences, Australian Garden, Energy Road, 23°10'44"N, 113°21'20"E, alt. 26 m, on bark, 20 January 2019, Z.T. Yao (LCUF GD19286; GenBank PP692376 for ITS, PP692476 for nuLSU and PP659692 for mtSSU).

Habitat and distribution. Growing on tree bark of pantropical forests. Previously reported from the U.S.A (Müller 1885). Newly reported for China.

Notes. The morphology and anatomy characteristics of the Chinese specimens correspond to *Pyrenula breutelii* (Müll. Arg.) Aptroot described from St Thomas, *Breutel*, ex hb. Hampe. *Pyrenula* macularis is distinguished by larger ascomata (0.3–1.5 mm), larger ascospores (35–45 × 14–16) µm and less locules (1–3) (Zahlbruckner 1930). In the protolog, TLC and KI result was not mentioned and molecular sequences were not provided. Here, we provide TLC, KI result and ITS and nuLSU sequences. Because the difference in ascospores between *P. macularis* and *P. breutelii* is not very significant, *P. macularis* was

synonymized with *P. breutelii* (Aptroot 2012; Aptroot et al. 2013). But the phylogenetic result and TLC result proves they are two different species. This is the first report of *P. breutelii* in China. Although *P. breutelii* clustered with *P. thelomorpha* with high support (1/100), they can be distinguished easily in anatomical characters. *P. thelomorpha* has no red or orange oil in over-mature ascospores and more locules (8 rows of c. 3–8 locules) (Aptroot 2009).

***Pyrenula macularis* (Zahlbr.) R.C. Harris**
MycoBank No: 134429
Fig. 6

Basionym. *Anthracothecium maculare* Zahlbr., *Mycologia* 22: 70 (1930).

Holotype. Yauco, Porto Rico [Puerto Rico], 30 Dec. 1915.

Description. Thallus corticolous, crustose, olive-green in the field and khaki after drying, surface dull, corticate with abundant pseudocyphellae, UV-. Apothecia perithecioid, conical, dispersed, aggregated occasionally when crowded, with crystals, immersed in the thallus, small, to 0.3 mm wide at the early developmental stage, then the sides partly covered by the thallus. Excipulum carbonized when mature and falls apart when over-mature. Ostioles apical, white. Hamathecium not inspersed, IKI+ red. Ascospores 8 per ascus, subbiserial, fusiform, with pointed or blunt ends, (33–)37–50 × (13–)14–16 µm, hyaline to brown, muriform, with c. 8 × 1–3 locules, lumina rounded, old spores containing globules of red oily substance.

Chemistry. Thallus UV-. TLC with solvent C showed unidentified black spots at Rf two, four and five under 254 nm ultraviolet light on fresh plate; unidentified green spot at the dividing line of Rf four and five on charred plate under daylight; unidentified red spots at Rf three, four and red spots at Rf five on charred plate under 365 nm ultraviolet light (Suppl. material 4).

Additional specimens examined. China • Hunan Province, Wugang City, Yun Shan, Shuanghua Pavilion, 26°39'28"N, 110°36'37"E, alt. 730 m, on bark of *Zelkova serrata*, 28 April 2018, Z.F. Jia (LCUF HNX18016; GenBank PP692368 for ITS). China • Hunan Province, Wugang City, Yun Shan, Shuanghua Pavilion, 26°39'28"N, 110°36'37"E, alt. 730 m, on bark of *Zelkova serrata*, 28 April 2018, Z.F. Jia (LCUF HNX18017; GenBank PP692369 for ITS). China • Hunan Province, Wugang City, Yun Shan, Shuanghua Pavilion, 26°39'28"N, 110°36'37"E, alt. 730 m, on bark of *Zelkova serrata*, 28 April 2018, Z.F. Jia (LCUF HNX18018; GenBank PP659691 for mtSSU, PP692370 for ITS and PP692473 for nuLSU).

Habitat and distribution. Growing on exposed tree in pantropical forest. Previously reported from Porto Rico (Zahlbruckner 1930), U.S.A. (Harris 1989), Australia (Aptroot 2009), Puntarenas (Aptroot et al. 2008), Muri Lagoon (Mccarthy 2000), HongKong (Aptroot and Seaward 1999) and Taiwan (Aptroot 2003) of China.

Notes. The morphology and anatomy characteristics of the Chinese specimens correspond to *Pyrenula macularis* (Zahlbr.) R.C. Harris described from Yauco, Porto Rico. *P. breutelii* is distinguished by different lichen substances (Suppl. material 4), smaller ascomata (0.3–0.5 mm), smaller ascospores ((23–)25–37(–41) × (10–)12–15(–18)) µm and more locules (1–4). *P. macularis* (no. nr. 5 and 6) has two more black spots at Rf two under 254 nm ultraviolet light on fresh plate than *P. breutelii* (no. nr. 2 and 3) (Suppl. material 4). In the

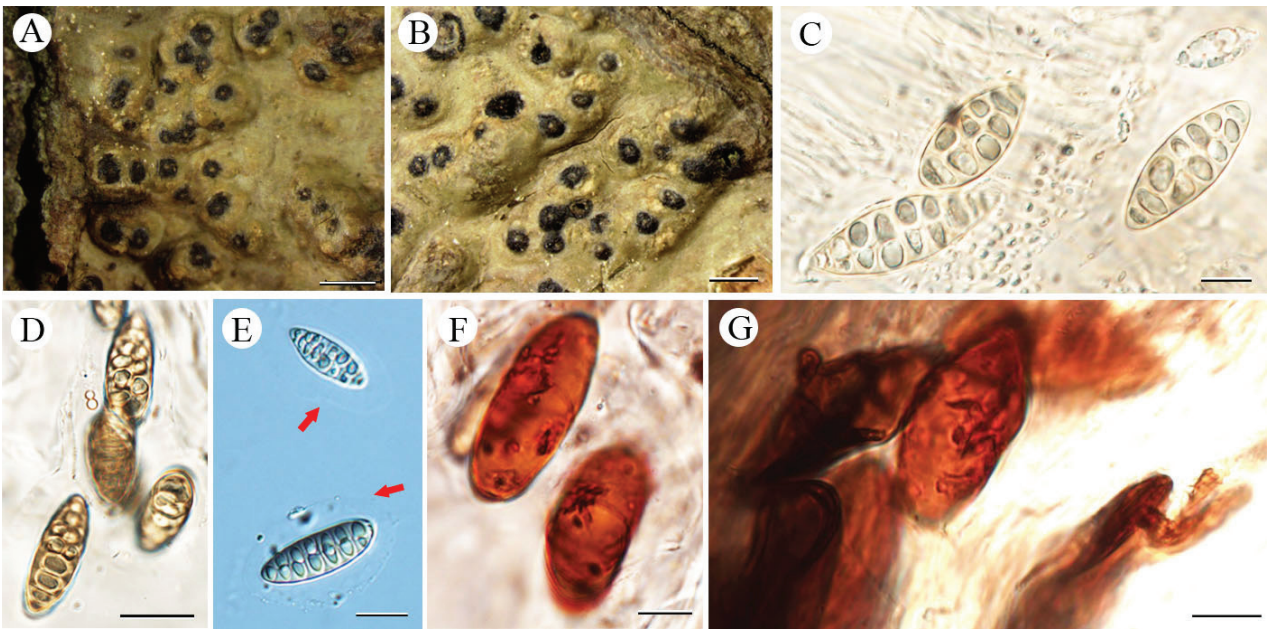

Figure 6. *Pyrenula macularis* (LCUF HNX18017) **A, B** thallus with ascomata and pseudocyphellae **C, D** ascospores at different development stages **E** ascospores with gelatinous halo shown by red arrows **F, G** over-mature ascospores with orange oil. Scale bars: 1 mm (**A, B**); 10 µm (**C**); 20 µm (**D, E**); 10 µm (**F, G**).

protolog, TLC and KI result was not mentioned and molecular sequences were not provided. Here, we provide TLC, KI result and ITS, nuLSU sequences. This species has previously been reported in China only in Hong Kong (Aptroot and Seaward 1999) and Taiwan (Aptroot 2003). Because the difference in ascospores between *P. macularis* and *P. breutelii* is not very significant, *P. macularis* was synonymous with *P. breutelii* (Aptroot 2012; Aptroot et al. 2013). But the phylogenetic result and TLC results prove they are two different species.

Discussion

Because the differences in ascospores between *Pyrenula macularis* and *P. breutelii* are not very significant, *P. macularis* was considered synonymous with *P. breutelii* (Aptroot 2012; Aptroot et al. 2013). But both the phylogenetic and the TLC results prove they are two different species. Similarly, if without molecular phylogenetic analysis and rigorous TLC trials, *P. submacularis* M.Z. Dou & Z.F. Jia, sp. nov. and *P. yunguiensis* M.Z. Dou & Z.F. Jia, sp. nov. might be classified into the same species, and *P. submacularis* M.Z. Dou & Z.F. Jia, sp. nov. might be classified as *P. macularis*. It is obvious that phylogenetic analysis and metabolite detection are crucial in the taxonomic study of *Pyrenula*, but they have been thus far limited to very few specimens, which may partly explain the delimitation problems in *P. quassiicola*, *P. mamillana*, *P. minor*, *P. aspistea* and other taxa revealed in previous and our phylogenetic analysis of this genus (Gueidan et al. 2016; Weerakoon et al. 2012). The delimination of the five species in this study suggests that it is significant to pay attention to the chemical substances in distinguishing phylogenetically informative characters and revealing near-cryptic diversification (Lücking et al. 2021) of *Pyrenula*.

Meanwhile, I carried out the TLC experiments of some remote species as Suppl. materials 5, 6. The *Pyrenula* sp., which was one new record in China

unpublished and included in the Group 2 of phylogenetic tree, did not produce the same set of terpenoids as the five species described in this article. But it showed two white spots at Rf 2 on the plate C, which might represent the same chemical substances as that *P. macularis* produced. The other species were included in other families, and did not produce the same chemicals as the five species. This seems to suggest that the likelihood of producing the same chemical is positively related to the distance of phylogenetic relationships. In Southern China, there are abundant subtropical to tropical evergreen resources (Zhu 2017). This habitat is favorable for the pyrenocarpous lichens, including *Pyrenula*. However, the genus has not been sufficiently studied in China. Most of *Pyrenula* reported in China were in the checklist of the lichens of Hong Kong and Taiwan (Aptroot and Seaward 1999; Aptroot 2003). Furthermore, the vast majority of *Pyrenula* reported in China were new records and had no molecular data. Our research suggests high species richness of *Pyrenula* is expected to be found when the taxonomic studies of this genus were carried out systematically in China.

Key to the species of *Pyrenula* reported in China

Key A (Ascospores submuriform to muriform).
Key B (Ascospores only transversely septate).

Key A

1 Thallus yellow to orange; anthraquinones pigments K+ pink to purplish ..... ***Pyrenula ochraceoflava* (Nyl.) R.C. Harris**
– Thallus K– or yellowish, anthraquinones absent **2**
2 Ostioles lateral **3**
– Ostioles apical **4**
3 Ascospores < 70 µm long ..... ***Pyrenula astroidea* (Fée) R.C. Harris**
– Ascospores > 70 µm long ..... ***Pyrenula schiffneri* (Zahlbr.) Aptroot**
4 Ascospores < 25 µm long **5**
– Ascospores > 25 µm long **6**
5 Thallus UV+yellow ..... ***Pyrenula confinis* (Nyl.) R.C. Harris**
– Thallus UV ..... ***Pyrenula parvinuclea* (Meyen & Flot.) Aptroot**
6 Old ascospores with orange oil **7**
– Old ascospores without orange oil **11**
7 Ascospores 4/ascus, 70–100(–106) × (17–)21–27(–41) µm, 10–12 × 3–14 locules ..... ***Pyrenula rufotetraspora* M.Z. Dou & Z.F. Jia, sp. nov.**
– Ascospores 8/ascus **8**
8 TLC with solvent C showed one spot with fluorescence at Rf five under 365 nm ultraviolet light, ascospores 40–65 × 16–21(–28) um, 7–9 × 2–7 locules ..... ***Pyrenula submacularis* M.Z. Dou & Z.F. Jia, sp. nov.**
– TLC with solvent C showed no fluorescent spot at Rf five under 365 nm ultraviolet light **9**
9 Most ascospores < 50 µm long **10**
– Ascospores 50–70(–80) × 17–22(–26) µm, 8 × 2–4 locules ..... ***Pyrenula yunguiensis* M.Z. Dou & Z.F. Jia, sp. nov.**

10 Ascospores (23–)25–37(–41) × (10–)12–15(–18) µm, 8 × 1–4 locules, TLC with solvent C showed no black spot at Rf two under 254 nm ultraviolet light ..... ***Pyrenula breutelii* (Müll. Arg.) Aptroot**
– Ascospores (33–)37–50 × (13–)14–16 µm, 8 × 1–3 locules, TLC with solvent C showed two black spots at Rf two under 254 nm ultraviolet light ... .***Pyrenula macularis* (Zahlbr.) R.C. Harris**
11 Ascospores > 80 µm long, mostly 2/ascus **12**
– Ascospores < 80 µm long, mostly 4–8/ascus.....**13**
12 Thallus without pseudocyphellae, ascospores 80–140(–155) µm long..... .....***Pyrenula platystoma* (Müll. Arg.) Aptroot**
– Thallus with pseudocyphellae, ascospores 115–180 µm long..... .....***Pyrenula duplicans* (Nyl.) Aptroot**
13 Locules relatively large and angular, with up to 6 between 2 primary septa.....***Pyrenula leucostoma* Ach.**
– Locules mostly round, at least in the central part of the ascospore with more than 6 between 2 primary septa ....***Pyrenula pyrenuloides* (Mont.) R.C. Harris**

Key B

1 Ostioles pointing in various directions, mostly eccentric to lateral; ascomata sometimes with several chambers connected to joint ostioles.....**2**
– Ostioles apical or, when eccentric, all pointing in the same direction; ascomata with one chamber or each chamber with own ostiole **4**
2 Terminal locules directly against the exospore wall; ascospores 16–25 µm long .....***Pyrenula circumfiniens* Vain.**
– Terminal locules separated from the exospore wall by endospore thickening.....**3**
3 Ascospores 35–45 µm long .....***Pyrenula adacta* Fée**
– Ascospores 18–30 µm long ..... ***Pyrenula acutispora* Kalb & Hafell**
4 Ascospores at least seemingly 4–7-septate; old ascospores with orange oil, thallus often with pseudocyphellae ....***Pyrenula sexlocularis* (Nyl.) Müll. Arg.**
– Ascospores all distinctly 3-septate.....**5**
5 Ascospores (45–)50–60 µm long, thallus without papillae but with pseudocyphellae .....***Pyrenula immissa* (Stirt.) Zahlbr.**
– Ascospores mostly < 50 µm long.....**6**
6 Ascomata erumpent, c. 0.4–0.8 mm diam; thallus with red patches or completely red; ascospores 27–35 µm long.....***Pyrenula cruenta* (Mont.) Vain.**
– Ascomata and thallus without external pigments **7**
7 Ascomata mostly aggregated, with fused walls but with separate ostioles.....**8**
– Ascomata mostly simple, only aggregated as by chance when crowded.... **10**
8 Old ascospores with red oil; hamathecium inspersed, ascospores 28.5–50 × 10–20 µm .....***Pyrenula inspersa* M.Z. Dou & Z.F. Jia**
– Old ascospores without red oil.....**9**
9 Ascospores mostly 21–25 µm long.....***Pyrenula leucotrypa* (Nyl.) Upreti**
– Ascospores mostly 15–20 µm long.....***Pyrenula anomala* (Ach.) Vain.**

10 Old ascospores with orange oil **11**
– Old ascospores without orange oil **14**
11 Ascospores < 35 µm long **12**
– Ascospores > 35 µm long **13**
12 Terminal locules directly against the exospore wall ..... ***Pyrenula apiculata* M.Z. Dou & Z.F. Jia**
– Terminal locules separated from the exospore wall by endospore thickening ..... ***Pyrenula bahiana* Malme**
13 Hamathecium IKI-; no substances detected by TLC ..... ***Pyrenula thailandica* Aptroot**
– Hamathecium IKI+ red; TLC showed an unidentified spot at Rf four under 254 nm ultraviolet light using solvent C ..... ***Pyrenula thailandicoides* M.Z. Dou & Z.F. Jia**
14 Terminal locules all directly against the exospore wall **15**
– Terminal locules mostly (at least in mature ascospores) separated from the exospore wall by endospore thickening **19**
15 Thallus UV+ yellow ..... ***Pyrenula pseudobufonia* (Rehm) R.C. Harris**
– Thallus UV **16**
16 Hamathecium inspersed **17**
– Hamathecium not inspersed ..... ***Pyrenula nitidula* (Bres.) R.C. Harris**
17 Ascospores all < 16 µm long ..... ***Pyrenula cayennensis* Müll. Arg.**
– Ascospores partly > 16 µm long **18**
18 Hamathecium inspersed only in the upper part .. ***Pyrenula acutalis* R.C. Harris**
– Hamathecium totally inspersed ... ***Pyrenula fetivica* (Krempelh.) Müll. Arg**
19 Hamathecium inspersed **20**
– Hamathecium not inspersed **24**
20 Central ascospore locules elongated ..... ***Pyrenula subelliptica* (Tuck.) R.C. Harris**
– Central ascospore locules transversely lenticular to rounded **21**
– Ascomata mostly < 0·7 mm diam; ascospores 18–20 µm long; thallus and ascomata without any anthraquinone ..... ***Pyrenula subglabrata* (Nyl.) Müll. Arg.**
– Ascomata mostly > 0·7 mm diam **22**
22 Ascospores mostly 10–20 µm long ..... ***Pyrenula mamillana* (Ach.) Trevis.**
– Ascospores mostly > 20 µm long **23**
23 Ascospores rounded, uniseriate in the ascus ..... ***Pyrenula massariospora* (Starb.) R.C. Harris**
– Ascospores at least at one end pointed, biseriate in the ascus ..... ***Pyrenula acutalis* R.C. Harris**
24 Thallus UV+yellow ..... ***Pyrenula dermatodes* (Borrer) Schaer**
– Thallus UV− or greenish/whitish reflecting **25**
25 Ascospores mostly > 25 µm long **26**
– Ascospores mostly < 25 µm long **30**
26 Ascospores 36–45 µm long, without black granules at the tips ..... ***Pyrenula subducta* (Nyl.) Müll. Arg.**
– Ascospores < 40 µm long, without black granules at the tips **27**
27 Ascomata mostly > 0·7 mm diam ..... ***Pyrenula complanata* (Mont.) Trevis.**
– Ascomata mostly < 0·7 mm diam **28**

28 Ascospores 32–42 µm long ..... ***Pyrenula punctella* (Nyl.) Trevis.**
– Ascospores mostly 25–37 µm long..... **29**
29 Central locules much wider than long, ascomata conical, emergent, thallus without pseudocyphellae..... ***Pyrenula mastophora* (Nyl.) Müll. Arg.**
– Central locules more or less rounded, ascomata somewhat rounded, often partly immersed in the thallus, thallus often with pseudocyphellae..... ..... ***Pyrenula quassiaecola* (Fée) Fée**
30 Ascospores mostly 21–25 µm long..... **31**
– Ascospores mostly < 21 µm long..... **34**
31 Ascomata with red, KOH+ purple crystals inside; ascomata > 0·5 mm diam ..... ***Pyrenula nitida* (Weigel) Ach.**
– Ascomata without red crystals..... **32**
32 Ascospores with angular diamond-shaped locules..... ..... ***Pyrenula micheneri* R.C. Harris**
– Ascospores with rounded or quadrangular locules **33**
33 Ascospores with at least one pointed end .... ***Pyrenula acutispora* Kalb & Hafellner**
– Ascospores with rounded ends..... ..... ***Pyrenula submastophora* Ajay Singh & Upreti**
34 Ascospores mostly < 15 µm long..... **35**
– Ascospores mostly > 15 µm long..... **36**
35 Ascospores 6–8 µm wide..... ***Pyrenula brunnea* Fée**
– Ascospores 4–6 µm wide..... ***Pyrenula aspistea* (Ach.) Ach**
36 Ascomata > 0·7 mm diam ..... ***Pyrenula scutata* (Stirt.) Zahlbr.**
– Ascomata < 0·7 mm diam..... **37**
37 Ascospores with dark bands between the locules .... ***Pyrenula confoederata* R.C. Harris**
– Ascospores without dark bands..... ***Pyrenula aggregata* (Fée) Fée**

Additional information

Conflict of interest

The authors have declared that no competing interests exist.

Ethical statement

No ethical statement was reported.

Funding

This research was supported by the National Natural Science Foundation of China (No. 32300005).

Author contributions

M.-Z.D. conceived and designed the study. M.-Z.D. and J.-C.L. generated the DNA sequence data. M.-Z.D., Y.-S.H., J.-C.L. and A.A. performed the phenotypic assessment of the material. M.-Z.D., Z.-F.J. and A.A. analyzed the data. M.-Z.D. and Z.-F.J. checked issues related to nomenclatural articles. M.-Z.D. wrote the manuscript draft. M.-Z.D., Z.-F.J. and A.A. revised the manuscript. All authors have read and agreed to the published version of the manuscript.

Author ORCIDs

Mingzhu Dou https://orcid.org/0000-0001-5160-1517
Jiechen Li https://orcid.org/0009-0001-8819-8407
Yongshun Hu https://orcid.org/0009-0002-6764-4364
André Aptroot https://orcid.org/0000-0001-7949-2594

Data availability

Publicly available datasets were analyzed in this study. All resulting alignments were deposited in TreeBASE (http://purl.org/phylo/treebase/phylows/study/TB2:S31341). All newly generated sequences were deposited in GenBank (https://www.ncbi.nlm.nih.gov/genbank/ (accessed on 31 December 2025). All new taxa were deposited in MycoBank (https://www.mycobank.org/ (accessed on 30 June 2025)).

References

Acharius E (1814) Synopsis methodica lichenum. Litteris et sumptibus Svanborg et soc., Lund.

Aptroot A (2003) Pyrenocarpous lichens and related non-lichenized ascomycetes from Taiwan. The Journal of the Hattori Botanical Laboratory 93: 155–173.

Aptroot A (2009) Pyrenulaceae. Fl. Australia 57: 449–480. https://www.anbg.gov.au/abrs/lichenlist/VOLUME%2057/Pyrenula%20macularis_d.html

Aptroot A (2012) A world key to the species of *Anthracothecium* and *Pyrenula*. Lichenologist (London, England) 44(1): 5–53. https://doi.org/10.1017/S0024282911000624

Aptroot A (2021) World key to the species of Pyrenulaceae and Trypetheliaceae. Archive for lichenology 29: 1–91.

Aptroot A, Seaward MRD (1999) Annotated checklist of Hongkong lichens. Bryophyte Diversity and Evolution 17(1): 57–101. https://doi.org/10.11646/bde.17.1.12

Aptroot A, Lücking R, Sipman HJM, Umaña L, Chaves JL (2008) Pyrenocarpous Lichens with Bitunicate Asci. Bibliotheca Lichenologica 97: 1–162.

Aptroot A, Schumm F, Cáceres MES (2012) Six new species of *Pyrenula* from the tropics. Lichenologist (London, England) 44(5): 611–618. https://doi.org/10.1017/S0024282912000254

Aptroot A, Sipman HJM, Cáceres MEDS (2013) Twenty-one new species of *Pyrenula* from south America, with a note on over-mature ascospores. Lichenologist (London, England) 45(2): 169–198. https://doi.org/10.1017/S0024282912000734

Aptroot A, Sipman HJM, Mercado Diaz JA, Mendonça CDO, Feuerstein SC, Cunha-Dias IPR, Pereira TA, Cáceres MEDS (2018) Eight new species of Pyrenulaceae from the neotropics, with a key to 3-septate *Pyrgillus* species. Lichenologist (London, England) 50(1): 77–87. https://doi.org/10.1017/S0024282917000573

Dou MZ, Wu XH, Li M, Zhao X, Jia ZF (2018) *Gyalecta caudiospora* sp. nov. from China. Mycotaxon 133(4): 721–727. https://doi.org/10.5248/133.721

Dou MZ, Liu SN, Li JC, Aptroot A, Jia ZF (2024) Three new *Pyrenula* species with 3-septate ascospores with red orange oil when over-mature (Ascomycota, Pyrenulales, Pyrenulaceae) from China. MycoKeys 102: 107–125. https://doi.org/10.3897/mycokeys.102.113619

Fu JM, Wang ZL, Wang CX, Zhang LL (2018) New records of six *Pyrenula* species from China. Mycotaxon 133(3): 473–480. https://doi.org/10.5248/133.473

Fu JM, Aptroot A, Wang ZL, Zhang LL (2019) Four *Pyrenula* species new to China. Mycotaxon 134(1): 155–160. https://doi.org/10.5248/134.155

Gardes M, Bruns TD (1993) ITS primers with enhanced specificity for Basidiomycetes – application to the identification of mycorrhiza and rusts. Molecular Ecology 2(2): 113–118. https://doi.org/10.1111/j.1365-294X.1993.tb00005.x

Geiser DM, Gueidan C, Miadlikowska J, Lutzoni F, Kauff F, Hofstetter V, Fraker E, Schoch C, Tibell L, Untereiner WA, Aptroot A (2006) Eurotiomycetes: Eurotiomycetidae and Chaetothyriomycetidae. Mycologia 98(6): 1054–1065. https://doi.org/10.1080/15572536.2006.11832633

Gueidan C, Aptroot A, Cáceres MES, Binh NQ (2016) Molecular phylogeny of the tropical lichen family Pyrenulaceae: Contribution from dried herbarium specimens and FTA card samples. Mycological Progress 15(1): 1–21. https://doi.org/10.1007/s11557-015-1154-8

Harris RC (1989) A sketch of the family Pyrenulaceae in eastern north America. Memoirs of the New York Botanical Garden 49: 74–107.

Ingle KK, Uppadhyay V, Nayaka S, Trivedi S, Sahoo D (2018) New records and an updated key of *Pyrenula* from India. Cryptogam Biodiversity and Assessment 2456-0251: 37–46. https://doi.org/10.21756/cab.esp7

Katoh K, Standley DM (2013) MAFFT multiple sequence alignment software version 7: Improvements in performance and usability. Molecular Biology and Evolution 30(4): 772–780. https://doi.org/10.1093/molbev/mst010

Lanfear R, Frandsen PB, Wright AM, Senfeld T, Calcott B (2017) PartitionFinder 2: New methods for selecting partitioned models of evolution for molecular and morphological phylogenetic analyses. Molecular Biology and Evolution 34(3): 772–773. https://doi.org/10.1093/molbev/msw260

Li JC, Dou MZ, Jia ZF (2024) Two new records of the genus *Pyrenula* (Pyrenulaceae) from China. Journal of Liaocheng University (Natural Science Edition). https://doi.org/10.19728/j.issn1672-6634.2024050002

Lücking R, Leavitt SD, Hawksworth DL (2021) Species in lichen-forming fungi: Balancing between conceptual and practical considerations, and between phenotype and phylogenomics. Fungal Diversity 109(1): 99–154. https://doi.org/10.1007/s13225-021-00477-7

Lücking R, Álvaro-Alba WR, Moncada B, Marín-Canchala NL, Tunjano SS, Cárdenas-López D (2023) Lichens from the Colombian Amazon: 666 taxa including 28 new species and 157 new country records document an extraordinary diversity. The Bryologist 126(2): 242–303. https://doi.org/10.1639/0007-2745-126.2.242

Lutzoni F, Pagel M, Reeb V (2001) Major fungal lineages are derived from lichen symbiotic ancestors. Nature 411(6840): 937–940. https://doi.org/10.1038/35082053

Mangold A, Martín MP, Lücking R, Lumbsch HT (2008) Molecular phylogeny suggests synonymy of Thelotremataceae within Graphidaceae (Ascomycota: Ostropales). Taxon 57(2): 476–486. https://doi.org/10.1017/S0024282908007366

Mason-Gamer R, Kellogg E (1996) Testing for phylogenetic conflict among molecular datasets in the tribe Triticeae (Graminae). Systematic Biology 45(4): 524–545. https://doi.org/10.1093/sysbio/45.4.524

Mccarthy PM (2000) The lichens of Rarotonga, Cook Islands, South Pacific Ocean I: Pyrenocarpous taxa. Lichenologist (London, England) 32(1): 15–47. https://doi.org/10.1006/lich.1999.0212

Mendonça CDO, Aptroot A, Cáceres MEDS (2016) Six new species of the lichen genus *Pyrenula* (Pyrenulaceae) from northeast Brazil. Phytotaxa 286(3): 169. https://doi.org/10.11646/phytotaxa.286.3.4

Miranda-González R, Bungartz F, Lücking R, Gaya E, de Oliveira Mendonça C, Viñas-Portilla C, da Silva Cáceres ME, de los Angeles Herrera-Campos M (2022) Phylogeny of the *Pyrenula* ochraceoflava group (Pyrenulaceae) reveals near-cryptic diversification and the inclusion of the Mazaediothecium album aggregate. The Bryologist 125(4): 541–557. https://doi.org/10.1639/0007-2745-125.4.541

Mishra GK, Nayaka S, Upreti DK, Bajpai R (2022) *Pyrenula* awasthii sp. nov., containing lichexanthone and anthraquinone from India. Cryptogam Biodiversity and Assessment 6(01): 14–16.

Müller J (1885) Lichenologische Beiträge XXI. Flora(Regensburg) 68: 331–342.

Orange A, James PW, White FJ (2010) Microchemical methods for the identification of lichens. British Lichen Society, London, 101 pp. https://doi.org/10.1006/lich.2002.0376

Ronquist F, Teslenko M, van der Mark P, Ayres DL, Darling A, Hohna S, Larget B, Liu L, Suchard MA, Huelsenbeck JP (2012) MrBayes 3.2: Efficient Bayesian phylogenetic inference and model choice across a large model space. Systematic Biology 61(3): 539–542. https://doi.org/10.1093/sysbio/sys029

Sipman HJM (2023) Four new *Pyrenula* species from primary forests in the Guianas, South America, and their ascospore development. Folia Cryptogamica Estonica 60: 65–74. https://doi.org/10.12697/fce.2023.60.09

Soto-Medina EA, Aptroot A, Lücking R (2023) New species of lichen for Colombia tropical dry forest. Cryptogamie. Mycologie 44(7): 103–107. https://doi.org/10.5252/cryptogamie-mycologie2023v44a7

Stamatakis A (2014) RAxML version 8: A tool for phylogenetic analysis and post-analysis of large phylogenies. Bioinformatics (Oxford, England) 30(9): 1312–1313. https://doi.org/10.1093/bioinformatics/btu033

Vilgalys R, Hester M (1990) Rapid genetic identification and mapping of enzymatically amplifed ribosomal DNA from several cryptococcus species. Journal of Bacteriology 172(8): 4238–4246. https://doi.org/10.1128/jb.172.8.4238-4246.1990

Wang ZL, Yan SK, Tang R, Sun MJ, Zhang LL (2018) New records of Lepraria and *Pyrenula* from China. Mycotaxon 133(1): 89–96. https://doi.org/10.5248/133.89

Weerakoon G, Aptroot A, Lumbsch HT, Wolseley PA, Wijeyaratne SC, Gueidan C (2012) New molecular data on Pyrenulaceae from Sri Lanka reveal two well-supported groups within this family. Lichenologist (London, England) 44(5): 639–647. https://doi.org/10.1017/S0024282912000333

Wei JC (2020) The enumeration of lichenized fungi in China. China Forestry Publishing House, Beijing, 606 pp.

White T, Bruns T, Lee S, Taylor J (1990) Amplification and direct sequencing of fungal ribosomal RNA genes for phylogenetics. In: Innis MA, Gelfand DH, Snisky JJ, White TJ (Eds) PCR Protocols: a guide to methods and applications. Academic Press, New York, 315–322. https://doi.org/10.1016/B978-0-12-372180-8.50042-1

Xie CM, Zhao ZT, Cheng PF, Zhang LL (2021) Additional species of *Pyrenula* (Pyrenulaceae) from China. Herzogia 34(1): 93–100. https://doi.org/10.13158/heia.34.1.2021.93

Zahlbruckner A (1930) New species of lichens from Porto Rico. Mycologia 22(2): 69–79. https://doi.org/10.1080/00275514.1930.12016983

Zhang D, Gao FL, Jakovli I, Zou H, Wang GT (2020) Phylosuite: An integrated and scalable desktop platform for streamlined molecular sequence data management and evolutionary phylogenetics studies. Molecular Ecology Resources 20(1): 348–355. https://doi.org/10.1111/1755-0998.13096

Zhang Q, Qin XM, Lu YB, Li PW, Huang XY (2023) A comprehensive alignment-filtering methodology improves phylogeny particularly by filtering overly divergent segments. BioRxiv. https://doi.org/10.1101/2023.12.26.573321

Zhu H (2017) The tropical forests of southern China and conservation of biodiversity. Botanical Review 83(1): 87–105. https://doi.org/10.1007/s12229-017-9177-2

Zoller S, Scheidegger C, Sperisen C (1999) PCR primers for the amplification of mitochondrial small subunit ribosomal DNA of lichen-forming ascomycetes. Lichenologist (London, England) 31(5): 511–516. https://doi.org/10.1006/lich.1999.0220

Supplementary material 1

Information for the sequences download from NCBI used in this study

Authors: Mingzhu Dou

Data type: docx

Link: https://doi.org/10.3897/mycokeys.110.131741.suppl1

Supplementary material 2

Phylogenetic tree constructed through ML analyses based on mtSSU, ITS, and nuLSU for *Pyrenula*

Authors: Mingzhu Dou

Data type: pdf

Explanation note: *Cyphellophora europaea* and *Endocarpon pusillum* are the out-group taxa. Only significant values (higher than 70% BS) are shown.

Link: https://doi.org/10.3897/mycokeys.110.131741.suppl2

Supplementary material 3

TLC test using C solvent system

Authors: Mingzhu Dou

Data type: jpg

Explanation note: **a**: fresh plate under 254 nm ultraviolet light; **b**: charring plate under daylight; **c**: charring plate under 365 nm ultraviolet light. 0: standard substance (*Lethariella cladonioides*, norstictic acid at Rf four and atranorin at Rf seven). 1: Bark without thallus of HN18017; 2: HN18017 (*Pyrenula macularis*); 3: HN18018 (*P. macularis*). 4: Bark without thallus of FJ211750; 5: FJ211750 (*P. submacularis*); 6: FJ220211 (*P. submacularis*). 7: Bark without thallus of GZ18096; 8: GZ18096 (*P. yunguiensis*); 9: Other taxon; 10. Bark without thallus of YN221461; 11. YN221461 (*P. yunguiensis*). 12: Bark without thallus of GZ18377; 13: GZ18377 (*P. rufotetraspora*). 14: Bark without thallus of GD19285; 15: GD19285 (*P. breutelii*); 16: GD19286 (*P. breutelii*).

Link: https://doi.org/10.3897/mycokeys.110.131741.suppl3

Supplementary material 4

TLC test using C solvent system

Authors: Mingzhu Dou

Data type: jpg

Explanation note: **a**: fresh plate under 254 nm ultraviolet light; **b**: charring plate under daylight; **c**: charring plate under 365 nm ultraviolet light. The spots visible in 254 nm UV on the fresh plate are marked with pencil. 0: standard substance (*Lethariella cladonioides*, norstictic acid at Rf four and atranorin at Rf seven). 1: Bark without thallus of GD19285; 2: GD19285 (*Pyrenula breutelii*); 3: GD19286 (*P. breutelii*). 4: Bark without thallus of HNX18017; 5: HNX18017 (*P. macularis*); 6: HNX18018 (*P. macularis*). 7: Bark without thallus of FJ211750; 8: FJ211750 (*P. submacularis*); 9: Bark without thallus of FJ220211; 10: FJ220211 (*P. submacularis*). 11: Bark without thallus of GZ18096; 12: GZ18096 (*P. yunguiensis*); 13. Bark without thallus of YN221461; 14. YN221461 (*P. yunguiensis*). 15: Bark without thallus of GZ18377; 13: GZ18377 (*P. rufotetraspora*).

Link: https://doi.org/10.3897/mycokeys.110.131741.suppl4

Supplementary material 5

TLC test using C solvent system

Authors: Mingzhu Dou

Data type: jpg

Explanation note: a: fresh plate under 254 nm ultraviolet light; b: charring plate under daylight; c: charring plate under 365 nm ultraviolet light. 0: standard substance (*Lethariella cladonioides*, norstictic acid at Rf four and atranorin at Rf seven). a: 1: ZJ240446 (*Malmidea* sp.); 2: ZJ240088 (*Allographa* sp.); 3: ZJ240057 (*Phyllobaeis* sp.); 4: ZJ240058 (*Phyllobaeis* sp.); 5: ZJ240059 (*Phyllobaeis* sp.); 6: ZJ240060 (*Pyrrhospora* sp.); 7: ZJ240084 (*Allographa* sp.); 8: ZJ240097 (*Pyrrhospora.* sp.); 9: ZJ240098 (*Pyrrhospora* sp.); 10: ZJ240205 (*Pyrrhospora.* sp.); 11: ZJ240253 (*Allographa* sp.); 12: ZJ240318 (*Allographa* sp.); 13. ZJ240323 (*Allographa* sp.); 14. ZJ240478 (*Phyrrospora* sp.); 15: HN19676 (*Pyrenula* sp.); 13: HN19701 (*Pyrenula* sp.).

Link: https://doi.org/10.3897/mycokeys.110.131741.suppl5

Supplementary material 6

TLC test using C solvent system, charring plate under 365 nm ultraviolet light

Authors: Mingzhu Dou

Data type: jpg

Explanation note: 1: ZJ240681 (*Allographa* sp.); 2: ZJ240697 (*Graphis* sp.); 3: ZJ240679 (*Graphis* sp.); 4: ZJ240680 (*Graphis* sp.); 5: ZJ240691 (*Graphis* sp.); 6: ZJ240694 (*Graphis* sp.); 7: ZJ240528 (*Coenogonium* sp.); 8: ZJ232073 (*Thelotrema* sp.); 9: ZJ240421 (*Ocellularia* sp.); 10: ZJ240226 (*Platythecium* sp.); 11: ZJ240334 (*Coenogonium* sp.); 12: ZJ240325 (*Coenogonium* sp.); 13. FJ231826 (*Phyllobaeis* sp.); 14. HNX241177 (*Coenogonium* sp.).

Link: https://doi.org/10.3897/mycokeys.110.131741.suppl6

MycoKeys 110: 185–210 (2024)
DOI: 10.3897/mycokeys.110.134132

Research Article

Interesting mycoparasites and *Paradingleyomyces lepidopterorum* gen. et sp. nov. (Hypocreales, Polycephalomycetaceae) from Yunnan Province, China

Yi Wang[1,2,3], De-Ping Wei[2,3], Xing-Can Peng[2,3,4,5], Ji-Chuan Kang[1,2,3], Zeng-Zhi Li[6], Chun-Ru Li[6], Xian Zhang[2,3,4,5], Gui-Ying Wang[1,2,3], Yun Zhou[1,2,3], Xin-Sheng He[7], Putarak Chomnunti[5], Ting-Chi Wen[1,2,3,7]

1 *School of Pharmacy, Guizhou University, Guiyang 550025, Guizhou, China*
2 *State Key Laboratory of Green Pesticide, Key Laboratory of Green Pesticide and Agricultural Bioengineering, Ministry of Education, Guizhou University, Guiyang 550025, China*
3 *Engineering Research Center of Southwest Bio-Pharmaceutical Resources, Ministry of Education, Guizhou University, Guiyang 550025, China*
4 *Center of Excellence in Fungal Research, Mae Fah Luang University, Chiang Rai 57100, Thailand*
5 *School of Science, Mae Fah Luang University, Chiang Rai 57100, Thailand*
6 *Zhejiang BioAsia Life Science Institute, Pinghu 314200, China*
7 *School of Life Science and Engineering, Southwest University of Science and Technology, Mianyang 621010, China*
Corresponding authors: Ting-Chi Wen (tingchiwen@yahoo.com); Putarak Chomnunti (putarak.cho@mfu.ac.th)

Abstract

A novel genus, *Paradingleyomyces* was introduced to accommodate *Pa. lepidopterorum* **sp. nov.**, based on a multigene phylogenetic analysis and its distinct morphological characteristics. Maximum likelihood (ML) and Bayesian inference analyses (BI) of ITS, SSU, LSU, *tef-1α*, *rpb1*, and *rpb2* sequence data shown that *Pa. lepidopterorum* formed an independent lineage nested between *Perennicordyceps* and *Dingleyomyces*. Morphologically, *Paradingleyomyces* is distinguished from *Perennicordyceps* by the presence of a white subiculum on the stromata of *Ophiocordyceps* cf. *cochlidiicola*. Perithecia are produced sporadically from the base to the apex of the stromata, and the secondary ascospores exhibit a notable length-to-width ratio. These characteristics distinguish *Paradingleyomyces* from *Perennicordyceps* which exhibits tortuous, branched, clavate to cylindrical stromata with rhizomorphs, parasitism of coleopteran and hemipteran larvae, and colonizes a broader range of fungal hosts. Additionally, perithecia in *Perennicordyceps* typically arise from the middle to the upper regions of the stromata, with secondary ascospores displaying a comparatively lower length-to-width ratio. *Paradingleyomyces* is morphologically identical to *Dingleyomyces* in its direct production of superficial perithecia on the stromata of *Ophiocordyceps* species. However, the phylogenetic analysis indicates that *Paradingleyomyces* and *Dingleyomyces* are not congeneric. Moreover, this study introduces another novel species, *Polycephalomyces tengchongensis*, and a novel sexual morph of *Pleurocordyceps yunnanensis*. Dimorphic phialides and conidia of *Pleurocordyceps parvicapitata* were observed and described for the first time based on a fresh collection from Tengchong County, Yunnan Province, China.

Key words: Entomopathogenic fungi, new genus, phylogeny, taxonomy

OPEN ACCESS

Academic editor: Nattawut Boonyuen
Received: 7 August 2024
Accepted: 23 October 2024
Published: 15 November 2024

Citation: Wang Y, Wei D-P, Peng X-C, Kang J-C, Li Z-Z, Li C-R, Zhang X, Wang G-Y, Zhou Y, He X-S, Chomnunti P, Wen T-C (2024) Interesting mycoparasites and *Paradingleyomyces lepidopterorum* gen. et sp. nov. (Hypocreales, Polycephalomycetaceae) from Yunnan Province, China. MycoKeys 110: 185–210. https://doi.org/10.3897/mycokeys.110.134132

Introduction

Polycephalomyces was introduced as an entomopathogenic genus by Kobayasi (1941), based on the asexual morph of the *Po. formosus*, which was characterized by polycephalous synnemata with white to pale yellow conidial masses on the tips. Species of *Polycephalomyces* form parasitic associations with a wide range of hosts, including insects, fungi and myxomycetes (Shrestha et al. 2017; Xiao et al. 2023). Among these, *Ophiocordyceps* species are the most common hosts to *Polycephalomyces*. For instance, *Polycephalomyces sinensis* was found as a hyperparasite on *Ophiocordyceps sinensis*, *Po. ramosus* on *Hirsutella guignardii* and *Pleurocordyceps lianzhouensis* on *O. crinalis* (Massee 1895; Kobayasi 1941; Kepler et al. 2013; Wang et al. 2014). Members of *Polycephalomyces* were expanded to include sexual species that were phylogenetically distant from the *Ophiocordyceps* sensu stricto by Kepler et al. (2013). In this study, the sexual morph of *Polycephalomyces* was described as possessing firm, pliant, multifurcating stromata, perithecia that are either superficial or immersed in an apical or subapical pulvinate cushion, filiform asci and disarticulating ascospores. The taxonomic placement of *Polycephalomyces* remained uncertain until Quandt et al. (2014) classified it within the family Ophiocordycipitaceae based on phylogenetic analyses of combining SSU, LSU, *tef-1α*, *rpb1* and *rpb2* sequence. *Perennicordyceps* was later established by Matočec et al. (2014) to accommodate four species (*Perennicordyceps cuboidea*, *Pe. paracuboidea*, *Pe. prolifica*, and *Pe. ryogamiensis*), which were previously classified under *Polycephalomyces*, based on comprehensive morphological characteristics and molecular data analyses. *Perennicordyceps* is characterized by the presence of superficial perithecia and acremonium-like or hirsutella-like asexual morphs (Matočec et al. 2014; Hyde et al. 2018; Wei et al. 2022). Wang et al. (2021) established *Pleurocordyceps* to accommodate ten species that previously were placed in *Polycephalomyces*. An increasing number of polycephalomyces-like species have been added to *Polycephalomyces*, *Perennicordyceps*, and *Pleurocordyceps*, contributing to a more refined understanding of their natural classification and phylogenetic relationships (Wang et al. 2014; Wang et al. 2015a, 2015b; Liang et al. 2016; Crous et al. 2017a; Xiao et al. 2018, 2023; Yang et al. 2020). Xiao et al. (2023) constructed a backbone tree of Hypocreales using extensive taxon sampling, and the result clearly showed that *Polycephalomyces*, *Perennicordyceps*, and *Pleurocordyceps* form a monophyletic clade distinct from Ophiocordycipitaceae. As a result, a new family, Polycephalomycetaceae, was established to accommodate these three genera. It is worth noting that in the phylogenetic analysis conducted by Xiao et al. (2023), Polycephalomycetaceae was identified as a sister clade with Ophiocordycipitaceae. However, in the study conducted by Wei et al. (2022), Polycephalomycetaceae was found to form a sister clade to Clavicipitaceae. These contrasting findings suggest that the phylogenetic relationship between Polycephalomycetaceae and other hypocrealean families requires further confirmation through future research, incorporating more comprehensive taxon sampling. Therefore, discovering hidden or yet unknown species within Polycephalomycetaceae is essential for improving our understanding of this family's evolutionary position.

During our ongoing exploration of the diversity of entomopathogenic fungi and their associated fungi in Yunnan Province, China, several polycephalomyces-like species were found from various hosts including *Elaphomyces* sp., lepidopteran

larvae, *Ophiocordyceps nutans*, and *Perennicordyceps* cf. *elaphomyceticola*. This study aims to assess the phylogenetic relationships of these samples with existing species of Polycephalomycetaceae using a concatenated SSU, ITS, LSU, *tef-1α*, *rpb1* and *rpb2* sequences, as well as detailed morphological analyses. The morphological observations and phylogenetic analyses allowed us to introduce a new genus, *Paradingleyomyces*, a new species, *Polycephalomyces tengchongensis*, a new sexual morph of *Pleurocordyceps yunnanensis*, and a new collection of *Pleurocordyceps parvicapitata*. These findings expand our understanding of this unique group of entomopathogens and mycoparasites, offering fresh and novel insights into their morphology, ecology and evolutionary relationships.

Materials and methods

Morphological study and isolation

To explore the diversity of fungal resources, samples were collected from tropical and subtropical forests rich in evergreen trees diversity in southwestern China. Morphological studies followed the guidelines proposed by Senanayake et al. (2020). Specimens were placed in small plastic boxes and transported to the laboratory for isolation. Both specimens and colonies were photographed using a Canon 6D camera equipped with a 100 mm MACRO lens for detailed morphological documentation. Fruiting bodies were examined, and free-hand sections were prepared using a stereomicroscope (Leica S9E). Slides containing sectioning of the fertile parts were mounted for microscopic observation with a Leica DM2500 compound microscope equipped with a digital camera. Micro-morphological characters, including ascomata, perithecia, peridium texture, asci, ascospores, secondary ascospores, conidiophores, phialides, and conidia were photographed and measured by using the Leica microsystem for precise documentation and analysis. A small mass of tissue from the fertile parts of the fungus or insect bodies was transferred to potato glucose agar (PDA) plate using sterile inoculation needles and incubated at 25 °C to obtain pure isolates (Wen et al. 2014; Aini et al. 2020; Peng et al. 2024). Freshly collected specimens were dried using silica gel to preserve them as dry specimens. The cultures were deposited in the Herbarium of Kunming Institute of Botany Culture Collection (KUNCC; http://english.kib.cas.cn/) and the dry specimens were deposited in the Herbarium of Cryptogams, Kunming Institute of Botany of the Chinese Academy of Sciences (KUN; http://kun.kingdonia.org/).

DNA extraction, PCR amplification and sequencing

DNA was extracted from fresh specimens and cultures using the E.Z.N.A.™ Fungal DNA MiniKit (Omega Biotech, CA, USA) following the manufacturer's protocols. Polymerase chain reaction (PCR) was performed to amplify six loci: the small subunits nuclear of rDNA (SSU), the internal transcribed spacer (ITS), the large subunit nuclear of rDNA (LSU), the transcription elongation factor-1α (*tef-1α*), the partial RNA polymerase II largest subunit (*rpb1*) and the partial RNA polymerase II second largest subunit (*rpb2*). The primer pairs used for amplifying the six loci were as follows: NS1 and NS4 for SSU (White et al. 1990), ITS5 and ITS4 for ITS (White et al. 1990), LROR and LR5 for LSU (Vilgalys and Hester 1990), 983F and 2218R for *tef-1α* (Rehner and Buckley 2005), CRPB1A and RPB1Cr for *rpb*1 (Castlebury et al.

2004), and RPB2-5F and RPB2-7R for *rpb2* (Liu et al. 1999). Amplification reaction was performed in a 50 µL reaction volume containing 4 µL of DNA template, 2 µL of each forward and reverse primers (10 pM), 22 µL of 2×*Taq* PCR StarMix with Loading Dye (GenStar) and 20 µL of twice-sterilized water. The amplification conditions for ITS, LSU, SSU, *tef-1α*, *rpb1*, and *rpb2* were as follows: (1) 3 min at 94 °C, (2) 33 cycles of denaturation at 94 °C for 30 s, annealing (ITS at 52 °C for 50 s, SSU at 47 °C for 1 min 20 s, LSU at 50 °C for 30 s, *tef-1α* at 58 °C for 50 s, *rpb1* and *rpb2* at 51 °C for 40 s), and elongation (ITS at 72 °C for 45 s, SSU and LSU at 72 °C for 1min 50 s, *tef-1α* at 72 °C for 1 min, *rpb1* and *rpb2* at 72 °C for 1 min 20 s), and (3) final extension at 72 °C for 10 min. The PCR products were sent to Tsingke Biological Technology in Chongqing, China, for sequencing, and the resulting sequences were submitted to GenBank for the assignment of accession numbers.

Phylogenetic analysis

The newly generated sequences were checked and assembled using BioEdit v.7.0.5.3 (Hall et al. 2011). The assembled sequences were then subjected to BLAST searches in the GenBank database of National Center for Biotechnology Information (NCBI) to confirm their identities. Taxa used for phylogenetic analyses were chosen based on relevant publications and presented in Table 1. The individual gene was aligned using MAFFT (Katoh and Standley 2013). Trimal v1.2 was used to remove alignments sites that did not achieve a user specified gap score of 0.6 (Capella-Gutiérrez et al. 2009). The trimmed alignments were concatenated using FasParser 2.10.0 (Sun 2017). The final combined alignment was subjected to Maximum likelihood (ML) and Bayesian inference (BI) analyses. ML analysis was performed using IQ-TREE 1.6.12, with branch support estimated from 1000 ultrafast bootstraps replicates (Minh et al. 2020).MrModelTest v. 2.3 (Nylander 2004) was used to determine the best evolutionary model for Bayesian inference analysis according to the Akaike Information Standard (AIC). The best-fit models GTR+I+G, were determined for SSU, ITS, LSU, *tef1-α*, *rpb1*, and *rpb2*. The BI analysis was carried out using MrBayes on XSEDE (3.2.7a) through the CIPRES Science Gateway V 3.3 platform (Miller et al. 2010). Four Markov chain Monte Carlo (MCMC) simulations were run for 50,000,000 generations, sampling every 1000 generations and discarding the first 25% as burn-in. The remaining trees were used to calculate Bayesian posterior probabilities. The resulting trees were visualized using FigTree v1.4.3 (Rambaut 2012). To determine whether the taxa represented new species or new records, the guidelines of Jeewon and Hyde (2016) were followed.

Results

Phylogenetic analyses

The phylogenetic analysis was constructed using sequence data from six loci, representing 112 Polycephalomycetaceae taxa. The alignment comprised 5142 base pair (bp) characters, including gaps (1026 bp for SSU, 602 bp for ITS, 845 bp for LSU, 901 bp for *tef-1α*, 711 bp for *rpb1*, and 1057 bp for *rpb2*). Of these, 3648 characters were constant, 1310 variable characters parsimony-uninformative and 1936 characters parsimony-informative. The likelihood of the best-scoring ML tree was -26079.662.

Table 1. Accession numbers of taxa used in this study. Newly generated sequences are indicated in bold. [T] Represents type strain, type specimens or neotype.

Current name	Voucher	SSU	ITS	LSU	*tef-1α*	*rpb1*	*rpb2*	Reference
Dingleyomyces lloydii	PDD1212154[T]	OR647563	OR602634	OR602640	OR588853	OR588860	OR588858	Johnston and Park (2023)
Paradingleyomyces lepidopterorum	**HKAS 131926[T]**	–	**OR878363**	**OR828238**	–	**OR829674**	**OR880683**	**This study**
Paradingleyomyces lepidopterorum	**HKAS 131927**	–	**OR878364**	**OR828239**	**OR880679**	**OR829675**	–	**This study**
Paradingleyomyces lepidopterorum	**HKAS 131921**	–	–	**OR828242**	–	**OR829678**	–	**This study**
Perennicordyceps cuboidea	NBRC 103836	JN941721	JN943332	JN941420	AB972951	JN992455	AB972955	Schoch et al. (2012)
Perennicordyceps cuboidea	NBRC 101740	JN941724	JN943331	JN941417	KF049684	JN992458	–	Schoch et al. (2012)
Perennicordyceps cuboidea	TNS-F-18487	KF049609	–	KF049628	KF049683	–	–	Kepler et al. (2013)
Perennicordyceps cuboidea	NBRC 101739	–	AB378668	AB378649	–	–	–	Ban et al. (2009)
Perennicordyceps elaphomyceticola	NTUCC 17-022	–	MK840824	MK840813	MK839230	MK839221	MK839212	Yang et al. (2020)
Perennicordyceps elaphomyceticola	MFLU 21-0262	OQ172101	OQ172064	OQ172032	OQ459718	OQ459747	OQ459792	Xiao et al. (2023)
Perennicordyceps elaphomyceticola	MFLU 21-0263	OQ172102	OQ172065	OQ172033	OQ459719	OQ459748	OQ459793	Xiao et al. (2023)
Perennicordyceps elaphomyceticola	MFLU 21-0264	OQ172103	OQ172067	OQ172035	OQ459720	OQ459749	OQ459794	Xiao et al. (2023)
Perennicordyceps elaphomyceticola	MFLU 21-0266	OQ172112	OQ172068	OQ172036	OQ459732	OQ459760	OQ459806	Xiao et al. (2023)
Perennicordyceps elaphomyceticola	**KUNCC23-16074**	**PP129613**	**OR878367**	**OR828243**	–	**OR829679**	–	**This study**
Perennicordyceps lutea	KUMCC 3004	–	–	OQ474910	–	–	–	Xiao et al. (2023)
Perennicordyceps paracuboidea	NBRC 100942	JN941711	JN943337	JN941430	AB972954	JN992445	AB972958	Schoch et al. (2012)
Perennicordyceps paracuboidea	NBRC 101742	JN941710	JN943338	JN941431	KF049685	JN992444	KF049669	Schoch et al. (2012)
Perennicordyceps prolifica	NBRC 100744	JN941709	AB925942	JN941432	AB972952	JN992443	AB972956	Ban et al. (2015)
Perennicordyceps prolifica	NBRC 101750	JN941708	JN943340	JN941433	AB972953	JN992442	AB972957	Ban et al. (2015)
Perennicordyceps prolifica	TNS-F-18547	KF049613	KF049660	KF049632	KF049687	KF049649	KF049670	Kepler et al. (2013)
Perennicordyceps prolifica	NBRC 103839	JN941706	JN943342	JN941435	–	JN992440	–	Schoch et al. (2012)
Perennicordyceps prolifica	NBRC 103838	JN941707	JN943339	JN941434	–	JN992441	–	Schoch et al. (2012)
Perennicordyceps prolifica	TNS-F-18481	KF049612	KF049659	KF049631	KF049686	KF049648	–	Kepler et al. (2013)
Perennicordyceps prolifica	–	AB027324	–	AB027370	–	–	–	Nikoh and Fukatsu. (2000)
Perennicordyceps ryogamiensis	NBRC 103842	JN941701	JN943345	JN941440	–	JN992435	–	Schoch et al. (2012)
Perennicordyceps ryogamiensis	NBRC 101751	JN941703	JN943343	JN941438	KF049688	JN992437	–	Schoch et al. (2012)
Pleurocordyceps agarica	YHHPA1305[T]	KP276655	KP276651	–	KP276659	KP276663	KP276667	Wang et al. (2015a, b)
Pleurocordyceps agarica	YHCPA1303	KP276657	KP276653	–	KP276661	KP276665	KP276669	Wang et al. (2015a, b)
Pleurocordyceps agarica	YHCPA1307	KP276658	KP276654	–	KP276662	KP276666	KP276670	Wang et al. (2015a, b)
Pleurocordyceps aurantiacus	MFLUCC 17-2113[T]	MG136904	MG136916	MG136910	MG136874	MG136866	MG136870	Xiao et al. (2018)
Pleurocordyceps aurantiacus	MFLU 17-1393[T]	MG136907	MG136919	MG136913	MG136877	MG136868	MG136873	Xiao et al. (2018)
Pleurocordyceps aurantiacus	MFLU 21-0276	OQ172097	OQ172072	OQ172042	OQ459714	–	OQ459788	Xiao et al. (2023)
Pleurocordyceps aurantiacus	GACP 20-2306	OQ172098	OQ172069	OQ172041	OQ459715	–	OQ459789	Xiao et al. (2023)
Pleurocordyceps formosus	ARSEF 1424	KF049615	KF049661	KF049634	KF049689	KF049651	KF049671	Kepler et al. (2013)
Pleurocordyceps heilongtanensis	KUMCC 3008	OQ172111	OQ172091	OQ172063	OQ459731	OQ459759	OQ459805	Xiao et al. (2023)
Pleurocordyceps kanzashianus	–	AB027325	AB027371	AB027371	–	–	–	Kepler et al. (2013)
Pleurocordyceps lanceolatus	GACP 17-2004[T]	OQ172110	OQ172076	OQ172046	OQ459726	OQ459754	OQ459800	Xiao et al. (2023)
Pleurocordyceps lanceolatus	GACP 17-2005[T]	OQ172109	OQ172077	OQ172047	OQ459727	OQ459755	OQ459801	Xiao et al. (2023)
Pleurocordyceps lianzhouensis	HIMGD20918	KF226245	EU149921	KF226246	KF226248	KF226247	–	Zhang et al. (2007)
Pleurocordyceps lianzhouensis	GIMYY9603	KF226249	EU149922	KF226250	KF226252	KF226251	–	Zhang et al. (2007)
Pleurocordyceps marginaliradians	MFLUCC 17-2276	MG136909	MG136921	MG136915	MG136879	–	MG271930	Xiao et al. (2018)
Pleurocordyceps marginaliradians	MFLU 17-1582	MG136908	MG136920	MG136914	MG136878	MG136869	MG271931	Xiao et al. (2018)

Current name	Voucher	SSU	ITS	LSU	*tef-1α*	*rpb1*	*rpb2*	Reference
Pleurocordyceps nipponicus	BCC 1881	KF049618	–	KF049636	KF049692	–	KF049674	Kepler et al. (2013)
Pleurocordyceps nipponicus	NHJ 4268	KF049621	–	KF049639	KF049695	KF049654	KF049676	Kepler et al. (2013)
Pleurocordyceps nipponicus	BCC 2325	KF049622	KF049665	KF049640	KF049696	KF049655	KF049677	Kepler et al. (2013)
Pleurocordyceps nipponicus	BCC 18108	MF416624	KF049657	MF416569	MF416517	MF416676	MF416462	Kepler et al. (2013)
Pleurocordyceps nipponicus	NBRC 101408	JN941751	JN943303	JN941390	–	JN992485	–	Schoch et al. (2012)
Pleurocordyceps nipponicus	NBRC 101407	JN941752	JN943302	JN941389	–	JN992486	–	Schoch et al. (2012)
Pleurocordyceps nipponicus	NBRC 101406	JN941753	JN943301	JN941388	–	JN992487	–	Schoch et al. (2012)
Pleurocordyceps nipponicus	Cod-RE1202	MG031286	KX827757	MG031248	MG196133	MG196175	–	Sangdee et al. (2017)
Pleurocordyceps nipponicus	BCC 1682	KF049620	KF049664	KF049638	KF049694	–	–	Kepler et al. (2013)
Pleurocordyceps nutansis	MFLU 21-0275^{T}	OQ172119	OQ172073	OQ172048	–	–	–	Xiao et al. (2023)
Pleurocordyceps nutansis	GACP 19-1906	OQ172117	OQ172079	OQ172049	–	–	–	Xiao et al. (2023)
Pleurocordyceps onorei	BRA: CR23902^{T}	–	KU898841	–	–	–	–	Crous et al. (2017a)
Pleurocordyceps onorei	BRA: CR23904	–	KU898843	–	–	–	–	Crous et al. (2017a)
Pleurocordyceps parvicapitata	MFLU 21-0272	OQ172099	OQ172084	OQ172056	OQ459716	OQ459745	OQ459790	Xiao et al. (2023)
Pleurocordyceps parvicapitata	MFLU 21-0273	OQ172100	OQ172085	OQ172057	OQ459717	OQ459746	OQ459791	Xiao et al. (2023)
Pleurocordyceps parvicapitata	MFLU 21-0270	OQ172105	OQ172082	OQ172054	OQ459722	OQ459751	OQ459796	Xiao et al. (2023)
Pleurocordyceps parvicapitata	MFLU 21-0271^{T}	OQ172106	OQ172083	OQ172055	OQ459723	OQ459752	OQ459797	Xiao et al. (2019)
Pleurocordyceps parvicapitata	**HKAS 131924**	**PP129615**	**OR878368**	**OR835990**	**OR880682**	**OR880686**	–	**This study**
Pleurocordyceps parvicapitata	**KUNCC23-16075**	**PP129616**	**OR878369**	**OR835991**	–	**OR880687**	–	**This study**
Pleurocordyceps parvicapitata	**HKAS 131925**	–	**OR878366**	**OR828241**	**OR880680**	**OR829677**	**OR880684**	**This study**
Pleurocordyceps phaothaiensis	BCC84551	–	MF959731	MF959735	MF959739	MF959743	–	Crous et al. (2017a)
Pleurocordyceps phaothaiensis	BCC84552	–	MF959732	MF959736	MF959740	MF959744	–	Crous et al. (2017a)
Pleurocordyceps ramosopulvinatus	SU-65	–	–	DQ118742	DQ118753	DQ127244	–	Chaverri et al. (2005)
Pleurocordyceps ramosopulvinatus	EFCC 5566	–	KF049658	KF049627	KF049682	KF049645	–	Kepler et al. (2013)
Pleurocordyceps ramosopulvinatus	–	AB027326	AB027372	–	–	–	–	Nikoh and Fukatsu (2000)
Pleurocordyceps sinensis	CN 80-2	HQ832887	HQ832884	HQ832886	HQ832890	HQ832888	HQ832889	Wang et al. (2012)
Pleurocordyceps sinensis	GACP 20-2304	OQ172107	OQ172074	OQ172044	OQ459724	–	OQ459798	Xiao et al. (2023)
Pleurocordyceps sinensis	GACP 20-2305	OQ172108	OQ172075	OQ172045	OQ459725	OQ459753	OQ459799	Xiao et al. (2023)
Pleurocordyceps sinensis	MFLU 21-0267	OQ172121	OQ172081	OQ172051	OQ459741	OQ459767	OQ459813	Xiao et al. (2023)
Pleurocordyceps sinensis	MFLU 21-0269	OQ172122	OQ172080	OQ172050	OQ459742	OQ459768	OQ459814	Xiao et al. (2023)
Pleurocordyceps sinensis	GACP 19-2301	OQ172124	OQ172078	OQ172053	OQ459744	–	OQ459816	Xiao et al. (2023)
Pleurocordyceps sinensis	GZU 20-0865	OQ172096	OQ172071	OQ172043	OQ459713	–	–	Xiao et al. (2023)
Pleurocordyceps sinensis	HMAS 43720^{T}	NR_119928	NG_042573	–	–	–	–	Wang et al. (2012)
Pleurocordyceps sinensis	CGMCC 3.19069	MH454346	MH459160	–	–	–	–	Sun et al. (2019)
Pleurocordyceps sinensis	–	–	HQ918290	–	–	–	–	Zhu et al. (2010)
Pleurocordyceps sp.	JB07.08.16_08	KF049616	KF049662	KF049635	KF049690	KF049652	KF049672	Kepler et al. (2013)
Pleurocordyceps sp.	JB07.08.17_07b	KF049617	–	–	KF049691	KF049653	KF049673	Kepler et al. (2013)
Pleurocordyceps sp.	BCC 2637	KF049619	KF049663	KF049637	KF049693	–	KF049675	Kepler et al. (2013)
Pleurocordyceps sp.	GIMCC 3.570	JX006097	JX006099	JX006098	JX006100	JX006101	–	Wang et al. (2020)
Pleurocordyceps sp.	NBRC 109990	–	–	AB925968	–	–	–	Wang et al. (2020)
Pleurocordyceps sp.	NBRC 110224	–	AB925931	AB925969	–	–	–	Unpublished
Pleurocordyceps sp.	NBRC 109987	–	AB925947	AB925983	–	–	–	Unpublished
Pleurocordyceps sp.	NBRC 109988	–	AB925948	AB925984	–	–	–	Unpublished
Pleurocordyceps sp.	–	HM135166	HM135164	HM135165	–	–	–	Wang et al. (2020)
Pleurocordyceps sp.	NBRC 110223	–	AB925930	–	–	–	–	Unpublished
Pleurocordyceps vitellina	KUMCC 3006	–	OQ172089	OQ172061	OQ459729	OQ459757	OQ459803	Xiao et al. (2023)
Pleurocordyceps vitellina	KUMCC 3007	–	OQ172090	OQ172062	OQ459730	OQ459758	OQ459804	Xiao et al. (2023)
Pleurocordyceps yunnanensis	YHH PY1006^{T}	–	KF977849	–	KF977851	KF977853	KF977855	Wang et al. (2015a, b)

Current name	Voucher	SSU	ITS	LSU	*tef-1α*	*rpb1*	*rpb2*	Reference
Pleurocordyceps yunnanensis	**HAKS 131922**	**PP129614**	–	**OR828244**	**OR880681**	**OR829680**	–	**This study**
Pleurocordyceps yunnanensis	YHC PY1005	–	KF977848	–	KF977850	KF977852	KF977854	Wang et al. (2015a, b)
Polycephalomyces albiramus	GACP 21-XS08^{T}	OQ172115	OQ172092	OQ172037	OQ459735	OQ459761	OQ459807	Xiao et al. (2023)
Polycephalomyces albiramus	GACPCC 21-XS08^{T}	OQ172116	OQ172093	OQ172038	OQ459736	OQ459762	OQ459808	Xiao et al. (2023)
Polycephalomyces formosus	NBRC 100686	MN586821	MN586830	MN586839	MN598054	MN598045	MN598061	Wang et al. (2020)
Polycephalomyces formosus	NBRC 100687	MN586822	MN586831	MN586840	MN598055	MN598046	MN598062	Wang et al. (2020)
Polycephalomyces formosus	NBRC 103843	MN586823	MN586832	MN586841	MN598056	MN598047	MN598063	Wang et al. (2020)
Polycephalomyces formosus	NBRC 109993^{T}	MN586824	MN586833	MN586842	MN598057	MN598048	MN598064	Wang et al. (2021)
Polycephalomyces formosus	NBRC 109994	MN586825	MN586834	MN586843	MN598058	MN598049	MN598065	Wang et al. (2020)
Polycephalomyces formosus	GACP 21-WFKQ03	OQ172113	OQ172094	OQ172039	–	–	–	Xiao et al. (2023)
Polycephalomyces formosus	GACP 21-WFKQ04	OQ172114	OQ172095	OQ172040	–	–	–	Xiao et al. (2023)
Polycephalomyces ramosus	NBRC 101760	MN586818	MN586827	MN586836	MN598051	MN598042	MN598060	Wang et al. (2020)
Polycephalomyces ramosus	NBRC 109984	MN586819	MN586828	MN586837	MN598052	MN598043	–	Wang et al. (2020)
Polycephalomyces ramosus	NBRC 109985	MN586820	MN586829	MN586838	MN598053	MN598044	–	Wang et al. (2020)
Polycephalomyces ramosus	MFLU 18-0162^{T}	MK863043	MK863250	MK863050	MK860188	–	–	Unpublished
Polycephalomyces ramosus	NBRC 109983	–	AB925946	AB925982	–	–	–	Unpublished
Polycephalomyces ramosus	RUTPP	–	–	AY259543	–	–	–	Bischof et al. (2003)
Polycephalomyces ramosus	RCEF 6016	–	KC782530	–	–	–	–	Crous et al. (2017a)
Polycephalomyces tengchongensis	**HKAS 131923^{T}**	**PP129612**	**OR878365**	**OR828240**	–	**OR829676**	**OR880685**	**This study**
Polycephalomyces tomentosus	BL 4	KF049623	KF049666	KF049641	KF049697	KF049656	KF049678	Kepler et al. (2013)
Tolypocladium ophioglossoides	NBRC 100998	JN941735	JN943319	JN941406	AB968602	JN992469	AB968563	Ban et al. (2015)
Tolypocladium ophioglossoides	NBRC 106330	JN941734	JN943321	JN941407	AB968603	JN992468	AB968564	Ban et al. (2015)

Abbreviations: ARSEF: Agricultural Research Service Entomopathogenic Fungus Collection, USDA, USA; **BCC:** BIOTEC Culture Collection, Klong Luang, Thailand; **EFCC:** Entomopathogenic Fungal Culture Collection, Chuncheon, Korea; **GZUH/GACP:** Herbarium of Guizhou University, China; **GZUIFR:** Institute of Fungal Resources of Guizhou University, China; **HKAS:** Kunming Institute of Botany, Academia Sinica, China; **NBRC:** Biological Resource Center, the National Institute of Technology and Evaluation, Japan; **NHJ:** Nigel Hywel-Jones personal collection, Thailand; **MFLU:** Mae Fah Luang University, Thailand; **KUNCC:** Kunming Institute of Botany Culture Collection, China; **NTUCC:** National Taiwan University Cancer Center, China; **PDD:** Dried specimens have been deposited in the New Zealand Fungarium, New Zealand; **CGMC:** China General Microbiological Culture Collection Center, China; **JB:** Joseph Bischoff, personal collection, Britain; **TNS:** National Museum of Science and Nature, Tsukuba, Japan; **YHH/YHC:** Yunnan Herbal Herbarium, China; **RTUPP:** Rutgers Mycological Herbarium.

In the phylogenetic analyses (Fig. 1), two strains of *Tolypocladium ophioglossoides* (NBRC 100998 and NBRC 106330) were used as outgroup taxa. In the multi-locus phylogenetic tree (Fig. 1), our specimens were distributed across four clades, representing one new genus, one new species and three known species. The strain of *Paradingleyomyces lepidopterorum* (HKAS 131926, HKAS 131927 and HKAS 131921) formed a distinct clade, positioned between *Dingleyomyces* and *Perennicordyceps*, with maximum statistical support (MLBS = 100%, BIPP = 1.00). *Polycephalomyces tengchongensis* (HKAS 131923) branches off from *Polycephalomyces formosus* with significant support (MLBS = 100%, BIPP = 1.00). *Pleurocordyceps yunnanensis* (HKAS 131922) groups with *Pleurocordyceps yunnanensis* (YHH PY1006 and YHC PY1005) with strong support (MLBS = 84%, BIPP = 0.99). *Pleurocordyceps parvicapitata* (HKAS 131924), along with its isolate KUNCC23-16075 and the isolate KUNCC23-16074 (which was isolated from the sclerotium of specimen HKAS 131925) clusters with *Pleurocordyceps parvicapitata* with adequate support (MLBS = 90%, BIPP = 1.00). *Perennicordyceps elaphomyceticola* (HKAS 131925), which represents the host of *Pleurocordyceps parvicapitata* phylogenetically clusters with *Perennicordyceps elaphomyceticola* (MFLU 21-0262, MFLU 21-0263, MFLU 21-0264, MFLU 21-0266, and NTUCC 17-022) with strong support (MLBS = 100%, BIPP = 1.00).

Figure 1. Phylogenetic tree of Polycephalomycetaceae based on a concatenated data matrix of SSU, ITS, LSU, *tef-1a*, *rpb1*, and *rpb2*. Bootstrap values greater than or equal to 75% and Bayesian posterior probabilities greater than or equal to 0.80 are shown at the respective nodes. Newly added taxa from this study are highlighted in red.

Taxonomy

***Paradingleyomyces* Y. Wang tris & T. C. Wen, gen. nov.**
Index Fungorum: IF901540

Etymology. Morphologically resembling the genus *Dingleyomyces*.

Type species. *Paradingleyomyces lepidopterorum* Y. Wang tris & T. C. Wen, sp. nov.

Description. Parasitic on *Ophiocordyceps* cf. *cochlidiicola*. Sexual morph: Stroma absent. ***Perithecia*** forming from white subiculum covering stromata of *Ophiocordyceps* cf. *cochlidiicola*, superficial, scattered, brown, ovoid or ellipsoidal. ***Asci*** cylindrical with a thickened cap, attenuated toward the base. ***Ascospores*** filiform, hyaline, disarticulating into many cylindrical secondary ascospores at maturity. ***Secondary ascospores*** cylindrical, aseptate, smooth-walled, with truncated ends. Asexual morph: Undetermined.

Notes. Both *Paradingleyomyces* and *Dingleyomyces* are monotypic genera and share similar morphological characteristics, including the formation of superficial perithecia on a white subiculum, cylindrical asci with thickened caps, and filiform ascospores that disarticulate into cylindrical secondary ascospores. Additionally, the type species of both genera occur as hyperparasites on *Ophiocordyceps* species (Johnston and Park 2023). However, multigene phylogenetic analysis revealed that these two genera exhibit a paraphyletic relationship, indicating they are not congeneric. *Paradingleyomyces* can be easily distinguished from *Perennicordyceps* by its reduced stromata, whereas *Perennicordyceps* features cylindrical to clavate, branched stromata with prominent rhizomorphs immersed in the substrate, and perithecia forming from the middle to upper parts of the stromata (Ban et al. 2009; Xiao et al. 2019, 2023).

***Paradingleyomyces lepidopterorum* Y. Wang tris & T. C. Wen, sp. nov.**
Index Fungorum: IF901541
Fig. 2

Etymology. This epithet is named after the order of its primary host: Lepidoptera.

Description. Parasitic on *Ophiocordyceps* cf. *cochlidiicola*. ***Stromata*** of host fungus are 55–180 mm in length, 1–3 mm in width, multiple, unbranched, brown at base becoming off-white toward the apex, fibrous, narrowly cylindrical to filiform. Sexual morph: ***Subiculum*** white, cottony, covering the stromata of host fungus. ***Perithecia*** 240–690 × 110–360 µm ($\bar{x}$ = 430 × 228 µm, n = 25), emerging from subiculum, superficial, scattered or dense, flesh-colored, ovoid or ellipsoidal. ***Asci*** 150–400 × 3–8 µm ($\bar{x}$ = 289 × 5 µm, n = 30), cylindrical, hyaline, with an apical cap. ***Apical cap*** 3–5 × 1–4 µm ($\bar{x}$ = 3.8 × 2.3 µm, n = 40), hemispherical. ***Ascospores*** filiform, multiseptate, breaking into many secondary ascospores at maturity. ***Secondary ascospores*** 2–4 × 0.5–1 µm ($\bar{x}$ = 2.5 × 0.9 µm, n = 50), hyaline, aseptate, smooth-walled, cylindrical with truncated ends. Asexual morph: Undetermined.

Distribution. China: Yunnan Province.

Material examined. ***Holotype:*** China • Yunnan Province, Tengchong County, Houqiao Town; 5 Nov. 2022; Collected by Yi Wang; Parasitic on the stromata of

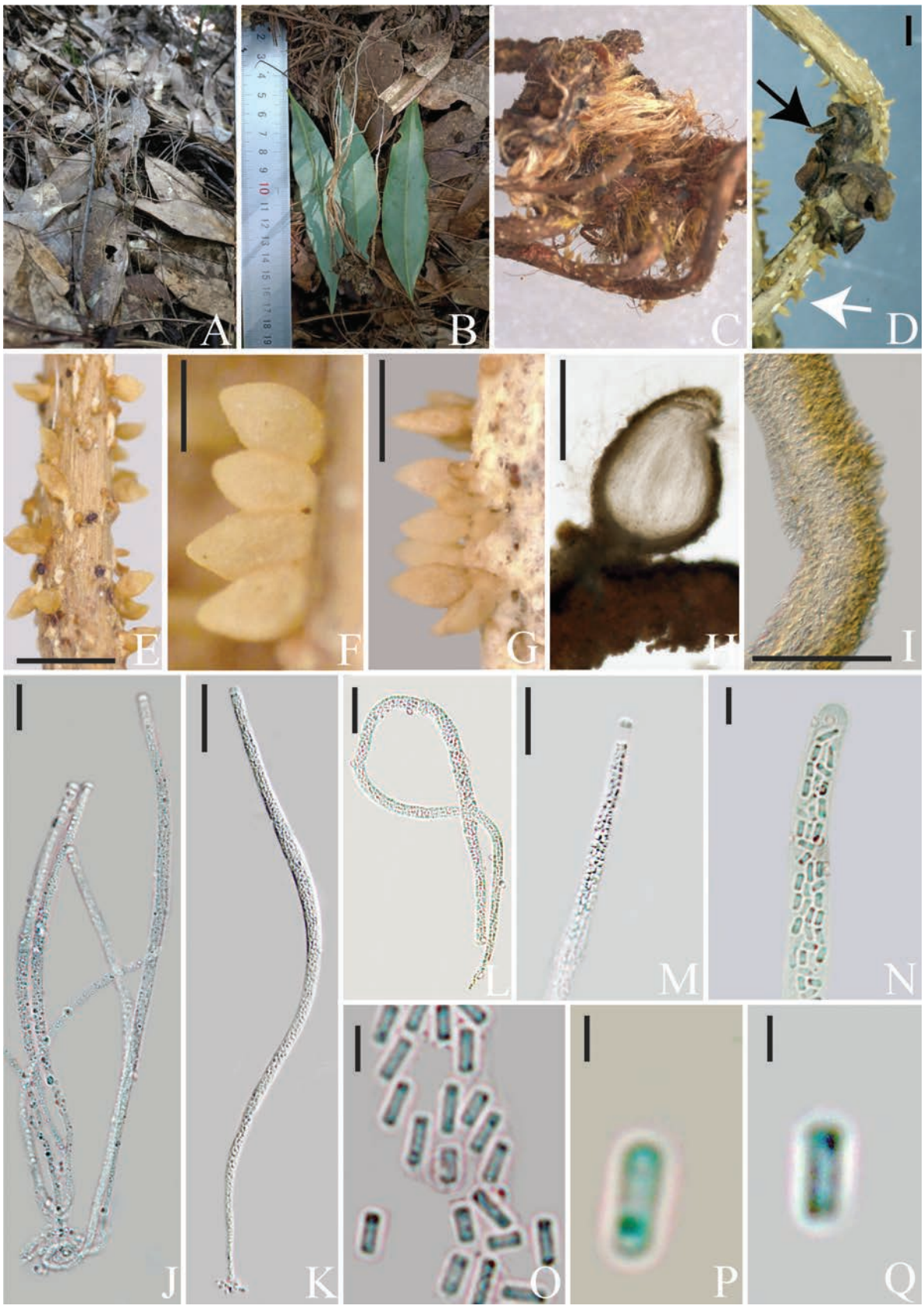

Figure 2. *Paradingleyomyces lepidopterorum* (HKAS 131926, **holotype**) **A** habitat **B** stromata growing from the host **C** host **D** perithecia of *Pa. lepidopterorum* (white arrow) and *Ophiocordyceps* cf. *cochlidiicola* (black arrow) **E–G** perithecia forming on white subiculum **H** vertical section of perithecium. I Peridium **J–L** asci **M, N** apical cap of asci **O–Q** secondary ascospores. Scale bars: 1 mm (**E–G**); 500 µm (**H**); 100 µm (**I**); 50 µm (**J, K**); 25 µm (**L**); 20 µm (**M, N**); 5 µm (**O–Q**).

Perennicordyceps cf. *elaphomyceticola*; GYY543H (HKAS 131926) • ***Paratypes:*** *ibid*; GYY543Z (HKAS131927), TC327 (HKAS 131921).

Notes. *Paradingleyomyces lepidopterorum* lives as a hyperparasite on the remnant stromata of *Ophiocordyceps* cf. *cochlidiicola*. The aging stromata of the host fungus become covered with the perithecia of the hyperparasitic fungus, which closely resemble those of the host. However, the key distinguishing feature is that the hyperparasitic perithecia are flesh-colored and grow on a white subiculum, whereas the host's perithecia are dark brown and directly connected to the stroma (Fig. 2D). *Paradingleyomyces lepidopterorum* and *Dingleyomyces lloydii* are morphologically very similar, but they can be easily distinguished from *Perennicordyceps* species by the presence of a white subiculum from which the perithecia arise (Table 2). In contrast, *Perennicordyceps* is characterized by cylindrical to clavate, branching stromata with the host and rhizomorphs embedded in the substrate. *Dingleyomyces lloydii* produce crown-like perithecia on the stromata of *Ophiocordyceps hauturu* and *O. robertsii*, while the perithecia of *Pa. lepidopterorum* sporadically form on the stromata of *O.* cf. *cochlidiicola*.

Polycephalomyces tengchongensis **Y. Wang tris & T. C. Wen, sp. nov.**
Index Fungorum: IF901449
Fig. 3

Etymology. Named after the location where the type specimen was found, Tengchong County, Yunnan Province.

Description. Parasitic on *Perennicordyceps* cf. *elaphomyceticola*. Sexual morph: Undetermined. Asexual morph: ***Synnemata*** 18.7 mm long, 1–2 mm wide, cylindrical, white, growing in small group on stromata of *Perennicordyceps* cf. *elaphomyceticola*. ***Fertile parts*** yellowish, with conidial mass forming on middle part of synnemata. ***Phialides*** dimorphic. ***α-phialides*** 9–20 × 1–2 µm ($\bar{x}$ = 12.3 × 1.2 µm, n = 45), phialidic, subulate, hyaline, smooth-walled, arranged in a parallel palisade-like layer around the fertile part. ***α-conidia*** 1–3 µm ($\bar{x}$ = 2 µm, n = 45), globose, hyaline.

Culture characters. Colonies on PDA attaining a diam. of 28–31 mm in 14 days at 25 °C, white, leathery, radially striate, reverse dark brown and turns pale outward. ***β-phialides*** 18–44 × 1–3 µm ($\bar{x}$ = 26.7 × 1.2 µm, n = 30), phialidic, lanceolate, smooth-walled. ***β-conidia*** 3–7 × 1.5–3 µm ($\bar{x}$ = 3.9 × 2.2 µm, n = 45), ellipsoidal to broadly fusiform, hyaline, aseptate, smooth-walled.

Material examined. China • Yunnan Province, Tengchong County, Houqiao Town; 5 Nov. 2022; Collected by Yi Wang; Parasitic on the stromata of *Perennicordyceps* cf. *elaphomyceticola*; GYY547 (HKAS 131923, ex-holotype living culture: KUNCC23-16073).

Notes. The newly described species *Polycephalomyces tengchongensis* is closely related to *Po. formosus* with strong support (MLBS = 100%, MIPP = 1.00, Fig. 1). However, *Polycephalomyces tengchongensis* is distinct from *Po. formosus* in several aspects. It parasitizes *Perennicordyceps* cf. *elaphomyceticola* and produces synnemata without well-defined stipe and a fertile head but features dimorphic phialides and conidia. In contrast, *Po. formosus* has stipitate synnemata with a fertile head at the tip and produces only one type of phialides and conidia (Xiao et al. 2023).

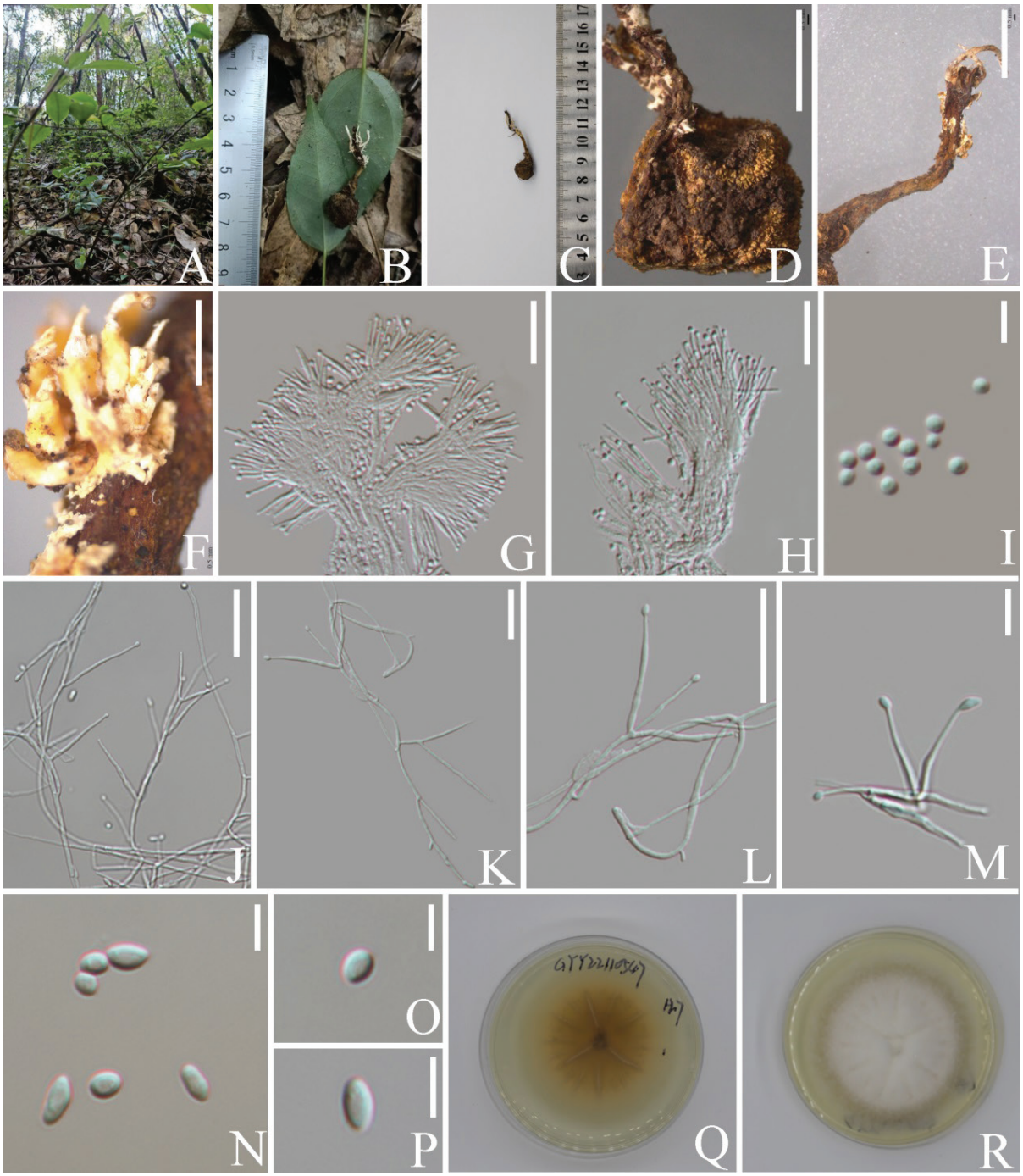

Figure 3. *Polycephalomyces tengchongensis* (**B–I** from HKAS 131923, **J–R** from KUNCC23-16073) **A** habitat **B–F** infected *Perennicordyceps* cf. *elaphomyceticola* showing synnemata of parasites **G, H** α-phialides **I** α-conidia **J–M** β-phialides **N–P** β-conidia **Q, R** reverse and front view of culture on PDA. Scale bars: 5 mm (**D–F**); 20 μm (**G, H**); 50 μm (**J–L**); 10 μm (**M**); 5 μm (**I, N–P**).

A comparison of nucleotide sequences between *Po. tengchongensis* and the ex-type of strain of *Po. formosus* (NBRC 109993) revealed 1% differences (6/584 bp) including three gaps in the ITS region, 0.3% (3/774 bp) differences including one gap in the LSU region, 2.3% differences (16/684 bp) including three gaps in the *rpb1* region and 1.6% differences (15/891bp) in the *rpb2* region. Collectively, the differences both in phenotypic profiles and nucleotides sequences support the establishment of *Polycephalomyces tengchongensis* as a new species.

Table 2. Morphological comparison between sexual species in *Paradingleyomyces*, *Perennicordyceps*, and *Dingleyomyces*.

Species	Host	Stromata (mm)	Perithecia (μm)	Asci (μm)	Apical cap (μm)	Secondary ascospores (μm)	References
Dingleyomyces lloydii	*Ophiocordyceps hauturu, Ophiocordyceps robertsii*	Reduced to white subiculum, flat, thin, irregular plates, often obscured by the perithecia, white or yellowish	300–950 × 300–650, superficial, ovoid, growing in small groups on white subiculum	200–450 × 6–10	2–3 diameter, 4 thickness	1.5–3 × 1–1.5	Dingley (1953); Mains (1958); Johnston and Park. (2023)
Perennicordyceps elaphomyceticola	*Elaphomyces* sp.	20–100 × 0.1–0.5, cylindrical, the colours vary from dark brown, titian red, brownish orange, yellow to pale	430–600 × 255–300, superficial, ovoid to ellipsoid, yellow when mature, pale when immature	365–420 × 5.0–7.6	2–3.5 × 3.3–5.2	1.5–3.2 × 1.4–2.3	Xiao et al. (2023)
Pe. cuboidea	Beetle larva or other *Cordyceps*	32–181 × 3–74, cylindrical, ochre yellow	400–500 × 250–330, superficial, lemon-shaped, glabrate	250–570 in length	3–5 in thickness	1.5–3 × 1–1.5	Ban et al. (2009)
Pe. prolifica	Cicada nymph	70.9–140.0× 0.8–2.2, thin cylindrical, brown	320–530 × 200–340, superficial, ovoid or ellipsoidal, grayish brown	430–650 in length	3–5 in thickness	2–3 × 1–2	Kobayasi and Shimizu (1963)
Pa. lepidopterorum	***Ophiocordyceps* cf. *cochlidiicola***	**Reduced to white subiculum**	**240–690 × 110–360, superficial, ovoid to ellipsoidal, brown**	**150–400 × 3–8**	**3–5 × 1–4**	**2–4 × 0.5–1**	**This study**
Pe. paracuboidea	Coleopteran larva	3.2–38.4 × 0.3–1.7, cylindrical	400–600 × 290–400, superficial, lemon-shaped, pale orangish brown	225–400 in length	3–6.3 in thickness	1.3–2.5 × 1–2	Ban et al. (2009)
Pe. ryogamiensis	Coleopteran larva	12–13 × 0.5, cylindrical, white, palely darkened, glabrate at the base	320–430 × 200–230, superficial, ovoid	450–610 in length	3.8–5 in thickness	2.5–5 × 1.5–2	Ban et al. (2009)

Pleurocordyceps parvicapitata **Y.P. Xiao, T.C. Wen & K.D. Hyde, in Xiao et al. Fungal Diversity 120: 50 (2023)**

Index Fungorum: IF559473

Figs 4, 5

Description. Parasitic on *Elaphomyces* sp. (Fig. 4). The host 6–10 mm in diam., dark brown or brown, spherical, hard, and rough on the surface. Sexual morph: ***Stromata*** 18–21 mm long, 1–2 mm wide, brown, multiple, fibrous. ***Stipe*** 8–15 mm long, 0.5–1 mm wide, brown, cylindrical, terminally or laterally carrying fertile cushions. ***Fertile cushions*** 0.5–1 mm in height, 1–2 mm in width, pale yellow to yellow, hemispherical. ***Perithecia*** 160–530 × 100–305 μm ($\bar{x}$ = 306 × 179 μm, n = 20), immersed, crowded, ovoid to obpyriform, ostiolate. ***Peridium*** 15–40 μm ($\bar{x}$ = 25 μm, n = 20) wide, three-layered, comprised of hyaline to pale yellow cells of ***textura intricate*** at outermost layer to ***textura angularis*** at middle layer to ***textura prismatica*** at inner layer. ***Asci*** 190–380 × 3–5 μm ($\bar{x}$ = 252 × 3.9 μm, n = 50), cylindrical, with thickened apex. ***Apical cap*** 1–2 × 2.5–4 μm ($\bar{x}$ = 1.7 × 3.4 μm, n = 60), hyaline. ***Ascospores*** filiform, multiseptate, hyaline, breaking into many secondary ascospores at maturity. ***Secondary ascospores*** 2–8 × 0.5–1 μm ($\bar{x}$ = 5.1 × 0.9 μm, n = 50), cylindrical, aseptate, straight, smooth-walled. Asexual morph: ***Synnemata*** cylindrical, off-white, gregarious, unbranched, occurring in close proximity to the fertile cushions. ***β-phialides*** up to 16 μm in length, 2 μm in width, cylindrical, attenuate toward the apex, phialidic, hyaline, smooth-walled. ***β-conidia*** 3–5 × 1–2 μm ($\bar{x}$ = 3.8 × 1.7 μm, n = 20), fusiform, hyaline, aseptate. Additionally, *Pleurocordyceps parvicapitata* parasitic on *Perennicordyceps elaphomyceticola* was found in proximity to the one on *Elaphomyces* sp. (Fig. 5). Sexual morph: ***Stromata*** not observed. ***Fertile cushion*** 0.5–1 mm long, 1–2 mm wide, directly growing on stromata of *Pe. elaphomyceticola*, pale yellow to yellow, surface wrinkle, rough due to the protruding perithecia. ***Perithecia*** 440–560 ×115–250 μm ($\bar{x}$ = 505 × 170 μm, n = 15) ovoid

Figure 4. *Pleurocordyceps parvicapitata* (**B–R** from HKAS 131924 **S–Z** from KUNCC23-16075) **A** habitat **B, C** stromata emerging from host **D** host (*Elaphomyces* sp.) **E** fertile cushions on stromata **F** enlargement of fertile cushion **G** cross-section through fertile cushion **H** perithecium **I** peridium **J, P** synnemata on stromata **K** asci **L** part of asci **M** ascus cap **N, O** secondary ascospores **Q, V, W** β-phialides **S** front and reverse view of culture on PDA **T** synnemata on culture **U, X** α-phialides **Y** α-conidia **Z** β-conidia. Scale Bars: 5 mm (**E**); 1 mm (**D, F**); 500 µm (**G, J, P**); 250 µm (**H**); 100 µm (**I**); 50 µm (**K, L**); 20 µm (**M, N, V, U, W**); 10 µm (**X**); 5 µm (**O, Q, R, Y, Z**).

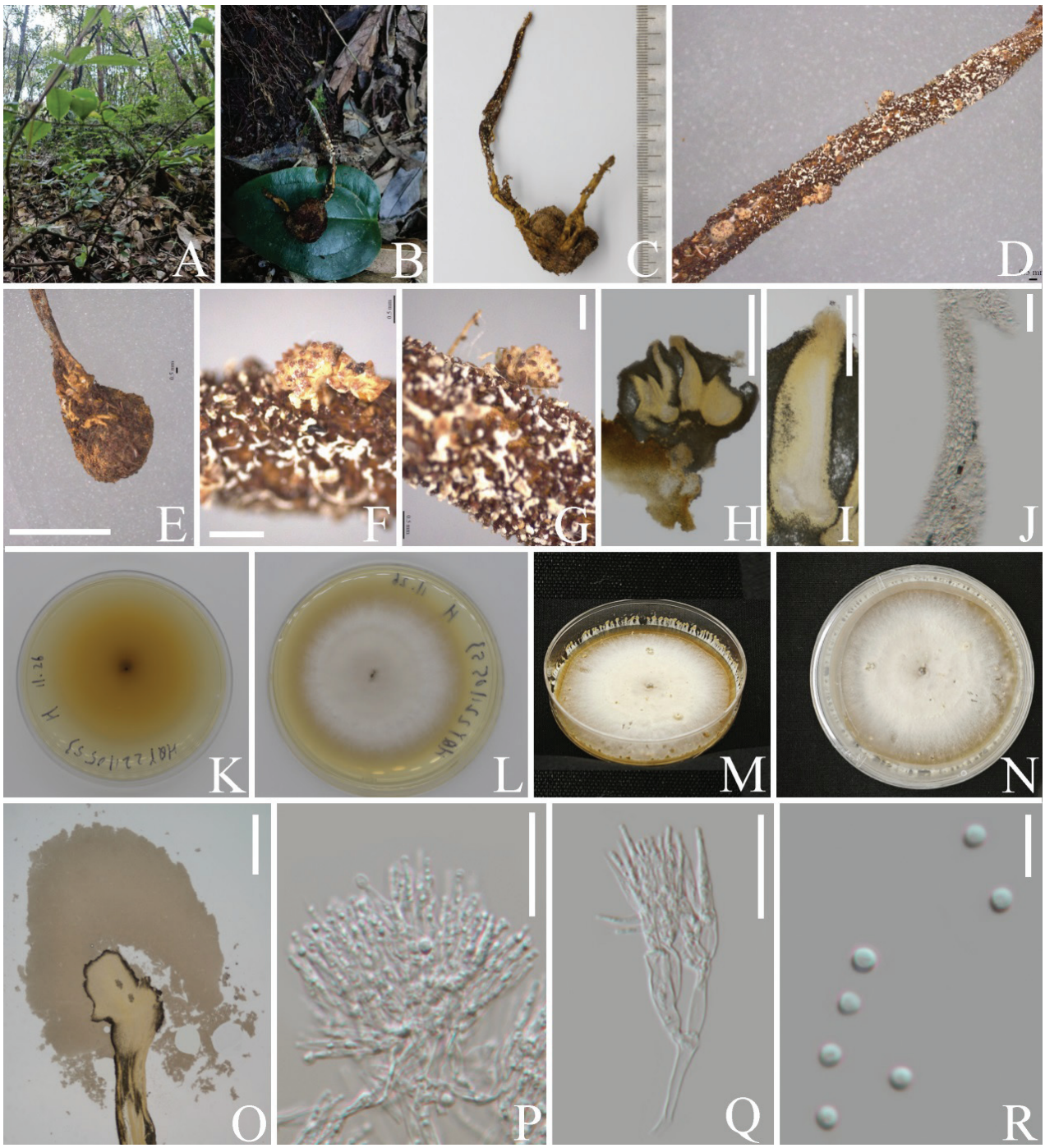

Figure 5. *Pleurocordyceps parvicapitata* (HKAS 131925) **A** habitat **B, C, E** host (*Perennicordyceps elaphomyceticola*) **D, F, G** fertile cushions growing on stromata of *Pe. elaphomyceticola* **H** cross-section through fertile cushion **I** perithecium **J** peridium **L** reverse and front view of culture on PDA after incubation for 14 days **M, N** front view of culture on PDA after incubation for 30 days **O** synnemata **P** conidiophores **Q** phialides **R** conidia. Scale bars: 1 mm (**E–G**); 500 µm (**H, I, O**); 20 µm (**J, P, Q**); 5 µm (**R**).

to obpyriform, immersed, gregarious. ***Peridium*** 15–42 µm ($\bar{x}$ = 25 µm, n = 20) wide, three-layered, comprised of hyaline to pale yellow cells of ***textura intricate*** at outermost layer to ***textura angularis*** at middle layer to ***textura prismatica*** at inner layer. Asci and ascospores were not observed due to the specimen being immature.

Culture characters. Colonies isolated from *Elaphomyces* sp. and *Perennicordyceps elaphomyceticola* present similar characteristics. Colonies on PDA

attaining 41–45 mm in diam. after incubation at 25 °C for 14 days, white, leathery, reverse grayish yellow. ***Synnemata*** emerging from margin of colony in annular distributions, 1–3 mm long, 1–2.5 mm wide, white, erected, apically branched. ***Conidial mass*** gathers at middle part or tip of synnemata, pale yellow, waterish. ***Phialides*** two-typed. ***α-phialides*** 10–28 × 1–2 μm ($\bar{x}$ = 15.7 × 1.5 μm, n = 50), hyaline, smooth-walled, subculate, caespitose, palisade-like. ***α-conidia*** 1–2 μm ($\bar{x}$ = 1.7 μm, n = 45), one-celled, hyaline, smooth-walled, globose. ***β-phialides*** 6–8 × 0.5–1 μm ($\bar{x}$ = 7.9 × 1.1 μm, n = 20), arising from hypha, solitary, lanceolate, hyaline, smooth-walled. ***β-conidia*** 2–6 × 1–2 μm ($\bar{x}$ = 3.8 × 0.8 μm, n = 35), fusiform, hyaline, aseptate, smooth-walled, asymmetrical.

Material examined. China • Yunnan Province, Tengchong County, Houqiao Town; 5 Nov. 2022; Collected by Yi Wang; Parasitic on *Elaphomyces* sp. buried in soil; GYY546 (HKAS 131924, living culture: KUNCC23-16075) • *ibid*; Parasitic on *Perennicordyceps elaphomyceticola*; 5 Nov. 2022; Collected by Yi Wang; GYY553 (HKAS 131925, living culture: KUNCC23-16074).

Notes. *Pleurocordyceps parvicapitata*, parasitic on *Elaphomyces* sp. and *Perennicordyceps elaphomyceticola*, was originally described by Xiao et al. (2023) based on specimens collected from Dadugang County, Xishuangbanna, Yunnan Province, China. The specimen associated with *Elaphomyces* sp. produces pale yellow to yellow, wrinkled fertile cushions that are laterally or terminally attached to stromata, along with cylindrical asci, filiform, disarticulating ascospores and cylindrical, smooth-walled secondary ascospores. In this study, we collected a specimen displaying the typical characteristics of *Pl. parvicapitata* from Tengchong County, Yunnan Province. Importantly, Xiao et al. (2023) described *Pl. parvicapitata* as having one type of phialides and conidia from dry specimen. In contrast, we examined the asexual morph from both our specimens and its pure culture, observing dimorphic phialides and conidia. Additionally, the specimen associated with *Perennicordyceps elaphomyceticola* was previously known only from its asexual morphs (Xiao et al. 2023), where the species was described as having pulvinate, yellowish conidiomata with one-type of phialides and conidia on the stromata of *Pe. elaphomyceticola*. In this study, we collected a sexual specimen from Tengchong County, Yunnan Province and its fertile cushion was similar to *Pl. parvicapitata* found on *Elaphomyces* sp. (Xiao et al. 2023). This is the first report of the sexual morph of *Pl. parvicapitata* on *Pe. elaphomyceticola*, which differs from previously described sexual morphs in that it directly forms a fertile cushion on the substrate. We have also supplemented this species with a pure culture which can be used for further research. These findings provide deeper insights into the morphological traits of *Pl. parvicapitata*.

Pleurocordyceps yunnanensis **(Hong Yu bis, Y.B. Wang & Y.D. Dai) Y.H. Wang, S. Ban, W.J. Wang, Yi Li, Ke Wang, P.M. Kirk & Y.J. Yao, in Wang et al. Journal of Systematics and Evolution 59(5): 1076 (2021)**

Index Fungorum: IF570681

Fig. 6

Description. Parasitic on *Ophiocordyceps nutans* (Ophiocordycipitaceae, Hypocreales) (Fig. 6). Sexual morph: ***Stromata*** 12–25 mm long, 0.5–1 mm wide, fibrous, brown, multiple, unbranched. ***Stipes*** 5–11 mm long, ca. 0.5 mm wide,

Figure 6. *Pleurocordyceps yunnanensis* (HAKS 131922) **A** habitat **B–D** stromata of *Pl. yunnanensis* growing from the host (*Ophiocordyceps nutans*) **E** fertile head **F** cross-section through fertile head **G** perithecium **H** peridium **I–K** asci **L, M** part of asci **N** part of ascospore **O, P** secondary ascospores. Scale bars: 5 mm (**C, D**); 1 mm (**E**); 100 µm (**F, G**); 50 µm (**H–K**); 20 µm (**L, M**); 5 µm (**N–P**).

brown to pale brown. ***Fertile head*** 1–2.5 mm long, 0.7–1.3 mm wide, yellowish to yellow, capitate, rough. ***Perithecia*** 160–390 × 55–170 µm ($\bar{x}$ = 269 × 115 µm, n = 20), immersed, crowded, ovoid to obpyriform, ostiolate yellow, thick-walled. ***Peridium*** 14–46 µm ($\bar{x}$ = 32 µm, n = 25) wide, three-layered, comprised of hyaline to yellowish cells of ***textura prismatica*** at outer layer to ***textura angularis*** at middle layer to ***textura porrecta*** at inner layer. ***Asci*** 95–235 × 3–6 µm ($\bar{x}$ = 172 × 5 µm, n = 40), 8-spored, with thickened cap. ***Ascospores*** filiform, hyaline, multiseptate, disarticulating into many secondary ascospores at maturity. ***Secondary ascospores*** 2.5–5 × 1–2 µm ($\bar{x}$ = 3.9 × 1.3 µm, n = 40), cylindrical, aseptate, hyaline, smooth-walled. Asexual morphs: see Wang et al. (2015a).

Material examined. China • Yunnan Province, Kunming City, the Wild Duck Lake Forest Park; 17 Sep. 2023; Collected by Yi Wang; Parasitic on *Ophiocordyceps nutans*; YYH13 (HAKS 131922).

Notes. The asexual morph of *Polycephalomyces yunnanensis* was first described by Wang et al. (2015a) from *Ophiocordyceps nutans* in Wild Duck Lake Forest Park, Kunming, Yunnan Province. This species was later transferred to *Pleurocordyceps* by Wang et al. (2021) based on molecular phylogenetic analyses. In this study, a sexual polycephalomyces-like fungus growing on *O. nutans* was obtained from the same location as the type specimen (Fig. 6). Phylogenetic analysis revealed that it groups with strains of *Pleurocordyceps yunnanensis* with strong support (Fig. 1). Therefore, we introduce our specimen as the new sexual morph of *Pl. yunnanensis*.

Discussion

Polycephalomycetaceae was introduced by Xiao et al. (2023) to encompass the genera *Pleurocordyceps*, *Perennicordyceps*, and *Polycephalomyces*. The monophyletic nature of these three genera has been confirmed through numerous phylogenetic studies (Tian et al. 2010; Wang et al. 2012; Kepler et al. 2013; Wang et al.2015a; Zhong et al. 2016; Crous et al. 2017a; Sobczak etal. 2017; Poinar and Vega 2020; Xiao et al. 2018, 2023). Johnston and Park (2023) introduced a new genus, *Dingleyomyces*, into Polycephalomycetaceae. *Dingleyomyces* is a monotypic genus, and typified by *Dingleyomyces lloydii*, a species that is hyperparasitic on *Ophiocordyceps hauturu* from New Zealand. *Dingleyomyces lloydii* was placed in a distant clade branching off from *Perennicordyceps* (Johnston and Park 2023). In this study, we introduce a new genus, *Paradingleyomyces* to accommodate *Pa. lepidopterorum* which forms a distinct clade nested between *Perennicordyceps* and *Dingleyomyces* (Fig. 1).

Perennicordyceps currently comprises six species, four identified based on their sexual morphology and two based on their asexual morphology. We have compared the sexual characteristics of *Pa. lepidopterorum* with the four sexual species of *Perennicordyceps*, as depicted in Fig. 7. Several distinctions between *Paradingleyomyces* and *Perennicordyceps* are observed: 1) *Pa. lepidopterorum* is characterized by the absence of stromata, while *Perennicordyceps* species exhibit branched, cylindrical to clavate, rhizomorphic stromata; 2) The host of *Pa. lepidopterorum* is *Ophiocordyceps* cf. *cochlidiicola*, whereas *Perennicordyceps* parasitize a broader range of host, including insect and fungi; 3) The perithecia of *Pa. lepidopterorum* form on a white subiculum and are distributed over the entire stromata of the host fungus, while in *Perennicordyceps* species,

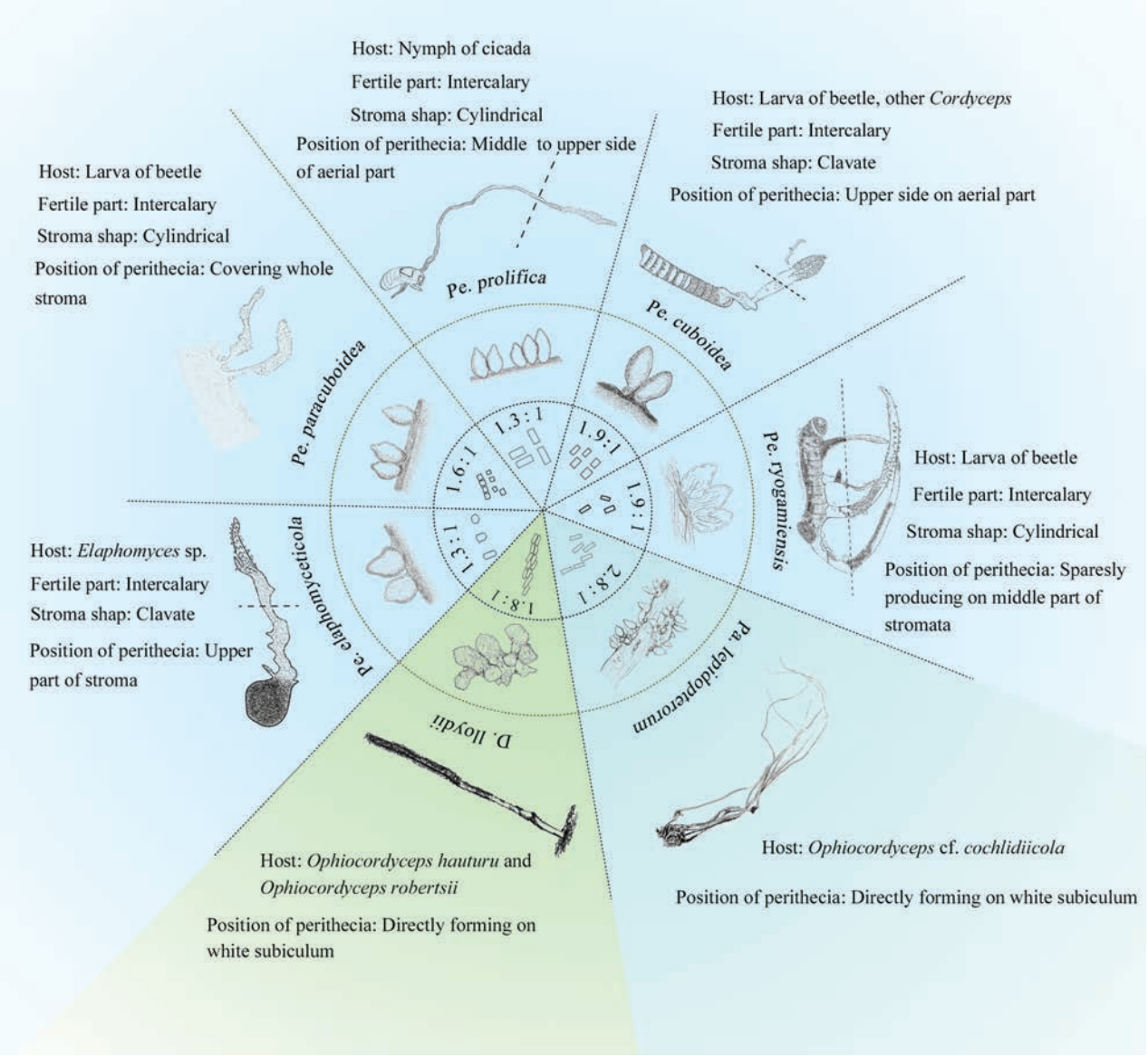

Figure 7. Morphological comparison of *Paradingleyomyces*, *Dingleyomyces* and *Perennicordyceps*. In *Perennicordyceps*, the dotted line below indicates burial in soil or woods. *Pe. cuboidea*, *Pe. prolifica*, *Pe. paracuboidea* and *Pe. ryogamiensis* were redrawn from Ban et al. (2009) and *Pe. elaphomyceticola* was redrawn from Xiao et al. (2023). *Pa. lepidopterorum* is a newly described species in this study. *D. lloydii* was redrawn from Johnston and Park (2023).

perithecia are densely formed from the middle to the upper part of the stromata; 4) The length-to-width ratio of secondary ascospores in *Pa. lepidopterorum* is 2.8: 1, which is greater than that observed in *Perennicordyceps* species. Consequently, we introduced *Paradingleyomyces* as a distinct genus rather than categorizing it within *Perennicordyceps*. Although *Dingleyomyces* has shares the poorly developed stromata connecting crowed perithecia to the stromata of *Ophiocordyceps hauturu* and *Ophiocordyceps robertsii*, giving a similar appearance to *Pa. lepidopterorum*, multigene phylogeny revealed a paraphyletic relationship between *Dingleyomyces* and *Paradingleyomyces*. Therefore, the establishment of *Paradingleyomyces* is well-supported by both morphological observations and phylogenetic analysis. The asexual morph of *Paradingleyomyces* is currently unknown, and future efforts should focus on exploring more hidden species within this genus.

Polycephalomyces was initially classified under Hypocreales *incertae sedis* (Kepler et al. 2013; Matočec et al. 2014). Up to 25 species were assigned to *Polycephalomyces*, but later some were transferred to *Pleurocordyceps* and *Perennicordyceps*, remaining eight species: *Po. albiramus*, *Po. formosus*, *Po. ramosus*, *Po. tomentosus*, *Po. baltica*, *Po. cylindrosporus*, *Po. ditmarii*, and *Po. paludosus* (Xiao et al. 2023). However, the phylogenetic relationships of the latter four species remain unclear due to a lack of molecular data. Notably, *Po. ramosus* and *Po. tomentosus* group with species of *Pleurocordyceps* in the study of Xiao et al. (2023) and this phylogenetic relationship is also observed in our study. Thus, the taxonomic status of *Po. ramosus* and *Po. tomentosus* remains questionable. In this study, we introduce a new species, *Polycephalomyces tengchongensis*, which is parasitic on *Perennicordyceps* cf. *elaphomyceticola* from Tengchong County, Yunnan Province, China. This new species is distinguished by a unique combination of features, including its host association, synnemata lacking a stipe and fertile head, and the presence of dimorphic phialides and conidia (see Table 3). The finding of *Po. tengchongensis* adds to the morphological diversity within the genus *Polycephalomyces*.

Pleurocordyceps was introduced by Wang et al. (2021) to accommodate ten species: *Pleurocordyceps agarica*, *Pl. aurantiacus*, *Pl. lianzhouensis*, *Pl. marginaliradians*, *Pl. nipponica*, *Pl. onorei*, *Pl. phaothaiensis*, *Pl. ramosopulvinatus*, *Pl. sinensis*, and *Pl. yunnanensis*, based on phylogenetic analysis. Wei et al. (2022) added a new species *Pleurocordyceps ophiocordycipiticola* which parasitizes *Ophiocordyceps cylindrospora* in Thailand. Xiao et al. (2023) introduced five additional species to this genus, including *Pl. heilongtanensis*, *Pl. lanceolata*, *Pl. nutantis*, *Pl. parvicapitata* and *Pl. vitellina*. Currently, *Pleurocordyceps* comprises 16 species, all of which have been verified by molecular phylogeny. The sexual morph of *Pleurocordyceps* is characterized by stipitate, fibrous stromata that produce pale yellow to yellow fertile cushion either laterally or terminally, with immersed ostiolate perithecia, cy-

Table 3. Distinguishing characteristics between *Po. tengchongensis* and other *Polycephalomyces* species.

Species	Host	Synnemata	Phialides (μm)	Conidia (μm)	Reference
Po. tengchongensis	***Perennicordyceps* cf. *elaphomyceticola* (Hypocreales, Polycephalomycetaceae)**	**Non-stipitate, without fertile head**	**Two-type, α-phialides 9–20 × 1–2, subulate; β-phialides 18–44 × 1–3, lanceolate**	**Two-type, α-conidia 1–3, globose; β-conidia 3–7 × 1.5–3, ellipsoidal to broadly fusiform**	**This study**
Po. albiramus	*Gryllotalpa* sp. (Orthoptera)	Stipitate, without fertile head	One-type, 12.8–18.3 × 1–2.2, narrowly subulate, awl-shaped	One-type 2.1–3.2 × 0.9–1.2, cylindrical to obovoid or subglobose	Xiao et al. (2023)
Po. baltica	Nymph or short-winged female bark louse	Stipitate, with fertile head	One-type, 3–4 long, flask-shaped	One-type, 3–4, globose	Poinar and Vega (2020)
Po. cylindrosporus	Coleoptera, Formicidae and Pentatomidae	Stipitate, with fertile head	One-type, 7–25 long	One-type, 2.5–4, cylindrical to bacilliform	Matočec et al. (2014)
Po. ditmarii	*Paravespula vulgaris* (Wasp), fly	Stipitate, with fertile head	One-type, 20–37 × 1.5–2.5, elongate, cylindrical, attenuating at the apex	One-type, 2.2–3 × 1.3–1.6, globose to subglobose to clavate	Van Vooren and Audibert (2005), Xiao et al. (2023)
Po. formosus	Coleopteran larvae or *Ophiocordyceps barnesii*	Stipitate, with fertile head	One-type, 6–25 × 1–1.2, cylindrical, tapering gradually	One-type, 2.5–3.2 × 1–1.2, ellipsoidal or ovoid	Kobayasi (1941)
Po. ramosus	Lepidopteran larvae or *Hirsutella guignardii*	Stipitate, with fertile head	Two-type, α-phialides 7–24 long, 1–2 at basal wide, cylindrical to narrowly lageniform; β-phialides 6–27 long, 2–3.5 at basal wide, 0.5–1 at neck width, narrowly lageniform or subulate	Two-type, α-conidia 2.4–3.2 × 1.6–2.4, ovoid; β-conidia 3.2–4 × 1.6–2, fusiform	Seifert (1985), Bischof et al. (2003)
Po. paludosus	Lepidopteran larva	Stipitate, with fertile head	One-type, 2–20 long, 1–1.5 at basal wide, subulate	One-type, 8–2.5 × 1.1–1.3, obovoid	Mains (1948)
Po. tomentosus	Myxomycetes	–	–	Three-type, globose or ellipsoidal or cylindrical	Seifert (1985)

lindrical asci, filiform disarticulating ascospores and cylindrical secondary ascospores. The asexual morph is characterized by stipitate, non-stipitate, or pulvinate synnemata, with or without fertile heads, generally displaying dimorphic phialides and conidia. Sexual morphs have been identified in six species including *Pl. marginaliradians* (Xiao et al. 2018), *Pl. nipponica*, *Pl. onorei* (Crous et al. 2017a), *Pl. parvicapitata* (Xiao et al. 2023), *Pl. phaothaiensis* (Crous et al. 2017b) and *Pl. ramosopulvinata* (Wang et al. 2021). The remaining 10 species of *Pleurocordyceps* have been described based on their asexual morphs. In this study, we report the sexual morph of *Pl. yunnanensis* from *Ophiocordyceps nutans* for the first time, collected from the same location as the type specimen. Ecologically, *Pleurocordyceps* species are particularly prone to infecting *Ophiocordyceps* or *Perennicordyceps* species, as well as their insect or fungal hosts. For instance, *Pl. parvicapitata* is known to infect *Perennicordyceps elaphomyceticola* and its host *Elaphomyces* sp. at the same region (Xiao et al. 2023). In this study, we once again obtained *Pl. parvicapitata* which infects both *Pe. elaphomyceticola* and its host *Elaphomyces* sp. from Tengchong County, Yunnan Province. This finding indicates that *Pl. parvicapitata* may be specific to *Pe. elaphomyceticola* and *Elaphomyces* sp. Additionally, we are the first to isolate and observe dimorphic phialides and conidia in *Pl. parvicapitata*, while Xiao et al. (2023) reported only one type of phialides and conidia from dried specimen. Therefore, the presence of dimorphs phialides and conidia should not be considered a reliable feature for species demarcation within *Pleurocordyceps*.

Additional information

Conflict of interest

The authors have declared that no competing interests exist.

Ethical statement

No ethical statement was reported.

Funding

This research was funded by the Science and Technology Foundation of Guizhou Province (No. [2019] 2451-3), the National Natural Science Foundation of China (No. 31760014), and Thailand Science Research and Innovation (TSRI) grant No.672A01014 from the Fundamental Fund for Basic Research, National Research Council of Thailand.

Author contributions

Investigation: YZ, GYW, XZ. Resources: XCP, XSH. Writing – original draft: TCW, YW. Writing – review and editing: DPW, JCK, CRL, PC, RCL, ZZL. All authors have read and agreed to the published version of the manuscript.

Author ORCIDs

Yi Wang https://orcid.org/0009-0006-5412-7893
De-Ping Wei https://orcid.org/0000-0002-3740-0142
Xing-Can Peng https://orcid.org/0000-0002-7271-7639
Ji-Chuan Kang https://orcid.org/0000-0002-6294-5793
Xian Zhang https://orcid.org/0009-0008-0919-4303
Putarak Chomnunti https://orcid.org/0000-0003-2989-1735
Ting-Chi Wen https://orcid.org/0000-0003-1744-5869

Data availability

All of the data that support the findings of this study are available in the main text.

References

Aini AN, Mongkolsamrit S, Wijanarka W, Thanakitpipattana D, Luangsa-Ard JJ, Budiharjo A (2020) Diversity of *Akanthomyces* on moths (Lepidoptera) in Thailand. MycoKeys 71: 1–22. https://doi.org/10.3897/mycokeys.71.55126

Ban S, Sakane T, Toyama K, Nakagiri A (2009) Teleomorph–anamorph relationships and reclassifcation of *Cordyceps cuboidea* and its allied species. Mycoscience 50(4): 261–272. https://doi.org/10.1007/S10267-008-0480-Y

Ban S, Sakane T, Nakagiri A (2015) Three new species of *Ophiocordyceps* and overview of anamorph types in the genus and the family Ophiocordycipitaceae. Mycological Progress 14(1): 1017. https://doi.org/10.1007/s11557-014-1017-8

Bischof JF, Sullivan RF, Hywel-Jones NL, White JF (2003) Resurrection of *Blistum tomentosum* and its exclusion from *Polycephalomyces* (Hyphomycetes, Deuteromycota) based on 28S rDNA sequence data. Mycotaxon 86: 433–444.

Capella-Gutiérrez S, Silla-Martínez JM, Gabaldón T (2009) TrimAl: A tool for automated alignment trimming in large-scale phylogenetic analyses. Bioinformatics 25(15): 1972–1973. https://doi.org/10.1093/bioinformatics/btp348

Castlebury LA, Rossman AY, Sung GH, Hyten AS, Spatafora JW (2004) Multigene phylogeny reveals new lineage for *Stachybotrys chartarum*, the indoor air fungus. Mycological Research 108(8): 864–872. https://doi.org/10.1017/S0953756204000607

Chaverri P, Bischof JF, Evans HC, Hodge KT (2005) *Regiocrella*, a new entomopathogenic genus with a pycnidial anamorph and its phylogenetic placement in the Clavicipitaceae. Mycologia 97(6): 1225–1237. https://doi.org/10.1080/15572536.2006.11832732

Crous PW, Wingfeld MJ, Burgess TI, Carnegie AJ, Hardy GESJ, Smith D, Summerel BA, Cano-Lira JF, Guarro J, Houbraken J, Lombard L, Martín MP, Sandoval-Denis M, Alexandrova AV, Barnes CW, Baseia IG, Bezerra JDP, Guarnaccia V, May TW, Hernández-Restrepo M, Stchigel AM, Miller AN, Ordoñez ME, Abreu VP, Accioly T, Agnello C (2017a) Fungal Planet description sheets: 625–715. Persoonia 39: 270–467. https://doi.org/10.3767/persoonia.2017.39.11

Crous PW, Wingfield MJ, Burgess TI, Hardy GESJ, Barber PA, Alvarado P, Barnes CW, Buchanan PK, Heykoop M, Moreno G, Thangavel R, Van der Spuy S, Barili A, Barrett S, Cacciola SO, Cano-Lira JF, Crane C, Decock C, Gibertoni TB, Guarro J, Guevara-Suarez M, Hubka V, Kolařík M, Lira CRS, Ordoñez ME, Padamsee M, Ryvarden L, Soares AM, Stchigel AM, Sutton DA, Vizzini A, Weir BS, Acharya K, Aloi F, Baseia IG, Blanchette RA, Bordallo JJ, Bratek Z, Butler T, Cano-Canal J, Carlavilla JR, Chander J, Cheewangkoon R, Cruz RHSF, Da Silva M, Dutta AK, Ercole E, Escobio V, Esteve-Raventós F, Flores JA, Gené J, Góis JS, Haines L, Held BW (2017b) Fungal Planet description sheets: 558–624. Persoonia 38(1): 240–384. https://doi.org/10.3767/003158517X698941

Dingley JM (1953) The Hypocreales of New Zealand. V. The genera *Cordyceps* and *Torrubiella*. Transactions and Proceedings of the Royal Society of New Zealand 81(3): 329–343.

Hall T, Biosciences I, Carlsbad C (2011) BioEdit: An important software for molecular biology. GERF Bulletin of Biosciences 2(1): 60–61. http://www.gerfbb.com/

Hyde KD, Chaiwan N, Norphanphoun C, Boonmee S, Camporesi E, Chethana KWT, Dayarathne MC, de Silva NI, Dissanayake AJ, Ekanayaka AH, Hongsanan S, Huang SK, Jayasiri SC, Jayawardena RS, Jiang HB, Karunarathna A, Lin CG, Liu JK, Liu NG, Lu

YZ, Luo ZL, Maharachchimbura SSN, Manawasinghe IS, Pem D, Perera RH, Phukhamsakda C, Samarakoon MC, Senwanna C, Shang QJ, Tennakoon DS, Thambugala KM, Tibpromma S, Wanasinghe DN, Xiao YP, Yang J, Zeng XY, Zhang JF, Zhang SN, Bulgakov TS, Bhat DJ, Cheewangkoon R, Goh TK, Jones EBG, Kang JC, Jeewon R, Liu ZY, Lumyong S, Kuo CH, McKenzie EHC, Wen TC, Yan JY, Zhao Q (2018) Mycosphere notes 169–224. Mycosphere: 9(2): 271–430. https://doi.org/10.5943/mycosphere/9/2/8

Jeewon R, Hyde KD (2016) Establishing species boundaries and new taxa among fungi: Recommendations to resolve taxonomic ambiguities. Mycosphere: 7(11): 1669–1677. https://doi.org/10.5943/mycosphere/7/11/4

Johnston PR, Park D (2023) *Dingleyomyces lloydii* (Hypocreales, Polycephalomycetaceae), gen. nov., comb. nov. New Zealand Journal of Botany 2023: 1–8. https://doi.org/10.1080/0028825X.2023.2291453

Katoh K, Standley DM (2013) MAFFT multiple sequence alignment software version 7: Improvements in performance and usability. Molecular Biology and Evolution 30(4): 772–780. https://doi.org/10.1093/molbev/mst010

Kepler R, Ban S, Nakagiri A, Bischof J, Hywel-Jones N, Owensby CA, Spatafora JW (2013) The phylogenetic placement of hypocrealean insect pathogens in the genus *Polycephalomyces*: An application of One Fungus One Name. Fungal Biology 117(9): 611–622. https://doi.org/10.1016/j.funbio.2013.06.002

Kobayasi Y (1941) The genus *Cordyceps* and its allies. Science Reports of the Tokyo Bunrika Daigaku 5: 53–260.

Kobayasi Y, Shimizu D (1963) Monographic studies of *Cordyceps* 2. Group parasitic on Cicadae. Bulletin of the National Science Museum, Tokyo 6: 286–314.

Liang ZQ, Chen WH, Liang JD, Han YF, Zou X (2016) Phenotypic polymorphism of the synnematous entomogenous fungi in an ant nest of *Ponera* I. Mycosystema 35(8): 906–917. https://doi.org/10.13346/j.mycosystema.150069

Liu YL, Whelen S, Hall BD (1999) Phylogenetic relationships among ascomycetes: Evidence from an RNA polymerase II subunit. Molecular Biology and Evolution 16(12): 1799–1808. https://doi.org/10.1093/oxfordjournals.molbev.a026092

Mains EB (1948) Entomogenous fungi. Mycologia 40(4): 402–416. https://doi.org/10.1080/00275514.1944.12017718

Mains EB (1958) Information concerning species of *Cordyceps* and *Ophionectria* in the Lloyd Herbarium. Lloydia 20(4): 219–227.

Massee G (1895) A revision of the genus *Cordyceps*. Annals of Botany 9(33): 1–44. https://doi.org/10.1093/oxfordjournals.aob.a090724

Matočec N, Kušan I, Ozimec R (2014) The genus *Polycephalomyces* (Hypocreales) in the frame of monitoring *Veternica cave* (Croatia) with a new segregate genus *Perennicordyceps*. Ascomycete.Org : Revue Internationale pour la Taxinomie des Ascomycota 6: 125–133.

Miller MA, Pfeiffer W, Schwartz T (2010) Creating the CIPRES Science Gateway for inference of large phylogenetic trees. Gateway Computing Environments Workshop (GCE), 1–8. https://doi.org/10.1109/GCE.2010.5676129

Minh BQ, Schmidt HA, Chernomor O, Schrempf D, Woodhams MD, Von Haeseler A, Lanfear R (2020) IQ-TREE 2: New models and efficient methods for phylogenetic inference in the genomic era. Molecular Biology and Evolution 37(5): 1530–1534. https://doi.org/10.1093/molbev/msaa015

Nikoh N, Fukatsu T (2000) Interkingdom host jumping underground: Phylogenetic analysis of entomoparasitic fungi of the genus *Cordyceps*. Molecular Biology and Evolution 17(4): 629–638. https://doi.org/10.1093/oxfordjournals.molbev.a026341

Nylander JA (2004) MrAIC [Internet] http://www.abc.se/~nylander/ [program distributed by the author]

Peng XC, Wen TC, Wei DP, Liao YH, Wang Y, Zhang X, Wang GY, Zhou Y, Tangtrakulwanich K, Liang JD (2024) Two new species and one new combination of *Ophiocordyceps* (Hypocreales, Ophiocordycipitaceae) in Guizhou. MycoKeys 102: 245–266. https://doi.org/10.3897/mycokeys.102.113351

Poinar G, Vega FE (2020) Entomopathogenic fungi (Hypocreales: Ophiocordycipitaceae) infecting bark lice (*Psocoptera*) in Dominican and Baltic amber. Mycology 11(1): 71–77. https://doi.org/10.1080/21501203.2019.1706657

Quandt CA, Kepler RM, Gams W, Araújo JPM, Ban S, Evans HC, Hughes D, Humber R, Hywel-Jones N, Li ZZ, Luangsa-Ard JJ, Rehner SA, Sanjuan T, Sato H, Shrestha B, Sung GH, Yao YJ, Zare R, Spatafora JW (2014) Phylogenetic-based nomenclatural proposals for Ophiocordycipitaceae (Hypocreales) with new combinations in *Tolypocladium*. IMA Fungus 5(1): 121–134. https://doi.org/10.5598/imafungus.2014.05.01.12

Rambaut A (2012) Figtree 1.4.3. http://tree.bio.ed.ac.uk/software/figtree/

Rehner SA, Buckley E (2005) A *Beauveria* Phylogeny inferred from nuclear ITS and EF1-α sequences: Evidence for cryptic diversification and links to *Cordyceps* teleomorphs. Mycologia 97(1): 84–98. https://doi.org/10.3852/mycologia.97.1.84

Sangdee A, Sangdee K, Seephonkai P, Jaihan P, Kanyaphum T (2017) Colony characteristics, nucleoside analog profiles, and genetic variations of medicinal fungus *Polycephalomyces nipponicus* (Ascomycetes) isolates from northeast Thailand. International Journal of Medicinal Mushrooms 19(5): 445–455. https://doi.org/10.1615/IntJMedMushrooms.v19.i5.60

Schoch CL, Seifert KA, Huhndorf S, Robert V, Spouge JL, Levesque CA, Chen W, Bolchacova E, Voigt K, Crous PW, Miller AN, Wingfield MJ, Aime MC, An KD, Bai FY, Barreto RW, Begerow D, Bergeron MJ, Blackwell M, Boekhout T, Bogale M, Boonyuen N, Burgaz AR, Buyck B, Cai L, Cai Q, Cardinali G, Chaverri P, Coppins BJ, Crespo A, Cubas P, Cummings C, Damm U, de Beer ZW, de Hoog GS, Del-Prado R, Dentinger B, Diéguez-Uribeondo J, Divakar PK, Douglas B, Dueñas M, Duong TA, Eberhardt U, Edwards JE, Elshahed MS, Fliegerova K, Furtado M, García MA, Ge ZW, Griffith GW, Griffiths K, Groenewald JZ, Groenewald M, Grube M, Gryzenhout M, Guo LD, Hagen F, Hambleton S, Hamelin RC, Hansen K, Harrold P, Heller G, Herrera C, Hirayama K, Hirooka Y, Ho HM, Hoffmann K, Hofstetter V, Högnabba F, Hollingsworth PM, Hong SB, Hosaka K, Houbraken J, Hughes K, Huhtinen S, Hyde KD, James T, Johnson EM, Johnson JE, Johnston PR, Jones EBG, Kelly LJ, Kirk PM, Knapp DG, Kõljalg U, Kovács GM, Kurtzman CP, Landvik S, Leavitt SD, Liggenstoffer AS, Liimatainen K, Lombard L, Luangsa-ard JJ, Lumbsch HT, Maganti H, Maharachchikumbura SSN, Martin MP, May TW, McTaggart AR, Methven AS, Meyer W, Moncalvo JM, Mongkolsamrit S, Nagy LG, Nilsson RH, Niskanen T, Nyilasi I, Okada G, Okane I, Olariaga I, Otte J, Papp T, Park D, Petkovits T, Pino-Bodas R, Quaedvlieg W, Raja HA, Redecker D, Rintoul TL, Ruibal C, Sarmiento-Ramírez JM, Schmitt I, Schüßler A, Shearer C, Sotome K, Stefani FOP, Stenroos S, Stielow B, Stockinger H, Suetrong S, Suh SO, Sung GH, Suzuki M, Tanaka K, Tedersoo L, Telleria MT, Tretter E, Untereiner WA, Urbina H, Vágvölgyi C, Vialle A, Vu TD, Walther G, Wang QM, Wang Y, Weir BS, Weiß M, White MM, Xu J, Yahr R, Yang ZL, Yurkov A, Zamora JC, Zhang N, Zhuang WY, Schindel D (2012) Nuclear ribosomal internal transcribed spacer (ITS) region as a universal DNA barcode marker for Fungi. Proceedings of the National Academy of Sciences of the United States of America 109(16): 6241–6246. https://doi.org/10.1073/pnas.1117018109

Seifert KA (1985) A monograph of *Stilbella* and some allied Hyphomycetes. Studies in Mycology 27: 1–235. https://doi.org/10.2307/3807446

Senanayake IC, Rathnayaka AR, Marasinghe DS, Calabon MS, Gentekaki E, Lee HB, Hurdeal VG, Pem D, Dissanayake LS, Wijesinghe SN, Bundhun D, Nguyen TT, Goonasekara ID, Abeywickrama PD, Bhunjun CS, Jayawardena RS, Wanasinghe DN, Jeewon R, Bhat DJ, Xiang MM (2020) Morphological approaches in studying fungi: Collection, examination, isolation, sporulation and preservation. Mycosphere: 11(1): 2678–2754. https://doi.org/10.5943/mycosphere/11/1/20

Shrestha B, Tanaka E, Hyun MW, Han JG, Kim CS, Jo JW, Han SK, Oh J, Sung JM, Sung GH (2017) Mycosphere Essay 19. *Cordyceps* species parasitizing hymenopteran and hemipteran insects. Mycosphere: 8(9): 1424–1442. https://doi.org/10.5943/mycosphere/8/9/8

Sobczak JF, Costa LFA, Carvalho JLVR, Salgado-Neto G, Moura-Sobczak JCMS, Messas YF (2017) The zombie ants parasitized by the fungi *Ophiocordyceps camponoti-atricipis* (Hypocreales: Ophiocordycipitaceae): new occurrence and natural history. Mycosphere: 8(9): 1261–1266. https://doi.org/10.5943/mycosphere/8/9/1

Sun YB (2017) FasParser: A package for manipulating sequence data. Zoological Research 38(2): 110–112. https://doi.org/10.24272/j.issn.2095-8137.2017.017

Sun JZ, Liu XZ, McKenzie EH, Jeewon R, Liu JK, Zhang XL, Zhao Q, Hyde KD (2019) Fungicolous fungi: terminology, diversity, distribution, evolution, and species checklist. Fungal Diversity 95(1): 1–94. https://doi.org/10.1007/s13225-019-00422-9

Tian LH, Hu B, Zhou H, Zhang WM, Qu LH, Chen YQ (2010) Molecular phylogeny of the entomopathogenic fungi of the genus *Cordyceps* (Ascomycota: Clavicipitaceae) and its evolutionary implications. Journal of Systematics and Evolution 48(6): 435–444. https://doi.org/10.1111/j.1759-6831.2010.00100.x

Van Vooren N, Audibert C (2005) Révision du complexe « *Cordyceps sphecocephala* ». 2e partie: Les mouches végétales. Bulletin Mensuel de la Societe Linneenne de Lyon 74(7): 221–254. https://doi.org/10.3406/linly.2005.13604

Vilgalys R, Hester M (1990) Rapid genetic identification and mapping of enzymatically amplified ribosomal DNA from several *Cryptococcus* species. Journal of Bacteriology 172(8): 4238–4246. https://doi.org/10.1128/jb.172.8.4238-4246.1990

Wang WJ, Wang XL, Li Y, Xiao SR, Kepler RM, Yao YJ (2012) Molecular and morphological studies of *Paecilomyces sinensis* reveal a new clade in clavicipitaceous fungi and its new systematic position. Systematics and Biodiversity 10(2): 221–232. https://doi.org/10.1080/14772000.2012.690784

Wang L, Li HH, Chen YQ, Zhang WM, Qu LH (2014) *Polycephalomyces lianzhouensis* sp. nov., a new species, co-occurs with *Ophiocordyceps crinalis*. Mycological Progress 13(4): 1089–1096. https://doi.org/10.1007/s11557-014-0996-9

Wang YB, Yu H, Dai YD, Chen ZH, Zeng WB, Yuan F, Liang ZQ (2015a) *Polycephalomyces yunnanensis* (Hypocreales), a new species of *Polycephalomyces* parasitizing *Ophiocordyceps nutans* and stink bugs (hemipteran adults). Phytotaxa 208: 34–44. https://doi.org/10.11646/phytotaxa.208.1.3

Wang YB, Yu H, Dai YD, Wu CK, Zeng WB, Yuan F, Liang ZQ (2015b) *Polycephalomyces agaricus*, a new hyperparasite of *Ophiocordyceps* sp. infecting melolonthid larvae in southwestern China. Mycological Progress 14(9): 1–9. https://doi.org/10.1007/s11557-015-1090-7

Wang YB, Wang Y, Fan Q, Duan DE, Zhang GD, Dai RQ, Dai YD, Zeng WB, Chen ZH, Li DD, Tang DX, Xu ZH, Sun T, Nguyen TT, Tran NL, Dao VM, Zhang LD, Dao VM, Zhang CM,

Huang LD, Liu YJ, Zhang XM, Yang DR, Sanjuan T, Liu XZ, Yang ZL, Yu H (2020) Multigene phylogeny of the family Cordycipitaceae (Hypocreales): New taxa and the new systematic position of the Chinese cordycipitoid fungus *Paecilomyces hepiali*. Fungal Diversity 103(1): 1–46. https://doi.org/10.1007/s13225-020-00457-3

Wang YH, Sayaka B, Wang WJ, Li Y, Wang K, Kirk PM, Bushley KE, Dong CH, Hawksworth DL, Yao YJ (2021) *Pleurocordyceps* gen. nov. for a clade of fungi previously included in *Polycephalomyces* based on molecular phylogeny and morphology. Journal of Systematics and Evolution 59(5): 1065–1080. https://doi.org/10.1111/jse.12705

Wei DP, Gentekaki E, Wanasinghe DN, Tang SM, Hyde KD (2022) Diversity, molecular dating and ancestral characters state reconstruction of entomopathogenic fungi in Hypocreales. Mycosphere: 13(2): 281–351. https://doi.org/10.5943/mycosphere/si/1f/8

Wen TC, Xiao YP, Li WJ, Kang JC, Hyde KD (2014) Systematic analyses of *Ophiocordyceps ramosissimum* sp. nov., a new species from a larvae of Hepialidae in China. Phytotaxa 161(3): 227–234. https://doi.org/10.11646/phytotaxa.161.3.6

White TJ, Bruns S, Lee S, Taylor J (1990) Amplification and direct sequencing of fungal ribosomal RNA genes for phylogenetics. PCR protocols: a guide to methods and applications 18(1): 315–322. https://doi.org/10.1016/B978-0-12-372180-8.50042-1

Xiao YP, Wen TC, Hongsanan S, Jeewon R, Luangsa-ard JJ, Brooks S, Wanasinghe DN, Long FY, Hyde KD (2018) Multigene phylogenetics of *Polycephalomyces* (Ophiocordycipitaceae, Hypocreales), with two new species from Thailand. Scientific Reports 8(1): 18087. https://doi.org/10.1038/s41598-018-36792-4

Xiao YP, Hongsanan S, Hyde KD, Brooks S, Xie N, Long FY, Wen TC (2019) Two new entomopathogenic species of *Ophiocordyceps* in Thailand. MycoKeys 47: 53–74. https://doi.org/10.3897/mycokeys.47.29898

Xiao YP, Wang YB, Hyde KD, Eleni G, Sun JZ, Yang Y, Meng J, Yu H, Wen TC (2023) Polycephalomycetaceae, a new family of clavicipitoid fungi segregates from Ophiocordycipitaceae. Fungal Diversity 120(1): 1–76. https://doi.org/10.1007/s13225-023-00517-4

Yang JI, Stadler M, Chuang WY, Wu S, Ariyawansa HA (2020) In vitro inferred interactions of selected entomopathogenic fungi from Taiwan and eggs of *Meloidogyne graminicola*. Mycological Progress 19(1): 97–109. https://doi.org/10.1007/s11557-019-01546-7

Zhang WM, Wang L, Tao MH, Chen YQ, Qu LH (2007) Two species of *Cordyceps* simultaneously parasitic on a larva of Lepidoptera. Mycosystema 26: 7–21.

Zhong X, Li SS, Peng QY, Zhang JS, Kan XT, Zhang GR, Liu X (2016) A *Polycephalomyces* hyperparasite of *Ophiocordyceps sinensis* leads to shortened duration of production and reduced numbers of host ascospores. Fungal Ecology 21: 24–31. https://doi.org/10.1016/j.funeco.2016.03.002

Zhu JS, Gao L, Li XH, Yao YS, Zhao JQ, Zhou YJ, Lu JH (2010) Maturational alteration of oppositely orientated rDNA and differential proliferation of GC-and AT-biased genotypes of *Ophiocordyceps sinensis* and *Paecilomyces hepiali* in natural *Cordyceps sinensis*. American Journal of Biomedical Sciences 2(3): 217–238. https://doi.org/10.5099/aj100300217

MycoKeys

MycoKeys 110: 211–236 (2024)
DOI: 10.3897/mycokeys.110.129228

Research Article

Thyridium lauri sp. nov. (Thyridiaceae, Thyridiales): a new pathogenic fungal species of bay laurel from Italy

Giuseppa Rosaria Leonardi[1], Dalia Aiello[1], Chiara Di Pietro[1], Antonio Gugliuzzo[1], Giovanna Tropea Garzia[1], Giancarlo Polizzi[1], Hermann Voglmayr[2]

1 *Department of Agriculture, Food and Environment, University of Catania, Via Santa Sofia 100, 95123 Catania, Italy*

2 *Department of Botany and Biodiversity Research, University of Vienna, Rennweg 14, 1030 Vienna, Austria*

Corresponding author: Dalia Aiello (dalia.aiello@unict.it)

Abstract

Laurus nobilis is an important Mediterranean tree and shrub native to Italy that is also commercially grown as spice and ornamental plant. Field surveys conducted since 2021 in Sicily (Italy) revealed that bay laurel plants in urban and private gardens and nurseries were severely affected by symptoms of stem blight and internal necrosis, which were associated with ambrosia beetle entry holes in the bark and internal wood galleries. The occurring ambrosia beetle was identified as *Xylosandrus compactus*, an invasive wood-boring pest previously reported from Sicily. Investigation of fungi from symptomatic tissues primarily resulted in the isolation of *Thyridium*-like colonies. The main symbiont of *X. compactus*, *Ambrosiella xylebori*, was also isolated from infested plants. Phylogenetic analyses of a combined matrix of ITS, LSU, *act1*, *rpb2*, *tef1*, and *tub2* gene regions revealed that the isolated *Thyridium*-like colonies represent a new fungal species within the genus *Thyridium*. Based on both phylogeny and morphology, the new isolated fungus is described as *Thyridium lauri* **sp. nov.** Moreover, two recently described species, *Phialemoniopsis hipposidericola* and *Phialemoniopsis xishuangbannaensis*, are transferred to the genus *Thyridium* due to the confirmed synonymy of both genera, as supported by molecular phylogenies. Pathogenicity test conducted on potted plants demonstrated that *T. lauri* is pathogenic to bay laurel, causing internal necrosis and stem blight. The new species was consistently re-isolated from the symptomatic tissue beyond the inoculation point, thereby fulfilling Koch's postulates. This study represents the first report of a new pathogenic fungus, *T. lauri*, causing stem blight and internal necrosis of bay laurel plants and associated with infestation of the invasive ambrosia beetle *X. compactus*.

Key words: Fungal diseases, *Laurus nobilis*, phylogeny, stem blight and internal necrosis, taxonomy, *Xylosandrus compactus*

Academic editor: Nattawut Boonyuen
Received: 7 June 2024
Accepted: 1 October 2024
Published: 15 November 2024

Citation: Leonardi GR, Aiello D, Di Pietro C, Gugliuzzo A, Tropea Garzia G, Polizzi G, Voglmayr H (2024) *Thyridium lauri* sp. nov. (Thyridiaceae, Thyridiales): a new pathogenic fungal species of bay laurel from Italy. MycoKeys 110: 211–236. https://doi.org/10.3897/mycokeys.110.129228

Introduction

Lauraceae is one of the largest families of trees and shrubs, distributed worldwide with approximately 55 genera and 3,000 species (Renner 2011; Zhang et al. 2023). This family includes economically important plants such as avocado (*Persea americana* Mill.), camphor (*Cinnamomum camphora* (L.) Sieb.), cinnamon (*Cinnamomum zeylanicum* Blume), and bay laurel (*Laurus nobilis* L.). Bay laurel,

also commonly known as sweet bay, is an evergreen tree or shrub naturally widespread across many countries of the Mediterranean basin, along the Atlantic coast of the Iberian Peninsula and the southern coast of the Black Sea (Giacobbe 1939; Rodríguez-Sánchez and Arroyo 2008). This plant is also cultivated in warm regions of the Americas, Eastern Asia, the Balkans, and Asia Minor (Batool et al. 2020; Singletary 2021). The economic importance of bay laurel lies in its use in public and private gardens as an ornamental tree or hedging plant (Raviv et al. 1982; Malaspina et al. 2022), as well as in its aromatic leaves, which serve as an important spice and flavoring agent in the culinary and food industries worldwide (Stefanaki and van Andel 2021). Traditionally, bay laurel leaves have been used in medicine by local people of Mediterranean countries for their biological properties, which are positively correlated with human health (Fang et al. 2005; Motti and de Falco 2021). Several recent studies have reported interest in the production of bay laurel plants due to the pharmacological and cosmetic properties of their essential oils and extracts (Lubbe and Verpoorte 2011; Ordoudi et al. 2022). Although bay laurel is investigated worldwide for its diverse potential uses, there is limited data available on fungal diseases affecting this plant. In Italy, leaf spots and stem blight caused by *Pestalotiopsis uvicola* (Speg.) Bissett, as well as crown and root rot caused by *Calonectria ilicicola* Boedijn & Reitsma have been reported on young potted plants (Vitale and Polizzi 2005; Polizzi et al. 2012). Furthermore, fungal diseases transmitted by bark and ambrosia beetles may pose a significant limitation to the cultivation of bay laurel on a global scale. Fungi closely associated with bark and ambrosia beetles are capable of infecting both the bark and wood tissues, resulting in severe diseases in the host tree. Among the fungi carried by these beetles, a quarantine pathogen is *Harringtonia lauricola* (T.C. Harr., Fraedrich & Aghayeva) Z.W. de Beer & M. Procter (formerly *Raffaelea lauricola*) (Ascomycota, Ophiostomatales) which causes a lethal vascular disease known as laurel wilt. This disease affects numerous species in the Lauraceae family, including bay laurel (Mayfield et al. 2008; Hughes et al. 2014, 2017; Eaton et al. 2023). This fungus has rapidly spread across the United States vectored by several species of ambrosia beetles, particularly *Xyleborus glabratus* Eichhoff (Coleoptera: Curculionidae), commonly known as the redbay ambrosia beetle (Ploetz et al. 2017).

Fungal species of the genus *Geosmithia*, particularly *Geosmithia langdonii* M. Kolařík, Kubátová & Pažoutová, *G. pallida* (G. Sm.) M. Kolařík, Kubátová & Pažoutová, and *G. putterillii* (Thom) Pitt (Ascomycota, Hypocreales), have been reported to be vectored by *Liparthrum colchicum* Semenov (Coleoptera: Curculionidae: Scolytinae), a phloem-feeding bark beetle, and are associated with dried twigs of bay laurel in France (Jordal et al. 2004; Kolarík et al. 2004, 2007) and Italy (Benvenuti et al. 2021; Vitale et al. 2021). *Ambrosiella xylebori* Brader ex Arx & Hennebert (Ascomycota, Ceratocystidaceae), along with *Fusarium* spp. and *Bionectria* sp., were involved in necrosis of twigs and branches of bay laurel infested by the ambrosia beetle *Xylosandrus compactus* (Eichhoff) (Coleoptera: Curculionidae) (Vannini et al. 2017). This invasive wood-boring insect pest, native to subtropical and tropical Asia, has been introduced to various subtropical regions worldwide, with its first report in the Mediterranean region coming from Italy in 2011 (FITOLAB 2011; Francardi et al. 2017). Currently, *X. compactus* is regarded as an emerging pest affecting various trees and ornamental plants in Italy (Francardi et al. 2017; Vannini et al. 2017; Gugliuzzo et al. 2019a, 2019b; Contarini et al. 2020), and bay laurel is reported as one of the preferred host plants of this am-

brosia beetle in the Mediterranean regions (Francardi et al. 2012; Barnouin et al. 2020; Riba-Flinch et al. 2021; Hızal et al. 2023). In Sicily, heavy infestations by *X. compactus* have primarily been reported on carob (*Ceratonia siliqua* L.), with less severe occurrences on bay laurel (Gugliuzzo et al. 2019c, 2023a).

Since 2021, bay laurel plants showing infestations of wood-boring insects associated with stem blight and internal necrosis have been observed in different nurseries of Sicily during field samplings following disease detection by farmers. From 2022 to 2024, additional surveys and observations were conducted in collaboration with the Regional Phytosanitary Service (Sicily, Italy) in street and park shrubs, private gardens, and nurseries with mother plants for tree propagation located in the Catania and Syracuse provinces. In most cases, the survey conduction revealed stem blight and internal necrosis, and the decline or death of numerous bay laurel trees, consistently accompanied by insect entry holes in the bark and internal galleries. As many fungal species have been reported worldwide for causing stem blight and internal necrosis of bay laurel associated with severe infestations of bark or ambrosia beetles, the aims of this study were to: i) characterize the fungal species associated with stem blight and internal necrosis of bay laurel plants; ii) assess their potential pathogenicity on healthy bay laurel plants; iii) identify the insect species co-occurring with these fungal phytopathogens in the diseased plants.

Materials and methods

Sampling, fungal isolation and beetle identification

Field samplings were carried out in June 2021 at nurseries located in Giarre (37°41.81'N, 15°11.52'E) and Mascali (37°44.85'N, 15°12.25'E) (Catania, Italy). Stem sections from 25 bay laurel plants exhibiting symptoms of stem blight, internal necrosis, and beetle infestations were randomly collected. Samples were then placed in sterile plastic bags and transferred to the laboratory of Plant Pathology at the Department of Agriculture, Food and Environment, University of Catania, for fungal isolation and insect identification. In the laboratory, 180 small wood fragments were collected from the discoloured inner woody tissues surrounding the outer portions of the beetle-bored galleries, excluding the interior of the galleries, which are typically inhabited by beetle-specific fungal symbionts. This approach was taken to focus on isolating the fungal species responsible for causing the disease. Each fragment was then divided into subsections (5 × 5 × 5 mm), with priority given to areas where the necrotic lesions were actively progressing (terminal discolored part). The subsections were sterilized in a 1.2% sodium hypochlorite solution for 60 s, rinsed once in sterile distilled water for 60 s, and air-dried in a laminar-flow hood on sterile paper. The surface-sterilized wood pieces were placed onto potato dextrose agar (PDA, Lickson, Vicari, Italy), supplemented with 100 mg L^{-1} of streptomycin sulphate (Sigma-Aldrich, St. Louis, MO, USA) to prevent bacterial growth, and then incubated at 25 ± 1 °C for ten days. The isolation frequency was calculated according to the formula: $F = (N_f/N_{tot}) \times 100$, where F is the frequency of putative fungal pathogen, N_f is the number of wood subfragments from which a fungal colony of interest emerged, and N_{tot} is the total number of wood subfragments cultured on PDA. Colonies of interest were subcultured on PDA plates to obtain pure cultures for macro- and microscopic observations and DNA extraction.

Twelve representative colonies of the most frequently recovered fungus were selected to obtain single-spore isolates and were stored in the collection of the Department of Agriculture, Food and Environment, Plant Pathology Section, University of Catania, for further analyses. Several beetles were extracted from the infested laurel stem sections, individually placed into sterile vials, and transferred to the Section of Applied Entomology of the same Department for beetle species identification. All adult beetles were then observed under a stereomicroscope for morphological identification, following the keys provided by Rabaglia et al. (2006).

Morphological characterization of fungal species

Three representative isolates (ALF2, ALF6, and ALF11) were selected for the description of pure cultures and morphological characterization. Cultures were grown on potato dextrose agar (PDA) and on cornmeal agar (Sigma, St Louis Missouri), amended with 2% (w/v) D(+)-glucose-monohydrate (CMD) at room temperature and ambient light. Colony features, such as texture, obverse and reverse colour, margin, and zonation were recorded. To examine sporulating structures, microscope slides were prepared in 3% KOH and observed at 100 × magnifications using a Zeiss Axio Imager.A1 compound microscope (Oberkochen, Germany) equipped with a Zeiss Axiocam 506 colour digital camera. Specifically, the length and width of conidia, as well as the length and width of conidiogenous cells (phialides) at their base, were measured, and the length-to-width ratio of conidia was calculated. Measurements of conidia are reported as maxima and minima in parentheses and the mean plus and minus the standard deviation of several measurements given in parentheses.

Holotype isolate (ALF11) was used to assess the effect of the temperature on mycelial growth rate. The fungal isolate was grown on PDA at 25 ± 1 °C for 14 days in the dark. Mycelial plugs, 5 mm in diameter, were obtained from the margins of actively growing colonies using a sterile cork borer and placed in the center of Petri plates, containing PDA amended with 100 mg L^{-1} of streptomycin sulphate. The plates were incubated at 5, 10, 15, 20, 25, 30, 35 and 40 ± 1 °C for 14 days in darkness. Five Petri plates were used as replicates for each temperature. Two perpendicular diameters were measured using a scale ruler at 7 and 14 days post-inoculation.

The isolates used in this study are maintained in the culture collection of the Department of Agriculture, Food, and Environment, University of Catania. Moreover, three representative isolates (AL2, ALF6 and ALF11) were deposited at the Westerdijk Fungal Biodiversity Institute (CBS), Utrecht, the Netherlands. Dried sporulating cultures were deposited as voucher specimens in the fungarium of the Department of Botany and Biodiversity Research, University of Vienna (WU-MYC).

DNA extraction, PCR amplification and sequencing

Collected isolates were grown on PDA for 14 days for the genomic DNA extraction. Mycelium was scraped off and processed according to the manufacturer's protocol using the Wizard Genomic DNA Purification Kit® (Promega Corporation, Madison, WI, USA). DNA samples were stored at 4 °C until use.

The following loci were amplified and sequenced: the complete internally transcribed spacer region (ITS1-5.8S-ITS2) rDNA gene with primers ITS5 and ITS4 (White et al. 1990); an approximately 0.9 kb fragment of the large-subunit (LSU) ribosomal RNA gene with primers LR0R (Moncalvo et al. 1995) and LR5 (Vilgalys and Hester 1990); a ca. 0.9 kb fragment of the partial alpha-actin (*act1*) gene with primers Act-1 and Act-5ra (Voigt and Wöstemeyer 2000); a ca. 0.9 kb fragment of the DNA-directed RNA polymerase II second largest subunit (*rpb2*) gene with primers RPB2-5F2 (Sung et al. 2007) and fRPB2-7cr (Liu et al. 1999); a ca. 0.8 kb fragment of the translation elongation factor 1-alpha (*tef1*) gene with primers TEF1_INTF (Jaklitsch 2009) and TEF1-LLErev (Jaklitsch et al. 2005); a ca. 0.5 kb fragment of the *tef1* gene with primers EF-688F and EF-1251R (Carbone and Kohn 1999); a ca. 0.85 kb fragment of the beta tubulin (*tub2*) gene with primers tub-intF (5'-AACAAGTAYGTYCCTCGCGCCGT-3') and T22D (Voglmayr et al. 2019) and a ca. 0.4 kb fragment of the same gene with primers bt2a and bt2b (Glass and Donaldson 1995).

The PCR amplification products were estimated visually by electrophoresis on 1% agarose gels and subsequently purified using an enzymatic PCR cleanup (Werle et al. 1994), as described in Voglmayr and Jaklitsch (2008). PCR products were sequenced in both directions by Macrogen Inc. (Seoul, South Korea) or at the Department of Botany and Biodiversity Research, University of Vienna, using the ABI PRISM Big Dye Terminator Cycle Sequencing Ready Reaction Kit v. 3.1 (Applied Biosystems, Warrington, UK) and the same primers as in PCR. Sequencing was performed on an automated DNA sequencer (3730xl Genetic Analyser, Applied Biosystems). The DNA sequences generated were assembled with Lasergene SeqMan Pro (DNASTAR, Madison, WI, USA) and deposited in GenBank (https://www.ncbi.nlm.nih.gov/) (Table 1).

Phylogenetic analyses

The sequences obtained in this study were compared with NCBI GenBank nucleotide database using the standard nucleotide Basic Local Alignment Search Tool (BLAST) (https://blast.ncbi.nlm.nih.gov/Blast.cgi). All single-spore isolates (ALF1, ALF2, ALF3, ALF4, ALF5, ALF6, ALF8, ALF10, ALF11, ALF14, ALF17, ALF19) were used for phylogenetic analyses within a combined matrix of ITS rDNA, LSU, *act*, *rpb2*, *tef1*, and *tub2* sequences. The newly generated sequences of each genomic region were aligned to reference sequences of *Thyridium* downloaded from GenBank, with two species from the Annulatascales and one species of *Myrmecridium* (Myrmecridiales) selected as the outgroup. For *Thyridium*, 10 accepted species and two recently described species of *Phialemoniopsis* for which sequences were available were included in the matrix, including ex-epitype and ex-holotype strains. The GenBank accession numbers of the sequences used in these analyses are given in Table 1.

Sequence alignments for phylogenetic analyses were produced with the server version of MAFFT (https://mafft.cbrc.jp/alignment/server/) and checked and refined using BioEdit Sequence alignment Editor 7.7.1.0 (Hall 1999). All six loci (ITS, LSU, *act1*, *rpb2*, *tef1*, *tub2*) were concatenated to a combined matrix using Phyutility v. 2.2 (Smith and Dunn 2008). The combined data matrix for phylogenetic analyses contained 4257 characters (528 nucleotides of ITS, 816 nucleotides of LSU, 839 nucleotides of *act1*, 879 nucleo-

Table 1. Information on fungal isolates deposited in GenBank and used in the phylogenetic analyses.

Taxon	Isolates[a]	Status[b]	Substrate/Host	GenBank accession numbers[c]					
				ITS	LSU	*act1*	*rpb2*	*tef1*	*tub2*
Annulusmagnus triseptatus	CBS 128831		decayed driftwood of *Alnus glutinosa*		GQ996540		JQ429258		
Ascitendus austriascus	CBS 131685		decayed driftwood of *Alnus glutinosa*		GQ996539		JQ429257		
Myrmecridium montsegurinum	JF 13180	HT	submerged wood of *Fraxinus excelsior*	KT991674	KT991664		KT991654		
Phialemoniopsis hipposidericola	KUMCC 21-0778	HT	*Hipposideros larvatus*	ON426882	OP363279	OQ930298			OR025957
Phialemoniopsis hipposidericola	KUMCC 21-0779		*Hipposideros larvatus*	ON426886	OP363283	OQ930299			OR025958
Phialemoniopsis xishuangbannaensis	KUMCC 21-0774	HT	*Hipposideros larvatus*	ON426881	OP363278	OQ930300			OR025959
Phialemoniopsis xishuangbannaensis	KUMCC 21-0775		*Hipposideros larvatus*	ON426884	OP363281	OQ930301			OR025960
Phialemoniopsis xishuangbannaensis	KUMCC 21-0776		*Hipposideros larvatus*	ON426885	OP363282	OQ930302			OR025961
Phialemoniopsis xishuangbannaensis	KUMCC 21-0777		*Hipposideros larvatus*	ON426883	OP363280	OQ930303			OR025962
Thyridium cornearis	CBS 131711	HT	human corneal fluid	KJ573445	KJ573450	HE599252		LC382144	HE599301
Thyridium cornearis	UTHSC 06-1465		shin aspirate	HE599285	HE599270	HE599253			HE599302
Thyridium curvatum	CBS 490.82	HT	skin lesion	AB278180	AB189156	HE599258		LC382142	HE599307
Thyridium curvatum	UTHSC R-3447		human eye	HE599291	FR745927	HE599259			HE599308
Thyridium endophyticum	ACCC 38979		lower stem of *Luffa cylindrica* (endophyte)	KT799556	KT799556	KT799553			KT799562
Thyridium endophyticum	ACCC 38980	HT	lower stem of *Luffa cylindrica* (endophyte)	KT799557	KT799560	KT799554			KT799563
Thyridium flavostromatum	MAFF 247509	HT	dead twigs of *Phyllostachys pubescens*	LC655959	LC655963	LC655979	LC655967	LC655971	LC655975
Thyridium hongkongense	HKU39	HT	the right forearm nodule biopsy of a human	KJ573442	KJ573447	KJ573452			KJ573457
Thyridium limonesiae	CBS 146752	HT	Skin nodule	MW050977	MW050976	MW349126			MW048608
Thyridium oculorum	CBS 110031	HT	human keratitis	KJ573444	KJ573449	HE599247		LC382145	HE599296
Thyridium oculorum	UTHSC 05-2527		peritoneal dialysis catheter	HE599281	HE599266	HE599249			HE599298
Thyridium pluriloculosum	CBS 131712	HT	human toe nail	HE599286	HE599271	HE599254		LC382141	HE599303
Thyridium pluriloculosum	MAFF 247508		dead wood of *Betula maximowicziana*	LC655960	LC655964	LC655980	LC655968	LC655972	LC655976
Thyridium pluriloculosum	UTHSC 09-3589		synovial fluid	HE599287	HE599272	HE599255			HE599304
Thyridium punctulatum	MAFF 239669		dead culms of *Phyllostachys pubescens*	LC655961	LC655965	LC655981	LC655969	LC655973	LC655977
Thyridium punctulatum	MAFF 247510	ET	dead twigs of *Phyllostachys nigra* var. *nigra*	LC655962	LC655966	LC655982	LC655970	LC655974	LC655978
Thyridium vestitum	CBS 125582		dead branches of *Pyrus communis*	MH863721	MH875182				
Thyridium vestitum	CBS 113027		dead bark of *Acer pseudoplatanus*		AY544671		DQ470890	DQ471058	
Thyridium lauri	**ALF1**		*Laurus nobilis*	**PP907005**	**PP907017**	**PP909726**	**PP909730**	**PP909742**	**PP909754**
T. lauri	**ALF2 (CBS 151896)**		*Laurus nobilis*	**PP907006**	**PP907018**		**PP909731**	**PP909743**	**PP909755**
T. lauri	**ALF3**		*Laurus nobilis*	**PP907007**	**PP907019**		**PP909732**	**PP909744**	**PP909756**
T. lauri	**ALF4**		*Laurus nobilis*	**PP907008**	**PP907020**		**PP909733**	**PP909745**	**PP909757**
T. lauri	**ALF5**		*Laurus nobilis*	**PP907009**	**PP907021**		**PP909734**	**PP909746**	**PP909758**
T. lauri	**ALF6 (CBS 151897)**		*Laurus nobilis*	**PP907010**	**PP907022**	**PP909727**	**PP909735**	**PP909747**	**PP909759**
T. lauri	**ALF8**		*Laurus nobilis*	**PP907011**	**PP907023**		**PP909736**	**PP909748**	**PP909760**

Taxon	Isolates[a]	Status[b]	Substrate/Host	GenBank accession numbers[c]					
				ITS	LSU	*act1*	*rpb2*	*tef1*	*tub2*
T. lauri	**ALF10**		*Laurus nobilis*	**PP907012**	**PP907024**		**PP909737**	**PP909749**	**PP909761**
T. lauri	**ALF11 (CBS 151898)**	HT	*Laurus nobilis*	**PP907013**	**PP907025**	**PP909728**	**PP909738**	**PP909750**	**PP909762**
T. lauri	**ALF14**		*Laurus nobilis*	**PP907014**	**PP907026**		**PP909739**	**PP909751**	**PP909763**
T. lauri	**ALF17**		*Laurus nobilis*	**PP907015**	**PP907027**		**PP909740**	**PP909752**	**PP909764**
T. lauri	**ALF19**		*Laurus nobilis*	**PP907016**	**PP907028**	**PP909729**	**PP909741**	**PP909753**	**PP909765**

[a] Strains and sequences generated in this study are shown in bold.
[b] ET = epitype; HT = holotype.
[c] ITS, internal transcribed spacer; LSU, large-subunit ribosomal RNA gene; *act1*, the partial alpha-actin gene; *rpb2*, DNA-directed RNA polymerase II second largest subunit gene; *tef1*, translation elongation factor 1-α; *tub2*, beta-tubulin.

tides of *rpb2*, 785 nucleotides of *tef1*, and 410 nucleotides of *tub2*). Maximum likelihood (ML) analyses were performed with RAxML (Stamatakis 2006), as implemented in raxmlGUI 2.0 (Silvestro and Michalak 2012), using the ML + rapid bootstrap setting and the GTRGAMMA+I substitution model which was selected as the most appropriate model by Modeltest. The matrix was partitioned for the different gene regions, and bootstrap analyses were done with 1,000 bootstrap replicates. For evaluation and interpretation of bootstrap support, values between 70% and 90% were considered moderate, above 90% as high, and 100% as the maximum. Maximum parsimony (MP) bootstrap analyses were performed with Phylogenetic Analyses Using Parsimony (PAUP) v. 4.0a169 (Swofford 2002). A total of 1,000 bootstrap replicates were implemented using five rounds of heuristic search with random sequence addition, followed by tree-bisection-reconnection (TBR) branch swapping. The MULTREES option was enabled, the steepest descent option was disabled, the COLLAPSE command was set to MINBRLEN, and each replicate was limited to 1 million rearrangements. All molecular characters were treated as unordered and assigned equal weight, with gaps considered as missing data. The COLLAPSE command was set to MINBRLEN.

Pathogenicity test

To assess the pathogenicity of *T. lauri*, two-year-old potted bay laurel plants grown under controlled growth chamber conditions were used. The holotype isolate (ALF11) was grown on PDA amended with 100 mg L^{-1} of streptomycin sulphate and incubated at 25 ± 1 °C for 30 days. The stems were surfaced disinfected with a 70% ethanol solution, and the bark was gently scraped using a sterile blade. The mycelial plug was then placed upside down onto the wound. Wounds were sealed with Parafilm to prevent desiccation. All inoculated plants were moved to a growth chamber with a 12 h photoperiod and maintained at 25 ± 1 °C. The plants were regularly watered and monitored monthly for symptom development. A total of nine plants were inoculated with *T. lauri* ALF11, while the control group consisted of an equal number of plants inoculated with sterile PDA. After four months, the phloem tissue was peeled back, and the lesion length extending both upward and downward from each inoculation site was measured. The mean and standard deviation were calculated. Pieces of necrotic tissue were cultured as previously described to fulfill the Koch's postulates, and the frequency of *Thyridium*-like colonies was determined.

Results

Sampling, fungal isolation and beetle identification

In the surveyed nurseries, bay laurel plants consistently showed symptoms of stem blight. The initial external symptoms observed included blight of the terminal leaves, beginning at the tips and progressing downward along the twigs. The leaves became dry as though suffering from lack of water and remained attached to twigs for several months (Fig. 1). In the most severe cases, the entire tree died. Symptomatic plants consistently exhibited bark necrosis surrounding small, circular entry holes bored by beetles, with diameters ranging from approximately 0.7 to 0.9 mm (Fig. 2a). Upon removing the bark from symptomatic stems or twigs with beetle entry holes, black to brown streaks of discoloration were observed in the sapwood, extending from the entry points into the surrounding wood (Fig. 2b–d). Longitudinal sections of the stem revealed discoloration extending upwards and downwards from the beetle galleries. Disease incidence, based on the number of plants showing symptoms of stem blight associated with ambrosia beetle attack in the nurseries where the disease was first observed (Mascali), ranged from approximately 30% to 40% of the 3,000

Figure 1. Symptoms of stem blight on bay laurel plants in nurseries located in Catania province **A** stem blight of twigs on a four-year-old tree, typically observed on a section of the canopy **B** stem blight of the lower part of plant **C** stem discoloration progressing from the tips to the lower part of the twig (red arrow).

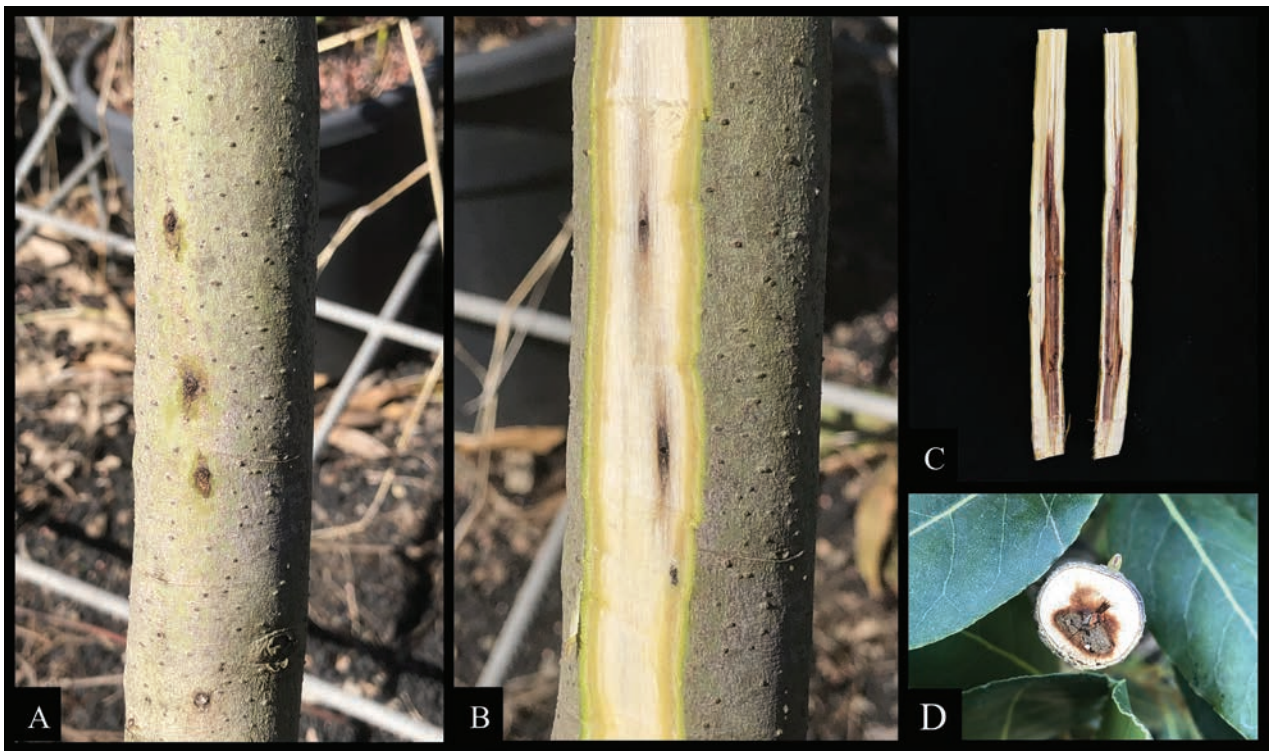

Figure 2. Details of symptoms on bay laurel trees **A, B** bark necrosis surrounding the small circular entry holes of *Xylosandrus compactus* **C, D** longitudinal and cross-section of twigs showing internal necrosis reaching the pith.

total plants. Two types of fungal colonies were consistently recovered from symptomatic tissue, with isolation frequencies ranging from 60 to 95% for *Thyridium*-like colonies and from 5 to 40% for *Ambrosiella*-like colonies. More than 300 adult beetle females were collected from diseased samples all of which were morphologically identified as *X. compactus*, the sole beetle species present in the sampled woody material.

Phylogenetic analyses and fungal species identification

Of the 4257 characters of the combined matrix used for phylogenetic analyses, 593 were parsimony informative (44 from ITS, 68 from LSU, 102 from *act1*, 259 from *rpb2*, 62 from *tef1*, and 51 from *tub2*), 364 were parsimony-uninformative and 3300 were constant. The ML tree (-lnL = 13574.613578) obtained by RAxML is shown in Fig. 3. Maximum Likelihood analyses resulted in a tree topology similar to that revealed by MP bootstrap analysis. The monophyly of the genus *Thyridium* was strongly supported, with 97% support in the ML analysis and 98% in the MP analysis, as was the monophyly of most *Thyridium* species included. However, the two non-type strains of *T. vestitum* (CBS 113027, CBS 125582) did not form a monophyletic clade, indicating that at least one of the two isolates is misidentified. The twelve isolates of this study formed a distinct monophyletic clade within *Thyridium*, representing a new species with maximum support. This clade was resolved as a sister group to a highly supported clade (96% ML, 95% MP) containing *T. curvatum*, *T. flavostromatum*, *T. hongkongense*, and *T. limonesiae*. While most terminal and basal nodes received high to maximum support, intermediate nodes were generally poorly supported.

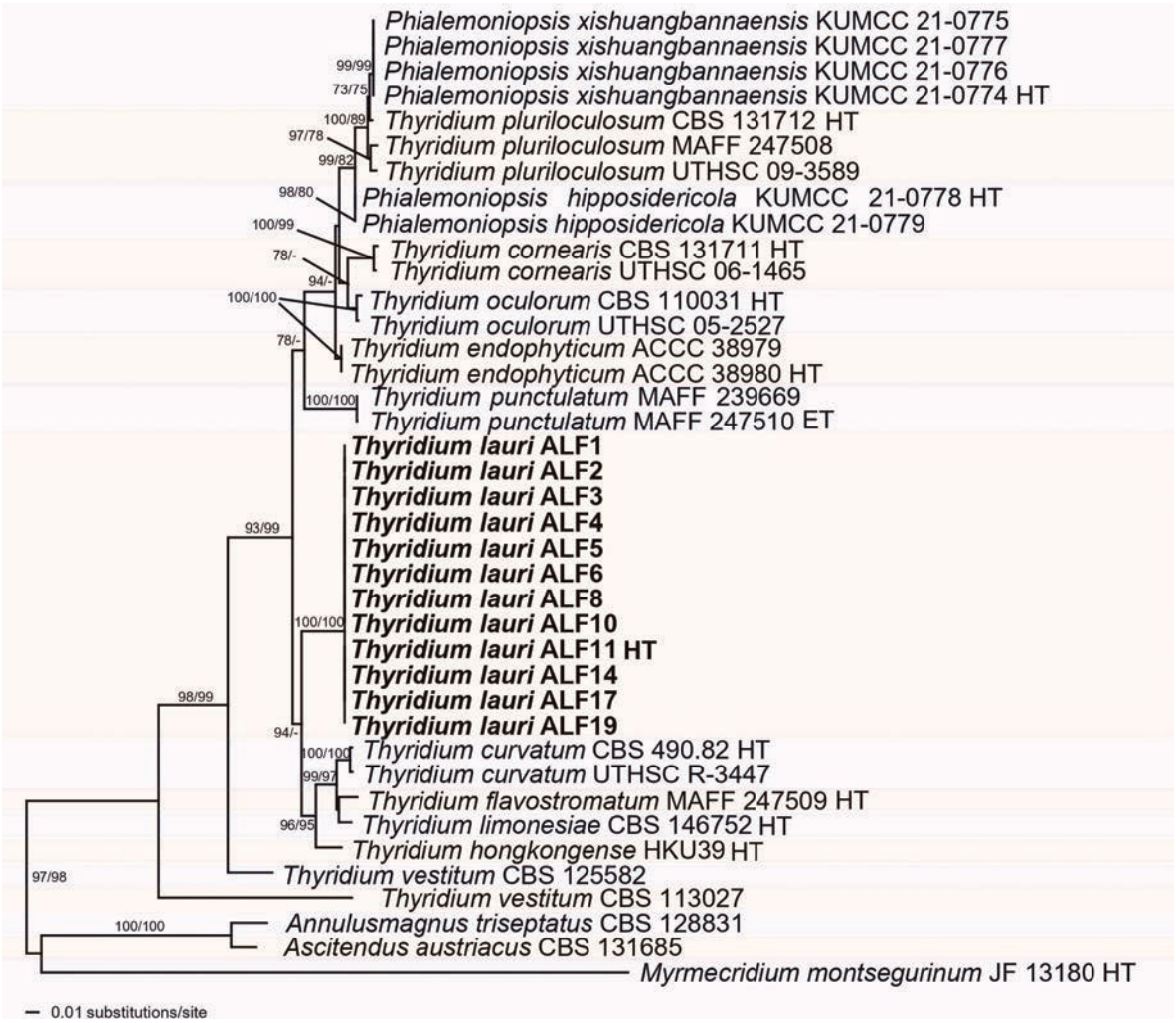

Figure 3. Phylogram of the best ML tree (-lnL = 13574.613578) revealed by RAxML from an analysis of the combined ITS-LSU-*act1-rpb2-tef1-tub2* matrix of *Thyridium*, showing the phylogenetic position of the new species from diseased *Laurus nobilis* (bold), with *Annulusmagnus triseptatus*, *Ascitendus austriacus* and *Myrmecridium montsegurinum* selected as outgroup to root the tree. Maximum Likelihood (ML) and Maximum Parsimony (MP) bootstrap support above 70% are given at first and second position, respectively, above or below the branches. ET = epitype; HT = holotype.

Pathogenicity test

The pathogenicity test confirmed that the new *Thyridium* species is pathogenic to bay laurel, causing internal necrosis and stem blight of all inoculated plants. The initial visible external symptoms included brown to black necrotic lesions at the inoculation site (Fig. 4), followed by the development of stem blight within four months. Internally, plants exhibited discoloration, characterized by brownish to blackish streaking in the sapwood, with a mean lesion length of 16.6 ± 7.1 cm. In addition, some inoculated and control plants exhibited brown exudates, which over time became crusty and adherent to the bark as a response to mechanical damage. Control plants displayed no internal symptoms, aside from minor wound oxidation. *Thyridium* was consistently re-isolated from necrotic tissue but was absent in the control treatments. The re-isolation frequency was 94%, and the emerging fungal colonies matched the originally inoculated *Thyridium* isolates based on morphological observations of the colony and conidia. Therefore, Koch's postulates were fulfilled.

Figure 4. Pathogenicity test on bay laurel **A** stems inoculated with *Thyridium lauri* isolate ALF11, showing symptoms of external lesion **B** internal necrosis with brownish to blackish streaking in the sapwood **C** control plant inoculated with sterile PDA.

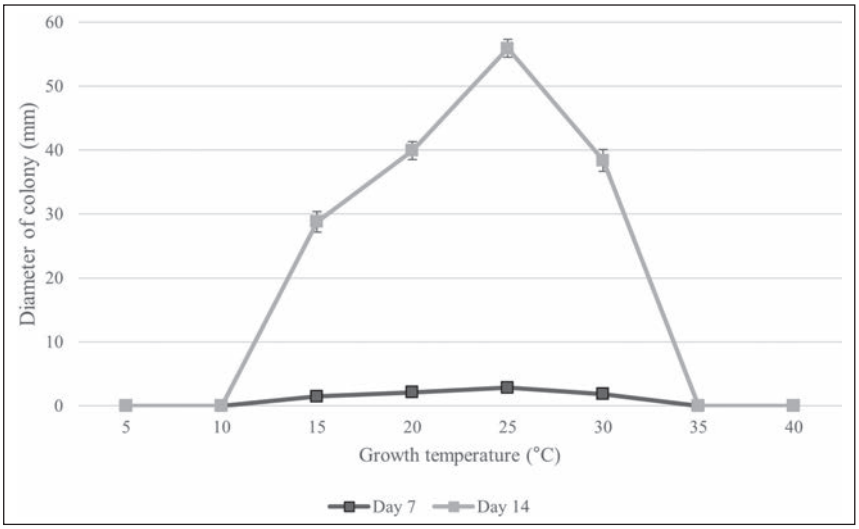

Figure 5. Effect of temperature on mycelial growth rate of *Thyridium lauri* ALF11 isolated from bay laurel. Data are means of five replicated Petri plates with bars indicating the standard error (SE).

Growth rate experiments

The growth rate experiments of *T. lauri* isolate ALF11 are shown in Fig. 5. The fungus grew slowly at 15 °C (29 mm diameter after 14 days). No mycelial growth was observed at 0, 5, 10, 35, and 40 °C while optimal growth occurred within the temperature range of 20 to 30 °C.

Taxonomy

***Thyridium lauri* Voglmayr, D. Aiello & G.R. Leonardi, sp. nov.**
MycoBank No: 854792
Figs 6, 7

Etymology. Referring to its host, *Laurus nobilis*.

Type. Italy • Sicily, Catania province, plant nursery located in Mascali, 37°44.85'N, 15°12.25'E, isolated from diseased corticated twigs of *Laurus nobilis*, 23 June 2021, G. Polizzi (holotype WU-MYC 0052725 dried culture; ex-holotype culture ALF11 = CBS 151898).

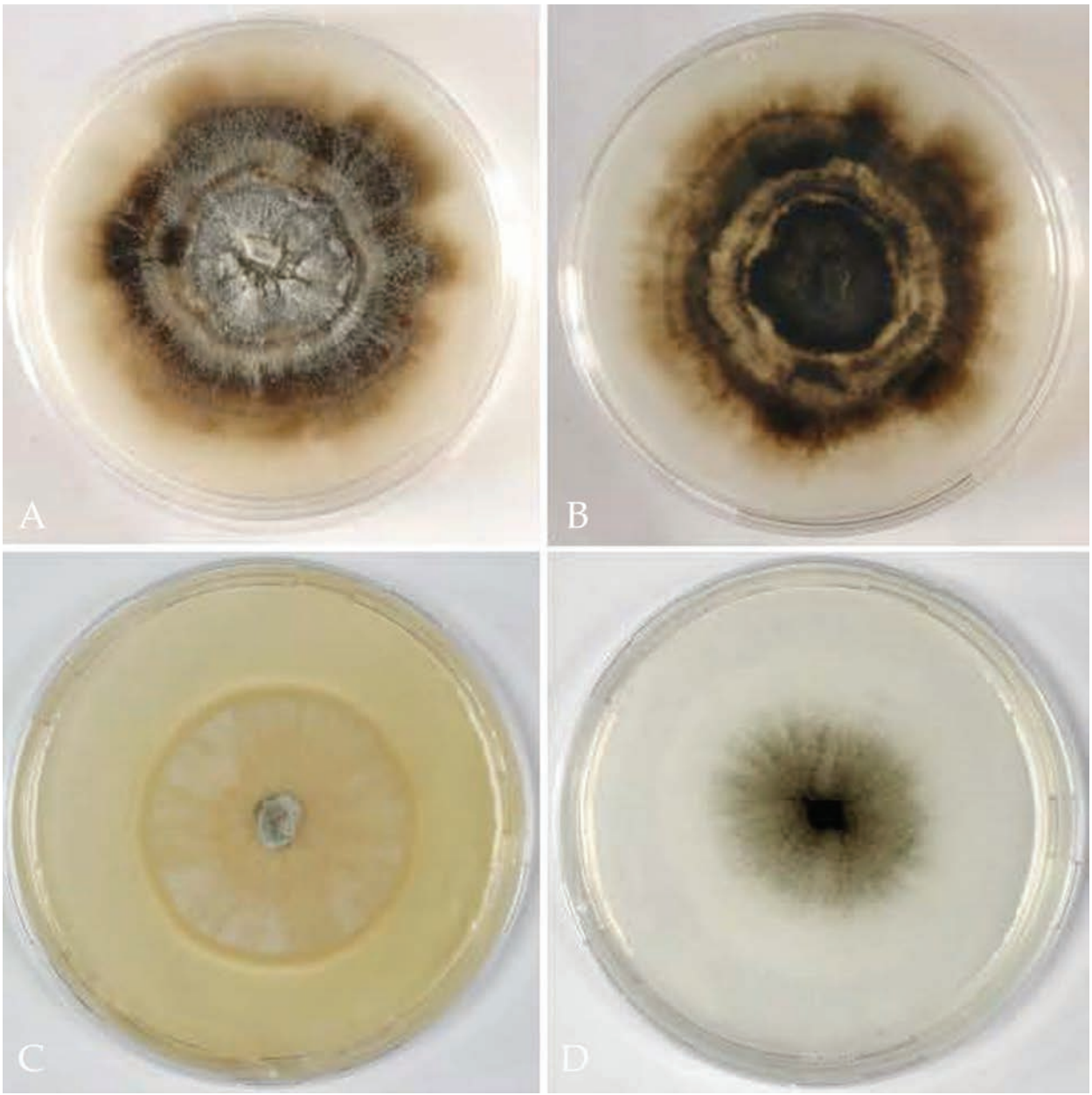

Figure 6. Colonies of *Thyridium lauri* (ALF 11, ex-holotype culture) **A** on PDA (1 month, 22 °C) **B** on PDA (1 month, 22 °C), reverse **C** on ½ PDA (21 days, 22 °C) **D** on CMD (21 days, 22 °C).

Description. On PDA reaching 54–56 mm diameter after 21 days, first pale creamy to yellowish, cottony in the centre, with dense whitish aerial mycelium after 14 days, after 1 month colonies ochraceous to umber brown in the centre, with distinct concentric lighter and darker zones, aerial mycelium white or grayish in the centre, sparse or lacking towards the margins, forming dry effused patches of branched aerial conidiophores interspersed with spot-like to effused patches of densely branched conidiophores immersed in white to cream slimy conidial masses; reverse dark umber brown in the centre, with lighter and darker brown concentric zones towards the margins. On CMD reaching 59–62 mm diameter after 21 days, colonies first whitish, from the centre becoming greenish brown with age, finally blackish brown in the centre, aerial mycelium sparse to absent, with scant erect branched conidiophores and strands of aggregated radial hyphae on the agar surface. Sporodochia and pycnidia not observed. Conidiation of three types, all of (sub)hyaline, thin-walled cells: (1) on tufts of aerial, several times loosely branched conidiophores, with straight elongate hyphal conidiophore cells and cylindrical to narrowly-ampulliform terminal or lateral conidiogenous cells (phialides) of variable length up to 50 µm long, producing conidia terminally; (2) on densely branched, interwoven-aggregated conidiophores, with knobby to sinuous conidiophore cells and terminal or lateral conidiogenous cells (polyphialides) of variable, irregular flexuous-knobby shape, 4–18 × 1.2–3.6 µm (n = 155), forming conidia terminally and/or laterally; and (3) on straight to bent adelophialides formed singly on hyphae at more or less right angles, 1–13 × 0.7–1.8 µm (n = 56), with a tiny pericline apical thickening, but without visible collarettes. Conidia hyaline to subhyaline, thin-walled, of two types: (1) subglobose to broadly ellipsoid, uni- to irregularly multiguttulate, commonly aggregated in spot-like to effuse slimy masses, produced on the branched conidiophore type (2), (2.2–)3.0–3.8(–4.8) × (2.0–)2.3–3.0(–3.7) µm, l/w = (1.0–)1.2–1.5(–1.9) (n = 211); (2) elongate, ellipsoid to allantoid, mostly biguttulate with a guttule near each end, mainly borne from adelophialides but also on conidiophore type (1), (2.3–)3.0–4.0(–4.9) × (1–)1.3–2.0(–2.8) µm, l/w = (1.2–)1.8–2.8(–4.0) (n = 169). Subglobose to broadly ellipsoid conidia mainly produced in masses on PDA in older parts of the colony; elongate to allantoid conidia commonly observed on CMD, more rarely on PDA, produced within 3–4 days mainly in the actively growing younger parts of the colony. On inoculation plugs of PDA cultures placed on CMD yeast-like cells observed 3 to 4 days after inoculation, developing by budding at one or two ends from swollen subglobose conidia. Sexual morph unknown.

Additional specimens examined. Italy • Sicily, Catania province, plant nursery located in Giarre, 37°41.81'N, 15°11.52'E, isolated from twig necrosis of *Laurus nobilis*, 10 June 2021, G. Polizzi (WU-MYC 0052726, dried culture ALF2; CBS 151896); • Catania province, plant nursery located in Giarre, 37°41.81'N, 15°11.52'E, isolated from twig necrosis of *Laurus nobilis*, 10 June 2021, G. Polizzi (WU-MYC 0052727, dried culture ALF6; CBS 151897).

Based on the results of molecular phylogenies (Fig. 3) and the synonymy of *Phialemoniopsis* with *Thyridium* two recently described *Phialemoniopsis* species are here combined in *Thyridium*.

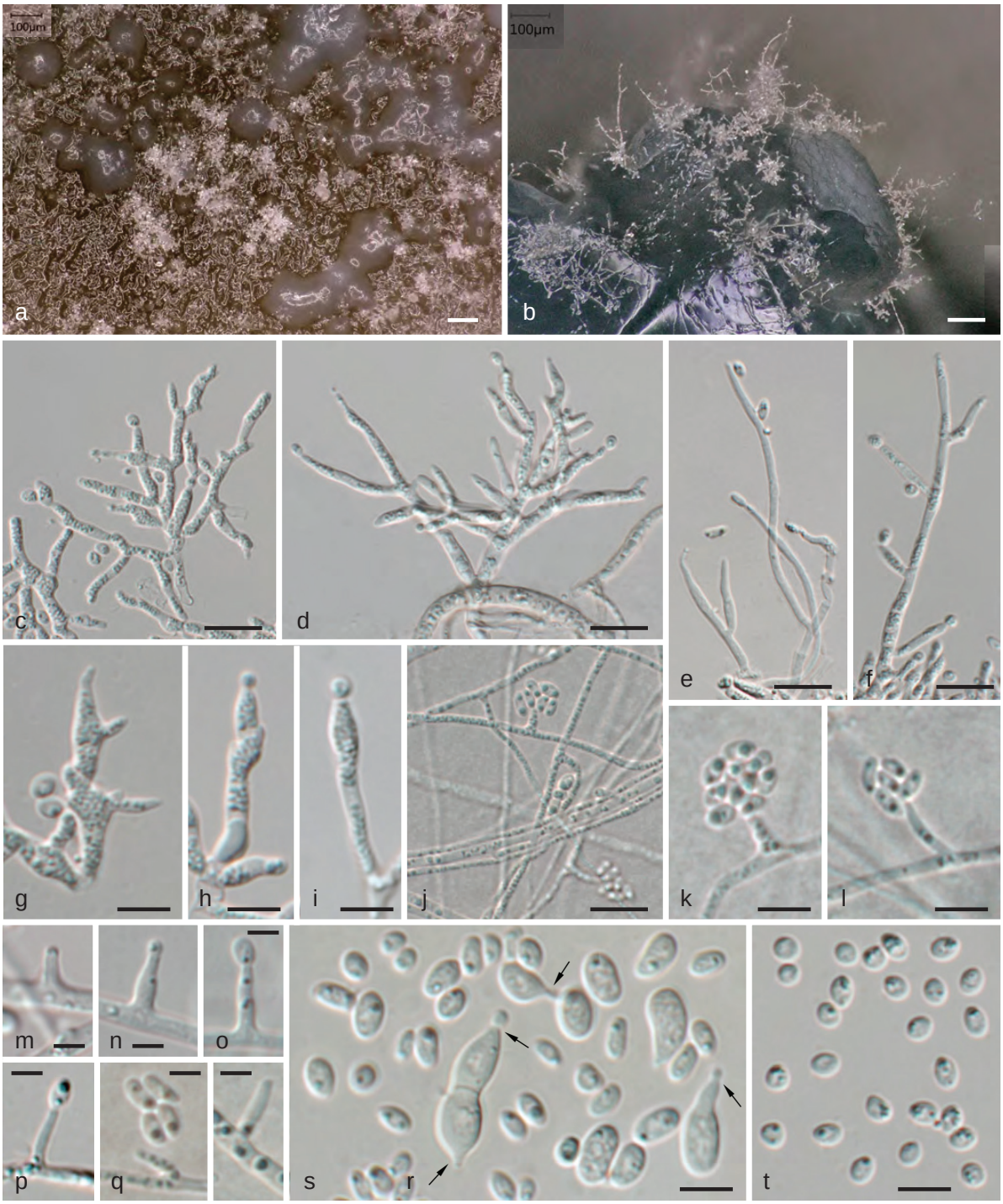

Figure 7. Morphology of *Thyridium lauri* (**a–c, e–h, t.** ALF6; **d, i, j, k, m–o, r, s.** ALF11; **l, p, q.** ALF2) **a** tufts of aerial conidiophore type 1 interspersed with patches of conidiophore type 2 submerged in slimy conidal masses (PDA, 1 month) **b** inoculation plug of PDA culture on CMD showing branched aerial conidiophore type 1 (11 days) **c** densely branched conidiophore type 2, showing flexuous-knobby conidiophore cells and irregular terminal and lateral conidiogenous cells (PDA, 1 month) **d–f** loosely branched conidiophore type 1 showing straight terminal and lateral conidiophore and conidiogenous cells (PDA, 1 month) **g, h** irregular conidiogenous cells from conidiophore type 2, showing terminal and lateral conidiation (PDA, 1 month) **i** ampulliform conidiogenous cell from conidiophore type 1 (CMD, 11 days) **j** surface mycelium with hyphal strand and adelophialides with ellipsoid-allantoid conidia (CMD, 11 days) **k–r** adelophialides on hyphae with ellipsoid-allantoid conidia (**k, l, p–r** CMD, 11 days; **m–o** PDA, 3 days) **s** swollen conidia showing yeast-like budding (arrows; PDA plug on CMD, 3 days) **t** subglobose conidia from conidiophore type 2 (PDA, 1 month). All from pure cultures grown at 22 °C. Scale bars: 100 µm (**a, b**); 10 µm (**c–f, j**); 5 µm (**g–i, k, l, s, t**); 3 µm (**m–r**).

Thyridium hipposidericola **(Karun., Tibpromma & X.F. Liu) Voglmayr, comb. nov.**
MycoBank No: 854793

Phialemoniopsis hipposidericola Karun., Tibpromma & X.F. Liu, in Liu et al. (2023). Basionym.

Thyridium xishuangbannaense **(Karun., Tibpromma & X.F. Liu) Voglmayr, comb. nov.**
MycoBank No: 854794

Phialemoniopsis xishuangbannaensis Karun., Tibpromma & X.F. Liu, in Liu et al. (2023). Basionym.

Discussion

This study revealed stem blight of bay laurel in Southern Italy as being associated with a new fungal species within the genus *Thyridium* (Sordariomycetes, Thyridiaceae). The isolates obtained from symptomatic tissues were identified based on the morphological characteristics and molecular phylogenetic analyses of the ITS, LSU, *act1*, *rpb2*, *tef1*, and *tub2* gene regions. Recently, Sugita and Tanaka (2022) provided a phylogenetic treatise on the genus *Thyridium*, which included the same six loci sequenced in our study. Molecular evidence and morphological similarities in the asexual morph revealed that the anamorph genus *Phialemoniopsis* is congeneric with *Thyridium*, leading to the reclassification of eight *Phialemoniopsis* species into *Thyridium* (Sugita and Tanaka 2022). Currently, molecular data for 10 *Thyridium* species and 2 *Phialemoniopsis* species originating from different substrates, including humans, animals, and plants, are available in GenBank. According to Index Fungorum (https://www.indexfungorum.org/Names/Names.asp; Accessed April 19, 2024), a total of 65 *Thyridium* species have been described, of which 44 are currently recognised within the genus *Thyridium*. However, sequence data are not yet available for the majority of these species, with 34 lacking molecular information. Two species of *Phialemoniopsis*, *P. hipposidericola* and *P. xishuangbannaensis*, recently described from bats in Southern China (Liu et al. 2023), are also classified within *Thyridum* based on molecular phylogenies (Fig. 3) and are therefore combined in *Thyridium* in this study.

In this study, the sequenced isolates formed a clade that is significantly distinct from all known *Thyridium* species with available sequence data, and are therefore described as a new species, *T. lauri*. Our isolates are phylogenetically close to *T. curvatum*, *T. flavostromatum*, *T. hongkongense*, and *T. limonesiae*, which were recovered from parts of human body (Perdomo et al. 2013; Tsang et al. 2014) or associated with human infections (Perdomo et al. 2013; Alvarez Martinez et al. 2021). *Thyridium lauri* shares similar morphological characteristics with other *Thyridium* species, with only minimal distinct traits observed. Nevertheless, the newly proposed species does not produce pycnidium-like conidiomata or chlamydospores unlike many phialemoniopsis-like asexual morphs of *Thyridium*. Similarly, no pycnidium-like conidiomata or chlamydospores have been observed in *T. curvatum* (Perdomo et al. 2013), *T. hongkongense* (Tsang et al. 2014), and *T. limonesiae* (Alvarez Martinez et al. 2021). *Thyridium lauri*

is characterised by the production of subglobose conidia aggregated in slimy masses and of yeast-like cells developing by budding from the same type of conidia. Moreover, it can be morphologically distinguished from the other species of the sister clade. The new species is distinguished from *T. hongkongense* by its larger elongate, ellipsoid to allantoid conidia (2.3–4.9 × 1.3–2.8 µm), while conidia of *T. hongkongense* are small, cylindrical, oval or rod- shaped, and slightly curved (2–3 × 1–2 µm) (Tsang et al. 2014). Similarly, *T. limonesiae* produces shorter cylindrical or oval conidia (2.3–4.9 × 1.4–2 µm) (Alvarez Martinez et al. 2021). Although *T. lauri* appears quite similar to *T. curvatum* in producing two types of conidia, *T. curvatum* is distinguished by its longer allantoid conidia (4–6 × 1–2 µm), shorter ellipsoid to ovoid conidia (1–2 × 0.5–1), and the presence of sporodochial conidiomata which were not found in *T. lauri* or *T. flavostromatum* (Perdomo et al. 2013). Within this sister group, *T. flavostromatum* produces the longest ellipsoid to allantoid conidia (2–7 × 1–2.5 µm) (Sugita and Tanaka 2022), characterised by a slightly apiculate base. Unlike *T. lauri*, *T. flavostromatum* produces solitary clamydospores.

In addition to the morphological characteristics, *T. lauri* can be distinguished from other species by its notable ecological traits. The new species was isolated from two different locations in Sicily, from the same host, and was confirmed to be pathogenic to bay laurel, as demonstrated by our pathogenicity tests. Notably, several anamorphic *Thyridium* species have been reported as opportunistic human pathogens, including *T. curvatum*, *T. hongkongense*, *T. limonesiae*, *T. oculorum*, *T. pluriloculosum* (Gams and McGinnis 1983; Rivero et al. 2009; Desoubeaux et al. 2014; Tsang et al. 2014; Alvarez Martinez et al. 2021; Patolia and Bansal 2021). These species have also been isolated from various environments, including soil samples (*T. curvatum*) (Perdomo et al. 2013), diesel fuel tank (*T. curvatum*) (Varaljay et al. 2019), seawater samples (*T. pluriloculosum*) (Taha et al. 2021), and marine sediment (*T. oculorum*) (Mahanty et al. 2019). A few *Thyridium* species reported as human pathogens have also been isolated from plant material at different reproductive stages. For example, *T. pluriloculosum* originally found in human nails as an asexual fungus (Perdomo et al. 2013) and reported to cause human infections (Patolia and Bansal 2021), was later rediscovered in its sexual state on the twigs of *Betula maximowicziana* (Sugita and Tanaka 2022). Other *Thyridium* species were isolated from plants (*T. curvatum*, *T. endophyticum*, *T. flavostromatum*, *T. punctulatum*) as non-pathogenic endophytes or saprobes (Halleen et al. 2007; Kaur et al. 2014; Su et al. 2016; Sugita and Tanaka 2022). Among these, *T. curvatum* and *T. oculorum* were also isolated from asymptomatic nursery material and young grapevines affected by Petri disease, respectively, but their importance in the grapevine decline has not yet been confirmed (Halleen et al. 2007; Ferreira et al. 2018). It is important to note that several *Thyridium* species, yet to be sequenced, have been described as sexual morphs from dead plant tissues. A review of the literature reveals that a single species, *T. nobile*, was recorded from twigs of a member of Laureaceae, *Laurus novocanariensis* (Petrak 1929). According to the USDA Fungus-Host database (https://fungi.ars.usda.gov; Accessed April 19, 2024), *Thyridium* has been recorded neither from *Laurus nobilis* nor from other Lauraceae. We are therefore confident that our species has not yet been described. The observed morphological differences, combined with the phylogenetic analyses and ecological characteristics, support the classification of these isolates as a new species.

The pathogenicity tests on bay laurel demonstrated that *T. lauri* is responsible for causing necrotic lesions in the stems, ultimately leading to stem blight. However, *Xylosandrus compactus* may also play a significant role in the development of symptoms. Notably, during our surveys, the symptoms of stem blight observed in bay laurel were consistently associated with the presence of entry holes and galleries created by the adults of the invasive ambrosia beetle, *X. compactus*.

As reported by several authors, the tunnelling activity in the wood, which disrupts the transport of water and nutrients, along with the introduction of ambrosia fungi presumed to be pathogenic to the host trees, likely contributes to the severe stem blight or even death of the plants (Ngoan et al. 1976; Paine et al. 1997; Bosso et al. 2012; Pennacchio et al. 2012; Greco and Wright 2015). In 2011, *X. compactus* was first recorded for Europe (Garonna et al. 2012) in urban parks of the Campania region in Italy. In Sicily, this ambrosia beetle was mainly found infesting carob trees (Gugliuzzo et al. 2019a), while in other regions of Italy it has also been found infesting many other host plants, including bay laurel (Francardi et al. 2012; Bateman et al. 2016; Vannini et al. 2017). As the crucial role of arthropods in disease epidemiology has been increasingly recognized worldwide (Moyo et al. 2014; Cruz et al. 2021; Heitmann et al. 2021; Berasategui et al. 2022; Lunde et al. 2023), it cannot be excluded that the beetles may actively disseminate the fungal propagules, or alternatively provide entry points for secondary fungal infections (Brader 1964). However, specific investigations are needed to verify these hypotheses. Previous studies have demonstrated that *X. compactus* inhabits the xylem, where it introduces specific mutualistic symbiotic fungi on which it relies for nutrition. The most consistently associated symbiotic fungal species, isolated from *X. compactus* and its several hosts worldwide, were *Ambrosiella xylebori* Brader ex Arx & Hennebert, *A. macrospora* (Francke-Grosm.) L.R. Batra, and *Fusarium* spp. (Muthappa and Venkatasubbaiah 1981; Bhat and Sreedharan 1988; Bosso et al. 2012; Bateman et al. 2016; Gugliuzzo et al. 2020, 2021). In this study, *Ambrosiella*-like colonies were isolated from symptomatic woody tissues in addition to *T. lauri*. In contrast, previous investigations did not reveal the presence of *Thyridium* involved in stem blight and internal necrosis associated with *X. compactus* (Vannini et al. 2017; Gugliuzzo et al. 2020; Benvenuti et al. 2021; Morales-Rodríguez et al. 2021; Vitale et al. 2022). However, some unidentified *Phialemonium* sp. and *Phialemoniopsis* sp. isolates were recorded in previous studies evaluating the fungal communities of *X. compactus* in the United States (Bateman et al. 2016) and Italy (Gugliuzzo et al. 2020). The ITS sequence of *Phialemonium* isolate Hulcr5398 (KU961666) (Bateman et al. 2016) matched very closely with *T. oculorum* (previously *Phialemoniopsis ocularis*, OR760549, HG933293), with a percentage identity of 99.6% in the BLAST search results. Moreover, phylogenetic analyses of the *Phialemonium* sp. isolate in our multigene matrix revealed that it was nested within the *T. oculorum* clade (data not shown), confirming its placement within *Thyridium*, although phylogenetically distant from *T. lauri*. While *Phialemoniopsis* and *Phialemonium* share highly similar morphologies, they phylogenetically belong to two distinct families within Sordariomycetes, Thyridiaceae and Cephalothecaceae, respectively (Perdomo et al. 2013; Hongsanan et al. 2017; Davolos et al 2019). Isolates morphologically identified as *Phialemonium* may, in fact, represent *Phialemoniopsis*, which is now considered a synonym of *Thyridium* (Sugita and Tanaka 2022).

One interesting finding is that the ITS of *Phialemoniopsis* isolate 50 (ON520570) (Gugliuzzo et al. 2020) was identical to *Thyridium* sp. (PP683252), and it matched very closely with *Phialemoniopsis* sp. isolates V18210, V18211, V18170, V18171 (ON413722, ON413723, ON415520, ON415521) and *Acremonium* sp. isolates Hulcr5037 (KU961664) and PB_AG_03 (OQ513933), with percentage identity ranging from 99 to 99.44% in the BLAST search results. Furthermore, phylogenetic analyses of the *Phialemonium* and *Acremonium* isolates in our multigene matrix, for which ITS and three LSU sequences are available in GenBank, showed that these isolates were nested within the *T. lauri* clade with high support (data not shown). This strongly suggests that they are members of *Thyridium* and are presumably very closely related, if not the same species. The *Acremonium* isolates Hulcr5037 and PB_AG_03, isolated from *X. compactus* in the United States (Bateman et al. 2016) and from *X. germanus* in Germany (Gugliuzzo et al. 2023b), respectively, were also reported to be one of the most prevalent fungi isolated from these beetles. However, their characterisation was based solely on the ITS sequences (Bateman et al. 2016; Gugliuzzo et al. 2023b). The other *Phialemoniopsis* sequences in GenBank that are highly similar to our ITS sequences originated from an unpublished study on fungi associated with *X. compactus* in the USA (ON413722, ON413723) and China (ON415520, ON415521). These remarkable findings suggest that the association of *T. lauri* and closely related fungal species with the beetle could be more widespread and stable, rather than attributed to a recent acquisition by the beetle from another host in the same area or to a recent introduction from other countries. The misidentification of the fungi commonly isolated from *X. compactus* may be attributed to the fact that earlier studies relied solely on ITS sequences, which were the only data available at the time, and *T. lauri* had not yet been described. This study enhances our understanding of the *Thyridium-Xylosandrus* association, and future multi-locus analyses of *Phialemoniopsis* and *Acremonium* isolates are necessary to accurately distinguish these species.

Interestingly, we observed a yeast-like phase of *T. lauri* when subcultured on a new medium, especially on inoculation plugs during the initial growth of the colony. It is known that symbiotic fungi of ambrosia beetles have evolved in a phase that facilitates the dissemination through the insect (Cassar and Blackwell 1996; Nel et al. 2021; Mayers et al. 2022). Several studies have demonstrated that ambrosia fungi are dimorphic, exhibiting both a mycelial phase and a yeast-phase, also referred to as the sprout-cell phase (Batra 1967). Specifically, *Harringtonia lauricola*, *Ceratocystis lunata*, and *Raffaela promiscua* have been reported in association with *Xyleborus affinis*, *Xylosandrus crassiusculus*, and *Xyleborinus saxesenii*, respectively, undergoing the dimorphic transition from filamentous to yeast-like growth, which was also observed *in vitro* (Batra 1967; Nel et al. 2021; Mayers et al. 2022; Joseph et al. 2023). This finding suggests that the newly described species may have a predisposition for developing associations with arthropods. In conclusion, this study identified a new pathogenic fungal species, *Thyridium lauri* sp. nov., responsible for causing stem blight and internal necrosis, in association with *X. compactus* infestations on bay laurel in Italy.

However, the ecological role of this fungus and its interaction with the beetle remain unclear. Further investigations are necessary to: (i) determine whether

X. compactus plays a role in the dissemination of *T. lauri* spores by isolating *T. lauri* from *X. compactus* adults infesting bay laurel and fulfilling Leach's postulates (Hulcr et al. 2020); and (ii) elucidate the potential symbiotic association between *T. lauri* and *X. compactus*.

Acknowledgement

The authors thank Dr. Alberto Fiorenza for his precious help during the laboratory and field procedures.

Additional information

Conflict of interest

The authors have declared that no competing interests exist.

Ethical statement

No ethical statement was reported.

Funding

This research was funded by Programma Ricerca di Ateneo MEDIT-ECO UNICT 2023-2024 Linea 2-University of Catania (Italy).

Author contributions

Conceptualization: G.P., D.A. Methodology: H.V., D.A. Validation: D.A., H.V., G.P. Formal analysis: G.R.L, H.V. Investigation: G.P., A.G., D.A., G.R.L, C.D.P., H.V. Resources: G.P., D.A., H.V. Data curation: G.R.L., H.V. Writing—original draft preparation: G.R.L. Writing—review and editing: D.A., H.V., G.P., A.G, G.T.G. Visualization: G.R.L. Supervision: G.P., D.A., H.V. Project administration: G.P., D.A. Funding acquisition: G.P., D.A. All authors have read and agreed to the published version of the manuscript.

Author ORCIDs

Giuseppa Rosaria Leonardi https://orcid.org/0000-0002-4676-5100
Dalia Aiello https://orcid.org/0000-0002-6018-6850
Chiara Di Pietro https://orcid.org/0009-0005-5746-8389
Antonio Gugliuzzo https://orcid.org/0000-0002-4118-2280
Giovanna Tropea Garzia https://orcid.org/0000-0002-2161-7021
Giancarlo Polizzi https://orcid.org/0000-0001-8630-2760
Hermann Voglmayr https://orcid.org/0000-0001-7666-993X

Data availability

The data obtained in this study are available in the main text and have been publicly uploaded to NCBI GenBank and MycoBank.

References

Alvarez Martinez D, Alberto C, Riat A, Schuhler C, Valladares P, Ninet B, Kraak B, Crous PW, Hou LW, Toutous Trellu L (2021) *Phialemoniopsis limonesiae* sp. nov. causing cutaneous phaeohyphomycosis in an immunosuppressed woman. Emerging Microbes & Infections 10(1): 400–406. https://doi.org/10.1080/22221751.2021.1892458

Barnouin T, Soldati F, Roques A, Faccoli M, Kirkendall LR, Mouttet R, Daubree JB, Noblecourt T (2020) Bark beetles and pinhole borers recently or newly introduced to France (Coleoptera: Curculionidae Scolytinae and Platypodinae). Zootaxa 4877(1): 51–74. https://doi.org/10.11646/zootaxa.4877.1.2

Bateman C, Sigut M, Skelton J, Smith KE, Hulcr J (2016) Fungal associates of the *Xylosandrus compactus* (Coleoptera: Curculionidae Scolytinae) are spatially segregated on the insect body. Environmental Entomology 45(4): 883–890. https://doi.org/10.1093/ee/nvw070

Batool S, Khera RA, Hanif MA, Ayub MA (2020) Bay Leaf. In: Hanif MA, Khan MM, Nawaz H, Byrne HJ (Eds) Medicinal plants of South Asia: novel sources for drug discovery. Elsevier, Amsterdam, 63–74. https://doi.org/10.1016/B978-0-08-102659-5.00005-7

Batra LR (1967) Ambrosia Fungi: A taxonomic revision and nutritional studies of some species. Mycologia 59(6): 976–1017. https://doi.org/10.1080/00275514.1967.12018485

Benvenuti C, Strangi A, Iovinella I, Barzanti GP, Simoni S, Vitale S, Luongo L, Francardi V, Roversi PF (2021) *Xylosandrus compactus* and *Liparthrum colchicum* (Coleoptera Scolytinae) in Tuscany: A preliminary screening of associated fungi. Redia–Journal of Zoology 104: 139–146. https://doi.org/10.19263/REDIA-104.21.14

Berasategui A, Breitenbach N, García-Lozano M, Pons I, Sailer B, Lanz C, Rodríguez V, Hipp K, Ziemert N, Windsor D, Salem H (2022) The leaf beetle *Chelymorpha alternans* propagates a plant pathogen in exchange for pupal protection. Current Biology 2(19): 4114–4127. https://doi.org/10.1016/j.cub.2022.07.065

Bhat SS, Sreedharan K (1988) Association of *Ambrosiella xylebori* Brader with the shothole borer *Xylosandrus compactus* Eichhoff a pest of robusta coffee. Journal of Caffeine Research 18: 54–57.

Bosso L, Senatore M, Varlese R, Ruocco M, Garonna AP, Bonanomi G, Mazzoleni S, Cristinzio G (2012) Severe outbreak of *Fusarium solani* on *Quercus ilex* vectored by *Xylosandrus compactus*. Journal of Plant Pathology 94: S485–S4105.

Brader L (1964) Etude de la relation entre le scolyte des rameaux du caféier *Xylosandrus compactus* Eichh (*X. morstatti* Hag) et sa plante-hôte. PhD Thesis, Wageningen University, Wageningen, The Netherlands.

Carbone I, Kohn L (1999) A method for designing primer sets for speciation studies in filamentous ascomycetes. Mycologia 91(3): 553–556. https://doi.org/10.1080/00275514.1999.12061051

Cassar S, Blackwell M (1996) Convergent origins of ambrosia fungi. Mycologia 88(4): 596–601. https://doi.org/10.1080/00275514.1996.12026690

Contarini M, Vannini A, Giarruzzo F, Faccoli M, Morales-Rodriguez C, Rossini L, Speranza S (2020) First record of *Xylosandrus germanus* (Blandford) (Coleoptera: Curculionidae Scolytinae) in the Mediterranean scrubland in Southern Italy and its co-presence with the co-generic species *X. compactus* (Eichhoff) and *X. crassiusculus* (Motschulsky). Bulletin OEPP. EPPO Bulletin. European and Mediterranean Plant Protection Organisation 50(2): 311–315. https://doi.org/10.1111/epp.12660

Cruz LF, Menocal O, Kendra PE, Carrillo D (2021) Phoretic and internal transport of *Raffaelea lauricola* by different species of ambrosia beetle associated with avocado trees. Symbiosis 84(2): 151–161. https://doi.org/10.1007/s13199-021-00776-2

Davolos D, Pietrangeli B, Persiani AM, Maggi O (2019) *Victoriomyces antarcticus* gen. nov. sp. nov. a distinct evolutionary lineage of the Cephalothecaceae (Ascomycota) based on sequence-based phylogeny and morphology. International Journal of Systematic and Evolutionary Microbiology 69(4): 1099–1110. https://doi.org/10.1099/ijsem.0.003275

Desoubeaux G, García D, Bailly E, Augereau O, Bacle G, De Muret A, Bernard L, Cano-Lira JF, Garcia-Hermoso D, Chandenier J (2014) Subcutaneous phaeohyphomycosis due to *Phialemoniopsis ocularis* successfully treated by voriconazole. Medical Mycology Case Reports 5: 4–8. https://doi.org/10.1016/j.mmcr.2014.04.001

Eaton MJ, Beale J, Long S, Dreaden TJ, Blevins A, Mayfield A, Buland M, Hadziabdic D, Crocker EV (2023) First report of laurel wilt caused by *Harringtonia lauricola* (previously *Raffaelea lauricola*) on northern spicebush in Kentucky and Tennessee. Plant Disease 107(4): 1221. https://doi.org/10.1094/PDIS-04-22-0868-PDN

Fang F, Sang S, Chen KY, Gosslau A, Ho CT, Rosen RT (2005) Isolation and identification of cytotoxic compounds from Bay leaf (*Laurus nobilis*). Food Chemistry 93(3): 497–501. https://doi.org/10.1016/j.foodchem.2004.10.029

Ferreira ABM, Leite LG, Hernandes JL, Harakava R, Padovani CR, Bueno CJ (2018) Colonization of vines by Petri disease fungi susceptibility of rootstocks to *Phaeomoniella chlamydospora* and their disinfection. Arquivos do Instituto Biológico 85(0). https://doi.org/10.1590/1808-1657000882017

FITOLAB (2011) *Xylosandrus compactus*. http://wwwagricolturaregionecampania.it/difesa/xylosandrus_2011html [accessed on 25 May 2024]

Francardi V, Pennacchio F, Santini L, Rumine P, Paoli A, Navarra A, Musetti N (2012) First report of *Xylosandrus compactus* on *Laurus nobilis* in Tuscany In: Giornate Fitopatologiche, Milano Marittima (Italy), March 2012.

Francardi V, Noal A, Francescato S, Pinto R, Bruni A, Loffredi L, Bucini D, Guarnieri D, Bellantuono M, Esposito N, Nuccitelli L, Binazzi F, Vitale S, Di Giambattistav G, Roversi PF, Pennacchio F (2017) Coexistence of *Xylosandrus crassiusculus* (Motschulsky) and *X. compactus* (Eichhoff) (Coleoptera Curculionidae Scolytinae) in the National Park of Circeo (Lazio Italy). Redia–Journal of Zoology 100: 149–155. https://doi.org/10.19263/REDIA-100.17.19

Gams W, McGinnis MR (1983) *Phialemonium* a new anamorph genus intermediate between *Phialophora* and *Acremonium.* Mycologia 75(6): 977–987. https://doi.org/10.1080/00275514.1983.12023783

Garonna AP, Dole SA, Saracino A, Mazzoleni S, Cristinzio G (2012) First record of the black twig borer *Xylosandrus compactus* (Eichhoff) (Coleoptera: Curculionidae Scolytinae) from Europe. Zootaxa 3251(1): 64–68. https://doi.org/10.11646/zootaxa.3251.1.5

Giacobbe A (1939) Ricerche geografiche ed ecologiche sul *Laurus nobilis* L. Archivio Botanico 15: 33–82.

Glass NL, Donaldson GC (1995) Development of primer sets designed for use with the PCR to amplify conserved genes from filamentous ascomycetes. Applied and Environmental Microbiology 61(4): 1323–1330. https://doi.org/10.1128/aem.61.4.1323-1330.1995

Greco EB, Wright MG (2015) Ecology biology and management of *Xylosandrus compactus* (Coleoptera: Curculionidae: Scolytinae) with emphasis on coffee in Hawaii. Journal of Integrated Pest Management 6(1): 7. https://doi.org/10.1093/jipm/pmv007

Gugliuzzo A, Criscione G, Garzia GT (2019a) Unusual behavior of *Xylosandrus compactus* (Coleoptera: Scolytinae) on carob trees in a mediterranean environment. Insects 10(3): 82. https://doi.org/10.3390/insects10030082

Gugliuzzo A, Criscione G, Siscaro G, Russo A, Tropea Garzia G (2019b) First data on the flight activity and distribution of the ambrosia beetle *Xylosandrus compactus* (Eichhoff) on carob trees in Sicily. Bulletin OEPP. EPPO Bulletin. European and Mediterranean Plant Protection Organisation 49(2): 340–351. https://doi.org/10.1111/epp.12564

Gugliuzzo A, Mazzeo G, Mansour R, Tropea Garzia G (2019c) Carob pests in the Mediterranean region: Bio-ecology natural enemies and management options. Phytoparasitica 47(5): 605–628. https://doi.org/10.1007/s12600-019-00766-7

Gugliuzzo A, Criscione G, Biondi A, Aiello D, Vitale A, Polizzi G, Tropea Garzia G (2020) Seasonal changes in population structure of the ambrosia beetle *Xylosandrus compactus* and its associated fungi in a southern Mediterranean environment. PLoS ONE 15(9): e0239011. https://doi.org/10.1371/journal.pone.0239011

Gugliuzzo A, Biedermann PH, Carrillo D, Castrillo LA, Egonyu JP, Gallego D, Haddi K, Hulcr J, Jactel H, Kajimura H, Kamata N, Meurisse N, Li Y, Oliver JB, Ranger CM, Rassati D, Stelinski LL, Sutherland R, Tropea Garzia G, Wright MG, Biondi A (2021) Recent advances toward the sustainable management of invasive *Xylosandrus* ambrosia beetles. Journal of Pest Science 94(3): 615–637. https://doi.org/10.1007/s10340-021-01382-3

Gugliuzzo A, Giuliano G, Rizzo R, Tropea Garzia G, Biondi A (2023a) Lethal and sublethal effects of synthetic and bioinsecticides toward the invasive ambrosia beetle *Xylosandrus compactus*. Pest Management Science 79(5): 1840–1850. https://doi.org/10.1002/ps.7365

Gugliuzzo A, Kreuzwieser J, Ranger CM, Tropea Garzia G, Biondi A, Biedermann PH (2023b) Volatiles of fungal cultivars act as cues for host-selection in the fungus-farming ambrosia beetle *Xylosandrus germanus*. Frontiers in Microbiology 14: 1151078. https://doi.org/10.3389/fmicb.2023.1151078

Hall TA (1999) BioEdit: A user-friendly biological sequence alignment editor and analysis program for Windows 95/98/NT. Nucleic Acids Symposium Series 41: 95–98.

Halleen F, Mostert L, Crous PW (2007) Pathogenicity testing of lesser-known vascular fungi of grapevines. Australasian Plant Pathology 36(3): 277–285. https://doi.org/10.1071/AP07019

Heitmann N, Glemnitz M, Lentzsch P, Platen R, Müller MEH (2021) Quantifying the role of ground beetles for the dispersal of *Fusarium* and *Alternaria* fungi in agricultural landscapes. Journal of Fungi 7(10): 863. https://doi.org/10.3390/jof7100863

Hızal E, Acer S, Altunışık S (2023) First record of the invasive alien species *Xylosandrus compactus* (Eichhoff) (Coleoptera: Curculionidae: Scolytinae) in Turkey. BioInvasions Records 12(1): 93–102. https://doi.org/10.3391/bir.2023.12.1.08

Hongsanan S, Maharachchikumbura SSN, Hyde KD, Samarakoon MC, Jeewon R, Zhao Q, Al-Sadi AM, Bahkali AH (2017) An updated phylogeny of Sordariomycetes based on phylogenetic and molecular clock evidence. Fungal Diversity 84(1): 25–41. https://doi.org/10.1007/s13225-017-0384-2

Hughes MA, Black A, Smith JA (2014) First report of laurel wilt caused by *Raffaelea lauricola* on bay laurel (*Laurus nobilis*) in the United States. Plant Disease 98(8): 1159–1159. https://doi.org/10.1094/PDIS-02-14-0194-PDN

Hughes MA, Riggins JJ, Koch FH, Cognato AI, Anderson C, Formby JP, Dreaden TJ, Ploetz RC, Smith JA (2017) No rest for the laurels: Symbiotic invaders cause un-precedented damage to southern USA forests. Biological Invasions 19(7): 2143–2157. https://doi.org/10.1007/s10530-017-1427-z

Hulcr J, Barnes I, De Beer ZW, Duong TA, Gazis R, Johnson AJ, Jusino MA, Kasson MT, Li Y, Lynch S, Mayers C, Musvuugwa T, Roets F, Seltmann KC, Six D, Vanderpool D, Villari C (2020) Bark beetle mycobiome: Collaboratively defined research priorities on a widespread insect-fungus symbiosis. Symbiosis 81(2): 101–113. https://doi.org/10.1007/s13199-020-00686-9

Jaklitsch WM (2009) European species of *Hypocrea* – Part I The green-spored species. Studies in Mycology 63: 1–91. https://doi.org/10.3114/sim.2009.63.01

Jaklitsch WM, Komon M, Kubicek CP, Druzhinina IS (2005) *Hypocrea voglmayrii* sp. nov. from the Austrian Alps represents a new phylogenetic clade in *Hypocrea*/*Trichoderma*. Mycologia 97(6): 1365–1378. https://doi.org/10.1080/15572536.2006.11832743

Jordal BH, Kirkendall LR, Harkestad K (2004) Phylogeny of a Macaronesian radiation: Host-plant use and possible cryptic speciation in *Liparthrum* bark beetles. Molecular Phylogenetics and Evolution 31(2): 554–571. https://doi.org/10.1016/j.ympev.2003.09.008

Joseph R, Bansal K, Keyhani NO (2023) Host switching by an ambrosia beetle fungal mutualist: Mycangial colonization of indigenous beetles by the invasive laurel wilt fungal pathogen. Environmental Microbiology 25(10): 1894–1908. https://doi.org/10.1111/1462-2920.16401

Kaur A, Rogers KD, Swenson DE, Dowd PF, Wicklow DT, Gloer JB (2014) Bioactive natural products from fungicolous Hawaiian isolates: Secondary metabolites from a *Phialemoniopsis* sp. Mycology 5(3): 120–129. https://doi.org/10.1080/21501203.2014.931309

Kolarík M, Kubátová A, Pažoutová S, Šrûtka P (2004) Morphological and molecular characterisation of *Geosmithia putterillii G. pallida* comb. nov. and *G. flava* sp. nov. associated with subcorticolous insects. Mycological Research 108(9): 1053–1069. https://doi.org/10.1017/S0953756204000796

Kolařík M, Kostovčík M, Pažoutová S (2007) Host range and diversity of the genus *Geosmithia* (Ascomycota: Hypocreales) living in association with bark beetles in the Mediterranean area. Mycological Research 111(11): 1298–1310. https://doi.org/10.1016/j.mycres.2007.06.010

Liu YJ, Whelen S, Hall BD (1999) Phylogenetic relationships among ascomycetes: Evidence from an RNA polymerse II subunit. Molecular Biology and Evolution 16(12): 1799–1808. https://doi.org/10.1093/oxfordjournals.molbev.a026092

Liu XF, Tibpromma S, Hughes AC, Chethana KWT, Wijayawardene NN, Dai DQ, Du TY, Elgorban AM, Stephenson SL, Suwannarach N, Xu JC, Lu L, Xu RF, Maharachchikumbura SSN, Zhao CL, Bhat DJ, Sun YM, Karunarathna SC, Mortimer PE (2023) Culturable mycota on bats in central and southern Yunnan Province China. Mycosphere 14(1): 497–662. https://doi.org/10.5943/mycosphere/14/1/7

Lubbe A, Verpoorte R (2011) Cultivation of medicinal and aromatic plants for specialty industrial materials. Industrial Crops and Products 34(1): 785–801. https://doi.org/10.1016/j.indcrop.2011.01.019

Lunde LF, Boddy L, Sverdrup-Thygeson A, Jacobsen RM, Kauserud H, Birkemoe T (2023) Beetles provide directed dispersal of viable spores of a keystone wood decay fungus. Fungal Ecology 63: 101232. https://doi.org/10.1016/j.funeco.2023.101232

Mahanty S, Bakshi M, Ghosh S, Chatterjee S, Bhattacharyya S, Das P, Das S, Chaudhuri P (2019) Green synthesis of iron oxide nanoparticles mediated by filamentous fungi isolated from Sundarban mangrove ecosystem India. BioNanoScience 9(3): 637–651. https://doi.org/10.1007/s12668-019-00644-w

Malaspina P, Betuzzi F, Ingegneri M, Smeriglio A, Cornara L, Trombetta D (2022) Risk of poisoning from garden plants: Misidentification between laurel and cherry laurel. Toxins 14(11): 726. https://doi.org/10.3390/toxins14110726

Mayers CG, Harrington TC, Biederman PHW (2022) Mycangia define the diverse ambrosia beetle-fungus symbiosis. In: Schultz TR, Gawne R, Peregrine PN (Eds) The convergent evolution of agriculture in humans and insects. MIT Press, Cambridge, 105–142. https://doi.org/10.7551/mitpress/13600.003.0013

Mayfield AE III, Smith JA, Hughes M, Dreaden TJ (2008) First report of laurel wilt disease caused by a *Raffaelea* sp. on avocado in Florida. Plant Disease 92(6): 976. https://doi.org/10.1094/PDIS-92-6-0976A

Moncalvo J, Wang H, Hseu R (1995) Phylogenetic relationships in *Ganoderma* inferred from the internal transcribed spacers and 25S ribosomal DNA sequences. Mycologia 87(2): 23–238. https://doi.org/10.1080/00275514.1995.12026524

Morales-Rodríguez C, Sferrazza I, Aleandri MP, Dalla Valle M, Speranza S, Contarini M, Vannini A (2021) The fungal community associated with the ambrosia beetle *Xylosandrus compactus* invading the mediterranean maquis in central Italy reveals high biodiversity and suggests environmental acquisitions. Fungal Biology 125(1): 12–24. https://doi.org/10.1016/j.funbio.2020.09.008

Motti R, de Falco B (2021) Traditional herbal remedies used for managing anxiety and insomnia in Italy: An ethnopharmacological overview. Horticulturae 7(12): 523. https://doi.org/10.3390/horticulturae7120523

Moyo P, Allsopp E, Roets F, Mostert L, Halleen F (2014) Arthropods vector grapevine trunk disease pathogens. Phytopathology 104(10): 1063–1069. https://doi.org/10.1094/PHYTO-11-13-0303-R

Muthappa BN, Venkatasubbaiah P (1981) Association of *Ambrosiella macrospora* with *Xylosandrus compactus* the shot-hole borer of Robusta coffee in India. Journal of Caffeine Research 11: 54.

Nel WJ, Wingfield MJ, de Beer ZW, Duong TA (2021) Ophiostomatalean fungi associated with wood boring beetles in South Africa including two new species. Antonie van Leeuwenhoek 114(6): 667–686. https://doi.org/10.1007/s10482-021-01548-0

Ngoan ND, Wilkinson RC, Short DE, Moses CS, Mangold JR (1976) Biology of an introduced ambrosia beetle *Xylosandrus compactus* in Florida. Annals of the Entomological Society of America 69(5): 872–876. https://doi.org/10.1093/aesa/69.5.872

Ordoudi SA, Papapostolou M, Nenadis N, Mantzouridou FT, Tsimidou MZ (2022) Bay Laurel (*Laurus nobilis* L.) essential oil as a food preservative source: Chemistry quality control activity assessment and applications to olive industry products. Foods 11(5): 752. https://doi.org/10.3390/foods11050752

Paine TD, Raffa KF, Harrington TC (1997) Interactions among scolytid bark beetles their associated fungi and live host conifers. Annual Review of Entomology 42(1): 179–206. https://doi.org/10.1146/annurev.ento.42.1.179

Patolia H, Bansal E (2021) Two rare cases of fungal bursitis due to *Phialemoniopsis piluloculosa*. IDCases 24: e01095. https://doi.org/10.1016/j.idcr.2021.e01095

Pennacchio F, Santini L, Francardi V (2012) Bioecological notes on *Xylosandrus compactus* (Eichhoff) (Coleoptera Curculionidae Scolytinae) a species recently recorded into Italy. Redia–Journal of Zoology 95: 67–77.

Perdomo H, García D, Gené J, Cano J, Sutton DA, Summerbell R, Guarro J (2013) *Phialemoniopsis* a new genus of Sordariomycetes and new species of *Phialemonium* and *Lecythophora*. Mycologia 105(2): 398–421. https://doi.org/10.3852/12-137

Petrak F (1929) Mykologische Beiträge zur Flora der kanarischen Inseln. Botanische Jahrbücher für Systematik, Pflanzengeschichte und Pflanzengeographie 62: 125–160.

Ploetz RC, Konkol JL, Narvaez T, Duncan RE, Saucedo RJ, Campbell A, Mantilla J, Carrillo D, Kendra PE (2017) Presence and prevalence of *Raffaelea lauricola* cause of laurel wilt in different species of ambrosia beetle in Florida USA. Journal of Economic Entomology 110: 347–354. https://doi.org/10.1093/jee/tow292

Polizzi G, Vitale A, Aiello D, Guarnaccia V, Crous P, Lombard L (2012) First report of *Calonectria ilicicola* causing a new disease on *Laurus* (*Laurus nobilis*) in Europe. Journal of Phytopathology 160(1): 41–44. https://doi.org/10.1111/j.1439-0434.2011.01852.x

Rabaglia RJ, Dole SA, Cognato AI (2006) Review of American Xyleborina (Coleoptera: Curculionidae: Scolytinae) occurring north of Mexico with an illustrated key. Annals

of the Entomological Society of America 99(6): 1034–1056. https://doi.org/10.1603/0013-8746(2006)99[1034:ROAXCC]2.0.CO;2

Raviv M, Putievsky E, Ravid U, Senderovitch D, Snir N, Roni R (1982) Bay laurel as an ornamental plant. Acta Horticulturae (132): 35–42. https://doi.org/10.17660/ActaHortic.1983.132.4

Renner SS (2011) Laurales. In: eLS (Ed.) John Wiley & Sons, Ltd. https://doi.org/10.1002/9780470015902.a0003695.pub2

Riba-Flinch JM, Leza M, Gallego D (2021) First records of *Xylosandrus compactus* (Coleoptera: Curculionidae Scolytinae) in the Iberian Peninsula: an expanding alien species. Zootaxa 4970(1): 161–170. https://doi.org/10.11646/zootaxa.4970.1.8

Rivero M, Hidalgo A, Alastruey-Izquierdo A, Cía M, Torroba L, Rodríguez-Tudela JL (2009) Infections due to *Phialemonium* species: Case report and review. Medical Mycology 47(7): 766–774. https://doi.org/10.3109/13693780902822800

Rodríguez-Sánchez F, Arroyo J (2008) Reconstructing the demise of Tethyan plants: climate-driven range dynamics of *Laurus* since the Pliocene. Global Ecology and Biogeography 17: 685–695.

Silvestro D, Michalak I (2012) RaxmlGUI: A graphical front-end for RAxML. Organisms, Diversity & Evolution 12(4): 335–337. https://doi.org/10.1007/s13127-011-0056-0

Singletary K (2021) Bay leaf: Potential health benefits. Nutrition Today 56(4): 202–208. https://doi.org/10.1097/NT.0000000000000493

Smith SA, Dunn CW (2008) Phyutility: A phyloinformatics tool for trees alignments and molecular data. Bioinformatics 24(5): 715–716. https://doi.org/10.1093/bioinformatics/btm619

Stamatakis E (2006) RAxML-VI-HPC: Maximum likelihood-based phylogenetic analyses with thousands of taxa and mixed models. Bioinformatics 22(21): 2688–2690. https://doi.org/10.1093/bioinformatics/btl446

Stefanaki A, van Andel T (2021) Mediterranean aromatic herbs and their culinary use. In: Galanakis CM (Ed.) Aromatic Herbs in Food. Academic Press, Cambridge, Massachusetts, USA, 93–121. https://doi.org/10.1016/B978-0-12-822716-9.00003-2

Su L, Deng H, Niu YC (2016) *Phialemoniopsis endophytica* sp. nov. a new species of endophytic fungi from *Luffa cylindrica* in Henan China. Mycological Progress 15(5): e48. https://doi.org/10.1007/s11557-016-1189-5

Sugita R, Tanaka K (2022) *Thyridium* revised: Synonymisation of *Phialemoniopsis* under *Thyridium* and establishment of a new order Thyridiales. MycoKeys 86: 147–176. https://doi.org/10.3897/mycokeys.86.78989

Sung GH, Sung JM, Hywel-Jones NL, Spatafora JW (2007) A multi-gene phylogeny of Clavicipitaceae (Ascomycota Fungi): Identification of localized incongruence using a combinational bootstrap approach. Molecular Phylogenetics and Evolution 44(3): 1204–1223. https://doi.org/10.1016/j.ympev.2007.03.011

Swofford DL (2002) PAUP*: Phylogenetic analysis using parsimony (*and other methods) Version 4 Sinauer Associates: Sunderland, MA, USA.

Taha H, Shivanand P, Zainudin MAA, Hadanan NA (2021) Identification of culturable marine fungi and bacteria from coastal region in Brunei Darussalam: Identification of culturable marine microbes. Biodiversitas (Surakarta) 22: 3. https://doi.org/10.13057/biodiv/d220332

Tsang CC, Chan JF, Ip PP, Ngan AH, Chen JH, Lau SK, Woo PC (2014) Subcutaneous phaeohyphomycotic nodule due to *Phialemoniopsis hongkongensis* sp. nov. Journal of Clinical Microbiology 52(9): 3280–3289. https://doi.org/10.1128/JCM.01592-14

Vannini A, Contarini M, Faccoli M, Valle MD, Rodriguez CM, Mazzetto T, Guarneri D, Vettraino AM, Speranza S (2017) First report of the ambrosia beetle *Xylosandrus compactus* and associated fungi in the Mediterranean maquis in Italy and new host–pest associations. Bulletin OEPP. EPPO Bulletin. European and Mediterranean Plant Protection Organisation 47(1): 100–103. https://doi.org/10.1111/epp.12358

Varaljay VA, Lyon WJ, Crouch AL, Drake CA, Hollomon JM, Nadeau LJ, Nunn HS, Stevenson BS, Bojanowski CL, Crookes-Goodson WJ (2019) Draft genome sequence of filamentous fungus *Phialemoniopsis curvata* isolated from diesel fuel. Microbiology Resource Announcements 8(30): 10–1128. https://doi.org/10.1128/MRA.00400-19

Vilgalys R, Hester M (1990) Rapid genetic identification and mapping of enzymatically amplified ribosomal DNA from several *Cryptococcus* species. Journal of Bacteriology 172(8): 4238–4246. https://doi.org/10.1128/jb.172.8.4238-4246.1990

Vitale A, Polizzi G (2005) Occurrence of *Pestalotiopsis uvicola* causing leaf spots and stem blight on bay laurel (*Laurus nobilis*) in Sicily. Plant Disease 89(12): 1362–1362. https://doi.org/10.1094/PD-89-1362A

Vitale S, Luongo L, Barzanti GP, Binazzi F, Petrucci M, Galli M, Pennacchio F, Francardi V (2021) First report of *Geosmithia pallida* and *G. langdonii* associated with *Liparthrum colchicum* in central Italy. Redia–Journal of Zoology 104: 167–170.

Vitale S, Toccafondi P, Luongo L, Binazzi F, Petrucci M, Francardi V, Landi S, Giovannini L, Simoni S, Roversi PF, Pennacchio F (2022) Fungi obtained from olive twig dieback and adults of the alien pest *Xylosandrus compactus* (Eichhoff) (Coleoptera Curculionidae Scolytinae). Redia–Journal of Zoology 105: 197–204. https://doi.org/10.19263/REDIA-105.22.25

Voglmayr H, Jaklitsch WM (2008) *Prosthecium* species with *Stegonsporium* anamorphs on Acer. Mycological Research 112(8): 885–905. https://doi.org/10.1016/j.mycres.2008.01.020

Voglmayr H, Jaklitsch WM, Mohammadi H, Kazemzadeh Chakusary M (2019) The genus *Juglanconis* (Diaporthales) on *Pterocarya*. Mycological Progress 18(3): 425–437. https://doi.org/10.1007/s11557-018-01464-0

Voigt K, Wöstemeyer J (2000) Reliable amplification of actin genes facilitates deep-level phylogeny. Microbiological Research 155(3): 179–195. https://doi.org/10.1016/S0944-5013(00)80031-2

Werle E, Schneider C, Renner M, Völker M, Fiehn W (1994) Convenient single-step one tube purification of PCR products for direct sequencing. Nucleic Acids Research 22(20): 4354–4355. https://doi.org/10.1093/nar/22.20.4354

White TJ, Bruns T, Lee S, Taylor J (1990) Amplification and direct sequencing of fungal ribosomal RNA genes for phylogenetics In: Innis MA, Gelfand DH, Sninsky JJ, White TJ (Eds) PCR Protocols: a guide to methods and amplifications. Academic Press, San Diego, 38: 315–322. https://doi.org/10.1016/B978-0-12-372180-8.50042-1

Zhang Y, Zhou J, Tng DY, Wang S, Wang Y, Peng Y, Liu H, Wang Z (2023) Phylogeny and systematics of *Sassafras* (Lauraceae), an interesting genus with disjunct distributions in eastern North America and East Asia. Plants 12(6): 1419. https://doi.org/10.3390/plants12061419

MycoKeys 110: 237–253 (2024)
DOI: 10.3897/mycokeys.110.133084

Research Article

Three new species of the genus *Kockovaella* (Cuniculitremaceae, Tremellales) from the phylloplane in China

Chun-Yue Chai[1,2], Zhi-Wen Xi[1,2], Qiu-Hong Niu[1,2], Feng-Li Hui[1,2]

1 *School of Life Science, Nanyang Normal University, Nanyang 473061, China*
2 *Research Center of Henan Provincial Agricultural Biomass Resource Engineering and Technology, Nanyang Normal University, Nanyang 473061, China*
Corresponding authors: Qiu-Hong Niu (qiuhongniu723@163.com); Feng-Li Hui (fenglihui@yeah.net)

Abstract

Kockovaella, in the family Cuniculitremaceae of the order *Tremellales*, is a globally distributed genus of blastoconidia-forming fungi. Currently, 23 species have been described and accepted as members of the genus. In this study, five yeast strains were isolated from plant leaf surfaces collected in the Fujian and Guizhou Provinces of China and identified through a combination of morphological and molecular methods. The related phenotypic features and molecular phylogenetic analyses based on ITS, LSU, and RPB1 sequences demonstrated that they were members of three novel *Kockovaella* species: *K. iteae* **sp. nov.**, *K. quanzhouensis* **sp. nov.**, and *K. sambucuse* **sp. nov.** These species were described in detail and discussed relative to other species. This study demonstrated the novel geographical distribution as well as the high species diversity of *Kockovaella* in China and offered more data for further studies in fungal systematics and evolution.

Key words: *Basidiomycota*, phylogenetic analysis, plant leaves, taxonomy, Tremellomycetes

Academic editor: Thorsten Lumbsch
Received: 25 July 2024
Accepted: 31 October 2024
Published: 20 November 2024

Citation: Chai C-Y, Xi Z-W, Niu Q-H, Hui F-L (2024) Three new species of the genus *Kockovaella* (Cuniculitremaceae, Tremellales) from the phylloplane in China. MycoKeys 110: 237–253. https://doi.org/10.3897/mycokeys.110.133084

Introduction

Kockovaella (*Tremellales*, Cuniculitremaceae), a ballistoconidiogenous anamorphic yeast genus, was first proposed by Nakase et al. (1991) to accommodate two species, *K. imperatae* and *K. thailandica*. Nine other species were subsequently identified in this genus (Canete-Gibas et al. 1998; Takashima and Nakase 1998; Luong et al. 2000; Fungsin et al. 2002). Prior phylogenetic investigations of the small subunit (SSU) rRNA gene demonstrated that *Kockovaella* was closely related to *Fellomyces* (Nakase et al. 1993). However, the division of *Kockovaella* and *Fellomyces* species into two genera is questionable because further phylogenetic studies indicate a close relationship between the species, and the only difference is the capacity of *Kockovaella* to produce ballistospores (Lopandic et al. 2011; Takashima and Nakase 2011). Nakase et al. (1993) and Nakase (2000) noted that the production of ballistospores may be influenced by cultivation methods and vary from clone to clone. Vegetative reproduction does not reflect the phylogenetic relationships, and a novel approach to the systematics of ballistosporous yeasts should be established (Lopandic et al.

2005a). Liu et al. (2015a) employed seven genes to reconstruct the phylogeny of most described anamorphic and teleomorphic tremellomycetous yeasts. Based on multi-gene phylogenies, eight nonballistoconidium-forming species previously assigned to *Fellomyces* (Lopandic et al. 2011) were transferred to *Kockovaella* (Liu et al. 2015a, b). The latest additions to the genus were *K. libkindii* from the cavity of the bromeliad *Vriesea minarum* in Brazil (Gomes et al. 2016), *K. haikouensis*, *K. ischaemi*, and *K. nitrophila* from the phylloplane in China (Li et al. 2020).

All species of the genus *Kockovaella* are asexual morphs, which are morphologically characterized by the production of blastoconidia on stalk-like conidiophores and budding cells. Some species may produce ballistoconidia and poorly developed pseudohyphae (Lopandic et al. 2011; Takashima and Nakase 2011; Liu et al. 2015b). Physiologically, members of the genus cannot undergo fermentation, possess Q-10 as a predominant ubiquinone, and assimilate diverse carbon sources, but not nitrate (Liu et al. 2015b). Species in this genus can be differentiated via phenotypic characteristics and phylogenetic analyses (Liu et al. 2015b; Li et al. 2020).

To date, 23 species have been accepted as members of the genus *Kockovaella*, with most reported in tropical and subtropical regions, especially in Asia (Lopandic et al. 2011; Takashima and Nakase 2011; Li et al. 2020). Previously, only four species, *K. chinensis*, *K. fuzhouensis*, *K. lichenicola*, and *K. sichuanensis*, were reported in Fujian and Sichuan Provinces of China (Yue 1982; Prillinger et al. 1997). Recently, Li et al. (2020) identified eight *Kockovaella* species in Hainan and Yunnan Provinces, including three new species. Despite these findings, the genus's diversity remains incompletely understood. In this study, five basidiomycetous yeast strains were obtained from Fujian and Guizhou Provinces. Phenotypic characteristics and molecular phylogenetic analyses determined that these strains represent three undescribed species of *Kockovaella*. The aim of the present study was to identify and describe these new taxa using an integrative taxonomic approach.

Materials and methods

Sample collection and yeast isolation

Leaf samples were collected in the Fujian and Guizhou Provinces of China. Yeast strains were isolated from leaf surfaces using the improved ballistospore-fall method outlined by Nakase and Takashima (1993). Fresh leaves were cut into small pieces and affixed with a thin layer of petroleum jelly to the inner lid of a Petri dish containing yeast extract-malt extract (YM) agar (0.3% yeast extract, 0.3% malt extract, 0.5% peptone, 1% glucose, and 2% agar). The mixture was supplemented with 0.01% chloramphenicol to limit bacterial growth. Plates were incubated at 20 °C and monitored daily to assess colony formation. Selected colonies were streaked onto YM agar plates for subsequent purification. Following purification, strains were suspended in YM broth supplemented with 20% (v/v) glycerol and stored at −80 °C for subsequent use. Cultures of the obtained isolates were preserved in the Microbiology Lab at Nanyang Normal University, Henan, China. All collected isolates and their origins are presented in Table 1.

Table 1. Yeast strains and origins investigated in this study.

Strain	Source	Location
Kockovaella iteae		
NYNU 239240^T	Leaf of *Itea yunnanensis*	East Mountain Park, Guiyang City, Guizhou Province, China (26°45'26"N, 106°21'31"E)
NYNU 239246	Leaf of *Itea yunnanensis*	East Mountain Park, Guiyang City, Guizhou Province, China (26°45'26"N, 106°21'31"E)
Kockovaella quanzhouensis		
NYNU 224192^T	Leaf of *Ilex asprella*	Qingyuan Mountain, Quanzhou City, Fujian Province, China (25°7'41"N, 118°44'7"E)
NYNU 22425	Leaf of *Myrica* sp.	Qingyuan Mountain, Quanzhou City, Fujian Province, China (25°7'41"N, 118°44'7"E)
Kockovaella sambucuse		
NYNU 22942^T	Leaf of *Sambucus chinensis*	Guiyang Botanical Garden, Guiyang City, Guizhou Province, China (26°34'51"N, 106°42'36"E)

Phenotypic characterization

Morphological, physiological, and biochemical characters were examined according to the standard methods described by Kurtzman et al. (2011). To induce sexual state, single or paired strains were mixed on corn meal agar (CMA; 2% cornmeal infusion and 2% agar), potato dextrose agar (PDA; 20% potato infusion, 2% glucose, and 1.5% agar), and V8 agar (10% V8 juice and 2% agar). The plates were then incubated at 20 °C for up to 8 weeks (Li et al. 2020). Ballistoconidium formation was tested using the inverted-plate method (do Carmo-Sousa and Phaff 1962) after two weeks of incubation on CMA at 17 °C. Glucose fermentation was tested in a liquid medium using Durham fermentation tubes. Carbon and nitrogen assimilation capacities were examined in a liquid medium, with nitrogen tests using a starved inoculum (Kurtzman et al. 2011). Growth at various temperatures (15, 20, 25, 30, 35, and 37 °C) was evaluated through cultivation on YM agar plates. Cell morphology was examined with a LEICA DM2500 camera (LECIA, Wetzlar, Germany) and LASV4.13 software. All new taxonomic descriptions and proposed names were submitted to the MycoBank database (http://www.mycobank.org; 17 June 2024).

DNA extraction, PCR amplification, and sequencing

Genomic DNA was extracted from each strain using the Ezup Column Yeast Genomic DNA Purification Kit, according to the manufacturer's directions (Sangon Biotech Co., Shanghai, China). The ITS region, D1/D2 domain of the LSU rRNA, and a partial segment RPB1 were amplified using the primers ITS1/ITS4 (White et al. 1990), NL1/NL4 (Kurtzman and Robnett 1998), and RPB1-Af and RPB1-Cr (Kurtzman and Robnett 2003), respectively. Amplifications were performed in a 25 µL reaction volume consisting of 9.5 µL of ddH_2O, 12.5 µL of Taq 2X PCR Master Mix with blue dye (Sangon Biotech Co., Shanghai, China), 1 µL of DNA template, and 1 µL of each primer. The ITS region and D1/D2 domain were amplified using an initial denaturation step of 2 min at 95 °C, followed by 35 cycles of 30 s at 95 °C, 30 s at 51 °C, 40 s at 72 °C, and a final extension of 10 min at 72 °C (Toome et al. 2013). Amplification of the partial RPB1 gene was performed using a touchdown PCR protocol as described by

Wang et al. (2014). PCR products were then purified and sequenced by Sangon Biotech Co., Ltd (Shanghai, China) using the same primers. The identity and accuracy of each sequence were determined by comparing them to sequences in GenBank. Assembly was performed with BioEdit v.7.1.3.0 (Hall 1999). All newly generated sequences were deposited in the GenBank database (https://www.ncbi.nlm.nih.gov/genbank/), and the accession numbers are presented in Table 2.

Table 2. Species name, strain numbers, and GenBank accession numbers included in phylogenetic analyses. Entries in bold represent newly generated sequences. The superscript ^{T} indicates type strain.

Taxa name	Strain number	Locality	GenBank accession numbers		
			ITS	LSU D1/D2	RPB1
Fellomyces borneensis	CBS 8282^{T}	Indonesia	NR_073336	NG_057663	KF036458
Fellomyces penicillatus	CBS 5492^{T}	Germany	NR_073217	NG_070551	KF036464
Fellomyces polyborus	CBS 6072^{T}	South Africa	NR_073238	NG_057660	KF036465
Fellomyces horovitziae	CBS 7515^{T}	Germany	NR_073234	NG_057659	KF036461
Kockovaella barringtoniae	CBS 9811^{T}	Thailand	KY103846	NG_058315	KF036487
Kockovaella calophylli	CBS 8962^{T}	Vietnam	NR_155238	NG_070554	KF036488
Kockovaella chinensis	CBS 8278^{T}	China	NR_073258	NG_069410	KF036459
Kockovaella cucphuongensis	JCM 10840^{T}	Vietnam	NR_155210	NG_068957	KF036489
Kockovaella distylii	CBS 8545^{T}	Japan	NR_077101	NG_057680	–
Kockovaella fuzhouensis	CBS 8243^{T}	China	AF444484	NG_058316	KF036460
Kockovaella haikouensis	CGMCC 2.3443^{T}	China	NR_174724	MK050274	MK849163
Kockovaella imperatae	CBS 7554^{T}	Thailand	NR_077104	AF189862	KF036490
Kockovaella iteae	**NYNU 239240^{T}**	**China**	**OR958773**	**OR958772**	**PP755337**
Kockovaella iteae	**NYNU 239246**	**China**	**PP752297**	**PP752296**	**PP755338**
Kockovaella ischaemi	CGMCC 2.3565^{T}	China	NR_174725	MK050276	MK849182
Kockovaella libkindii	CBS 12685^{T}	Brazil	JQ861271	JQ861271	–
Kockovaella lichenicola	CBS 8315^{T}	China	NR_073338	NG_069411	KF036462
Kockovaella litseae	JCM 10838^{T}	Vietnam	NR_155209	NG_068956	KF036491
Kockovaella machilophila	CBS 8607^{T}	Japan	NR_077099	NG_057681	KF036492
Kockovaella mexicana	CBS 8279^{T}	Mexico	NR_164408	KY108124	KF036463
Kockovaella nitrophila	CGMCC 2.3465^{T}	China	NR_174726	MK050278	MK050278
Kockovaella ogasawarensis	CBS 8544^{T}	Japan	NR_073264	NG_057679	–
Kockovaella phaffii	CBS 8608^{T}	Japan	NR_077098	NG_058317	KF036493
Kockovaella prillingeri	CBS 8308^{T}	Thailand	NR_073337	KY108126	KY108126
Kockovaella quanzhouensis	**NYNU 224192^{T}**	**China**	**OP278691**	**OP278690**	**PP755336**
Kockovaella quanzhouensis	**NYNU 22425**	**China**	**PP752295**	**PP752294**	**PP755335**
Kockovaella sacchari	CBS 8624^{T}	Thailand	NR_077102	NG_058318	**KF036494**
Kockovaella sambucuse	**NYNU 22942^{T}**	**China**	**OP566879**	**OP566878**	–
Kockovaella schimae	CBS 8610^{T}	Japan	NR_137140	NG_058319	KF036495
Kockovaella sichuanensis	CBS 8318^{T}	China	NR_073259	AF189879	KF036466
Kockovaella thailandica	CBS 7552^{T}	Thailand	NR_077103	NG_057650	KF036496
Kockovaella vietnamensis	JCM 10841^{T}	Vietnam	NR_077111	NG_058320	KF036497
Sterigmatosporidium polymorphum	CBS 8088^{T}	Germany	NR_111071	AF075480	KF036418

Phylogenetic analysis

In addition to the newly generated sequences, additional related sequences were also downloaded from GenBank (Table 2) for phylogenetic analyses. The combined ITS, LSU, and RPB1 sequence dataset was used to explore the phylogenetic positions of the newly isolated strains within *Kockovaella*. All *Kockovaella* and *Fellomyces* species listed in Table 2, with available ITS, LSU, and RPB1 sequences, were included as ingroup taxa. *Sterigmatosporidium polymorphum* CBS 8088 was used as the outgroup (Gomes et al. 2016). Because previous phylogenetic studies focusing on *Kockovaella* were mainly based on the ITS and LSU regions, a combined ITS and LSU sequences dataset, comprising all species of *Kockovaella* and *Fellomyces* in Table 2, was used to further differentiate species identities within this genus.

Individual locus sequences were aligned using MAFFT v.7.110 (Katoh and Standley 2013) under the G-INI-I option. Poorly aligned regions were excluded and adjusted manually using MEGA v.11 (Tamura et al. 2021). Aligned sequences of the different loci were concatenated with Phylosuit v.1.2.2 (Zhang et al. 2020). Alignments were improved through manual gap adjustments. Ambiguous areas were excluded from the analysis using Aliview (Larsson 2014).

Phylogenetic analyses were conducted using Maximum Likelihood (ML) and Bayesian Inference (BI) methods. The ML method was performed using RAxML v.8.2.3 (Stamatakis 2014) under a GTRGAMMA model with one thousand rapid bootstrap (BS) replicates. For the BI approach, ModelFinder (Kalyaanamoorthy et al. 2017) was used to infer the appropriate substitution model that would best fit the model of DNA evolution for all combined datasets. The BI method was conducted using MrBayes v.3.2.7a (Ronquist et al. 2012) via the CIPRES Science Gateway. Six simultaneous Markov chains were run for 50 million generations, with trees sampled every 1,000 th generation. The first 25% of trees were discarded as burn-in. The remaining trees were used to calculate the Bayesian posterior probabilities (BPPs) for each clade. The resulting trees were visualized with FigTree v.1.4.3 (Andrew 2016). Branches showing BS values ≥ 50% and BPPs ≥ 0.95 indicated at the nodes.

Results

Molecular phylogeny

The combined dataset of ITS, LSU, and RPB1 resulted in an alignment of 1930 characters (ITS: 1–496, LSU: 497–1118, RPB1: 1119–1930). Among them, there were 1120 constant, 155 variable but parsimony non-informative, and 655 parsimony informative characters. ModelFinder recommended the GTR+I+G evolution model for Bayesian inference. Both ML and BI methods produced similar topologies in the main lineages. The ML-derived topology, along with BS values and BPPs above 50% and 0.95, respectively, is presented (Fig. 1). The phylogeny confirmed *Kockovaella* as a distinct genus (BS/92%; BPP/1). The five newly isolated strains formed three distinct and well-supported groups, separate from other *Kockovaella* species.

The combined dataset of ITS and LSU sequences produced a concatenated alignment of 1,118 characters, including 817 constant, 88 variable but parsimony non-informative, and 213 parsimony informative characters. The GTR+I+G

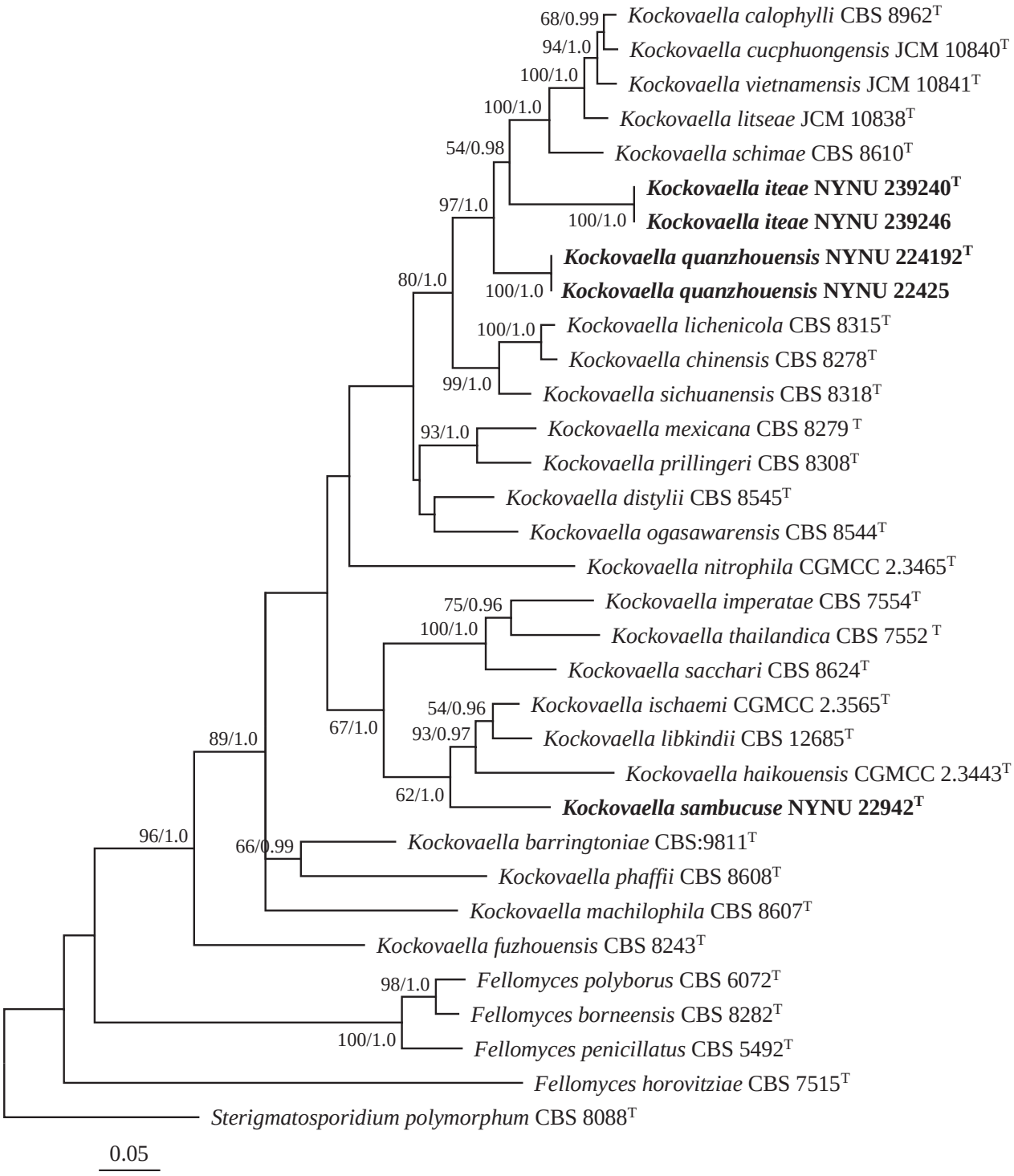

Figure 1. Maximum likelihood phylogenetic tree of *Kockovaella* generated from combined ITS, LSU, and RPB1 sequence data. The tree is rooted with *Sterigmatosporidium polymorphum* CBS 8088. Bootstrap values (BS ≥ 50% and BPPs ≥ 0.95) are displayed near branches. Type strain sequences are marked with (T). New species are highlighted in bold.

evolution model was also adopted for this dataset in Bayesian inference. The ML and BI methods yielded similar topologies in the main lineages. The ML-derived topology, with BS values and BPPs above 50% and 0.95, respectively, is shown (Fig. 2). This tree revealed 23 known *Kockovaella* species, while the newly isolated strains formed three independent groups, consistent with the combined ITS, LSU, and RPB1 dataset phylogeny.

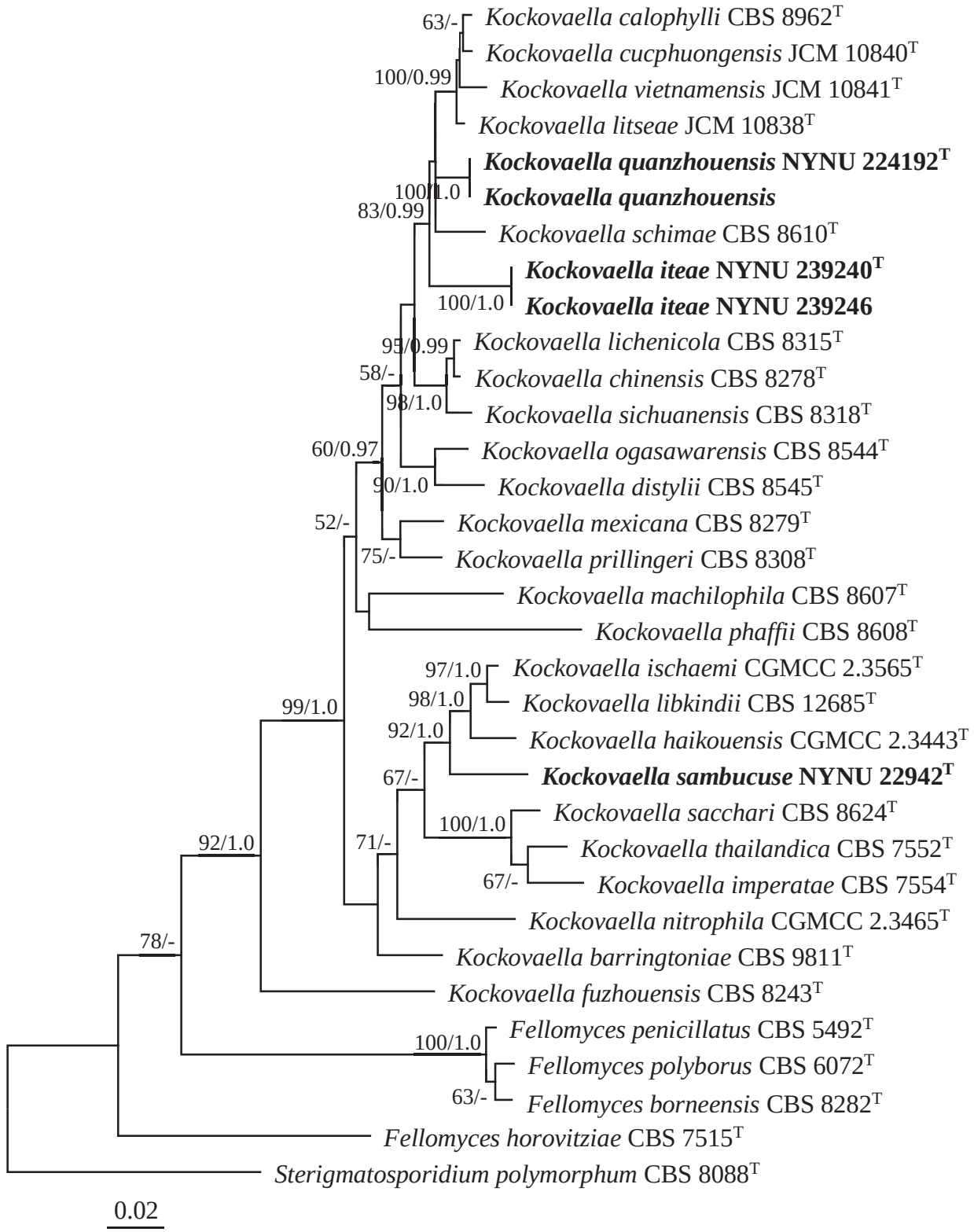

Figure 2. Maximum likelihood phylogenetic tree of *Kockovaella* generated from combined ITS and LSU sequence data. The tree is rooted with *Sterigmatosporidium polymorphum* CBS 8088. Bootstrap values (BS ≥ 50% and BPPs ≥ 0.95) are displayed near branches. Type strain sequences are marked with (T). New species are highlighted in bold.

Groups NYNU 224192 and NYNU 239240, each containing two strains, clustered with *K. calophylli*, *K. cucphuongensis*, *K. litseae*, *K. schimae*, and *K. vietnamensis* in all combined dataset trees (Figs 1, 2). Strains in the NYNU 224192

group had identical ITS and D1/D2 sequences, indicating that they are conspecific. Strains in the NYNU 239240 group, also with identical ITS and D1/D2 sequences, differed from the NYNU 224192 group by 8 nucleotide (nt) (~1.3%) substitutions and 29 nt (~5.8%) mismatches in the D1/D2 and ITS regions, respectively. These two groups differed from their five closest known species by 4–9 nucleotide (nt) (~0.7–1.5%) substitutions and 14–13 nt (~2.8–4.4%) mismatches in the D1/D2 and ITS regions, respectively. Strain NYNU 22942 clustered with *K. haikouensis*, *K. ischaemi*, and *K. libkindii* with 62% BS and 1.0 BPPs support in the combined ITS, LSU, and RPB1 phylogenetic tree (Fig. 1). It formed a well-supported clade with these species in the combined ITS and LSU dataset tree (92% BS, 1.0 BPPs; Fig. 2), differing from its nearest relatives by 9–10 nucleotide (nt) (~1.5–1.7%) substitutions and 25–27 nt (~4.7–5.1%) mismatches in the D1/D2 and ITS regions, respectively.

The above sequence comparisons suggested that the five novel strains represent three novel species within the genus *Kockovaella*.

Taxonomy

***Kockovaella iteae* C.Y. Chai & F.L. Hui, sp. nov.**
MycoBank No: 854381
Fig. 3

Etymology. The specific epithet *iteae* refers to *Itea*, the plant genus from which the type strain was isolated.

Type. China • Guizhou Prov.: Guiyang City, East Mountain Park, in the phylloplane of *Itea yunnanensis*, 15 Sept 2023, D. Lu, NYNU 239240 (holotype GDMCC 2.503^T preserved as a metabolically inactive state, culture ex-type PYCC 9996).

Description. On YM agar after 7 days at 20 °C, the streak culture is white to cream-colored, butyrous, smooth and glistening, with an entire margin. After 7 days in YM broth at 20 °C, cells are ellipsoidal or ovoid, 1.5–3.6 × 3.6–5.5 µm, single or pairs, and reproduced by polar budding and the formation of stalked conidia. The conidia are separated at the distal end of the stalks from parent cells. After 1 month at 20 °C, a ring and sediment are present. In Dalmau plate culture on CMA, pseudohyphae are not formed. Sexual structures are not observed on PDA, CMA or V8 agar. Ballistoconidia are symmetrical and apiculate, 1.8–2.4 × 2.7–3.3 µm. Glucose fermentation is absent. Glucose, inulin (delayed and weak), sucrose, raffinose, melibiose, galactose, lactose, trehalose, maltose, melezitose, cellobiose, salicin (delayed and weak), L-rhamnose, D-xylose, L-arabinose, D-arabinose (delayed), 5-keto-D-gluconate (delayed and weak), D-ribose (delayed), erythritol (delayed), ribitol, galactitol, D-mannitol, D-glucitol, myo-inositol, succinate, citrate, D-glucosamine, N-acetyl-D-glucosamine, 2-keto-D-gluconate (delayed), D-glucuronate, and glucono-1.5-lactone are assimilated as sole carbon sources. Methyl-α-D-glucoside, L-sorbose, methanol, ethanol, glycerol, DL-lactate, and D-gluconate are not assimilated. Ethylamine (delayed) and L-lysine are assimilated as sole nitrogen sources. Nitrate, nitrite, and cadaverine are not assimilated. Maximum growth temperature is 25 °C. Growth in vitamin-free medium is positive. Growth on 50% (w/w) glucose-yeast extract agar is negative. Starch-like substances are not produced. Urease activity is positive. Diazonium Blue B reaction is positive.

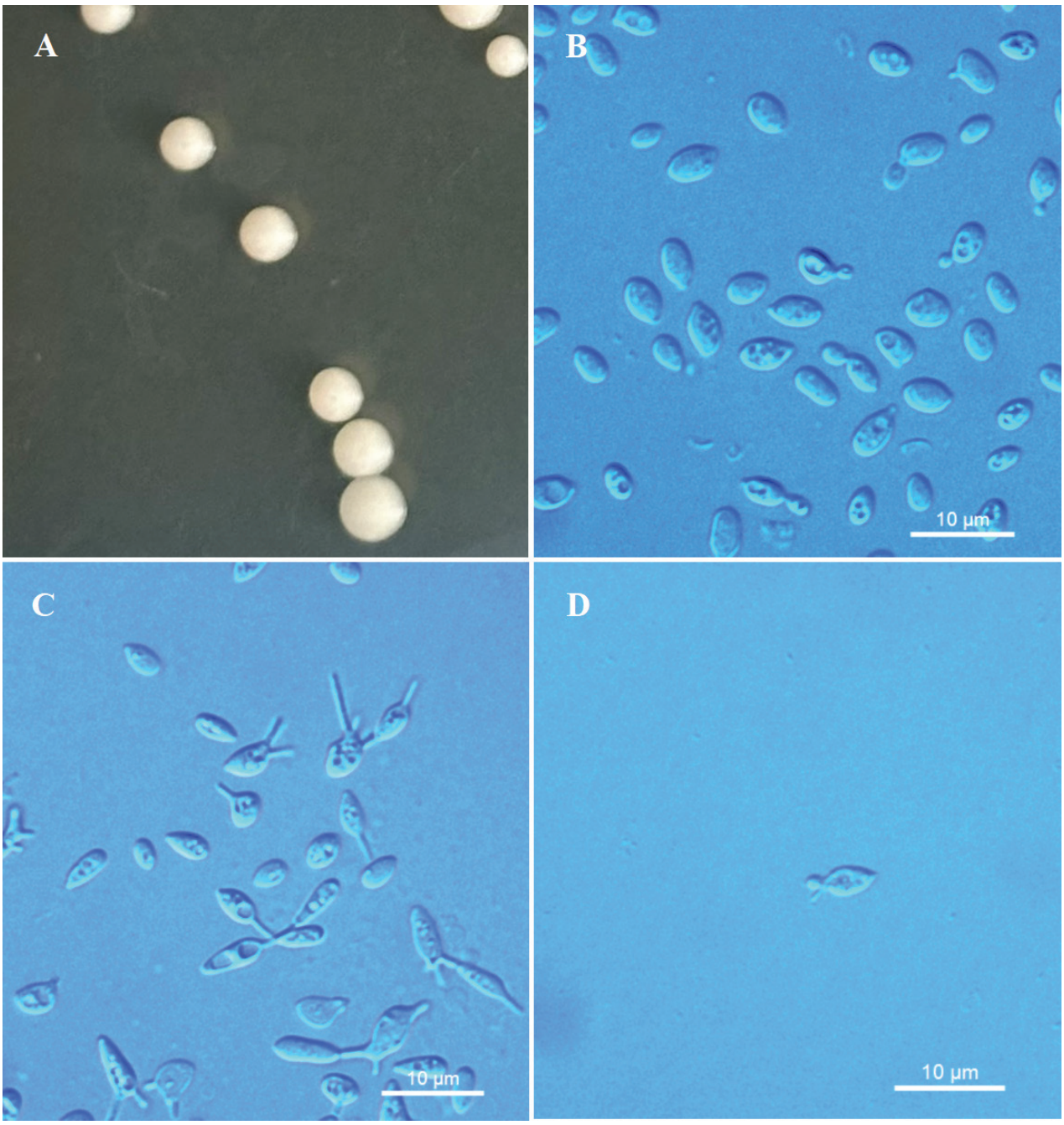

Figure 3. Morphological characteristics of *Kockovaella iteae* sp. nov. NYNU 239240^{T} **A** colony morphology on YM agar after growth for 7 d at 20 °C **B** budding cells after growth for 7 d in YM broth at 20 °C **C** stalked conidia on PDA after growth for 7 d at 20 °C **D** ballistoconidia on CM agar after growth for 7 d at 20 °C. Scale bars: 10 μm.

Additional strain examined. CHINA • Guizhou Prov.: Guiyang City, East Mountain Park, in the phylloplane of *Itea yunnanensis*, 15 Sept 2023, D. Lu, NYNU 239246.

GenBank accession numbers. holotype GDMCC 2.503^{T} (ITS: OR958773, D1/D2: OR958772, RPB1: PP755337); additional strains NYNU 239246 (ITS: PP752297, D1/D2: PP752296, RPB1: PP755338).

Note. Physiologically, *Kockovaella iteae* sp. nov. differs from six closely related species, *K. calophylli*, *K. cucphuongensis*, *K. litseae*, *K. quanzhouensis*, *K. schimae*, and *K. vietnamensis*, in its ability to assimilate inulin and ethylamine (Table 3).

Table 3. Physiological and biochemical characteristics differing between the new species and closely related species.

Characteristics	1	2*	3*	4*	5*	6*	7	8	9*	10*	11*
Carbon assimilation											
Inulin	d/w	–	–	–	–	–	–	–	–	+	–
L-Sorbose	–	–	d/w	W	w	d/w	d/w	d	–	–	–
D-Arabinose	d	d	w	D	d	d	–	+	-	w	+
Galactitol	+	+	d/w	D	d	w	–	+	+	+	+
Succinate	+	d/w	d	D	+	+	–	+	v	w	n
Citrate	+	d/w	d	D	w	w	–	+	–	v	–
Glucono-δ-lactone	+	d/w	d/w	D	w	w	–	+	n	n	n
Nitrogen assimilation											
Ethylamine	d	–	–	–	–	–	–	–	d	–	n
Cadaverine	–	–	–	–	–	–	–	–	+	+	n
Growth tests											
Growth at 30 °C	–	–	+	–	–	+	+	+	+	+	**n**

Species: 1, *K. iteae*; 2, *K. schimae*; 3, *K. calophylli*; 4, *K. cucphuongensis*; 5, *K. litseae*; 6, *K. vietnamensis*; 7, *K. quanzhouensis*; 8, *K. sambucuse*; 9, *K. haikouensis*; 10, *K. ischaemi*; 11, *K. libkindii.* +, positive reaction; –, negative reaction; d, delayed positive; w, weakly positive; n, data not available. All data from this study, except those marked with *, which were obtained from the original description (Lopandic et al. 2011; Takashima and Nakase 2011; Gomes et al. 2016).

***Kockovaella quanzhouensis* C.Y. Chai & F.L. Hui, sp. nov.**
MycoBank No: 854382
Fig. 4

Etymology. The specific epithet *qingyuanensis* refers to the geographic origin of the type strain, Qingyuan Mountain, Quanzhou, Fujian.

Type. China • Fujian Prov.: Quanzhou City, Qingyuan Mountain, in the phylloplane of *Ilex asprella*, 12 Mar 2022, W.T. Hu & S.B. Chu, NYNU 224192 (holotype GDMCC 2.325^{T} preserved as a metabolically inactive state, culture ex-type PYCC 9950).

Description. On YM agar after 7 days at 20 °C, the streak culture is cream to pale yellow, butyrous, smooth and glistening, with an entire margin. After 7 days in YM broth at 20 °C, cells are ovoid, 2.1–4.9 × 3.3–5.6 µm, single or pairs, and reproduced by polar budding and the formation of stalked conidia. The conidia are separated at the distal end of the stalks from parent cells. After 1 month at 20 °C, a ring and sediment are present. In Dalmau plate culture on CMA, pseudohyphae and hyphae are not formed. Sexual structures are not observed on PDA, CMA or V8 agar. Ballistoconidia are symmetrical and apiculate, 3.7–4.2 × 7.9–8.0 µm. Glucose fermentation is absent. Glucose, sucrose, raffinose, melibiose, galactose, lactose, trehalose, maltose, melezitose, cellobiose, L-sorbose (delayed and weak), L-rhamnose, D-xylose, L-arabinose, D-ribose, D-mannitol, D-glucitol, D-gluconate (delayed), D-glucosamine, N-acetyl-D-glucosamine, and D-glucuronate are assimilated as sole carbon sources. Inulin, methyl-α-D-glucoside, salicin, D-arabinose, 5-keto-D-gluconate, methanol, ethanol, glycerol, erythritol, ribitol, galactitol, myo-inositol, DL-lactate, succinate, citrate, 2-keto-D-gluconate, and glucono-1.5-lactone are not assimilated. L-Lysine is assimilated as sole nitrogen sources. Nitrate, nitrite, ethylamine, and

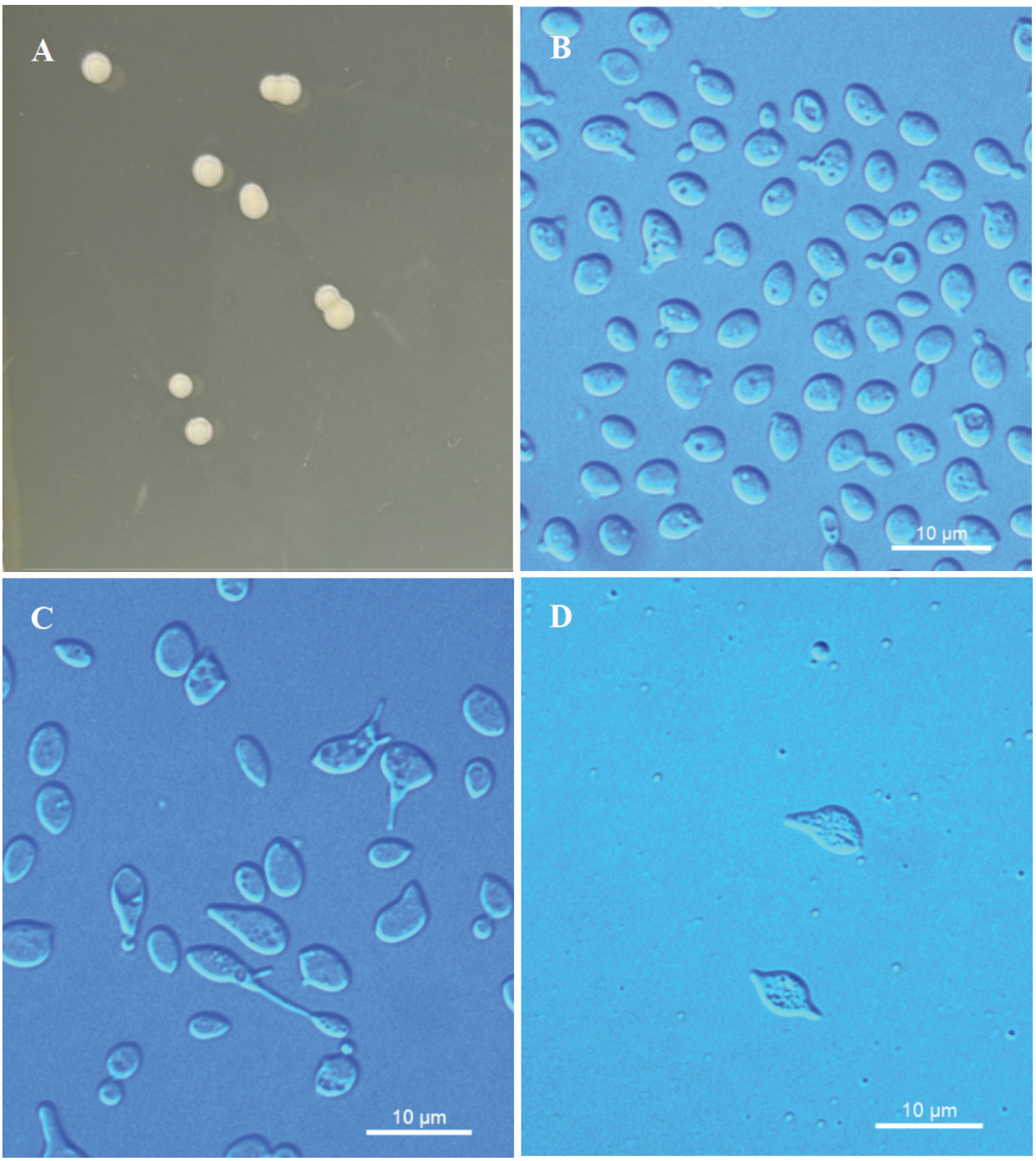

Figure 4. Morphological characteristics of *Kockovaella quanzhouensis* sp. nov. NYNU 224192^{T} **A** colony morphology on YM agar after growth for 7 d at 20 °C **B** budding cells after growth for 7 d in YM broth at 20 °C **C** stalked conidia on PDA after growth for 7 d at 20 °C **D** ballistoconidia on CM agar after growth for 7 d at 20 °C. Scale bars: 10 μm.

cadaverine are not assimilated. Maximum growth temperature is 30 °C. Growth in vitamin-free medium is positive. Growth on 50% (w/w) glucose-yeast extract agar is negative. Starch-like substances are not produced. Urease activity is positive. Diazonium Blue B reaction is positive.

Additional strain examined. China • Fujian Prov.: Quanzhou City, Qingyuan Mountain, in the phylloplane of *Myrica* sp., 12 Mar 2022, W.T. Hu & S.B. Chu, NYNU 22425.

GenBank accession numbers. holotype GDMCC 2.325^{T} (ITS: OP278691, D1/D2: OP278690, RPB1: PP755336); additional strains NYNU 22425 (ITS: PP752295, D1/D2: PP752294, RPB1: PP755335).

Note. Physiologically, *Kockovaella quanzhouensis* sp. nov. differs from six closely related species, *K. calophylli*, *K. cucphuongensis*, *K. litseae*, *K. iteae*, *K. schimae*, and *K. vietnamensis*, in its inability to assimilate D-arabinose, galactitol, succinate, citrate and glucono-1.5-lactone (Table 3).

***Kockovaella sambucuse* C.Y. Chai & F.L. Hui, sp. nov.**

MycoBank No: 854383

Fig. 5

Etymology. The specific epithet *sambucuse* refers to *Sambucus*, the plant genus from which the type strain was isolated.

Type. China • Guizhou Prov.: Guiyang City, Guiyang Botanical Garden, in the phylloplane of *Sambucus chinensis*, Aug 2022, L. Zhang and F.L. Hui, NYNU 22942 (holotype GDMCC 2.313^{T} preserved as a metabolically inactive state, culture ex-type PYCC 9951).

Description. On YM agar after 7 days at 20 °C, the streak culture is white to cream-colored, butyrous, smooth and glistening, with an entire margin. After 7 days in YM broth at 20 °C, cells are ovoid, 2.1–3.3 × 3.3–4.7 µm, and single or pairs, budding is polar. After 1 month at 20 °C, a ring and sediment are present. In Dalmau plate culture on CMA, pseudohyphae and hyphae are not formed. Sexual structures are not observed on PDA, CMA or V8 agar. Ballistoconidia are ellipsoidal or somewhat kidney-shaped, 3.4–4.9 × 5.2–6.8 µm. Glucose fermentation is absent. Glucose, sucrose, raffinose, melibiose, galactose, lactose, trehalose, maltose, melezitose, cellobiose, salicin, L-sorbose (delayed), L-rhamnose (delayed), D-xylose, L-arabinose, D-arabinose, D-ribose, glycerol (delayed), ribitol, galactitol, D-mannitol, D-glucitol, DL-lactate (delayed and weak), succinate, citrate, D-glucosamine, N-acetyl-D-glucosamine, 2-keto-D-gluconate (weak), D-glucuronate and glucono-1.5-lactone are assimilated as sole carbon

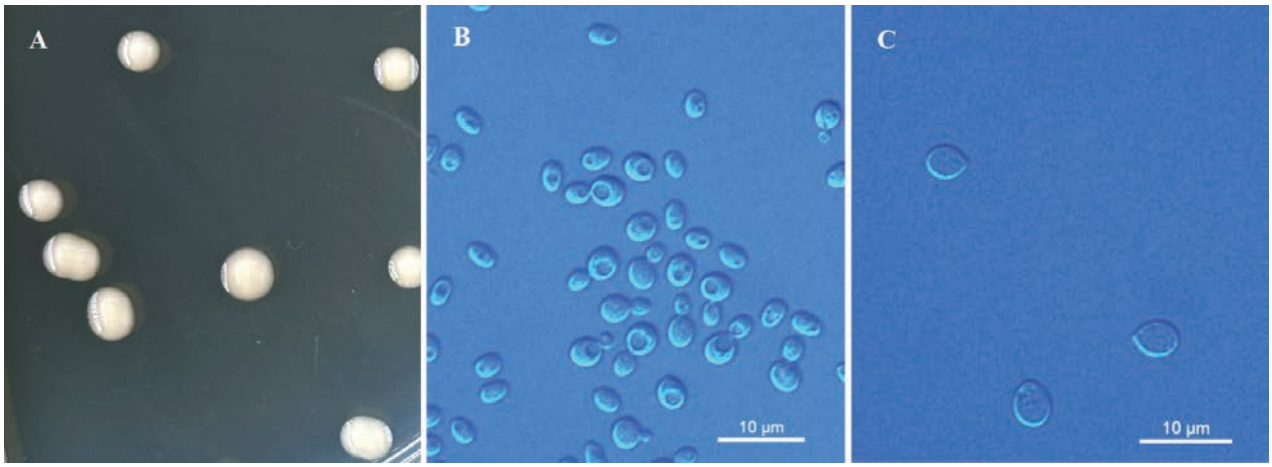

Figure 5. Morphological characteristics of *Kockovaella sambucuse* sp. nov. NYNU 22942^{T} **A** colony morphology on YM agar after growth for 7 d at 20 °C **B** budding cells after growth for 7 d in YM broth at 20 °C **C** ballistoconidia on CM agar after growth for 7 d at 20 °C. Scale bars: 10 µm.

sources. Inulin, methyl-α-D-glucoside, 5-keto-D-gluconate, methanol, ethanol, erythritol, myo-inositol, and D-gluconate are not assimilated. L-Lysine is assimilated as sole nitrogen sources. Nitrate, nitrite, ethylamine and cadaverine are not assimilated. Maximum growth temperature is 30 °C. Growth in vitamin-free medium is positive. Growth on 50% (w/w) glucose-yeast extract agar is negative. Starch-like substances are not produced. Urease activity is positive. Diazonium Blue B reaction is positive.

GenBank accession numbers. holotype GDMCC 2.313^{T} (ITS: OP566879, D1/D2: OP566878).

Note. Physiologically, *Kockovaella sambucuse* sp. nov. differs from three closely related species, *K. haikouensis*, *K. ischaemi*, and *K. libkindii*, in its ability to assimilate L-sorbose and its inability to assimilate cadaverine (Table 3).

Discussion

Phylogenetic analyses grouped 26 species of *Kockovaella* together (Figs 1, 2), including three new species from China: *K. iteae* sp. nov., *K. quanzhouensis* sp. nov., and *K. sambucuse* sp. nov. Our results are consistent with previous observations (Gomes et al. 2016; Li et al. 2020), and provide additional insights into the phylogeny and taxonomy of *Kockovaella*.

Kockovaella sambucuse sp. nov. described in this study was represented by only one strain from our isolations. Despite a number of samples collected in different locations for two consecutive years, we were unable to confirm the occurrence of this yeast to obtain additional strains. The description of single-strain species will add to an understanding of yeast phylogeny and species diversity, which would be unknown if new species descriptions were limited to those taxa for which multiple strains were available (Kurtzman 2010).

Fellomyces horovitziae was first reported in Germany by Spaaij et al. (1991) based on phenotypic characteristics. However, our phylogenetic analysis did not support its placement in *Fellomyces*, despite its morphological similarity to other species in the genus, as it forms conidia on stalks (Lopandic et al. 2011). This result is similar to the results of previous phylogenetic analyses based on the single LSU sequence and the combined ITS and LSU sequences (Gomes et al. 2016; Li et al. 2020). Therefore, further analyses using more molecular or genomic data are needed to clarify its phylogenetic position.

Kockovaella species are widely distributed across various habitats. They are commonly identified as epiphytic fungi on flowers (Yue 1982), leaves (Canete-Gibas et al. 1998; Hamamoto et al. 1998; Takashima and Nakase 1998; Luong et al. 2000; Fungsin et al. 2002; Lopandic et al. 2011; Li et al. 2020), and lichens (Prillinger et al. 1997; Lopandic et al. 2005b) in temperate and subtropical climate regions. *K. libkindii*, for example, has been found in water cavities (Gomes et al. 2016), where it forms a minor component of the yeast community, likely vectored by insects visiting these microhabitats (Gomes et al. 2016). In this study, three new *Kockovaella* species were associated with plant leaves, similar to other species in the genus. Other species identified from these samples include *Bullera alba*, *Derxomyces boekhoutii*, *Erythrobasidium primogenitum*, *Moesziomyces antarcticus*, *Moesziomyces aphidis*, *Symmetrospora coprosmae*, and *Tilletiopsis washingtonensis*, all common representatives in the phyllosphere (Nakase 2000; Kruse et al. 2017). The discovery of these three

new species highlights the widespread natural distribution of *Kockovaella* species on plants, emphasizing the need for extensive sampling and detailed molecular and phenotypic analyses to fully understand their global diversity.

Conclusions

In the present study, five phyllosphere-inhabiting yeast strains were identified as three new *Kockovaella* species, *K. iteae* sp. nov., *K. quanzhouensis* sp. nov., and *K. sambucuse* sp. nov., based on morphological and molecular phylogenetic analyses, which provides us with further understanding of this genus diversity in China. In the future, we firmly believe that more and more species of the genus will be isolated from more plants around the world.

Acknowledgments

The authors are very grateful to their colleagues at the School of Life Science, Nanyang Normal University, including Dan Lu for providing specimens; Ting Lei for help with phylogenetic analysis; Shan Liu and Ya-Zhuo Qiao for help with morphological observations.

Additional information

Conflict of interest

The authors declare that the research was conducted in the absence of any commercial or financial relationships that could be construed as a potential conflict of interest.

Ethical statement

No ethical statement was reported.

Funding

This research was funded by the National Natural Science Foundation of China (Project No. 31570021) and the Program for the Outstanding Youth Science Fund Project of Henan province (Project No. 222300420014).

Author contributions

C.-Y.C.: Investigation, Methodology, Writing – original draft. Z.-W.X.: Molecular experiments, Data analysis. Q.-H.N.: Funding acquisition, Resources, Software, Validation, Writing – review & editing. F.-L.H.: Funding acquisition, Resources, Writing – review & editing. All authors have read and agreed to the published version of the manuscript.

Author ORCIDs

Chun-Yue Chai https://orcid.org/0000-0003-0284-5560
Qiu-Hong Niu https://orcid.org/0000-0003-1695-7117
Feng-Li Hui https://orcid.org/0000-0001-7928-3055

Data availability

The datasets presented in this study can be found in online repositories. The names of the reposi-tory/repositories and accession number(s) can be found in the article.

References

Andrew R (2016) FigTree: Tree figure drawing tool Version 1.4.3. Institute of Evolutionary Biology, United Kingdom, University of Edinburgh Press.

Canete-Gibas CF, Takashima M, Sugita T, Nakase T (1998) Three new species of *Kockovaella* isolated from plants collected in the Ogasawara Islands. The Journal of General and Applied Microbiology 44(1): 11–18. https://doi.org/10.2323/jgam.44.11

do Carmo-Sousa L, Phaff HJ (1962) An improved method for the detection of spore discharge in the Sporobolomycetaceae. Journal of Bacteriology 83(2): 434–435. https://doi.org/10.1128/jb.83.2.434-435.1962

Fungsin B, Hamamoto M, Arunpairojana V, Sukhumavasi J, Atthasampunna P, Nakase T (2002) *Kockovaella barringtoniae* sp. nov., a new basidiomycetous yeast species isolated from a plant leaf collected in a tropical rain forest in Thailand. International Journal of Systematic and Evolutionary Microbiology 52(1): 281–284. https://doi.org/10.1099/00207713-52-1-281

Gomes FCO, Safar SVB, Santos ARO, Lachance MA, Rosa CA (2016) *Kockovaella libkindii* sp. nov., a yeast species isolated from water tanks of bromeliad. International Journal of Systematic and Evolutionary Microbiology 66(12): 5066–5069. https://doi.org/10.1099/ijsem.0.001471

Hall TA (1999) Bioedit: A user-friendly biological sequence alignment editor and analysis program for Windows 95/98/NT. Nucleic Acids Symposium Series 41: 95–98.

Hamamoto M, Kuroyanagi T, Nakase T (1998) *Fellomyces ogasawarensis* sp. nov. and *Fellomyces distylii* sp. nov., yeasts isolated from a plant in Japan. International Journal of Systematic Bacteriology 48(1): 287–293. https://doi.org/10.1099/00207713-48-1-287

Kalyaanamoorthy S, Minh BQ, Wong TKF, Von Haeseler A, Jermiin LS (2017) Modelfinder: Fast model selection for accurate phylogenetic estimates. Nature Methods 14(6): 587–589. https://doi.org/10.1038/nmeth.4285

Katoh K, Standley DM (2013) MAFFT multiple sequence alignment software version 7: Improvements in performance and usability. Molecular Biology and Evolution 30(4): 772–780. https://doi.org/10.1093/molbev/mst010

Kruse J, Doehlemann G, Kemen E, Thines M (2017) Asexual and sexual morphs of *Moesziomyces* revisited. IMA Fungus 8(1): 117–129. https://doi.org/10.5598/imafungus.2017.08.01.09

Kurtzman CP (2010) Description of new yeast species - Is one strain enough? The Bulletin of BISMiS 1(1): 17–24.

Kurtzman CP, Robnett CJ (1998) Identification and phylogeny of ascomycetous yeasts from analysis of nuclear large subunit (26S) ribosomal DNA partial sequences. Antonie van Leeuwenhoek 73(4): 331–371. https://doi.org/10.1023/A:1001761008817

Kurtzman CP, Robnett CJ (2003) Phylogenetic relationships among yeasts of the 'Saccharomyces complex' determined from multigene sequence analyses. FEMS Yeast Research 3(4): 417–432. https://doi.org/10.1016/S1567-1356(03)00012-6

Kurtzman CP, Fell JW, Boekhout T (2011) Methods for isolation, phenotypic characterization and maintenance of yeasts. In: Kurtzman CP, Fell JW, Boekhout T (Eds) The Yeasts – a Taxonomic Study, 5th edn., Vol. 1. Amsterdam, Elsevier, 87–110. https://doi.org/10.1016/B978-0-444-52149-1.00007-0

Larsson A (2014) AliView: A fast and lightweight alignment viewer and editor for large datasets. Bioinformatics 30(22): 3276–3278. https://doi.org/10.1093/bioinformatics/btu531

Li AH, Yuan FX, Groenewald M, Bensch K, Yurkov AM, Li K, Han PJ, Guo LD, Aime MC, Sampaio JP, Jindamorakot S, Turchetti B, Inacio J, Fungsin B, Wang QM, Bai FY (2020) Diversity and phylogeny of basidiomycetous yeasts from plant leaves and soil: Proposal of two new orders, three new families, eight new genera and one hundred and seven new species. Studies in Mycology 96: 17–140. https://doi.org/10.1016/j.simyco.2020.01.002

Liu XZ, Wang QM, Theelen B, Groenewald M, Bai FY, Boekhout T (2015a) Phylogeny of tremellomycetous yeasts and related dimorphic and filamentous basidiomycetes reconstructed from multiple gene sequence analyses. Studies in Mycology 81(1): 1–26. https://doi.org/10.1016/j.simyco.2015.08.001

Liu XZ, Wang QM, Göker M, Groenewald M, Kachalkin AV, Lumbsch HT, Millanes AM, Wedin M, Yurkov AM, Boekhout T, Bai FY (2015b) Towards an integrated phylogenetic classification of the Tremellomycetes. Studies in Mycology 81(1): 85–147. https://doi.org/10.1016/j.simyco.2015.12.001

Lopandic K, Molnár O, Prillinger H (2005a) Application of ITS sequence analysis, RAPD and AFLP fingerprinting in characterising the yeast genus *Fellomyces.* Microbiological Research 160(1): 13–26. https://doi.org/10.1016/j.micres.2004.09.005

Lopandic K, Molnár O, Prillinger H (2005b) *Fellomyces mexicanus* sp. nov., a new member of the yeast genus Fellomyces isolated from lichen *Cryptothecia rubrocincta* collected in Mexico. Microbiological Research 160(1): 1–11. https://doi.org/10.1016/j.micres.2004.09.004

Lopandic L, Prillinger H, Wuczkowski M (2011) *Fellomyces* Y. Yamada & Banno (1984). In: Kurtzman CP, Fell JW, Boekhout T (Eds) The Yeasts – a Taxonomic Study, 5th edn., Vol. 3. Amsterdam, Elsevier, 1759–1772. https://doi.org/10.1016/B978-0-444-52149-1.00142-7

Luong DT, Takashima M, Van P, Dung NL, Nakase T (2000) Four new species of *Kockovaella* isolated from plant leaves collected in Vietnam. The Journal of General and Applied Microbiology 46(6): 297–310. https://doi.org/10.2323/jgam.46.297

Nakase T (2000) Expanding world of ballistosporous yeasts: Distribution in the phyllosphere, systematics and phylogeny. The Journal of General and Applied Microbiology 46(4): 189–216. https://doi.org/10.2323/jgam.46.189

Nakase T, Takashima M (1993) A simple procedure for the high frequency isolation of new taxa of ballistosporous yeasts living on the surfaces of plants. RIKEN Review 3: 33–34.

Nakase T, Itoh M, Takematsu A, Mikata K, Banno I, Yamada Y (1991) *Kockovaella*, a new ballistospore-forming anamorphic yeast genus. The Journal of General and Applied Microbiology 37(2): 175–197. https://doi.org/10.2323/jgam.37.175

Nakase T, Takematsu A, Yamada Y (1993) Molecular approaches to the taxonomy of ballistosporous yeasts based on the analysis of the partial nucleotide sequences of 18S ribosomal ribonucleic acids. The Journal of General and Applied Microbiology 39(2): 107–134. https://doi.org/10.2323/jgam.39.107

Prillinger H, Kraepelin G, Lopandic K, Schweigkofler W, Molnár O, Weigang F, Dreyfuss MM (1997) New species of *Fellomyces* isolated from epiphytic lichen species. Systematic and Applied Microbiology 20(4): 572–584. https://doi.org/10.1016/S0723-2020(97)80029-X

Ronquist F, Teslenko M, van der Mark P, Ayres DL, Darling A, Höhna S, Larget B, Liu L, Suchard MA, Huelsenbeck JP (2012) MrBayes3.2: Efficient Bayesian phylogenetic inference and model choice, across a large model space. Systematic Biology 61(3): 539–542. https://doi.org/10.1093/sysbio/sys029

Spaaij F, Weber G, Roeijmans HJ, van Eijk GW, Oberwinkler F (1991) *Fellomyces horovitziae* sp. nov., a new basidiomycetous yeast species isolated from a *Xenasmatel-*

la basidiocarp. Antonie van Leeuwenhoek 59(4): 293–298. https://doi.org/10.1007/BF00583682

Stamatakis A (2014) RAxML Version 8: A tool for phylogenetic analyses and post analyses of large phylogenies. Bioinformatics 30(9): 1312–1313. https://doi.org/10.1093/bioinformatics/btu033

Takashima M, Nakase T (1998) *Bullera penniseticola* sp. nov. and *Kockovaella sacchari* sp. nov., two new yeast species isolated from plants in Thailand. International Journal of Systematic Bacteriology 48(3): 1025–1030. https://doi.org/10.1099/00207713-48-3-1025

Takashima M, Nakase T (2011) *Kockovaella* Nakase, Banno & Y. Yamada (1991). In: Kurtzman CP, Fell JW, Boekhout T (Eds) The Yeasts – a Taxonomic Study, 5th edn., Vol. 3. Amsterdam, Elsevier, 1781–1794. https://doi.org/10.1016/B978-0-444-52149-1.00145-2

Tamura K, Stecher G, Kumar S (2021) MEGA11: Molecular Evolutionary Genetics Analysis Version 11. Molecular Biology and Evolution 38(7): 3022–3027. https://doi.org/10.1093/molbev/msab120

Toome M, Roberson RW, Aime MC (2013) *Meredithblackwellia eburnean* gen. et sp. nov., Kriegeriaceae fam. nov. and Kriegeriales ord. nov. toward resolving higher-level classification in Microbotryomycetes. Mycologia 105(2): 486–495. https://doi.org/10.3852/12-251

Wang QM, Theelen B, Groenewald M, Bai FY, Boekhout T (2014) Moniliellomycetes and Malasseziomycetes, two new classes in Ustilaginomycotina. Persoonia 33(1): 41–47. https://doi.org/10.3767/003158514X682313

White TJ, Bruns T, Lee S, Taylor J (1990) Amplification and direct sequencing of fungal ribosomal RNA genes for phylogenetics. In: Innis MA, Gelfand DH, Sninsky JJ, White TJ (Eds) PCR Protocols: A Guide to Methods and Applications. Academic Press, New York, 315–322. https://doi.org/10.1016/B978-0-12-372180-8.50042-1

Yue JZ (1982) A new species of *Sterigmatomyces*. Acta Mycologica Sinica 1(2): 79–87. https://doi.org/10.13346/j.mycosystema.1982.02.004

Zhang D, Gao F, Jakovlić I, Zou H, Zhang J, Li WX, Wang GT (2020) PhyloSuite: An integrated and scalable desktop platform for streamlined molecular sequence data management and evolutionary phylogenetics studies. Molecular Ecology Resources 20(1): 348–355. https://doi.org/10.1111/1755-0998.13096

MycoKeys

MycoKeys 110: 255–272 (2024)
DOI: 10.3897/mycokeys.110.129120

Research Article

Unveiling species diversity within early-diverging fungi from China II: Three new species of *Absidia* (Cunninghamellaceae, Mucoromycota) from Hainan Province

Meng-Fei Tao[1], Zi-Ying Ding[1], Yi-Xin Wang[1], Zhao-Xue Zhang[2], Heng Zhao[3], Zhe Meng[1], Xiao-Yong Liu[1,4]

1 *College of Life Sciences, Shandong Normal University, Jinan, 250358, China*
2 *Shandong Provincial Key Laboratory for Biology of Vegetable Diseases and Insect Pests, College of Plant Protection, Shandong Agricultural University, Taian, 271018, China*
3 *School of Ecology and Nature Conservation, Beijing Forestry University, Beijing 100081, China*
4 *State Key Laboratory of Mycology, Institute of Microbiology, Chinese Academy of Sciences, Beijing 100101, China*

Corresponding authors: Zhe Meng (zmeng@sdnu.edu.cn); Xiao-Yong Liu (liuxy@sdnu.edu.cn)

Abstract

Absidia is distributed worldwide and primarily isolated from soil, feces, and decaying plants. The genus was initially classified into Absidiaceae and then Mucoraceae, and currently belongs to Cunninghamellaceae and is further divided into *Absidia* s.s., *Lichtheimia*, and *Lentamyces*. Three new species of *Absidia* s.s. are identified and described from soil in Hainan Province of China based on morphological characteristics, molecular data, and maximum growth temperatures as well. They are named based on distinct shapes of projections on columellae: *A. crystalloides* **sp. nov.** (crystal-like), *A. pacifica* **sp. nov.** (pacifier-like), *A. pateriformis* **sp. nov.** (bowling-like). In SSU-ITS-LSU-TEF-*Act* phylogram, the *A. crystalloides* is closely related to *A. oblongispora* and *A. heterospora*, the *A. pacifica* is a sister group with *A. edaphica*, and the *A. pateriformis* has a close relationship with *A. jiangxiensis*. This study enriches the species diversity of *Absidia* in China.

Key words: Basal fungi, fungal diversity, molecular phylogeny, Mucorales taxonomy

Academic editor: Thorsten Lumbsch
Received: 6 June 2024
Accepted: 1 November 2024
Published: 20 November 2024

Citation: Tao M-F, Ding Z-Y, Wang Y-X, Zhang Z-X, Zhao H, Meng Z, Liu X-Y (2024) Unveiling species diversity within early-diverging fungi from China II: Three new species of *Absidia* (Cunninghamellaceae, Mucoromycota) from Hainan Province. MycoKeys 110: 255–272. https://doi.org/10.3897/mycokeys.110.129120

Introduction

The genus *Absidia* Tiegh. 1878 belongs to Mucoromycota, Mucoromycetes, *Mucorales*, Cunninghamellaceae (http://www.indexfungorum.org/, accessed on 15 March 2024). The type species of this genus is *A. reflexa* Tiegh. 1878 (van Tieghem 1876). Its classification has been a subject of controversy for over a century. *Absidia* was initially classified in the family Absidiaceae (von Arx 1982) and later in the family Mucoraceae (Benny et al. 2001). Eventually, it was included in the family Cunninghamellaceae (Ashton 2009). Recently, *Absidia* s.l. was divided into *Absidia* s.s., *Lichtheimia* Vuill, and *Lentamyces* Kerst. Hoffm. & K. Voigt based on growth temperature, molecular phylogeny, and morphological characteristics (Hoffmann et al. 2007; Hoffmann and Voigt 2009; Hoffmann 2010). The *Absidia* is distributed globally, with reports

of its presence in Estonia (1621), Australia (839), Czechia (688), Argentina (514), and Lithuania (422) (https://www.gbif.org/, accessed on 15 March 2024). The genus is primarily found in soil, but it can also be detected in feces, air, decaying plants, and waste materials (Zhang et al. 2018; Lima et al. 2020; Zong et al. 2021; Hurdeal et al. 2021, 2023). Currently, there are 131 records of *Absidia* species, varieties and subspecies (http://www.indexfungorum.org/, accessed on 15 March 2024). Zhao et al. (2023) discovered 15 novel *Absidia* species from Beijing, Yunnan, Qinghai, and Xinjiang of China, along with three Chinese new record species. This significant contribution has substantially augmented the Chinese database on *Absidia* species resources and enhanced the taxonomic framework of Mucoromycota (Zhao et al. 2023). *Absidia* is frequently employed in the biotransformation of various types of natural products, including hydroxylation, glycosylation, reduction reactions, and more. Both *A. caerulea* and *A. glauca* can be utilized for the biotransformation of flavones and flavanones (Sordon et al. 2019). *A. spinosa* is applied in the biotransformation of cresol red (Kristanti et al. 2016). Additionally, it should be noted that species in those genera closely related to *Absidia* plays a vital role as a pathogen causing human mucormycosis (Constantinides et al. 2008); specifically, *A. corymbifera* (=*Lichtheimia corymbifera*) is associated with meningitis (Mackenzie et al. 1988) and keratitis (Varona et al. 2015). The typical characteristics of *Absidia* include stolons, rhizoids, sporangia, sporangiophores, etc. The sporangiophores can be branched or unbranched and may grow erect or curved. If a collar is present, it is easily noticeable. One or two protrusions are present on columellae. It produces zygospores that are typically spherical in shape (van Tieghem 1876; Hoffmann et al. 2007; Zong et al. 2021; Zhao et al. 2023).

While investigating soil microbial resources in Hainan Province, three novel *Absidia* species (*A. crystalloides* sp. nov., *A. pacifica* sp. nov., and *A. pateriformis* sp. nov.) were discovered. These new species are illustrated in this article based on morphological features, molecular phylogeny, and maximum growth temperatures.

Materials and methods

Sample collection and strain isolation

The strains were isolated from soil samples collected from Jianfengling Mountains and Bawangling Mountains in Hainan Province in October 2023. Samples were subjected to the moist-chamber culture and plate dilution coating methods (Zhao et al. 2022a, 2022b). The moist-chamber culture involved evenly sprinkling 1 g of soil onto the surface of PDA plates (potato 200 g, dextrose 20 g, agar 20 g, distilled water 1000 mL), sealing with a parafilm, inverting the plates, and incubating at 25 °C in darkness. After three days, microscopic observation was conducted, and the target strain was purified using an inoculating loop upon the formation of sporangia of *Absidia*. The plate dilution coating included taking 1 g of soil, diluting with 1 mL of sterile water through swirling and shaking until reaching dilutions of 10^{-2}, 10^{-3}, and 10^{-4}. Subsequently, 200 µL of the diluted solutions (10^{-3} and 10^{-4}) were evenly applied onto the surface of PDA plates using sterile triangle spreaders. The plates were sealed with a

parafilm and inverted for cultivation at 25 °C in darkness. After three days, purification of target strains was performed. The target strain was stored in four freezing tubes and preserved in a refrigerator at a temperature of 4 °C. The purified strains were preserved in the China General Microbiological Culture Collection Center, Beijing, China (CGMCC). Additionally, they were stored in the Shandong Agricultural University Culture Collection (SAUCC) and Shandong Normal University, Jinan, China (XG). The dried cultures were maintained in the Herbarium Mycologicum Academiae Sinicae, Beijing, China (HMAS).

Morphology and maximum growth temperature

The PDA cultured colonies were incubated at a temperature of 25 °C, and on the seventh day of colony growth, photographs were captured from both the front and back using a digital camera (Canon Powershot G7X). The colonies were allowed to grow for a period of five to six days, and then their microscopic morphology was observed using Olympus SZX10 stereomicroscope and Olympus BX53 microscope. Morphological features were assessed by measuring 20 variables, including minimum and maximum values. Two strains were inoculated on PDA containing 0.1% lecithin for pairing experiments, and the petri dishes were sealed with parafilm to maintain moisture. To determine the maximum growth temperature, a gradient method (Zheng et al. 2007, 2009; Zheng and Liu 2009; Zong et al. 2021; Zhao et al. 2022b) was employed whereby the colonies were initially cultured at 25 °C for two days followed by an increase in temperature by 1 °C each day until no further growth was observed. This determined the maximum temperature. The species were classified and described, and the taxonomic information was uploaded to Fungal Name repository (https://nmdc.cn/fungalnames/).

DNA extraction, PCR amplification, and sequencing

In this study, the CTAB method (Doyle and Doyle 1990; Guo et al. 2000) was employed for DNA extraction. Subsequently, the extracted DNA underwent polymerase chain reaction (PCR) targeting five segments, namely SSU (small subunit), ITS (internal transcribed spacer), LSU (large subunit of ribosomal DNA), TEF-1α (translation elongation factor 1 alpha), and *Act* (actin). For PCR amplification, five primer pairs were utilized: NS1/NS4, ITS4/ITS5, LR0R/LR5, EF1-983F/TEF1LLErev, and Act-1/Act-4R (Table 1). The amplification reaction solution (25 μL) contained 12.5 μL 2× Hieff Canace Plus PCR Master Mix with dye (Yeasen Biotechnology, Shanghai, China, Cat No. 10154ES03), 9.5 μL ddH_2O, 1 μL forward primer (10 μM), 1 μL reverse primer (10 μM) and 1 μL DNA template (1 ng/μL). The PCR programs are listed in Table 1. Following PCR amplification, the products were subjected to electrophoresis using 2% agarose gels and observed under UV light to confirm successful amplification (Zhang et al. 2021). Amplified products were purified through recovery using a Gel Extraction Kit (Cat# AE0101-C, Shandong Sparkjade Biotechnology Co., Ltd.). Tsingke Biotechnology Co., Ltd. (Qingdao, China) was responsible for DNA sequencing and primer synthesis. MEGA v. 7.0 (Kumar et al. 2016) was employed for sequence assembly. Finally, the sequence was compared against NCBI (National Center for Biotechnology Information) database to search relatives.

Table 1. Experimental condition of PCR used in this study.

Loci	PCR primers	Primer sequence (5' – 3')	PCR cycles	References
SSU	NS1; NS4	GTA GTC ATA TGC TTG TCT C C; CTT CCG TCA ATT CCT TTA AG	95 °C 5 min; (94 °C 60 s, 54 °C 50 s, 72 °C 60 s) × 37 cycles; 72 °C 10 min	(White et al. 1990)
ITS	ITS5; ITS4	GGA AGT AAA AGT CGT AAC AAG G; TCC TCC GCT TAT TGA TAT GC	95 °C 5 min; (95 °C 30 s, 55 °C 30 s, 72 °C 1 min) × 35 cycles; 72 °C 10 min	(White et al. 1990)
LSU	LR0R; LR5	GTA CCC GCT GAA CTT AAG C; TCC TGA GGG AAA CTT CG	95 °C 5 min; (94 °C 30 s, 52 °C 45 s, 72 °C 90 s) × 30 cycles; 72 °C 10 min	(Hurdeal et al. 2023)
TEF-1α	EF1-983F; TEF1LLErev	GCYCCYGGHCAYCGTGAYTTYAT; AACTTGCAGGCAATGTGG	95 °C 5 min; (95 °C 30 s, 55 °C 60 s,72 °C 60 s) × 30 cycles; 72 °C 10 min	(Rehner and Buckley 2005; Jaklitsch et al. 2005)
Act	Act-1; Act-4R	TGG GAC GAT ATG GAI AAI ATC TGG CA; TC ITC GTA TIC TIG CTI IGA IAT CCA CA T	95 °C 3 min; (95 °C 60 s, 55 °C 60 s,72 °C 60 s) × 30 cycles; 72 °C 10 min	(Voigt and Wöstemeyer 2000)

Phylogenetic analyses

Referring to the newly published article about *Absidia* (Zhao et al. 2023), the sequences were downloaded for phylogenetic analysis from the NCBI (https://www.ncbi.nlm.nih.gov/), and the GenBank accession numbers of the sequences used are shown in Table 2. All sequences were compared and manually corrected using MEGA v.7.0 (Kumar et al. 2016). The phylogeny of *Absidia* was inferred using the maximum likelihood (ML), Bayesian inference (BI), and maximum parsimony (MP) algorithms. ML analysis was conducted using RaxML 8.2.4 in CIPRES Science Gateway V. 3.3 (https://www.phylo.org/), with 1,000 bootstrap replicates (Miller et al. 2010; Stamatakis 2014). Eight cold Markov chains ran simultaneously for two million generations using the GTR + I + G model for BI analysis, and sampling once every 1,000 generations (Huelsenbeck and Ronquist 2001; Nylander 2004). MP analysis was performed for 1,000 bootstrap replicates by the heuristic search option with reconnection and bisection (Swofford 2002). The result of phylogenetic analysis was checked and adjusted using FigTree v.1.4.4 (http://tree.bio.ed.ac.uk/software/figtree), followed by beautifying the phylogenetic tree with Adobe Illustrator CC 2019. Base differences among the three new species and related species were calculated with MEGA7, with evolutionary distances and standard deviations being shown below and above the diagonal line, respectively. (Kumar et al. 2016).

Result

Phylogeny

Phylogenetic analyses of SSU, ITS, LSU rDNA, TEF-1α and *Act* were conducted for a total of 91 sequences, composing 36 species of *Absidia* and two outgroups, *Cunninghamella blakesleeana* (CBS 782.68) and *C. elegans* (CBS 167.53). The phylogenetic analysis encompassed a total of 4,785 characters, with 516 of SSU, 996 of ITS, 1,874 of LSU, 743 of TEF-1α, 660 of *Act* characters (Suppl. material 2). Among these, there were 2,712 constant and 515 variable but parsimony-uninformative characters, while the remaining 1558 characters were parsimony-informative. Both the maximum likelihood (ML) and Bayesian Inference (MB) method yielded highly similar trees with almost identical topologies. The phylogenetic relationship was represented using the topological structure obtained from ML analyses, with a final optimization likelihood of -53757.555363 (Fig. 1). The six strains of *Absidia* isolated in this study were divided into three individual branches representing *A. pacifica*, *A. crystalloides*, and *A. pateriformis*. In order to further resolve the three

Table 2. GenBank accession numbers of sequences used in this study.

Species	Strains	GenBank accession numbers				
		ITS	LSU	TEF-1α	Act	SSU
Absidia abundans	XY09265	ON074697	ON074681	NA	NA	NA
A. abundans	CGMCC 3.16255*	NR_182590	ON074683	NA	NA	NA
A. abundans	XY09274	ON074696	ON074682	NA	NA	NA
A. aguabelensis	URM 8213*	NR_189383	NG_241934	NA	NA	NA
A. alpina	CGMCC 3.16104	OL678133	NA	NA	NA	NA
A. ampullacea	CGMCC 3.16054	MZ354138	MZ350132	NA	NA	NA
A. anomala	CBS 125.68*	MH859085	MH870799	NA	NA	NA
A. anomala	FSU5798	EF030523	NA	NA	EF030535	NA
A. biappendiculata	CBS 187.64	MZ354153	MZ350147	MZ357420	MZ357438	NA
A. bonitoensis	URM 7889*	MN977786	MN977805	NA	NA	NA
A. brunnea	CGMCC 3.16055*	MZ354139	MZ350133	MZ357403	MZ357421	NA
A. caatinguensis	URM 7156*	NR_154704	NG_058582	NA	NA	NA
A. caerulea	XY00608	OL620081	NA	NA	NA	NA
A. caerulea	XY00729	OL620082	NA	NA	NA	NA
A. caerulea	CBS101.36	MH855718	MH867230	NA	NA	NA
A. caerulea	FSU767	AY944870	NA	NA	NA	NA
A. californica	CBS 314.78	JN205816	MH872902	NA	NA	NA
A. californica	FSU4748	AY944873	EU736301	EU736247	EU736224	EU736274
A. californica	FSU4747	AY944872	EU736300	EU736246	AY944758	EU736273
A. chinensis	CGMCC 3.16057	MZ354141	MZ350135	NA	MZ357422	NA
A. chinensis	CGMCC 3.16056*	MZ354140	MZ350134	NA	NA	NA
A. cinerea	CGMCC 3.16062	MZ354146	MZ350140	MZ357407	MZ357427	NA
A. cornuta	URM 6100*	NR_172976	MN625255	NA	NA	NA
A. crystalloides	**CGMCC3.27496***	**PP377803**	**PP373736**	**PP790574**	**PP790582**	**PP779723**
A. crystalloides	**SAUCC693201**	**PP377804**	**PP373737**	**PP790573**	**PP790581**	**PP779722**
A. cuneospora	CBS 101.59*	MH857828	MH869361	NA	NA	NA
A. cylindrospora	CBS 100.08	JN205822	JN206588	NA	NA	NA
A. digitula	CGMCC 3.16058*	MZ354142	MZ350136	MZ357404	MZ357423	NA
A. edaphica	MFLUCC 20-0088	NR_172305	NG_075367	NA	MT410739	NG_074951
A. frigida	CGMCC 3.16201*	NR_182565	OM030223	NA	NA	NA
A. fusca	CBS 102.35*	NR_103625	NG_058552	NA	NA	NA
A. gemella	CGMCC 3.16202*	OM108488	OM030224	NA	NA	NA
A. glauca	CBS 129233	MH865253	MH876693	NA	NA	NA
A. glauca	CBS 101.08*	MH854573	MH866105	NA	NA	NA
A. glauca	FSU660	AY944879	EU736302	EU736248	EU736225	EU736275
A. globospora	CGMCC 3.16031*	NR_189829	MW671544	MZ357412	MZ357431	NA
A. globospora	CGMCC 3.16035	MW671538	MW671545	MZ357413	MZ357432	NA
A. globospora	CGMCC 3.16036	MW671539	MW671546	MZ357414	MZ357433	NA
A. heterospora	SHTH021	JN942683	JN982936	NA	NA	JQ004928
A. jiangxiensis	CGMCC 3.16105*	OL678134	PP780377	PP790569	PP790577	PP779719
A. jindoensis	CNUFC-PTI1-1	MF926622	MF926616	MF926513	MF926510	MF926626
A. koreana	EML-IFS45-1*	KR030062	KR030056	KR030060	KR030058	KT321298
A. koreana	XY00816	OL620083	ON123771	NA	NA	NA
A. koreana	XY00596	OL620084	NA	NA	NA	NA
A. lobata	CGMCC 3.16256	ON074690	ON074679	NA	NA	NA
A. longissima	CGMCC 3.16203*	NR_182566	OM030225	NA	NA	NA
A. macrospora	FSU4746	AY944882	EU736303	EU736249	AY944760	EU736276
A. medulla	CGMCC 3.16034	NR_189832	MW671549	MZ357417	MZ357436	NA
A. montepascoalis	URM 8218	NR_172995	NA	NA	NA	NA
A. multispora	URM 8210*	MN953780	MN953782	NA	NA	NA
A. nigra	CBS 127.68*	NR_173068	MZ350146	MZ357419	MZ357437	NA

Species	Strains	GenBank accession numbers				
		ITS	LSU	TEF-1α	Act	SSU
A. nigra	CGMCC 3.16059	MZ354143	MZ350137	MZ357405	MZ357424	NA
A. nigra	CGMCC 3.16060	MZ354144	MZ350138	MZ357406	MZ357425	NA
A. oblongispora	CGMCC 3.16061	MZ354145	MZ350139	NA	MZ357426	NA
A. ovalispora	CGMCC 3.16019	NR_176748	MW264131	NA	NA	NA
A. pacifica	**CGMCC3.27497***	**PP377802**	**PP373735**	**PP839793**	**PP790579**	**PP779720**
A. pacifica	**SAUCC413601**	**PP377801**	**PP373734**	**PP839794**	**PP790580**	**PP779721**
A. panacisoli	SYPF 7183*	MF522181	MF522180	MF624251	NA	MF522179
A. pararepens	XY00631	OL620085	ON123774	NA	NA	NA
A. pararepens	XY00615	OL620086	NA	NA	NA	NA
A. pararepens	XY05899	OL620087	NA	NA	NA	NA
A. pararepens	CCF 6352	MT193669	MT192308	NA	NA	NA
A. pateriformis	**CGMCC3.27495***	**PP377805**	**PP373738**	**PP790575**	**PP790583**	**PP779724**
A. pateriformis	**SAUCC634702**	**PP377806**	**PP373739**	**PP790576**	**PP790584**	**PP779725**
A. pernambucoensis	URM<BRA>7219	MN635568	MN635569	NA	NA	NA
A. pseudocylindrospora	EML-FSDY6-2	KU923817	KU923814	NA	KU923815	KU923819
A. psychrophilia	FSU4745	AY944874	EU736306	EU736252	AY944762	EU736279
A. purpurea	CGMCC 3.16106	OL678135	NA	NA	NA	NA
A. radiata	CGMCC 3.16257	ON074698	ON074684	NA	NA	NA
A. radiata	XY09330-1	ON074699	ON074685	NA	NA	NA
A. repens	CBS 115583*	NR_103624	NG_058551	NA	NA	NA
A. saloaensis	URM 8209*	MN953781	MN953783	NA	NA	NA
A. sichuanensis	CGMCC 3.16258*	NR_182589	ON074688	NA	NA	NA
A. soli	MFLU-20-0414*	MT396373	MT393988	NA	NA	MT394049
A. spinosa	FSU551	AY944887	EU736307	EU736253	EU736227	EU736280
A. stercoraria	EML-DG8-1*	KU168828	KT921998	KT922002	KT922000	NG_065640
A. sympodialis	CGMCC 3.16063*	MZ354147	MZ350141	NA	NA	NA
A. sympodialis	CGMCC 3.16064	MZ354148	MZ350142	MZ357408	NA	NA
A. terrestris	FMR 14989*	LT795003	LT795005	NA	NA	NA
A. turgida	CGMCC 3.16032*	NR_189830	NG_241931	MZ357415	MZ357434	NA
A. varians	CGMCC 3.16065*	MZ354149	MZ350143	MZ357409	MZ357428	NA
A. virescens	CGMCC 3.16066*	MZ354150	MZ350144	MZ357410	MZ357429	NA
A. virescens	CGMCC 3.16067	MZ354151	MZ350145	MZ357411	MZ357430	NA
A. xinjiangensis	CGMCC 3.16107*	OL678136	NA	NA	NA	NA
A. yunnanensis	XY09528	ON074701	ON074686	NA	NA	NA
A. yunnanensis	CGMCC 3.16259*	NR_182591	NG_149054	NA	NA	NA
A. zonata	CGMCC 3.16033*	NR_189831	MW671548	MZ357416	MZ357435	NA
A. zygospora	RSPG 214	KC478527	NA	NA	NA	NA
A. zygospora	ANG28	DQ914420	NA	NA	NA	NA
Cunninghamella blakesleeana	CBS 782.68	JN205869	MH870950	NA	NA	NA
C. elegans	CBS 167.53	MH857146	HM849700	NA	NA	NA

Notes: The newly discovered species identified in the study are in bold. Ex-type strains are marked with a "*". NA stands for "not available".

new species and their related species, genetic distances of each DNA marker were calculated and shown in the Suppl. material 1: PDF. The *A. pacifica* is closely related to *A. edaphica* (MLBV = 100, BIPP = 1.00), with genetic distances of 0.739 (ITS), 0.699 (LSU), 0.008 (*Act*), and 0.003 (SSU). The *A. crystalloides* is closely related to *A. oblongispora* and *A. heterospora* (MLBV = 100, BIPP = 1.00), with genetic distances of 0.760 (ITS), 0.716 (LSU), and 0.008 (*Act*) from *A. oblongispora*, and 0.657 (ITS), 0.721 (LSU), and 0.000 (SSU) from *A. heterospora*. The *A. pateriformis* is closely related to *A. jiangxiensis* (MLBV = 100, BIPP = 1.00), with genetic distances of 0.724 (ITS), 0.763 (LSU), 0.002 (TEF-1α), 0.018 (*Act*), and 0.003 (SSU).

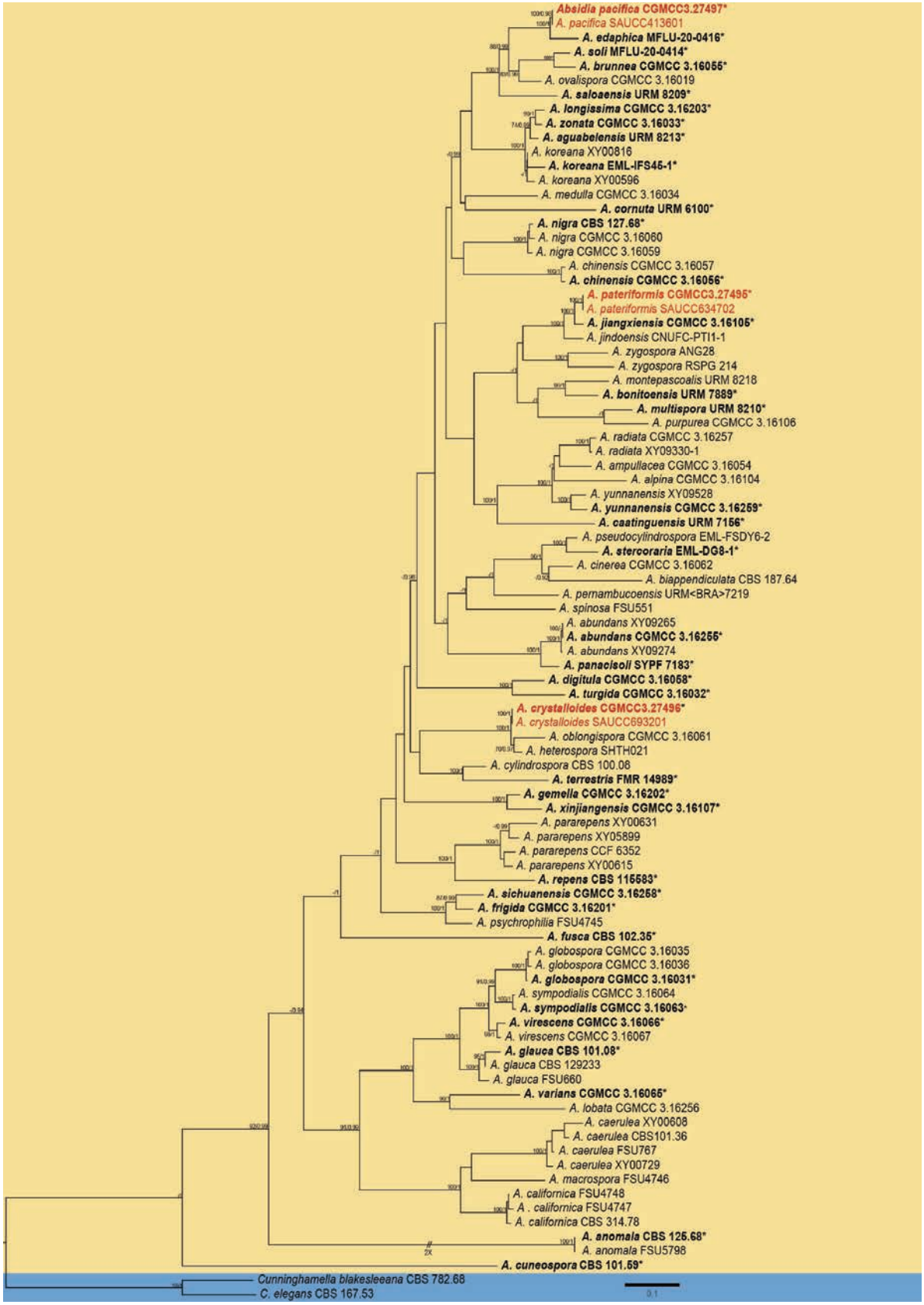

Figure 1. The maximum likelihood phylogram of *Absidia* based on SSU, ITS, LSU rDNA, TEF-1α and *Act* sequences with *Cunninghamella blakesleeana and C. elegans* as outgroups. The branches are marked with the Maximum Likelihood Bootstrap Value (left, MLBV ≥ 70%) and Bayesian Inference Posterior Probability (right, BIPP ≥ 0.90) at nodes. The six newly identified strains are denoted in red. Ex-type or ex-epitype strains are indicated with "*".

Taxonomy

The present study reported three novel species, namely *Absidia pacifica* sp. nov., *A. crystalloides* sp. nov., and *A. pateriformis* sp. nov., from soil samples collected in Hainan, China. They are described and illustrated as follows.

***Absidia pacifica* M.F. Tao, H. Zhao & X.Y. Liu, sp. nov.**
Fungal Names: FN 571915
Fig. 2

Type. China • Hainan Province, Changjiang County, Bawangling National Forest Park (19.08593°N, 109.12275°E), from soil, 14 Oct 2023, M.F. Tao and X.Y. Liu, holotype HMAS 352924, ex-holotype living culture CGMCC3.27497, living cultures XG06955-16 or SAUCC6955-16.

Etymology. The epithet *pacifica* (Lat.) refers to the pacifier-shaped projections.

Description. Mycelia hyaline at first, becoming brownish when mature, aseptate or irregularly septate with age, branched. Stolons hyaline to brownish, smooth, branched, 4.2–8.8 µm in diameter. Rhizoids well-developed, root-like, hyaline, simply branched. Stolons present. Sporangiophores growing from stolons, erect or slightly bent, unbranched, hyaline, single or 2–6 in whorls, 79.1–128.7 µm long, 3.0–6.5 µm wide, sometimes with a swelling beneath sporangia, with a septum 11.3–29.6 µm below apophyses. Apophyses obvious, small, hyaline, slightly pigmented, 4.6–8.4 µm wide at the base and 9.8–20.0 µm wide at the top. Sporangia globose, smooth, dark brown, deliquescent-walled, 23.6–39.2 µm long, 19.0–33.7 µm wide. Collars absent or present. Columellae mostly globose, occasionally oval, 12.8–22.1 µm long, 9.5–21.8 µm wide. Projections pacifier-like, 4.1–7.5 µm long, 1.8–3.9 µm wide. Sporangiospores variously shaped, mostly cylindrical or subglobose, smooth, hyaline, 2.8–6.2 µm long, 2.0–3.9 µm wide. Chlamydospores absent. Zygospores not found.

Culture characteristics. Colonies on PDA at 25 °C for 7 days, reaching 85 mm in diameter, exhibiting an average growth rate of approximately 11.4–12.1 mm/d, white initially, brown with age, irregularly concentrically zonate with ring, flower-shaped, irregularly in reverse, with adjoining satellite colonies at edge.

Maximum growth temperature. 35 °C.

Additional specimen examined. China • Hainan Province, Changjiang County, Seven Forks (19.11750°N, 109.15000°E), from soil, 11 Apr 2023, M.F. Tao and X.Y. Liu, living culture XG04136-4 or SAUCC413601; • China, Hainan Province, Changjiang County, Bawangling National Forest Park (19.08593°N, 109.12275°E), from soil, 14 Oct 2023, M.F. Tao and X.Y. Liu, living culture XG06955-15 or SAUCC6955-15.

Notes. Phylogenetically, *A. pacifica* was closely related to *A. edaphica*. Morphologically, the sporangiophores of *A. pacifica* was longer than that of *A. edaphica* (3.0–6.5 µm vs 2.5–5.4 µm), and the distance between the septum and apophysis was shorter in *A. pacifica* than that in *A. edaphica* (11.3–29.6 µm vs 20–33.5 µm). The columellae of *A. pacifica* were larger than those of *A. edaphica* (9.5–21.8 × 12.8–22.1 µm vs 5–9.5 × 6.5–20 µm). Additionally, some columellae in *A.pacifica* lacked a collar structure. The overall length of spores in *A.pacifica* was slightly larger than that in *A. edaphica* (2.8–6.2 µm

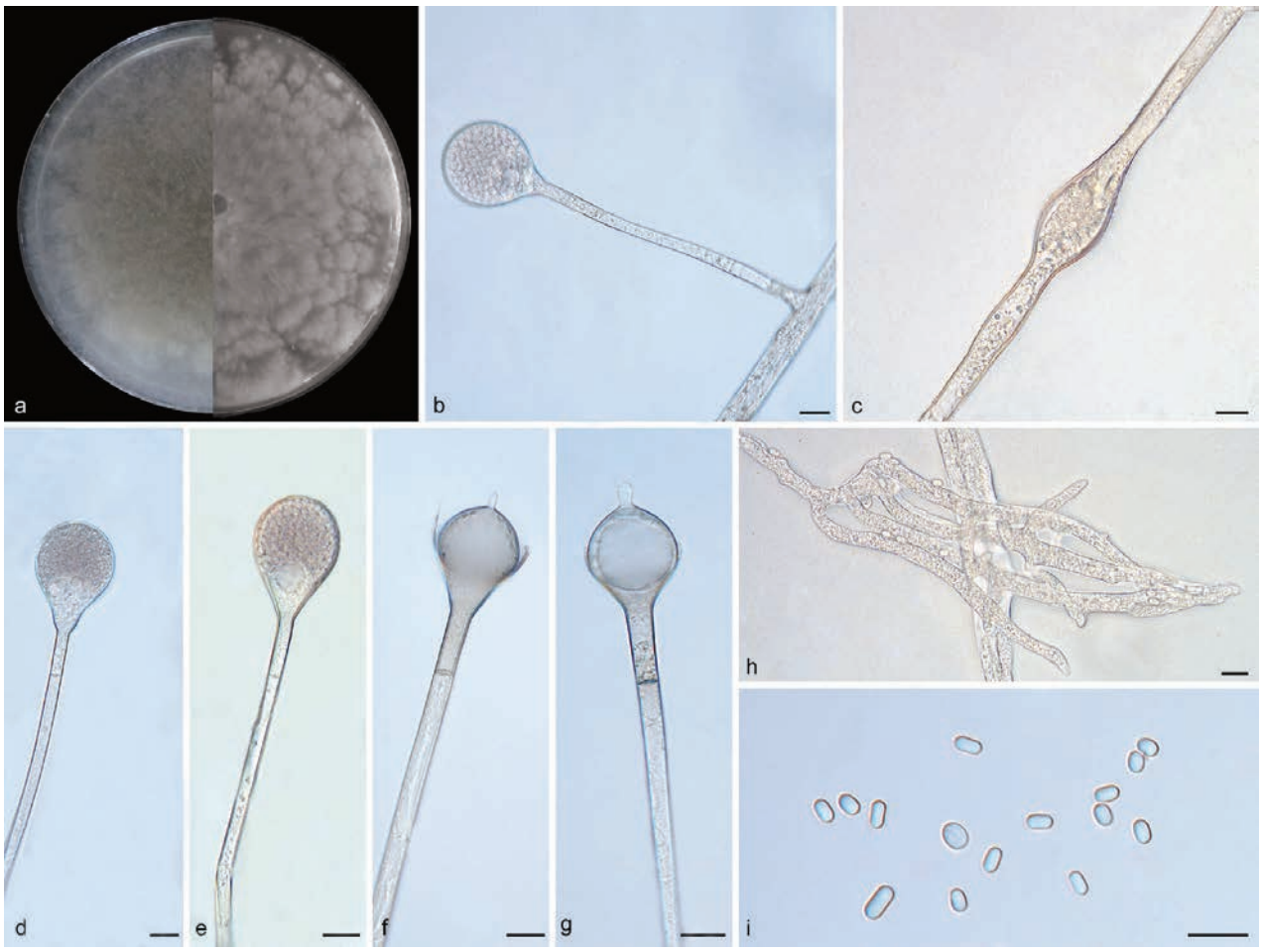

Figure 2. *Absidia pacifica* (holotype: HMAS 352924) **a** obverse and reverse of the culture on PDA **b, d, e** sporangia **c** swellings in hyphae **f, g** columellae **h** rhizoids **i** sporangiospores. Scale bars: 10 μm (**b–i**).

vs 3.5–5.5 μm), and the shape of sporangiospores in *A. pacifica* was more diverse. Physiologically, the maximum growth temperature for *A. pacifica* was lower than that of *A. edaphica* (35 °C vs 36 °C) (Hurdeal et al. 2021).

Absidia crystalloides **M.F. Tao, H. Zhao & X.Y. Liu, sp. nov.**
Fungal Names: FN 571916
Fig. 3

Type. China • Hainan Province, Changjiang County, Bawangling National Forest Park (19.08593°N, 109.12275°E), from soil, 14 Oct 2023, M.F. Tao and X.Y. Liu, holotype HMAS 352925, ex-holotype living culture CGMCC3.27496, living cultures XG06948-15 or SAUCC6948-15.

Etymology. The epithet *crystalloides* (Lat.) refers to the crystal-like projections.

Description. Mycelia white at first and gradually turning to dark brown, branched, subhyaline to hyaline, aseptate or irregularly septate with age. Rhizoids well-developed, root-like, branched. Stolons hyaline, branched, brownish, smooth, 3.1–7.8 μm in diameter. Sporangiophores growing on stolons, mostly unbranched or simply branched, erect or slightly bent, smooth, single or 2–4 in whorls, 55.8–109.3 μm long, 2.6–4.7 μm wide, with one septum 12.8–24.1 μm below sporan-

gia. Sporangia mainly globose, rarely pyriform, dark brown, smooth, subhyaline, deliquescent-walled, 23.0–28.0 µm long, 23.4–28.0 µm wide. Apophyses distinct, light brown, subhyaline, 3.9–9.4 µm wide at the base and 7.4–17.8 µm wide at the top. Collars clearly present, hyaline. Columellae subglobose to globose, smooth, 9.7–12.6 µm long, 11.7–19.5 µm wide. Projections present or absent, if present, single, crystal-like, 3.1–3.5 µm long, 1.8–2.2 µm wide. Sporangiospores smooth, hyaline, oval or fabiform, exhibiting a slight constriction at the center, 3.1–4.1 µm long, 2.1–2.8 µm wide. Chlamydospores absent. Zygospores not found.

Culture characteristics. Colonies on PDA at 25 °C for 7 days, reaching 65 mm in diameter, exhibiting an average growth rate of approximately 8.6–9.3 mm/d, white initially, gradually becoming dark brown when mature, irregularly concentrically zonate with ring, irregularly in reverse.

Maximum growth temperature. 32 °C.

Additional specimen examined. China • Hainan Province, Changjiang County, Bawangling National Forest Park (19.08593°N, 109.12275°E), from soil, 14 Oct 2023, M.F. Tao and X.Y. Liu, living culture XG06932-1 or SAUCC693201, XG06948-17 or SAUCC6948-17.

Notes. Phylogenetically, *A. crystalloides* was closely related to *A. oblongispora* and *A. heterospora*. Compared with *A. oblongispora*, the *A. crystalloides* exhibited a smaller stolon diameter (3.1–7.8 µm vs 4.0–9.5 µm), the septum was po-

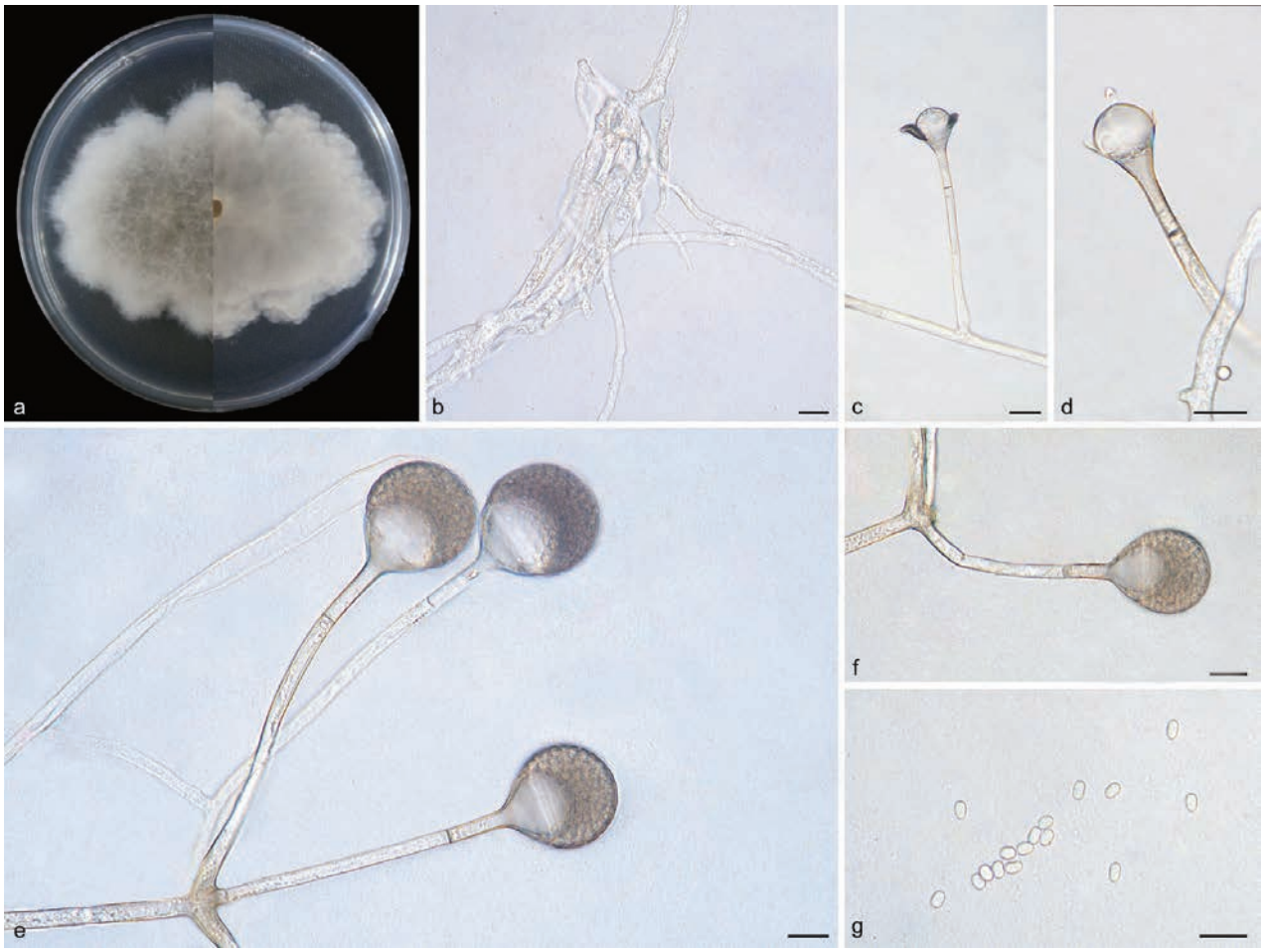

Figure 3. *Absidia crystalloides* (holotype: HMAS 352925) **a** obverse and reverse of the culture on PDA **b** rhizoids **c, d** columellae **e, f** sporangia **g** sporangiospores. Scale bars: 10 µm (**b–g**).

sitioned at a greater distance from apophyses (12.8–24.1 µm vs 9.5–16.0 µm), while sporangiophores were located at a shorter distance (55.8–109.3 µm vs 33.0–300.0 µm), apophyses had a wider base width (3.9–9.4 µm vs 3.5–7.5 µm). Physiologically, the maximum growth temperature of *A. crystalloides* was higher (32 °C vs 31 °C). In comparison to *A. heterospora*, the *A. crystalloides* possessed two forms of sporangiospores and had a smaller columella diameter (11.7–19.5 µm vs 10.5–34 µm) (Hesseltine and Ellis 1964; Zhao et al. 2023).

Absidia pateriformis **M.F. Tao, H. Zhao & X.Y. Liu, sp. nov.**
Fungal Names: FN 571917
Fig. 4

Type. China • Hainan Province, Ledong County, Jianfengling National Forest Park (18.74540°N, 108.96716°E), from soil, 13 Oct 2023, M.F. Tao and X.Y. Liu, holotype HMAS 352926, ex-holotype living culture CGMCC3.27495, living cultures XG06347-1 or SAUCC6347D-1.

Etymology. The *pateriformis* (Lat.) refers to its bowling-like projections.

Description. Mycelia white at first and gradually turning to light brown, aseptate or septate, branched. Rhizoids well-developed, root-like, simply branched.

Figure 4. *Absidia pateriformis* (holotype: HMAS 352926) **a** obverse and reverse of the culture on PDA **b** sporangiospores **c** rhizoids **d** columellae **e–g** sporangia. Scale bars: 10 µm (**b–g**).

Stolons hyaline, branched, smooth, 4.4–9.2 μm in diameter. Sporangiophores growing on stolons, erect or slightly bent, mostly unbranched or simply branched, smooth, single or 2–4 in whorls, 33.4–156.5 μm long, 2.7–6.8 μm wide. Sporangia globose to pyriform, smooth, hyaline, deliquescent-walled, 16.8–30.6 μm long, 11.2–26.7 μm wide, and with a septum 9.4–20.6 μm below sporangia. Apophyses obvious, gradually widening from the base to the top, 3.8–11.4 μm wide at the base and 7.1–24.3 μm wide at the top, light brown, hyaline. Collars absent or present. Columellae mostly globose, occasionally oval, 10.9–25.1 μm long, 8.2–21.0 μm wide. Projections obvious, bowling-like, hyaline, single, 3.3–6.7 μm long, 1.2–4.0 μm wide. Sporangiospores smooth, hyaline, oval or globose, 3.1–4.2 μm long, 2.7–4.0 μm wide. Chlamydospores absent. Zygospores not found.

Culture characteristics. Colonies on PDA at 25 °C for 7 days, reaching 80 mm in diameter, exhibiting an average growth rate of approximately 10.7–11.4 mm/day, initially white, gradually becoming light brown and greenish when mature, regularly in reverse, petaloid at edge.

Maximum growth temperature. 30 °C.

Additional specimen examined. China • Hainan Province, Ledong County, Jianfengling National Forest Park (18.74540°N, 108.96716°E), from soil, 13 Oct 2023, M.F. Tao and X.Y. Liu, living culture XG06347D-2, SAUCC634702 or SAUCC6347D-2.

Notes. In the molecular phylogeny, *A. pateriformis* was closely related to *A. jiangxiensis*. Morphologically, the sporangiophores of *A. pateriformis* were at most four-wheeled and branched, while those of *A. jiangxiensis* were at most six-wheeled and unbranched. Additionally, the maximum length of the sporangiophores in *A. jiangxiensis* was significantly greater than that in *A. pateriformis* (156.5 μm vs 280.0 μm). The sporangia size was also smaller in *A. pateriformis* (16.8–30.6 × 11.2–26.7 μm vs 16.5–48 × 16.5–44 μm), with only one projection observed instead of two and a narrower columellae (8–21 μm vs 10–34 μm). Zygospores were not observed in *A. pateriformis* (Zhao et al. 2023).

Discussion

Absidia is predominantly distributed in soil environments (Richardson 2009). In this study, we investigated the soil in Hainan Province. Based on morphology, growth temperature dynamics and molecular phylogenetic analyses, we identified three novel species in the genus *Absidia*, namely *A. pacifica* sp. nov., *A. crystalloides* sp. nov., and *A. pateriformis* sp. nov. The inclusion of these three taxa altered the topology of the *Absidia* tree. Through joint data analysis of SSU, ITS, LSU, TEF-1α and *Act*, the placement of these new species in the evolutionary tree was robustly supported (*A. pacifica* 100% MLBV and 0.98 BIPP; *A. crystalloides* 100% MLBV and 1.00 BIPP; *A. pateriformis* 100% MLBV and 1.00 BIPP; Fig. 1). The phylogenetic analysis also revealed a close relationship between *A. pacifica* and *A. edaphica* (100% MLBV, 1.00 BIPP), whereas *A. crystalloides* exhibited a close affinity to both *A. oblongispora* and *A. heterospora* (100% MLBV, 1.00 BIPP), and *A. pateriformis* demonstrated a strong association with *A. jiangxiensis* (100% MLBV, 1.00 BIPP). Simultaneously, we observed certain variations in morphological structure and physiology, which served as the basis for species identification. The three newly discovered species and their related counterparts exhibited varying degrees of discrepancy in sporangiophores, sporangia, projections, sporangiospores, and other structures. Furthermore, the maximum growth

temperatures were found to be distinguishable among these species. These dissimilarities served as the foundation for the identification of novel species.

Currently, the phylogenetic analysis of *Absidia* primarily employed a combined analysis of SSU, ITS, LSU, TEF-1α, and *Act*. Previous studies demonstrated that due to the significant variation among *Absidia* species, relying solely on ITS for identifying *Absidia* species might yield inaccurate results; therefore, it was essential to incorporate LSU or other gene markers in the analysis process. Nucleotide sequences of SSU ITS, LSU, TEF-1α, and *Act* fragments served as robust tools for *Absidia* identification (White et al. 1990; Hoffmann et al. 2007, 2013; Ariyawansa et al. 2015).

Early on, *Lichtheimia* was initially classified as *Absidia* due to its morphological resemblance, Hoffmann et al. (2007) categorized *Absidia* into three groups based on their maximum growth temperature: thermotolerant (≥37 °C), mesophilic (25 °C–34 °C), and mycoparasitic (≤30 °C). The thermotolerant strains were subsequently reclassified as *Lichtheimia*. Currently, there were hardly any identified strains of *Absidia* capable of growing at a maximum temperature of 37 °C (Zhao et al. 2022b, 2023). This study further confirmed this conclusion by demonstrating that the maximum growth temperatures for *A. pacifica*, *A. crystalloides*, and *A. pateriformis* were 35 °C, 32 °C and 30 °C, respectively.

In China, the majority of *Absidia* species were predominantly distributed in Xinjiang, Taiwan, and Yunnan, primarily inhabiting tropical, subtropical, and temperate regions (Zhao et al. 2022b). However, due to its limited tolerance for high temperatures, most *Absidia* species found in tropical areas were typically restricted to cool and humid environments such as forest soil and dung (Cordeiro et al. 2020; Lima et al. 2021). The discovery of the three new species in this study was exclusively made in the tropical forest soil of Hainan Island. This finding further validated the remarkable species diversity of *Absidia* within tropical and subtropical regions while also providing valuable insights for future exploration into additional *Absidia* strains.

Additional information

Conflict of interest

The authors have declared that no competing interests exist.

Ethical statement

No ethical statement was reported.

Funding

This study was supported by the National Natural Science Foundation of China (Nos. 32170012, 32300011, 32470004), Ji'nan City's 'New University 20 Policies' Initiative for Innovative Research Teams Project (202228028), Innovative Agricultural Application Technology Project of Jinan City (CX202210), and Key Technological Innovation Program of Shandong Province, China (2022CXGC020710)

Author contributions

M.F. Tao was responsible for DNA sequencing, photo editing and paper drafting; Z.Y. Ding was responsible for data analyses; Y.X. Wang and Z.X. Zhang collected soil samples; H. Zhao named the new species and revised the paper; Z. Meng was responsible

for data analyses and manuscript revision; X.Y. Liu took charge of naming the new species, conceiving and revising the paper, and providing funding.

Author ORCIDs

Meng-Fei Tao https://orcid.org/0009-0008-9053-1310
Zi-Ying Ding https://orcid.org/0009-0003-1618-5740
Yi-Xin Wang https://orcid.org/0009-0001-5231-914X
Zhao-Xue Zhang https://orcid.org/0000-0002-4824-9716
Heng Zhao https://orcid.org/0000-0003-2938-5613
Xiao-Yong Liu https://orcid.org/0000-0002-8808-010X

Data availability

All of the data that support the findings of this study are available in the main text or Supplementary Information.

References

Ariyawansa HA, Hyde KD, Jayasiri SC, Buyck B, Chethana KWT, Dai DQ, Dai YC, Daranagama DA, Jayawardena RS, Lücking R, Ghobad-Nejhad M, Niskanen T, Thambugala KM, Voigt K, Zhao RL, Li G-J, Doilom M, Boonmee S, Yang ZL, Cai Q, Cui Y-Y, Bahkali AH, Chen J, Cui BK, Chen JJ, Dayarathne MC, Dissanayake AJ, Ekanayaka AH, Hashimoto A, Hongsanan S, Jones EBG, Larsson E, Li WJ, Li Q-R, Liu JK, Luo ZL, Maharachchikumbura SSN, Mapook A, McKenzie EHC, Norphanphoun C, Konta S, Pang KL, Perera RH, Phookamsak R, Phukhamsakda C, Pinruan U, Randrianjohany E, Singtripop C, Tanaka K, Tian CM, Tibpromma S, Abdel-Wahab MA, Wanasinghe DN, Wijayawardene NN, Zhang J-F, Zhang H, Abdel-Aziz FA, Wedin M, Westberg M, Ammirati JF, Bulgakov TS, Lima DX, Callaghan TM, Callac P, Chang C-H, Coca LF, Dal-Forno M, Dollhofer V, Fliegerová K, Greiner K, Griffith GW, Ho H-M, Hofstetter V, Jeewon R, Kang JC, Wen T-C, Kirk PM, Kytövuori I, Lawrey JD, Xing J, Li H, Liu ZY, Liu XZ, Liimatainen K, Lumbsch HT, Matsumura M, Moncada B, Nuankaew S, Parnmen S, de Azevedo Santiago ALCM, Sommai S, Song Y, de Souza CAF, de Souza-Motta CM, Su HY, Suetrong S, Wang Y, Wei S-F, Wen TC, Yuan HS, Zhou LW, Réblová M, Fournier J, Camporesi E, Luangsa-ard JJ, Tasanathai K, Khonsanit A, Thanakitpipattana D, Somrithipol S, Diederich P, Millanes AM, Common RS, Stadler M, Yan JY, Li XH, Lee HW, Nguyen TTT, Lee HB, Battistin E, Marsico O, Vizzini A, Vila J, Ercole E, Eberhardt U, Simonini G, Wen H-A, Chen X-H, Miettinen O, Spirin V, Hernawati (2015) Fungal diversity notes 111–252: Taxonomic and phylogenetic contributions to fungal taxa. Fungal Diversity 75(1): 27–274. https://doi.org/10.1007/s13225-015-0346-5

Ashton H (2009) Ainsworth and Bisby's Dictionary of the Fungi (10th edn). Reference Reviews 23(5): 42–42. https://doi.org/10.1108/09504120910969104

Benny GL, Humber RA, Morton JB (2001) Zygomycota: Zygomycetes. In: McLaughlin DJ, McLaughlin EG, Lemke PA (Eds) Systematics and Evolution, 1st edn. Springer, Berlin, Heidelberg, 113–146. https://doi.org/10.1007/978-3-662-10376-0_6

Constantinides J, Misra A, Nassab R, Wilson Y (2008) *Absidia corymbifera* fungal infection in burns: A case report and review of the literature. Journal of Burn Care & Research; Official Publication of the American Burn Association 29(2): 416–419. https://doi.org/10.1097/BCR.0b013e318166da78

Cordeiro TR, Nguyen TT, Lima DX, Silva SC, Lima CL, Leitão JD, Gurgel L, Lee HB, Santiago AL (2020) Two new species of the industrially relevant genus *Absidia* (Mucorales)

from soil of the Brazilian Atlantic Forest. Acta Botanica Brasílica 34(3): 549–558. https://doi.org/10.1590/0102-33062020abb0040

Doyle JJ, Doyle JL (1990) Isolation of plant DNA from fresh tissue. Focus (San Francisco, Calif.) 12: 13–15. https://doi.org/10.2307/2419362

Guo LD, Hyde KD, Liew ECY (2000) Identification of endophytic fungi from Livistona chinensis based on morphology and rDNA sequences. The New Phytologist 147(3): 617–630. https://doi.org/10.1046/j.1469-8137.2000.00716.x

Hesseltine CW, Ellis JJ (1964) The Genus *Absidia*: *Gongronella* and cylindrical-spored species of *Absidia*. Mycologia 56(4): 568–601. https://doi.org/10.1080/00275514.1964.12018145

Hoffmann K (2010) Identification of the genus *Absidia* (Mucorales, Zygomycetes): a comprehensive taxonomic revision. In: Gherbawy Y, Voigt K (Eds) Molecular Identification of Fungi, 1st, edn. Springer, Berlin, 439–460. https://doi.org/10.1007/978-3-642-05042-8-19

Hoffmann K, Voigt K (2009) *Absidia parricida* plays a dominant role in biotrophic fusion parasitism among mucoralean fungi (Zygomycetes): *Lentamyces*, a new genus for *A. parricida* and *A. zychae*. Plant Biology 11(4): 537–554. https://doi.org/10.1111/j.1438-8677.2008.00145.x

Hoffmann K, Discher S, Voigt K (2007) Revision of the genus *Absidia* (Mucorales, Zygomycetes) based on physiological, phylogenetic, and morphological characters; thermotolerant *Absidia* spp. form a coherent group Mycocladiaceae fam. nov. Mycological Research 111(10): 1169–1183. https://doi.org/10.1016/j.mycres.2007.07.002

Hoffmann K, Pawłowska J, Walther G, Wrzosek M, de Hoog GS, Benny GL, Kirk PM, Voigt K (2013) The family structure of the Mucorales: A synoptic revision based on comprehensive multigene-genealogies. Persoonia 30(1): 57–76. https://doi.org/10.3767/003158513X666259

Huelsenbeck JP, Ronquist F (2001) MRBAYES: Bayesian inference of phylogenetic trees. Bioinformatics (Oxford, England) 17(8): 754–755. https://doi.org/10.1093/bioinformatics/17.8.754

Hurdeal V G, Gentekaki E, Lee H B, Jeewon R, Hyde K D, Tibpromma S, Mortimer P E, Xu J (2021) Mucoralean fungi in Thailand: novel species of *Absidia* from tropical forest soil. Cryptogamie Mycol 42: 39–61. https://doi.org/10.5252/CRYPTOGAMIE-MYCOLOGIE2021V42A4

Hurdeal VG, Jones EBG, Gentekaki E (2023) *Absidia* zygospora (Mucoromycetes), a new species from nan province, Thailand. Studies in Fungi 8(1): 0. https://doi.org/10.48130/SIF-2023-0015

Jaklitsch WM, Komon M, Kubicek CP, Druzhinina IS (2005) *Hypocrea voglmayrii* sp. nov. from the Austrian Alps represents a new phylogenetic clade in *Hypocrea*/*Trichoderma*. Mycologia 97(6): 1365–1378. https://doi.org/10.1080/15572536.2006.11832743

Kristanti RA, Fikri Ahmad Zubir MM, Hadibarata T (2016) Biotransformation studies of cresol red by *Absidia spinosa* M15. Journal of Environmental Management 172: 107–111. https://doi.org/10.1016/j.jenvman.2015.11.017

Kumar S, Stecher G, Tamura K (2016) MEGA7: Molecular evolutionary genetics analysis version 7.0 for bigger datasets. Molecular Biology and Evolution 33(7): 1870–1874. https://doi.org/10.1093/molbev/msw054

Lima DX, Cordeiro TR, de Souza CA, de Oliveira R, Lee HB, Souza-Motta CM, Santiago AL (2020) Morphological and molecular evidence for two new species of *Absidia* from neotropic soil. Phytotaxa 446(1): 61–71. https://doi.org/10.11646/phytotaxa.446.1.8

Lima CL, Lima DX, Cordeiro TR, Lee HB, Nguyen TT, Gurgel L, Santiago AL (2021) *Absidia bonitoensis* (Mucorales, Mucoromycota), a new species isolated from the soil of an upland Atlantic Forest in Northeastern Brazil. Nova Hedwigia 112(1–2): 241–251. https://doi.org/10.1127/nova_hedwigia/2021/0614

Mackenzie DW, Soothill JF, Millar JH (1988) Meningitis caused by *Absidia corymbifera*. The Journal of Infection 17(3): 241–248. https://doi.org/10.1016/S0163-4453(88)96570-X

Miller MA, Pfeiffer W, Schwartz T (2010) Creating the CIPRES Science Gateway for inference of large phylogenetic trees. 2010 Gateway Computing Environments Workshop (GCE), 1–8. https://doi.org/10.1109/GCE.2010.5676129

Nylander J A A (2004) MrModeltest v2. [Program distributed by the author] http://www.abc.se/–nylander/mrmodeltest2/mrmodeltest2.html

Rehner SA, Buckley E (2005) A Beauveria phylogeny inferred from nuclear ITS and EF1-α sequences: Evidence for cryptic diversification and links to Cordyceps teleomorphs. Mycologia 97(1): 84–98. https://doi.org/10.3852/mycologia.97.1.84

Richardson M (2009) The ecology of the Zygomycetes and its impact on environmental exposure. Clinical Microbiology and Infection 15(5): 2–9. https://doi.org/10.1111/j.1469-0691.2009.02972.x

Sordon S, Popłoński J, Tronina T, Huszcza E (2019) Regioselective O-glycosylation of flavonoids by fungi Beauveria bassiana, *Absidia coerulea* and *Absidia glauca*. Bioorganic Chemistry 93: 102750. https://doi.org/10.1016/j.bioorg.2019.01.046

Stamatakis A (2014) RAxML version 8: A tool for phylogenetic analysis and post-analysis of large phylogenies. Bioinformatics (Oxford, England) 30(9): 1312–1313. https://doi.org/10.1093/bioinformatics/btu033

Swofford D L (2002) PAUP*. Phylogenetic analysis using parsimony (*and other methods). Version 4.0b10. https://doi.org/10.1111/j.0014-3820.2002.tb00191.x

van Tieghem P (1876) Troisieme memoire sur les Mucorinees. Ann Sci Nat Bot Ser 6(4): 312–398.

Varona DM, Sánchez JC, Muñoz LA, Cantos EM, Moraleda LR (2015) Keratitis caused by *Absidia corymbifera* in an immunocompetent male with no corneal injuries. Archivos de la Sociedad Española de Oftalmología 90(3): 139–141. https://doi.org/10.1016/j.oftal.2014.02.020

Voigt K, Wöstemeyer J (2000) Reliable amplification of actin genes facilitates deep-level phylogeny. Microbiological Research 155(3): 179–195. https://doi.org/10.1016/S0944-5013(00)80031-2

von Arx JA (1982) On Mucoraceae s. str. and other families of the *Mucorales*. Sydowia 35: 10–26.

White TJ, Bruns T, Lee S, Taylor J (1990) Amplification and direct sequencing of fungal ribosomal RNA genes for phylogenetics. In: Innis MA, Gelfand D, Sninsky J et al. (Eds) PCR Protocols: A Guide to Methods and Applications. Academic Press, New York, USA, 315–322. https://doi.org/10.1016/B978-0-12-372180-8.50042-1

Zhang TY, Yu Y, Zhu H, Yang SZ, Yang TM, Zhang MY, Zhang YX (2018) *Absidia panacisoli* sp. nov., isolated from rhizosphere of Panax notoginseng. International Journal of Systematic and Evolutionary Microbiology 68(8): 2468–2472. https://doi.org/10.1099/ijsem.0.002857

Zhang Z, Liu R, Liu S, Mu T, Zhang X, Xia J (2021) Morphological and phylogenetic analyses reveal two new species of Sporocadaceae from Hainan, China. MycoKeys 88: 171–192. https://doi.org/10.3897/mycokeys.88.82229

Zhao H, Nie Y, Zong T, Dai Y, Liu X (2022a) Three new species of *Absidia* (Mucoromycota) from China based on phylogeny, morphology and physiology. Diversity 14(2): 132. https://doi.org/10.3390/d14020132

Zhao H, Nie Y, Zong T, Wang Y, Wang M, Dai Y, Liu X (2022b) Species diversity and ecological habitat of *Absidia* (Cunninghamellaceae, Mucorales) with emphasis on five new species from forest and grassland soil in China. Journal of Fungi (Basel, Switzerland) 8(5): 471. https://doi.org/10.3390/jof8050471

Zhao H, Nie Y, Zong T, Wang K, Lv M, Cui Y, Tohtirjap A, Chen J, Zhao C, Wu F, Cui B, Yuan Y, Dai Y, Liu X (2023) Species diversity, updated classification and divergence times of the phylum Mucoromycota. Fungal Diversity 123(1): 49–157. https://doi.org/10.1007/s13225-023-00525-4

Zheng RY, Liu XY (2009) Taxa of *Pilaira* (Mucorales, Zygomycota) from China. Nova Hedwigia 88(1–2): 255–267. https://doi.org/10.1127/0029-5035/2009/0088-0255

Zheng R Y, Chen G Q, Huang H et al. (2007) A monograph of *Rhizopus*. Sydowia 59: 273.

Zheng RY, Liu XY, Li RY (2009) More *Rhizomucor* causing human mucormycosis from China: *R. chlamydosporus* sp. nov. Sydowia 61: 135–147.

Zong TK, Zhao H, Liu XL, Ren LY, Zhao CL, Liu XY (2021) Taxonomy and phylogeny of four new species in *Absidia* (Cunninghamellaceae, Mucorales) from China. Frontiers in Microbiology 12: 677836. https://doi.org/10.3389/fmicb.2021.677836

Supplementary material 1

Estimates of evolutionary divergence between sequence based on ITS, LSU, TEF, ACT, SSU

Authors: Meng-Fei Tao

Data type: pdf

Explanation note: Estimates of evolutionary divergence between sequence based on ITS, LSU, TEF, ACT and SSU. Three new species and their relatives were selected to study, and the number of base differences per site from between sequences are shown. Standard error estimate(s) are shown above the diagonal. Evolutionary analyses were conducted in MEGA7.

Link: https://doi.org/10.3897/mycokeys.110.129120.suppl1

Supplementary material 2

The combined ITS + LSU + TEF + ACT + SSU sequence matrix used in this study

Authors: Meng-Fei Tao

Data type: fas

Explanation note: Phylogenetic analyses of SSU, ITS, LSU rDNA, TEF-1α and Act were conducted for a total of 91 sequences, composing 36 species of Absidia and two outgroups, Cunninghamella blakesleeana (CBS 782.68) and C. elegans (CBS 167.53). The phylogenetic analysis encompassed a total of 4,785 characters, with 516 of SSU, 996 of ITS, 1,874 of LSU, 743 of TEF-1α, 660 of Act characters.

Link: https://doi.org/10.3897/mycokeys.110.129120.suppl2

MycoKeys

MycoKeys 110: 273–285 (2024)
DOI: 10.3897/mycokeys.110.136048

Research Article

20 years of bibliometric data illustrates a lack of concordance between journal impact factor and fungal species discovery in systematic mycology

R. Henrik Nilsson[1], Arnold Tobias Jansson[1], Christian Wurzbacher[2], Sten Anslan[3,4], Pauline Belford[5], Natàlia Corcoll[6], Alexandra Dombrowski[1], Masoomeh Ghobad-Nejhad[7], Mikael Gustavsson[6], Daniela Gómez-Martínez[6], Faheema Kalsoom Khan[8], Maryia Khomich[9], Charlotte Lennartsdotter[1], David Lund[10], Breyten Van Der Merwe[11], Vladimir Mikryukov[4], Marko Peterson[4], Teresita M. Porter[12], Sergei Põlme[4], Alice Retter[13,14], Marisol Sanchez-Garcia[15], Sten Svantesson[1,8], Patrik Svedberg[6], Duong Vu[16], Martin Ryberg[8], Kessy Abarenkov[17], Erik Kristiansson[10]

1 *Department of Biological and Environmental Sciences, Gothenburg Global Biodiversity Centre, University of Gothenburg, Box 463, 405 30 Göteborg, Sweden*
2 *Chair of Urban Water Systems Engineering, Technical University of Munich, Am Coulombwall 3, 85748 Garching, Germany*
3 *Department of Biological and Environmental Science, University of Jyväskylä, Survontie 9, 40014 Jyväskylän yliopisto, Finland*
4 *Institute of Ecology and Earth Sciences, University of Tartu, Liivi 2, 50409 Tartu, Estonia*
5 *Department of Computer Science and Engineering, Interaction Design, University of Gothenburg, Lindholmsplatsen 1, 41756 Göteborg, Sweden*
6 *Department of Biological and Environmental Sciences, FRAM Centre for Future Chemical Risk Assessment and Management Strategies, University of Gothenburg, Box 463, 405 30 Göteborg, Sweden*
7 *Department of Biotechnology, Iranian Research Organization for Science and Technology (IROST), P. O. Box 3353-5111, Tehran, Iran*
8 *Systematic Biology, Department of Organismal Biology, Evolutionary Biology Center, Uppsala University, Norbyvägen 18 D, 752 36 Uppsala, Sweden*
9 *Department of Clinical Science, University of Bergen, Box 7804, 5020 Bergen, Norway*
10 *Department of Mathematical Sciences, Chalmers University of Technology and University of Gothenburg, Göteborg, Sweden*
11 *Department of Chemical Engineering, Stellenbosch University, Private Bag X1, Stellenbosch, South Africa*
12 *Toronto, Ontario, Canada*
13 *Department of Functional and Evolutionary Ecology, University of Vienna, Djerassiplatz 1, A-1030 Vienna, Austria*
14 *Leibniz Institute for Freshwater Ecology and Inland Fisheries, IGB, Zur alten Fischerhuette 2, 16775 Neuglobsow, Germany*
15 *Department of Forest Mycology and Plant Pathology, Swedish University of Agricultural Sciences, Box 7026, 750 07 Uppsala, Sweden*
16 *Westerdijk Fungal Biodiversity Institute, Uppsalalaan 8, 3584 CT Utrecht, Netherlands*
17 *Natural History Museum, University of Tartu, Vanemuise 46, Tartu 51014, Estonia*

Corresponding author: R. Henrik Nilsson (henrik.nilsson@bioenv.gu.se)

Abstract

Journal impact factors were devised to qualify and compare university library holdings but are frequently repurposed for use in ranking applications, research papers, and even individual applicants in mycology and beyond. The widely held assumption that mycological studies published in journals with high impact factors add more to systematic mycology than studies published in journals without high impact factors nevertheless lacks evidential underpinning. The present study uses the species hypothesis system of the UNITE database for molecular identification of fungi and other eukaryotes to trace the publication history and impact factor of sequences uncovering new fungal species hypotheses. The data show that journal impact factors are poor predictors of discovery potential in systematic mycology. There is no clear relationship between journal impact factor and the discovery of new species hypotheses for the years 2000–2021. On the contrary, we found journals with low, and even no, impact factor to account for substantial parts of the species hypothesis landscape, often discovering new fungal taxa that are only later picked up by journals with high impact factors. Funding agencies and hir-

Academic editor: Thorsten Lumbsch
Received: 31 August 2024
Accepted: 18 October 2024
Published: 20 November 2024

Citation: Nilsson RH, Jansson AT, Wurzbacher C, Anslan S, Belford P, Corcoll N, Dombrowski A, Ghobad-Nejhad M, Gustavsson M, Gómez-Martínez D, Kalsoom Khan F, Khomich M, Lennartsdotter C, Lund D, Van Der Merwe B, Mikryukov V, Peterson M, Porter TM, Põlme S, Retter A, Sanchez-Garcia M, Svantesson S, Svedberg P, Vu D, Ryberg M, Abarenkov K, Kristiansson E (2024) 20 years of bibliometric data illustrates a lack of concordance between journal impact factor and fungal species discovery in systematic mycology. MycoKeys 110: 273–285. https://doi.org/10.3897/mycokeys.110.136048

ing committees that insist on upholding journal impact factors as a central funding and recruitment criterion in systematic mycology should consider using indicators such as research quality, productivity, outreach activities, review services for scientific journals, and teaching ability directly rather than using publication in high impact factor journals as a proxy for these indicators.

Key words: Bibliometrics, impact factor, mycology, systematics, taxonomy

Introduction

The concept of journal impact factors (IFs) was introduced in the 1970s as a means to qualify and compare university library holdings (Garfield 2006; Casadevall and Fang 2014). It was argued that since a journal's IF is computed as the average number of recent citations to papers recently published in that journal, the IF indicates the relative importance of that journal. IFs could thus be used as guidance for cost-efficient trimming of library holdings – and, by computing average IFs for entire libraries, for ranking libraries according to the perceived importance of their holdings. By and large, the IF concept was well received by the librarian community by virtue of offering some degree of objectivity in what up to that point had been a signally subjective enterprise (Archambault and Larivière 2009). However, it did not take long before the IF concept was invested with meaning and significance far beyond its intended jurisdiction and saw use to rank individual research papers and even researchers according to perceived importance (Simons 2008). A researcher's average or cumulative IF could be used, many hiring committees and research funding agencies started to argue, to rank candidates or applicants in a reasonably objective, and above all time- and cost-efficient, manner. Heavily laden with mystical import, the IF concept soon took a firm grip on the research landscape (McKiernan et al. 2019).

Over time, parts of the scientific community warmed to the idea that IFs may be an unwarrantably simplistic predictor of past and future research performance (Dong et al. 2005; Krell 2000; Lăzăroiu 2013). Indeed, there are countless examples of pivotal research papers that were published in journals with no, or low, or moderate impact factors – and substandard, faulty, or downright fraudulent papers published in high-IF journals (Trikalinos et al. 2008; Brembs 2018). But still, in the year 2024, the use of IFs as indicators of scientific performance and potential holds significant traction in the scientific community. Many of the present authors regularly serve in various evaluation committees for promotions, academic positions, and research grants in systematic mycology and beyond. In this capacity we are typically asked to rank applicants or applications in order of relevance to the matter at hand. We're instructed – and happy – to consider a multitude of parameters, including research performance, previous grants, stays abroad, time spent on parental leave, teaching, supervision, review services, and outreach. But often enough, when the committee finally convenes to negotiate a joint position, IFs tend to surface as the most decisive – and sometimes the only – parameter of relevance. The oracular emphasis laid on IFs at the expense of all other parameters is a perennial source of amazement to us. It effectively punishes researchers and research groups who ever spent any time doing anything other than maximizing IFs (Rushforth

and de Rijcke 2015; Johann et al. 2024). But is it really the case that mycological discovery scales in a linear way with impact factor so that by choosing the application/applicant with the highest impact factor statistics, we get the most mycology for the money? Several of us have struggled to look ourselves in the mirror following committee meetings of this kind.

In the context of systematic mycology, down-prioritizing researchers and research groups without a strong track record of high-IF publications would make sense if, indeed, low-IF publications and no-IF publications do not contribute much, or anything, to systematic mycology. Conversely, if it is the case that also (or even primarily) low- and no-IF publications make substantial contributions to this field, then the usefulness of IFs as a decisive indicator in systematic mycology would be illusory and, in fact, directly counterproductive. Is there data to form some sort of evidential underpinning for the contribution of IFs to systematic mycology? We argue that there is. The UNITE database for molecular identification of eukaryotes clusters all public, full-length fungal barcode (nuclear ribosomal internal transcribed spacer, or ITS) sequences in the International Nucleotide Sequence Database Collaboration (Arita et al. 2021) into roughly species-level entities referred to as species hypotheses (SHs; Abarenkov et al. 2024). These SHs can be thought of as digital twins of the underlying species, and meticulous record and rich metadata are kept for all sequences in each SH, including the publication history of each sequence. Theory can thus be pitted against experiment by querying the IF of the constituent sequences of SHs. Is it really the case that new species of fungi are primarily found in high-IF publications, for instance? And is the trend of IFs versus mycosystematical discovery linear, just like parts of the mycological community seem so happy to assume? Do scientific outlets without formal IFs really contribute nothing to mycology? The present study sets out to assess whether the reliance put on IFs in systematic mycology holds up to empirical scrutiny. Our results suggest that the use of IFs as arbiters of scientific quality and discovery potential in systematic mycology is not consistent with the image of rationality that we feel systematic mycology should seek to project.

Materials and methods

The full flow of operation behind the UNITE database is described elsewhere (Kõljalg et al. 2013, 2020; Abarenkov et al. 2024). In brief, UNITE clusters the ITS sequences of the International Nucleotide Sequence Database Collaboration (INSDC) jointly with UNITE-contributed environmental DNA (eDNA, DNA obtained from mixed/bulk samples) ITS sequences into species hypotheses at distance thresholds 0.5% through to 3.0% in steps of 0.5%. These operational taxonomic units can be thought of as entities roughly at the species level. The sequences and the SHs are available for web-based interaction as well as for download in various formats (https://unite.ut.ee/repository.php).

The 1,258,182 Sanger sequencing-derived sequences of UNITE eukaryotic release 10 were found to be distributed across 182,847 SHs at the default 1.5% sequence dissimilarity level. We targeted sequences submitted to the INSDC in the interval 2000–2021. All 43,057 non-singleton SHs whose first (earliest date of INSDC deposition) sequence was annotated (by default or by subse-

quent third-party sequence annotation) as fungal were targeted. These SHs comprised a total of 506,103 sequences. All other SHs were considered to represent non-fungal eukaryotes and are not treated any further in this study. We examined all sequences computationally for information on publication of origin. A total of 23,710 (55.1%) fungal SHs were first discovered through a sequence for which a published study of origin was specified in INSDC, leaving 19,347 (44.9%) of the initial-SH-discovery sequences with a publication status of the "Unpublished" or "Direct submission" kind. Some proportion of these seemingly unpublished sequences can be expected to be published but not updated with publication information in INSDC (Durkin et al. 2020). We thus subjected all 19,347 such seemingly unpublished sequences to manual Google and Google Scholar searches to see if they in fact had been published. In these queries, we used the INSDC accession number, the author names, and the title of the study (as available).

Official journal impact factors were compiled from ISI Web of Science for the period 2000–2021 for all journals sporting sequences in all SHs deemed to be fungal. The annual median impact factor for mycology was inferred from the 33 mycological journals in ISI's journal category "Mycology". Each sequence was assigned the impact factor of its outlet and the year of publication in the IF window 2000–2021. Two alternative approaches were adopted for sequences published in an outlet without a formal IF for the year of publication. In the "strict median" approach, they were not assigned any IF value and were excluded from estimates of median IFs. In the "relaxed median" approach, they were assigned an IF of 0.0 and were included in estimates of median IFs. IFs were considered down to the three decimal digits supported by ISI Web of Science. As a baseline, we also analyzed all formal fungal species descriptions 2000–2021 for impact factor using GBIF (https://www.gbif.org/) and MycoBank (Robert et al. 2013).

Results

We found 43,057 non-singleton UNITE SHs to be fungal. The first (oldest) sequence in each such SH was examined for publication information. More than half (23,710; 55.1%) of these were found to be annotated to publication of origin, leaving 19,347 (44.9%) of the "Unpublished" and "Direct submission" kind. We were able to track down 10,203 (52.7%) of these to a published study of origin, giving us a final dataset of 33,913 published sequences, each representing a first, initial discovery of an SH. These 33,913 sequences were found to come from 6,878 studies. Sequences only released through B.Sc./M.Sc./Ph.D. theses were scored as unpublished. The unpublished sequences are not considered any further in this study. The SH-derived sequences of the study were found to have been published in well over 1,500 different journals and outlets, ranging from top-tier international journals with an IF of over 30 to what seemed to be regional or even local journals without an online presence.

In total, 28,662 (84.5%) of the sequences that were the first to evince a new SH discovery were published in a scientific journal with a formal IF that year, leaving 5,251 (15.5%) of the sequences published in an outlet without. Out of those 5,251 sequences, 2,223 (42.3%) were published in a journal that did not have a formal IF at the time of publication, but that eventually obtained one af-

ter an average of 4.7 years, leaving 3,028 (57.7%) of the without-IF-sequences published in an outlet that never had a formal IF (2000–2021). The *strict* and *relaxed* median IFs of sequences discovering new SHs over time are displayed in Fig. 1a. Fig. 1b visualizes the difference between the strict/relaxed approaches and the median IF in mycology. Fig. 2 shows the proportion of SHs whose initial discovery was reported in a journal without a formal IF, and with an IF below the mycological median, respectively, over time. Fig. 3 provides a window on the IF trend inside SHs by plotting the IFs of subsequent recoveries of the SH following its initial discovery. To account for the trend of increasing IFs in mycology over time, the data in Fig. 3 was normalized by subtracting the median impact factor of the journals in ISI's category "Mycology".

11,386 (33.6%) SHs contained sequences that were released through two or more distinct studies, all of which either lacked a formal IF or had an IF below the median mycological IF the year of publication. Similarly, 2,048 (6.0%) SHs were found to be known from two or more distinct studies, all of which had an IF above the median mycological IF the year of publication. 313 (0.9%) SHs were found to be known from two or more distinct studies, none of which were published in an outlet with a formal IF. In analogy, 12,477 (36.8%) SHs were found to be known from two or more distinct studies, all of which were published in an outlet with a formal IF at the year of publication. 1,260 (3.7%) non-singleton SHs were recovered both from journals with and without formal IFs. The results of the analysis of the impact factors of formal fungal species descriptions 2000–2021 are given in Suppl. material 1.

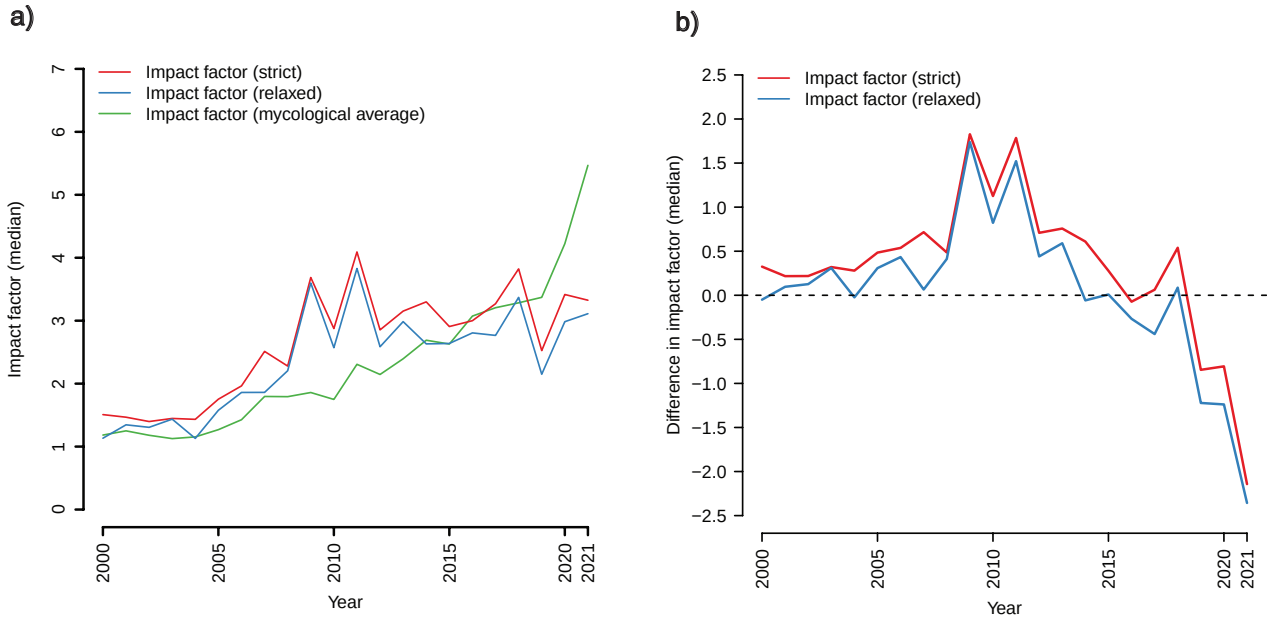

Figure 1. a the median impact factor of initial discoveries of UNITE species hypotheses (SHs). For the red curve, only sequences published in a journal with a formal impact factor from the year of publication were included in the calculation. For the blue curve, also sequences published in journals without a formal impact factor from the year of publication were included with their impact factor set to 0.0. The green curve shows the average impact factor of the journals in ISI's category "Mycology" over time **b** the median impact factor of initial discoveries of SHs visualized as the difference in IF from the median mycological IF (dashed line) over time. The post-2015 drop in relative impact factor is presumably explained by the trend of increasing IFs in ISI's category "Mycology" over time and mycologists' apparent struggle to take advantage of this trend when publishing.

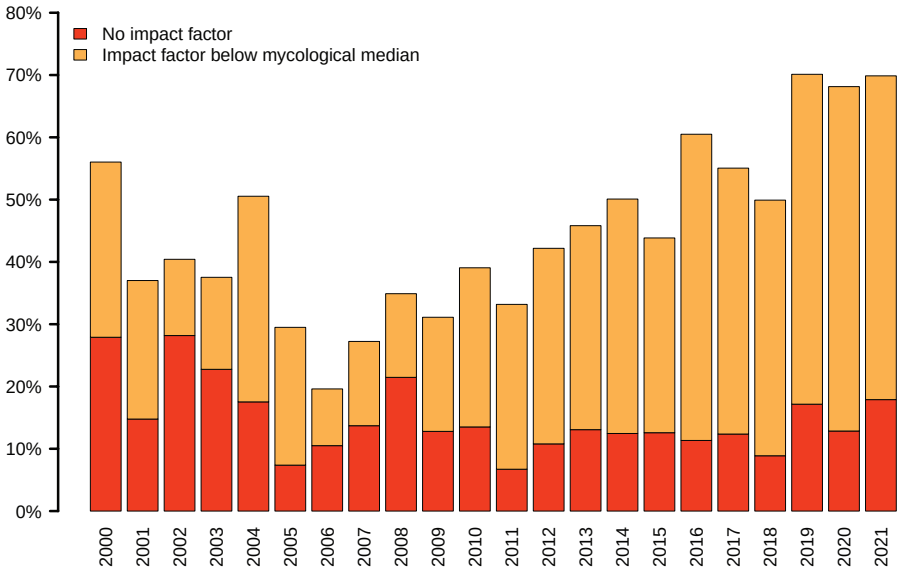

Figure 2. The proportion of SHs whose initial discovery was reported in a journal without a formal IF (red) or with an IF below the mycological median (orange) over time.

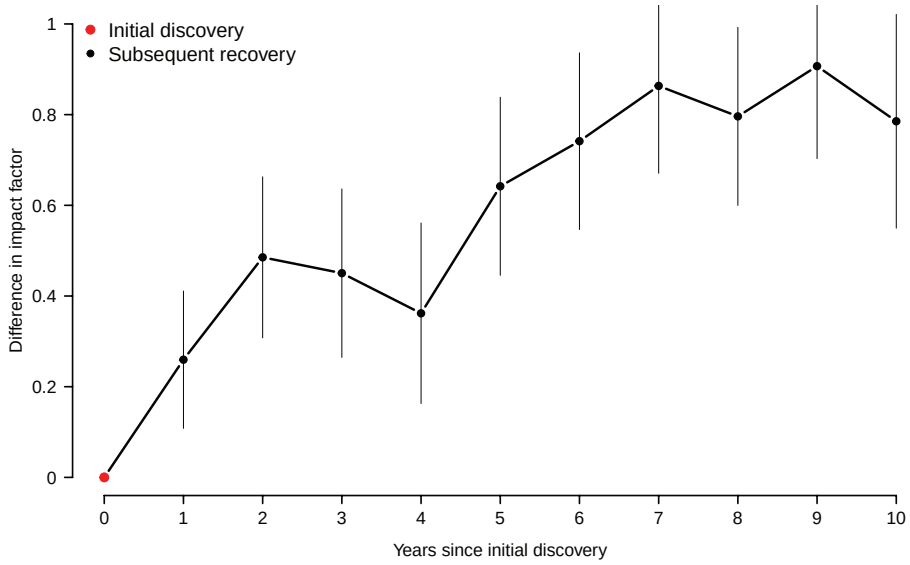

Figure 3. The median IFs of sequences inside SHs over time. SHs were discovered at year 0. The SHs were then inspected for subsequent recoveries in journals with a formal IF, and the value plotted is the median of all such recoveries. To account for the trend of increasing IFs in mycology, the data was normalized by subtracting the median impact factor of the journals in ISI's category "Mycology". The unit of the y axis is difference in IF. The error bars show 95% confidence intervals.

Discussion

The present study examined the relation of journal IFs to discovery potential in systematic mycology. Our results are largely dispiriting – there seems to be no meaningful correlation between IFs and mycosystematical discovery potential as measured as the discovery of new SHs in UNITE. On the contrary, at least in systematic mycology, journal IFs come across as a concept divested of meaning, or at least the meaning ascribed to it in the committee meetings that many of the present authors regularly attend. For instance, for the last 10 years, the majority of new SHs were first reported from journals with an IF below the median mycological IF in a trend that is accentuated over time (Fig. 2). Similarly,

formal description of species seems to be a perpetually below-median exercise (Suppl. material 1). In some sense this indicates that journals with an IF above the mycological median do not play an important role in systematic mycology, yet these high-IF journals are what we tend to put a premium on in mycosystematical committees, at least in our experience. The non-trivial proportion of SHs recovered only from no-IF and below-median-IF studies suggests that mycological research traditions and choices of taxonomic target groups differ widely – in fact, disparately – across and among those who study fungi in one capacity or another. Indeed, to some extent, different groups of fungi are studied in no/below-median-IF journals compared to above-median-IF journals. Suppressing mycological research published in no/low-IF outlets is thus tantamount to advocating a paraphyletic view of the fungal kingdom. Such a stance does not blend well with contemporary phylogenetic thinking, where wide and representative taxon sampling is identified as a non-negotiable cornerstone (e.g., Heath et al. 2008).

In an IF-centred world, important mycological findings would be announced in high-IF journals, and those results would only later trickle down and be subsumed into studies published in journals of lesser, or no, IFs. Our results take umbrage with such a contention (Fig. 3). Indeed, publications in high-IF journals seem to draw from the results of publications that were not published in high-IF journals in a way not usually considered in the committee meetings we attend. Figs 1–3 and Suppl. material 1 jointly suggest that the majority of non-trivial discoveries in systematic mycology – particularly in recent years – are being presented in journals that can be called "below average" or even "objectionable" in the sense of lacking a formal IF altogether. That makes – it seems to us – the practice of prioritizing "above average" journal publications in committee situations inimical to systematic mycology. Clearly, journal IFs and species discovery make uneasy bedfellows. The discovery and description of new species are essential for laying the groundwork for scientific progress, yet they do not necessarily resonate well with the short timeframe for IFs and the criteria used by high-IF journals for publication.

Our results do not necessarily suggest that the mycological community should prioritize low/no-IF researchers and research teams, but rather that IFs are a superficially deep, but deeply superficial, measure of mycosystematical discovery potential. If it, indeed, is mycosystematical discovery potential that we wish to promote, then time's provision of further and better particulars seems to call for abandoning oversimplified shortcuts in the assessment of a researcher's previous production. Maybe, in fact, there are no shortcuts (Bertuzzi and Drubin 2013). Maybe committees really have to go through a few of the applicants' main papers in detail to assess the quality and the scientific explanatory power of their findings. Maybe the committee really needs to examine and compare the citations to each individual paper to further quantify and qualify the import of those papers on mycology. And maybe the proposed research project will have to be given more than fleeting attention after all. That would clearly be a very time-consuming approach – presumably a horrifying thought to many, the present authors included. This is, nevertheless, what our results seem to suggest.

Ranking candidates based on IFs furthermore perpetuates the 'Matthew effect' whereby candidates who happen to publish in high impact journals early in

their career accrue more recognition and cumulative advantage relative to other candidates (Petersen et al. 2011; Rushforth and de Rijcke 2015). This is problematic when candidates have early career advantages not directly related to their research potential. Given many institutions' commitments to Diversity, Equity, and Inclusion (DEI), the elimination of IF-bias in highly specialized fields where this metric has been shown to be a poor indicator of research contributions should be a priority. The self-correcting nature of science reflects openness to revision when new data come to light, something that we feel should apply also to the evaluation of science. Considering our work and others, committees that insist on making decisions that are heavily weighted by IFs should also consider the risk of bias entrenched in current processes (Boutron et al. 2023).

This study makes the simplification to define "systematic mycology" as the field that discovers and describes new species and groups of fungi – which is what the present study quantifies. We are well aware that systematic mycology covers more than just that, and that the discovery of new SHs in UNITE and formal description of species do not do full justice to the discipline. At the same time, it would seem like a stretch to argue that the discovery and formal description of new species and groups of fungi, unlike all other aspects of systematic mycology, scale poorly to IFs. Instead, we hypothesize that our data speak reasonably well for all of systematic mycology in arguing against the use of IFs as a decisive indicator in systematic mycology. Our study made heavy use of the UNITE SH system, which is based on the formal fungal barcode, the nuclear ribosomal ITS region (Schoch et al. 2012). While we agree that the ITS region is by all accounts the best choice of a singular fungal barcode, it is nevertheless a genetic marker that does not reflect species boundaries perfectly throughout the fungal kingdom (Abarenkov et al. 2016). We used the dynamic SH release of UNITE in an attempt at avoiding the use of static similarity thresholds for automated designations of operational taxonomic units, but it is inevitable that some degree of taxonomic artificiality marks our results (Nilsson et al. 2019).

Our approach was to some extent haunted by missing data – at the onset of the project, a full 19,347 (44.9%) of the sequences representing initial discoveries of species hypotheses were not annotated with a study of origin. We spent more than three months trying to restore this information, but we often found ourselves struggling with journals without a digital presence, journals in other languages than the present set of co-authors had access to, special characters, conflicting information, and the sheer magnitude of the task at hand. In the end, we were able to restore the publication information for 10,203 sequences, reducing the share of "unpublished" sequences from 49.7% to 21.2%. We find it remarkable that upwards of half of the public fungal barcode sequences older than two years were un-annotated to begin with in this regard. Durkin et al. (2020) provided data to suggest that systematic mycology does not maximize its scientific and outreach potential, and the present study lends further weight to those claims. Another source of bias in our results comes from our decision to target only the INSDC and Sanger-sequencing-derived sequences in UNITE. In addition to these sequences, UNITE also features five very large metabarcoding datasets published in high-profile journals (Nilsson et al. 2023). We felt that if we were to also include metabarcoding studies in our approach, then we would have to include not just five high-profile – but all extant – metabarcoding studies to get an unbiased view. However, there is no centralized resource

where all metabarcoding datasets are available in an accessible way, and the prospects for clustering billions or even trillions of sequences into the UNITE SH system would furthermore have been bleak. The present paper thus reflects the Sanger sequencing view of systematic mycology.

Conclusion

Mycologists regularly report feeling compelled to publish in high-IF journals by virtue of professionalism. Our data suggest that if we by professionalism mean keeping the best interest of systematic mycology in mind, then journal IFs are at a particular risk of misinterpretation – and are regularly ascribed a weight that endangers progress in the field. We eagerly anticipate a future where applications and candidates are assessed in a more integrative way than simple summary metrics obtained from journal IFs, and where mycological contributions are quantified in a way agnostic of the very journal in which they happened to be published. Our non-trivial experience of serving in various evaluation committees is dispiriting in this regard, painting a bleak picture for the future of systematic mycology in a time when the understanding of fungal diversity is more important than ever.

Acknowledgements

GBIF and MycoBank are acknowledged for assistance with bibliographic data for species descriptions.

Additional information

Conflict of interest

The authors have declared that no competing interests exist.

Ethical statement

No ethical statement was reported.

Funding

This work was supported by Vetenskapsrådet (2023-03456) and Artdatabanken (2023.4.3-30).

Author contributions

All authors have contributed equally.

Author ORCIDs

R. Henrik Nilsson https://orcid.org/0000-0002-8052-0107
Arnold Tobias Jansson https://orcid.org/0000-0002-9100-9814
Christian Wurzbacher https://orcid.org/0000-0001-7418-0831
Sten Anslan https://orcid.org/0000-0002-2299-454X
Pauline Belford https://orcid.org/0009-0005-5297-483X
Natàlia Corcoll https://orcid.org/0000-0002-1660-9422
Masoomeh Ghobad-Nejhad https://orcid.org/0000-0002-7807-4187
Mikael Gustavsson https://orcid.org/0000-0003-0635-8321
Daniela Gómez-Martínez https://orcid.org/0000-0001-8834-8930

Faheema Kalsoom Khan https://orcid.org/0000-0002-4891-953X
Maryia Khomich https://orcid.org/0000-0002-6840-5739
Charlotte Lennartsdotter https://orcid.org/0009-0008-2780-4881
David Lund https://orcid.org/0000-0003-4075-7529
Breyten Van Der Merwe https://orcid.org/0000-0003-0546-5619
Vladimir Mikryukov https://orcid.org/0000-0003-2786-2690
Teresita M. Porter https://orcid.org/0000-0002-0227-6874
Sergei Põlme https://orcid.org/0000-0002-9658-1166
Alice Retter https://orcid.org/0009-0004-3758-4123
Marisol Sanchez-Garcia https://orcid.org/0000-0002-0635-6281
Sten Svantesson https://orcid.org/0000-0003-3435-3659
Patrik Svedberg https://orcid.org/0000-0001-6622-5366
Duong Vu https://orcid.org/0000-0001-7960-2765
Martin Ryberg https://orcid.org/0000-0002-6795-4349
Kessy Abarenkov https://orcid.org/0000-0001-5526-4845
Erik Kristiansson https://orcid.org/0000-0002-8609-2414

Data availability

All of the data that support the findings of this study are available in the main text or Supplementary Information.

References

Abarenkov K, Adams RI, Laszlo I, Agan A, Ambrosio E, Antonelli A, Bahram M, Bengtsson-Palme J, Bok G, Cangren P, Coimbra V, Coleine C, Gustafsson C, He J, Hofmann T, Kristiansson E, Larsson E, Larsson T, Liu Y, Martinsson S, Meyer W, Panova M, Pombubpa N, Ritter C, Ryberg M, Svantesson S, Scharn R, Svensson O, Töpel M, Unterseher M, Visagie C, Wurzbacher C, Taylor AFS, Kõljalg U, Schriml L, Nilsson RH (2016) Annotating public fungal ITS sequences from the built environment according to the MIxS-Built Environment standard–a report from a May 23–24, 2016 workshop (Gothenburg, Sweden). MycoKeys 16: 1–15. https://doi.org/10.3897/mycokeys.16.10000

Abarenkov K, Nilsson RH, Larsson K-H, Taylor AFS, May TW, Frøslev TG, Pawlowska J, Lindahl B, Põldmaa K, Truong C, Vu D, Hosoya T, Niskanen T, Piirmann T, Ivanov F, Zirk A, Peterson M, Cheeke TE, Ishigami Y, Jansson AT, Stjernegaard Jeppesen T, Kristiansson E, Mikryukov V, Miller JT, Oono R, Ossandon FJ, Paupério J, Saar I, Schigel D, Suija A, Tedersoo L, Kõljalg U (2024) The UNITE database for molecular identification and taxonomic communication of fungi and other eukaryotes: Sequences, taxa and classifications reconsidered. Nucleic Acids Research 52(D1): D791–D797. https://doi.org/10.1093/nar/gkad1039

Archambault É, Larivière V (2009) History of the journal impact factor: Contingencies and consequences. Scientometrics 79(3): 635–649. https://doi.org/10.1007/s11192-007-2036-x

Arita M, Karsch-Mizrachi I, Cochrane G (2021) The international nucleotide sequence database collaboration. Nucleic Acids Research 49(D1): D121–D124. https://doi.org/10.1093/nar/gkaa967

Bertuzzi S, Drubin DG (2013) No shortcuts for research assessment. Molecular Biology of the Cell 24(10): 1505–1506. https://doi.org/10.1091/mbc.e13-04-0193

Boutron I, Page MJ, Higgins JPT, Altman DG, Lundh A, Hróbjartsson A (2023) Considering bias and conflicts of interest among the included studies. In: Higgins JPT, Thom-

as J, Chandler J, Cumpston M, Li T, Page MJ, Welch VA (Eds) Cochrane Handbook for Systematic Reviews of Interventions version 6.4 Cochrane, 2023. www.training.cochrane.org/handbook

Brembs B (2018) Prestigious science journals struggle to reach even average reliability. Frontiers in Human Neuroscience 12: 327726. https://doi.org/10.3389/fnhum.2018.00037

Casadevall A, Fang FC (2014) Causes for the persistence of impact factor mania. mBio 5(2): 10–1128. https://doi.org/10.1128/mBio.00064-14

Dong P, Loh M, Mondry A (2005) The" impact factor" revisited. Biomedical Digital Libraries 2(1): 1–8. https://doi.org/10.1186/1742-5581-2-7

Durkin L, Jansson T, Sanchez M, Khomich M, Ryberg M, Kristiansson E, Nilsson RH (2020) When mycologists describe new species, not all relevant information is provided (clearly enough). MycoKeys 72: 109–128. https://doi.org/10.3897/mycokeys.72.56691

Garfield E (2006) The history and meaning of the journal impact factor. Journal of the American Medical Association 295(1): 90–93. https://doi.org/10.1001/jama.295.1.90

Heath TA, Hedtke SM, Hillis DM (2008) Taxon sampling and the accuracy of phylogenetic analyses. Journal of Systematics and Evolution 46(3): 239–257. https://doi.org/10.3724/SP.J.1002.2008.08016

Johann D, Neufeld J, Thomas K, Rathmann J, Rauhut H (2024) The impact of researchers' perceived pressure on their publication strategies. Research Evaluation 2024: rvae011. https://doi.org/10.1093/reseval/rvae011

Kõljalg U, Nilsson RH, Abarenkov K, Tedersoo L, Taylor AFS, Bahram M, Bates ST, Bruns TD, Bengtsson-Palme J, Callaghan TM, Douglas B, Drenkhan T, Eberhardt U, Dueñas M, Grebenc T, Griffith GW, Hartmann M, Kirk PM, Kohout P, Larsson E, Lindahl BD, Lücking R, Martín MP, Matheny PB, Nguyen NH, Niskanen T, Oja J, Peay KG, Peintner U, Peterson M, Põldmaa K, Saag L, Saar I, Schüßler A, Scott JA, Senés C, Smith ME, Suija A, Taylor DL, Telleria MT, Weiss M, Larsson K-H (2013) Towards a unified paradigm for sequence-based identification of fungi. Molecular Ecology 22(21): 5271–5277. https://doi.org/10.1111/mec.12481

Kõljalg U, Nilsson RH, Schigel D, Tedersoo L, Larsson K-H, May TW, Taylor AFS, Stjernegaard Jeppesen T, Frøslev TG, Lindahl BD, Põldmaa K, Saar I, Suija A, Savchenko A, Yatsiuk I, Adojaan K, Ivanov F, Piirmann T, Pöhönen R, Zirk A, Abarenkov K (2020) The taxon hypothesis paradigm—On the unambiguous detection and communication of taxa. Microorganisms 8(12): 1910. https://doi.org/10.3390/microorganisms8121910

Krell F-T (2000) Impact factors aren't relevant to taxonomy. Nature 405(6786): 507–508. https://doi.org/10.1038/35014664

Lăzăroiu G (2013) The misuse of journal impact factors in evaluating scientific output. Contemporary Readings in Law and Social Justice 2: 164–169.

McKiernan EC, Schimanski LA, Muñoz Nieves C, Matthias L, Niles MT, Alperin JP (2019) Use of the Journal Impact Factor in academic review, promotion, and tenure evaluations. eLife 8: e47338. https://doi.org/10.7554/eLife.47338

Nilsson RH, Larsson KH, Taylor AFS, Bengtsson-Palme J, Jeppesen TS, Schigel D, Kennedy P, Picard K, Glöckner FO, Tedersoo L, Saar I, Kõljalg U, Abarenkov K (2019) The UNITE database for molecular identification of fungi: Handling dark taxa and parallel taxonomic classifications. Nucleic Acids Research 47(D1): D259–D264. https://doi.org/10.1093/nar/gky1022

Nilsson RH, Ryberg M, Wurzbacher C, Tedersoo L, Anslan S, Põlme S, Spirin V, Mikryukov V, Svantesson S, Hartmann M, Lennartsdotter C, Belford P, Khomich M, Retter

A, Corcoll N, Gómez Martinez D, Jansson T, Ghobad-Nejhad M, Vu D, Sanchez-Garcia M, Kristiansson E, Abarenkov K (2023) How, not if, is the question mycologists should be asking about DNA-based typification. MycoKeys 96: 143–157. https://doi.org/10.3897/mycokeys.96.102669

Petersen AM, Jung WS, Yang JS, Stanley HE (2011) Quantitative and empirical demonstration of the Matthew effect in a study of career longevity. Proceedings of the National Academy of Sciences of the United States of America 108(1): 18–23. https://doi.org/10.1073/pnas.1016733108

Robert V, Vu D, Amor ABH, van de Wiele N, Brouwer C, Jabas B, Szoke S, Dridi A, Triki M, Daoud S, Chouchen O, Vaas L, de Cock A, Stalpers JA, Stalpers D, Verkley GJM, Groenewald M, dos Santos FB, Stegehuis G, Li W, Wu L, Zhang R, Ma J, Zhou M, Gorjón SP, Eurwilaichitr L, Ingsriswang S, Hansen K, Schoch C, Robbertse B, Irinyi L, Meyer W, Cardinali G, Hawksworth DL, Taylor JW, Crous PW (2013) MycoBank gearing up for new horizons. IMA Fungus 4(2): 371–379. https://doi.org/10.5598/imafungus.2013.04.02.16

Rushforth A, de Rijcke S (2015) Accounting for impact? The journal impact factor and the making of biomedical research in the Netherlands. Minerva 53(2): 117–139. https://doi.org/10.1007/s11024-015-9274-5

Schoch CL, Seifert KA, Huhndorf S, Robert V, Spouge JL, Levesque CA, Chen W, Bolchacova E, Voigt K, Crous PW, Miller AN, Wingfield MJ, Aime MC, An K-D, Bai F-Y, Barreto RW, Begerow D, Bergeron M-J, Blackwell M, Boekhout T, Bogale M, Boonyuen N, Burgaz AR, Buyck B, Cai L, Cai Q, Cardinali G, Chaverri P, Coppins BJ, Crespo A, Cubas P, Cummings C, Damm U, de Beer ZW, de Hoog GS, Del-Prado R, Dentinger B, Diéguez-Uribeondo J, Divakar PK, Douglas B, Dueñas M, Duong TA, Eberhardt U, Edwards JE, Elshahed MS, Fliegerova K, Furtado M, García MA, Ge Z-W, Griffith GW, Griffiths K, Groenewald JZ, Groenewald M, Grube M, Gryzenhout M, Guo L-D, Hagen F, Hambleton S, Hamelin RC, Hansen K, Harrold P, Heller G, Herrera C, Hirayama K, Hirooka Y, Ho H-M, Hoffmann K, Hofstetter V, Högnabba F, Hollingsworth PM, Hong S-B, Hosaka K, Houbraken J, Hughes K, Huhtinen S, Hyde KD, James T, Johnson EM, Johnson JE, Johnston PR, Jones EBG, Kelly LJ, Kirk PM, Knapp DG, Kõljalg U, Kovács GM, Kurtzman CP, Landvik S, Leavitt SD, Liggenstoffer AS, Liimatainen K, Lombard L, Luangsa-ard JJ, Lumbsch HT, Maganti H, Maharachchikumbura SSN, Martin MP, May TW, McTaggart AR, Methven AS, Meyer W, Moncalvo J-M, Mongkolsamrit S, Nagy LG, Nilsson RH, Niskanen T, Nyilasi I, Okada G, Okane I, Olariaga I, Otte J, Papp T, Park D, Petkovits T, Pino-Bodas R, Quaedvlieg W, Raja HA, Redecker D, Rintoul TL, Ruibal C, Sarmiento-Ramírez JM, Schmitt I, Schüßler A, Shearer C, Sotome K, Stefani FOP, Stenroos S, Stielow B, Stockinger H, Suetrong S, Suh S-O, Sung G-H, Suzuki M, Tanaka K, Tedersoo L, Telleria MT, Tretter E, Untereiner WA, Urbina H, Vágvölgyi C, Vialle A, Vu TD, Walther G, Wang Q-M, Wang Y, Weir BS, Weiß M, White MM, Xu J, Yahr R, Yang ZL, Yurkov A, Zamora J-C, Zhang N, Zhuang W-Y, Schindel D (2012) Nuclear ribosomal internal transcribed spacer (ITS) region as a universal DNA barcode marker for Fungi. Proceedings of the National Academy of Sciences of the United States of America 109(16): 6241–6246. https://doi.org/10.1073/pnas.1117018109

Simons K (2008) The misused impact factor. Science 322(5899): 165–165. https://doi.org/10.1126/science.1165316

Trikalinos NA, Evangelou E, Ioannidis JP (2008) Falsified papers in high-impact journals were slow to retract and indistinguishable from nonfraudulent papers. Journal of Clinical Epidemiology 61(5): 464–470. https://doi.org/10.1016/j.jclinepi.2007.11.019

Supplementary material 1

Supplementary item

Authors: R. Henrik Nilsson, Arnold Tobias Jansson, Christian Wurzbacher, Sten Anslan, Pauline Belford, Natàlia Corcoll, Alexandra Dombrowski, Masoomeh Ghobad-Nejhad, Mikael Gustavsson, Daniela Gómez-Martínez, Faheema Kalsoom Khan, Maryia Khomich, Charlotte Lennartsdotter, David Lund, Breyten Van Der Merwe, Vladimir Mikryukov, Marko Peterson, Teresita M. Porter, Sergei Põlme, Alice Retter, Marisol Sanchez-Garcia, Sten Svantesson, Patrik Svedberg, Duong Vu, Martin Ryberg, Kessy Abarenkov, Erik Kristiansson

Data type: pdf

Explanation note: **a** the median impact factor of formal fungal species descriptions 2000-2021. For the red curve, only descriptions published in a journal with a formal impact factor from the year of publication were included in the calculation. For the blue curve, also descriptions published in journals without a formal impact factor from the year of publication were included with their impact factor set to 0.0. The green curve shows the average impact factor of the journals in ISI's category "Mycology" over time **b** the median impact factor of formal species descriptions visualized as the difference in IF from the median mycological IF (dashed line) over time **c** the proportion of formal description of species in journals without a formal IF (red) or with an IF below the mycological median (orange) over time.

Link: https://doi.org/10.3897/mycokeys.110.136048.suppl1

MycoKeys

MycoKeys 110: 287–317 (2024)
DOI: 10.3897/mycokeys.110.130260

Research Article

Unveiling species diversity within early-diverging fungi from China III: Six new species and a new record of *Gongronella* (Cunninghamellaceae, Mucoromycota)

Yi-Xin Wang[1], Heng Zhao[2], Yang Jiang[1], Xin-Ye Liu[1], Meng-Fei Tao[1], Xiao-Yong Liu[1,3]

1 *College of Life Sciences, Shandong Normal University, Jinan 250358, China*
2 *School of Ecology and Nature Conservation, Beijing Forestry University, Beijing 100083, China*
3 *State Key Laboratory of Mycology, Institute of Microbiology, Chinese Academy of Sciences, Beijing 100101, China*
Corresponding author: Xiao-Yong Liu (liuxy@sdnu.edu.cn)

Abstract

Gongronella had accommodated only two species for more than half a century and as many as 17 new species have been described in this genus since 2015. However, no systematic studies were conducted for this genus so far. The distribution, substrate and morphology of all known species in *Gongronella* are analysed herein. Meanwhile, with the support of phylogenetic and morphological evidence, six new species (*G. abortosporangia* **sp. nov.**, *G. apophysata* **sp. nov.**, *G. bawanglingensis* **sp. nov.**, *G. inconstans* **sp. nov.**, *G. pingtangensis* **sp. nov.** and *G. reniformis* **sp. nov.**) are proposed and *G. pamphilae* is recorded from China for the first time. The phylogenetic tree was constructed using ITS+LSU+TEF+ACT+RPB1 and the results were basically the same as ITS+LSU. All species of *Gongronella*, except *G. namwonensis* from fresh water, were isolated from soil. The genus is distributed worldwide, mainly in tropical and subtropical regions. A synoptic key is provided for a total of 24 species (18 species previously published and six species newly described herein), except for *G. banzhaoae* due to unavailable protologue, type and living culture. No morphologies were described when *G. pamphilae* was proposed. Thanks to the strains isolated in this study, *G. pamphilae* is included in the key and reported as a Chinese new record. This is the first comprehensive taxonomy and phylogeny of the genus *Gongronella*.

Key words: Mucoromycota, molecular phylogeny, new taxa, soil-borne fungi, taxonomy

Academic editor: Thorsten Lumbsch
Received: 22 June 2024
Accepted: 4 November 2024
Published: 20 November 2024

Citation: Wang Y-X, Zhao H, Jiang Y, Liu X-Y, Tao M-F, Liu X-Y (2024) Unveiling species diversity within early-diverging fungi from China III: Six new species and a new record of *Gongronella* (Cunninghamellaceae, Mucoromycota). MycoKeys 110: 287–317. https://doi.org/10.3897/mycokeys.110.130260

Introduction

The genus *Gongronella* Ribaldi has a great potential in biological applications due to the ability of producing bioactive substance such as chitosan (Wang et al. 2008; Zhou et al. 2008), dissolving phosphate and degrading metalaxyl (Doilom et al. 2020; Martins et al. 2020). *Gongronella* sp. w5, a well-known strain in this genus, can induce fungi *Panus rudis* (Wei et al. 2010) and *Coprinopsis cinerea* (Pan et al. 2014; Hu et al. 2019; Liu et al. 2022) to produce laccase, secrete organic acids for improving the acquisition of phosphate in plants and thus promote their growth (Dong et al. 2018; Wang et al. 2021) and synthesise various bioactive enzymes, such as β-glucosidase and invertase (Zhou et al. 2020; Mai et al. 2021).

This genus was established in 1952 and typified with *Gongronella urceolifera* Ribaldi (Ribaldi 1952). It belongs to Mucoromycota Doweld, Mucoromycetes Doweld, *Mucorales* Dumort, Cunninghamellaceae Naumov ex R.K. Benj. (Tedersoo et al. 2018). Before 2015, the taxonomy of *Gongronella* was stagnant, accommodating only two species *G. urceolifera* (= *G. butleri*) and *G. lacrispora*. Since 2015, as many as 17 species have been described successively (Hesseltine and Ellis 1961; Adamcik et al. 2015; Ariyawansa et al. 2015; Li et al. 2016; Tibpromma et al. 2017; Dong et al. 2019; Zhang et al. 2019; Crous et al. 2020; de Freitas et al. 2020; Doilom et al. 2020; Martins et al. 2020; Wang et al. 2023a; Zhao et al. 2023). At present, *Gongronella* contains 19 species, nearly half of which were initially found from China (Table 1). In the GlobalFungi database, there are a total of 3,039 sample records for the genus *Gongronella* covering Asia (1,566, 51.53%), North America (571, 18.79%), Europe (433, 14.58%), South America (261, 8.59%), Africa (123, 4.05%), Australia (64, 2.11%) and Atlantic Ocean (1, 0.03%) (https://globalfungi.com/, accessed on 18 October 2024). Considering geographical climate, most samples were collected from tropical and subtropical regions (https://globalfungi.com/, accessed on 17 October 2024). In conclusion, the species of *Gongronella* were distributed worldwide and mainly concentrated in tropical and subtropical regions in Asia.

Regarding substrate of nomenclatural types within the genus *Gongronella*, *G. namwonensis* was isolated from fresh water and the other 18 species were all isolated from soil (Crous et al. 2020; Doilom et al. 2020). According to the GlobalFungi database, substrates include soil (1852, 60.94%), topsoil (475, 15.63%), root (403, 13.26%), rhizosphere soil (204, 6.71%), root + rhizosphere soil (52, 1.71%), litter (22, 0.72%), sediment (10, 0.33%), shoot (9, 0.3%) and deadwood (7, 0.23%), (https://globalfungi.com/, accessed on 19 October 2024). Although the GlobalFungi database showed more kinds of substrates of *Gongronella*, most strains were still isolated from a variety of soil samples.

In this study, 14 strains of the genus *Gongronella* were isolated from soil in Hainan, Yunnan, Sichuan and Guizhou Provinces from China. According to ITS+LSU+TEF+RPB1 molecular phylogenetic analyses and morphological comparisons, these strains were classified into six new species and one was identified as new record species to China. The morphological information of all described species of *Gongronella* was reviewed and compared.

Table 1. The origin of taxonomic types in *Gongronella*.

Countries	Type numbers	Percentage (%)
China	9	47.4
Korea	3	15.8
Brazil	3	15.8
Australia	2	10.5
Portugal	1	5.3
UK	1	5.3

Note: These data are from the Index Fungorum (http://www.indexfungorum.org/, accessed on 9 December 2023) and Wang et al. (2023).

Materials and methods

Isolation and morphology

Soil samples were collected in Hainan Province (April 2023 and October 2023), Sichuan Province (June 2023) and Guizhou Province (August 2023). Strains were isolated from the soil samples by a combination of soil dilution and single spore isolation.

About 1 g soil sample was mixed with 10 ml sterile water to prepare 10^{-1} soil suspension. One millilitre of 10^{-1} suspension was transferred to 9 ml of sterile water to obtain a 10^{-2} soil suspension. In the same way, 10^{-3} and 10^{-4} soil suspensions were made. The final 10^{-3} and 10^{-4} soil suspensions (200 ml) were pipetted on the surface of Rose-Bengal Chloramphenicol Agar (RBC: peptone 5.00 g/l, glucose 10.00 g/l, KH_2PO_4 1.00 g/l, $MgSO_4 \cdot 7H_2O$ 0.50 g/l, rose red 0.05 g/l, chloramphenicol 0.10 g/l, agar 15.00 g/l) (Corry et al. 1995), dispersed evenly with sterilised coating rods and cultured at 25 °C in the dark for 2–5 days. Upon colonies were visible, they were transferred onto Potato Dextrose Agar (PDA: glucose 20.00 g/l, potato 200.00 g/l, agar 20.00 g/l, pH 7). When sporangia were produced, sporangiospores were suspended with sterile water and streaked with a sterilised inoculation ring. The plates were cultured at 25 °C in darkness and single spore colonies were transferred on to a new PDA plate for subculturing. To ensure the formation of zygospores, pairing experiments were carried out by adding 0.1% lecithin to PDA and sealing Petri dishes to retain moisture. The microscopic morphological characteristics of fungi were observed with an optical microscope (Olympus BX53) and photographed with a high-definition colour digital camera (Olympus DP80). All strains were stored with 10% sterilised glycerine at 4 °C. Each morphological character was statistically calculated from 30 measurements (Zhang et al. 2022). Cultures were deposited in the China General Microbiological Culture Collection Center, Beijing, China (CGMCC) and the Shandong Agricultural University Culture Collection, Taian, China (SAUCC). Specimens were deposited in the Herbarium Mycologicum Academiae Sinicae, Beijing, China (HMAS). Taxonomic information for the new taxa was registered in the Fungal Name repository (https://nmdc.cn/fungalnames/).

DNA extraction and amplification

Genomic DNA was extracted from mycelia using the CTAB method and BeaverBeads Plant DNA Kit (Cat. No.: 70409-20; BEAVER Biomedical Engineering Co., Ltd.) (Doyle et al. 1990; Guo et al. 2000; Wang et al. 2023b). ITS, LSU, TEF, ACT and RPB1 were amplified by polymerase chain reaction using ITS4/ITS5, LR0R/LR7, EF1-728F/EF1-986R, ACT-512F/ACT-783R and RPB1-Af/RPB1-Cr primer pairs, respectively (Table 2). Amplification was performed in a final volume of 20 µl, containing 10 µl 2× Hieff Canace® Plus PCR Master Mix (Yeasen Biotechnology, Cat No. 10154ES03), 0.5 µl of forward and reverse primers each (10 µM) (TsingKe, Beijing, China), 1 µl template genomic DNA (about 1 µM) and 8 µl distilled deionised water. Molecular loci, PCR primers and programmes used in this study are listed in Table 2. The PCR products were electrophoresed with 1% agarose gel. The DNA fragments were stained with GelRed and observed under

Table 2. Molecular loci, PCR primers and programmes used in this study.

Loci	PCR primers	Sequence (5'–3')	PCR cycles	References
ITS	ITS5	GGA AGT AAA AGT CGT AAC AAG G	95 °C 5 min; (95 °C 30 s, 55 °C 30 s, 72 °C 1 min) × 35 cycles; 72 °C 10 min	White et al. (1990)
	ITS4	TCC TCC GCT TAT TGA TAT GC		
LSU	LR0R	GTA CCC GCT GAA CTT AAG C	95 °C 5 min; (95 °C 50 s, 47 °C 30 s, 72 °C 1.5 min) × 35 cycles; 72 °C 10 min	Vilgalys and Hester (1990)
	LR7	TAC TAC CAC CAA GAT CT		
TEF	EF1-728F	CAT CGA GAA GTT CGA GAA GG	95 °C 5 min; (95 °C 30 s, 55 °C 60 s, 72 °C 1 min) × 30 cycles; 72 °C 10 min	Carbone and Kohn (1999); O'Donnell et al. (1998)
	EF2	GGA RGT ACC AGT SAT CAT GTT		
RPB1	RPB1-Af	GAR TGY CCD GGD CAY TTY GG	95 °C 3 min; (94 °C 40 s, 60 °C 40 s, 72 °C 2 min) × 9 (94 °C 45 s, 55 °C 1.5 min, 72 °C 2 min) × 37 cycles; 72 °C 10 min	Stiller and Hall (1997)
	RPB1-Cr	CCN GCD ATN TCR TTR TCC ATR TA		
ACT	ACT-512F	ATG TGC AAG GCC GGT TTC GC	95 °C 3 min; (95 °C 1 min, 55 °C 1 min, 72 °C 1 min) × 30 cycles; 72 °C 10 min	Voigt and Wostemeyer (2000)
	ACT-783R	TAC GAG TCC TTC TGG CCC AT		

ultraviolet light. Then a gel extraction kit (Cat# AE0101-C; Shandong Sparkiade Biotechnology Co., Ltd.) was used for gel recovery. Sanger sequencing was carried out by Biosune Company Limited (Shanghai, China). Consensus sequences were assembled using MEGA v.7.0 (Kumar et al. 2016). All sequences generated in this study were deposited at GenBank under the accession numbers in Table 3.

Relative sequences were obtained by BLAST search in the GenBank nucleotide database of NCBI website (Kumar et al. 2016). Sequences both generated herein and retrieved from GenBank (Table 3) were aligned using MAFFT 7 online service (http://mafft.cbrc.jp/alignment/server/, 20 October 2023) (Katoh et al. 2019). The ITS, LSU, TEF, ACT and RPB1 sequences were analysed individually and jointly. The optimal evolutionary model for each partition was determined and included in the analysis using MrModelTest v.2.3 (Nylander 2004). Phylogenetic history was reconstructed using Maximum Likelihood (ML) algorithm with RaxML-HPC2 on XSEDE 8.2.12 (Stamatakis 2014; Zhao et al. 2024) and Bayesian Inference (BI) algorithm with MrBayes 3.2.7a (Huelsenbeck and Ronquist 2001; Ronquist and Huelsenbeck 2003; Ronquist et al. 2012). ML was performed for 1,000 bootstrap replicates with the GTRGAMMA model of nucleotide evolution. BI was performed using a quick start algorithm with an automatic stop option. The Bayesian analysis consisted of 5,000,000 generations with four parallel runs with the option of stopping rules and a sampling frequency of 100 generations. The burn-in score was set to 0.25 and the posterior probability (PP) was determined from the remaining trees. Initial adjustments of phylogenetic trees were made using FigTree v.1.4.4 (http://tree.bio.ed.ac) and the layout of the trees was finished using Adobe Illustrator CC 2019 (https://adobe.com/products/illustrator).

Results

Phylogenetic analyses

The sequence matrix included 43 strains in 25 species of *Gongronella*, with *Cunninghamella echinulata* CBS 156.28 as outgroup. A total of 4,080 characters comprised ITS rDNA (1–989), LSU rDNA (990–1967), TEF (1968–2172), ACT (2173–2948) and RPB1 (2949–4080). Amongst these characters, 2,866 were constant, 562 variable, but parsimony non-informative and 652 parsimony

Table 3. Information of strains used in this study.

Species	Strains	Substrates	Countries	GenBank accession numbers				
				ITS	LSU	ACT	TEF	RPB1
Gongronella abortosporangia	**CGMCC 3.27028***	**Soil**	**China**	**PP195847**	**PP195948**	**PP933938**	**PP850088**	**PP842883**
	SAUCC 4064-2	**Soil**	**China**	**PP195848**	**PP195949**	**PP933939**	**PP850089**	**PP842882**
G. apophysata	**CGMCC 3.27031***	**Soil**	**China**	**PP195853**	**PP195954**	**PP933947**	**PP850099**	**PP842878**
	SAUCC 4846-3	**Soil**	**China**	**PP195854**	**PP195955**	**PP933948**	**PP850100**	**PP842877**
G. banzhaoae	BRIP 75171a*	Soil	Australia	OR271908	OR259049	n.a.	n.a.	n.a.
G. bawanglingensis	**CGMCC 3.27033***	**Soil**	**China**	**PP195857**	**PP195958**	**PP933951**	**PP850103**	**PP883965**
	SAUCC 6946-1	**Soil**	**China**	**PP195858**	**PP195959**	**PP933952**	**PP850104**	**PP883964**
G. brasiliensis	URM 7487*	Soil	Brazil	NR_155148	KY114932	n.a.	n.a.	n.a.
	URM 7488	Soil	Brazil	KY114931	KY114933	n.a.	n.a.	n.a.
G. butleri	CBS 216.58*	Soil	UK	JN206285	MH869292	n.a.	n.a.	n.a.
G. chlamydospora	CGMCC 3.16118*	Soil	China	OL678157	n.a.	n.a.	n.a.	PP898292
G. eborensis	MUM 10.262*	Soil	Portugal	KT809408	MN947301	n.a.	n.a.	n.a.
	MUM 10.263	Soil	Portugal	GU244500	MN947302	n.a.	n.a.	n.a.
G. guangdongensis	CGMCC 2.15212*	Soil	China	NR_158464	MN947303	n.a.	n.a.	n.a.
	CGMCC 2.15213	Soil	China	KC462740	MN947304	n.a.	n.a.	n.a.
G. hydei	KUMCC 18.0198*	Rhizosphere soil	China	NR_171964	MT907273	n.a.	n.a.	n.a.
G. inconstans	**CGMCC 3.27029***	**Soil**	**China**	**PP195849**	**PP195950**	**PP933941**	**PP850091**	**PP842874**
	SAUCC 4113-3	**Soil**	**China**	**PP195850**	**PP195951**	**PP933942**	**PP850092**	**PP842873**
G. koreana	EML-TS2Bp*	Soil	Korea	KP636529	KP636530	KP636527	n.a.	n.a.
	EML-TS2Bp-2	Soil	Korea	KP835545	KP835542	KP835543	n.a.	n.a.
G. lacrispora	ATCC 24412*	Soil	Brazil	GU244498	JN206609	n.a.	n.a.	n.a.
G. multiramosa	CGMCC 3.26216*	Soil	China	OR733546	OR733611	PP933937	PP850087	PP842881
	SAUCC 4056-4	Soil	China	OR733545	OR733610	n.a.	n.a.	n.a.
G. multispora	CGMCC 3.16119*	Soil	China	OL678158	n.a.	n.a.	n.a.	pm
G. namwonensis	CNUFC WW2-12*	Fresh water	Korea	NR_175640	MN658482	n.a.	n.a.	n.a.
G. oleae	CGMCC 3.26217*	Soil	China	OR742078	OR733608	PP933945	PP850097	PP850080
	SAUCC 4164-2	Soil	China	OR742079	OR733609	PP933946	PP850098	PP850079
G. orasabula	EML-QF12-1*	Soil	Korea	NR_148087	KT936263	KT936265	n.a.	n.a.
	EML-QF12-2	Soil	Korea	KT936270	KT936264	n.a.	n.a.	n.a.
G. pamphilae	BRIP 74936a*	Soil	Australia	OR271909	OR259050	n.a.	n.a.	n.a.
	CGMCC 3.27027	**Soil**	**China**	**PP195845**	**PP195946**	**PP933935**	**PP850086**	**PP850081**
	SAUCC 4031-2	**Soil**	**China**	**PP195846**	**PP195947**	**PP933936**	**PP850085**	**PP850082**
G. pedratalhadensis	URM 8182*	Soil	Brazil	MN912512	MN912508	n.a.	n.a.	n.a.
G. pingtangensis	**CGMCC 3.27032***	**Soil**	**China**	**PP195855**	**PP195956**	**PP933949**	**PP850101**	**PP842880**
	SAUCC 5676-2	**Soil**	**China**	**PP195856**	**PP195957**	**PP933950**	**PP850102**	**PP842879**
G. qichaensis	CGMCC 3.26218*	Soil	China	OR733544	OR733607	n.a.	**PP850093**	**PP850084**
	SAUCC 4137-3	Soil	China	OR733543	OR733606	n.a.	**PP850094**	**PP850083**
G. reniformis	**CGMCC 3.27030***	**Soil**	**China**	**PP195851**	**PP195952**	**PP933943**	**PP850095**	**PP842875**
	SAUCC 4142-5	**Soil**	**China**	**PP195852**	**PP195953**	**PP933944**	**PP850096**	**PP842876**
G. sichuanensis	CGMCC 3.19651*	Soil	China	MK813373	MK813855	MK820625	n.a.	n.a.
	CGMCC 3.19652	Soil	China	MK813374	MK813856	MK820626	n.a.	n.a.
G. zunyiensis	CGMCC 3.19899*	Soil	China	MN453856	MN453853	n.a.	n.a.	n.a.
	CGMCC 3.19900	Soil	China	MN453857	MN453854	n.a.	n.a.	n.a.
Cunninghamella echinulata	CBS 156.28*	n.a.	n.a.	JN205895	MH877699	n.a.	n.a.	n.a.

Notes: New species established in this study are in bold. Ex-type or ex-holotype strains are labelled with a star mark "*". The abbreviation "n.a." stands for "not available"

informative characters (Suppl. material 1). MrModelTest suggested that the Dirichlet fundamental frequency and GTR+I+G evolution pattern for both partitions were adopted in Bayesian Inference. The topology of the Bayesian tree was consistent with that of the ML tree and, therefore, was used as a representative to summarise the evolutionary history within the genus *Gongronella* (Fig. 1). *G. abortosporangia* was closely related to *G. multiramosa* with a high support (BIPP = 0.95). *G. pingtangensis* was closely related to *G. namwonensis* with a high support (BIPP = 1). *G. reniformis* was closely related to *G. pamphilae* and *G. brasiliensis* with a high support (MLBV = 75, BIPP = 0.99). The *G. bawanglingensis* (MLBV = 100, BIPP = 1) is closely related to *G. qichaensis* and *G. inconstans*. *G. inconstans* (MLBV = 99, BIPP = 1) is closely related to *G. qichaensis* with a high support (BIPP = 0.96). *G. apophysata* is closely related to *G. zunyiensis*.

Taxonomy

Gongronella abortosporangia **Yi Xin Wang, H. Zhao & X.Y. Liu, sp. nov.**
Fungal Names: FN 571253
Fig. 2

Etymology. The epithet "*abortosporangia*" (Latin) refers to the abortive sporangia.

Type. China • Hainan Province, Lingshui Li Autonomous County, Qixian Yaochi Yexi Hot Spring (18.70161°N, 109.69318°E), from soil sample, 10 April 2023, Yi-Xin Wang (holotype HMAS 352726, ex-holotype strain CGMCC 3.27028).

Description. Colonies growing slowly on PDA in darkness at 25 °C, reaching 49.2–52.4 mm in diameter in seven days, white, regular at edge and cottony in the centre, reversely milky white. Rhizoids hyaline, branched, irregularly shaped, with oil droplets. Stolons absent. Sporangiophores on aerial mycelia, erect or slightly curved, unbranched or branched (1–6 times), 4.0–96.8 × 1.0–4.2 µm, hyaline, smooth, mostly aseptate, sometimes one-septate and rarely two-septate, occasionally containing a line of oil droplets. Sterile (aborted) sporangia abundant, mainly on the top of short lateral branches of sporangiophores, mostly gourd-shaped, 11.6–16.7 × 5.5–17.7 µm, partially elliptical with a slight shrinkage, 12.5–18.0 × 6.7–10.6 µm, occasionally clavate, 20.1–22.7 × 9.5–10.4 µm. Fertile sporangia hyaline or light yellow, spherical, 7.0–23.2 µm in diameter, smooth and deliquescent-walled, leaving a collar after releasing sporangiospores. Columellae mostly hemispherical, 2.5–4.2 × 3.6–7.4 µm, sometimes sub-hemispherical, 1.3–3.9 × 3.6–5.5 µm, hyaline, smooth. Apophyses hyaline, smooth, variously shaped, mostly cup-shaped, 1.9–8.6 × 2.1–6.7 µm, partially hemispherical, 2.7–5.5 × 2.8–7.4 µm, occasionally pear-shaped, 8.2 × 7.2 µm. Sporangiospores not uniform, hyaline, smooth, ovoid, 2.6–3.5 × 1.7–2.1 µm, reniform, 2.9–3.5 × 1.7–2.3 µm. Chlamydospores gourd-shaped, 20.3–29.3 × 6.4–9.3 µm. Giant cells intercalary, globular, subglobular, 2.6–4.6 µm in diameter. Zygospores not found.

Additional specimen examined. China • Hainan Province, Lingshui Li Autonomous County, Benhao Town (18.70161°N, 109.69318°E), from soil sample, 10 April 2023, Yi-Xin Wang (living culture SAUCC 4064-2).

GenBank accession numbers. CGMCC 327028 (ITS, PP195847; LSU, PP195948; TEF, PP850088; ACT, PP933938; RPB1, PP842883), SAUCC 4064-2 (ITS, PP195848; LSU, PP195949; TEF, PP850089; ACT, PP933939; RPB1, PP842882).

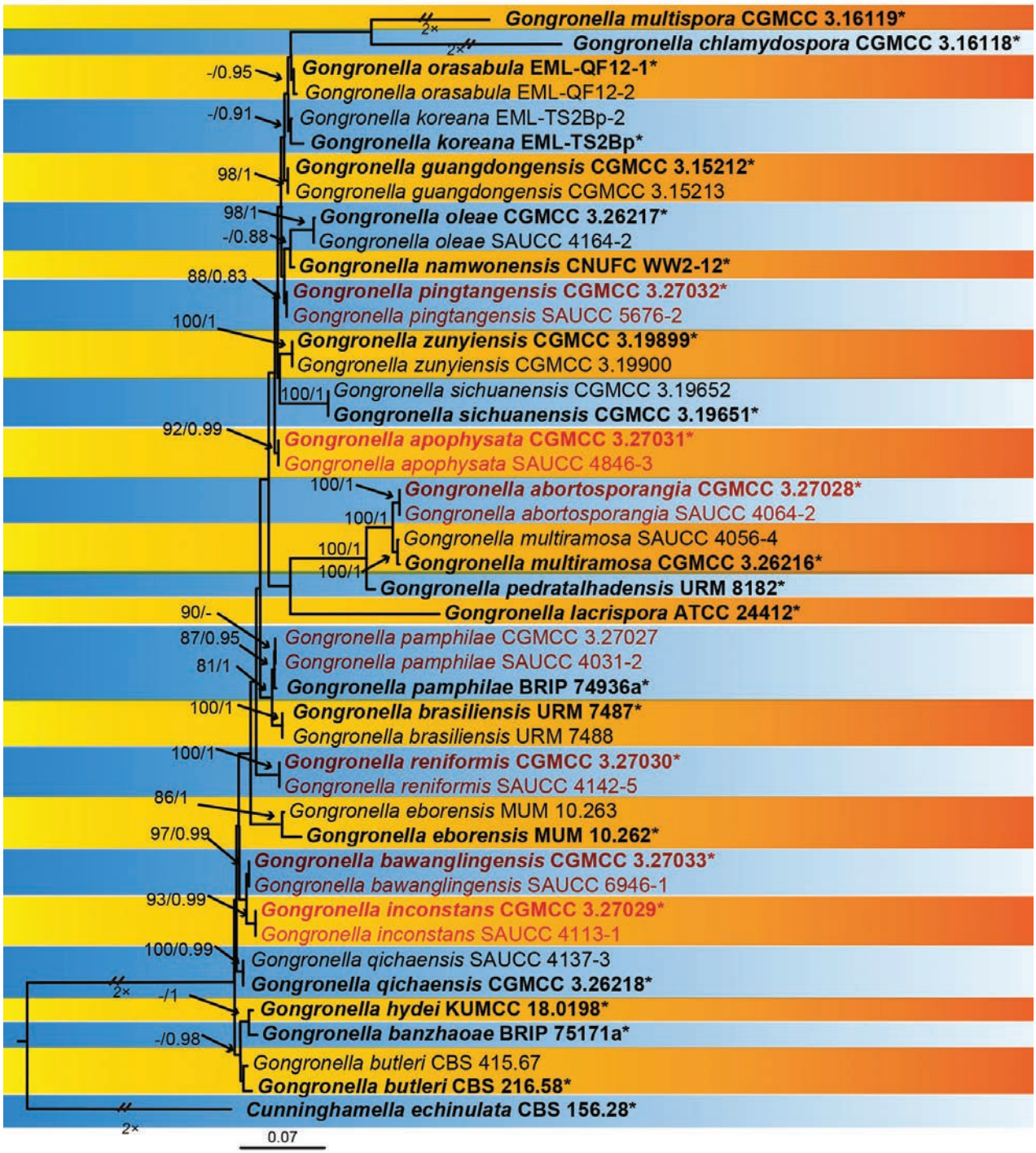

Figure 1. A Maximum Likelihood (ML) phylogenetic consensus tree inferred from DNA sequences of ITS, LSU, TEF, ACT and RPB1, showing relationships amongst species of *Gongronella* with *Cunninghamella echinulata* CBS 156.28 as outgroup. The Maximum Likelihood bootstrap value (MLBV) and Bayesian Inference posterior probability (BIPP) are successively shown at the nodes and separated by a slash "/". Strains marked with a star "*" are ex-types or ex-holotypes. The strains isolated and sequenced in this study are shown in red. Branches shortened to fit the page are represented by double slashes "//" and folds "×". The scale in the bottom centre indicates 0.2 substitutions per site.

Notes. Based on phylogenetic analyses of ITS+LSU+TEF+ACT+RPB1 sequences, the two isolates of the new species *Gongronella abortosporangia* formed an independent clade with high supports (MLBV = 100; Fig. 1), which is closely related to *G. multiramosa* (BIPP = 0.95; Fig. 1). This new species differs morphologically

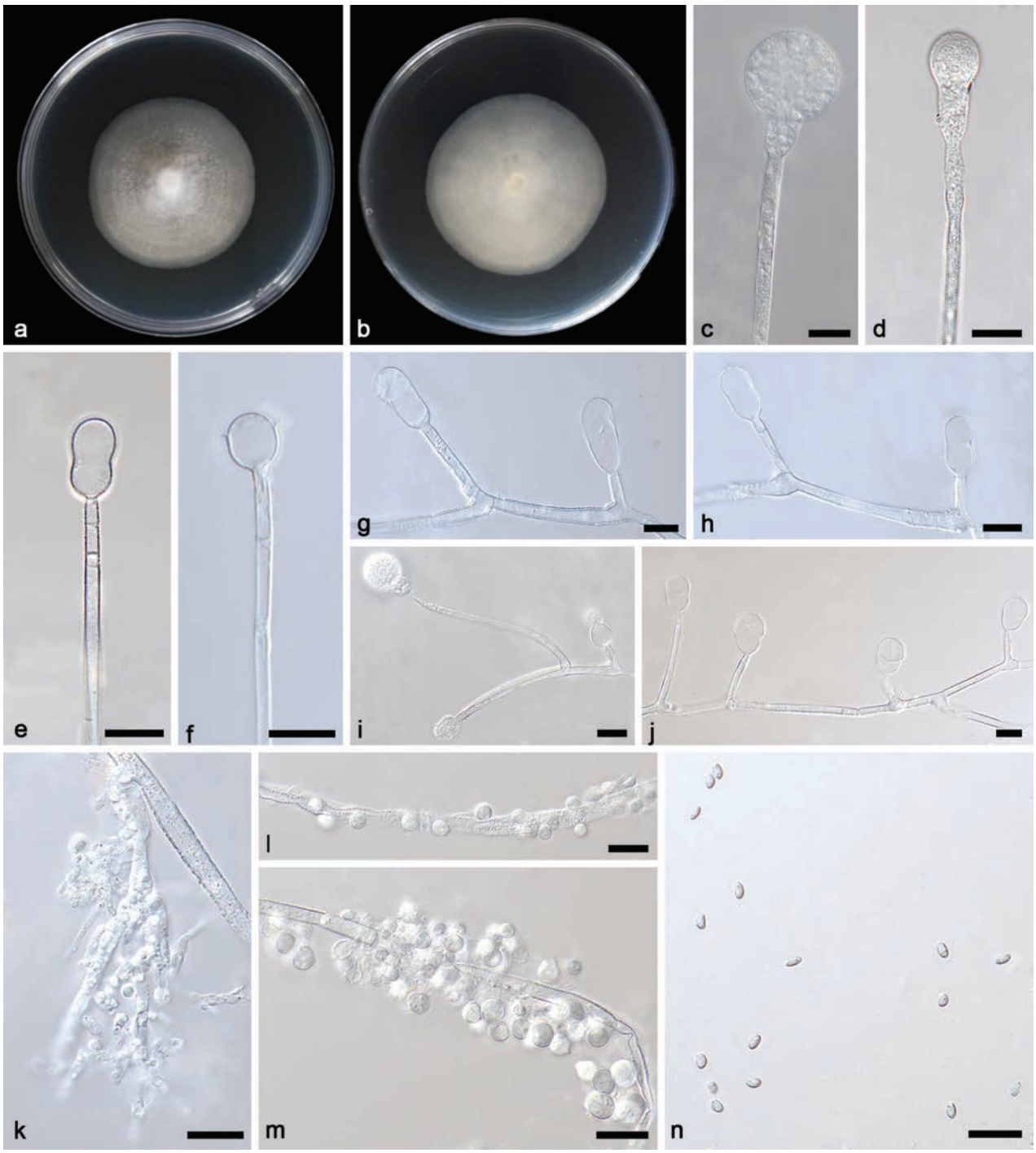

Figure 2. *Gongronella abortosporangia* ex-holotype CGMCC 3.27028 **a**, **b** colonies on PDA (**a** obverse **b** reverse) **c** an unbranched sporangiophore with a mature sporangium **d** an unbranched sporangiophore with an immature sporangium **e** an aborted sporangium with two septa **f** columellae, collars and apophyses **g**, **h**, **j** branched sporangiophores with sterile (aborted) sporangia **i** a branched sporangiophore with a mature sporangium, columellae, collars and apophyses **k** rhizoids **l**, **m** giant cells **n** sporangiospores. Scale bars: 10 µm (**c–n**).

from *G. multiramosa* in sporangium, septum, columella, collar and apophysis (Wang et al. 2023a). The *G. abortosporangia* is different from *G. multiramosa* in shape and size of sterile sporangia, the former being variously shaped, mostly gourd-shaped, 11.6–16.7 × 5.5–17.7 µm, partially elliptical with a slight shrinkage, 12.5–18.0 × 6.7–10.6 µm, occasionally clavate, 20.1–22.7 × 9.5–10.4 µm, while

the latter being only ovoid, 9.6 × 6.2 µm in diameter. In fertile sporangia, *G. abortosporangia* has a smaller minimum diameter than *G. multiramosa* (7.0 µm vs. 15.5 µm). *G. abortosporangia* has more septa on sporangiophores compared to *G. multiramosa* (0–2 vs. 0–1). Although *G. abortosporangia* is similar in shape of columellae to *G. multiramosa*, it is shorter in length (hemispherical, 3.6–7.4 µm vs. 8.0–9.8 µm, sub-hemispherical, 3.6–5.5 µm vs. 7.6–10.0 µm). The *G. abortosporangia* has shorter collars than *G. multiramosa*, 0.6–3.9 µm vs. 1.3–7.2 µm. The *G. abortosporangia* is similar in shape of apophyses to *G. multiramosa*. However, they are different from each other in main pattern and size: The former mostly cup-shaped (1.9–8.6 × 2.1–6.7 µm vs. 4.6–7.0 × 8.5–10.0 µm) and partially hemispherical (2.7–5.5 × 2.8–7.4 µm vs. 4.4–5.6 × 8.5–9.0 µm) and the latter opposite. Combining morphological and molecular phylogenetic analyses, we classified the two isolates as a new species *G. abortosporangia* allied to *G. multiramosa*.

***Gongronella apophysata* Yi Xin Wang, H. Zhao & X.Y. Liu, sp. nov.**
Fungal Names: FN 571631
Fig. 3

Etymology. The epithet "*apophysata*" (Latin) refers to various shapes of apophyses.

Type. China • Sichuan Province, Emeishan City, Leshan City, Ehong Road, near the Xu family residence (29.59211°N, 103.37776°E), from soil sample, 25 June 2023, Yi-Xin Wang (holotype HMAS 352728, ex-holotype strain CGMCC 3.27031).

Description. Colonies growing slowly on PDA in darkness at 25 °C, reaching 35.8–42.4 mm in diameter in seven days, white, irregular at edge and cottony in the centrr, reversely milky white. Rhizoids hyaline, branched, irregularly shaped. Stolons absent. Sporangiophores on aerial mycelia, erect or slightly curved, unbranched or slightly branched (1–2 times), 11.2–190.9 × 1.6–3.9 µm, hyaline, smooth, mostly aseptate or one-septate, occasionally two-septate. Sterile (aborted) sporangia predominantly on the top of short lateral branches of sporangiophores, gourd-shaped, 14.0 × 8.3 µm. Fertile sporangia hyaline or light yellow, spherical, 12.5–40.5 µm in diameter, smooth and deliquescent-walled, leaving a collar after releasing sporangiospores. Columellae elliptic, 2.6–4.0 × 2.1–5.5 µm, sub-hemispherical, 1.4–2.7 × 2.2–4.3 µm, hyaline, smooth. Apophyses hyaline, smooth, variously shaped, mostly ellipsoidal to olive-shaped, 2.3–17.3 × 2.4–10.0 µm, partially subglobose, 4.6–10.2 × 4.3–10.0 µm, occasionally gourd-shaped, 11.4 × 4.9 µm. Sporangiospores not uniform, hyaline, smooth, mostly reniform, 3.2–5.5 × 1.7–3.1 µm, ovoid, 2.5–3.7 × 1.7–2.6 µm, occasionally subglobose, 1.7–2.5 µm. Chlamydospores present, not uniform, gourd-shaped, ellipsoidal and suborbicular, mostly gourd-shaped, 23.5–35.4 × 10.8–14.0 µm, partially ellipsoidal, 18.6–21.4 × 10.3–18.5 µm. Giant cells in the rhizoids, intercalary, globose, 4.4–10.5 µm in diameter. Zygospores not found.

Additional specimen examined. China • Sichuan Province, Emeishan City, Leshan City, Ehong Road, near the Xu family residence (29.59211°N, 103.37776°E), from soil sample, 25 June 2023, Yi-Xin Wang (living culture SAUCC 4846-3).

GenBank accession numbers. CGMCC 3.27031 (ITS, PP195853; LSU, PP195954; TEF, PP850099; ACT, PP933947; RPB1, PP842878), SAUCC 4846-3 (ITS, PP195854; LSU, PP195956; TEF, PP850100; ACT, PP933948; RPB1, PP842877).

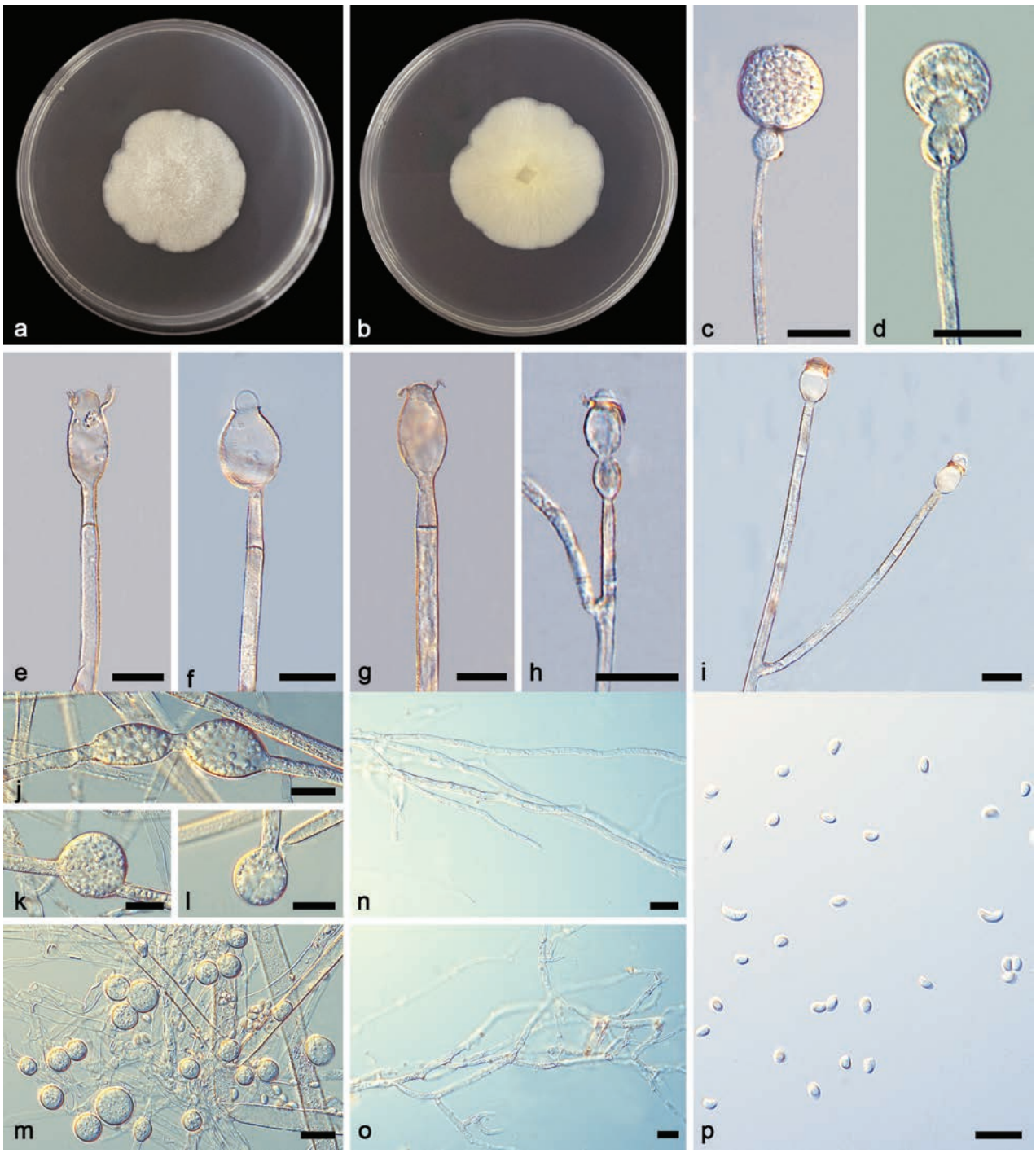

Figure 3. *Gongronella apophysata* ex-holotype CGMCC 3.27031 **a**, **b** colonies on PDA (**a** obverse **b** reverse) **c** an unbranched sporangiophore with a fertile sporangium **d** an unbranched sporangiophore with an immature sporangium **e–g** columellae, collars, apophyses and septa **h** branched sporangiophores with columellae, collars and apophyses **i** branched sporangiophores with columellae, collars and apophyses **j–l** chlamydospores **m** giant cells **n**, **o** rhizoids **p** sporangiospores. Scale bars: 10 μm (**c–p**).

Notes. Based on phylogenetic analyses of ITS+LSU+TEF+ACT+RPB1 sequences, the two isolates of the new species *Gongronella apophysata* form an independent clade with high support (MLBV = 98; Fig. 1), which is closely related to *G. zunyiensis*. In ITS, *G. apophysata* differs from the type species of *G. zunyiensis* by 13 base pairs. This new species differs morphologically

from *G. zunyiensis* in sporangium, columellae, apophyses and chlamydospore (Dong et al. 2019). *G. apophysata* has larger sporangia than *G. zunyiensis* (12.5–40.5 µm vs. 11.0–19.5 µm). *G. apophysata* differs from *G. zunyiensis* in the shape of columellae, the former being elliptic and the latter being hemispherical and globose. As for apophyses, *G. apophysata* and *G. zunyiensis* are remarkably different in shape and size, the former variously shaped, mostly ellipsoidal to olivary, 2.3–17.3 × 2.4–10.0 µm, partially subglobose, 4.6–10.2 × 4.3–10.0 µm, occasionally gourd-shaped, 11.4 × 4.9 µm and the latter hemispherical, 1.5–3.5 × 1.0–3.0 µm. *G. apophysata* is remarkably different from *G. zunyiensis* in shape and size of chlamydospores, the former being not uniform, mostly gourd-shaped, 23.5–35.4 × 10.8–14.0 µm, partially ellipsoidal, 18.6–21.4 × 10.3–18.5 µm and the latter being terminal or lateral, globose or subglobose, 7.0–10.5 µm in diameter. Combining morphological and molecular phylogenetic analyses, we classified the two isolates together as a new species *G. apophysata* allied to *G. zunyiensis*.

Gongronella bawanglingensis **Yi Xin Wang, H. Zhao & X.Y. Liu, sp. nov.**
Fungal Names: FN 571903
Fig. 4

Etymology. The epithet "*bawanglingensis*" (Latin) refers to the location where the type was collected, Bawangling National Forest Park.

Type. China • Hainan Province, Changjiang Li Autonomous County, Bawangling National Forest Park (19.08593°N, 109.12275°E), from soil sample, 14 October 2023, Yi-Xin Wang (holotype HMAS 352730, ex-holotype strain CGMCC 3.27033).

Description. Colonies growing slowly on PDA in darkness at 25 °C, reaching 45.6–48.8 mm in diameter in seven days, white, cottony in the centre, on the reverse milky white. Rhizoids hyaline, branched, irregularly shaped. Stolons absent. Sporangiophores on aerial mycelia, erect or slightly curved, unbranched or slightly branched (up to 3 times), sympodially branched, 1.3–4.5 µm in width, hyaline, smooth, mostly aseptate or one-septate, no more than four-septate. Sterile (aborted) sporangia mainly on the top of short lateral branches of sporangiophores, mostly gourd-shaped. Fertile sporangia hyaline or light yellow, spherical, 4.2–18.5 µm in diameter, smooth and deliquescent-walled, leaving a collar after releasing sporangiospores. Columellae mostly hemispherical, 1.6–5.1 × 2.1–7.2 µm, sometimes arch-shaped, 1.4–3.7 × 2.6–8.8 µm, occasionally spherical, 2.3–6.1 × 2.5–8.1 µm, hyaline, smooth. Collars mostly distinct, 0.7–5.9 µm. Apophyses hyaline, smooth, variously shaped, mostly oval, 3.9–20.6 × 3.3–12.9 µm, sometimes subglobose, 4.8–12.2 × 4.7–12.3 µm, occasionally gourd-shaped. Sporangiospores not uniform, hyaline, smooth, mostly ovoid, 2.5–3.6 × 1.7–2.6 µm, partially reniform, 2.6–3.3 × 1.9–2.2 µm. Chlamydospores not uniform, gourd-shaped, 15.1–24.6 × 7.4–12.9 µm, ellipsoidal, 15.1–18.6 × 8.3–14.0 µm, suborbicular, 12.6–13.5 µm in diameter. Giant cells intercalary, globular, 3.2–6.9 µm in diameter. Zygospores not found.

Additional specimen examined. China • Hainan Province, Changjiang Li Autonomous County, Bawangling National Forest Park (19.08593°N, 109.12275°E), from soil sample, 14 October 2023, Yi-Xin Wang (living culture SAUCC 6946-1).

Figure 4. *Gongronella bawanglingensis* ex-holotype CGMCC 3.27033 **a**, **b** colonies on PDA (**a** obverse **b** reverse) **c**, **d** an unbranched sporangiophore with a fertile sporangium **e** branched sporangiophores with sterile (aborted) sporangia **f** branched sporangiophores with immature sporangia **g–i** columellae, collars, apophyses and septa **j**, **k** branched sporangiophores with columellae, collars and apophyses **l**, **m** chlamydospores **n** giant cells **o** rhizoids **p** sporangiospores. Scale bars: 10 μm (**c–p**).

GenBank accession numbers. CGMCC 3.27033 (ITS, PP195857; LSU, PP195958; TEF, PP50103; ACT, PP933951; RPB1, PP883965), and SAUCC 6946-1 (ITS, PP1195858; LSU, PP195959; TEF, PP850104; ACT, PP933952; RPB1, PP883964).

Notes. Based on phylogenetic analyses of ITS+LSU+TEF+ACT+RPB1 sequences, the two isolates of the new species *Gongronella bawanglingensis* form an independent clade with full support (MLBV = 100, BIPP = 1; Fig. 1), which is closely

related to *G. inconstans* and *G. qichaensis*. In ITS, *G. bawanglingensis* differs from *G. inconstans* by 21 base pairs. This new species differs morphologically from *G. inconstans* in columella, apophysis, colour and sporangiospore. *G. bawanglingensis* and *G. inconstans* are similar in the dominant shape of columellae, but the former is longer than that of the latter (2.1–7.2 µm vs. 2.0–3.9 µm). As for apophyses, *G. bawanglingensis* and *G. inconstans* are remarkably different from each other in shape and size, the former mostly oval, 3.9–20.6 × 3.3–12.9 µm, sometimes subglobose, 4.8–12.2 × 4.7–12.3 µm, occasionally gourd-shaped, the latter mostly long fusiform, 7.6–17.4 × 5.4–4.7 µm, sometimes oval, 5.5–8.8 × 4.4–6.3 µm, rarely egg-shaped, 5.0–6.4 × 4.2–5.7 µm. As for collars, the *G. inconstans* are more distinct than *G. bawanglingensis* (2.0–17.0 µm vs. 0.7–5.9 µm). As for sporangiospores, *G. bawanglingensis* and *G. inconstans* are similar in dominant shape, but the former is smaller in size than the latter (ovoid, 2.5–3.6 × 1.7–2.6 µm vs. 2.7–4.9 × 1.8–3.5 µm, reniform, 2.6–3.3 × 1.9–2.2 µm vs. 3.1–4.1 × 2.0–4.5 µm). Additionally, the *G. inconstans* has more shapes, except ovoid and reniform. In ITS, *G. bawanglingensis* differs from *G. qichaensis* by 28 base pairs. This new species differs morphologically from *G. qichaensis* in sporangium, columellae and apophysis (Wang et al. 2023a). The *G. bawanglingensis* has evidently smaller sporangia than *G. qichaensis*, 4.2–18.5 µm vs. 7.9–36.7 µm. In columella and apophysis, the two species have evident differences in shape. Combining morphological and molecular phylogenetic analyses, we classified the two isolates together as a new species *G. bawanglingensis* allied to *G. inconstans* and *G. qichaensis*.

Gongronella inconstans **Yi Xin Wang, H. Zhao & X.Y. Liu, sp. nov.**
Fungal Names: FN 571905
Fig. 5

Etymology. The epithet "*inconstans*" (Latin) refers to the inconstant shape of apophyses.

Type. China • Hainan Province, Lingshui Li Autonomous County (18.69850°N, 109.88098°E), from soil sample, 7 Apr 72023, Yi-Xin Wang (holotype HMAS 352731, ex-holotype strain CGMCC 3.27029).

Description. Colonies growing slowly on PDA in darkness at 25 °C, reaching 31.2–36.8 mm in diameter in seven days, white, regular at edge and cottony, reversely milky white. Rhizoids hyaline, branched, irregular, ubiquitous. Stolons absent. Sporangiophores on aerial mycelia, erect or slightly curved, unbranched or slightly branched (2–3 times), 1.7–3.9 µm width, hyaline, smooth, mostly aseptate. Fertile sporangia hyaline or light yellow, spherical, 8.8–21.4 µm in diameter, smooth and deliquescent-walled, leaving a collar after releasing sporangiospores. Columellae mostly hemispherical, 1.2–2.4 × 2.0–3.9 µm, sometimes spherical, 3.2–7.2 × 3.4–7.2 µm, hyaline, smooth. Collars distinct, 2.0–17.0 µm wide. Apophyses hyaline, smooth, variously shaped, mostly long fusiform, 7.6–17.4 × 4.7–5.4 µm, sometimes oval, 5.5–8.8 × 4.4–6.3 µm, rarely egg-shaped, 5.0–6.4 × 4.2–5.7 µm. Sporangiospores not uniform, hyaline, smooth, mostly ovoid, 2.7–4.9 × 1.8–3.5 µm, sometimes reniform, 3.1–4.1 × 2.0–4.5 µm or subglobose, 2.4–4.1 µm in diameter, occasionally irregular, 5.0–8.0 × 2.5–3.2 µm. Chlamydospores present, gourd-shaped and irregular. Giant cells intercalary, globular, 4.2–8.0 µm in diameter. Zygospores not found.

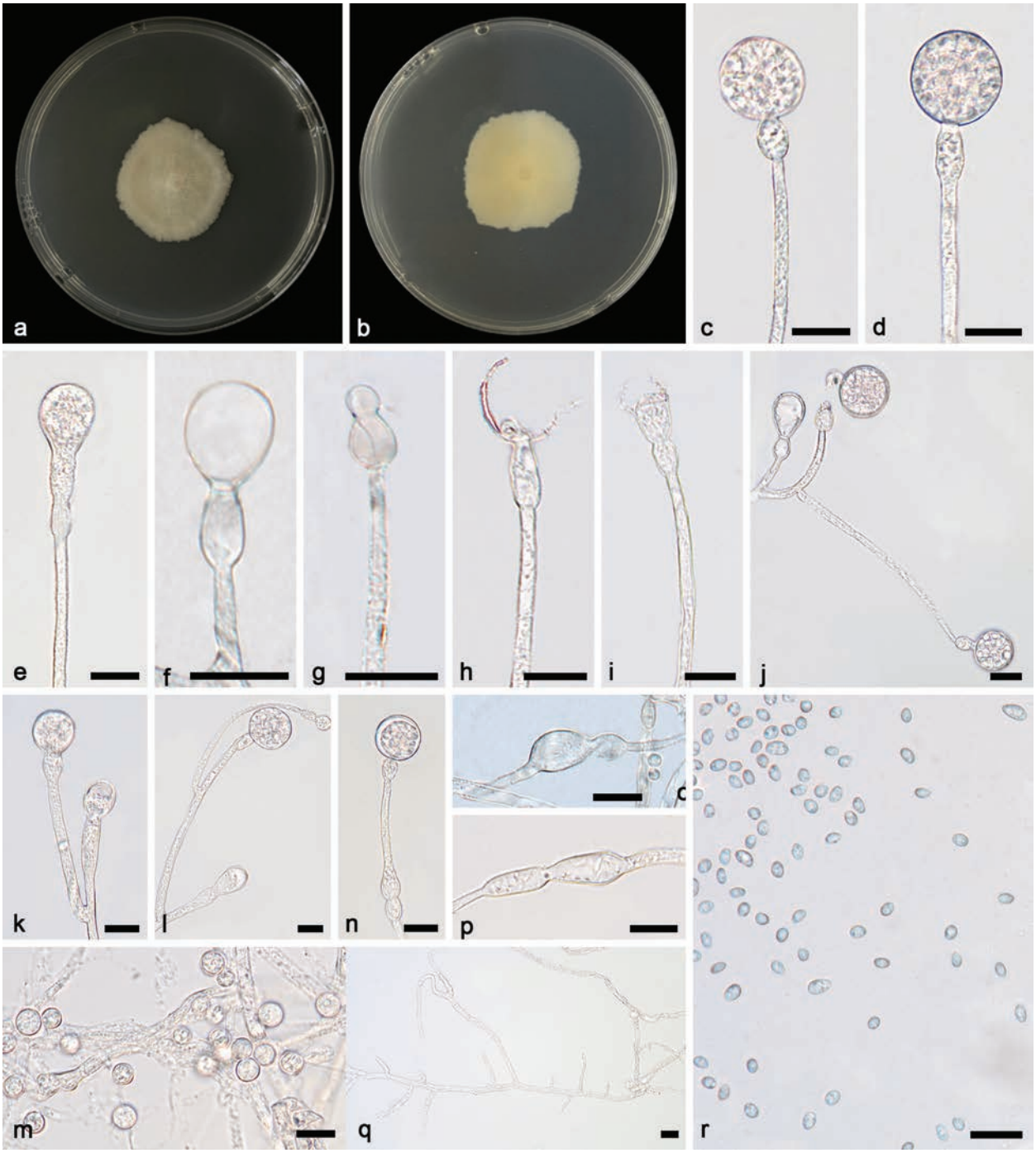

Figure 5. *Gongronella inconstans* ex-holotype CGMCC 3.27029 **a**, **b** colonies on PDA (**a** obverse **b** reverse) **c**, **d** an unbranched sporangiophore with a fertile sporangium **e** an unbranched sporangiophore with a premature sporangium **f** branched sporangiophores with aborted sporangia **g–i** columellae, collars, apophyses **j–l** branched sporangiophores with fertile sporangia, columellae, collars and apophyses **n** fertile sporangium with protuberance **o, p** chlamydospores **m** giant cells **q** rhizoids **r** sporangiospores. Scale bars: 10 μm (**c–r**).

Additional specimen examined. China • Hainan Province, Lingshui Li Autonomous County (18.69850°N, 109.88098°E), from soil sample, 7 April 2023, Yi-Xin Wang (living culture SAUCC 4113-1).

GenBank accession numbers. CGMCC 3.27029 (ITS, PP1955849; LSU, PP195950; TEF, PP850091; ACT, PP933941; RPB1, PP842874), and SAUCC 4113-1 (ITS, PP105850; LSU, PP195951; TEF, PP850092, ACT, PP933942; RPB1, PP842873).

Note. Based on phylogenetic analyses of ITS+LSU+TEF+ACT+RPB1 sequences, the two isolates of the new species *Gongronella inconstans* form an independent clade with full support (MLBV = 100, BIPP = 1; Fig. 1), which is closely related to *G. qichaensis* with high support (BIPP = 0.96; Fig. 1). In ITS, *G. inconstans* differs from *G. qichaensis* by 28 base pairs. This new species differs morphologically from *G. inconstans* in sporangium, columellae and apophysis. As for sporangium, the *G. inconstans* is smaller than the *G. qichaensis*, 8.8–21.4 µm vs. 7.9–36.7 µm. The *G. inconstans* and *G. qichaensis* are different in size and shape of columellae (Wang et al. 2023a). The *G. inconstans* mostly hemispherical, 1.2–2.4 × 2.0–3.9 µm, sometimes spherical, 3.2–7.2 × 3.4–7.2 µm. Additionally, the columellae of *G. qichaensis* is mostly ellipsoidal, 0.8–6.5 × 1.2–8.1 µm, sometimes sub-hemispherical to curved, 1.0–2.0 × 2.5–4.5 µm. *G. inconstans* and *G. qichaensis* are evidently different in apophysis shape. The former mostly long fusiform, sometimes oval-shaped and rarely egg shaped. The latter mostly pear-shaped to oval, partially elliptical or sub-globose. Combining morphological and molecular phylogenetic analyses, we classified the two isolates together as a new species: *G. inconstans* allied to *G. qichaensis*.

***Gongronella pamphilae* Y.P. Tan, Bishop-Hurley & R.G. Shivas**
Fungal Names: FN 900776
Fig. 6

Etymology. Named after Pamphilae of Epidaurus (ca. 1st century AD), a historian of Egyptian descent who lived in Greece.

Description. Colonies growing slowly on PDA in darkness at 25 °C, reaching 36.6–44.6 mm in diameter in seven days, white, regular at edge and cottony in the centre, reversely milky white. Rhizoids hyaline, branched, irregular. Stolons absent. Sporangiophores on aerial mycelia, erect or slightly curved, unbranched or slightly branched (1–2 times), 3.7–154.9 × 1.4–4.1 µm, hyaline, smooth, mostly aseptate, no more than two-septate. Fertile sporangia hyaline or light yellow, spherical, 13.8–30.8 µm in diameter, smooth and deliquescent-walled, leaving a collar after releasing sporangiospores. Columellae mostly hemispherical, 1.8–4.7 × 2.0–7.7 µm, sometimes arc-shaped, 0.5–1.6 × 3.3–4.6 µm, occasionally subglobose, 4.8–6.4 × 5.9–6.9 µm, hyaline, smooth. Collars distinct, 1.0–5.1 µm wide. Apophyses hyaline, smooth, variously shaped, mostly subglobose, 5.7–8.1 × 5.6–9.0 µm, sometimes ellipsoidal, 4.8–6.9 × 4.8–6.1 µm. Sporangiospores not uniform, hyaline, smooth, reniform, 3.0–5.5 × 1.8–3.4 µm, ovoid, 2.5–5.6 × 1.8–3.7 µm. Chlamydospores present, ellipsoidal. Giant cells intercalary, globose, 4.0–8.1 µm in diameter. Zygospores not found.

Additional specimen examined. China • Hainan Province, Lingshui Li Autonomous County, Shizhi Village Road (18.70178°N, 109.83679°E), from soil sample, 10 April 2023, Yi-Xin Wang (specimen HMAS 352732, living culture CGMCC 3.27027, SAUCC 4031-2).

GenBank accession numbers. CGMCC 3.27027 (ITS, PP195845; LSU, PP195946; TEF, PP850086; ACT, PP933935; RPB1, PP850081), and SAUCC 4031-2 (ITS, PP195846; LSU, PP195947; TEF, PP850085; ACT, PP933936; RPB1, PP850082).

Note. Based on phylogenetic analyses of ITS+LSU+TEF+ACT+RPB1 DNA sequences, the two isolates of the new record species *Gongronella pamphilae* form

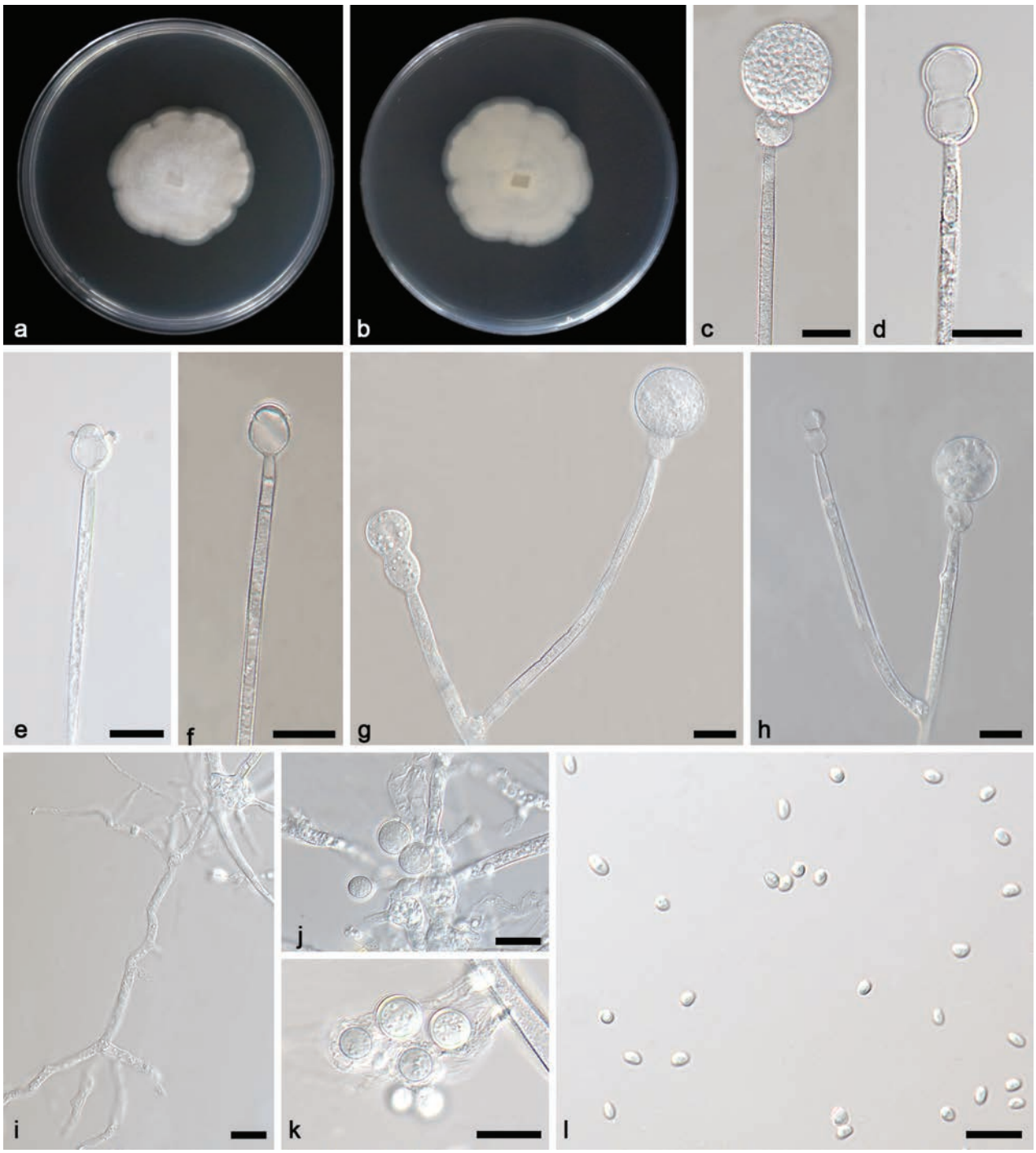

Figure 6. *Gongronella pamphilae* ex-living culture CGMCC 3.27027 **a**, **b** colonies on PDA (**a** obverse **b** reverse) **c** an unbranched sporangiophore with a fertile sporangium **d** an unbranched sporangiophore with an aborted sporangium **e, f** an unbranched sporangiophore with columellae, apophyses and collars **g, h** branched sporangiophores with columellae, collars, apophyses **i** Rhizoids **j, k** giant cells **l** sporangiospores. Scale bars: 10 µm (**c–l**).

an independent clade with full support (MLBV = 100; Fig. 1), which is closely related to *G. pamphilae* (MLBV = 100; BI = 1, Fig. 1). In ITS, the two isolates differ from *G. pamphilae* by only 2 base pairs. As no morphological descriptions were provided for the *G. pamphilae* in its protologue, we classified the two isolates together as members of *G. pamphilae* just based on molecular phylogenetic analyses. Consequently, we provide herein a supplemental description for the species.

***Gongronella pingtangensis* Yi Xin Wang, H. Zhao & X.Y. Liu, sp. nov.**
Fungal Names: FN 571904
Fig. 7

Etymology. The epithet "*pingtangensis*" (Latin) refers to the location where the type was collected, Pingtang County.

Type. China • Qiannan Buyi and Miao Autonomous Prefecture, Pingtang County, Kapu Maonan Town (25.79510°N, 107.38631°E), from soil sample, 7 August 7 2023, Yi-Xin Wang (holotype HMAS 352732, ex-holotype strain CGMCC 3.27032).

Description. Colonies growing slowly on PDA in darkness at 25 °C, reaching 38.8–45.6 mm in diameter in seven days, white, cottony, in reverse milky white. Rhizoids hyaline, branched, irregular. Stolons absent. Sporangiophores on aerial mycelia, erect or slightly curved, unbranched, or slightly branched (1–4 times), sympodially branched, 1.4–5.9 µm in width, hyaline, smooth, mostly aseptate or one-septate. Sterile (aborted) sporangia predominantly on the top of short lateral branches of sporangiophores. Fertile sporangia hyaline or light yellow, spherical, 14.2–27.1 µm in diameter, smooth and deliquescent-walled, leaving a collar after releasing sporangiospores. Columellae mostly hemispherical, 2.3–4.0 × 2.8–6.9 µm, partially arch-shaped, 0.9–1.5 × 4.1–4.9 µm, rarely spherical, 4.4–6.0 × 5.1–6.9 µm, hyaline, smooth. Collars mostly distinct, 0.6–8.7 µm wide. Apophyses hyaline, smooth, variously shaped, mostly oval, 7.1–19.8 × 6.9–15.9 µm, partially bowling pin-shaped, 15.6–17.5 × 8.5–9.4 µm, rarely egg-shaped, 4.6–9.8 × 3.6–8.7 µm. Sporangiospores not uniform, hyaline, smooth, mostly ovoid, 2.8–3.9 × 2.0–2.5 µm, sometimes reniform, 2.9–3.6 × 1.9–2.4 µm and globose, 2.1–2.7 µm in diameter, occasionally irregular, 4.8–6.2 × 2.1–2.8 µm. Chlamydospores absent. Giant cells in rhizoids, intercalary, globose, 5.2–6.8 µm in diameter. Zygospores not found.

Additional specimen examined. China • Qiannan Buyi and Miao Autonomous Prefecture, Pingtang County, Kapu Maonan Town (25.79510°N, 107.38631°E), from soil sample, 7 August 2023, Yi-Xin Wang (living culture SAUCC 5676-2).

GenBank accession numbers. CGMCC 3.27032 (ITS, PP195855; LSU, PP195956; TEF, PP850101; ACT, PP933949; RPB1, PP842880), and SAUCC 5676-4 (ITS, PP195856; LSU, PP195957; TEF, PP850102; ACT, PP933950; RPB1, PP842879).

Note. Based on phylogenetic analyses of ITS+LSU+TEF+ACT+RPB1 sequences, the two isolates of the new species *G. pingtangensis* form an independent clade with high support (MLBV = 100, BIPP = 0.84; Fig. 1), which is closely related to *G. namwonensis* with high support (BIPP = 1; Fig. 1). In ITS, *G. pingtangensis* differs from *G. namwonensis* by 14 base pairs. This new species differs morphologically from *G. namwonensis* in columellae, apophysis and giant cell (Crous et al. 2020). *G. pingtangensis* and *G. namwonensis* greatly differ from each other in shape of columellae, the former being mostly hemispherical, partially arch-shaped, rarely spherical and the latter being globose, subglobose, hemispherical, nipple-like and ellipsoidal. As for apophyses, *G. pingtangensis* and *G. namwonensis* obviously differ from each other in shape, the former being mostly oval, partially bowling pin-shaped, rarely egg-shape and the latter being subglobose and ellipsoid, sometimes with a truncated base. As for giant cells, the *G. namwonensis* varies in shape more than *G. pingtangensis*. Combining morphological and molecular phylogenetic analyses, we classified the two isolates together as a new species *G. pingtangensis* allied to *G. namwonensis*.

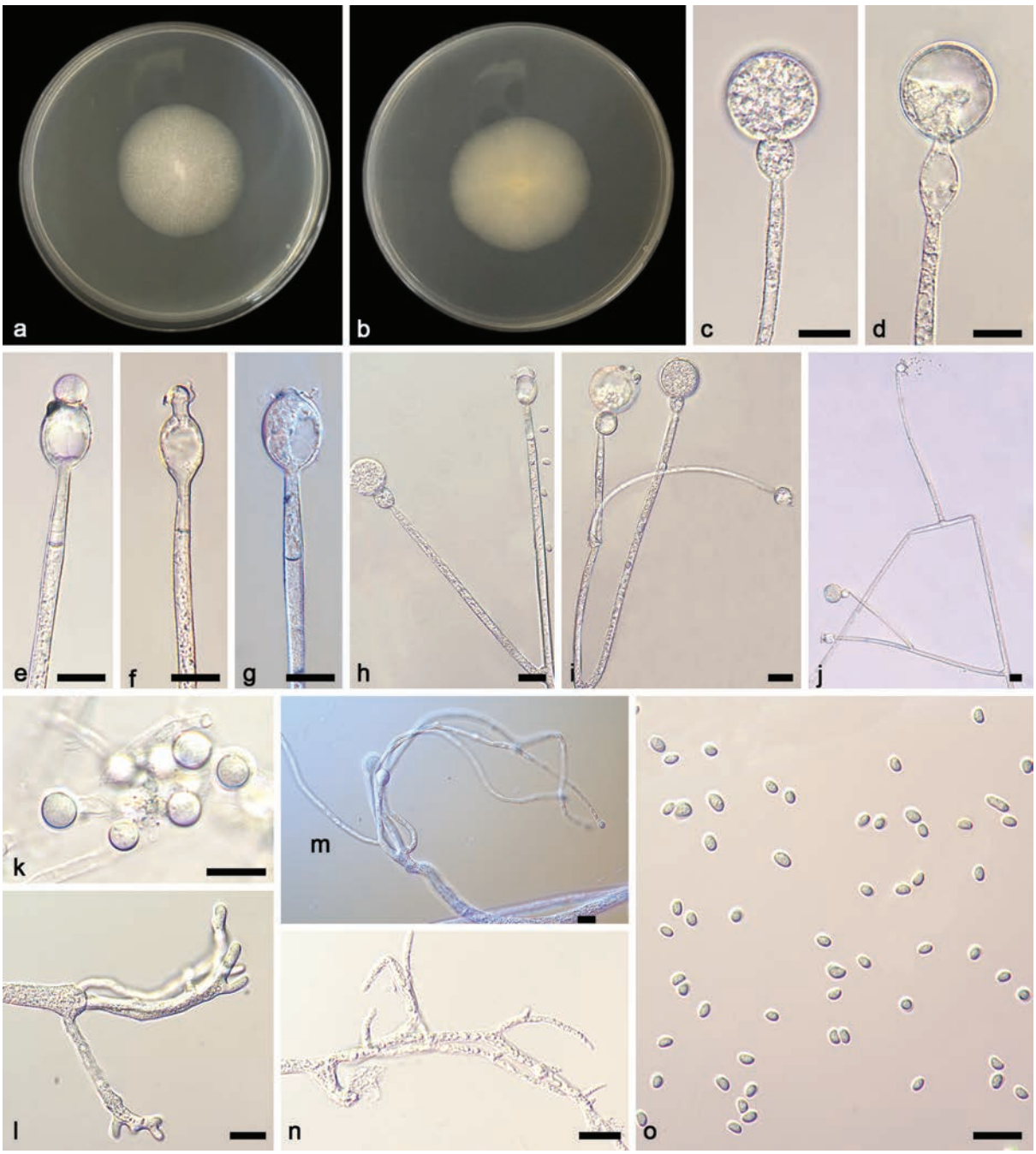

Figure 7. *Gongronella pingtangensis* ex-holotype CGMCC 3.27032 **a**, **b** colonies on PDA (**a** obverse **b** reverse) **c**, **d** an unbranched sporangiophore with a fertile sporangium **e–g** columellae, collars, apophyses and septa **h–j** branched sporangiophores with fertile sporangia, columellae, collars, apophyses and septa **k** giant cells **i–n** rhizoids **o** sporangiospores. Scale bars: 10 μm (**c–o**).

Gongronella reniformis **Yi Xin Wang, H. Zhao & X.Y. Liu, sp. nov.**
Fungal Names: FN 571630
Fig. 8

Etymology. The epithet "*reniformis* " (Latin) refers to the reniform sporangiospores.

Type. China • Hainan Province, Changjiang Li Autonomous County, Qicha Town (19.11750°N, 109.15000°E), from soil sample, 11 April 2023, Yi-Xin Wang (holotype HMAS 352727, ex-holotype strain CGMCC 3.27030).

Description. Colonies on PDA in darkness at 25 °C growing slowly, reaching 39.4–41.8 mm in diameter in seven days, white, regular at edge and cottony in the centre, on reverse milky white. Rhizoids hyaline, branched, irregular, sometimes with giant cells in the terminal. Stolons absent. Sporangiophores on aerial mycelia, erect or slightly curved, unbranched or slightly branched (1–3 times), 3.4–157.9 × 0.8–3.4 µm, hyaline, smooth, mostly aseptate, partially no more than two-septate. Sterile (aborted) sporangia predominantly on the top of short lateral branches of sporangiophores, gourd-shaped, 15.0–19.9 × 3.1–10.9 µm. Fertile sporangia hyaline or light yellow, spherical, 7.9–26.0 µm in diameter, smooth and deliquescent-walled, leaving a collar after releasing sporangiospores. Columellae mostly elliptic, 1.7–4.6 × 1.4–5.2 µm, sometimes sub-hemispherical, 1.4–2.6 × 3.3–4.9 µm, hyaline, smooth. Collars distinct, 2.1–4.3 µm. Apophyses hyaline, smooth, variously shaped, pear-shaped, 3.3–8.5 × 3.0–7.3 µm, ellipsoidal, 4.6–10.1 × 2.9–7.8 µm. Sporangiospores not uniform, hyaline, smooth, mostly reniform, 2.8–3.5 × 1.8–2.3 µm, occasionally ovoid, 3.1–3.4 × 1.7–2.0 µm. Chlamydospores, mostly ellipsoidal, 7.3–12.5 × 6.1–11.2 µm, sometimes irregular. Giant cells intercalary, globose, 3.5–10.0 µm in diameter. Zygospores not found.

Additional specimen examined. China • Hainan Province, Changjiang Li Autonomous County, Qicha Town (19.11750°N, 109.15000°E), from soil sample, 11 April 2023, Yi-Xin Wang (living culture SAUCC 4142-5).

GenBank accession numbers. CGMCC 3.27030 (ITS, PP195851; LSU, PP195952; TEF, PP850095; ACT, PP933943; RPB1, PP84875), SAUCC 4142-5 (ITS, PP195852; LSU, PP195953; TEF, PP850096; ACT, PP933944; RPB1, PP842876).

Notes. Based on phylogenetic analyses of ITS+LSU+TEF+ACT+RPB1 sequences, the two isolates of the new species *Gongronella reniformis* form an independent clade with full support (MLBV = 100, BIPP = 1; Fig. 1), which is close to *G. pamphilae* and *G. brasiliensis* with a high support (MLBV = 89, BIPP = 1; Fig. 1). Comparing ITS sequences showed that *G. reniformis* is relatively closely related to *G. pamphilae* (44 bp of dissimilarity) and *G. brasiliensis* (40 bp of dissimilarity). There were no morphological descriptions of *G. pamphilae* in its protologue, so the morphological comparison was made between *G. reniformis* and the *G. pamphilae* strains identified in this study. This new species differs morphologically from *G. pamphilae* in sporangium, columellae, apophysis, sporangiospore. The sporangium of *G. reniformis* is smaller than that of *G. pamphilae* (7.9–26.0 µm vs. 13.8–30.8 µm). *G. reniformis* and *G. pamphilae* are different from each other mainly in shape and size of columellae, the former being mostly elliptic, 1.7–4.6 × 1.4–5.2 µm, sometimes sub-hemispherical, 1.4–2.6 × 3.3–4.9 µm and the latter being mostly hemispherical, 1.8–4.7 × 2.0–7.7 µm, sometimes arc-shaped, 0.5–1.6 × 3.3–4.6 µm. The *G. reniformis* and *G. pamphilae* are different from each other in dominant shape and size of apophyses, the former being pear-shaped, 3.3–8.5 × 3.0–7.3 µm and ellipsoidal, 4.6–10.1 × 2.9–7.8 µm, the latter being spherical, 5.7–8.1 × 5.6–9.0 µm and ellipsoidal, 4.8–6.9 × 4.8–6.1 µm. The sporangiospores of *G. reniformis* are smaller than those of *G. pamphilae* (reniform, 2.8–3.5 × 1.8–2.3 µm vs. 3.0–5.5 × 1.8–3.4 µm, ovoid, 3.1–3.4 × 1.7–2.0 µm vs. 2.5–5.6 × 1.8–3.7 µm). This new species differs morphologically from *G. brasiliensis* in sporangiophore, columellae and giant cells (Tibpromma et al. 2017). In sporangiophores, the *G. renformis* differs from the *G. brasiliensis* in size, 3.4–157.9 × 0.8–3.4 µm vs. 26.5–320.0 × 2.5–5.0 µm. As for columellae,

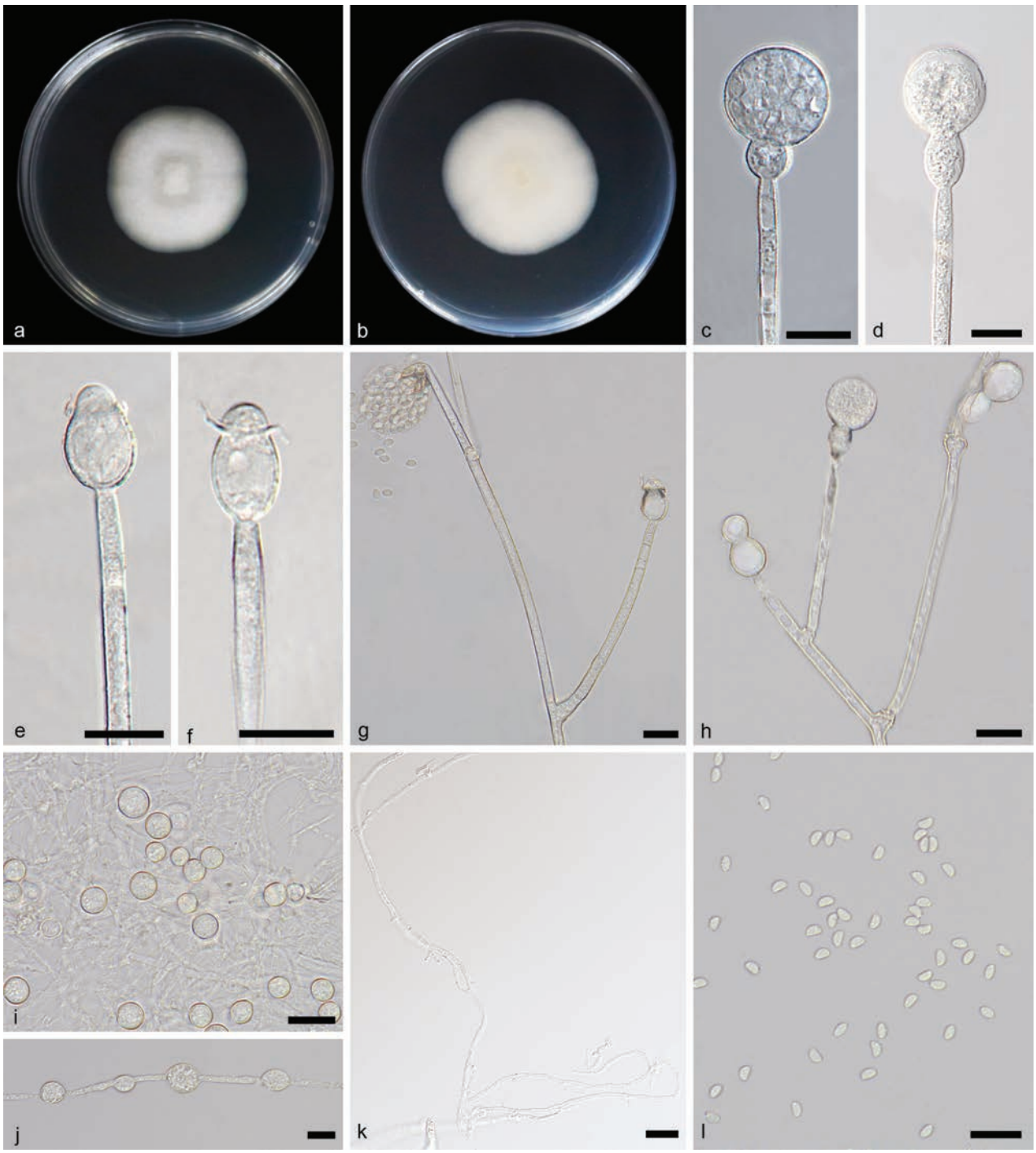

Figure 8. *Gongronella reniformis* ex-holotype CGMCC 3.27030 **a**, **b** colonies on PDA (**a** obverse **b** reverse) **c** an unbranched sporangiophore with a fertile sporangium **d** an unbranched sporangiophore with an immature sporangium **e**, **f** columellae, collars and apophyses **g** branched sporangiophores with shedding sporangia, columellae, collars, apophyses and septa **h** branched sporangiophores with fertile sporangia and sterile (aborted) sporangia **i** giant cells **j** chlamydospore **k** rhizoids **l** sporangiospores. Scale bars: 10 μm (**c–l**).

the *G. renformis* and *G. brasiliensis* are different in shape. The former mostly elliptic, sometimes sub-hemispherical. The latter globose, subglobose and conical-cylindrical. The *G. renformis* is evidently smaller than *G. brasiliensis* in giant cells, 3.5–10.0 μm vs. up to 48 μm. Combining morphological and molecular phylogenetic analyses, we classified the two isolates as a new species *G. reniformis*.

Morphological comparisons and key to the species of *Gongronella*

Together with the six new species proposed in this study, a total of 25 species of *Gongronella* have been described worldwide. Except *G. banzhaoae*, morphological comparisons were made amongst 18 species published before and six species newly proposed in this study (Table 4). We provide herein a synoptic key for these species. Characteristics adopted in the key include colonies, sporangiophores, sporangia, columellae, apophyses, sporangiospores and giant cells.

1 Giant cells known **2**
– Giant cells unknown **15**
2 Aborted sporangia known **3**
– Aborted sporangia unknown ..... ***G. hydei***
3 Fertile sporangia > 25 µm diameter **4**
– Fertile sporangia < 25 µm diameter **10**
4 Sporangiospores mainly not reniform **5**
– Sporangiospores mainly reniform **7**
5 Columellae mainly ellipsoidal ..... ***G. qichaensis***
– Columellae mainly not ellipsoidal **6**
6 Fertile sporangia 14.2–27.1 µm ..... ***G. pingtangensis***
– Fertile sporangia, 13.0–41.0 µm ..... ***G. lacrispora***
7 Sporangiospores > 4 µm wide **8**
– Sporangiospores < 4 µm wide **10**
8 Sporangiophores branched ≥ 3 times ..... ***G. namwonensis***
– Sporangiophores branched < 3 times **9**
9 Columellae mainly globose and subglobose, 4.0–8.0 µm ..... ***G. brasiliensis***
– Columellae mainly hemispherical, 1.8–4.7 × 2.0–7.7 µm ..... ***G. pamphilae***
10 Apophyses mainly reniform, 2.8–3.5 × 1.8–2.3 µm ..... ***G. reniformis***
– Apophyses mainly reniform, 3.2–5.5 × 1.7–3.1 µm ..... ***G. apophysata***
11 Sporangiophores branched > 3 times **12**
– Sporangiophores branched ≤ 3 times **14**
12 Giant cells > 6 µm diameter **13**
– Giant cells < 6 µm diameter ..... ***G. abortosporangia***
13 Columellae mainly subspherical and ovoid, 2.6–5.2 × 3.2–6.5 µm ..... ***G. oleae***
– Columellae mainly hemispherical, 4.4–5.6 × 8.5–9.0 µm ..... ***G. multiramosa***
14 Apophyses oval, subglobose and gourd-shaped ..... ***G. bawanglingensis***
– Apophyses long fusiform, oval and egg-shaped ..... ***G. inconstans***
15 Fertile sporangia > 25 µm diameter **16**
– Fertile sporangia < 25 µm diameter **17**
16 Apophyses vasiform, 5.0–15.0 × 4.5–15.0 µm ..... ***G. pedratalhadensis***
– Apophyses ellipsoidal to subglobose, 4.5–8.5 × 4.5–6.0 µm ..... ***G. sichuanensis***
17 Columellae hemispherical **18**
– Columellae not hemispherical **19**
18 Apophyses urn-shaped to subglobose, 6.0–12.0 × 6.0–10.0 µm ..... ***G. chlamydospora***
– Apophyses oval, 7.0–10 × 8.0–8.7 µm ..... ***G. butleri***
19 Sporangiospores ≥ 3.5 µm long **20**
– Sporangiospores < 3.5 µm long **21**

20 Apophyses globose to subglobose, 3.5–6.5 × 3.0–7.0 µm..... ***G. eborensis***
– Apophyses pyriform to subglobose, 8.0–12.0 × 7.0–9.5 µm... ***G. multispora***
21 Sporangiospores ≥ 4 µm width, mostly not bean-shaped **22**
– Sporangiospores < 4 µm width, mostly bean-shaped.....**23**
22 Columellae hemispherical, spherical or ovoid, 2.5–12.0 × 2.0–12.0 µm ....***G. guangdongensis***
– Columellae hemispherical and globose, 2.0–3.0 × 3.5–7.0 µm..... .....***G. zunyiensis***
23 Sporangiospores 2.0–3.5 × 2.0–2.5 µm.....***G. orasabula***
– Sporangiospores 1.7–2.1 × 2.1–3.8 µm.....***G. koreana***

Discussion

Southern China is located in tropical and subtropical areas, which belong to tropical monsoon climate and subtropical monsoon climate. All the samples used in this study were collected from these areas, including Hainan, Sichuan, Yunnan and Guizhou Provinces. This is consistent with the geographical distribution of the species of *Gongronella*, mainly inhabiting tropical and subtropical regions.

The genus *Gongronella* was established in 1952 and its type *Gongronella urceolifera* was synonymised with *Gongronella butleri* whose basionym is *Absidia butleri* (Ribaldi 1952). Numbers of this genus have increased rapidly recently, with as many as 17 species being described between 2015 and 2024 and the genus currently has a total of 25 members including the six new species proposed herein, all of which are listed in Table 3. However, there are no systematic analyses of the morphological characteristics of the species of *Gongronella*. In this study, the morphological characteristics of the 24 species of *Gongronella* were comparatively analysed (Table 4), except *G. banzhaoae*. Since *G. banzhaoae* only has molecular data and no morphological description, it is not compared in this study.

Since 2019, phylogenetic analyses of *Gongronella* have mainly been conducted on the basis of morphological characteristics and ITS+LSU sequence (Zhang et al. 2019). In this study, new TEF, ACT and RPB1 protein-coding sequences were added for the construction of phylogenetic trees and the results were basically consistent with previous studies based on ITS+LSU. Twelve strains were grouped into six individual clades and two strains were grouped along with *G. pamphilae*. Compared with *G. multiramosa*, *G. abortosporangia* has more abundant and various aborted sporangia, smaller fertile sporangia and smaller columellae (Wang et al. 2023a). Compared with *G. pamphilae*, *G. reniformis* has smaller sporangia and sporangiospores, as well as different shapes of columellae and apophyses. Compared with *G. brasiliensis*, *G. reniformis* has smaller sporangiophores, different columella shapes and smaller giant cells (Tibpromma et al. 2017). Compared with *G. zunyiensis*, *G. apophysata* has larger sporangia, as well as different shapes of columellae, apophyses and chlamydospores (Dong et al. 2019). Compared with *G. inconstans*, *G. bawanglingensis* has smaller sporangiospores, larger columellae, different shapes and sizes of apophyses. Compared with *G. qichaensis*, the *G. bawanglingensis* has smaller sporangia, different columellae and apophysis shapes (Wang et al. 2023a). *G. pingtangensis* and *G. namwonensis* are different in size and shape of columellae (hemispherical vs. globose) and apophyses (oval vs. subglobose). *G. namwonensis* has more shapes of giant cells (Crous et al. 2020).

Table 4. Morphological comparisons of *Gongronella* species.

Species	Colonies	Sporangiophores	Sporangia	Columellae	Apophyses	Sporangiospores	Giant cell	Reference
G. abortosporangia	PDA: dark 25 °C 7 d 24.6–26.2 mm diam., white, regular at edge and cottony in the centre, in reverse milky white	unbranched or branched 1–6 times, 4.0–96.8 × 1.0–4.2 µm, mostly aseptate, partially 1-septate, rarely 2-septate, occasionally containing a line of oil droplets	Aborted: mostly gourd-shape, 11.6–16.7 × 5.5–17.7 µm, partially elliptical with slight shrinkage, 12.5–18.0 × 6.7–10.6, occasionally clavate, 20.1–22.7 × 9.5–10.4 µm; Fertile: 7.0–23.2 µm diam	mostly hemispherical, 2.5–4.2 × 3.6–7.4 µm, sometimes sub-hemispherical, 1.3–3.9 × 3.6–5.5 µm	mostly cup-shaped, 1.9–8.6 × 2.1–6.7 µm, partially hemispherical, 2.7–5.5 × 2.8–7.4 µm, occasionally pear-shaped, 8.2 × 7.2 µm	ovoid, 2.6–3.5 × 1.7–2.1 µm, reniform, 2.9–3.5 × 1.7–2.3 µm	intercalary, globular, subglobular, 2.6–4.6 µm diam.	This study
G. apophysata	PDA: dark 25 °C 7 d 17.9–21.2 mm in diam., white, irregular at edge and cottony in centre, in reverse milky white	unbranched or branched 1–2 times, 11.2–190.9 × 1.6–3.9 µm, mostly aseptate or 1-septate, occasionally 2-septate	Aborted: gourd-shape, 14.0 × 8.3 µm; Fertile: spherical, 12.5–40.5 µm diam.	elliptic, 2.6–4.0 × 2.1–5.5 µm, sub-hemispherical, 1.4–2.7 × 2.2–4.3 µm	mostly ellipsoidal to olivary, 2.3–17.3 × 2.4–10.0 µm, partially subglobose, 4.6–10.2 × 4.3–10.0 µm, occasionally gourd-shaped, 11.4 × 4.9 µm	mostly reniform, 3.2–5.5 × 1.7–3.1 µm, ovoid, 2.5–3.7 × 1.7–2.6 µm, occasionally sub-orbicular, 1.7–2.5 µm	intercalary, globular, 4.4–10.5 µm diam.	This study
G. bawanglingensis	PDA: dark 25 °C 7 d 22.8–24.4 mm diam., white, cottony in centre, in reverse milky white	unbranched or sympodially branched 1–3 times, 1.3–4.5 µm wide, mostly aseptate or 1-septate, occasionally up to 4-septate	Aborted: mostly gourd-shaped; Fertile: spherical, 4.2–18.5 µm diam.	mostly hemispherical, 1.6–5.1 × 2.1–7.2 µm, some arch-shaped, 1.4–3.7 × 2.6–8.8 µm, spherical, 2.3–6.1 × 2.5–8.1 µm	oval-shaped, 3.9–20.6 × 3.3–12.9 µm, subglobose-shaped, 4.8–12.2 × 4.7–12.3 µm, occasionally gourd-shaped	mostly ovoid, 2.5–3.6 × 1.7–2.6 µm, reniform, 2.6–3.3 × 1.9–2.2 µm	intercalary, globular, 3.2–6.9 µm diam.	This study
G. brasiliensis	MEA: 25 °C 7 d 1.0–2.0 mm high 60.0 mm diam., white, cottony, irregular at edge, reverse cream to buff	26.5–320.0 × 2.5–5.0 µm, solitary, arising from stolons or in whorls of two, often with a single branch, 1- or 2-septate below apophyses	Aborted: globose, 5.0–17.0 µm diam.; Fertile: globose, subglobose, 9.5–30.0 µm diam.	globose, subglobose, (3.0–)4.0–8.0(–9.0) µm, conical-cylindrical, 1.5–2.5 × 2.0–3.0 µm, some very small, up to 1 µm diam.	globose, (3.0–)4.0–5.0(–6.0) µm diam., vase-shaped, (3.0–)4.0 × 12.0(–14.5) µm, ellipsoidal, 5.0–10.0(–12.0) × 3.0–7.0(–8.5) µm	reniform, 1.5–4.0 × 1.5–2.5 µm, ellipsoid to fusiform, 2.0–6.5 × 1.5–3.0 µm, ellipsoid with a flattened end, 2.5–7.5 × 1.5–4.0 µm	globose, subglobose, ovoid, some hypha-like, irregularly swollen, up to 48.0 µm diam.	Tibpromma et al. (2017)
G. butleri	White turf	simply or irregularly branched, 2.1–3.1 µm wide, always 1-septate	Fertile: globose, 16.5–22.7 µm		swollen, oval-shaped, 7.0–10 × 8.0–8.7 µm	oval to flattened on one side to reniform, 2.5–7.2 × 1.7–4.7 µm		Ribaldi (1952), Babu et al. (2015)
G. chlamydospora	PDA: 27 °C 11 d 90.0 mm diam., floccose, at first white, then drab grey	unbranched or simply branched, hyaline, slightly constricted at top	Fertile: globose, 8.5–17.0 µm diam.	ovoid to depressed subglobose, 3.0–5.5 × 3.5–6.5 µm	urn-shaped to subglobose, 6.0–12.0 × 6.0–10.0 µm	ellipsoid, reniform or irregular, 2.0–3.0 × 1.0–2.0 µm		Zhao et al. (2023)
G. eborensis	PDA: 25 °C 5 d 28.0–32.0 mm diam.	46.0–94.0 × 1.5–3.0 µm, irregularly or simply branched, always 1-septate under apophyses	Fertile: globose to subglobose, 7.5–16.0 × 7.0–13.0 µm	hemispherical to subglobose, 11.5–5.5 × 8.2–3.2 µm	globose to subglobose, 3.5–6.5 × 3.0–7.0 µm	reniform to fusiform-elliptical, 2.6–3.8 × 1.2–1.6 µm		Martins et al. (2020)
G. guangdongensis	PDA: 25 °C 13 d 1–2 mm high, 50.0 mm diam., white or pale, irregular at edge; in reverse buff to honey	irregularly or simply branched, 28.0–100.0 × 2.0–2.5 µm, always 1-septate	Aborted: sometimes present; Fertile: always globose, 14.0–21.5 µm diam.	hemispherical, spherical or ovoid, 2.5–12.0 × 2.0–12.0 µm	hemispherical, 5.5–9.0 µm in diam.	globose, 2.0–3.0 µm in diam.		Adamcik et al. (2015)

Species	Colonies	Sporangiophores	Sporangia	Columellae	Apophyses	Sporangiospores	Giant cell	Reference
G. hydei	PDA: 25 °C 7 d 60.0–65.0 mm diam., circular, entire at edge, flat or effuse, dense, white;	up to 120.0 µm long, 1.6–3.2 µm wide, mostly unbranched, occasionally branched, mostly 1-septate	Fertile: globose to subglobose, 10.5–18.8 × 10.0–17.5 µm	hemispherical, sometimes tiny, 1.7–4.7 × 2.2–6.3 µm	cuboid-shaped with truncate at the base, 2.5–3.9 × 3.5–5.1 µm; cup-shaped rounded at the base, 2.7–6.2 × 3.8–7.8 µm; cup-shaped truncate at the base, 3.7–7.3 × 3.8–7.3 µm	reniform, 2.4–3.8 × 1.5–2.3 µm, ellipsoidal to fusiform, 2.6–3.4 × 1.8–3.4 µm	globose, guttulate, up to 25.0 µm diam.	Doilom et al. (2020)
G. inconstans	PDA: dark 25 °C 7 d 15.6–18.4 mm diam., white, regular at edge, cottony, in reverse milky white	unbranched or branched 2–3 times, 1.7–3.9 µm wide, mostly aseptate	Aborted: existence; Fertile: spherical, 8.8–21.4 µm diam.	mostly hemispherical, 1.2–2.4 × 2.0–3.9 µm, sometimes spherical, 3.2–7.2 × 3.4–7.2 µm	variously shaped, mostly long fusiform, 7.6–17.4 × 4.7–5.4 µm, sometimes oval-shaped, 5.5–8.8 × 4.4–6.3 µm, rarely egg-shaped, 5.0–6.4 × 4.2–5.7 µm	ovoid, 2.7–4.9 × 1.8–3.5 µm, reniform, 3.1–4.1 × 2.0–4.5 µm, some subcircular, 2.4–4.1 µm, occasionally irregular, 5.0–8.0 × 2.5–3.2 µm	intercalary, globular, 4.2–8.0 µm diam.	This study
G. koreana	PDA: 25 °C 7 d 31.5–33.0 mm diam., light white at first, cotton white with age, reverse from light-coloured to white	2.5–2.8 µm wide, mostly branched, 1-septate	Fertile: globose, 12.3–15.5 × 12.4–15.6 µm diam.	hemispherical, 1.2–2.3 × 2.6–3.3 µm	typically pyriform, 5.4–6.5 × 5.9–7.1 µm	mostly bean-shaped, 1.7–2.1 × 2.1–2.8 µm		Ariyawansa et al. (2015)
G. lacrispora	25 °C 13 d 50.0 mm in diam., 1–3 mm high, thickly floccose to felty, irregular at edge, at first white, then grey or pale grey, later pale wine colour	up to 6.5 µm wide, rarely septate	Aborted: sometimes present; Fertile: typically perfectly globose, 13.0–41.0 µm diam	dorsiventrally flattened to spherical, 2.5–13.0 × 4.5–20.0 µm	hemispherical, 4.0–8.6 µm. in diam.	lacrymoid to narrowly napiform, 2.8-4.5 × 5.5-9.0 µm	intercalary, globose to irregular, often with vacuoles or oil droplets, 20.0-37.0 × 60.0 µm	Hesseltine and Ellis (1961)
G. multiramosa	PDA: dark 25 °C 7 d 21.6–25.6 mm diam., white, regular at edge, cottony in centre, reverse milky white	unbranched or sympodially branched up to 7 times, 4.7–128.4 × 2.6–3.9 µm, usually 1-septate, occasionally containing a line of oil droplets	Aborted: ovoid, 9.6 × 6.2 µm diam.; Fertile: spherical, 15.5–23.2 µm diam.;	mostly hemispherical, 3.6–5.7 × 8.0–9.8 µm, sometimes sub-hemispherical, 3.0; –3.9 × 7.6–10.0 µm	mostly hemispherical, 4.4–5.6 × 8.5–9.0 µm, partially cup-shaped,4.6–7.0 × 8.5–10.0 µm	subspherical, 1.7–2.6 µm, ovoid, 2.6–3.3 × 1.7–2.3 µm, few reniform, 2.7–3.4 × 1.3–1.9 µm	globular, sub-spherical, 3.0–6.7 µm diam.	Wang et al. (2023a)
G. multispora	PDA: 27 °C 10 d 80.0 mm diam., 10.0 mm high, from white to yellowish, in reverse crusty, yellow	unbranched or sympodially branched, 2–3 in whorls and swollen on the base, 1 to several septate	Fertile: globose, 12.0–17.0 µm diam.	hemispherical, 2.0–4.5 × 2.0–4.0 µm	pyriform to subglobose, 8.0–12.0 × 7.0–9.5 µm	ellipsoid, fusiform, cylindrical, reniform subglobose to globose or irregular, 2.5–3.5 × 1.5–2.5 µm		Zhao et al. (2023)
G. namwonensis	MEA:25 °C 7 d 55.0 mm diam. (28 °C 5 d 90.0 mm diam), white, in reverse cream	simply or sympodially or monopodially branched, up to 1 mm long and 5.0 µm wide, in whorls of 2 or 3 times, mostly 1-septate	Aborted: sometimes formed; Fertile: globose, up to 30.0 µm diam.	globose, subglobose, 3.5–7.0 µm diam., hemispherical,; 1.8–5.5 × 2.5–8.5 µm, nipple-like, ellipsoidal, 2.0–3.8 × 2.0–5.0 µm	globose (2.5–)5.0–9.5(–12.0); µm, subglobose and ellipsoid, some with a truncated base,; 7.5–14.5 × 5.5–12.0 µm	reniform, ellipsoidal, some ovoid, 2.5–3.5 × 1.7–2.5 µm, rarely irregular, up to 6 × 2.5 µm	globose, subglobose and branched	Crous et al. (2020)
G. oleae	PDA: dark 25 °C 7 d, 16.3–17.0 mm diam., white, regular at edge, cottony in centre, inreverse milky white	unbranched or branched 3–4 times, 7.0–96.8 × 0.9–3.5 µm, mostly aseptate, sometimes 1-septate	Aborted: 7.0–7.8 µm diam.; Fertile: spherical, 8.8–24.5 µm diam.;	mostly sub-spherical or ovoid, 2.6–5.2 × 3.2–6.5 µm, sometimes hemi-spherical, 0.4–3.3 × 2.8–5.3 µm	pear-shaped, 4.4–5.6 × 8.5–9.0 µm, cup-shaped, 4.6–7.0 × 8.5–10.0 µm, elliptical or subspherical, 2.7–8.0 × 2.8–9.1 µm	ovoid, 2.40–3.34 × 1.51–2.35 µm, reniform, 2.58–4.99 × 1.48–2.24 µm	terminal, globular, sub-spherical, 3.2–6.5 µm diam.	Wang et al. (2023a)

Species	Colonies	Sporangiophores	Sporangia	Columellae	Apophyses	Sporangiospores	Giant cell	Reference
G. orasabula	SMA: 25 °C 5 d, 33.0–35.0 mm, initial white, later off-white, irregular at edge, in reverse white	35.0–200.0 × 2.5–4.0 µm, simply branched 1–3 times	Fertile: globose to subglobose or calabash vase-shaped, 12.0–20.0 × 12.5–22.0 µm	hemispherical, 2.0–3.0 × 3.0–4.0 µm	globose, subglobose to pyriform, 5.0–10.0 × 4.5–8.5 µm	mostly bean-shaped, 2.0–3.5 × 2.0–2.5 µm		Li et al. (2016)
G. pamphilae	PDA: dark 25 °C 7 d 18.3–22.3 mm in diam., white, regular at edge and cottony in centre, in reverse milky white	unbranched or branched 1–2 times, 3.7–154.9 × 1.4–4.1 µm, mostly aseptate, occasionally 1- or 2-septate	Aborted: existence; Fertile: spherical, 13.8–30.8 µm diam.	mostly hemispherical, 1.8–4.7 × 2.0–7.7 µm, sometimes arc-shaped, 0.5–1.6 × 3.3–4.6 µm, spherical, 4.8–6.4 × 5.9–6.9 µm	spherical, 5.7–8.1 × 5.6–9.0 µm, ellipsoidal, 4.8–6.9 × 4.8–6.1 µm	reniform, 3.0–5.5 × 1.8–3.4 µm, ovoid, 2.5–5.6 × 1.8–3.7 µm	intercalary, globular, 4.0–8.1 µm diam	This study
G. pedratalhadensis	PDA: 25 °C 7 d 5.5 mm high, 45.0 mm diam., white, irregular at edge, in reverse pale	sympodially branched 1–2 times, 9.5–30.0 × 2.5–7.0 µm, mostly 1-septate below sporangia, rarely two or more septate	Aborted: existence; Fertile: globose 17.0–35.0(40.0) µm diam.	mostly hemispherical, some short hemispherical or subglobose, 5.0–15.0 × 4.0–21.5 µm	vasiform, short or long, 5.0–15.0 × 4.5–15.0 µm	bean-shaped, 2.5–3.5 × 1.5–2.5 µm, rarely irregular, 2.5–3.5 × 2.0–3.0 µm		de Freitas et al. (2020)
G. pingtangensis	PDA: dark 25 °C 7 d 19.4–22.8 mm diam., white, cottony, in reverse milky white	unbranched or sympodially branched 1–4 times, 1.4–5.9 µm wide, aseptate or 1-septate	Aborted: existence; Fertile: spherical, 14.2–27.1 µm diam.;	mostly hemispherical, 2.3–4.0 × 2.8–6.9 µm, some arch-shaped, 0.9–1.5 × 4.1–4.9 µm, spherical, 4.4–6.0 × 5.1–6.9 µm	mostly oval-shaped, 7.1–19.8 × 6.9–15.9 µm, some bowling pin-shaped, 15.6–17.5 × 8.5–9.4 µm, egg-shaped, 4.6–9.8 × 3.6–8.7 µm	mostly ovoid, 2.8–3.9 × 2.0–2.5 µm, some reniform, 2.9–3.6 × 1.9–2.4 µm, spherical, 2.1–2.7 µm, occasionally large irregularly shaped, 4.8–6.2 × 2.1–2.8 µm	intercalary, globular, 5.2–6.8 µm diam.	This study
G. qichaensis	PDA: dark, 25 °C 7 d 20.3–22.7 mm diam., white, cottony, regular at edge, in reverse milky white	unbranched or branched 1–2 times, 17.3–141.2 × 0.7–4.3 µm, usually aseptate, occasionally 2-septate	Aborted: ovoid,12.2–13.7 µm in diam.; Fertile: spherical, 7.9–36.7 µm diam.	ellipsoidal, 0.8–6.5 × 1.2–8.1 µm, sometimes sub-hemispherical to curved, 1.0–2.0 × 2.5–4.5 µm	mostly pear-shaped to oval, 4.6–13.4 × 3.4–10.7 µm, partially elliptical or sub-spherical, 6.0–11.3 × 4.8–9.0 µm	mostly ellipsoidal, 3.0–4.2 × 2.1–2.8 µm, sometimes reniform, 2.8–3.7 × 2.3–2.8 µm, few spherical, 2.4–3.3 µm	intercalary or terminal, globular, sub-spherical, 3.5–6.7 µm diam.	Wang et al. (2023a)
G. reniformis	PDA: dark 25 °C 7 d 19.7–20.9 mm diam., white, regular at edge and cottony in centre in reverse milky white	unbranched or branched 1–3 times, 3.4–157.9 × 0.8–3.4 µm, mostly aseptate, occasionally 1- or 2-septate	Aborted: gourd-shape, 15.0–19.9 × 3.1–10.9 µm; Fertile: spherical, 7.9–26.0 µm diam.	mostly elliptic, 1.7–4.6 × 1.4–5.2 µm, sometimes sub-hemispherical, 1.4–2.6 × 3.3–4.9 µm	pear-shaped, 3.3–8.5 × 3.0–7.3 µm, ellipsoidal, 4.6–10.1 × 2.9–7.8 µm	mostly reniform, 2.8–3.5 × 1.8–2.3 µm, ovoid, 3.1–3.37 × 1.7–2.0 µm	intercalary, globular, 3.5–10.0 µm diam.	This study
G. sichuanensis	PDA: 25 °C 14 d 4.0–5.0 mm high, 67.0–68.0 mm diam., white, regular at edge, in reverse grey	solitary or simply branched, 28.0–46.5 × 1.0–3.0 µm, 1- or 2-septate	Fertile: globose, subglobose, 10.5–26.5 µm diam.	hemispherical, 1.5–3.5 × 1.0–3.0 µm	ellipsoidal to subglobose, 4.5–8.5 × 4.5–6.0 µm in diam.	reniform, ovoid or ellipsoidal, 1.5–2.0 × 1.0–1.5 µm		Zhang et al. (2019)
G. zunyiensis	PDA: 25 °C 14 d 3.0–6.0 mm high, 70.0–75.0 mm diam., white, villiform, irregular at edge, in reverse grey-white	1.5–4.0 µm wide, branched several times, usually aseptate	Fertile: subglobose to globose, 11.0–19.5 µm diam.	hemispherical and globose, 2.0–3.0 × 3.5–7.0 µm	subglobose, 3.5–9.5 µm, conical-cylindrical, 4.0–7.0 × 5.0–9.0 µm	subglobose, reniform, 1.5–2.0 × 2.0–3.5 µm		Dong et al. (2019)

These significant morphological differences, coupled with those phylogenetically independent clades, ensure their novelty (Wang et al. 2023a). As for *G. pamphilae*, two strains were grouped into an independent separate clade and there are only two base pairs of difference in ITS rDNA sequences. As no morphological descriptions were provided for *G. pamphilae* in its protologue, we classified the two isolates together as the new record species of *G. pamphilae* only based on molecular phylogenetic analyses.

In summary, the molecular phylogenetic and morphological results support the identification of the six new species for the 12 strains cultured in this study, namely *G. abortosporangia*, *G. reniformis*, *G. apophysata*, *G. bawanglingensis*, *G. pingtangensis*, *G. inconstans* and two strains as new record species of *G. pamphilae*, complementing the morphological description of *G. pamphilae*. TFE, ACT and RPB1 protein-coding sequences were newly added to construct the phylogenetic evolutionary tree and the results were basically consistent with ITS+LSU results. The morphology of members of the genus *Gongronella* was systematically described herein, with a morphological description table being established for the described strains of *Gongronella* and the new strains described in this study (Table 4).

Acknowledgements

We thank Zhao-Xue Zhang (Shandong Agricultural University), Xin-Yi Wang (Shandong Normal University) and Shu-Bin Liu (Beijing Forestry University) for soil collection.

Additional information

Conflict of interest

The authors have declared that no competing interests exist.

Ethical statement

No ethical statement was reported.

Funding

This study was supported by the National Natural Science Foundation of China (Nos. 32170012, 32300011, 32470004), Ji'nan City's 'New University 20 Policies' Initiative for Innovative Research Teams Project (202228028), Innovative Agricultural Application Technology Project of Jinan City (CX202210) and Key Technological Innovation Program of Shandong Province, China (2022CXGC020710)

Author contributions

Y.X. Wang took charge of the microscopy, DNA sequencing, data analyses and drafted the paper; H. Zhao made specimens, proposed new species and revised the paper; Y. Jiang, Xin-Y. Liu and M.F. Tao collected samples and isolated cultures; Xiao-Y. Liu proposed new species, revised the paper and provided funding.

Author ORCIDs

Yi-Xin Wang https://orcid.org/0009-0001-5231-914X
Heng Zhao https://orcid.org/0000-0003-2938-5613

Yang Jiang https://orcid.org/0009-0003-1292-610X
Xin-Ye Liu https://orcid.org/0009-0004-9396-1763
Xiao-Yong Liu https://orcid.org/0000-0002-8808-010X

Data availability

The sequences were deposited in the GenBank database.

References

Adamcik S, Cai L, Chakraborty D, Chens X, Cotter HV, Dai D, Daii Y, Das K, Deng C, Ghobad-Nejhad M, Hyde K, Langer E, Deepna LKP, Liu F, Liu S, Liu T, Lv W, Lv S, Machado A, Buyck B (2015) Fungal biodiversity profiles 1–10. Cryptogamie. Mycologie 36(2): 121–166. https://doi.org/10.7872/crym/v36.iss2.2015.121

Ariyawansa H, Hyde K, Jayasiri S, Buyck B, Kandawatte T, Dai D, Dai Y, Daranagama D, Jayawardena R, Lücking R, Ghobad-Nejhad M, Niskanen T, Thambugala K, Voigt K, Zhao R, Li G, Doilom M, Boonmee S, Yang Z, Chen X (2015) Fungal diversity notes 111–252: Taxonomic and phylogenetic contributions to fungal taxa. Fungal Diversity 75(1): 27–274. https://doi.org/10.1007/s13225-015-0346-5

Babu AG, Kim SW, Adhikari M, Yadav DR, Um YH, Kim C, Lee HB, Lee YS (2015) A new record of *Gongronella butleri* isolated in Korea. Mycobiology 43(2): 166–169. https://doi.org/10.5941/MYCO.2015.43.2.166

Carbone I, Kohn LM (1999) A method for designing primer sets for speciation studies in filamentous ascomycetes. Mycologia 91(3): 553–556. https://doi.org/10.1080/00275514.1999.12061051

Corry J E L, Curtis G D W, Baird R M, 1995. Rose bengal chloramphenicol (RBC) agar, in Progress in Industrial Microbiology. Elsevier, 431–433. https://doi.org/10.1016/S0079-6352(05)80079-7

Crous P, Wingfield M, Chooi Y, Gilchrist C, Lacey E, Pitt J, Roets F, Swart W, Cano J, Valenzuela-Lopez N, Hubka V, Shivas R, Stchigel AM, Holdom D, Jurjević Ž, Kachalkin A, Lebel T, Lock C, Martín M, Groenewald JZ (2020) Fungal Planet description sheets: 1042-1111. Persoonia 44(1): 301–459. https://doi.org/10.3767/persoonia.2020.44.11

de Freitas LMS, de Oliveira RJV, Leite TRC, Nguyen TTT, Lim HJ, Lee HB, de Santiago ALCMA (2020) *Gongronella pedratalhadensis*, a new species of *Mucorales* (Mucoromycota) isolated from the Brazilian Atlantic Forest, with an identification key for the genus. Sydowia 73: 61–68.

Doilom M, Guo J, Phookamsak R, Mortimer PE, Karunarathna SC, Dong W, Liao C, Yan K, Pem D, Suwannarach N, Promputtha I, Lumyong S, Xu J (2020) Screening of phosphate-solubilizing fungi from air and soil in Yunnan, China: Four novel species in *Aspergillus*, *Gongronella*, *Penicillium*, and *Talaromyces*. Frontiers in Microbiology 11: 585215. https://doi.org/10.3389/fmicb.2020.585215

Dong Y, Sun Q, Zhang Y, Wang X, Liu P, Xiao Y, Fang Z (2018) Complete genome of *Gongronella* sp. w5 provides insight into its relationship with plant. Journal of Biotechnology 286: 1–4. https://doi.org/10.1016/j.jbiotec.2018.08.022

Dong CB, Zhang ZY, Chen WH, Han YF, Huang JZ, Liang ZQ (2019) *Gongronella zunyiensis* sp. nov. (Cunninghamellaceae, *Mucorales*) isolated from rhizosphere soil in China. Phytotaxa 425: 290–296. https://doi.org/10.11646/phytotaxa.425.5.4

Doyle JJ, Doyle JL, Brown AHD (1990) Chloroplast DNA phylogenetic affinities of newly described species in *Glycine* (*Leguminosae:* Phaseoleae). Systematic Botany 15(3): 466–471. https://doi.org/10.2307/2419362

Guo LD, Hyde KD, Liew ECY (2000) Identification of endophytic fungi from *Livistona chinensis* based on morphology and rDNA sequences. The New Phytologist 147(3): 617–630. https://doi.org/10.1046/j.1469-8137.2000.00716.x

Hesseltine CW, Ellis JJ (1961) Notes on *Mucorales*, especially *Absidia.* Mycologia 53(4): 406–426. https://doi.org/10.1080/00275514.1961.12017970

Hu J, Zhang Y, Xu Y, Sun Q, Liu J, Fang W, Xiao Y, Kües U, Fang Z (2019) *Gongronella* sp. w5 elevates *Coprinopsis cinerea* laccase production by carbon source syntrophism and secondary metabolite induction. Applied Microbiology and Biotechnology 103(1): 411–425. https://doi.org/10.1007/s00253-018-9469-4

Huelsenbeck JP, Ronquist F (2001) MRBAYES: Bayesian inference of phylogenetic trees. Bioinformatics (Oxford, England) 17(8): 754–755. https://doi.org/10.1093/bioinformatics/17.8.754

Katoh K, Rozewicki J, Yamada KD (2019) MAFFT online service: Multiple sequence alignment, interactive sequence choice and visualization. Briefings in Bioinformatics 20(4): 1160–1166. https://doi.org/10.1093/bib/bbx108

Kumar S, Stecher G, Tamura K (2016) MEGA7: Molecular evolutionary genetics analysis version 7.0 for bigger datasets. Molecular Biology and Evolution 33(7): 1870–1874. https://doi.org/10.1093/molbev/msw054

Li GJ, Hyde KD, Zhao RL, Hongsanan S, Abdel-Aziz FA, Abdel-Wahab MA, Alvarado P, Alves-Silva G, Ammirati JF, Ariyawansa HA, Baghela A, Bahkali AH, Beug M, Bhat DJ, Bojantchev D, Boonpratuang T, Bulgakov TS, Camporesi E, Boro MC, Ceska O, Chakraborty D, Chen JJ, Chethana KWT, Chomnunti P, Consiglio G, Cui BK, Dai DQ, Dai YC, Daranagama DA, Das K, Dayarathne MC, De Crop E, De Oliveira RJV, de Souza CAF, de Souza JI, Dentinger BTM, Dissanayake AJ, Doilom M, Drechsler-Santos ER, Ghobad-Nejhad M, Gilmore SP, Góes-Neto A, Gorczak M, Haitjema CH, Hapuarachchi KK, Hashimoto A, He MQ, Henske JK, Hirayama K, Iribarren MJ, Jayasiri SC, Jayawardena RS, Jeon SJ, Jerônimo GH, Jesus AL, Jones EBG, Kang JC, Karunarathna SC, Kirk PM, Konta S, Kuhnert E, Langer E, Lee HS, Lee HB, Li WJ, Li XH, Liimatainen K, Lima DX, Lin CG, Liu JK, Liu XZ, Liu ZY, Luangsa-ard JJ, Lücking R, Lumbsch HT, Lumyong S, Leaño EM, Marano AV, Matsumura M, McKenzie EHC, Mongkolsamrit S, Mortimer PE, Nguyen TTT, Niskanen T, Norphanphoun C, O'Malley MA, Parnmen S, Pawłowska J, Perera RH, Phookamsak R, Phukhamsakda C, Pires-Zottarelli CLA, Raspé O, Reck MA, Rocha SCO, de Santiago ALCMA, Senanayake IC, Setti L, Shang QJ, Singh SK, Sir EB, Solomon KV, Song J, Srikitikulchai P, Stadler M, Suetrong S, Takahashi H, Takahashi T, Tanaka K, Tang LP, Thambugala KM, Thanakitpipattana D, Theodorou MK, Thongbai B, Thummarukcharoen T, Tian Q, Tibpromma S, Verbeken A, Vizzini A, Vlasák J, Voigt K, Wanasinghe DN, Wang Y, Weerakoon G, Wen HA, Wen TC, Wijayawardene NN, Wongkanoun S, Wrzosek M, Xiao YP, Xu JC, Yan JY, Yang J, Da Yang S, Hu Y, Zhang JF, Zhao J, Zhou LW, Peršoh D, Phillips AJL, Maharachchikumbura SSN (2016) Fungal diversity notes 253–366: Taxonomic and phylogenetic contributions to fungal taxa. Fungal Diversity 78(1): 1–237. https://doi.org/10.1007/s13225-016-0366-9

Liu J, Peng C, Han Q, Wang M, Zhou G, Ye B, Xiao Y, Fang Z, Kües U (2022) *Coprinopsis cinerea* uses laccase Lcc9 as a defense strategy to eliminate oxidative stress during fungal-fungal interactions. Applied and Environmental Microbiology 88(1): e01760–e21. https://doi.org/10.1128/AEM.01760-21

Mai Z, Wang L, Zeng Q (2021) Characterization of a novel isoflavone glycoside-hydrolyzing β-glucosidase from mangrove soil metagenomic library. Biochemical and Biophysical Research Communications 569: 61–65. https://doi.org/10.1016/j.bbrc.2021.06.086

Martins MR, Santos C, Soares C, Santos C, Lima N (2020) *Gongronella eborensis* sp. nov., from vineyard soil of Alentejo (Portugal). International Journal of Systematic and Evolutionary Microbiology 70(5): 3475–3482. https://doi.org/10.1099/ijsem.0.004201

Nylander J (2004) MrModeltest V2. program distributed by the author. Bioinformatics (Oxford, England) 24: 581–583. https://doi.org/10.1093/bioinformatics/btm388

O'Donnell K, Kistler HC, Cigelnik E, Ploetz RC (1998) Multiple evolutionary origins of the fungus causing Panama disease of banana: Concordant evidence from nuclear and mitochondrial gene genealogies. Proceedings of the National Academy of Sciences of the United States of America 95(5): 2044–2049. https://doi.org/10.1073/pnas.95.5.2044

Pan K, Zhao N, Yin Q, Zhang T, Xu X, Fang W, Hong Y, Fang Z, Xiao Y (2014) Induction of a laccase Lcc9 from *Coprinopsis cinerea* by fungal coculture and its application on indigo dye decolorization. Bioresource Technology 162: 45–52. https://doi.org/10.1016/j.biortech.2014.03.116

Ribaldi M (1952) Sopra un interessante zigomicete terricolo: *Gongronella urceolifera* n. gen. et n. sp. Rivista di Biologia 44(1): 157–166.

Ronquist F, Huelsenbeck JP. 2003. MrBayes 3: Bayesian phylogenetic inference under mixed models. Bioinformatics (Oxford, England) 19(12): 1572–1574. https://doi.org/10.1093/bioinformatics/btg180

Ronquist F, Teslenko M, van der Mark P, Ayres DL, Darling A, Höhna S, Larget B, Liu L, Suchard MA, Huelsenbeck JP (2012) MrBayes 3.2: Efficient Bayesian phylogenetic inference and model choice across a large model space. Systematic Biology 61(3): 539–542. https://doi.org/10.1093/sysbio/sys029

Stamatakis A (2014) RAxML version 8: A tool for phylogenetic analysis and post-analysis of large phylogenies. Bioinformatics (Oxford, England) 30(9): 1312–1313. https://doi.org/10.1093/bioinformatics/btu033

Stiller JW, Hall BD (1997) The origin of red algae: Implications for plastid evolution. Proceedings of the National Academy of Sciences of the United States of America 94(9): 4520–4525. https://doi.org/10.1073/pnas.94.9.4520

Tedersoo L, Sánchez-Ramírez S, Kõljalg U, Bahram M, Döring M, Schigel D, May T, Ryberg M, Abarenkov K (2018) High-level classification of the *Fungi* and a tool for evolutionary ecological analyses. Fungal Diversity 90(1): 135–159. https://doi.org/10.1007/s13225-018-0401-0

Tibpromma S, Hyde KD, Jeewon R, Maharachchikumbura SSN, Liu J, Bhat DJ, Jones EBG, McKenzie EHC, Camporesi E, Bulgakov TS, Doilom M, de Azevedo Santiago ALCM, Das K, Manimohan P, Gibertoni TB, Lim YW, Ekanayaka AH, Thongbai B, Lee HB, Yang J-B, Kirk PM, Sysouphanthong P, Singh SK, Boonmee S, Dong W, Raj KNA, Latha KPD, Phookamsak R, Phukhamsakda C, Konta S, Jayasiri SC, Norphanphoun C, Tennakoon DS, Li J, Dayarathne MC, Perera RH, Xiao Y, Wanasinghe DN, Senanayake IC, Goonasekara ID, de Silva NI, Mapook A, Jayawardena RS, Dissanayake AJ, Manawasinghe IS, Chethana KWT, Luo Z-L, Hapuarachchi KK, Baghela A, Soares AM, Vizzini A, Meiras-Ottoni A, Mešić A, Dutta AK, de Souza CAF, Richter C, Lin C-G, Chakrabarty D, Daranagama DA, Lima DX, Chakraborty D, Ercole E, Wu F, Simonini G, Vasquez G, da Silva GA, Plautz Jr HL, Ariyawansa HA, Lee H, Kušan I, Song J, Sun J, Karmakar J, Hu K, Semwal KC, Thambugala KM, Voigt K, Acharya K, Rajeshkumar KC, Ryvarden L, Jadan M, Hosen MI, Mikšík M, Samarakoon MC, Wijayawardene NN, Kim NK, Matočec N, Singh PN, Tian Q, Bhatt RP, de Oliveira RJV, Tulloss RE, Aamir S, Kaewchai S, Marathe SD, Khan S, Hongsanan S, Adhikari S, Mehmood T, Bandyopadhyay TK, Svetasheva TY, Nguyen TTT, Antonín V, Li W-J, Wang Y, Indoliya Y, Tkalčec Z,

Elgorban AM, Bahkali AH, Tang AMC, Su H-Y, Zhang H, Promputtha I, Luangsa-ard J, Xu J, Yan J, Ji-Chuan K, Stadler M, Mortimer PE, Chomnunti P, Zhao Q, Phillips AJL, Nontachaiyapoom S, Wen T-C, Karunarathna SC (2017) Fungal diversity notes 491–602: Taxonomic and phylogenetic contributions to fungal taxa. Fungal Diversity 83(1): 1–261. https://doi.org/10.1007/s13225-017-0378-0

Vilgalys R, Hester M (1990) Rapid genetic identification and mapping of enzymatically amplified ribosomal DNA from several *Cryptococcus* species. Journal of Bacteriology 172(8): 4238–4246. https://doi.org/10.1128/jb.172.8.4238-4246.1990

Voigt K, Wostemeyer J (2000) Reliable amplification of actin genes facilitates deep-level phylogeny. Microbiological Research 155(3): 179–195. https://doi.org/10.1016/S0944-5013(00)80031-2

Wang J, Zhou W, Yuan H, Wang Y (2008) Characterization of a novel fungal chitosanase Csn2 from *Gongronella* sp. JG. Carbohydrate Research 343(15): 2583–2588. https://doi.org/10.1016/j.carres.2008.08.004

Wang X, Fang J, Liu P, Liu J, Fang W, Fang Z, Xiao Y (2021) *Mucoromycotina* fungi possess the ability to utilize plant sucrose as a carbon source: Evidence from *Gongronella* sp. w5. Frontiers in Microbiology 11: 591697. https://doi.org/10.3389/fmicb.2020.591697

Wang YX, Zhao H, Ding ZY, Ji XY, Zhang ZX, Wang S, Zhang XG, Liu XY (2023) Three new species of *Gongronella* (Cunninghamellaceae, *Mucorales*) from soil in Hainan, China based on morphology and molecular phylogeny. Journal of Fungi (Basel, Switzerland) 9(12): 1182. https://doi.org/10.3390/jof9121182

Wang S, Liu X, Xiong C, Gao S, Xu W, Zhao L, Song C, Liu X, James TY, Li Z, Zhang X (2023) ASF1 regulates asexual and sexual reproduction in *Stemphylium eturmiunum* by DJ-1 stimulation of the PI3K/AKT signaling pathway. Fungal Diversity 123(1): 159–176. https://doi.org/10.1007/s13225-023-00528-1

Wei F, Hong Y, Liu J, Yuan J, Fang W, Peng H, Xiao Y (2010) *Gongronella* sp. induces overproduction of laccase in *Panus rudis*. Journal of Basic Microbiology 50(1): 98–103. https://doi.org/10.1002/jobm.200900155

White T, Bruns T, Lee S, Taylor J, Innis M, Gelfand D, Sninsky J (1990) Amplification and direct sequencing of fungal ribosomal RNA genes for phylogenetics, in PCR protocols: a guide to methods and applications, 315–322. https://doi.org/10.1016/B978-0-12-372180-8.50042-1

Zhang ZY, Han YF, Chen WH, Liang ZQ (2019) *Gongronella sichuanensis* (Cunninghamellaceae, *Mucorales*), a new species isolated from soil in China. Phytotaxa 416: 167–174. https://doi.org/10.11646/phytotaxa.416.2.4

Zhang ZX, Liu RY, Liu SB, Mu TC, Zhang XG, Xia JW (2022) Morphological and phylogenetic analyses reveal two new species of Sporocadaceae from Hainan, China. MycoKeys 88: 171–192. https://doi.org/10.3897/mycokeys.88.82229

Zhao H, Nie Y, Zong T, Wang K, Lv M, Cui Y, Tohtirjap A, Chen J, Zhao C, Wu F, Cui B, Yuan Y, Dai Y, Liu X (2023) Species diversity, updated classification and divergence times of the phylum Mucoromycota. Fungal Diversity 123(1): 49–157. https://doi.org/10.1007/s13225-023-00525-4

Zhao H, Nie Y, Huang B, Liu XY (2024, October 14) Unveiling species diversity within early-diverging fungi from China I: Three new species of *Backusella* (Backusellaceae, Mucoromycota). MycoKeys 109: 285–304. https://doi.org/10.3897/mycokeys.109.126029

Zhou W, Yuan H, Wang J, Yao J (2008) Production, purification and characterization of chitosanase produced by *Gongronella* sp. JG. Letters in Applied Microbiology 46(1): 49–54. https://doi.org/10.1111/j.1472-765X.2007.02262.x

Zhou G, Peng C, Liu X, Chang F, Xiao Y, Liu J, Fang Z (2020) Identification and immobilization of an invertase with high specific activity and sucrose tolerance ability of *Gongronella* sp. w5 for high fructose syrup preparation. Frontiers in Microbiology 11: 633. https://doi.org/10.3389/fmicb.2020.00633

Supplementary material 1

The combined ITS+LSU+TEF+ACT+RPB1 sequence matrix used in this study

Authors: Yi-Xin Wang

Data type: fas

Explanation note: The sequence matrix included 43 strains in 25 species of *Gongronella*, with *Cunninghamella echinulata* CBS 156.28 as outgroup. A total of 4,080 characters comprised ITS rDNA (1–989), LSU rDNA (990–1967), TEF rDNA (1968–2172), ACT rDNA (2173–2948) and RPB1 rDNA (2949–4080). Among them, there were 2866 constant, 562 variable but parsimony non-informative and 652 parsimony informative characters.

Link: https://doi.org/10.3897/mycokeys.110.130260.suppl1

MycoKeys 110: 319–360 (2024)
DOI: 10.3897/mycokeys.110.136844

Research Article

Re-evaluation of *Ceratostomella* and *Xylomelasma* with introduction of two new species (Sordariomycetes)

Martina Réblová[1], Jana Nekvindová[2], Miroslav Kolařík[3], Željko Jurjević[4], Michal Kolář[5], Vít Hubka[3,6]

1 *Department of Taxonomy, Institute of Botany, The Czech Academy of Sciences, 252 43 Průhonice, Czech Republic*
2 *Institute of Clinical Biochemistry and Diagnostics, University Hospital Hradec Králové, 500 05 Hradec Králové, Czech Republic*
3 *Laboratory of Fungal Genetics and Metabolism, Institute of Microbiology, The Czech Academy of Sciences, 142 20 Prague 4, Czech Republic*
4 *EMSL Analytical, Inc., 200 Route 130 North, Cinnaminson, New Jersey 08077, USA*
5 *Laboratory of Genomics and Bioinformatics, Institute of Molecular Genetics, The Czech Academy of Sciences, 142 20 Prague 4, Czech Republic*
6 *Department of Botany, Faculty of Science, Charles University, 128 00 Prague 2, Czech Republic*
Corresponding author: Martina Réblová (martina.reblova@ibot.cas.cz)

Abstract

In this study, we assessed the phylogenetic relationships among members of *Ceratostomella* and the morphologically similar genus *Xylomelasma*, currently classified within the Sordariomycetes. Our phylogenetic analyses, utilising three and five gene markers, revealed that species from these two genera are congeneric, supporting the transfer of *Xylomelasma* to *Ceratostomella*. Consequently, we propose two new combinations: *C. sordida* **comb. nov.** and *C. novae-zelandiae* **comb. nov.** In addition, we identified two cryptic species within the *C. sordida* species complex, which are described as *C. crypta* **sp. nov.** and *C. melanospora* **sp. nov.** Traditional micromorphological characters have proven insufficient for differentiating these new species; however, they are clearly distinguishable by molecular data, particularly using the internal transcribed spacer region ITS1-5.8S-ITS2 (ITS) of the nuclear rRNA cistron, and genes encoding the second largest subunit of RNA polymerase II (*rpb2*), and translation elongation factor 1-α (*tef1-α*) as primary and secondary barcodes. This study provides new insights into the morphological characteristics of *Ceratostomella*, identifying the ascogenous system as an important diagnostic trait at the generic level, which distinguishes *Ceratostomella* from morphologically similar fungi. *Ceratostomella* is currently recognised with eight species. We also investigated the relationship between *Ceratostomella* and the closely related *Barbatosphaeria*. The lack of statistical support in the Maximum likelihood analysis is discussed and the inclusion of *Ceratostomella* in Barbatosphaeriaceae is not supported. *Ceratostomella* is accepted as a genus *incertae sedis*, while Barbatosphaeriaceae remains a monotypic family. The global diversity of *Ceratostomella* is inferred from metabarcoding data and published field observations. Biogeographic analysis indicates that members of *Ceratostomella* are widespread, found in soil and decaying wood, as well as in air, dust, roots, shoots, and water across temperate, subtropical and tropical regions in both the Northern and Southern Hemispheres. We are concurrently publishing whole-genome analyses of three ex-type strains of *Ceratostomella*, i.e. *C. crypta*, *C. melanospora* and *C. sordida*. This effort aims to establish a new standard for high-quality taxonomic studies, which, in accordance with current trends, should incorporate whole-genome sequencing data for future research and application. Our findings underscore the importance of integrating morphological, biogeographic and molecular data for accurate species delineation and highlight the complexity within the genus *Ceratostomella*.

Academic editor: Andrew Miller
Received: 11 September 2024
Accepted: 17 October 2024
Published: 21 November 2024

Citation: Réblová M, Nekvindová J, Kolařík M, Jurjević Ž, Kolář M, Hubka V (2024) Re-evaluation of *Ceratostomella* and *Xylomelasma* with introduction of two new species (Sordariomycetes). MycoKeys 110: 319–360. https://doi.org/10.3897/mycokeys.110.136844

Key words: Ascogenous hyphae, biogeography, cryptic species, molecular systematics, saprobes, Sordariomycetes, two new species

Introduction

Ceratostomella (Saccardo 1878) was introduced to encompass species with simple diagnostic features, such as dark rostrate ascomata and hyaline, aseptate ascospores. According to MycoBank (Crous et al. 2004), 111 species have historically been assigned to this genus. However, the following studies have revealed that *Ceratostomella* is phenotypically more diverse than previously thought (e.g. Sydow and Sydow 1919; Elliott 1923; Melin and Nannfeldt 1934; Moreau 1952; Hunt 1956; Booth 1957; Dennis 1988; Samuels and Barr 1997; Réblová 2006; De Beer et al. 2013; Réblová et al. 2018). It includes taxa with both evanescent and persistent asci, as well as hyaline or pigmented ascospores. Additionally, it encompasses various types of interthecial filaments and, where known, asexual morphs characterised by annellidic, holoblastic, phialidic, and tretic conidiogenesis. The enormous species variability within *Ceratostomella* has posed a challenging task for mycologists, who have made numerous attempts to classify its species. Various studies using molecular data (see below) have demonstrated that *Ceratostomella* represents a heterogeneous species assemblage exhibiting phenotypic convergence. Despite their similar phenotypes, these species belong to several phylogenetically distinct lineages.

Of the numerous species ascribed to *Ceratostomella*, only a handful represents the core of the genus. Réblová (2006) redefined *Ceratostomella* through comparative morphology and phylogenetic analyses of ribosomal DNA sequences from two representative species, *C. cuspidata* and *C. pyrenaica*. Molecular data for the lectotype species, *C. rostrata*, designated by Clements and Shear (1931), are not available. *Ceratostomella* is characterised by non-stromatic perithecial ascomata with an upright cylindrical, sulcate neck, thick leathery to carbonaceous ascomatal wall, persistent clavate asci arising from supportive, discrete ascogenous cells, usually inconspicuous apical annulus, broadly cellular paraphyses, and brown, aseptate, suballantoidal, irregularly ellipsoidal, globose or reniform ascospores arranged in fascicle or 2–3-seriately within the ascus. The asexual morphs are unknown, and the axenic cultures derived from ascospores remained sterile. *Ceratostomella* thrives in strongly decayed wood or decaying *Polyporales* basidiomata and is primarily distributed in temperate regions of both hemispheres. The genus was classified as *incertae sedis* within *Sordariomycetidae* with four species accepted (Réblová 2006), and later, together with *Barbatosphaeria* and *Xylomelasma*, placed in the family Barbatosphaeriaceae by Zhang et al. (2017).

The revision of other *Ceratostomella* species with persistent asci prompted their reclassification in several unrelated genera within Sordariomycetes. These include *Barbatosphaeria* in Barbatosphaeriaceae (Réblová 2008; Réblová et al. 2015b), *Calyptosphaeria*, *Lentomitella*, *Spadicoides* and *Torrentispora* in *Xenospadicoidales* (Réblová et al. 2018), *Ceratosphaeria* in *Magnaporthales* (von Niessl 1876), *Chaetosphaeria* in Chaetosphaeriales (Booth 1957; Huhndorf and Fernández 2005), *Clohiesia* in *Annulatascales* (Réblová et al. 2018), *Daruvedia* in *Pyrenulales* (Dennis 1988), *Natantiella* (*incertae sedis*) (Réblová and Štěpánek

2009), *Jattaea* and *Togniniella* in Calosphaeriales (Réblová et al. 2004, 2015a; Réblová 2011), *Phaeoacremonium* in Togniniales (Gramaje et al. 2015), *Phomatospora* in *Phomatosporales* (Réblová et al. 2018), *Pseudorhynchia* in *Hypocreales* (Samuels and Barr 1997), and *Wallrothiella* in *Amplistromatales* (Réblová and Seifert 2004). Other species with evanescent asci and hyaline ascospores have been reclassified into several genera such as *Ceratocystis*, *Huntiella* and *Thielaviopsis* of *Microascales* and *Ceratocystiopsis*, *Grosmannia*, *Leptographium*, *Ophiostoma* and *Pesotum* of *Ophiostomatales*; these species including their synonymy are listed in De Beer et al. (2013, 2014). Unravelling the phylogenetic relationships of many other *Ceratostomella* species remains a complex task. This complexity arises from the lack of living cultures, insufficient diagnoses, ambiguous or lost holotypes, and the scarcity of recent collections. The entire taxonomic history of *Ceratostomella* was detailed in Réblová et al. (2018).

Xylomelasma (Réblová 2006) is remarkably similar to *Ceratostomella* in both morphology and ecology. The genus was typified by *X. sordida*, and *X. novae-zelandiae* was accepted as a second species. Both genera share similar ascospores and persistent asci that float freely within the centrum at maturity, robust paraphyses, rostrate non-stromatic ascomata with thick wall and occasional occurrence of Munk pores in the wall cells. In addition, they exhibit identical ascogenous apparatus, consisting of oval, clavate or obclavate, discrete cells from which asci arise as an outgrowth. *Xylomelasma* was distinguished from *Ceratostomella* by its ellipsoidal ascospores that are obliquely uniseriate, occasionally biseriate in the ascus, more or less cylindrical paraphyses, distinct apical annulus and ascomata with both sulcate and non-sulcate necks. Based on single-gene nuclear large and small subunit rDNA (LSU and SSU) phylograms, *Ceratostomella* and *Xylomelasma* were shown to be closely related, although they did not form a monophyletic clade (Réblová 2006). However, in the phylogenetic analyses based on the concatenated data set of LSU, SSU, and the second largest subunit of RNA polymerase II (*rpb2*) DNA sequences, a strongly supported relationship between the two genera was confirmed (Réblová et al. 2018). Currently, *Xylomelasma* contains four species, including *X. moderata* (Vassiljeva and Stephenson 2014) and *X. shoalensis* (Hernández-Restrepo et al. 2016).

During a survey of ascomycetes, we collected specimens of *C. cuspidata* and *C. pyrenaica* from Belgium and New Zealand, along with four collections preliminarily identified as *X. sordida* from wood in advanced stages of decay in the Czech Republic, and from a swab from generating station in the USA. Axenic cultures were derived from all collections. Furthermore, we re-examined the holotype of *X. novae-zelandiae*, which lacks a living culture as the ascospores never germinated *in vitro*, and we successfully extracted DNA from the ascomata.

The aim of this study is to investigate the relationships between *Ceratostomella* and *Xylomelasma*, as well as among the four '*X. sordida*' strains isolated by us, using comparative morphological studies and novel DNA sequences. Additionally, we sought to re-evaluate the morphological traits originally used to delimit both genera. To achieve this, we generated new sequences for nuclear rDNA ITS1-5.8S-ITS2 (ITS barcode), nuclear LSU and SSU rDNA, *rpb2*, and the intermediate section of the coding region of translation elongation factor 1-α (*tef1-α*) from all available ex-type and non-type strains of *Ceratostomella* and *Xylomelasma* and subjected them to phylogenetic analyses.

In our integrative taxonomic approach, we combine both phylogenetic and morphological data. With the capability of utilising GlobalFungi (Větrovský et al. 2020), we also incorporate geographical and ecological information. A crucial next step in advancing taxonomic standards and refining fungal classification is the concurrent publication of whole-genome sequence (WGS) data for type strains. This approach allows for more comprehensive comparisons between taxa, including with those so-called 'fungal dark taxa'—fungi that lack observable morphological structures, cannot be cultured under laboratory conditions, and are primarily detected through DNA sequencing, particularly via environmental metabarcoding (Nilsson et al. 2019). The current topic of significant discussion is the potential introduction of DNA-based typification (e.g. Nilsson et al. 2023), with WGS data serving as an alternative typification material. For such a system to function effectively, WGS data must also be available for the currently described diversity. In response to the call by Zhou (2024), we publish short-read WGS data for representative strains of *Ceratostomella*, supporting this emerging trend in fungal taxonomy.

Materials and methods

Fungal strains and morphological studies

Material was obtained from temperate regions in both the Northern and Southern Hemispheres, including a swab from the USA and collections on wood from temperate broadleaf and mixed forests in Belgium, Czech Republic, and New Zealand. Dried specimens were deposited into the Fungarium of the Institute of Botany CAS (**PRA**) in Průhonice, Czech Republic and New Zealand Fungarium (**PDD**) in Auckland, New Zealand. Cultures were deposited in Westerdijk Fungal Biodiversity Institute (**CBS**) in Utrecht, the Netherlands, and Culture Collection of Fungi (**CCF**), Faculty of Science, Charles University in Prague, Czech Republic. Other herbarium material was obtained from Fungarium of the Illinois Natural History Survey (**ILLS**) in Champaign, Illinois, USA. Along with our collections and literature references, data on the host and geographic distribution of the species studied were obtained from the MyCoPortal (http://www.mycoportal.org/portal/index.php, Miller and Bates 2017, accessed on October 14, 2024). Taxonomic novelties were registered in MycoBank. Table 1 presents the studied strains, their sources, and the GenBank accession numbers for the sequences obtained in this study.

Structures of the fungi on the host and living cultures were examined with an Olympus SZX12 dissecting microscope (Olympus America, Inc., Melville, NY, USA). Dry ascomata were rehydrated with water, and the gelatinous centrum was extracted using the tip of a needle. Microscopic preparations were mounted in 90% lactic acid, water, and Melzer's reagent. Measurements were taken from specimens mounted in Melzer's reagent and means ± standard deviation (SD) were calculated for sizes of asci and ascospores based on a minimum of 20–25 measurements. Microscopic observations were conducted using an Olympus BX51 light microscope. Nomarski differential interference contrast (DIC) and phase contrast (PC) were used for observations and measurements. Microphotographs were captured using an Olympus DP70 camera with Imaging Software Cell^D (Olympus). Colony macrophotographs were captured with a Canon EOS 77D digital camera with Canon EF 100 mm f/2.8L Macro IS USM

Table 1. Taxa, isolate information and new sequences determined for this study (in bold) and additional sequences retrieved from GenBank.

Taxon	Source	Status	Country	Host	Substrate	GenBank accession numbers					Ref.
						ITS	nucLSU	nucSSU	*rpb2*	*tef1-α*	
Ceratostomella crypta	CBS 131683	T	Czech Republic	unidentified	decayed wood	KT991679	KM492871	KM492860	KM492910	**PQ213498**	1,2
C. crypta	CBS 131684	P	Czech Republic	unidentified	decayed wood	**PQ215754**	**PQ215747**	**PQ215922**	**PQ213489**	**PQ213499**	
C. crypta	CCF 5710	P	USA	n/a	generating station (swab)	**PQ215755**	**PQ215748**	**PQ215923**	—	—	
Ceratostomella cuspidata	ICMP 17629		New Zealand	*Nothofagus* sp.	decayed wood/ bark	KT991671	FJ617558	KT991642	KT991651	**PQ213500**	1,3
C. cuspidata	IFBL 57.31		Belgium	unidentified	decayed wood	**PQ215756**	**PQ215749**	**PQ215924**	**PQ213490**	**PQ213501**	
Ceratostomella melanospora	CBS 147993	T	Czech Republic	*Fagus sylvatica*	decayed wood	**PQ215757**	**PQ215750**	**PQ215925**	**PQ213491**	**PQ213502**	
Ceratostomella novae-zelandiae	PDD 81433	T	New Zealand	*Nothofagus* sp.	decayed wood/ bark	**PQ215758**	**PQ215751**	**PQ215926**	—	—	
Ceratostomella pyrenaica	CBS 117116	P	Czech Republic	*Acer campestre*	decayed wood	**PQ215759**	DQ076323	DQ076324	**PQ213492**	**PQ213503**	4
C. pyrenaica	PRA-21825		Czech Republic	*Quercus* sp.	decayed wood	**PQ215760**	**PQ215752**	**PQ215927**	—	**PQ213504**	
C. pyrenaica	CBS 129343		Czech Republic	*Quercus* sp.	decayed wood	KT991672	KY931835	KY931893	KY931863	—	2,4
Ceratostomella sordida	CBS 116000	T	France	*Alnus glutinosa*	decayed wood	**PQ215761**	AY761087	AY761090	KY931929	**PQ213505**	4,5
Neotracylla pini	CBS 146010	T	Malaysia	*Pinus tecunumanii*	needles	—	**PQ215753**	**PQ215928**	**PQ213493**	—	
Tracylla aristata	CBS 141404	E	Australia	*Eucalyptus regnans*	leaves	—	OL654186	**PQ215929**	**PQ213494**	—	6
Tracylla eucalypti	CBS 144429	T	Colombia	*Eucalyptus urophylla*	leaves	—	OL654187	**PQ215930**	**PQ213495**	—	6

Notes: T, E, P indicate ex-holotype, ex-epitype and ex-paratype strains.
References: 1 = Réblová et al. 2015b; 2 = Réblová et al. 2016; 3 = Réblová and Štěpánek 2009; 4 = Réblová et al. 2018; 5 = Réblová 2006; 6 = Réblová et al. 2021.

objective (Canon Europe Ltd., Middlesex, UK) with daylight spectrum 5500K 16W LED lights. Images were processed using Adobe Photoshop CS6 software (Adobe Systems, San Jose, CA, USA).

One isolate from a swab and five cultures derived from ascospores of fresh specimens were prepared in the context of this study; unfortunately, those of *C. cuspidata* IFBL 57.31 and *C. pyrenaica* PRA-21825 are no longer viable. Axenic cultures were prepared as outlined by Jurjević et al. (2015) and Réblová and Nekvindová (2023). In order to assess colony characteristics, diffusible pigments and growth patterns, strains were cultivated on cornmeal dextrose agar (CMD) (cornmeal agar, Oxoid Limited, Basingstoke, UK, supplemented with 2% w/v dextrose), MLA (Modified Leonian's agar) (Malloch 1981), oatmeal agar (OA), and potato-carrot agar (PCA) (Crous et al. 2019a). In addition, other nutrient media such as Modified cellulose agar (MCA), malt extract agar (MEA), and potato-dextrose agar (PDA) (HealthLink, Jacksonville FL, USA; currently Hardy diagnostics), were also used to incubate cultures. To measure the size of the colonies *in vitro*, an agar plug with 2-week-old mycelium was placed at the centre and at the edge of new 9 cm and 6 cm Petri dishes. Colony diameter was measured from cultures that were two and four weeks old. Colony characteristics were determined based on 4-week-old cultures incubated in the dark at

23 °C. To assess the growth at higher temperatures, the cultures were incubated at 30, 35, 37 and 41 °C on MEA, PDA, and OA for a period of two weeks. To induce sporulation, strains were also inoculated on cornmeal agar (CMA, Crous et al. 2019a) supplemented with sterile stems of *Urtica dioica* and exposed to alternating UV light and darkness in 12-hour intervals.

Gene markers, DNA extraction, PCR amplification, and sequencing

The relationships between *Ceratostomella* and *Xylomelasma*, as well as intraspecific and interspecific relationships within *Ceratostomella* were evaluated using five gene markers. These include the internal transcribed spacer ITS1-5.8S-ITS2 of the nuclear rRNA cistron used as a primary barcode for fungi (Schoch et al. 2012); the nuclear large subunit rDNA gene (D1–D3 domains, approximately 1800 base pairs) and the nuclear small subunit rDNA gene, which are commonly employed for studying relationships within the *Ascomycota* at the generic and higher taxonomic levels (e.g. Schoch et al. 2009). Additionally, genes encoding the second largest subunit of RNA polymerase II (DNA-directed RNA polymerase) and the intermediate section of the translation elongation factor 1-α were used, as they are effective in distinguishing interspecific relationships in fungi (e.g. Robert et al. 2011; Stielow et al. 2015).

Protocols for DNA extraction and PCR amplification of ITS, LSU, SSU, *rpb2*, and *tef1-α* were conducted following the methods described by Réblová and Nekvindová (2023). Automated sequencing was carried out by Eurofins Genomics Europe Sequencing Service (Cologne, Germany). Analyses of raw sequence data and assembly of sequence contigs were performed using Sequencher v. 5.4.6 (Gene Codes Corp., Ann Arbor, MI, USA). In Suppl. material 1, we provide the accession numbers of sequences for members of Sordariomycetes obtained from GenBank, most of which have been previously published in other studies (Ranghoo et al. 1999; Suh and Blackwell 1999; Huhndorf et al. 2004; Réblová and Seifert 2004; Réblová et al. 2004, 2011, 2015a,b, 2016, 2018, 2020, 2021; Miller and Huhndorf 2005; Réblová 2006, 2011, 2013; Shenoy et al. 2006, 2010; Yaguchi et al. 2006; Zhang et al. 2006, 2017; Arzanlou et al. 2007; Spatafora et al. 2007; Damm et al. 2008; Plattner et al. 2009; Réblová and Štěpánek 2009; Thongkantha et al. 2009; Ferrer et al. 2012; Jaklitsch et al. 2013; Untereiner et al. 2013; Klaubauf et al. 2014; Tsang et al. 2014; Hernández-Restrepo et al. 2016; Senanayake et al. 2016; Yang et al. 2017; Réblová and Štěpánek 2018; Song et al. 2018; Crous et al 2019b; Luo et al. 2019; Lu et al. 2020; Hyde et al. 2021).

The ex-type strains of *C. crypta* CBS 131683, *C. melanospora* CBS 147993 and *C. sordida* CBS 116000 were selected for whole-genome DNA sequencing. Genomic DNA was extracted from 5-day-old cultures grown on MEA agar plates using the NucleoSpin® Soil isolation kit (Macherey–Nagel, Düren, Germany). Library preparation (2 × 300 bp Illumina paired-end) was carried out, and sequencing was performed on a NextSeq 2000 instrument (Illumina) following the manufacturer's protocol. The quality of the raw sequencing data was assessed using FastQC v. 0.11.9 (Andrews 2010) (Accessed on 23 Aug. 2024), and low-quality reads were filtered out using Trimmomatic v. 0.39 (Bolger et al. 2014) based on the quality control results (FastQC 0.11.9). The high-quality reads were then assembled de novo using SPAdes v4.0.0 (Bankevich et al. 2012). Genome assembly quality was assessed using QUAST v. 5.2.0 (Gurevich

et al. 2013), and completeness was evaluated with BUSCO v. 5.7.1.1 (Seppey et al. 2019) against the fungi_odb10.2019-11-20 dataset. Genome annotation was conducted using the Funannotate pipeline v. 1.18.16 (Palmer and Stajich 2020) to predict and annotate gene models within the target genome. Functional annotation was performed using InterProScan v. 5.69-101.0 (Jones et al. 2014) and EggNOG-mapper v. 2.1.9 (Huerta-Cepas et al. 2019). The genome identities were confirmed by comparing extracted ITS barcode sequences.

Phylogenetic and barcode analyses

The gene sequences were aligned using MAFFT v. 7.487 (Katoh and Standley 2013) implemented in the CIPRES Science Gateway v. 3.3 (Miller et al. 2010) and manually corrected in BioEdit v. 7.1.8 (Hall 1999), if necessary. Phylogenetic analyses were executed using software packages available on the CIPRES Science Gateway v. 3.3. First, we conducted separate single-marker Maximum likelihood (ML) analyses with RAxML-HPC v. 8.2.12 (Stamatakis 2014). Since we did not detect any conflicting clades between these analyses, the individual sequence alignments were concatenated into two final alignments (deposited in TreeBASE, study number 31694) and subjected to phylogenetic analyses. Partitions, for which we assumed rate heterogeneity, were evaluated using MrModeltest v. 2.4 (Nylander 2004) to determine the best partitioning scheme for our datasets and to select the best-fit models under Akaike information criteria.

In the first phylogenetic analysis of LSU-SSU-*rpb2* sequences, the alignment comprised 107 ingroup strains and included a total of 4 676 characters including gap regions, with 2 452 unique character sites (RAxML). Eighty-six nucleotides (nt) at the beginning of LSU and 70 nt at the beginning of SSU were excluded from the analyses due to the incompleteness of many sequences retrieved from GenBank. Three members of the *Savoryellales* (*Hypocreomycetidae*), such as *Bactrodesmium abruptum*, *Bactrodesmium diversum*, and *Neoascotaiwania terrestris*, were selected as the outgroup, based on previous research and known relationships within the Sordariomycetes, and availability of molecular data (Réblová et al. 2020). The GTR+I+G best-fit model of nucleotide evolution was selected for each partition.

In the second phylogenetic analysis of ITS-LSU-SSU-*rpb2*-*tef1*-*α* sequences, the alignment included 11 strains representing 6 species of *Ceratostomella*, encompassing a total of 6 161 characters including gap regions, and 1 099 unique character sites (RAxML). Seventy nucleotides at the beginning of SSU were excluded from the analysis due to the incompleteness of many sequences. The outgroup was selected from members of Chaetosphaeriaceae, specifically *Curvichaeta curvispora* and *Menispora uncinata*, based on known relationships from the first analysis and the availability of DNA sequences. The following best-fit models of nucleotide evolution were selected for each partition: GTR+I for ITS, LSU, *tef1*-*α*; HKY+I for SSU; and GTR+G for *rpb2*.

The Maximum likelihood analysis was performed with RAxML-HPC v. 8.2.12 with a GTRCAT approximation. Statistical support for the nodes was determined by non-parametric bootstrapping (BS) with 1 000 replicates. The Bayesian Inference (BI) analysis was performed with MrBayes v. 3.2.7 (Ronquist et al. 2012). Two Bayesian searches were conducted using default parameters. The B-MCMCMC (Bayesian-Metropolis-coupled Markov chain Monte Carlo) analyses lasted until the average standard deviation of split frequencies was below

0.01, with trees saved every 1 000 generations with a burn-in of 25%. The BI and ML phylogenetic trees were compared visually in terms of topological conflicts between the supported clades. Nodes supported by values of ≥ 75% ML Bootstrap (BS) and ≥ 0.95 BI Posterior Probability (PP) were deemed well-supported. Phylogenetic trees were visualised in FigTree v. 1.4.3 (Rambaut 2010) and SeaView v. 5.0.5 (Gouy et al. 2010) and edited in Microsoft PowerPoint.

The identity/similarity for ITS, *rpb2* and *tef1-α* sequences of members of *Ceratostomella* was calculated using BioEdit. Histograms of intraspecific and interspecific distances were created for ITS, *rpb2* and *tef1-α* markers to illustrate the extent of overlap for each gene (the so-called barcode gap). A matrix of pairwise distances was computed in MEGA v. 11.0.13 software (Tamura et al. 2021) using the p-distance model with gap deletion (pairwise deletion option) (Kimura 1980). The histograms were plotted in GraphPrism v. 7.03 (Graphpad Software, La Jolla, California) using a bin size of 0.003 (ITS), 0.002 (*rpb2*) and 0.001 (*tef1-α*).

Biogeography assessment using published environmental sequences

The biogeography of six out of the eight known *Ceratostomella* species with available ITS sequences was examined following the workflow outlined by Réblová et al. (2022). We utilised the GlobalFungi database (Větrovský et al. 2020), release 5 (16.11.2023), which comprises 84 972 samples from 846 studies, encompassing 593 399 355 unique ITS1 or ITS2 sequences. Since the GlobalFungi database contains separate ITS1 and ITS2 sequences, we analysed these regions independently. To ensure consistency with the ITS spacers stored in GlobalFungi, which were originally extracted using the ITSx extractor (Bengtsson-Palme et al. 2013), we used the ITSx extractor implemented in the SEED2 platform (Větrovský et al. 2018) to extract the spacers from our data. To identify *Ceratostomella* species in GlobalFungi, we conducted an exact hit similarity search in the database with all unique ITS1 and ITS2 haplotypes from our study, searching for published environmental sequences that match in both length and sequence.

Results

Phylogenetic and barcode analyses

In the first phylogenetic analysis, based on a three-gene dataset (LSU-SSU-*rpb2*), we assessed the relationships among *Ceratostomella*, *Xylomelasma*, and representatives of the Sordariomycetes. Phylogenetic trees constructed through BI and ML analyses displayed broad congruence, with the ML tree depicted in Fig. 1. The nodes with support values ≥ 75% ML BS and ≥ 0.95 BI PP were considered well-supported. The phylogram revealed 40 well-supported lineages representing 33 families or orders and seven genera *incertae sedis* belonging to three major, strongly supported clades, i.e. *Diaporthomycetidae* (98% ML BS /1.0 PP), *Sordariomycetidae* (83/0.98) and *Sordariomycetidae incertae sedis* (95/1.0). Members of *Ceratostomella* and *Xylomelasma* formed a monophyletic, strongly supported and fully resolved clade (95%/1.0) in the *Sordariomycetidae incertae sedis*. This clade included two strains of *C. cuspidata* (ICMP 17629, IFBL 57.31), three strains of *C. pyrenaica* (CBS 117116, CBS 129343, PRA-21825), the ex-type strains of *X. sordida* CBS 116000 and *X. novae-zelandiae* PDD 81433, and

four new isolates initially identified as *X. sordida*. While the two *Ceratostomella* species formed a strongly supported subclade (100/1.0), the original representatives of *Xylomelasma* were not monophyletic. *Xylomelasma sordida* formed a species complex (98/1.0) as a sister to *Ceratostomella*, whereas *X. novae-zelandiae* clustered on a basal branch. These results support the conclusion that both genera are congeneric and that *Xylomelasma* represents a synonym of the older name *Ceratostomella*, with two new combinations proposed, *C. sordida* and *C. novae-zelandiae*. Four new strains acquired in this study represent two cryptic species that are morphologically indistinguishable from *C. sordida*. These strains are described below as *C. crypta* (ex-type strain CBS 131683, CBS 131684, CCF 5710) and *C. melanospora* (ex-type strain CBS 147993). Additionally, *X. shoalensis* holotype ILLS 76895 is shown to be conspecific with *C. sordida* CBS 116000, with their LSU (760 nt long fragment) exhibiting 99.2% sequence similarity. The *Ceratostomella* clade is a sister (62/0.99) to *Barbatosphaeria* (Barbatosphaeriaceae) (94/1.0), though this relationship is not statistically supported in the ML analysis. Other close relatives of *Ceratostomella* include members of the clade (94/1) containing *Ophiostomatales* (100/1) and *Natantiella ligneola* CBS 123470.

In the second phylogenetic analysis, we utilised a five-gene dataset (ITS-LSU-SSU-*rpb2*-*tef1-α*) to focus on the relationships among *Ceratostomella* species. Both ML and BI trees were congruent, with the ML tree shown in Fig. 2. Compared to the first analysis (Fig. 1), the *Ceratostomella* clade differed in the position of *C. novae-zelandiae*, which appeared on a separate branch as a sister (99/1.0) to the *C. cuspidata* and *C. pyrenaica* subclade (100/1.0). The *C. sordida* species complex consisted of three morphologically indistinguishable species that can be clearly differentiated by molecular data. The low sequence similarity of ITS, *rpb2*, and *tef1-α* markers, along with the high evolutionary divergence among these markers within the *C. sordida* species complex warrant the recognition of three distinct species, including the newly identified *C. crypta* and *C. melanospora*. *Ceratostomella crypta* was represented by three isolates in the phylogenetic analysis; the strain CBS 131684 exhibited the following sequence similarities with the ex-type strain and the other isolate CCF 5710: 99.6% in ITS, 100% in LSU, SSU, and *tef1-α*, and 99.8% in *rpb2*. *Ceratostomella sordida* and *C. crypta* exhibited sequence similarities of 89.3–90.8% in ITS, 90.4% in *rpb2*, and 96.3% in *tef1-α*. *Ceratostomella sordida* and *C. melanospora* showed similarities of 78% in ITS, 85.2% in *rpb2*, and 96.5% in *tef1-α*. *Ceratostomella crypta* and *C. melanospora* demonstrated similarities of 70–76.9% in ITS, 84.7–84.9% in *rpb2*, and 93.8% in *tef1-α*.

We recognised a clear barcoding gap in all three markers: ITS, *rpb2* and *tef1-α* (Fig. 3). Regarding species differences in genetic divergence among the three barcodes within the *C. sordida* species complex, the divergence was generally lower between *C. sordida* and *C. crypta* (ITS: 7.5–7.7%, *rpb2*: 9.6%, *tef1-α*: 3.6–3.7%) compared to the higher divergence encountered between *C. sordida* and *C. melanospora* (ITS: 23.7%, *rpb2*: 15%, *tef1-α*: 6.5%). The genetic divergence between the new species, *C. melanospora* and *C. crypta*, ranged from 6.2% in *tef1-α*, 15.1–15.3% in *rpb2* to 23.9% in ITS. The estimates of genetic divergences between *C. melanospora*/*C. sordida* and *C. melanospora*/*C. crypta* in ITS and *rpb2* were the highest within the *C. sordida* species complex. The estimates of evolutionary divergence are provided in the Suppl. material 2.

Whole-genome sequences for the three representative strains were successfully obtained, BioProject: PRJNA1170903. The number of scaffolds ranged from

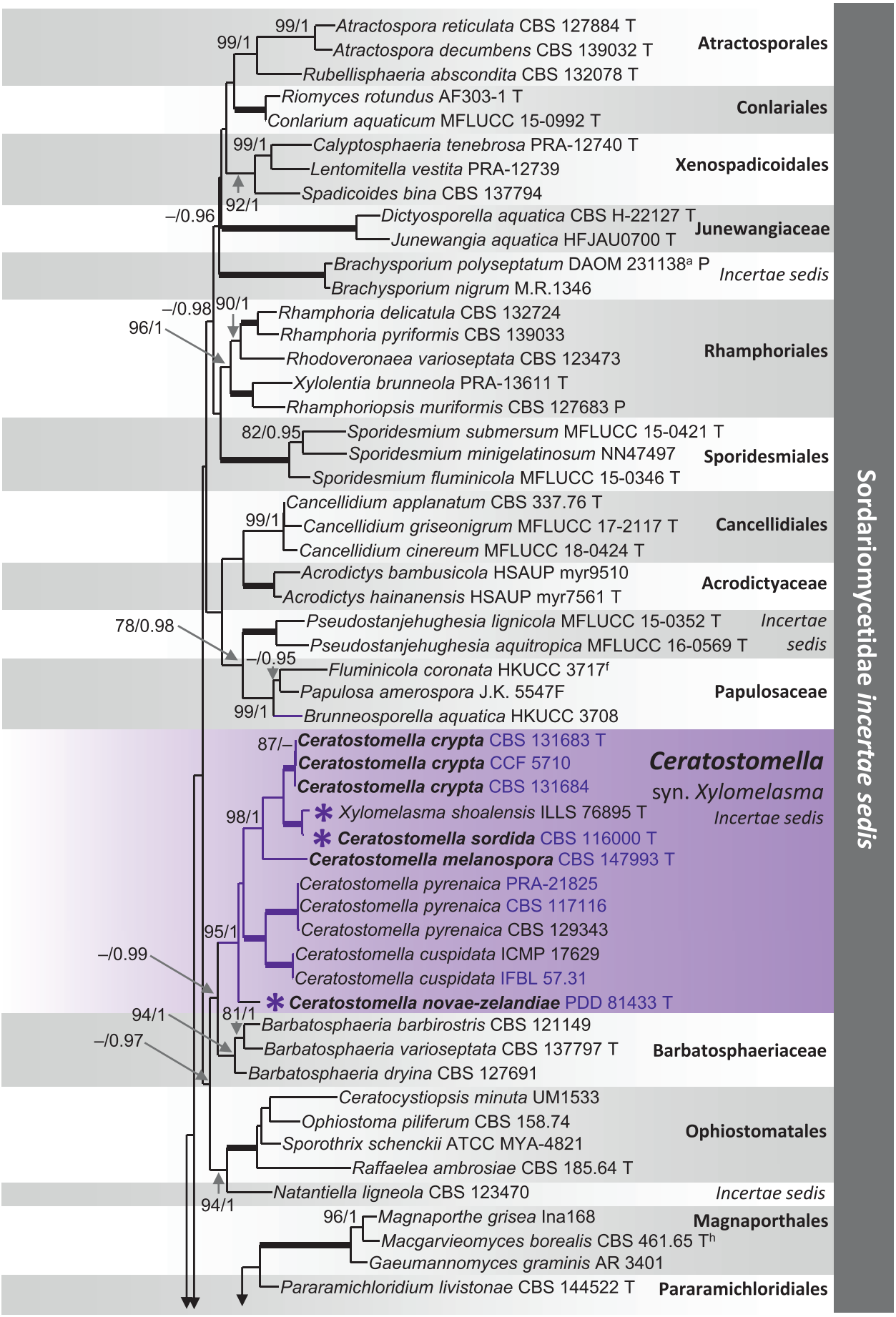
Atractospora reticulata CBS 127884 T
Atractospora decumbens CBS 139032 T
Rubellisphaeria abscondita CBS 132078 T
Atractosporales
Riomyces rotundus AF303-1 T
Conlarium aquaticum MFLUCC 15-0992 T
Conlariales
Calyptosphaeria tenebrosa PRA-12740 T
Lentomitella vestita PRA-12739
Spadicoides bina CBS 137794
Xenospadicoidales
Dictyosporella aquatica CBS H-22127 T
Junewangia aquatica HFJAU0700 T
Junewangiaceae
Brachysporium polyseptatum DAOM 231138[a] P
Brachysporium nigrum M.R.1346
Incertae sedis
Rhamphoria delicatula CBS 132724
Rhamphoria pyriformis CBS 139033
Rhodoveronaea varioseptata CBS 123473
Xylolentia brunneola PRA-13611 T
Rhamphoriopsis muriformis CBS 127683 P
Rhamphoriales
Sporidesmium submersum MFLUCC 15-0421 T
Sporidesmium minigelatinosum NN47497
Sporidesmium fluminicola MFLUCC 15-0346 T
Sporidesmiales
Cancellidium applanatum CBS 337.76 T
Cancellidium griseonigrum MFLUCC 17-2117 T
Cancellidium cinereum MFLUCC 18-0424 T
Cancellidiales
Acrodictys bambusicola HSAUP myr9510
Acrodictys hainanensis HSAUP myr7561 T
Acrodictyaceae
Pseudostanjehughesia lignicola MFLUCC 15-0352 T
Pseudostanjehughesia aquitropica MFLUCC 16-0569 T
Incertae sedis
Fluminicola coronata HKUCC 3717[f]
Papulosa amerospora J.K. 5547F
Brunneosporella aquatica HKUCC 3708
Papulosaceae
Ceratostomella crypta CBS 131683 T
Ceratostomella crypta CCF 5710
Ceratostomella crypta CBS 131684
Xylomelasma shoalensis ILLS 76895 T
Ceratostomella sordida CBS 116000 T
Ceratostomella melanospora CBS 147993 T
Ceratostomella pyrenaica PRA-21825
Ceratostomella pyrenaica CBS 117116
Ceratostomella pyrenaica CBS 129343
Ceratostomella cuspidata ICMP 17629
Ceratostomella cuspidata IFBL 57.31
Ceratostomella novae-zelandiae PDD 81433 T
Ceratostomella
syn. Xylomelasma
Incertae sedis
Barbatosphaeria barbirostris CBS 121149
Barbatosphaeria varioseptata CBS 137797 T
Barbatosphaeria dryina CBS 127691
Barbatosphaeriaceae
Ceratocystiopsis minuta UM1533
Ophiostoma piliferum CBS 158.74
Sporothrix schenckii ATCC MYA-4821
Raffaelea ambrosiae CBS 185.64 T
Ophiostomatales
Natantiella ligneola CBS 123470
Incertae sedis
Magnaporthe grisea Ina168
Macgarvieomyces borealis CBS 461.65 T[h]
Gaeumannomyces graminis AR 3401
Magnaporthales
Pararamichloridium livistonae CBS 144522 T
Pararamichloridiales
Sordariomycetidae incertae sedis
99/1
99/1
99/1
92/1
–/0.96
–/0.98
90/1
96/1
82/0.95
99/1
78/0.98
–/0.95
99/1
87/–
98/1
95/1
–/0.99
94/1
81/1
–/0.97
94/1
96/1

557 to 9491, with genome completeness, based on conserved fungal genes, between 98.5% and 98.9%. Genome sizes varied from 38.9 to 52.4 Mbp. The annotated genomes have been deposited in the NCBI database, and the quality and completeness of the assembled whole genomes are presented in Table 2.

Biogeography of *Ceratostomella*

Members of *Ceratostomella* thrive on decaying wood and decaying basidiomata of *Polyporales*. They have also been detected in environmental samples predominantly isolated from air and soil, as well as from deadwood, shoots, roots and water across various habitats. Representatives of the genus *Ceratostomella* are distributed worldwide, primarily in temperate regions of the Northern and Southern Hemispheres, with some occurrences in subtropical (*C. cuspidata*, *C. sordida*) and tropical (*C. sordida*) zones of Asia, Australasia, Europe and North America and South America. According to GlobalFungi, the most common species appears to be *C. sordida*, which is the only species found across various biomes in temperate, subtropical and tropical regions. *Ceratostomella sordida* was identified in 126 samples, compared to other species with known DNA sequences: *C. pyrenaica* (50 samples), *C. cuspidata* (28), *C. crypta* (10), *C. melanospora* (7), and *C. novae-zelandiae* (2). For detailed information, see Suppl. material 3.

Taxonomy

***Ceratostomella* Sacc., Michelia 1: 370. 1878.**

Xylomelasma Réblová, Mycologia 98: 87. 2006. Synonym.

Lectotype species. *Ceratostomella rostrata* (Tode) Sacc., Syll. Fung. 1: 409. 1882 (Lectotype designated by Clements and Shear 1931).

Description. *Sexual morph*. Ascomata perithecial, non-stromatic, venter globose to subglobose, superficial, semi-immersed or immersed, glabrous, roughened or tuberculate, dark brown to black, usually surrounded by sparse mycelium; hyphae growing out of the sides and bottom of the venter. Necks rostrate, central, cylindrical, straight to slightly flexuous, perpendicular or oblique to almost decumbent toward the substrate, sulcate or glabrous. Ostiolum periphysate. Ascomatal wall leathery to carbonaceous, two-layered. Outer layer consisting of brown, thick-walled cells, textura prismatica to textura angularis to textura epidermoidea, often with a distinct, external crustose layer of heavily pigmented, dark brown cells with opaque walls. Inner layer consisting of thin-

Figure 1. Maximum Likelihood phylogenetic tree of members of the Sordariomycetes based on analysis of LSU, SSU, and *rpb2* DNA sequences. Species names given in bold are taxonomic novelties; the newly acquired strains and those with novel sequences are highlighted in blue font; T, E and P denote ex-holotype, ex-epitype and ex-paratype strains; [a] paratype of *Cryptadelphia polyseptata*, [b] holotype of *Calosphaeriophora pulchella*, [c] holotype of *Poroconiochaeta discoidea*, [d] holotype of *Coniochaetidium ostreum*, [e] holotype of *Cryptendoxyla hypophloia*, [f] Nom. inval., Art. 36.1(c) (Melbourne), [g] holotype of *Jattaea prunicola*, and [h] holotype of *Diplorhinotrichum juncicola*. Thickened branches indicate branch support with ML BS = 100% and PP values = 1.0. Branch support of nodes ≥ 75% ML and ≥ 0.95 PP is indicated above or below branches. A hyphen (–) indicates values lower than 75% ML BS or 0.95 PP. Purple asterisk before the name indicates former members of the genus *Xylomelasma* within the *Ceratostomella* clade.

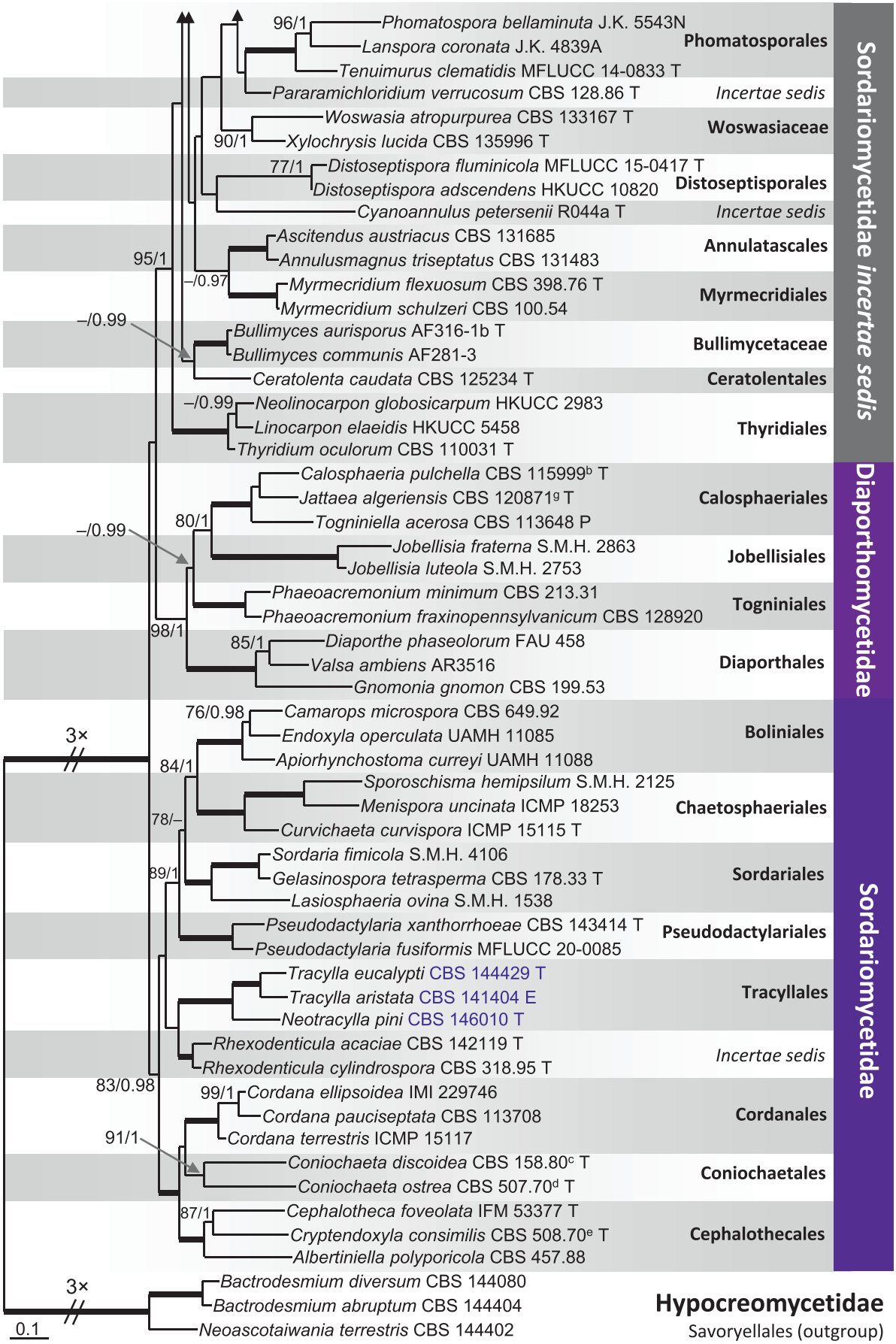

Figure 1. Continued.

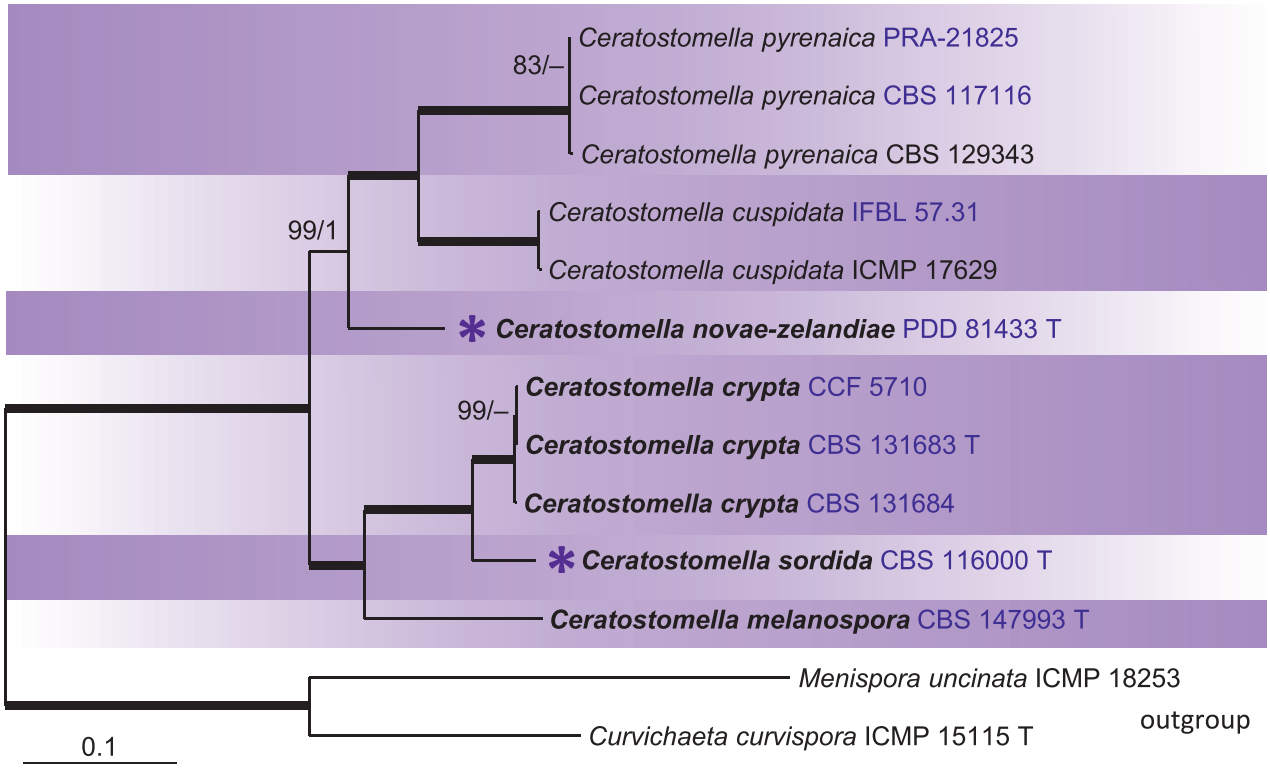

Figure 2. Maximum Likelihood phylogenetic tree of members of *Ceratostomella* based on analysis of ITS, LSU, SSU, *rpb2* and *tef1-α* DNA sequences. Species names given in bold are taxonomic novelties; the newly acquired strains and those with novel sequences are highlighted in blue font. Thickened branches indicate branch support with ML BS = 100% and PP values = 1.0. Branch support of nodes ≥ 75% ML and ≥ 0.95 PP is indicated above or below branches. A hyphen (–) indicates values lower than 75% ML BS or 0.95 PP. Purple asterisk before the name indicates former members of the genus *Xylomelasma* within the *Ceratostomella* clade.

Table 2. Quality and completeness of the obtained whole genome sequences, BioProject: PRJNA1170903.

Strain	Taxon	GenBank biosample numbers	Dataset Complete (BUSCO) (%)	Scaffold N50	Contigs N50	Number of scaffolds	Total length (genome size, bp)
CBS 131683	*C. crypta*	SAMN44110716	98.9	205990	201397	9491	52431894
CBS 147993	*C. melanospora*	SAMN44110894	98.6	315073	299955	1285	38866519
CBS 116000	*C. sordida*	SAMN44113309	98.5	614896	586589	557	49647797

ner-walled, subhyaline to hyaline, elongated and compressed cells. Ascogenous hyphae with croziers, with several lateral and terminal dehiscent cells produced sequentially and simultaneously, from each ascogenous cell one ascus arises as an outgrowth. Paraphyses abundant, unbranched, septate, hyaline, broad-celled and constricted at the septa, wider near the base, tapering, apically free, longer than the asci, disintegrating with age. Asci unitunicate, persistent, clavate to cylindrical-clavate, short-stipitate, truncate to broadly rounded at the apex, tapering toward the base from the sporiferous part, floating freely within the centrum at maturity, with a shallow, sometimes indistinct, non-amyloid apical annulus, 8-spored. Ascus stipe usually contains non-refractive material deposited at the bottom part, visible after ascus dehiscence from the ascogenous cell. Ascospores variable in shape, suballantoid, ellipsoidal to irregularly ellipsoidal, globose or reniform, straight or curved, often flattened on one side, hyaline when young, becoming pale brown to brown before discharge from the ascus,

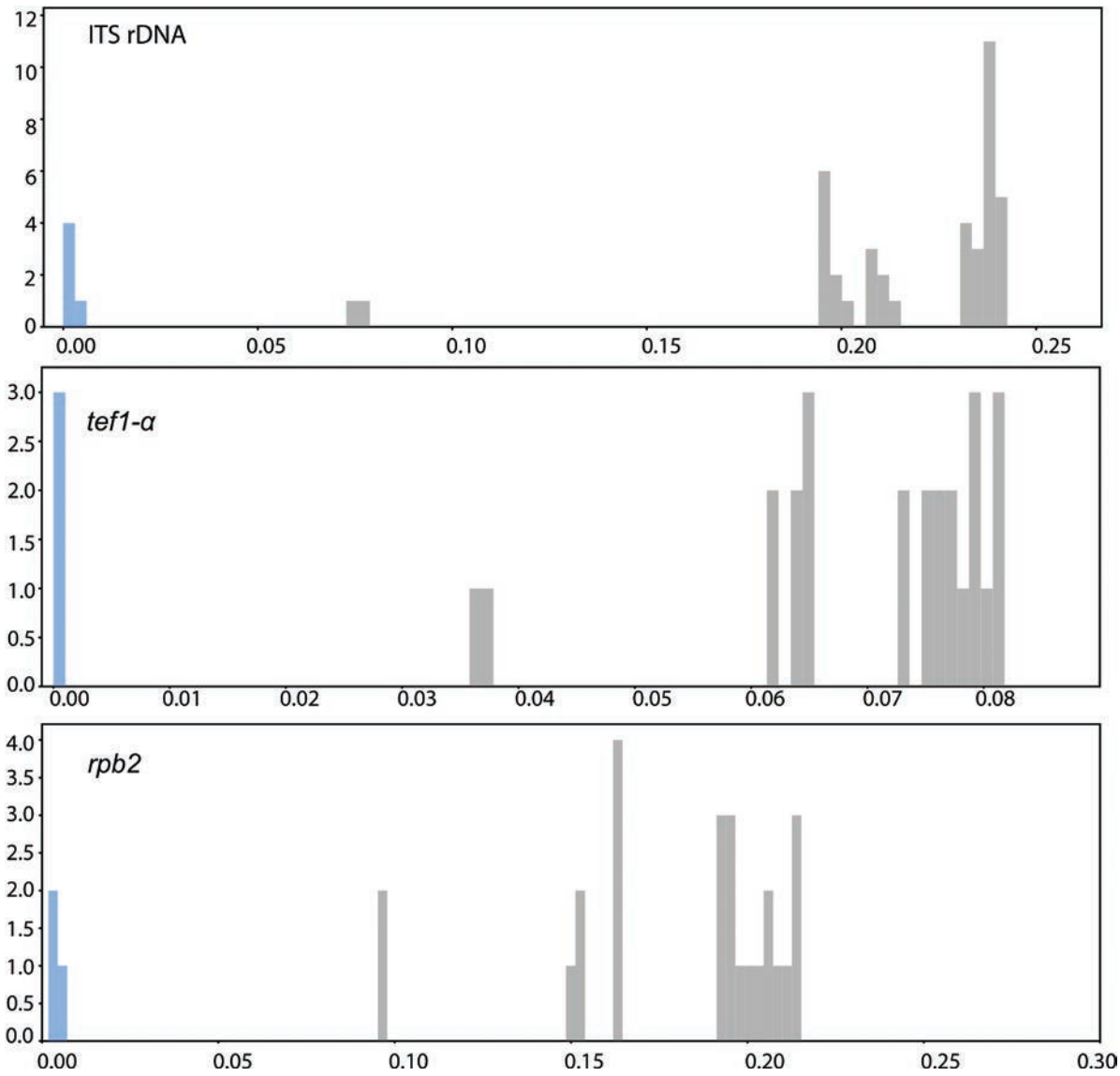

Figure 3. Barcoding gap. The frequency distribution graphs of the Kimura 2-parameter distances of ITS, *rpb2* and *tef1-α* DNA sequences (i.e. barcoding gaps). The intraspecific distances are shown as blue bars and interspecific distances as grey bars.

aseptate, smooth, sometimes with indistinct terminal pores at one or both ends, arranged in a fascicle in the upper part of the ascus or 2–3-seriate or uniseriate within the ascus. (Partially adopted from Réblová 2006.) ***Asexual morph*.** Hyphomycetous, dematiaceous; in culture only sterile mycelium was observed.

Accepted species. *Ceratostomella crypta*, *C. cuspidata*, *C. melanospora*, *C. novae-zelandiae*, *C. pyrenaica*, *C. rhynchophora*, *C. rostrata,* and *C. sordida*.

Notes. Species of *Ceratostomella* exhibit a variety of ascospore shapes, including suballantoid to reniform in *C. cuspidata*, suballantoid non-apiculate in *C. rostrata*, ellipsoidal slightly apiculate in *C. crypta*, *C. melanospora*, *C. rhynchophora*, and *C. sordida*, and ellipsoidal to oblong in *C. pyrenaica*. Réblová (2006) also described *Ceratostomella* sp. M.R. 2592, which has globose ascospores; however, this species lacks molecular data to confirm its placement in the genus. The key to identifying *Ceratostomella* species was provided by Réblová (2006). Table 3 displays morphological characteristics of *Ceratostomella* species accepted in the genus.

Table 3. Morphological characteristics of *Ceratostomella* spp.

Taxon	Ascomata size*	Munk pores	Neck	Asci size	Ascospores size	Shape	Sample (GF)**	Ref.
C. crypta	350–500	No	sulcate	66–77(–81.5) × 7.5–9.5(–10)	8.5–11 × (4–)4.5–5.5	ellipsoidal, slightly apiculate	10	1
C. cuspidata	380–500	Yes	sulcate	21–30 × (5–)6–7	4–5 × 2–3	suballantoid to reniform	28	2
C. melanospora	300–480	No	sulcate	63–78 × 6.5–8(–8.5)	(8–)8.5–10.5(–11) × 4–5	ellipsoidal, slightly apiculate	7	1
C. novae-zelandiae	310–340	No	smooth	50–60(–65) × 7–8(–9)	7–8 × (3.5–)4–5	ellipsoidal, slightly apiculate	2	2
C. pyrenaica	400–550	No	sulcate	(30–)33–40 × 5.5–7	7–9 × 3–4	ellipsoidal to oblong, slightly curved and apiculate	50	2
C. rhynchophora	500–650	No	sulcate	(33–)35–44 × 7–8.5(–10)	6–7 × (3.5–)4–5	ellipsoidal, slightly apiculate, sometimes flattened on one side	n/a	2
C. rostrata	650–750	Yes	sulcate	(26–)30–39 × 5–6	4.5–6 × 1.5–2	allantoid to suballantoid	n/a	2
C. sordida	490–550	Yes	sulcate	(58–)60–76(–81) × 7–10(–13)	9–12 × 4–6	ellipsoidal, slightly apiculate	126	2

* Size of ascomata (diam), asci and ascospores is given in µm.
**GF = GlobalFungi database; the number indicates the total number of samples with identical sequences detected in GlobalFungi.
n/a = data not available.
References: 1 = This study; 2 = Réblová 2006.

***Ceratostomella crypta* Réblová, Hubka & Jurjević, sp. nov.**
MycoBank No: 855703
Figs 4–6

Etymology. *Cryptus* (Latin) meaning hidden, secret; referring to cryptic nature of this species, which is morphologically indistinguishable from *C. melanospora* and *C. sordida*.

Type. Czech Republic • South Moravian Region, Břeclav district, obora Soutok near Lanžhot; on decaying deciduous wood; 23 Oct 2004; M. Réblová M.R. 2911 (holotype PRA-21820!, ex-type culture CBS 131683).

Description. *Sexual morph*. Ascomata non-stromatic, grouped, immersed with only necks protruding, sometimes partially erumpent with bases semi-immersed. Venter 350–500 µm diam, subglobose, upright, dark brown to black, with sparse brown, septate, slightly flexuous hairs 3.5–4.5 µm wide sparsely covering the sides and bottom. Neck 100–120 µm wide, up to 860 µm long, central, cylindrical, upright, tapering at the top, sulcate along the upper half or the whole length. Ostiole periphysate. Ascomatal wall fragile to leathery, 51–72(–82) µm thick, two-layered. Outer layer consisting of thick-walled, dark brown, polyhedral cells with opaque walls of textura prismatica, with several cells forming the external crustose layer ca. 9–14 µm thick, cells tend to be more flattened and paler towards the interior. Inner layer consists of several rows of thin-walled, hyaline, flattened cells. Paraphyses abundant, longer than the asci, becoming partially disintegrated with age, septate, slightly constricted at the septa, hyaline, 5–9.5 µm wide, wider near the base, tapering to ca. 3.5 µm. Asci 66–77(–81.5) × 7.5–9.5(–10) µm (mean ± SD = 74.9 ± 4.4 × 8.7 ± 0.8 µm), 57.5–71.5(–86) µm (mean ± SD = 65.8 ± 2.6 µm) long in the sporiferous part; asci containing mostly collapsed ascospores are generally smaller in size 61–71.5(–74) × 7–8.5 µm (mean ± SD = 66.4 ± 2.9 × 7.8 ± 0.6 µm), 50.5–59 µm (mean ± SD = 54.3 ± 3.5 µm) long in the sporiferous part, broadly rounded to truncate at the apex, cylindrical, with a short tapering stipe, apical annulus non-amyloid, 2.5 µm wide, 1–1.5 µm high, 8-spored. Ascospores 8.5–11 × (4–)4.5–5.5 µm (mean ± SD = 9.5 ± 0.7 × 5 ± 0.3 µm), ellipsoidal, slightly apiculate

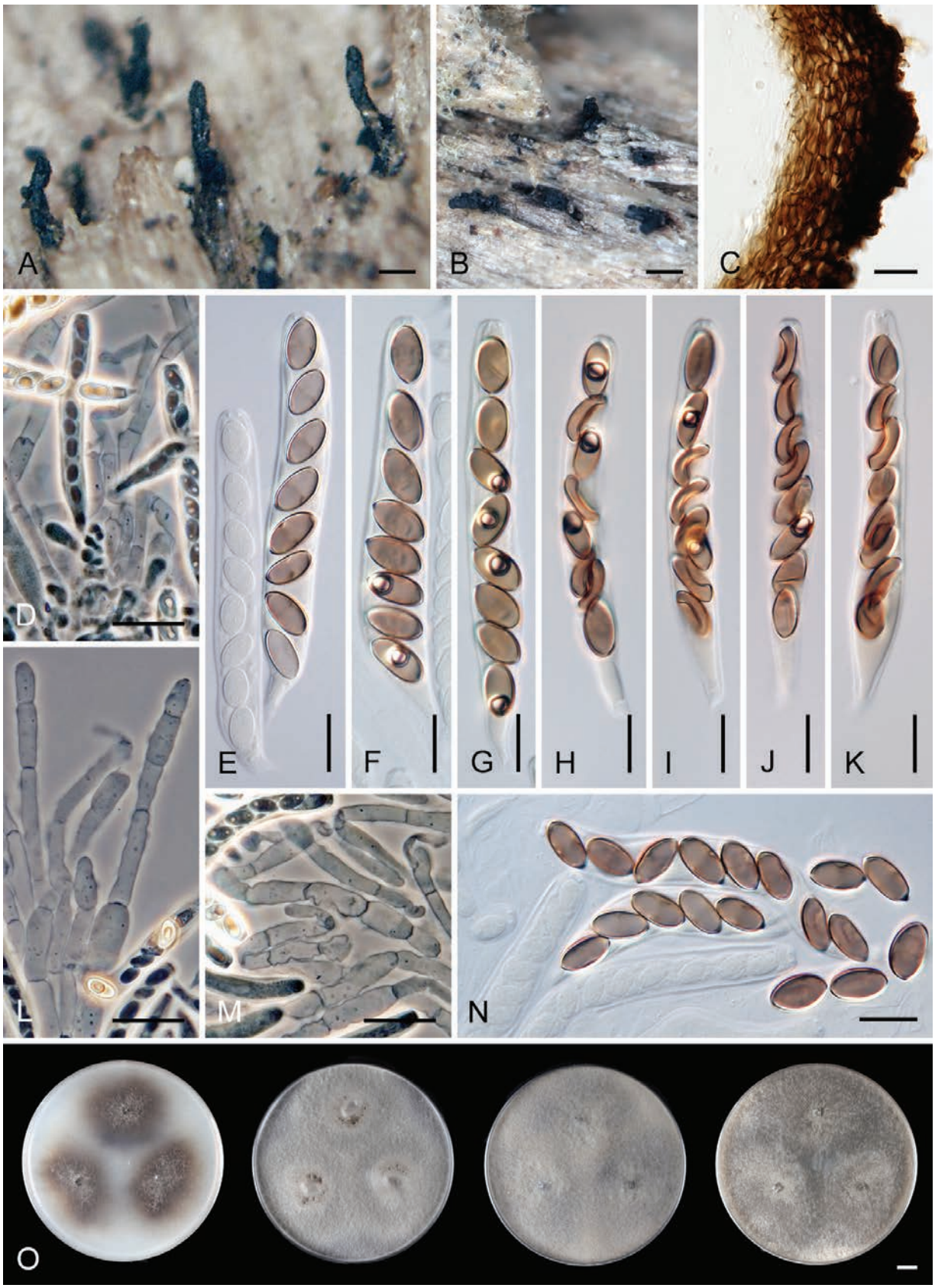

Figure 4. *Ceratostomella crypta* (**A–N** from holotype PRA-21820 **O** from ex-type strain CBS 131683) **A, B** ascomata **C** a longitudinal section of the ascomatal wall **D** asci with paraphyses and ascogenous cells **E–K** asci with ascospores **L, M** paraphyses **N** ascospores **O** colony morphology at 23 °C after 4 weeks on CMD, MLA, OA and PCA (from left to right). Images: on natural substrate (**A–N**). Scale bars: 500 µm (**A, B**); 20 µm (**C, D, L, M**); 10 µm (**E–K, N**); 1 cm (**O**).

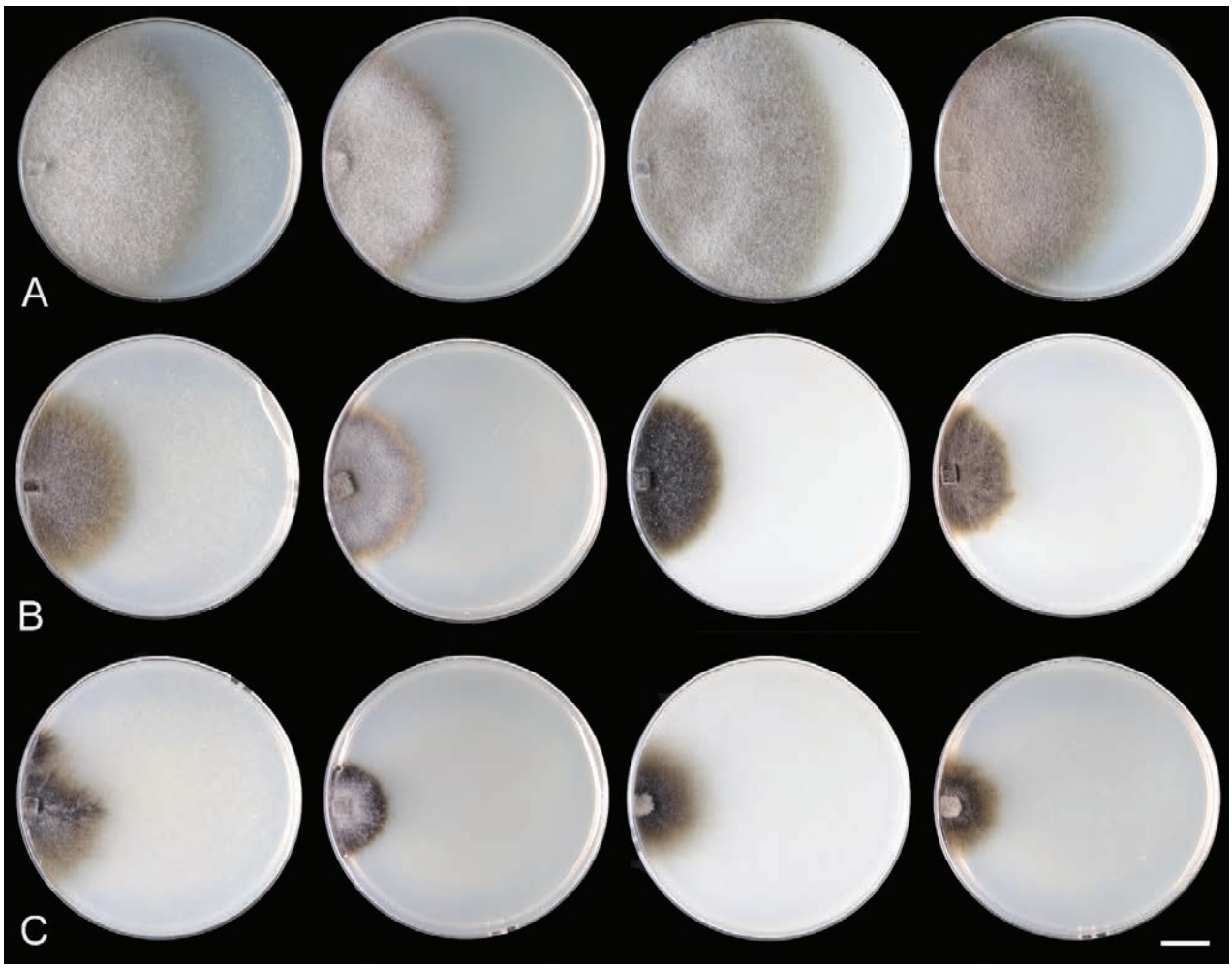

Figure 5. Growth rates *in vitro* of *Ceratostomella* spp. **A** *C. crypta* CBS 131683 **B** *C. sordida* CBS 116000 **C** *C. melanospora* CBS 147993. Colonies on CMD, MLA, OA and PCA (from left to right) after two weeks. Scale bar: 1 cm.

at both ends, brown, aseptate, smooth, with an inconspicuous germ pore at one or both ends, sometimes with one oil drop, often collapsing, obliquely uniseriate or partially overlapping within the ascus. ***Asexual morph*.** Unknown.

Characteristics in culture (after 2/4 wk at 23 °C). On CMD colonies 70–72 mm/mycelium fully covered the plate, circular, flat, margin effuse to fimbriate with a sparse growth, cobwebby, grey-brown, reverse of the same colour. On MLA colonies 50–51 mm diam/mycelium fully covered the plate, margin entire to fimbriate, circular, flat, margin entire, lanose, olivaceous grey, reverse dark olivaceous brown. On OA colonies 83–85 mm diam/mycelium fully covered the plate, circular, margin entire to fimbriate, lanose, olivaceous grey, reverse dark brown. On PCA colonies 62–64 mm diam/mycelium fully covered the plate, circular, flat, margin diffuse, cobwebby, grey-brown, reverse dark brown. Sporulation was absent on all media.

Temperature dependent growth at 30, 35, 37, 41 °C was assessed as colony diam on MEA, PDA, and OA, respectively, after a period of two weeks: 30 °C >90 mm/>90 mm/>90 mm, 35 °C >90 mm/>90 mm/>90 mm, 37 °C >90 mm/>90 mm/>90 mm, 41 °C 46–48 mm/40–41 mm/26–27 mm.

On MCA, colonies are effuse, with commonly submerged subhyaline hyphae that later become vein-like, ranging in colour from brown to dark olivaceous

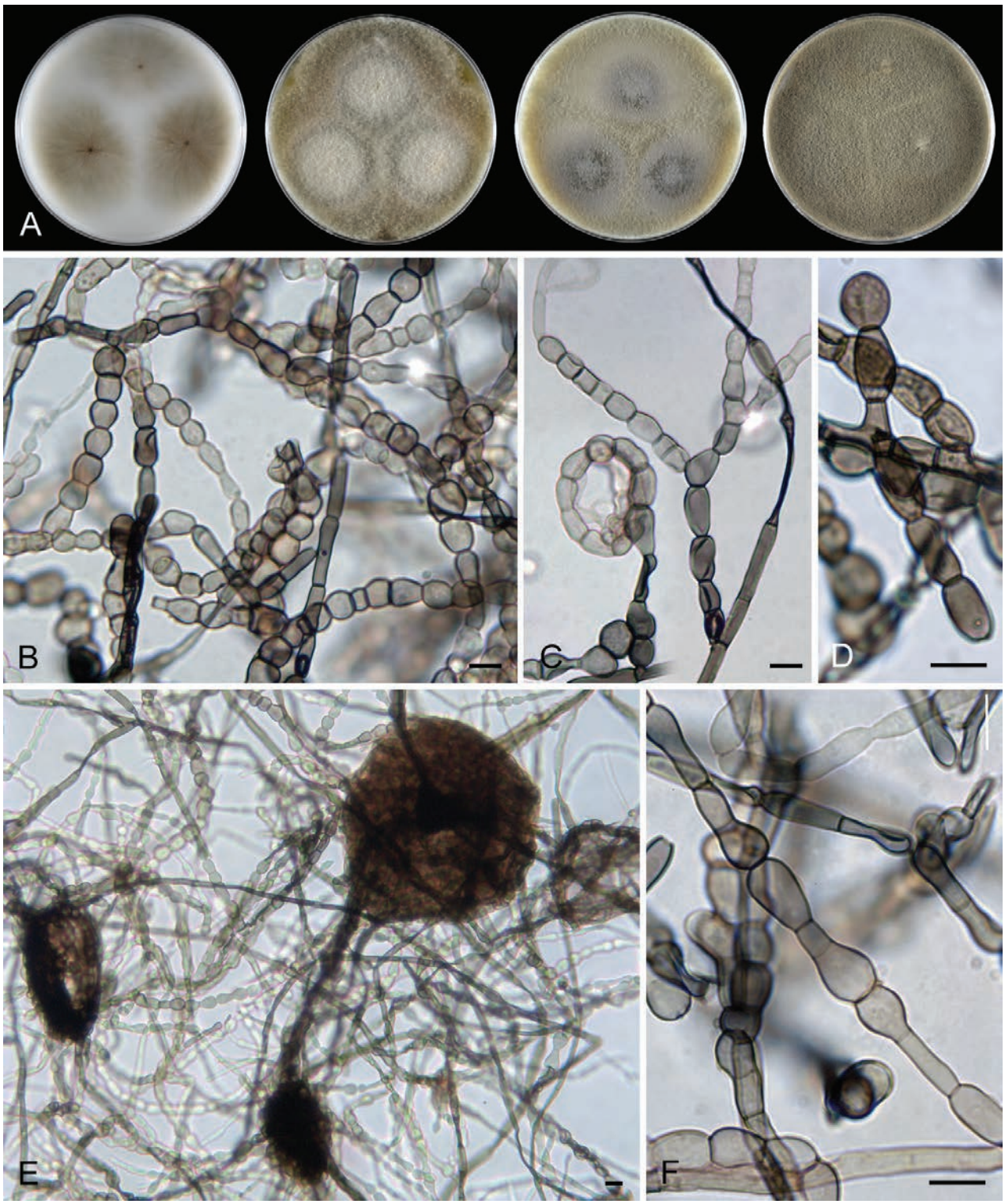

Figure 6. *Ceratostomella crypta* (CCF 5710) **A** colony morphology at 37 °C after 2 weeks on MCA, MEA, OA and PDA (from left to right) **B, D–F** pigmented monilioid hyphae on CA. **C** monilioid hyphae on MEA. Scale bars: 1 cm (**A**); 10 µm (**B–F**).

brown, 3–7 µm in diameter, smooth and septate, with occasional tuberose formations. These hyphae often branch to form monilioid hyphae composed of thick-walled cells, varying in shape from nearly rectangular to subglobose. Branching of monilioid hyphae often occurs at right angles, coiling hyphae are also present.

Additional specimens examined. Czech Republic • South Moravian Region: Břeclav district, obora Soutok near Lanžhot; on decaying deciduous wood; 23 Oct 2004; M. Réblová M.R. 2916 (PRA-21821, culture CBS 131684). USA • South Carolina: swab from generating station; Jul 2014; Ž. Jurjević 2471 (culture CCF 5710 = CBS 142809).

Habitat and geographical distribution. Saprobe on decaying deciduous wood in the Czech Republic; it was also isolated from a swab from generating station in the USA (South Carolina). According to GlobalFungi, the species is distributed predominantly in the temperate region of the Northern Hemisphere. Identical sequences were found in 10 samples isolated from air, sediment, soil, and water in various habitats including cropland, forest, shrubland, wetland, anthropogenic, and aquatic environments in the USA (California, Louisiana, North Carolina, and Tennessee).

Notes. Distinguishing *C. crypta* from other species within the *C. sordida* complex presents significant challenges. Nonetheless, *C. crypta* can be reliably differentiated through analysis of ITS, *rpb2*, and *tef1-α* sequences. Moreover, *in vitro* observations revealed that *C. crypta* demonstrates the highest growth rate within its species complex (Fig. 5). It is worth noting that *C. crypta* is unique as its mycelium completely colonizes culture plates within a two-week period when cultivated on MEA and PDA, and within a four-week period when cultivated on CMD, MLA, and PCA media at 23 °C compared to *C. melanospora* and *C. sordida*. In addition, *C. crypta* grows well at 37 °C and exhibits a growth also at 41 °C (Fig. 6). The mycelium of *Ceratostomella* spp. *in vitro* is pigmented and remains sterile. In *C. crypta*, we observed monilioid hyphae, either branched or unbranched, growing from the septate hyphae. On MEA and MCA, monilioid hyphae are more dominant compared to those on PDA. Occasionally, these hyphae appear tuberose (budding-like), a feature that becomes more pronounced with age (Fig. 6F).

Ceratostomella crypta is represented by three isolates in our phylogeny. Two strains that were isolated from ascospores originate from the same locality in the Czech Republic, while the third is from the USA and is only known in its asexual state. In the Czech specimens, ascospores were observed either strongly collapsed within the asci (CBS 131683, Fig. 4G–K) or mostly retaining their full shape (CBS 131684, Fig. 4E, F) after rehydration, considerably impacting the ascus size. In the closely related species, such as *C. melanospora* and *C. sordida*, the difference in ascus size is less pronounced based on ascospore shape.

***Ceratostomella cuspidata* (Fr.) Réblová, Mycologia 98: 77. 2006.**

Sphaeria cuspidata Fr., Syst. Mycol. 2: 220. 1823. Basionym.
≡ *Ceratostoma cuspidatum* (Fr.) Sacc., Syll. Fung. 1: 474. 1882.

Description. See Réblová (2006).

Specimens examined. Belgium • Locality and date unknown; B. Declerque (IFBL 57.31, culture no longer viable). New Zealand • West Coast Region, Westland District, Mount Aspiring National Park, Makarora Bush Walk, 500 m N of NP Headquarters in Makarora; decaying wood of *Nothofagus* sp.; 30 Mar 2005; M. Réblová M.R. 2964/NZ 629 (PDD 123700, culture ICMP 17629).

Habitat and geographical distribution. Saprobe on decaying wood of *Nothofagus* sp., *Quercus* sp., and other unidentified hosts, known in the Czech Republic, New Zealand, Norway and Sweden (Fries 1823; Réblová 2006; MyCoPortal). According to GlobalFungi, *C. cuspidata* is distributed in temperate and subtropical regions in both the Northern and Southern Hemispheres. Identical sequences were found in 28 samples isolated from air and soil in forest and anthropogenic habitats, and occasionally in croplands, grasslands, and shrublands biomes in Australia, Indonesia and New Zealand. The environmental data suggest that *C. cuspidata* is especially widespread in Australasia.

Notes. In our phylogeny, the species is represented by two isolates from Belgium and New Zealand. *Ceratostomella cuspidata* is well distinguishable from other species by its suballantoid to reniform ascospores, often flattened on one side, measuring 4–5 × 2–3 µm (Réblová 2006). The ascospores are arranged in a fascicle or they are 2–3-seriate in the sporiferous part of the ascus. *Ceratostomella rostrata* closely resembles *C. cuspidata* but stands out due to its larger ascomata and narrower allantoid to suballantoid ascospores.

Ceratostomella melanospora **Réblová, sp. nov.**
MycoBank No: 855704
Figs 7, 8

Etymology. *Melanos* (Greek) meaning black, dark, *spora* (Latin) from Ancient Greek *sporá*, meaning a seed, referring to brown ascospores.

Type. Czech Republic • Pardubice Region, Chrudim district, Železné hory Mts. Protected Landscape Area, Horní Bradlo, Malá Střítež settlement, Polom National Nature Reserve; 600 m alt.; on decaying wood of *Fagus sylvatica*; 9 Oct 2020; M. Réblová M.R. 4088 (holotype PRA-21822!, ex-type culture CBS 147993).

Description. ***Sexual morph*****.** Ascomata non-stromatic, densely grouped or solitary, superficial, semi-immersed or immersed with only neck protruding. Venter 300–480 µm diam, subglobose, upright or lying horizontally in the host tissue, dark brown to black, with brown, septate, slightly flexuous hairs 2.5–4 µm wide sparsely covering the sides and bottom. Neck 90–100 µm wide, up to 500 µm long, central, cylindrical, upright, glabrous, tapering, apex sulcate; the neck is sometimes slightly wider near the top. Ostiole periphysate. Ascomatal wall fragile to leathery, 55–65 µm thick, two-layered. Outer layer consisting of thick-walled, dark brown, polyhedral cells with opaque walls of textura prismatica, with several cells forming the external crustose layer ca. 8–13 µm thick, cells tend to be more flattened and paler towards the interior. Inner layer consists of several rows of thin-walled, hyaline, flattened cells. Paraphyses abundant, longer than the asci, may become partially disintegrated with age, septate, constricted at the septa, hyaline, (5–)6.5–10.5 µm wide, wider near the base, tapering to 3–4 µm. Asci 63–78 × 6.5–8(–8.5) µm (mean ± SD = 70.8 ± 4.2 × 7.2 ± 0.7 µm), 51–60(–62.5) µm (mean ± SD = 57.0 ± 3.3 µm) long in the sporiferous part; truncate at the apex, cylindrical, with a short tapering stipe, apical annulus non-amyloid, ca. 2.5 µm wide, 1–1.5 µm high, 8-spored. Ascospores (8–)8.5–10.5(–11) × 4–5 µm (mean ± SD = 9.3 ± 0.7 × 4.5 ± 0.3 µm), ellipsoidal, slightly apiculate at both ends, brown, aseptate, smooth, with an

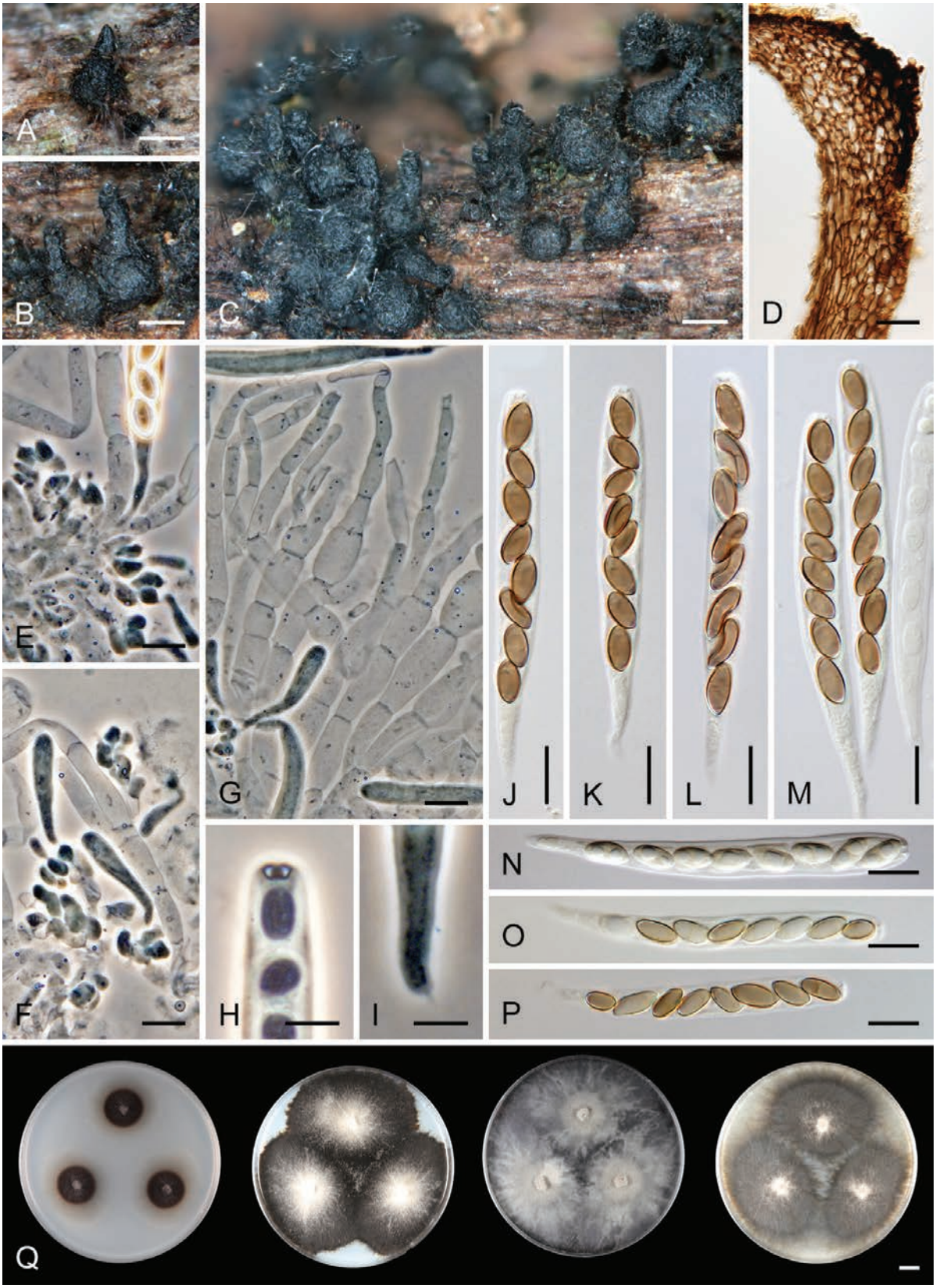

Figure 7. *Ceratostomella melanospora* (**A–P** from holotype PRA-21822 **Q** from ex-type strain CBS 147993) **A–C** ascomata **D** a longitudinal section of the ascomatal wall **E, F** asci with ascogenous cells **G** paraphyses **H** ascal apex **I** stipe of the ascus **J–M** asci with ascospores **N–O** asci of different ages with maturing ascospores **Q** colony morphology at 23 °C after 4 weeks on CMD, MLA, OA and PCA (from left to right). Images: on natural substrate (**A–P**). Scale bars: 500 µm (**A–C**); 20 µm (**D**); 10 µm (**E–G, J–P**); 5 µm (**H, I**); 1 cm (**Q**).

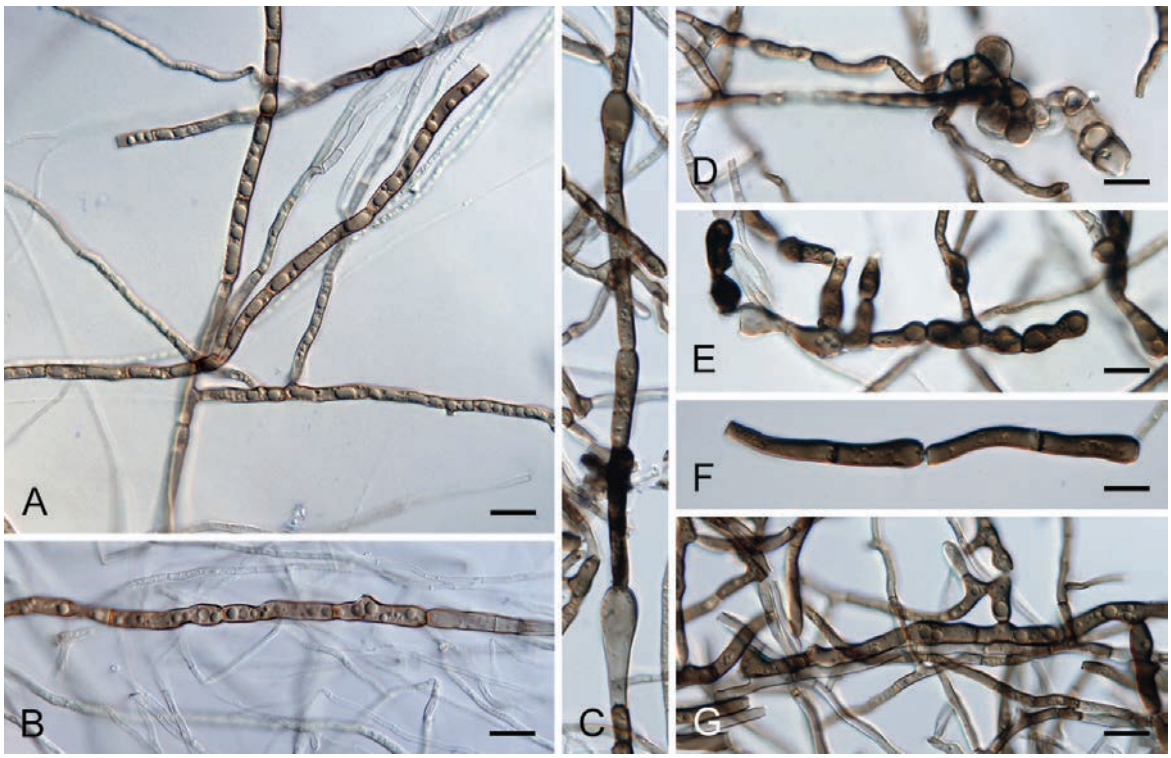

Figure 8. Vegetative mycelium of *Ceratostomella* spp. on MLA **A, B** *C. melanospora* CBS 147993 **C–G** *C. sordida* CBS 116000. Scale bars: 10 µm (**A–G**).

inconspicuous germ pore at one or both ends, occasionally with one oil drop, often collapsing, obliquely uniseriate or partially overlapping, or partially 2-seriate within the ascus. ***Asexual morph*.** Unknown.

Culture characteristics (after 2/4 wk at 23 °C). On CMD colonies 30–32 mm/64–70 mm diam, circular, flat, margin diffuse, cobwebby, mucoid towards the margin, dark brown, with an outer beige zone of conspicuous submerged growth, reverse of the same colour. On MLA colonies 20–21 mm/48–50 mm diam, circular, flat margin fimbriate to somewhat lobate, floccose and whitish grey centrally, cobwebby to mucoid and dark olivaceous grey towards the periphery, reverse of the same colour. On OA colonies 28–30 mm/73–75 mm diam, circular, flat, margin diffuse, lanose and pale olivaceous grey at the centre, sparse to cobwebby and olivaceous black towards the margin, reverse dark brown. On PCA colonies 17–18 mm/53–54 mm diam, circular, flat, margin rhizoidal, submerged, floccose and beige-grey centrally, cobwebby and dark brown towards the margin, reverse dark brown. Sporulation was absent on all media.

Temperature dependent growth at 30, 35, 37, 41 °C was assessed as colony diam on MEA, PDA, and OA, respectively, after a period of two weeks: 30 °C 27–29 mm/23–24 mm/23 mm, 35 °C no growth/no growth/no growth, 37 °C no growth/no growth/no growth, 41 °C no growth/no growth/no growth.

On MLA, colonies are effuse, with submerged hyphae 1–2 µm in diameter. These hyphae are hyaline to subhyaline, sparsely branched, septate, smooth, intertwined with vein-like dark brown hyphae, 3–4.5 µm in diameter. Monilioid hyphae were not observed.

Habitat and geographical distribution. This species is a saprobe on decaying wood of *Fagus sylvatica* and is known to occur in the Czech Republic. According to GlobalFungi, identical sequences were identified in seven environ-

mental samples obtained from various localities within the temperate zone of the Northern Hemisphere. These samples were primarily isolated from air and soil in cropland and forest biomes, with occasional findings in anthropogenic habitats in Canada, China, Italy, and Sweden.

Notes. *Ceratostomella melanospora* is characterised by ellipsoidal, slightly apiculate, mid-brown ascospores arranged 1-seriately, occasionally partially 2-seriately in the ascus. The species is micromorphologically indistinguishable from *C. crypta* and *C. sordida* but differs by the colony characteristics and can also be clearly differentiated by ITS, *rpb2*, and *tef1-α* sequences. Pigmented monilioid hyphae, which formed abundantly in the culture of *C. crypta* and to some extent in *C. sordida*, were not observed in *C. melanospora* (Fig. 8).

***Ceratostomella novae-zelandiae* (Réblová) Réblová, comb. nov.**
MycoBank No: 855705
Fig. 9

Xylomelasma novae-zelandiae Réblová [as '*novaezelandiae*'], Mycologia 98: 87. 2006. Basionym.

Description. See Réblová (2006).

Specimen examined. New Zealand • West Coast Region, Westland District, Haast 300 km SW of Greymouth, Jackson River valley, track to the Lake Ellery; on decaying wood of a stump of *Nothofagus* sp.; 10 Mar 2003; M. Réblová M.R. 2787/NZ 297 (holotype PDD 81433!).

Habitat and geographical distribution. Saprobe occurring on decaying wood of *Nothofagus* sp. in New Zealand (Réblová 2006). According to GlobalFungi, identical sequences were found in two samples isolated from soil in temperate broadleaf forest habitats in New Zealand and Chile.

Notes. *Ceratostomella novae-zelandiae* is distinguished from the other two species in the *C. sordida* complex by its smaller asci, measuring 50–60(–65) × 7–8(–9) µm, and smaller ascospores, measuring 7–8 × (3.5–)4–5 µm.

***Ceratostomella pyrenaica* Réblová & J. Fourn., Mycologia 98: 78. 2006.**

Description. See Réblová (2006).

Specimens examined. Czech Republic • South Moravian Region, Hodonín district, Mikulčice, Skařiny Nature Reserve; on decaying wood of a trunk of *Acer campestre*; 24 Oct 2004; M. Réblová, M.R. 2912 (paratype PRA-21823, CBS 117116); • *Ibid*.; Břeclav district, Valtice, Rendez-vous National Nature Monument; on decaying wood of a branch of *Quercus* sp.; 20 Nov. 2010; M. Réblová M.R. 3566 (PRA-21824, CBS 129343); • *Ibid*.; Břeclav district, Milovice, Křivé jezero Nature Reserve, road near Panenský mlýn; on decaying wood of a trunk of *Quercus* sp.; 17 Nov 2010; M. Réblová M.R. 3584 (PRA-21825).

Habitat and geographical distribution. Saprobe on decaying deciduous wood of *Acer campestre*, *Alnus glutinosa*, *Quercus* sp. and other unidentified hosts, and on decaying basidioma of *Trametes gibbosa*, known from the Czech Republic, Belgium and France (Réblová 2006; MyCoPortal; this study). Accord-

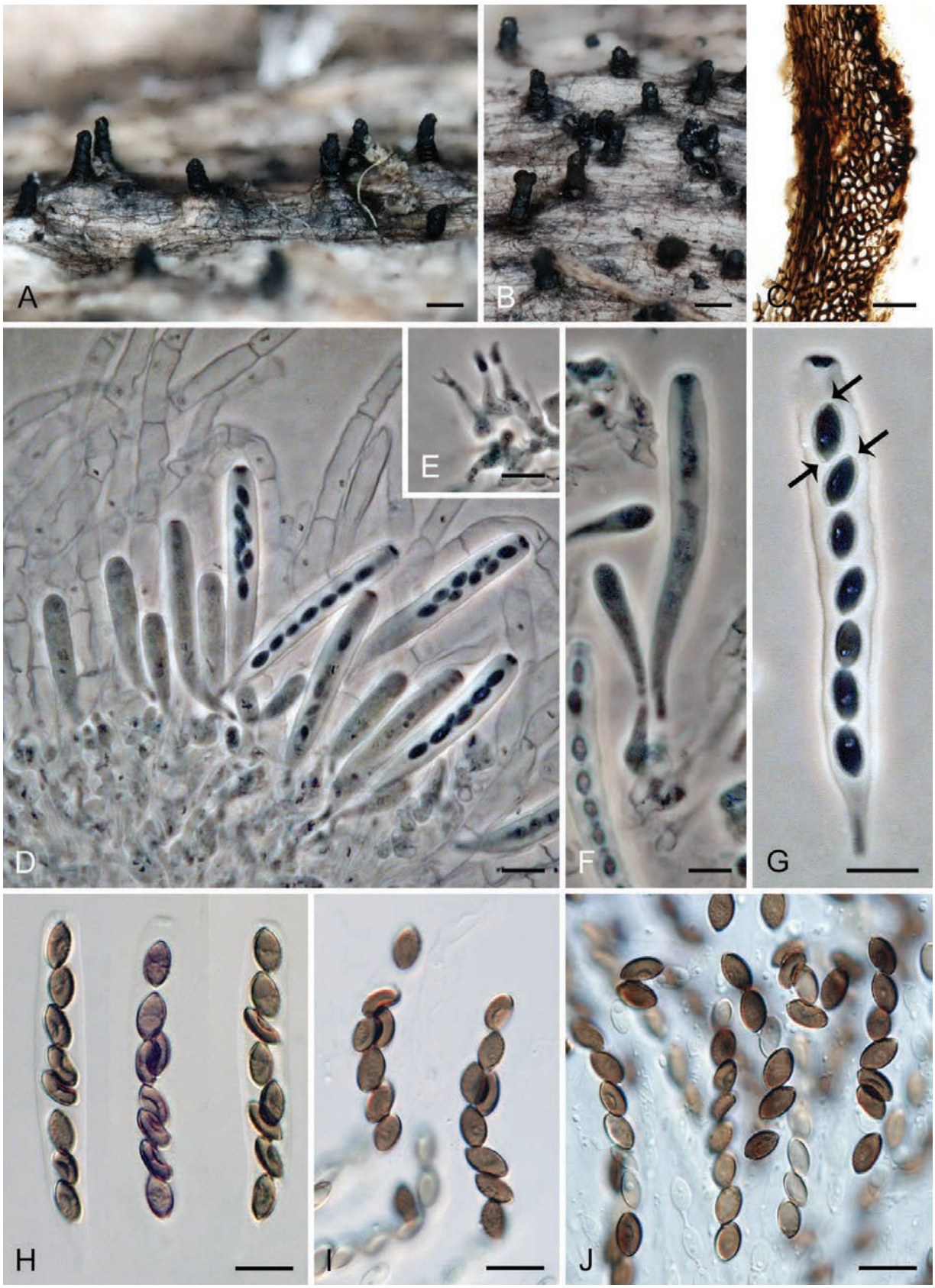

Figure 9. *Ceratostomella novae-zelandiae* (holotype PDD 81433) **A, B** ascomata **C** a longitudinal section of the ascomatal wall **D–F** paraphyses, ascogenous cells, and asci **G** young ascus (arrows indicate ends of ascospores with pores, where the outer wall becomes thinner) **H–J** asci with ascospores. Images: on natural substrate (**A–J**). Scale bars: 500 µm (**A, B**); 20 µm (**C**); 10 µm (**D–J**).

ing to GlobalFungi, identical sequences were found in 50 samples collected in temperate and subtropical regions. These samples mainly originated from air, soil, but also shoots, roots and deadwood. *Ceratostomella pyrenaica* is commonly found in croplands and forests, also in grasslands, woodlands and anthropogenic habitats in Croatia, Czech Republic, Italy and the USA (Hawaii, Michigan, and North Carolina).

Notes. *Ceratostomella pyrenaica* is well distinguished from other species by its ellipsoidal to oblong ascospores, which are slightly curved, apiculate at both ends and flattened on one side, pale brown, measuring 7–9 × 3–4 µm.

Ceratostomella rhynchophora **(De Not.) Réblová, Mycologia 98: 78. 2006.**

Sordaria rhynchophora De Not., Comment. Soc. Crittog. Ital. 2(3): 480. 1867. Basionym.
≡ *Ceratostoma rhynchophora* (De Not.) W. Kirschstein, Krypt.-Fl. Brandenburg 7: 249. 1911.
= *Ceratostoma notarisii* Sacc., Nuovo Giorn. Bot. Ital. 7: 308. 1875.

Description. See Réblová (2006).

Specimens examined. France • Pyrénés Atlantiques, Ariège, Rimont, Las Muros; on decaying wood of *Prunus domestica*; 3 Feb 2002; J. Fournier J.F. 02022 (PRA-21826) • *Ibid*.; 21 Apr 2002; J. Fournier J.F. 02070 (PRA-21827).

Habitat and geographical distribution. Saprobe on decaying wood of *Betula papyrifera*, *Prunus domestica*, and on decaying basidioma of *Fomes fomentarius*, known in Canada, France, Italy, and Poland (De Notaris 1867; Réblová 2006; MyCoPortal).

Notes. The neotype of this species (Italy, decaying wood of *Prunus domestica*, P.A. Saccardo, PAD; as *Ceratostoma notarisii*) was designated by Réblová (2006). The species is characterised by ellipsoidal, slightly apiculate ascospores, sometimes flattened on one side, measuring 6–7 × (3.5–)4–5 µm. The ascospores are mid-brown, with a minute pore at each end, and are arranged 1–2-seriately or in a fascicle within the ascus. Given the shape of the ascospores, the species resembles members of the *C. sordida* complex, but it clearly differs by having smaller ascospores.

Ceratostomella rostrata **(Tode) Sacc., Syll. Fung. 1: 408. 1882.**

Sphaeria rostrata Tode, Fungi Mecklenb. Sel. 2:14. 1791. Basionym.
≡ *Dryinosphaera rostrata* (Tode) Dumort., Comment. bot.: 88. 1822.
≡ *Cryptosphaeria rostrata* (Tode) Ces. & De Not., Comm. Soc. crittog. Ital. 1(fasc. 4): 231. 1863.
≡ *Ceratostoma rostratum* (Tode) Fuckel, Jahrb. Nassau. Ver. Naturk. 23–24:127. 1870.
≡ *Cerastoma rostratum* (Tode) Quél., Mém. Soc. Émul. Montbéliard, Sér. 2, 5: 521. 1875.
≡ *Ceratosphaeria rostrata* (Tode) Sacc., Syll. Fung. 2: 227. 1883. (as '[Kickx] Sacc.').
≡ *Cerastostomella rostrata* (Tode) Massee, Grevillea 17(84): 73. 1889.

≡ *Endoxyla rostrata* (Tode) Munk, Dansk Bot. Ark. 17: 196. 1957.
= *Ceratostoma grumsinianum* W. Kirschst., Ann. Mycol. 34:199. 1936.
= *Wegelina polyporina* M.E. Barr, Cryptogamie, Bryol. Lichenol. 19:170. 1998.[1]

Description. See Réblová (2006).

Habitat and geographical distribution. Saprobe on decaying basidioma of *Fomes fomentarius* and decaying wood of *Acer saccharum*, *Acer* sp., *Coriaria* sp., *Fraxinus* sp., *Morus* sp., *Ostrya* sp., *Quercus pedunculata*, *Quercus* sp., *Populus tremuloides*, *Robinia pseudoacacia*, *Ulmus glabra*, *Ulmus* sp., and other unknown hosts, known in Belgium, Canada, Czech Republic, Denmark, Finland, France, Netherlands, Norway, Germany, Poland, Sweden, Switzerland, and the USA (Tode 1791; Kirschstein 1936; Barr 1998; Réblová 2006; MyCoPortal).

Notes. Réblová (2006) designated the lectotype (illustration; Tode 1791: fig. 79) and epitype (Fries´s Scleromyceti Sueciae 116, decayed wood, PRM 666367) of *C. rostrata*. Untereiner (1993), in her revision of the genus *Endoxyla*, cited *Ceratostomella ampullasca* (Saccardo 1882) and *Endoxyla laevirostris* (Munk 1965) as synonyms of *C. rostrata*. However, recent collections and molecular DNA data have revealed that these two species are conspecific and were reclassified as *Natantiella ligneola* (Réblová and Štěpánek 2009). There are numerous records of *C. rostrata* in MyCoPortal; however, these may represent species of *Endoxyla*, as the synonymy of this species was only recently clarified. Accurate identification would require a thorough examination of the herbarium specimens cited, which are housed in various collections around the world.

Ceratostomella rostrata is somewhat similar to *C. cuspidata*; however, it differs in having larger ascomata and pale brown, allantoid to suballantoid, narrower ascospores measuring 4.5–6 × 1.5–2 µm. These ascospores are typically arranged in a fascicle in the upper part of the ascus or are 2–3-seriate within the ascus. Molecular data for this species are not available.

***Ceratostomella sordida* (Réblová) Réblová, comb. nov.**
MycoBank No: 855706
Figs 8, 10

Xylomelasma sordida Réblová, Mycologia 98: 88. 2006. Basionym.

Description. See Réblová (2006).

Characteristics in culture (after 2/4 wk at 23 °C). On CMD colonies 38–40 mm/72–73 mm diam, circular, flat, margin diffuse to slightly fimbriate, cobwebby, olivaceous-brown, reverse of the same colour. On MLA colonies 35–36 mm/76–80 mm diam, circular, flat, sub-entire with a tendency towards a fimbriate edge, lanose, zonate, whitish grey centrally with an olivaceous brown intermediate zone, dark olivaceous grey towards the periphery, reverse dark olivaceous. On OA colonies 34–35 mm/77–79 mm diam, flat, margin diffuse, floccose to cobwebby, olivaceous grey to olivaceous brown, aerial hyphae with

1 Synonymy adopted from Réblová (2006).

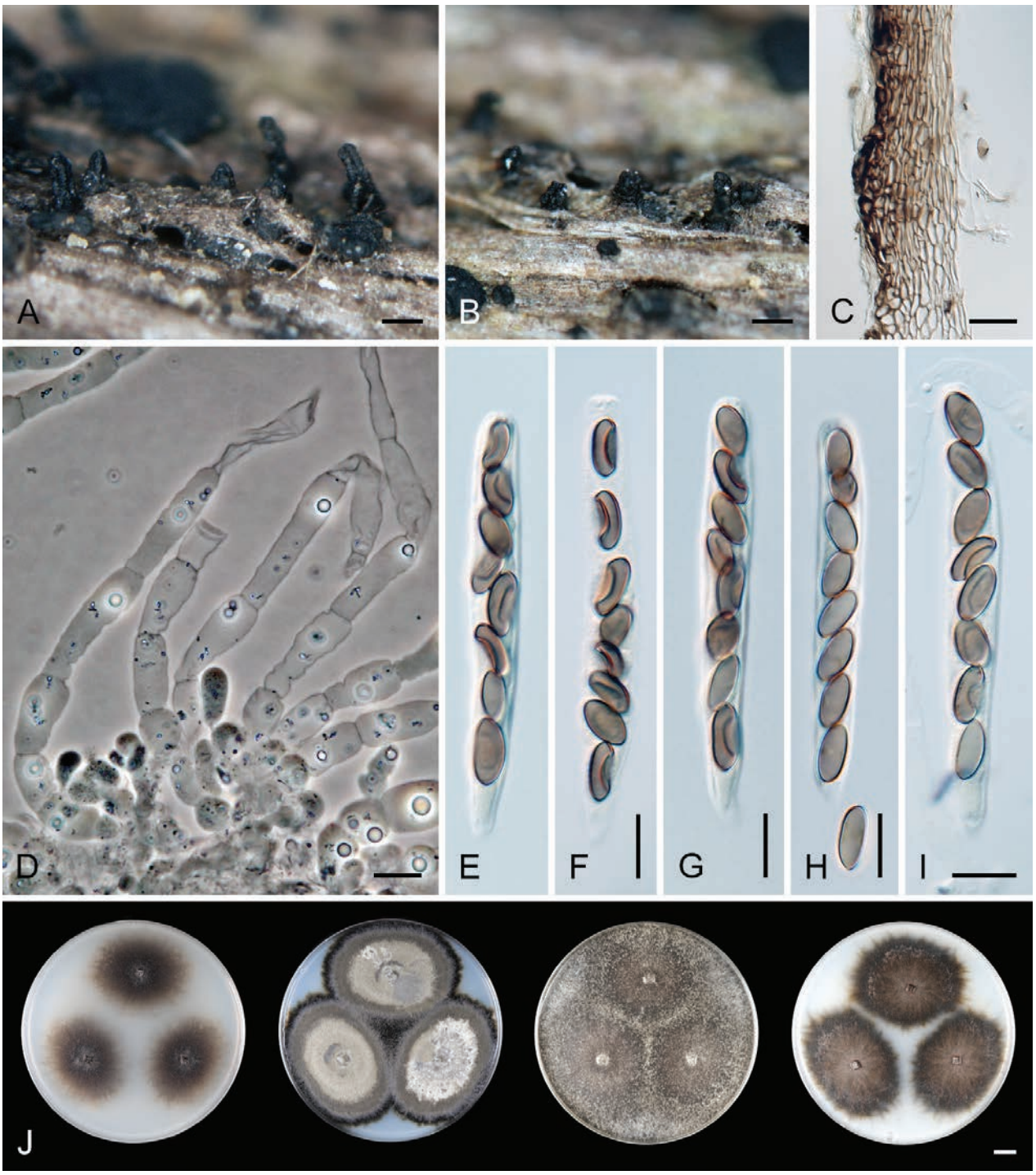

Figure 10. *Ceratostomella sordida* (**A–I** from holotype PRM 902275 **J** from ex-type strain CBS 116000) **A, B** ascomata **C** a longitudinal section of the ascomatal wall **D** paraphyses with ascogenous cells **E–I** asci with ascospores **J** colony morphology at 23 °C after 4 weeks on CMD, MLA, OA and PCA (from left to right). Images: on natural substrate (**A–I**). Scale bars: 500 µm (**A, B**); 20 µm (**C**); 10 µm (**D–I**); 1 cm (**J**).

numerous colourless droplets, reverse of the same colour. On PCA colonies 30–31 mm/58–60 mm diam, circular, flat, margin rhizoidal, sparse to cobwebby, whitish brown at the centre, dark brown towards the periphery, reverse dark brown. Sporulation was absent on all media.

Temperature dependent growth at 30, 35, 37, 41 °C was assessed as colony diam on MEA, PDA, and OA, respectively, after a period of two weeks: 30 °C 58–60

mm/55–58 mm/49–50 mm, 35 °C 60–61 mm/58–59 mm/46–47 mm, 37 °C 37–39 mm/30 mm/14–19 mm, 41 °C germination only/ 5–7 mm/no growth.

On MLA, colonies are effuse, with submerged hyphae 1.5–3 µm in diameter; hyphae are smooth, branched, septate, subhyaline to pale brown, intertwined with dark brown, vein-like hyphae with occasional tuberose formations, 4–6.5 µm in diameter. Dark brown monilioid hyphae 5.5–9 µm in diameter, composed primarily of rectangular cells, occur rarely.

Specimen examined. France • Pyrénés Atlantiques: Ariège, Lescure, Bois du Pas du Baup; 500 m alt.; on rotten wood of *Alnus glutinosa*; 24 Feb 2004; J. Fournier J.F. 04020 (holotype PRM 902275!, ex-type culture CBS 116000).

Habitat and geographical distribution. Saprobe that decomposes the wood of *Alnus glutinosa*, *Eucalyptus viminalis*, *Fagus sylvatica*, *Populus* sp. and other unidentified hosts. It has been found in Argentina, Canada, Czech Republic, Denmark, France, Hungary, New Zealand and Norway (Réblová 2006; MyCoPortal). According to GlobalFungi, *C. sordida* is distributed worldwide in temperate, subtropical and tropical regions of Asia, Australasia, Europe and North and South America. Identical sequences were found in 126 samples isolated mainly in cropland and forest habitats, but also in air, dust, deadwood, grassland, roots, shoots, soil (including rhizosphere soil), tundra, water, and aquatic and anthropogenic habitats in Argentina, Austria, Brazil, Canada, China, Costa Rica, France, French Guyana, Italy, Indonesia, Japan, New Zealand, Papua New Guinea, Romania, Russia, Spain, Sweden, Switzerland, South Korea, and the USA (California, Florida, Iowa, Louisiana, North Carolina, Oklahoma, Pennsylvania, and Tennessee).

Notes. In culture, *C. sordida* rarely forms short monilioid hyphae (Fig. 8), in contrast to *C. crypta*, where these hyphae form frequently and are much longer (Fig. 6). We re-examined the holotype of *C. sordida* (Réblová 2006), focusing on the measurements of both asci and ascospores. Despite fully rehydrating the centrum of the aged material, we observed that the ascospores were slightly smaller 8–10.5 × (3.5–)4–5 µm compared to the previously recorded dimensions of 9–12 × 4–6 µm. Similarly, the asci showed a narrower width of 6.5–8 µm, contrasting with the previously reported range of 7–10(–13) µm. For accuracy, we provide both measurements in the fresh and aged material. Two species introduced in this study, *C. crypta* (CBS 131683, CBS 131684) and *C. melanospora* (CBS 147993), were hidden among the herbarium material labelled as C. *sordida*.

Excluded or ambiguous species

***Xylomelasma moderata* Lar.N. Vassiljeva & S.L. Stephenson, Mycosphere 5: 223. 2014. Nom. inval., Art. F.5.1 (Shenzhen).**

Notes. The species was collected on unidentified decaying wood in the USA (Virginia) (Vassiljeva and Stephenson 2014). However, it was not validly published as an identifier issued by a recognised repository was not cited in the protologue. The species is morphologically distinct from *Ceratostomella* and, based on available morphological data, it represents *Calyptosphaeria subdenudata* (Réblová et al. 2018).

***Xylomelasma shoalensis* A.N. Mill., Y. Marín & Stchigel, Sydowia 68: 224. 2016.**

Specimen examined. USA – Illinois • Montgomery County, Shoal Creek Conservation Area; 39.1871, -89.5963; on 6 cm. diam. decorticated branch on the ground; 4 Apr 2004; A.N. Miller ANM 1 (holotype ILLS 76895!).

Notes. The only available LSU sequence (KX290919, Hernández-Restrepo et al. 2016) of *X. shoalensis* indicates that the species is a member of *Ceratostomella* (Fig. 1). Based on the sequence similarity with *X. sordida* (99.2%), they are likely conspecific. However, according to its diagnosis, this species does not match the generic delimitation of *Ceratostomella*. *Xylomelasma shoalensis* was described with immersed, globose to subglobose and smaller (175–265 µm diam) ascomata featuring a rostrate, slender, non-sulcate neck and hyaline to yellowish-brown, oblong to suballantoid, septate ascospores in unitunicate asci. Its LSU sequence was not obtained from a mycelium of an axenic culture but directly from ascomata on the host. It is evident that morphology belongs to a different genus and species. We examined the holotype, but no traces of a *Ceratostomella*-like fungus could be found. Therefore, due to this ambiguity, *X. shoalensis* is excluded from *Ceratostomella*.

Discussion

Phylogenetic analyses utilising three and five molecular markers, respectively, revealed that *Ceratostomella* (Saccardo 1878) and *Xylomelasma* (Réblová 2006) are congeneric. The analysed species included *C. cuspidata* and *C. pyrenaica* representing *Ceratostomella*, along with the ex-type strains of *X. sordida*, the type of *Xylomelasma*, and *X. novae-zelandiae*. In both phylogenies, *Ceratostomella* consisted of three subclades: *Ceratostomella*, the *C. sordida* species complex, and *C. novae-zelandiae*. However, the position of *C. novae-zelandiae* varied between the two data sets; it either clustered on a basal branch or as a sister to the *Ceratostomella* subclade. *Ceratostomella novae-zelandiae* was originally placed in *Xylomelasma* based on morphological similarities, as no living culture or DNA data were available at the time (Réblová 2006). In this study, DNA was successfully extracted from ascomata of the holotype of *X. novae-zelandiae* PDD 81433 and new ITS, LSU, and SSU sequences were generated. However, the amplification of protein-coding genes was not successful. *Ceratostomella* is currently recognised with eight species which are listed here. Another species, referred to as *Ceratostomella* sp., was placed in the genus by Réblová (2006). It is characterised by its unique globose ascospores, which are distinct from the reported ascospore variability. This species has not been formally described due to the limited herbarium material that could serve as a holotype and lack of a living culture. Recollection and molecular data of this species are needed to support its placement in the genus.

Ceratostomella and *Xylomelasma* exhibit high morphological similarity, with differences primarily in the position of ascospores within the ascus, the variable visibility of the apical annulus, the ornamentation of the neck, and the morphology of the paraphyses. However, the phylogenetic analysis revealed that *Ceratostomella* exhibits greater variability in these morphological traits than previously recognised, supporting the reclassification of *Xylomelasma* as a synonym of *Ceratostomella*. Smaller ascospores, ranging from suballantoid

to reniform shapes, tend to be arranged 2–3-seriately or form fascicles in the sporiferous part of the ascus, whereas ellipsoidal and globose ascospores are generally 1–2-seriate within the ascus. The ascospores are aseptate, glabrous and hyaline when young, becoming brown at maturity before being released from the asci. Characters such as the terminal germination pores are particularly well-visible in immature hyaline ascospores (Fig. 9G). A common characteristic of *Ceratostomella* ascospores is their frequent collapsing apparently upon drying, which may influence the size of the sporiferous part of the ascus.

Species of *Ceratostomella* typically possess a thick ascomatal wall, often adorned with tubercles on the exterior. This wall is composed of thick-walled, dark brown to dark reddish-brown cells, which may contain Munk pores (*C. cuspidata*, *C. rostrata*, and *C. sordida*). The neck in all species is sulcate and ornamented with 4–5 ridges at the top, except for *C. novae-zelandiae*, which has a glabrous neck. The apical, non-amyloid annulus is present in all species and is most visible with phase contrast microscopy, although its visibility can vary. In the former *Xylomelasma* species, *C. sordida* and *C. novae-zelandiae*, the paraphyses are composed of slightly longer cells, but are similarly constricted, primarily in the lower part.

A prominent morphological trait shared by both genera is the ascogenous system. This system comprises short ascogenous hyphae with lateral and terminal discrete cells from which asci emerge as outgrowths. The asci and ascogenous cells are connected by a tapering stipe; its bottom part is sometimes visible as a thread-like connective between the ascus and ascogenous cell. The stipe eventually disintegrates at maturity, allowing the asci to float freely in the centrum. The ascus stipe often contains non-refractive material deposited at the basal part, which becomes visible after the ascus dehisces from the ascogenous cell.

The morphology of the ascogenous system can be peculiar in some taxa and has significant diagnostic value at the genus level. These taxonomically important traits include the attachment of asci to ascogenous hyphae, the presence or absence of discrete cells from which asci arise, and the overall architecture of these formations. For instance, members of the order Calosphaeriales, many of which include former *Ceratostomella* species, (including genera such as *Calosphaeria*, *Flabellascus*, *Jattaea*, *Pleurostoma*, and *Togniniella*) and Togniniales (*Phaeoacremonium*) possess morphologically distinct ascoma centrums specific to each genus (Barr 1985; Barr et al. 1993; Mostert et al. 2006; Réblová 2011; Réblová et al. 2015a).

Another example of a distinct ascogenous apparatus is found in the genus *Barbatosphaeria* of Barbatosphaeriaceae, which encompasses several species initially classified in *Ceratostomella*. This feature was first observed in *B. fagi* by Samuels and Candoussau (1996) and later recognised as a diagnostic feature of the genus by Réblová et al. (2015b). In *Barbatosphaeria*, the asci taper towards a slender stipe, with the basal part of the stipe conspicuously swollen. This swollen base remains attached to the ascogenous hyphae after the mature ascus is liberated and floats freely in the centrum. The attachment of asci to ascogenous hyphae and the mechanism of ascus dehiscence in *Barbatosphaeria* is somewhat similar to that of *Ceratostomella*, its closest relative, although the stipe in *Barbatosphaeria* is more robust and does not transform into a thread-like filament. The ascogenous cells present in *Ceratostomella* are

absent in *Barbatosphaeria*. However, the attached torso of the swollen base of the ascus stipe in *Barbatosphaeria* mimics these cells and may represent an evolutionary pathway, leading to the development of discrete ascogenous cells.

Phylogenetic analyses using three distinct barcodes have uncovered two cryptic species within the *C. sordida* complex, now identified as *C. crypta* and *C. melanospora*. By analysing five genes: the slow-evolving rDNA genes LSU and SSU, alongside a rapidly evolving ITS gene (primary fungal barcode, Schoch et al. 2012) and the slow-evolving protein-coding genes *rpb2* and *tef1-α* (non-rDNA secondary barcodes, Stielow et al. 2015), we were able to elucidate the phylogenetic relationships within the *C. sordida* species complex (Fig. 2). These findings were corroborated by phylogenetic analysis based on the LSU, SSU, and *rpb2* genes (Fig. 1), further validating the distinctiveness of the new species within the complex.

Traditional diagnostic morphological characters have proven insufficient for characterising species within *C. sordida* complex. *Ceratostomella crypta* and *C. melanospora* are morphologically indistinguishable from *C. sordida* and from each other in terms of ascospores, asci, paraphyses, and ascomata, but they can be clearly differentiated by molecular data and the size of their genome. In culture, their vegetative mycelium was darkly pigmented and fast-growing, with all species remaining sterile on various nutrient media and when exposed to UV light. Although no significant morphological differences could be identified among members of the *C. sordida* species complex on the natural substrate, *C. crypta* typically formed monilioid hyphae (Fig. 6) and demonstrated the fastest growth rate *in vitro* (Fig. 5). Notably, within the same time frame, the mycelium of *C. crypta* covered the entire plate (or nearly the entire plate) when grown on MEA, OA and PDA (in two weeks) and CMD, MLA, OA and PCA (in four weeks) compared to *C. melanospora* and *C. sordida*. Interestingly, *C. crypta* and *C. sordida* exhibited growth at 37 °C, which is one of the four key criteria for a fungal strategy to colonize and parasitize the tissues of humans and other mammals (Köhler et al. 2015). Additionally, *C. crypta* demonstrated growth at 41 °C on MEA, OA, and PDA, whereas *C. sordida* exhibited growth at this temperature only on PDA.

The closest relative to *Ceratostomella* recruits from *Barbatosphaeria*. *Ceratostomella* and *Barbatosphaeria* form sister clades; however, their relationship is not statistically supported (–/0.99). This grouping (–/1.0) was first identified in the molecular systematic study of *Barbatosphaeria*, where it received strong support in BI analysis but no statistical support in ML analysis (Réblová et al. 2015b). Zhang et al. (2017) proposed the family Barbatosphaeriaceae to include *Barbatosphaeria*, *Ceratostomella* and *Xylomelasma*), although the grouping was supported only in the BI analysis. The lack of statistical support from ML analysis for this monophyly does not warrant the inclusion of *Ceratostomella* in Barbatosphaeriaceae, as proposed by Zhang et al. (2017). Currently, *Ceratostomella* is accepted as a genus *incertae sedis*, while Barbatosphaeriaceae remains a monotypic family. We suggest that better taxon sampling of species, currently unknown to us, is needed to provide support for the inclusion of *Ceratostomella* in Barbatosphaeriaceae.

Ceratostomella shares several morphological similarities with the genus *Melanospora* (Corda 1837) of the family Ceratostomataceae (*Melanosporales*, *Hypocreomycetidae*), such as ascomata with a rostrate neck (which may

be adorned with coronal setae or lack them) and dull brown, aseptate ascospores with terminal pores. However, *Melanospora* distinctly differs from *Ceratostomella* by its evanescent asci, the absence of paraphyses, and the presence of pseudoparenchyma in the centrum (Luttrell 1951; Cannon and Hawksworth 1982). *Ceratostomella* also exhibits certain similarities to the genus *Cannonia* (Taylor and Hyde 1999), including dark ascomata with long necks and brown ellipsoidal ascospores. Nonetheless, *Cannonia* can be distinguished from *Ceratostomella* by its ascospores with a full-length germ slit, filiform paraphyses, the presence of a rudimentary stroma, and a dark clypeus around the base of the neck. Additionally, *Ceratostomella* differs from both genera in the morphology of its ascogenous system.

Conclusions

This study provides new morphological, molecular, and biogeographical data, offering deeper insights into the genus *Ceratostomella* and clarifying interspecific relationships. Based on phylogenetic analyses and comparative morphological studies, we have transferred the genus *Xylomelasma* to *Ceratostomella*, proposed two new combinations, and described two new species. We recognise eight species within the genus. Members of *Ceratostomella* are distributed worldwide in temperate, subtropical and tropical zones of Asia, Australasia, Europe and North and South America. Based on field observations (Réblová 2006; this study) and metabarcoding data in GlobalFungi (Větrovský et al. 2020), *C. sordida* emerges as the most common species of *Ceratostomella* among those with available DNA sequence data. It was identified in 126 environmental samples and several herbarium collections. On the other hand, *C. novae-zelandiae* is recognised as a rare species. It has been identified in only one field record from New Zealand and two environmental samples from GlobalFungi (Chile and New Zealand), confirming the occurrence of this species in the Southern Hemisphere. To improve the standards and reproducibility of our research, we are publishing WGS data. This not only supports future descriptions of new 'dark taxa' from environmental DNA samples but also facilitates the classification of *Ceratostomella* diversity. By characterising all representatives of the genus through genomic data, future taxonomic efforts will be more streamlined and accurate.

Despite these advances, information on the asexual morph remains lacking, as it did not form in any of the analysed species (Réblová 2006; this study). We advocate the use of dual barcoding, particularly employing ITS primary barcode and secondary barcodes such as *tef1-α* and *rpb2*, to differentiate among members of *Ceratostomella*, especially among morphologically indistinguishable species. Additionally, further research focusing on comprehensive taxon sampling and exploring environmental DNA could enhance our understanding of the diversity and ecological roles of these fungi.

Acknowledgements

Curators and collection managers Dana Lančová (PRA), Trix Merkx (CBS), Andrew N. Miller (ILLS) and Adrienne Stanton (PDD), are acknowledged for assistance with obtaining living cultures and herbarium loans and depositing new herbarium specimens and newly acquired strains.

Additional information

Conflict of interest

The authors have declared that no competing interests exist.

Ethical statement

No ethical statement was reported.

Funding

This study was supported by the project of the Czech Academy of Sciences 'Strategie AV21 MycoLife – svět hub', and as long-term research development projects of the Czech Academy of Sciences, Institute of Botany (RVO 67985939) (M.R.) and the University Hospital Hradec Králové MH CZ – DRO (UHHK, 00179906) (J.N.).

Author contributions

Conceptualization: MR. Data curation: ŽJ, MR. Formal analysis: MK, MR, MK, JN. Funding acquisition: MR. Investigation: JN, MR, ŽJ, VH. Methodology: JN, MR, ŽJ, MK, MK, VH. Resources: ŽJ, MR, MK, JN. Software: MK. Validation: MR. Visualization: MR. Writing - original draft: ŽJ, MK, MR, VH.

Author ORCIDs

Martina Réblová https://orcid.org/0000-0001-5229-1709
Jana Nekvindová https://orcid.org/0000-0002-2861-5483
Miroslav Kolařík https://orcid.org/0000-0003-4016-0335
Željko Jurjević https://orcid.org/0000-0002-5556-4722
Michal Kolář https://orcid.org/0000-0002-4593-1525
Vít Hubka https://orcid.org/0000-0003-4583-6496

Data availability

All of the data that support the findings of this study are available in the main text or Supplementary Information.

References

Andrews S (2010) Babraham bioinformatics-FastQC a quality control tool for high throughput sequence data. https://www.bioinformatics.babraham.ac.uk/projects/fastqc

Arzanlou M, Groenewald JZ, Gams W, Braun U, Shin HD, Crous PW (2007) Phylogenetic and morphotaxonomic revision of *Ramichloridium* and allied genera. Studies in Mycology 58: 57–93. https://doi.org/10.3114/sim.2007.58.03

Bankevich A, Nurk S, Antipov D, Gurevich AA, Dvorkin M, Kulikov AS, Lesin VM, Nikolenko SI, Pham S, Prjibelski AD, Pyshkin AV, Sirotkin AV, Vyahhi N, Tesler G, Alekseyev MA, Pevzner PA (2012) SPAdes: A new genome assembly algorithm and its applications to single-cell sequencing. Journal of Computational Biology 19(5): 455–477. https://doi.org/10.1089/cmb.2012.0021

Barr ME (1985) Notes on the Calosphaeriales. Mycologia 77(4): 549–565. https://doi.org/10.1080/00275514.1985.12025141

Barr ME (1998) *Wegelina*, a reinstated genus in the Calosphaeriales. Cryptogamie. Bryologie, Lichenologie 19: 169–173.

Barr ME, Rogers JD, Ju MJ (1993) Revisionary studies in the Calosphaeriales. Mycotaxon 48: 529–535.

Bengtsson-Palme J, Ryberg M, Hartmann M, Branco S, Wang Z, Godhe A, De Wit P, Sánchez-García M, Ebersberger I, Sousa F, Amend AS, Jumpponen A, Unterseher M, Kristiansson E, Abarenkov K, Bertrand YJK, Sanli K, Eriksson KM, Vik U, Veldre V, Nilsson RH (2013) Improved software detection and extraction of ITS1 and ITS2 from ribosomal ITS sequences of fungi and other eukaryotes for analysis of environmental sequencing data. Methods in Ecology and Evolution 4(10): 914–919. https://doi.org/10.1111/2041-210X.12073

Bolger AM, Lohse M, Usadel B (2014) Trimmomatic: A flexible trimmer for Illumina Sequence Data. Bioinformatics 30(15): btu170. https://doi.org/10.1093/bioinformatics/btu170

Booth C (1957) Studies of Pyrenomycetes: I. Four species of *Chaetosphaeria*, two with *Catenularia* conidia. II. *Melanopsamma pomiformis* and its *Stachybotrys* conidia. Mycological Papers 68: 1–27.

Cannon PF, Hawksworth DL (1982) A re-evaluation of *Melanospora* Corda and similar Pyrenomycetes, with a revision of the British species. Botanical Journal of the Linnean Society 84(2): 115–160. https://doi.org/10.1111/j.1095-8339.1982.tb00363.x

Clements FE, Shear CL (1931) The genera of fungi. HW Wilson, New York, 496 pp.

Corda ACJ (1837) Icones fungorum hucusque cognitorum I. J.G. Calve, Prague, 32 pp. [Tab. I–VII.]

Crous PW, Gams W, Stalpers JA, Robert V, Stegehuis G (2004) MycoBank: An online initiative to launch mycology into the 21st century. Studies in Mycology 50: 19–22.

Crous PW, Verkley GJM, Groenewald JZ, Houbracken J (2019a). Fungal Biodiversity. Westerdijk Laboratory Manual Series No. 1. Westerdijk Fungal Biodiversity Institute, Utrecht, 425 pp.

Crous PW, Schumacher RK, Akulov A, Thangavel R, Hernández-Restrepo M, Carnegie AJ, Cheewangkoon R, Wingfield MJ, Summerell BA, Quaedvlieg W, Coutinho TA, Roux J, Wood AR, Giraldo A, Groenewald JZ (2019b) New and Interesting Fungi. 2. Fungal Systematics and Evolution 3(1): 57–134. https://doi.org/10.3114/fuse.2019.03.06

Damm U, Crous PW, Fourie PH (2008) A fissitunicate ascus mechanism in the Calosphaeriaceae, and novel species of *Jattaea* and *Calosphaeria* on *Prunus* wood. Persoonia 20(1): 39–52. https://doi.org/10.3767/003158508X313940

De Beer ZW, Seifert KA, Wingfield MJ (2013) A nomenclator for ophiostomatoid genera and species in the Ophiostomatales and Microascales. CBS Biodiversity Series 12: 245–322.

De Beer ZW, Duong TA, Barnes I, Wingfield BD, Wingfield MJ (2014) Redefining *Ceratocystis* and allied genera. Studies in Mycology 79(1): 187–219. https://doi.org/10.1016/j.simyco.2014.10.001

De Notaris G (1867) Nuove reclute per la Pirenomicetologia italica. Commentario della Società Crittogamologica Italiana 2(3): 477–492.

Dennis RWG (1988) A new genus for *Sphaeria bacillata* Cooke. Belarra 2: 25–28.

Elliott JA (1923) The ascigerous stage of the sweet potato black rot fungus. Phytopathology 13: 56–56.

Fries EM (1823) Systema Mycologicum 2(2): 275–620.

Ferrer A, Miller AN, Sarmiento C, Shearer CA (2012) Three new genera representing novel lineages of Sordariomycetidae (Sordariomycetes, Ascomycota) from tropical freshwater habitats in Costa Rica. Mycologia 104(4): 865–879. https://doi.org/10.3852/11-111

Gouy M, Guindon S, Gascuel O (2010) SeaView version 4: A multiplatform graphical user interface for sequence alignment and phylogenetic tree building. Molecular Biology and Evolution 27(2): 221–224. https://doi.org/10.1093/molbev/msp259

Gramaje D, Mostert L, Groenewald JZ, Crous PW (2015) *Phaeoacremonium*: From esca disease to phaeohyphomycosis. Fungal Biology 119(9): 759–783. https://doi.org/10.1016/j.funbio.2015.06.004

Gurevich A, Saveliev V, Vyahhi N, Tesler G (2013) QUAST: Quality assessment tool for genome assemblies. Bioinformatics 29(8): 1072–1075. https://doi.org/10.1093/bioinformatics/btt086

Hall TA (1999) BioEdit 5.0.9: A user-friendly biological sequence alignment editor and analysis program for Windows 95/98/NT. Nucleic Acids Symposium Series 41: 95–98.

Hernández-Restrepo M, Schumacher RK, Wingfield MJ, Ahmad I, Cai L, Duong TA, Edwards J, Gené J, Groenewald JZ, Jabeen S, Khalid AN, Lombard L, Madrid H, Marin-Felix Y, Marincowitz S, Miller AN, Rajeshkumar KC, Rashid A, Sarwar S, Stchigel AM, Taylor PWJ, Zhou N, Crous PW (2016) Fungal Systematics and Evolution: FUSE 2. Sydowia 68: 193–230. https://doi.org/10.12905/0380.sydowia68-2016-0193

Huerta-Cepas J, Szklarczyk D, Heller D, Hernández-Plaza A, Forslund SK, Cook H, Mende DR, Letunic I, Rattei T, Jensen LJ, von Mering C, Bork P (2019) eggNOG 5.0: A hierarchical, functionally and phylogenetically annotated orthology resource based on 5090 organisms and 2502 viruses. Nucleic Acids Research 47(D1): D309–D314. https://doi.org/10.1093/nar/gky1085

Huhndorf SM, Fernández FA (2005) Teleomorph-anamorph connections: *Chaetosphaeria raciborskii* and related species, and their *Craspedodidymum*-like anamorphs. Fungal Diversity 19: 23–49.

Huhndorf SM, Miller AN, Fernández FA (2004) Molecular systematics of the Sordariales: The order and the family Lasiosphaeriaceae redefined. Mycologia 96(2): 368–387. https://doi.org/10.1080/15572536.2005.11832982

Hunt J (1956) Taxonomy of the genus *Ceratocystis*. Lloydia 19: 1–58.

Hyde KD, Bao DF, Hongsanan S, Chethana KWT, Yang J, Suwannarach N (2021) Evolution of freshwater Diaporthomycetidae (Sordariomycetes) provides evidence for five new orders and six new families. Fungal Diversity 107(1): 71–105. https://doi.org/10.1007/s13225-021-00469-7

Jaklitsch WM, Réblová M, Voglmayr H (2013) Molecular systematics of *Woswasia atropurpurea* gen. et sp. nov. (*Sordariomycetidae*), a fungicolous ascomycete with globose ascospores and holoblastic conidiogenesis. Mycologia 105(2): 476–485. https://doi.org/10.3852/12-244

Jones P, Binns D, Chang H-Y, Fraser M, Li W, McAnulla C, McWilliam H, Maslen J, Mitchell A, Nuka G, Pesseat S, Quinn AF, Sangrador-Vegas A, Scheremetjew M, Yong S-Y, Lopez R, Hunter S (2014) InterProScan 5: Genome-scale protein function classification. Bioinformatics 30(9): 1236–1240. https://doi.org/10.1093/bioinformatics/btu031

Jurjević Ž, Kubátová A, Kolařík M, Hubka V (2015) Taxonomy of *Aspergillus* section *Petersonii* sect. nov. encompassing indoor and soilborne species with predominant tropical distribution. Plant Systematics and Evolution 301(10): 2441–2462. https://doi.org/10.1007/s00606-015-1248-4

Katoh K, Standley DM (2013) MAFFT multiple sequence alignment software version 7: Improvements in performance and usability. Molecular Biology and Evolution 30(4): 772–780. https://doi.org/10.1093/molbev/mst010

Kimura M (1980) A simple method for estimating evolutionary rates of base substitutions through comparative studies of nucleotide sequences. Journal of Molecular Evolution 16(2): 111–120. https://doi.org/10.1007/BF01731581

Kirschstein W (1936) Beiträge zur Kenntnis der Ascomyceten und ihrer Nebenformen besonders aus der Mark Brandenburg und dem Bayerischen Walde. Annales Mycologici 34: 180–210.

Klaubauf S, Tharreau D, Fournier E, Groenewald JZ, Crous PW, de Vries RP, Lebrun MH (2014) Resolving the polyphyletic nature of *Pyricularia* (Pyriculariaceae). Studies in Mycology 79(1): 85–120. https://doi.org/10.1016/j.simyco.2014.09.004

Köhler JR, Casadevall A, Perfect J (2015) The spectrum of fungi that infects humans. Cold Spring Harbor Perspectives in Medicine 5(1): a019273. https://doi.org/10.1101/cshperspect.a019273

Lu YZ, Zhang JY, Lin CG, Luo ZL, Liu JK (2020) *Pseudodactylaria fusiformis* sp. nov. from freshwater habitat in China. Phytotaxa 446: 95–102. https://doi.org/10.11646/phytotaxa.446.2.2

Luo ZL, Hyde KD, Liu JK, Maharachchikumbura SSN, Jeewon R, Bao DF, Bhat DJ, Lin CG, Li WL, Yang J, Liu NG, Lu YZ, Jayawardena RS, Li JF, Su HY (2019) Freshwater Sordariomycetes. Fungal Diversity 99(1): 451–660. https://doi.org/10.1007/s13225-019-00438-1

Luttrell ES (1951) Taxonomy of the Pyrenomycetes. The University of Missouri Studies 24: 1–120.

Malloch D (1981) Moulds: Their isolation, cultivation and identification. University of Toronto Press, Toronto, 97 pp.

Melin E, Nannfeldt JA (1934) Researches into the blueing of ground wood-pulp. Svenska Skogsvårdsföreningens Tidskrift 32: 397–616.

Miller AN, Bates ST (2017) The Mycology Collections Portal (MyCoPortal). IMA Fungus 8(2): 65–66. https://doi.org/10.1007/BF03449464

Miller AN, Huhndorf SM (2005) Multi-gene phylogenies indicate ascomal wall morphology is a better predictor of phylogenetic relationships than ascospore morphology in the Sordariales (Ascomycota, Fungi). Molecular Phylogenetics and Evolution 35(1): 60–75. https://doi.org/10.1016/j.ympev.2005.01.007

Miller MA, Pfeiffer W, Schwartz T (2010) Creating the CIPRES Science Gateway for inference of large phylogenetic trees. Proceedings of the Gateway Computing Environments Workshop (GCE), 14 Nov. 2010, New Orleans, 8 pp. https://doi.org/10.1109/GCE.2010.5676129

Moreau C (1952) Coexistence des formes *Thielaviopsis* et *Graphium* chez une souche de *Ceratocystis major* (van Beyma) nov. comb. Remarques sur les variations des *Ceratocystis*. Revue de Mycologie 17: 17–25. [Supplement Colonial]

Mostert L, Groenewald JZ, Summerbell RC, Gams W, Crous PW (2006) Taxonomy and pathology of *Togninia* (Diaporthales) and its *Phaeoacremonium* anamorphs. Studies in Mycology 54: 1–118. https://doi.org/10.3114/sim.54.1.1

Munk A (1965) On some species of *Endoxyla* found in Denmark. Botanisk Tidsskrift 61: 56–70.

Niessl G von (1876) Notizen über neue und kritische Pyrenomyceten. Verhandlungen des naturforschenden Vereines in Brünn 14: 165–218.

Nilsson RH, Larsson KH, Taylor AFS, Bengtsson-Palme J, Jeppesen TS, Schigel D, Kennedy P, Picard K, Glöckner FO, Tedersoo L, Saar I, Kõljalg U, Abarenkov K (2019) The UNITE database for molecular identification of fungi: Handling dark taxa and parallel taxonomic classifications. Nucleic Acids Research 47(D1): D259–D264. https://doi.org/10.1093/nar/gky1022

Nilsson RH, Ryberg M, Wurzbacher C, Tedersoo L, Anslan S, Põlme S, Spirin V, Mikryukov V, Svantesson S, Hartmann M, Lennartsdotter C, Belford P, Khomich M, Retter

A, Corcoll N, Gómez Martinez D, Jansson T, Ghobad-Nejhad M, Vu D, Sanchez-Garcia M, Kristiansson E, Abarenkov K (2023) How, not if, is the question mycologists should be asking about DNA-based typification. MycoKeys 96: 143–157. https://doi.org/10.3897/mycokeys.96.102669

Nylander JAA (2004) MrModeltest v2. Program distributed by the author. Evolutionary Biology Centre, Uppsala University, Sweden.

Palmer JM, Stajich JE (2020) Funannotate v1.8.1: eukaryotic genome annotation. Zenodo. https://doi.org/10.5281/zenodo.4054262

Plattner A, Kim JJ, Reid J, Hausner G, Lim YW, Yamaoka Y, Breuil C (2009) Resolving taxonomic and phylogenetic incongruence within species *Ceratocystiopsis minuta*. Mycologia 101(6): 878–887. https://doi.org/10.3852/08-132

Rambaut A (2010) FigTree v.1.3.1. Institute of Evolutionary Biology, University of Edinburgh, Edinburgh.

Ranghoo VM, Hyde KD, Liew ECY (1999) Family placement of *Ascotaiwania* and *Ascolacicola* based on DNA sequences from the large subunit rRNA gene. Fungal Diversity 2: 159–168.

Réblová M (2006) Molecular systematics of *Ceratostomella* sensu lato and morphologically similar fungi. Mycologia 98(1): 68–93. https://doi.org/10.1080/15572536.2006.11832714

Réblová M (2008) *Barbatosphaeria* gen. et comb. nov., a new genus for *Calosphaeria barbirostris*. Mycologia 99(5): 723–732. https://doi.org/10.1080/15572536.2007.11832536

Réblová M (2011) New insights into the systematics and phylogeny of the genus *Jattaea* and similar fungi of the Calosphaeriales. Fungal Diversity 49(1): 167–198. https://doi.org/10.1007/s13225-011-0099-8

Réblová M (2013) Two taxonomic novelties in the Sordariomycetidae: *Ceratolenta caudata* gen. et sp. nov. and *Platytrachelon abietis* gen. et comb. nov. for *Ceratosphaeria abietis*. Mycologia 105(2): 462–475. https://doi.org/10.3852/12-199

Réblová M, Nekvindová J (2023) New genera and species with chloridium-like morphotype in the Chaetosphaeriales and Vermiculariopsiellales. Studies in Mycology 106(1): 199–258. https://doi.org/10.3114/sim.2023.106.04

Réblová M, Seifert KA (2004) *Cryptadelphia* (Trichosphaeriales), a new genus for holomorphs with *Brachysporium* anamorphs and clarification of the taxonomic status of *Wallrothiella*. Mycologia 96(2): 343–367. https://doi.org/10.1080/15572536.2005.11832981

Réblová M, Štěpánek V (2009) New fungal genera, *Tectonidula* gen. nov. for *Calosphaeria*-like fungi with holoblastic-denticulate conidiogenesis and *Natantiella* gen. nov. for three species segregated from *Ceratostomella*. Mycological Research 113(9): 991–1002. https://doi.org/10.1016/j.mycres.2009.06.003

Réblová M, Štěpánek V (2018) Introducing the Rhamphoriaceae, fam. nov. (Sordariomycetes), two new genera, and new life histories for taxa with *Phaeoisaria*- and *Idriella*-like anamorphs. Mycologia 110(4): 750–770. https://doi.org/10.1080/00275514.2018.1475164

Réblová M, Mostert L, Gams W, Crous PW (2004) New genera in the Calosphaeriales: *Togniniella* and its anamorph *Phaeocrella*, and *Calosphaeriophora* as anamorph of *Calosphaeria*. Studies in Mycology 50: 533–550.

Réblová M, Gams W, Seifert KA (2011) Monilochaetes and allied genera of the Glomerellales, and a reconsideration of families in the Microascales. Studies in Mycology 68: 163–191. https://doi.org/10.3114/sim.2011.68.07

Réblová M, Jaklitsch W, Réblová K, Štěpánek V (2015a) Phylogenetic reconstruction of the Calosphaeriales and Togniniales using five genes and predicted RNA secondary structures of ITS, and *Flabellascus tenuirostris* gen. et sp. nov. PLoS ONE 10(12): e0144616. https://doi.org/10.1371/journal.pone.0144616

Réblová M, Réblová K, Štěpánek V (2015b) Molecular systematics of *Barbatosphaeria* (Sordariomycetes): Multigene phylogeny and secondary ITS structure. Persoonia 35(1): 21–38. https://doi.org/10.3767/003158515X687434

Réblová M, Fournier J, Štěpánek V (2016) Two new lineages of aquatic ascomycetes: *Atractospora* gen. nov. and *Rubellisphaeria* gen. et sp. nov., and a sexual morph of *Myrmecridium montsegurinum* sp. nov. Mycological Progress 15(3): 1–18. https://doi.org/10.1007/s11557-016-1166-z

Réblová M, Miller AN, Réblová K, Štěpánek V (2018) Phylogenetic classification and generic delineation of *Calyptosphaeria* gen. nov., *Lentomitella*, *Spadicoides* and *Torrentispora* (Sordariomycetes). Studies in Mycology 89(1): 1–62. https://doi.org/10.1016/j.simyco.2017.11.004

Réblová M, Hernández-Restrepo M, Fournier J, Nekvindová J (2020) New insights into the systematics of *Bactrodesmium* and its allies and introducing new genera, species and morphological patterns in the Pleurotheciales and Savoryellales (Sordariomycetes). Studies in Mycology 95: 415–466. https://doi.org/10.1016/j.simyco.2020.02.002

Réblová M, Kolařík M, Nekvindová J, Réblová K, Sklenář F, Miller AN, Hernández-Restrepo M (2021) Phylogenetic reassessment, taxonomy, and biogeography of *Codinaea* and similar fungi. Journal of Fungi 7(12): 1097. https://doi.org/10.3390/jof7121097

Réblová M, Hernández-Restrepo M, Sklenář F, Nekvindová J, Réblová K, Kolařík M (2022) Consolidation of *Chloridium*: New classification into eight sections with 37 species and reinstatement of the genera *Gongromeriza* and *Psilobotrys*. Studies in Mycology 103(1): 87–212. https://doi.org/10.3114/sim.2022.103.04

Robert V, Szöke S, Eberhardt U, Cardinali G, Meyer W, Seifert KA, Lévesque CA, Lewis CT (2011) The quest for a general and reliable fungal DNA barcode. The Open and Applied Informatics Journal 5(1): 45–61. https://doi.org/10.2174/1874136301105010045

Ronquist F, Teslenko M, van der Mark P, Ayres DL, Darling A, Höhna S, Larget B, Liu L, Suchard MA, Huelsenbeck JP (2012) MrBayes 3.2: Efficient Bayesian phylogenetic inference and model choice across a large model space. Systematic Biology 61(3): 539–542. https://doi.org/10.1093/sysbio/sys029

Saccardo PA (1878) Fungi Veneti novi vel critici. Series IX. Michelia 1: 361–445.

Saccardo PA (1882) Sylloge Pyrenomycetum. Vol. I. Sylloge Fungorum 1: 1–768.

Samuels GJ, Barr ME (1997) Notes on and additions to the Niessliaceae (Hypocreales). Canadian Journal of Botany 75(12): 2165–2176. https://doi.org/10.1139/b97-928

Samuels GJ, Candoussau F (1996) Heterogeneity in the Calosphaeriales: A new *Calosphaeria* with *Ramichloridium*- and *Sporothrix*-like synanamorphs. Nova Hedwigia 62: 47–60.

Schoch CL, Sung GH, López-Giráldez F, Townsend JP, Miadlikowska J, Hofstetter V, Robbertse B, Matheny PB, Kauff F, Wang Z, Gueidan C, Andrie RM, Trippe K, Ciufetti LM, Wynns A, Fraker E, Hodkinson BP, Bonito G, Groenewald JZ, Arzanlou M, de Hoog GS, Crous PW, Hewitt D, Pfister DH, Peterson K, Gryzenhout M, Wingfield MJ, Aptroot A, Suh SO, Blackwell M, Hillis DM, Griffith GW, Castlebury LA, Rossman AY, Lumbsch HT, Lücking R, Büdel B, Rauhut A, Diederich P, Ertz D, Geiser DM, Hosaka K, Inderbitzin P, Kohlmeyer J, Volkmann-Kohlmeyer B, Mostert L, O'Donnell K, Sipman H, Rogers JD, Shoemaker RA, Sugiyama J, Summerbell RC, Untereiner W, Johnston PR, Stenroos S, Zuccaro A, Dyer PS, Crittenden PD, Cole MS, Hansen K, Trappe JM, Yahr R, Lutzoni F, Spatafora JW (2009) The Ascomycota tree of life: A phylum-wide phylogeny clarifies

the origin and evolution of fundamental reproductive and ecological traits. Systematic Biology 58(2): 224–239. https://doi.org/10.1093/sysbio/syp020

Schoch CL, Seifert KA, Huhndorf S, Robert V, Spouge JL, Levesque CA, Chen W, Bolchacova E, Voigt K, Crous PW, Miller AN, Wingfield MJ, Aime MC, An K-D, Bai F-Y, Barreto RW, Begerow D, Bergeron M-J, Blackwell M, Boekhout T, Bogale M, Boonyuen N, Burgaz AR, Buyck B, Cai L, Cai Q, Cardinali G, Chaverri P, Coppins BJ, Crespo A, Cubas P, Cummings C, Damm U, de Beer ZW, de Hoog GS, Del-Prado R, Dentinger B, Diéguez-Uribeondo J, Divakar PK, Douglas B, Dueñas M, Duong TA, Eberhardt U, Edwards JE, Elshahed MS, Fliegerova K, Furtado M, García MA, Ge Z-W, Griffith GW, Griffiths K, Groenewald JZ, Groenewald M, Grube M, Gryzenhout M, Guo L-D, Hagen F, Hambleton S, Hamelin RC, Hansen K, Harrold P, Heller G, Herrera C, Hirayama K, Hirooka Y, Ho H-M, Hoffmann K, Hofstetter V, Högnabba F, Hollingsworth PM, Hong S-B, Hosaka K, Houbraken J, Hughes K, Huhtinen S, Hyde KD, James T, Johnson EM, Johnson JE, Johnston PR, Jones EBG, Kelly LJ, Kirk PM, Knapp DG, Kõljalg U, Kovács GM, Kurtzman CP, Landvik S, Leavitt SD, Liggenstoffer AS, Liimatainen K, Lombard L, Luangsa-ard JJ, Lumbsch HT, Maganti H, Maharachchikumbura SSN, Martin MP, May TW, McTaggart AR, Methven AS, Meyer W, Moncalvo J-M, Mongkolsamrit S, Nagy LG, Nilsson RH, Niskanen T, Nyilasi I, Okada G, Okane I, Olariaga I, Otte J, Papp T, Park D, Petkovits T, Pino-Bodas R, Quaedvlieg W, Raja HA, Redecker D, Rintoul TL, Ruibal C, Sarmiento-Ramírez JM, Schmitt I, Schüßler A, Shearer C, Sotome K, Stefani FOP, Stenroos S, Stielow B, Stockinger H, Suetrong S, Suh S-O, Sung G-H, Suzuki M, Tanaka K, Tedersoo L, Telleria MT, Tretter E, Untereiner WA, Urbina H, Vágvölgyi C, Vialle A, Vu TD, Walther G, Wang Q-M, Wang Y, Weir BS, Weiß M, White MM, Xu J, Yahr R, Yang ZL, Yurkov A, Zamora J-C, Zhang N, Zhuang W-Y, Schindel D (2012) Nuclear ribosomal internal transcribed spacer (ITS) region as a universal DNA barcode marker for fungi. Proceedings of the National Academy of Sciences of the United States of America 109(16): 6241–6246. https://doi.org/10.1073/pnas.1117018109

Senanayake IC, Al-Sadi AM, Bhat JD, Camporesi E, Dissanayake AJ, Lumyong S, Maharachchikumbura SSN, Hyde KD (2016) Phomatosporales ord. nov. and Phomatosporaceae fam. nov., to accommodate *Lanspora*, *Phomatospora* and *Tenuimurus*, gen. nov. Mycosphere 7(5): 628–641. https://doi.org/10.5943/mycosphere/7/5/8

Seppey M, Manni M, Zdobnov EM (2019) BUSCO: Assessing Genome Assembly and Annotation Completeness. In: Kollmar M (Ed.) Methods in molecular biology. Springer, New York, 227–245. https://doi.org/10.1007/978-1-4939-9173-0_14

Shenoy BD, Jeewon R, Wu WP, Bhat DJ, Hyde KD (2006) Ribosomal and RPB2 DNA sequence analyses suggest that *Sporidesmium* and morphologically similar genera are polyphyletic. Mycological Research 110(8): 916–928. https://doi.org/10.1016/j.mycres.2006.06.004

Shenoy BD, Jeewon R, Wang HK, Amandeep K, Ho WH, Bhat DJ, Crous PW, Hyde KD (2010) Sequence data reveals phylogenetic affinities of fungal anamorphs *Bahusutrabeeja*, *Diplococcium*, *Natarajania*, *Paliphora*, *Polyschema*, *Rattania* and *Spadicoides*. Fungal Diversity 44(1): 161–169. https://doi.org/10.1007/s13225-010-0059-8

Song HY, Zhong PA, Liao JL, Wang ZH, Hu DM, Huang YJ (2018) *Junewangia aquatica* (Junewangiaceae), a new species from freshwater habitats in China. Phytotaxa 336(3): 272–278. https://doi.org/10.11646/phytotaxa.336.3.5

Spatafora JW, Sung GH, Sung JM, Hywel-Jones NL, White Jr JF (2007) Phylogenetic evidence for an animal pathogen origin of ergot and the grass endophytes. Molecular Ecology 16(8): 1701–1711. https://doi.org/10.1111/j.1365-294X.2007.03225.x

Stamatakis A (2014) RAxML Version 8: A tool for phylogenetic analysis and post-analysis of large phylogenies. Bioinformatics 30(9): 1312–1313. https://doi.org/10.1093/bioinformatics/btu033

Stielow JB, Lévesque CA, Seifert KA, Meyer W, Iriny L, Smits D, Renfurm R, Verkley GJ, Groenewald M, Chaduli D, Lomascolo A, Welti S, Lesage-Meessen L, Favel A, Al-Hatmi AM, Damm U, Yilmaz N, Houbraken J, Lombard L, Quaedvlieg W, Binder M, Vaas LA, Vu D, Yurkov A, Begerow D, Roehl O, Guerreiro M, Fonseca A, Samerpitak K, van Diepeningen AD, Dolatabadi S, Moreno LF, Casaregola S, Mallet S, Jacques N, Roscini L, Egidi E, Bizet C, Garcia-Hermoso D, Martín MP, Deng S, Groenewald JZ, Boekhout T, de Beer ZW, Barnes I, Duong TA, Wingfield MJ, de Hoog GS, Crous PW, Lewis CT, Hambleton S, Moussa TA, Al-Zahrani HS, Almaghrabi OA, Louis-Seize G, Assabgui R, McCormick W, Omer G, Dukik K, Cardinali G, Eberhardt U, de Vries M, Robert V (2015) One fungus, which genes? Development and assessment of universal primers for potential secondary fungal DNA barcodes. Persoonia 35(1): 242–263. https://doi.org/10.3767/003158515X689135

Suh S-O, Blackwell M (1999) Molecular phylogeny of the cleistothecial fungi placed in Cephalothecaceae and Pseudeurotiaceae. Mycologia 91(5): 836–848. https://doi.org/10.1080/00275514.1999.12061089

Sydow H, Sydow P (1919) Mycologische Mitteilungen. Annales Mycologici 17: 33–47.

Tamura K, Stecher G, Kumar S (2021) MEGA11: Molecular Evolutionary Genetics Analysis version 11. Molecular Biology and Evolution 38(7): 3022–3027. https://doi.org/10.1093/molbev/msab120

Taylor JE, Hyde KD (1999) *Cannonia* gen. nov., from palms in the Southern Hemisphere. Mycological Research 103(11): 1398–1402. https://doi.org/10.1017/S0953756299008795

Thongkantha S, Jeewon R, Vijaykrishna D, Lumyong S, McKenzie EHC, Hyde KD (2009) Molecular phylogeny of Magnaporthaceae (Sordariomycetes) with a new species *Ophioceras chiangdaoense* from *Dracaena loureiroi* in Thailand. Fungal Diversity 34: 157–173.

Tode HJ (1791). Fungi Mecklenburgenses Selecti 2: 1–64. https://doi.org/10.5962/bhl.title.148599

Tsang C-C, Chan JFW, Ip PPC, Ngan AHY, Chen JHK, Lau SKP, Woo PCY (2014) Subcutaneous phaeohyphomycotic nodule due to a novel *Phialemoniopsis* species, *Phialemoniopsis hongkongensis* sp. nov. Journal of Clinical Microbiology 52: 3280–3289. https://doi.org/10.1128/JCM.01592-14

Untereiner WA (1993) A taxonomic revision of the genus Endoxyla. Mycologia 85(2): 294–310. https://doi.org/10.1080/00275514.1992.12026274

Untereiner WA, Bogale M, Carter A, Bud Platt HW, Hanson SÅ, Læssøe T, Stepánek V, Réblová M (2013) Molecular phylogeny of Boliniales (Sordariomycetes) with an assessment of the systematics of *Apiorhynchostoma*, *Endoxyla* and *Pseudovalsaria*. Mycologia 105: 564–588. https://doi.org/10.3852/12-326

Vassiljeva LN, Stephenson SL (2014) Notes on pyrenomycetous fungi in the Mountain Lake area of southwestern Virginia. Mycosphere 5(1): 218–227. https://doi.org/10.5943/mycosphere/5/1/11

Větrovský T, Baldrian P, Morais D (2018) SEED 2: A user-friendly platform for amplicon high-throughput sequencing data analyses. Bioinformatics 34(13): 2292–2294. https://doi.org/10.1093/bioinformatics/bty071

Větrovský T, Morais D, Kohout P, Lepinay C, Algora C, Awokunle Hollá S, Bahnmann BD, Bílohnědá K, Brabcová V, D'Alò F, Human ZR, Jomura M, Kolařík M, Kvasničková J, Lladó S, López-Mondéjar R, Martinović T, Mašínová T, Meszárošová L, Michalčíková

L, Michalová T, Mundra S, Navrátilová D, Odriozola I, Piché-Choquette S, Štursová M, Švec K, Tláskal V, Urbanová M, Vlk L, Voříšková J, Žifčáková L, Baldrian P (2020) GlobalFungi, a global database of fungal occurrences from high-throughput-sequencing metabarcoding studies. Scientific Data 7(1): 228. https://doi.org/10.1038/s41597-020-0567-7

Yaguchi T, Sano A, Yarita K, Suh MK, Nishimura K, Udagawa S-I (2006) A new species of *Cephalotheca* isolated from a Korean patient. Mycotaxon 96: 309–322.

Yang J, Maharachchikumbura SSN, Liu JK, Hyde KD, Jones EBG, Al-Sadi AM, Liu ZY (2017) *Pseudostanjehughesia aquitropica* gen. et sp. nov. and *Sporidesmium* sensu lato species from freshwater habitats. Mycological Progress 17(5): 591–616. https://doi.org/10.1007/s11557-017-1339-4

Zhang N, Castlebury LA, Miller AN, Huhndorf SM, Schoch CL, Seifert KA, Rossman AY, Rogers JD, Kohlmeyer J, Volkmann-Kohlmeyer B, Sung GH (2006) An overview of the systematics of the Sordariomycetes based on a four-gene phylogeny. Mycologia 98(6): 1076–1087. https://doi.org/10.1080/15572536.2006.11832635

Zhang H, Dong W, Hyde KD, Maharachchikumbura SSN, Hongsanan S, Bhat DJ, Al-Sadi AM, Zhang D (2017) Towards a natural classification of Annulatascaceae-like taxa: Introducing Atractosporales ord. nov. and six new families. Fungal Diversity 85(1): 75–110. https://doi.org/10.1007/s13225-017-0387-z

Zhou L-W (2024) The strategy for naming fungal 'dark taxa' may involve a transition period and genomics. Fungal Biology Reviews 48: 100358. https://doi.org/10.1016/j.fbr.2024.100358

Supplementary material 1

Taxa, isolate information and sequences retrieved from GenBank

Author: Martina Réblová

Data type: pdf

Link: https://doi.org/10.3897/mycokeys.110.136844.suppl1

Supplementary material 2

Estimates of evolutionary divergence between ITS rDNA, *rpb2* and *tef1-α* sequences

Author: Miroslav Kolařík

Data type: pdf

Link: https://doi.org/10.3897/mycokeys.110.136844.suppl2

Supplementary material 3

Biogeographical distribution, substrate, habitat and other detailed metadata for *Ceratostomella* species with available ITS sequences inferred from the GlobalFungi database

Author: Martina Réblová

Data type: pdf

Link: https://doi.org/10.3897/mycokeys.110.136844.suppl3

MycoKeys 110: 361–383 (2024)
DOI: 10.3897/mycokeys.110.134154

Research Article

Unveiling two new species of *Trichoderma* (Hypocreales, Hypocreaceae) that cause green mold disease on *Stropharia rugosoannulata* from Guizhou Province, China

Entaj Tarafder[1,2,3], Zhang Wenjun[1,2,3], Samantha C. Karunarathna[4], Abdallah M. Elgorban[5], Man Huilian[1,2,3], Wu Nan[6], Xiangyu Zeng[1,2], Wang Yong[1,2], Feng-Hua Tian[1,2,3]

1 *Department of Plant Pathology, College of Agriculture, Guizhou University, Guiyang, China*
2 *Institute of Edible Mushroom, Guizhou University, Guiyang, China*
3 *Engineering Research Center of Chinese Ministry of Education for Edible and Medicinal Fungi, Jilin Agricultural University, Changchun 130118, China*
4 *Center for Yunnan Plateau Biological Resources Protection and Utilization, College of Biological Resource and Food Engineering, Qujing Normal University, Qujing, Yunnan 655011, China*
5 *Department of Botany and Microbiology, College of Science, King Saud University, Riyadh 11451, Saudi Arabia*
6 *School of Life Science and Technology, Heilongjiang Bayi Agricultural Reclamation University, Daqing 163316, China*

Corresponding author: Feng-Hua Tian (fhtian@gzu.edu.cn)

Abstract

Stropharia rugosoannulata is an important edible mushroom in China, but green mold disease has caused significant production and economic losses. In this study, two new pathogens *Trichoderma strophariensis* and *T. viridistromatis* were identified as the causal agents of this disease. During October-November 2023, six strains of the fungal pathogen were isolated from infected fruiting bodies of *S. rugosoannulata* and identified based on morphological characteristics and molecular phylogenetic analyses of internal transcribed spacer (nrITS), the second largest RNA polymerase II subunit (*rpb2*) and the partial translation elongation factor 1-alpha (*tef1-α*) region. The representative isolates of the pathogenic green mold *Trichoderma* species were used to perform a pathogenicity test with spore suspensions, resulting in symptoms similar to those observed in the cultivated field. The same pathogens were successfully re-isolated, thereby fulfilling Koch's postulates. Detailed morphological descriptions, illustrations, culture characteristics, and comparisons with morphologically similar and closely related species are provided.

Key words: Ascomycetes, novel taxa, pathogen, phylogeny, taxonomy

Academic editor:
Sajeewa Maharachchikumbura
Received: 7 August 2024
Accepted: 26 October 2024
Published: 22 November 2024

Citation: Tarafder E, Wenjun Z, Karunarathna SC, Elgorban AM, Huilian M, Nan W, Zeng X, Yong W, Tian F-H (2024) Unveiling two new species of *Trichoderma* (Hypocreales, Hypocreaceae) that cause green mold disease on *Stropharia rugosoannulata* from Guizhou Province, China. MycoKeys 110: 361–383. https://doi.org/10.3897/mycokeys.110.134154

Introduction

Stropharia rugosoannulata (Wine-cap mushroom), a renowned edible mushroom, also known as Daqiugaigu in Chinese, has been widely cultivated in Poland, Germany, Russia and the United States (Huang et al. 2023). China imported a strain of *S. rugosoannulata* from Poland in the 1980s and began widespread cultivation in the 1990s (Yan et al. 2020). In recent years, *S. rugosoannulata* has been rapidly promoted and widely cultivated throughout China (Gu et al. 2024). With the increasing scale of cultivation, the annual yield of *S. rugosoannulata* in China has exceeded 210,000 tons per year (Huang et al. 2023). However, the emergence of various diseases during the cultivation of *S. rugosoannulata* has driven researchers to in-

tensify their efforts to optimize its growth conditions. Our investigation observed green mold disease on the soil surface and fruiting bodies of *S. rugosoannulata* from three different localities. This disease incidence can lead to mushroom rot and a decline in yield and quality. The dedication of researchers to addressing this issue is a reassuring sign for the future of *S. rugosoannulata* cultivation.

Green mold disease is a major prevalent disease that frequently arises during mushroom development and is characterized by green, villiform mycelia on the surface (Li et al. 2013). *Trichoderma* Pers. (Hypocreales, Ascomycota) is a saprobic fungus found in soil, healthy plants, wood, and other fungi and plays a crucial role as the causative agent of green mold disease. *Trichoderma* species are widely used to combat fungal pathogens (Hasan et al. 2012; Liu et al. 2012; Li et al. 2013; Abo-Elyousr et al. 2014; Poveda et al. 2019), produce antibiotics, enzymes, and biofuel (Degenkolb et al. 2008; Jun et al. 2011; Wijayawardene et al. 2022). Additionally, *Trichoderma* species contribute to the bioremediation of xenobiotic compounds in water and soil (Katayama and Matsumura 1993; Harman et al. 2004; Ezzi and Lynch 2005). Currently, *Trichoderma* comprises more than 500 species globally, based on the literature search (Jaklitsch 2009; Jaklitsch and Voglmayr 2015; Jambhulkar et al. 2024), legitimate names in the Mycobank (https://www.mycobank.org.) and in the Species Fungorum database (www.speciesfungorum.org; accessed on 23 October 2024).

Trichoderma has two types of species with differing ascospore colours, namely hyaline and green ascospores. Chaverri and Samuels (2004) pioneered comprehensive research on green-spored *Trichoderma* species, providing foundational insight into their taxonomy and systematics. Subsequently, Jaklitsch and Voglmayr (2015) proposed a comprehensive classification primarily based on molecular phylogenetic analyses rather than the color of ascospores, dividing them into six subclades: *Ceramicum*, *Chlorosporum*, Harzianum, *Helium*, *Spinulosum*, and *Strictipile*. However, other researchers have not recognized this classification, largely due to the inconsistencies between molecular sequence data and morphological characteristics, as highlighted by Chen and Zhuang (2017). Bustamante et al. (2021) used multi-locus phylogenetic analyses alongside four DNA-based approaches to accurately delimit species within the *Trichoderma* Harzianum lineage, including most green-spored species.

The present study was conducted based on the pathogen of the green mold disease, aiming to characterize and identify the isolates. Six isolates were isolated from soil samples and fruiting bodies of *S. rugosoannulata* cultivated fields in three different regions of Guizhou Province, China. The study described two new species and compared their morphological characteristics among closely related species. A combined dataset of ITS, *rpb2*, and *tef1-α* was used for the thorough phylogenetic analyses, ensuring the reliability of the results.

Materials and methods

Pathogen collection, isolation, and maintenance

Infected fruiting bodies of *S. rugosoannulata* were collected from mushroom-cultivated fields at Baiyun and Shuicheng counties (23°4'23.6352"N, 120°37'39.7812"E and 24°55'39.936"N, 121°11'30.264"E), Guizhou Province,

China in October-November 2023. Field photographs of the fresh specimens were taken with a Canon EOS 1200D (Canon, Japan) or Sony DSC-W830 (Sony, Japan) camera. The specimens were packed in aluminium foil and transferred to the Plant Pathology Laboratory at Guizhou University for isolation. Fungal pathogens on infected fruiting bodies were isolated using the spread plate and tissue isolation method following Wang et al. (2019). Purified cultures were incubated on potato dextrose agar (PDA), malt extract agar (MEA), and synthetic low nutrient agar (SNA) plates at 25, 30, and 35 °C. The holotype specimen was deposited in the Herbarium of the Department of Plant Pathology, Agricultural College, Guizhou University (HGUP). All single ex-type strains were deposited in the Culture Collection of the Guizhou University, China (GUCC) Department of Plant Pathology at Agriculture College and maintained in 25% (v/v) glycerol at −80 °C for long-term preservation (Zeng et al. 2022). Index Fungorum numbers were registered for the new taxa (https://www.indexfungorum.org/names/Names.asp).

Pathogenicity assays

A pathogenicity test was conducted by inoculating fungal mycelial blocks and spore suspensions from six strains isolated from Baiyun, Shuicheng, and Anshun counties onto the soil surface and fruiting bodies of *S. rugosoannulata*, following the updated protocol of Tian et al. (2017). All strains were incubated at 25 °C for 10 days. Control checks (CK) included PDA blocks and distilled water, replacing the mycelial blocks and spore suspensions. Photographs of the inoculated soils were taken after one, seven, and 10 days to monitor the development of any green mycelia. After the 10-day incubation, fungal pathogens were re-examined and re-isolated from the diseased areas to fulfill Koch's postulates, ensuring accurate identification of pathogenicity (Zhang et al. 2015; Xie et al. 2024). The experiment was repeated three times to validate the results and account for variability.

Morphological studies

Micro-morphological observations were performed from culture photographs of fresh stromata, which were taken using an ultra-depth field stereomicroscope (digital microscope system Keyence VHX-7000) to illustrate the macrostructures. Sections were made using a stereomicroscope (Leica DM2500) and mounted in water or a rehydrated 5% KOH solution. The cultures were incubated at 25 °C in darkness (Põldmaa 2011; Wei et al. 2024). Approximately 30 morphological measurements of new species were made for each feature using the ZEN 3.0 (blue edition) (Jena, Germany) software (Zeiss Scope 5 with color camera AxioCam 208) with differential interference contrast (DIC) optics to observe the morphological characteristics (Jaklitsch and Voglmayr 2015; Fu et al. 2024; Zeng et al. 2024). Colony characteristics, i.e., color and texture on PDA (Potato dextrose agar; 200 g potatoes, 20 g dextrose, 20 g agar per L), MEA (malt extract agar; 30 g malt extract, 5 g mycological peptone, 15 g agar per L) and synthetic low nutrient agar (SNA) plates at 25, 30 and 35 °C were observed and noted over 14 days.

Molecular studies

DNA extraction, Polymerase Chain Reaction (PCR) and sequencing

The genomic DNA was extracted from the colony of the isolates cultured at 25 °C, PDA for seven days using a CwBiotech Plant Genomic DNA Kit (Changping, Beijing, China) following the manufacturer's protocol.

The internal transcribed spacer (nrITS), the second largest RNA polymerase II subunit (*rpb2*) and the partial translation elongation factor 1-alpha (*tef1-α*) regions were amplified using the primer pairs ITS5/ITS4, EF1-728F/TEF1LLErev, and fRPB2-5F/fRPB2-7cR, respectively (White et al. 1990; Carbone and Kohn 1999; Liu et al. 1999; Jaklitsch et al. 2005). A 25 mL reaction mixture containing 1.6 mL dNTP mix (2.5 mM/mL), 0.2 mL Taq polymerase (5 U/mL), 2 mL polymerase buffer (10 /mL), 1 ml forward and reverse primers (10 mM/mL), and 1 mL DNA template was used for PCR experiments. Amplifications were carried out in a T100™ Thermal Cycler (BIO-RAD), which was configured for an initial denaturation at 95 °C for 3 minutes, followed by 34 cycles of 1 minute at 95 °C, 30 seconds at 55 °C, 1-minute extension at 72 °C, and a final extension at 72 °C for 10 minutes. Sangon Biotech (Shanghai) Co., Ltd. sequenced PCR products using the same PCR primers used in amplification operations. The newly generated sequences were checked with BioEdit v.7.2.5 (Hall 1999) and deposited in the NCBI GenBank nucleotide database for future reference.

The amplified sequences were subjected to BLASTn searches in the GenBank nucleotide database for comparison. Subsequently, closely related sequences of the taxa exhibiting zero E-values were retrieved from the database to generate the dataset. Besides, the sequences used by earlier studies on *Trichoderma* (Zeng et al. 2022) were also obtained from the database to prepare the final dataset (Table 1).

Dataset representation

Sequences of the closely related taxa with zero E-value were searched from the BLASTn analyses in the NCBI GenBank nucleotide database. A preliminary BLAST search with the newly amplified sequences of the collected specimens showed the highest sequence similarity with the members of the *Trichoderma* Pers. Hence, a dataset was prepared based on the highest-scored hits of the BLAST search plus the datasets used in the earlier studies on *Trichoderma* (Zeng et al. 2022).

Sequence alignment and phylogenetic analyses

The newly generated reverse and forward sequences were reassembled manually using BioEdit version 7.0.5.3 (Hall 1999) and were aligned with MAFFT v.7.427 (Katoh et al. 2019) in an online platform (https://www.ebi.ac.uk/Tools/msa/mafft/). The aligned sequences were imported to MEGA v.7.0 (Kumar et al. 2016) for manual improvement and trimming of both ends.

A quick phylogenetic analyses of DNA fragments (ITS, *rpb2* and *tef1-α*) from 128 strains were performed with alignments and associated data matrices, including six isolates in this study (GUCC TB1117, GUCC TB1118, GUCC TB1119, GUCC TB1120, GUCC TB1121 and GUCC TB1122) and 122 reference strains (Table 1) by using offline software 'One-click Fungal Phylogenetic Tool'

Table 1. Names, strain numbers, locations, and corresponding GenBank accession numbers of the taxa used in the phylogenetic analysis.

Species	Strain	Geographic origin	GenBank Accession Numbers		
			ITS	*rpb2*	*tef1-α*
T. achlamydosporum	YMF 1.06226	China	MN977791	MT052180	MT070156
T. aerugineum	CBS 120541 T	Austria	FJ860720	FJ860516	FJ860608
T. afarasin	DIS 314F	Cameroon	FJ442259	FJ442778	FJ463400
T. afroharzianum	CBS 466.94	Netherlands	KP009262	KP009150	KP008851
T. aggregatum	HMAS 248863	China	KY687946	KY688001	KY688062
T. aggressivum	CBS 100525	United Kingdom	-	AF545541	AF534614
T. alni	CBS 120633 T	United Kingdom	EU518651	EU498349	EU498312
T. alpinum	HMAS 248821 T	China	KY687906	KY687958	KY688012
T. amazonicum	IB 95	Peru	-	HM142368	HM142377
T. anaharzianum	YMF 1.00383	China	MH113931	MH158995	MH183182
T. asiaticum	YMF 1.00352	China	MH113930	MH158994	MH183183
T. atrobrunneum	S3	Italy	-	KJ665241	KJ665376
T. atrogelatinosum	CBS 237.63 T	New Zealand	MH858272	KJ842201	KJ871083
T. attinorum	LESF 236	USA	-	KT278971	KT279039
T. aureoviride	CPK 2848	Germany	FJ860733	FJ860523	FJ860615
T. azevedoi	CEN1422 T	Brazil	MK714902	MK696821	MK696660
T. bannaense	HMAS 248840 T	China	KY687923	KY687979	KY688037
T. breve	HMAS 248844 T	China	KY687927	KY687983	KY688045
T. brevicrassum	HMAS 248871 T	China	KY687954	KY688008	KY688064
T. britannicum	CBS 253.62 T	United Kingdom	MH858149	KF134787	KF134796
T. brunneoviride	CBS 121130	Germany	EU518659	EU498357	EU498316
T. byssinum	HMAS 248838 T	China	KY687921	KY687977	KY688035
T. catoptron	GJS 02-76 T	Sri Lanka	AY737766	AY391900	AY391963
T. ceraceum	GJS 95-159 T	North Carolina	AF275332	AF545508	AF534603
T. ceramicum	CBS 114576 T	Austria	FJ860743	FJ860531	FJ860628
T. ceratophylli	YMF 1.04621	China	MK327581	MK327580	MK327579
T. cerinum	S357	France	-	KF134788	KF134797
T. chlamydosporicum	HMAS 248850	China	KY687933	KY687989	KY688052
T. chlorosporum	GJS 88-33 T	USA	-	AY391903	AY391966
T. christiani	CBS 132572 T	Spain	-	KJ665244	KJ665439
T. chromospermum	HMAS 252535	China	KF923304	KF923315	KF923292
T. cinnamomeum	GJS 97-237	USA	AY737759	AY391920	AY391979
T. compactum	CBS 121218 T	China	-	KF134789	KF134798
T. concentricum	HMAS 248833 T	China	KY687915	KY687971	KY688027
T. corneum	GJS 97-82 ET	Thailand	-	KJ665252	KJ665455
T. costaricense	PC 21 T	Costa Rica	AY737754	AY391921	AY391980
T. cremeoides	S112 T	Italy	-	KJ665253	KJ665456
T. cremeum	GJS 91-125 T	USA	AY737760	AF545511	AF534598
T. cuneisporum	GJS 91-93 T	USA	AY737763	AF545512	AF534600
T. dacrymycellum	WU 29044	Germany	FJ860749	FJ860533	FJ860633
T. danicum	CBS 121273 T	Denmark	FJ860750	FJ860534	FJ860634
T. epimyces	CBS 120534 T	Austria	EU518663	EU498360	EU498320
T. estonicum	GJS 96-129 T	Estonia	AY737767	AF545514	AF534604
T. ganodermatis	HMAS 248856	China	KY687939	KY687995	KY688060
T. gelatinosum	GJS 88-17	France	AY737775	AF545516	AF534579
T. gliocladium	CBS 130009 T	Italy	MH865622	KJ665271	KJ665502
T. guizhouense	S278	Croatia	-	KF134791	KF134799
T. hainanense	HMAS 248837 T	China	KY687920	KY687976	KY688033
T. harzianum	CBS 226.95 T	Austria	AY605713	AF545549	AF534621
T. hausknechtii	CBS 133493 T	France	-	KJ665276	KJ665515
T. helicolixii	CBS 133499 T	Greece	-	KJ665278	KJ665517
T. helicum	DAOM 230021	Austria	-	DQ087239	KJ871125

Species	Strain	Geographic origin	GenBank Accession Numbers		
			ITS	*rpb2*	*tef1-α*
T. hirsutum	HMAS 248834 T	China	KY687916	KY687972	KY688029
T. hunanense	HMAS 248841 T	China	KY687924	KY687980	KY688039
T. hymenopellicola	GUCC202008	China	MZ330754	ON088663	ON102007
T. hymenopellicola	GUCC202009	China	MZ330755	ON088664	ON102008
T. hymenopellicola	GUCC202010	China	MZ330756	ON088661	ON102005
T. hymenopellicola	GUCCTB626	China	ON074580	ON088662	ON102006
T. hymenopellicola	GUCCTB625	China	ON074583	-	ON102011
T. inaequilaterale	YMF 1.06203	China	MN977795	MT052186	MT070152
T. ingratum	HMAS 248822 T	China	KY687917	KY687973	KY688018
T. inhamatum	CBS 273.78 T	Colombia	-	FJ442725	AF348099
T. italicum	CBS 132567 T	Italy	-	KJ665282	KJ665525
T. jaklitschii	CP61-2 T	Peru	-	MW480149	MW480140
T. lentiforme	DIS 94D	Peru	-	FJ442749	FJ463379
T. lentinulae	CGMCC 3.19847 T	China	-	MN605867	MN605878
T. liberatum	HMAS 248831 T	China	KY687913	KY687969	KY688025
T. linzhiense	HMAS 248846 T	China	KY687929	KY687985	KY688047
T. lixii	CBS 110080 T	USA	AF443920	KJ665290	FJ716622
T. longibrachiatum	CBS 816.68 T	Austria	Z31019	DQ087242	EU401591
T. longifialidicum	LESF 552	USA	-	KT278955	KT279020
T. longipile	DAOM 177227 T	Austria	AY865630	AF545550	AF534622
T. longisporum	HMAS 248843	China	KY687926	KY687982	KY688043
T. lycogaloides	WU 32096 T	French Guiana	-	KF134792	KF134800
T. parepimyces	CBS 122769 T	Austria	FJ860800	FJ860562	FJ860664
T. parestonicum	CBS 120636 T	Austria	FJ860803	FJ860565	FJ860667
T. peberdyi	CEN1426 T	Brazil	MK714906	MK696825	MK696664
T. peruvianum	CP15-2 T	Peru	-	MW480153	MW480145
T. perviride	HMAS 273786 T	China	-	KX026962	KX026954
T. phyllostachydis	CBS 114071 T	Austria	FJ860809	FJ860570	FJ860673
T. pinicola	SFC20130926-S233 T	South Korea	MH050354	MH025993	MH025981
T. pleuroti	CBS 124387 T	USA	-	HM142372	HM142382
T. pleuroticola	CBS 124383 T	USA	-	HM142371	HM142381
T. polypori	HMAS 248855 T	China	KY687938	KY687994	KY688058
T. priscilae	CBS 131487 T	Austria	-	KJ665333	KJ665691
T. propepolypori	YMF 1.06224	China	MN977789	MT052181	MT070158
T. pseudoasiaticum	YMF 1.06200 T	China	MN977792	MT052183	MT070155
T. pseudocandidum	PC 59 T	Costa Rica	AY737757	AY391899	AY737742
T. pseudodensum	HMAS 248828 T	China	KY687910	KY687967	KY688023
T. pseudogelatinosum	CNU N309 T	South Korea	-	HM920173	HM920202
T. purpureum	HMAS 273787 T	China	-	KX026961	KX026953
T. pyramidale	CBS 135574 T	Italy	-	KJ665334	KJ665699
T. rifaii	DIS 337F ET	Panama	-	FJ442720	FJ463321
T. rosulatum	HMAS 252548	China	KF729995	KF730005	KF729984
T. rufobrunneum	HMAS 266614 T	China	KF729998	KF730010	KF729989
T. rugulosum	SFC20180301-1 T	South Korea	MH050353	MH025986	MH025984
T. shennongjianum	HMAS 245009	China	-	KT735259	KT735253
T. silvae-virgineae	CBS 120922	Austria	-	FJ860587	FJ860696
T. simile	YMF 1.06201	China	MN977793	MT052184	MT070154
T. simmonsii	S7	Italy	-	KJ665337	KJ665719
T. simplex	HMAS 248842 T	China	KY687925	KY687981	KY688041
T. sinuosum	CPK 1595	Austria	FJ860838	FJ179619	FJ860697
T. solum	HMAS 248848 T	China	KY687931	KY687987	KY688050
T. spinulosum	CBS 311.50 T	Austria	FJ860844	FJ860591	FJ860701
T. spirale	DAOM 183974 T	Thailand	EU280068	AF545553	EU280049
T. stipitatum	HMAS 266612	China	KF730002	KF730011	KF729990
T. stramineum	GJS 02-84 T	Sri Lanka	AY737765	AY391945	AY391999

Species	Strain	Geographic origin	GenBank Accession Numbers		
			ITS	*rpb2*	*tef1-α*
T. strictipile	CPK 1601	Austria	-	FJ860594	FJ860704
T. strophariensis	**GUCC TB1117 T**	**China**	**PP920011**	**PP954941**	**PP954947**
T. strophariensis	**GUCC TB1118**	**China**	**PP920012**	**PP954942**	**PP954948**
T. strophariensis	**GUCC TB1119**	**China**	**PP920013**	**PP954943**	**PP954949**
T. subazureum	YMF 1.06207	China	MN977799	MT052190	MT070148
T. subuliforme	YMF 1.06204	China	MN977796	MT052187	MT070151
T. sulawesense	GJS 85-228	USA	-	AY391954	AY392002
T. surrotundum	GJS 88-73 T	USA	AY737769	AF545540	AF534594
T. tawa	GJS 97-174 T	Thailand	AY737756	AY391956	AY392004
T. tenue	HMAS 273785 T	China	-	KX026960	KX026952
T. thailandicum	GJS 97-61 T	Thailand	AY737772	AY391957	AY392005
T. thelephoricola	CBS 120925	Austria	FJ860858	FJ860600	FJ860711
T. tibetense	HMAS 245010	China	-	KT735261	KT735254
T. tomentosum	CBS 120637	Austria	-	FJ860532	FJ860629
T. tropicosinense	HMAS 252546	China	KF923302	KF923313	KF923286
T. undatipile	HMAS 248854	China	KY687937	KY687993	KY688056
T. velutinum	CPK 298 T	Nepal	-	KF134794	KJ665769
T. vermifimicola	CGMCC 3.19694 T	China	MN594473	MN605871	MN605882
T. virens	DAOM 167652 T	USA	EU330955	AF545547	AF534619
T. virescentiflavum	PC 278	Costa Rica	AY737768	AY391959	AY392007
T. viridistromatis	**GUCC TB1120 T**	**China**	**PP922277**	**PP954944**	**PP954950**
T. viridistromatis	**GUCC TB1121**	**China**	**PP926290**	**PP954945**	**PP954951**
T. viridistromatis	**GUCC TB1122**	**China**	**PP922285**	**PP954946**	**PP954952**
T. xixiacum	CGMCC 3.19697 T	China	MN594476	MN605874	MN605885
T. zayuense	HMAS 248835 T	China	KY687918	KY687974	KY688031
T. zelobreve	CGMCC 3.19695 T	China	MN594474	MN605872	MN605883
T. zeloharzianum	YMF 1.00268	China	MH113932	MH158996	MH183181

Note: Newly sequenced strains are shown in bold. T denotes type cultures.

(OFPT-https://ofpt.guhongxin.com) following its default protocol (Zeng et al. 2023). The final Maximum likelihood analysis was performed with RAxML-HPC2 v. 8.2.12 (Stamatakis 2014) on the CIPRES Science Gateway platform using the GTR+I+G model with 1,000 bootstrap replicates and Bayesian analyses were conducted with MrBayes v.3.2.2 (Ronquist et al. 2012) using MCMC methods (Geyer 1991) under a GTR+I+G model. Markov chains were run for 2 × 106 generations, saving a tree every 100th generation with all the remaining parameters set to default. Bayesian analyses reached a standard deviation of split frequency of 0.0048 at the end of the specified number of generations. For both analyses, the initial 25% of trees recovered (10,000 trees) were excluded as the burn-in, while the remaining 30,002 trees were utilized to estimate the posterior probabilities for the group. ML bootstrap values (MLBS) ≥ 70% and Bayesian posterior probabilities (PP) values ≥ 0.95 are displayed in the phylogenetic tree. The resulting trees were visualized in FigTree v1.4.3 (Rambaut 2016).

Results

Pathogenicity tests

Both soil inoculating groups of covering mycelial blocks and soil mixed with spore suspension of isolates GUCC TB1117 and GUCC TB1120 exhibited similar symptoms of green mold disease in the field after seven days (Fig. 1g), while

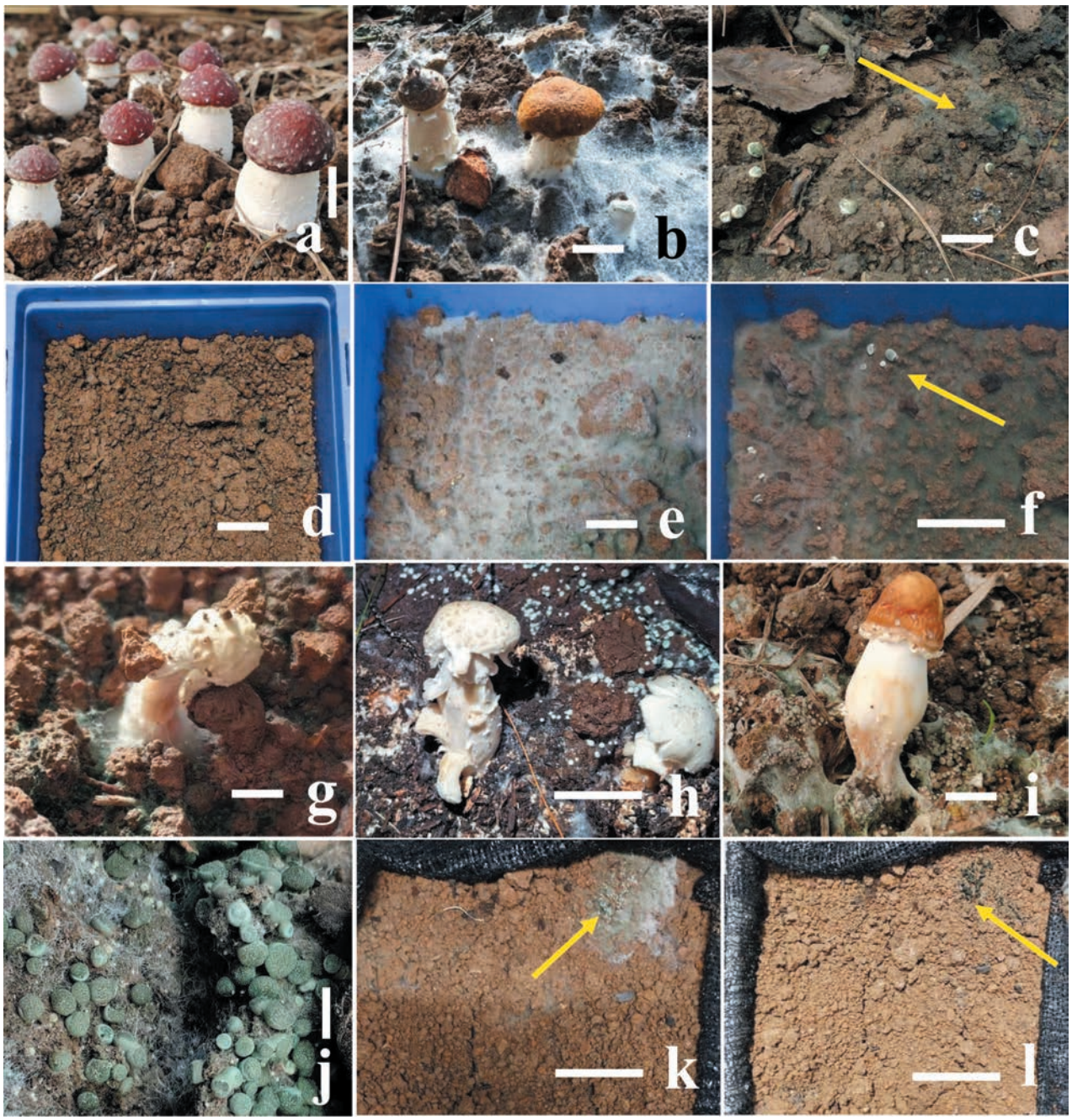

Figure 1. Field symptoms of green mold disease on *Stropharia rugosoannulata* and pathogenicity tests of isolates GUCC TB1117 and GUCC TB1120 with spore suspension **a** healthy fruiting bodies of *S. rugosoannulata* **b** field symptoms of green mold disease on *S. rugosoannulata* **c** large stroma of the pathogen *T. stropharіensis* (GUCC TB1117) **d** control, no disease after seven days of inoculation with distilled water **e–g** pathogenicity tests after spraying with 0.5 mL spore suspension (1×10^6 conidia mL^{-1}) **e, f** hyphal blocks and pathogen stroma (F = yellow arrow) appear on the surface of the soil after five days of inoculation **g** whole rotten fruiting bodies after seven days of inoculation **h, i** rotten fruiting bodies of *S. rugosoannulata* in the field with *T. viridistromatis* (GUCC TB1120) **j** Aggregated stroma of the pathogen *T. viridistromatis* (GUCC TB1120) with typical green symptoms **k, l** yellow arrows showing pathogen hyphal blocks and stroma appear on the surface of the soil after five days of inoculation. Scale bars: 20 mm (**a–e**); 10 mm (**f**); 20 mm (**g**); 10 mm (**h**); 20 mm (**l, j**); 10 mm (**k, l**).

the control group did not have (Fig. 1d). The green mycelia can be observed on the surface of the mushroom tray after 3–5 days and spread fast, covering the whole surface of the substrate and turning green within 10 days (Fig. 1e, f).

The rate of isolates GUCC TB1117 and GUCC TB1120 infecting mushroom tray is about 50%, similar to its incidence in the field. The same fungal pathogen had been observed and re-isolated from these symptoms, which fulfills Koch's postulates (Fig. 1).

Phylogenetic analyses

The phylogenetic analyses were conducted using a combined dataset of nrITS, *rpb2*, and *tef1-α* sequences. A total of 128 sequences were aligned, and this resulted in a dataset consisting of 2934 nucleotides; after the ends of the individual alignments were trimmed, the size of the aligned dataset was as nrITS 610 bp, *rpb2* was 1080 bp, and *tef1-α* was 1244 bp respectively. The best-fit substitution model of each gene is ITS (TIM2+F+R4), *rpb2* (TIM3e+I+G4) and *tef1-α* (TIM+F+R4). The RAxML analysis of the combined dataset yielded a best-scoring tree with a final ML optimization likelihood value of –37957.575772. Estimated base frequencies are as follows: A = 0.233134, C = 0.285526, G = 0.253003, and T = 0.228336; substitution rates AC = 1.134637, AG = 4.477934, AT = 1.149518, CG = 1.048786, CT = 6.335323, and GT = 1.000000; proportion of invariable sites I = 0.544721; and gamma distribution shape parameter a = 0.951765. The Bayesian analysis ran 29,64000 generations before the average standard deviation for split frequencies reached 0.00998. The analysis generated 59,282 trees, from which 44,462 were sampled after burn-in, and the 99% credible set contains 35,309 trees. Our new strains belong to a distinct clade that is genetically distant from *T. britannicum*, *T. aerugineum*, *T. danicum*, and *T. spinulosum* and is divided into four subclades represented by our newly generated strains (Fig. 2). DNA base pair differences also supported the phylogenetic placements of these novel taxa (Table 2).

Table 2. The DNA base differences of our isolates and related taxa in different loci.

Species	Strain number	ITS (1–610 bp)	*rpb2* (611–1690 bp)	*tef1-α* (1691-2934 bp)
Trichoderma stropharіensis	GUCC24-0002	0	0	0
Trichoderma stropharіensis	GUCC24-0003	0	0	0
Trichoderma stropharіensis	GUCC24-0004	0	0	0
Trichoderma britannicum	CBS 25362	28 (gaps: 4)	48 (gap: 0)	64 (gap: 25)
Trichoderma aerugineum	CBS 120541	16 (gaps: 9)	78 (gap: 0)	67 (gap: 11)
Trichoderma danicum	CBS 121273	25 (gaps: 8)	99 (gaps: 0)	105 (gaps: 3)
Trichoderma spinulosum	CBS 31150	21 (gaps: 8)	82 (gaps: 0)	108 (gap: 7)
Trichoderma viridistromatis	GUCC24-0005	0	0	0
Trichoderma viridistromatis	GUCC24-0006	0	0	0
Trichoderma viridistromatis	GUCC24-0007	0	0	0
Trichoderma britannicum	CBS 25362	17 (gaps: 5)	20 (gap: 0)	55 (gaps: 21)
Trichoderma aerugineum	CBS 120541	10 (gaps:10)	79 (gap: 0)	78 (gaps: 11)
Trichoderma danicum	CBS 121273	25 (gaps: 8)	95 (gap: 0)	113 (gap: 0)
Trichoderma spinulosum	CBS 31150	22 (gaps: 8)	73 (gaps: 0)	109 (gaps: 7)

Figure 2. A phylogram was constructed using ML analysis, utilizing a combined ITS, *rpb2*, and *tef1-α* sequences dataset. The green-spored *T. longibrachiatum* (CBS81668) was used as the outgroup taxon following Zeng et al. (2022). The tree with the highest score according to RAxML, with a final probability value of *-lnL* = 37957.575772, is displayed. Maximum Likelihood (ML) values equal to or greater than 70% and Bayesian Inference (BI) values equal to or greater than 0.90 are given above the nodes (ML values on the left side of '/' in regular font and BI values on right side of '/' in italics). Type strain sequences are indicated in red bold, while newly generated sequences are shown in black bold. Strain numbers for the sequences are shown in the tree following the taxon name. 'T' denotes ex-holotype strains.

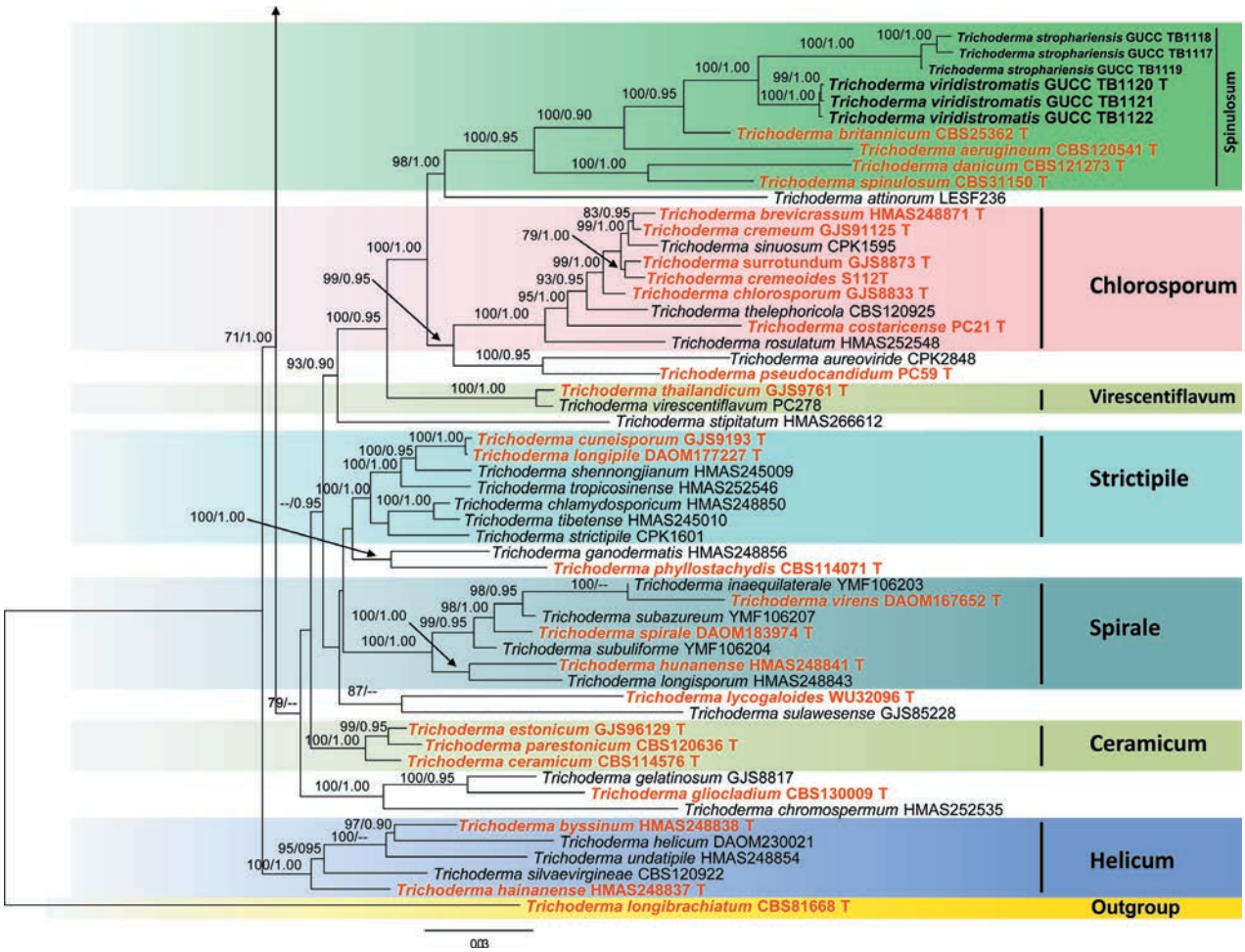

Figure 2. Continued.

Taxonomy

***Trichoderma stropharienses* E. Tarafder & F.H. Tian, sp. nov.**
Fungal Names: FN 902311
Figs 3, 4

Diagnosis. *Trichoderma stropharienses* differs from *T. britannicum* by smaller stromata (0.9–2.2 × 0.8–2 mm) with dark green surface, margin free; surface finely rugose or tubercular, brownish between black ascomata; ostiolar dots absent, inconspicuous or convex to distinctly papillate measuring (27–)35–64(–90) mm diam. Additionally, it is easily distinguished from *T. viridistromatis* by its relatively larger ascospores (8.4–16.9 × 5.5–8.1 µm) and conidia (8.5–25.5 × 5.7–17.9 µm). Phylogenetically, *T. stropharienses* forms a distinct clade and is closely related to *T. viridistromatis*, *T. britannicum*, and *T. aerugineum* with 100% ML and 0.90 BYPP statistical support (Fig. 1).

Holotype. HGUP 24-0001.

Etymology. The specific epithet '*stropharienses*' refers to the occurrence of the new taxon in cultivated mushrooms *Stropharia rugosoannulata*.

Description. *Stromata*, when fresh 1–14 mm in diameter, 1–11 mm thick (n = 10), solitary to sometimes aggregated, discoid or undulate, with brownish margin and pale red, depressed center when young, becoming reddish with ru-

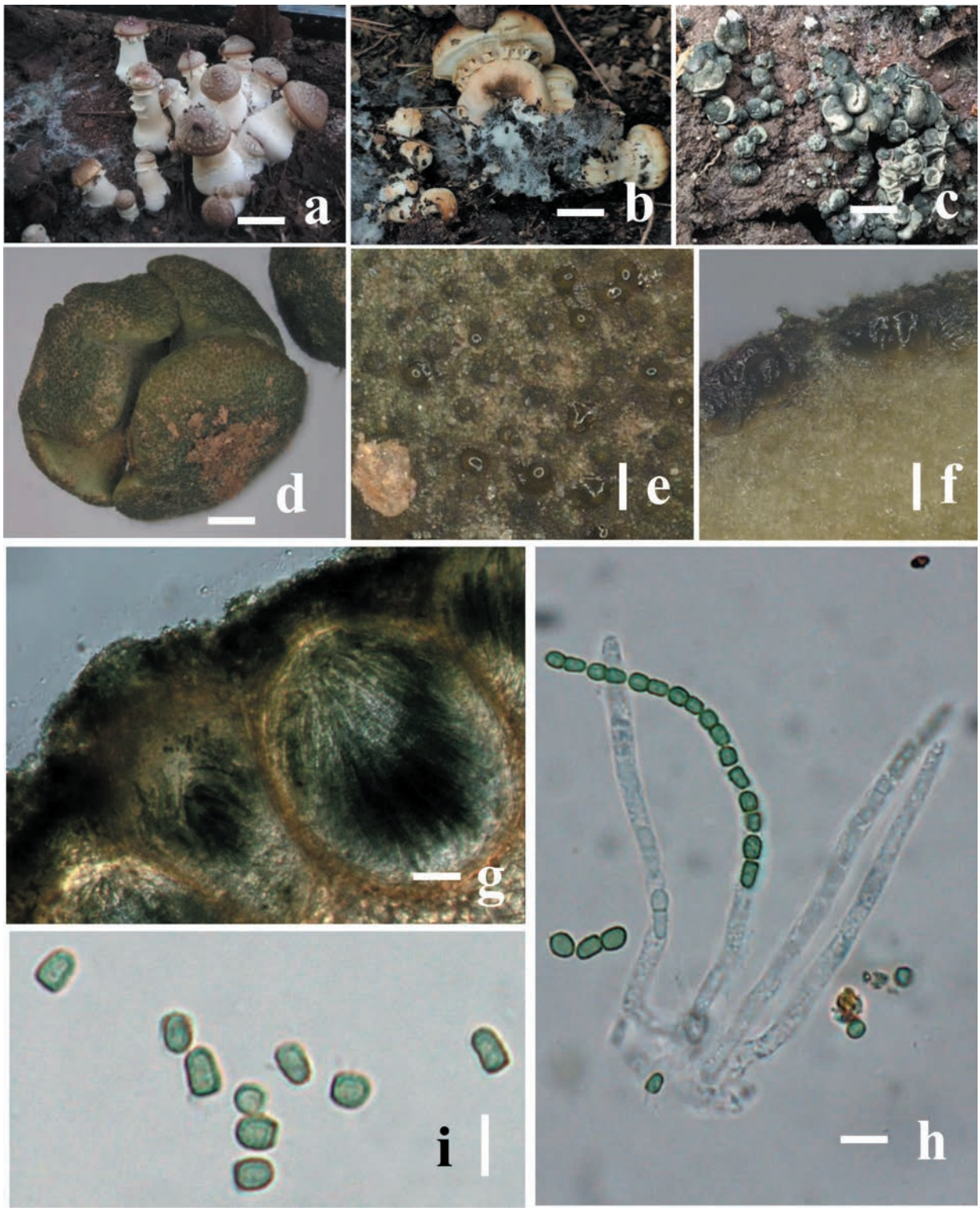

Figure 3. Morphology of *Trichoderma strophariensis* (HGUP 24-0001, GUCC 24-0002) **a, b** disease in the field habitat **c** fresh stromata on natural habitat **d** dry stromata **e** ostiolar dots on stromata surface **f** cortical and subcortical tissues in section **g** ascomatal tissue in section **h** asci with ascospores **i** ascospores. Scale bars: 10 mm (**a, b**); 20 mm (**c**); 100 mm (**d–f**); 50 µm (**g**); 20 µm (**h, i**).

gose surface when mature. Attached to the host by hyphae, easily detached; sides often attenuated downward, surrounded at the base by white cottony mycelium when young. Surface finely rugose, tubercular, brownish between black

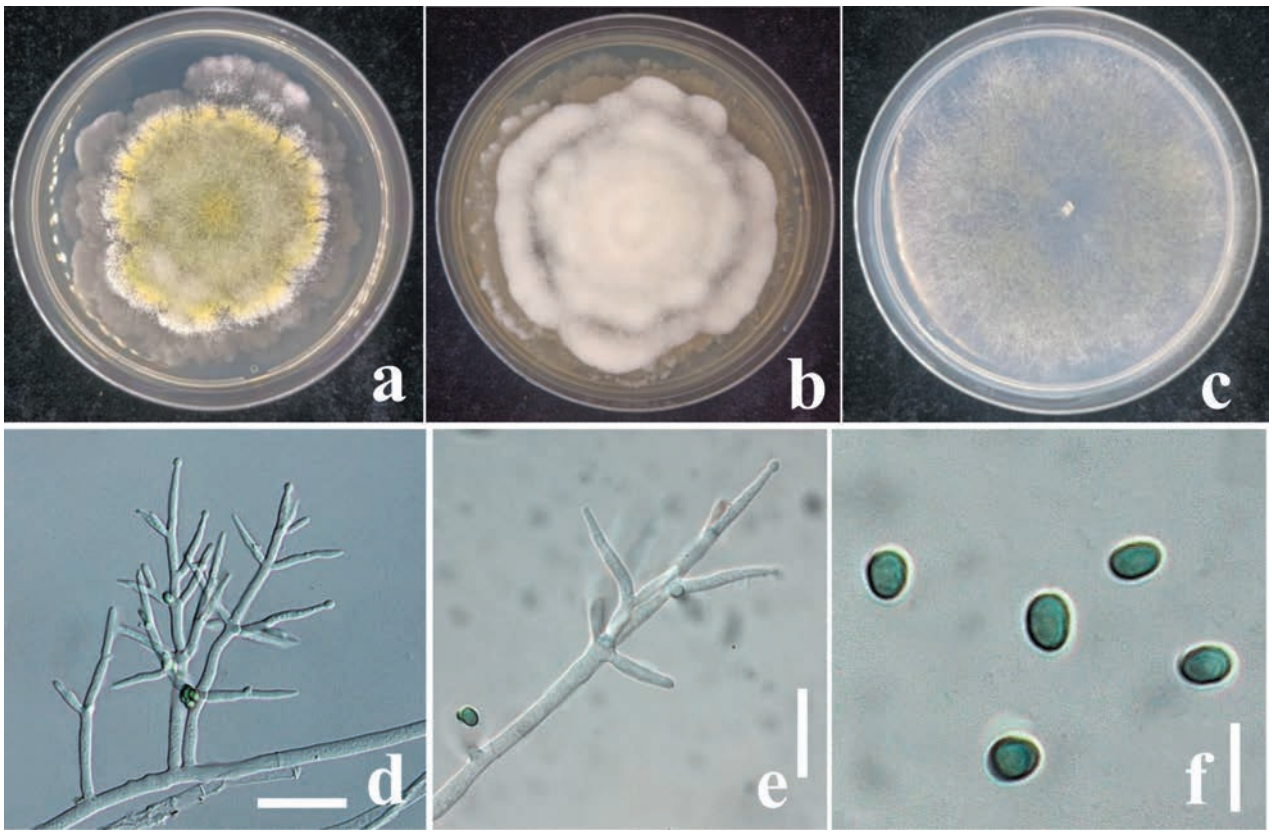

Figure 4. a cultures on MEA (five days) **b** cultures on PDA (five days) **c** cultures on SNA (4 days) **d** conidiophores **e** phialides **f** conidia. Scale bars: 10 µm (**d, e**); 5 µm (**f**).

ascomata; Ostiolar dots are convex to umbilicate, greenish, overall colors light green, darker green when dry, surface and spores green when mature. ***Ostiole*** 14–21 µm wide at apex, 41–59 µm high (n = 30). ***Ascomata*** (139–)175–295(–347) × (113–)151–248(–290) µm (n = 20), flask-shaped or sub-globose, crowded. ***Peridium*** 18–28 µm thick at the base and sides (n = 40), light brown. ***Asci*** (67–)110–146(–207) × (3.7–)5.8–7.7(–9.4) µm, stipe (3–)7–11(–18) µm long (n = 50), containing 16-ascospores, apex slightly thickened, hyaline, cylindrical. ***Ascospores*** (8.4–)9.2–11.6(–16.9) × (5.5–)6.6–7.8(–8.1) µm, l/w (1.2–)1.4–1.6(–2.1) (n = 90), green, verruculose; sub-globose, oblong, elongated, thick-walled.

Culture characteristics. Optimal growth at 25 °C on all media, poor and limited growth at 30 °C, no growth at 35 °C.

On MEA and PDA growth is slow, colony creamy white, finely farinose by scant effuse conidiation; on PDA reverse brownish, surface turning greenish-brown. On MEA at 25 °C after five days colony radius 5–7 mm; colony circular, dense, thick, first whitish, becoming zonate after a few weeks, turning olive-green to brown with yellow greenish, farinose center; conidiation effuse, on short odd verticillium like conidiophores. On SNA colony radius at 25 °C after 2 weeks 6–9 mm; colony dense, hyaline, turning greenish or olivaceous from conidia. Conidiation following growth, effuse, on aerial hyphae and short odd verticillium-like conidiophores, spreading from the plug. ***Conidiophores*** simple, 1–4 level are branched and tapered at the tips, bearing few asymmetric side branches, terminated by solitary phialides of 2–3 divergent phialides. ***Phialides*** (10.5–)37–44(–55) × (1.5–)2.5–11(–12.5) µm (n = 50), mostly gregarious,

cylindrical, less commonly subfusiform, often thickest near the base. ***Conidia*** (8.5–)12.5–16.4(–25.5) × (5.7–)6.5–10.7(–17.9) µm (n = 70), one-celled, variable shape and size, typically oblong and pale olive green when fully mature, sub-globose, oval or ellipsoid and hyaline when immature, straight or slightly curved, sides sometimes pinched, smooth; base often truncate, thick-walled.

Habitat. On mushroom cultivated field, associated with *Stropharia rugosoannulata*.

Distribution. China, Guizhou Province, Guiyang City, and Liupanshui City; Guizhou City in Anshun Province.

Material examined. China • Guizhou, Liupanshui City, Shuicheng District, 2°55'39.36"N, 120°11'30.64"E, on soil surfaces of *Stropharia rugosoannulata* cultivated field, 16-November-2023, E. Tarafder and F.H. Tian (HGUP 24-0001, holotype); ex-type living cultures GUCC TB1117, GUCC TB1118 and GUCC TB1119.

GenBank accession numbers. GUCC TB1117 (ITS: PP920011; *rpb2*: PP954941; *tef1-α*: PP954947); GUCC TB1118 (ITS: PP920012; *rpb2*: PP954942; *tef1-α*: PP954948); GUCC TB1119 (ITS: PP920013; *rpb2*: PP954943; *tef1-α*: PP954949).

Notes. Morphologically, our new isolates are most similar to *T. danicum* in the size of stromata (5–20 mm) but can be distinguished by its generally smaller ascospores and conidia (Table 3); the presence of deeper color of stromata and ascospores, less pigment on media, and faster growth rate on PDA and SNA. However, our new isolates differ from *T. britannicum* by smaller stromata (0.9–2.2 mm) with dark green surfaces (Jaklitsch, 2009). In addition, it differs from other new species (*T. viridistromatis*) in producing cylindrical, less commonly subfusiform phialides (10.5–55 × 1.5–12.5 µm) and larger conidia (8.5–25.5 × 5.7–17.9 µm), typically oblong, subglobose, oval, sometimes ellipsoid and pale olive green after maturity. Phylogenetically, our isolate (HGUP 24-0001) forms an independent clade and clustering with *Trichoderma britannicum*, *T. aerugineum*, *T. danicum*, *T. viridistromatis*, and *T. spinulosum* within the Spinulosum lineage with 100% ML and 1.00 BYPP statistical support (Fig. 2). It exhibits 4% sequence differences (28/610 nucleotides, four gaps) in the ITS region, 4% differences (48/1080 nucleotides, no gaps) in the *rpb2* gene, and 5% differences (64/1244 nucleotides, twenty-five gaps) in *tef1-α* gene when compared with *T. britannicum*. Additionally, the differences between our isolate with *T. viridistromatis* are 4% (29/610 nucleotides, four gaps) in the ITS region, 4%

Table 3. Morphological comparison of *Trichoderma britannicum*, *T. aerugineum*, *T. strophariensis*, *T. danicum*, *T. viridistromatis*, and *T. spinulosum*.

Taxon (holotype)	Ascospores	Conidia	Substratum	References
T. britannicum	10–16 × 4.5–6.2 µm	4.7–19.3 × 4–6.2 µm	Decaying wood of broadleaf trees	Jaklitsch et al. 2014
T. aerugineum	8–12 × 4–6 µm	3–5 × 2–4 µm	Decaying wood	Chaverri and Samuels (2004)
T. strophariensis	**8.4–16.9 × 5.5–8.1 µm**	**8.5–25.5 × 5.7–17.9 µm**	**mushroom species (*Stropharia*)**	**This study**
T. danicum	3–5 × 2.5–4.4 µm	3–3.5 × 2.7–3 µm	On pine wood	Jaklitsch 2009
T. viridistromatis	3.4–5.6 × 2.4–3.3 µm	2.8–4 × 1.7–3.2 µm	mushroom species (*Stropharia*)	This study
T. spinulosum	5–7 × 3–4 µm	3.5–4.7 × 3–3.7 µm	On stems of *Chelidonium majus*	Jaklitsch and Voglmayr 2015

(46/1080 nucleotides, no gaps) differences in the *rpb2* gene, and 5% (65/1244 nucleotides, twenty-five gaps) differences in the *tef1-α* gene. In contrast, the differences in our isolate with *T. danicum* are more than 4% (25/610 nucleotides, eight gaps) in the ITS region, 9% (99/1080 nucleotides, no gaps) in *rpb2* gene, and 8% (105/1244 nucleotides, three gaps) in *tef1-α* gene (Table 2). Therefore, based on both morphological and phylogenetic distinctions, *T. stropharіensis* is introduced as a new species from cultivated mushrooms.

Trichoderma viridistromatis **E. Tarafder & F.H. Tian, sp. nov.**
Fungal Names: FN 902312
Figs 5, 6

Diagnosis. *Trichoderma viridistromatis* differs from *T. aerugineum* by its smaller stromata (0.5–2 mm diam, to ca. 1 mm thick in *T. aerugineum*) and bigger phialides measuring 7–23 × 2.4–4 µm in *T. aerugineum*. In addition, it is easily distinguished from *T. stropharіensis* by its smaller ascospores (3.4–5.6 × 2.4–3.3 µm) and conidia (2.8–4 × 1.7–3.2 µm). Phylogenetically, *T. viridistromatis* forms a distinct clade and is closely related to *T. stropharіensis*, *T. britannicum*, and *T. aerugineum* with 100% ML and 0.90 BYPP statistical support (Fig. 1).

Holotype. HGUP 24-0004.

Etymology. The epithet "*viridistromatis*" refers to an entirely green-colored stroma.

Description. ***Stromata***, when fresh 1–7 mm in diam., 0.5–2 mm thick (n = 10), mostly gregarious, aggregated, discoid or undulate, becoming pulvinate, compact; outline circular to oblong; margin attached or free, surface smooth when immature without ostiolar dots, with yellowish margin and pale red, depressed center when young, becoming reddish with rugose surface when mature. Outline circular, oblong or irregularly lobed. Surface smooth, tubercular or rugose, when young finely velvety. Ostiolar dots absent, ostiolar openings sometimes visible, (16–)20–30(–32) µm (n = 30) wide, inconspicuous, pale, more distinct and shinier after rehydration. ***Ostioles*** (18–)24–30(–45) µm long, plane with the surface, (8–)12–19(–23) µm wide at the apex (n = 30). ***Ascomata*** (69–)75–85(–96) × (36–)41–55(–60) µm (n = 30), numerous, 5–7 per mm stroma length, sub-globose or flask-shaped. ***Peridium*** (7–)11–19(–22) µm (n = 60) thick at the base and sides; hyaline to pale yellowish. ***Asci*** (63–)74–81(–85) × (3.2–)4.2–5(–5.5) µm, stipe (4–)5–11(–14) µm (n = 30) long, containing 16-ascospores, apex not thickened, hyaline, cylindrical. ***Ascospores*** (3.4–)3.6–4.3(–5.6) × (2.4–)2.8–3.1(–3.3) µm, l/w 1–1.1(–1.2) (n = 34), hyaline, verruculose, single-celled, non-septate, sub-globose, oblong or slightly tapered downwards, thick-walled.

Culture characteristics. Optimal growth at 25 °C on all media, poor and limited growth at 30 °C, no growth at 35 °C. Although MEA exhibited good growth, precultures were made on it.

On MEA and PDA, growth is slow, colony is creamy white, finely farinose by scant effuse conidiation; on PDA, reverse brownish, surface turning greenish-brown. On MEA at 25 °C after five days colony radius 5–7 mm; colony circular, dense, thick, first whitish, becoming zonate after a few weeks, turning olive-green to brown with yellow-greenish, farinose center; conidiation effuse, on short odd

verticillium like conidiophores. On SNA colony radius at 25 °C after 2 weeks 6–9 mm; colony dense, hyaline, turning greenish or olivaceous from conidia. Conidiation following growth, effuse, on aerial hyphae and short odd verticillium-like conidiophores, spreading from the plug. ***Conidiophores*** simple, 1–4 level, are branched and tapered at the tips, bearing few asymmetric side branches, terminated by solitary phialides of 2–3 divergent phialides. ***Phialides*** (5.5–)7–10(–14) × (1.6–)2.5–2.9(–3.5) µm (n = 32), mostly gregarious, lageniform, less commonly subfusiform, not thickest near the base. ***Conidia*** (2.8–)3.1–3.7(–4) × (1.7–)2.2–2.7(–3.2) µm (n = 70), variable shape and size, typically oblong and pale yellowish green when fully mature, oval, ellipsoid and hyaline when immature, straight or slightly curved, sides sometimes pinched, smooth; base often truncate.

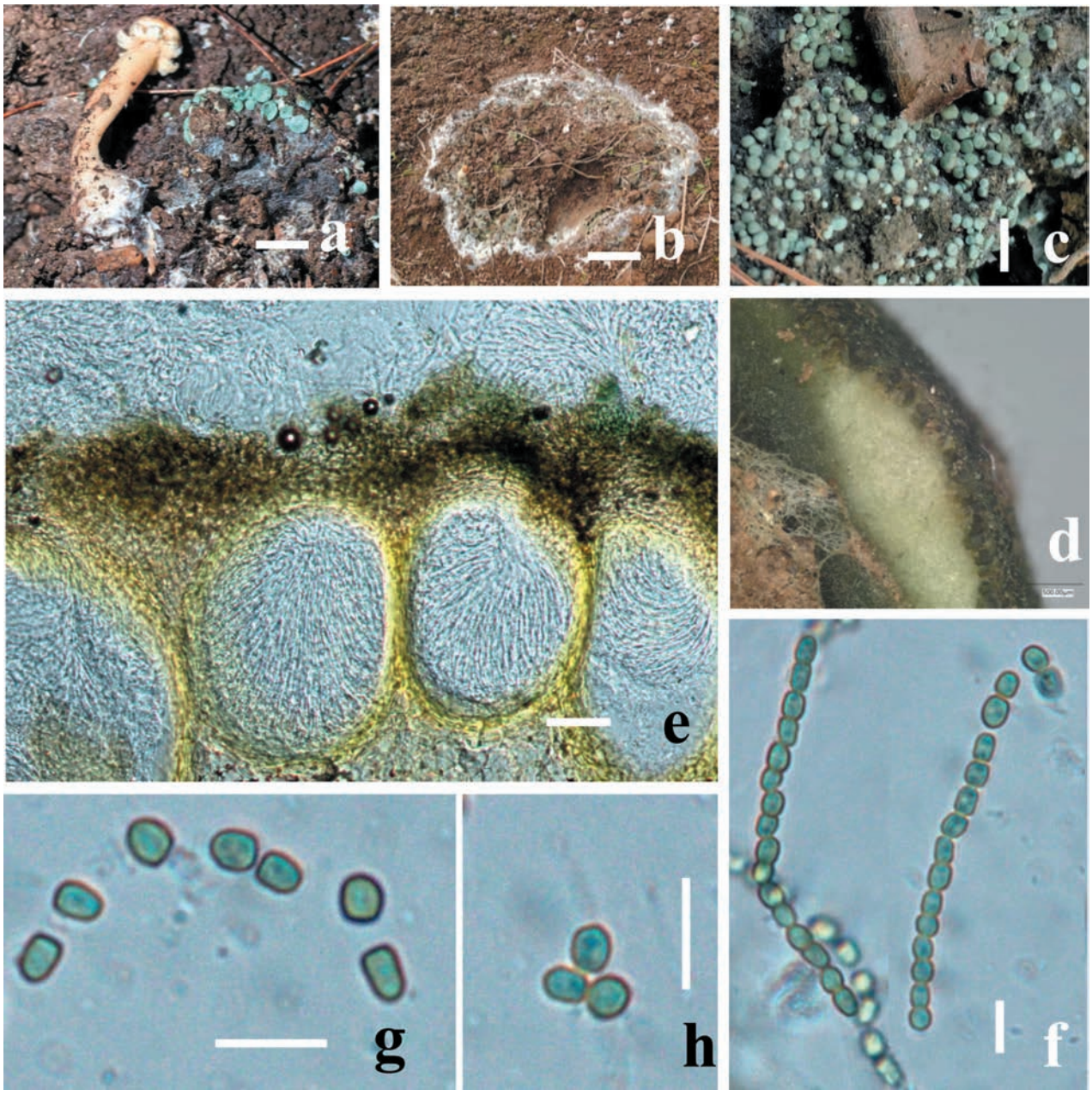

Figure 5. Morphology of *Trichoderma viridistromatis* (HGUP 24-0004, GUCC 24-0005) **a, b** diseased in the field, **c** fresh stromata on natural substrate **d** cortical and subcortical tissues **e** ascomatal tissue in section **f** asci with ascospores **g, h** ascospores. Scale bars: 10 mm (**a–c**); 1,000 µm (**d**); 50 µm (**e**); 20 µm (**f–h**).

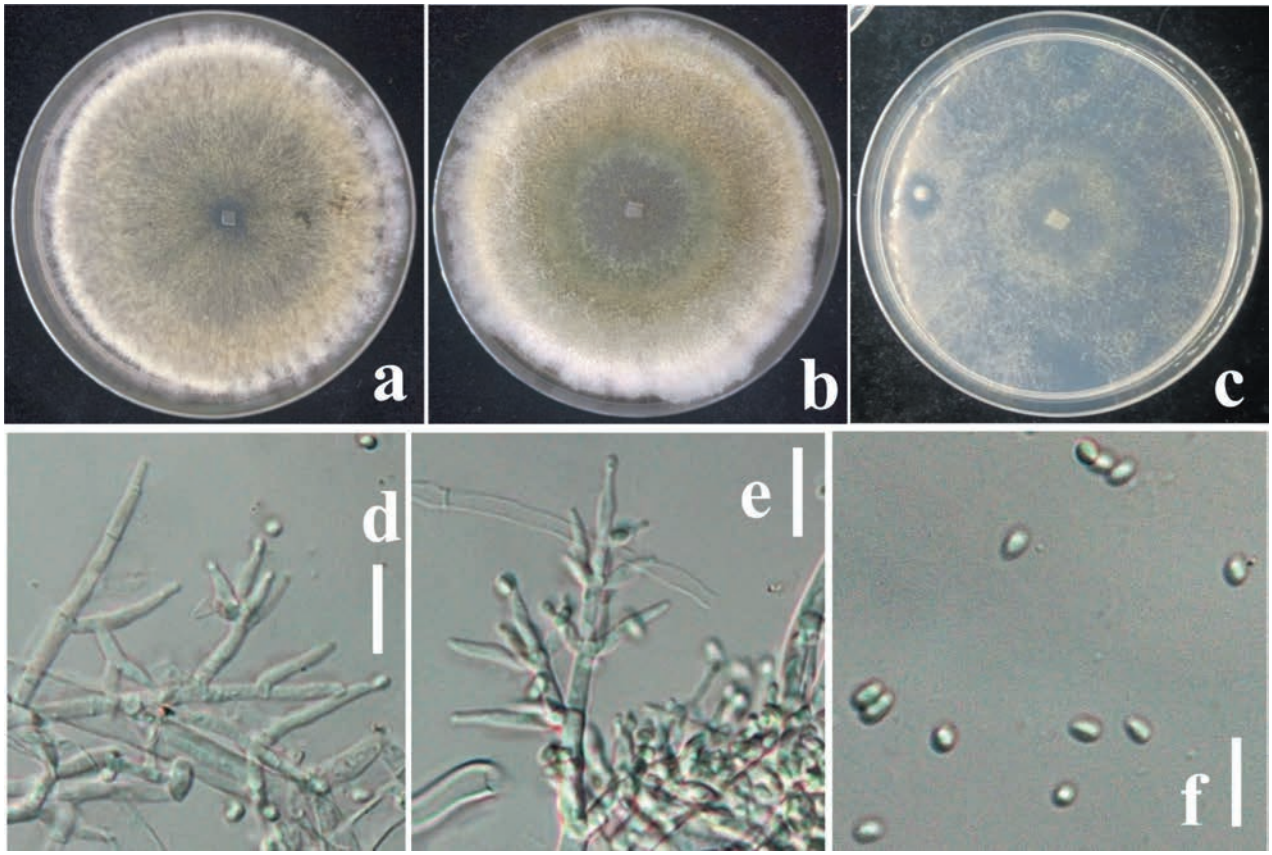

Figure 6. a cultures on MEA (five days) **b** cultures on PDA (five days) **c** cultures on SNA (four days) **d** conidiophores **e** phialides **f** conidia. Scale bars: 10 µm (**d, e**); 5 µm (**f**).

Habitat. On mushroom cultivated field, associated with *Stropharia rugosoannulata*.

Distribution. China, Guizhou Province, Guiyang City, and Liupanshui City; Guizhou City in Anshun Province.

Material examined. China • Guizhou, Liupanshui City, Shuicheng District, 24°55'39.936"N, 121°11'30.264"E, on soil surfaces of *Stropharia rugosoannulata* cultivated field, 16-November-2023, E. Tarafder and F.H. Tian (HGUP 24-0004, holotype); ex-type living cultures GUCC TB1120, GUCC TB1121 and GUCC TB1122.

GenBank accession numbers. GUCC TB1120 (ITS: PP922277; *rpb2*: PP954944; *tef1-α*: PP954950); GUCC TB1121 (ITS: PP926290; *rpb2*: PP954945; *tef1-α*: PP954951); GUCC TB1122 (ITS: PP922285; *rpb2*: PP954946; *tef1-α*: PP954952)

Notes. Morphologically, our newly described taxon *Trichoderma viridistromatis* shares common characteristics with *T. aerugineum* (CBS120541) and *T. britannicum*, a species previously isolated from dead stems and leaves of *Calamagrostis epigejos*. However, *T. viridistromatis* differs from *T. aerugineum* by having smaller stromata (0.5–2 mm in diameter, compared to ca. 1 mm thick in *T. aerugineum*) and larger phialides (7–23 × 2.4–4 µm in *T.* aerugineum) and ascospores (8–12 × 4–6 µm; Table 4) (Chaverri and Samuels 2004). Additionally, it can be distinguished from *T. stropharіensis* by its larger stromata (1–14 mm in diameter, 1–11 mm thick in *T. stropharіensis*) and significantly larger subglobose to elongated ascospores (8.4–16.9 × 5.5–8.1 µm).

Table 4. Morphological comparison of *Trichoderma britannicum*, *T. aerugineum*, *T. viridistromatis*, *T. spinulosum*, and *T. strophariensis*.

Taxon (holotype)	Ascospores	Conidia	Substratum	References
T. britannicum	10–16 × 4.5–6.2 µm	4.7–19.3 × 4–6.2 µm	Decaying wood of broadleaf trees	Jaklitsch et al. 2014
T. aerugineum	8–12 × 4–6 µm	3–5 × 2–4 µm	Decaying wood	Chaverri and Samuels (2004)
T. viridistromatis	**3.4–5.6 × 2.4–3.3 µm**	**2.8–4 × 1.7–3.2 µm**	**mushroom species (*Stropharia*)**	**This study**
T. spinulosum	5–7 × 3–4 µm	3.5–4.7 × 3–3.7 µm	On stems of *Chelidonium majus*	Jaklitsch and Voglmayr 2015
T. strophariensis	8.4–16.9 × 5.5–8.1 µm	8.5–25.5 × 5.7–17.9 µm	mushroom species (*Stropharia*)	This study

In comparison, *T. britannicum* has discoid, convex to turbinate stromata surrounded by light brown radial mycelium and much larger one-celled ascospores (10–16 × 4.5–6.2 µm; Table 4) (Jaklitsch et al. 2014). The phylogenetic positions of the new taxon (Fig. 2) demonstrated that *Trichoderma viridistromatis* is closely related to *T. strophariensis*, *T. britannicum*, and *T. aerugineum*, with strong statistical support (Fig. 2). However, our isolate differs from *T. britannicum* with 3% (17/610 nucleotides, with five gaps) in ITS region, 2% (20/1080 nucleotides, no gaps) in *rpb2* gene, and 4% (55/1244 nucleotides, twenty-one gaps) in *tef1-α* gene. Moreover, the difference in our collections with *T. aerugineum* is more than 2% (10/610 nucleotides, ten gaps) in the ITS region, 7% (79/1080 nucleotides, no gaps) in the *rpb2* gene, and 6% (78/1244 nucleotides, eleven gaps) in *tef1-α* gene (Table 2). Additionally, the differences between our isolate with *T. strophariensis* are 4% (29/610 nucleotides, four gaps) in ITS region, 4% (46/1080 nucleotides, no gaps) differences in *rpb2* gene, and 5% (65/1244 nucleotides, twenty-five gaps) differences in *tef1-α* gene also supported *T. viridistromatis* to be a distinct species compared to *T. strophariensis* and *T. britannicum* respectively.

Discussion

Green mold is a prevalent disease in mushroom cultivation that disrupts the average growth of mushroom fruiting bodies or mycelium and inhibits the average growth of mushrooms (Zeng et al. 2022). The discovery of two new *Trichoderma* species causing green mold disease significantly advances our understanding of fungal pathogens in mushroom cultivation. This finding underscores the urgent need for effective disease management strategies in agriculture. The pathogenicity of HGUP 24-0001 and HGUP 24-0004 on *Stropharia rugosoannulata* was confirmed in controlled field tests, where both strains caused symptoms consistent with green mold disease. The rapid development of green mycelia covering the mushroom trays fulfilled Koch's postulates. In this study, the rapid colonization of mushroom trays by green mycelia is a clear indicator of the aggressive interaction between the pathogens and the host, a situation of intense concern, leading to significant damage to the mushroom fruiting bodies. The occurrence of mold diseases affecting *S. rugosoannulata*, highlights the significant economic losses due to fungal infections in mushroom cultivation (Huang et al. 2023). The infection rate of both isolates in the mushroom trays mirrors their incidence in the field, indicating a potentially

significant agricultural impact. A detailed observation of symptoms, from initial mycelial growth to full substrate colonization, provides a comprehensive timeline of disease progression and is crucial for effective disease management in mushroom cultivation (Zhang et al. 2022).

Morphological analysis of the newly identified *Trichoderma* species revealed distinct characteristics. The typical symptoms of green mold disease were greenish mycelial growth and rotting of the fruiting bodies of the mushrooms. Moreover, molecular phylogenetic analyses of the nuclear ribosomal internal transcribed spacer (nrITS) region, the second largest subunit of RNA polymerase II (*rpb2*), the partial translation elongation factor 1-alpha (*tef1-α*) provided conclusive evidence for the delineation of the two new *Trichoderma* species, and these isolates were separated from previously identified and described species of *T. britannicum*, *T. aerugineum*, *T. danicum*, and *T. spinulosum* and properly placed within the distinct clades (Fig. 2). This molecular approach not only confirmed the novelty of the species but also highlighted the genetic diversity within the genus *Trichoderma*. This study successfully identified and described two new species of *T. strophariensis* and *T. viridistromatis* as the causal agents of green mold disease in *Stropharia rugosoannulata* in Guizhou Province, China.

The discovery of these new pathogens emphasizes the need for continuous monitoring and research on fungal diseases affecting economically important mushrooms. Integrating morphological and molecular identification techniques provides a robust framework for identifying and characterizing new fungal pathogens, ultimately improving disease management practices. Future studies should continue to explore the agricultural and biotechnological potential of these and other *Trichoderma* species, contributing to a deeper understanding and sustainable management of fungal pathogens in agriculture. This new pathogen can infect the mycelia of *S. rugosoannulata* at an early stage and the entire fruit body at maturity, making it a challenging competitor in the field. However, our significant findings also reveal an unexpected diversity of *Trichoderma* in China, highlighting the need for further research and inspiring future investigations.

Acknowledgements

Samantha C. Karunarathna thanks the "Yunnan Revitalization Talents Support Plan" (High-End Foreign Experts Program), the National Natural Science Foundation of China (NSFC 32260004), and the Key Laboratory of Yunnan Provincial Department of Education of the Deep-Time Evolution on Biodiversity from the Origin of the Pearl River for their support. The authors extend their appreciation to the Researchers Supporting Project (number RSP2024R56), King Saud University, Riyadh, Saudi Arabia.

Additional information

Conflict of interest

The authors have declared that no competing interests exist.

Ethical statement

No ethical statement was reported.

Funding

This research was funded by Guizhou Provincial Basic Research Program (Natural Science) ZK[2023] general 087 and the National Natural Science Foundation of China, grant number NSFC 32000013 & 32260044; Guizhou Provincial Support Fund of Science and Technology, grant number Support of QKH [2021] General 199; Guizhou Department, grant number Qianjiaoji [2022] 071; Guizhou Province Edible Fungi Industry Technology System (GZMARS-SYJ-2024-2026); Researchers Supporting Project (number RSP2024R56), King Saud University, Riyadh, Saudi Arabia.

Author contributions

Conceptualization, ET., FT; Data curation, ET., ZW., MH, FT.; Formal analysis, ET., FT., XZ., SCK.; Investigation, ET., ZW., FT.; Methodology, ET., ZW., SCK., WN., YW.; Project administration and resources, FT.; Software, ET., SCK., AME, MH, XZ.; Supervision, FT.; Writing original draft, ET.; Writing review and editing, ET., SCK., AME., WN., YW., XZ.; Funding acquisition, FT., XZ.; The first draft of the manuscript was written by ET and all authors commented on previous versions of the manuscript. All authors read and approved the final manuscript.

Author ORCIDs

Entaj Tarafder https://orcid.org/0000-0002-3680-3433
Zhang Wenjun https://orcid.org/0009-0005-8310-0537
Samantha C. Karunarathna https://orcid.org/0000-0001-7080-0781
Abdallah M. Elgorban https://orcid.org/0000-0003-3664-7853
Man Huilian https://orcid.org/0009-0006-7894-1873
Wu Nan https://orcid.org/0009-0006-1192-4171
Xiangyu Zeng https://orcid.org/0000-0003-1341-1004
Wang Yong https://orcid.org/0000-0003-3831-2117
Feng-Hua Tian https://orcid.org/0000-0002-6962-9531

Data availability

Sequence data generated for the present study have been deposited in GenBank with the accession number(s) can be found below: https://www.ncbi.nlm.nih.gov/genbank/, GUCC TB1117 (ITS: PP920011; rpb2: PP954941; tef1-α: PP954947); GUCC TB1118 (ITS: PP920012; rpb2: PP954942; tef1-α: PP954948); GUCC TB1119 (ITS: PP920013; rpb2: PP954943; tef1-α: PP954949); GUCC TB1120 (ITS: PP922277; rpb2: PP954944; tef1-α: PP954950); GUCC TB1121 (ITS: PP926290; rpb2: PP954945; tef1-α: PP954951); GUCC TB1122 (ITS: PP922285; rpb2: PP954946; tef1-α: PP954952). All of the data that support the findings of this study are available in the main text.

References

Abo-Elyousr KA, Abdel-Hafez SI, Abdel-Rahim IR (2014) Isolation of *Trichoderma* and evaluation of their antagonistic potential against *Alternaria porri*. Journal of Phytopathology 162(9): 567–574. https://doi.org/10.1111/jph.12228

Bustamante DE, Calderon MS, Leiva S, Mendoza JE, Arce M, Oliva M (2021) Three new species of *Trichoderma* in the *Harzianum* and *Longibrachiatum* lineages from Peruvian cacao crop soils based on an integrative approach. Mycologia 113(5): 1056–1072. https://doi.org/10.1080/00275514.2021.1917243

Carbone I, Kohn LM (1999) A method for designing primer sets for speciation studies in filamentous ascomycetes. Mycologia 91(3): 553–556. https://doi.org/10.1080/00275514.1999.12061051

Chaverri P, Samuels GJ (2004) *Hypocrea*/*Trichoderma* (Ascomycota, Hypocreales, Hypocreaceae): Species with green ascospores. Studies in Mycology 48: 1–116.

Chen K, Zhuang WY (2017) Discovery from a large-scaled survey of *Trichoderma* in soil of China. Scientific Reports 7(1): 9090. https://doi.org/10.1038/s41598-017-07807-3

Degenkolb T, Dhren HV, Nielsen KF, Samuels GJ, Brückner H (2008) Recent advances and future prospects in peptaibiotics, hydrophobin, and mycotoxin research, and their importance for chemotaxonomy of *Trichoderma* and *Hypocrea.* Chemistry & Biodiversity 5(5): 671–680. https://doi.org/10.1002/cbdv.200890064

Ezzi MI, Lynch JM (2005) Biodegradation of cyanide by *Trichoderma* spp. and *Fusarium* spp. Enzyme and Microbial Technology 36(7): 849–854. https://doi.org/10.1016/j.enzmictec.2004.03.030

Fu S, Sun JE, Tarafder E, Wijayawardene NN, Hu Y, Wang Y, Li Y (2024) Pezizomycotina species associated with rotten plant materials in Guizhou Province, China. MycoKeys 106: 265–285. https://doi.org/10.3897/mycokeys.106.125920

Geyer CJ (1991) Markov chain Monte Carlo maximum likelihood. In: Keramidas EM (Ed.) Computing Science and Statistics: Proceedings of the 23rd Symposium on the Interface. Interface Foundation, Fairfax Station, 156–163.

Gu M, Chen Q, Zhang Y, Zhao Y, Wang L, Wu X, Zhao M, Gao W (2024) Evaluation of Genetic Diversity and Agronomic Traits of Germplasm Resources of *Stropharia rugosoannulata.* Horticulturae 10(3): 213. https://doi.org/10.3390/horticulturae10030213

Hall TA (1999) BioEdit: A user-friendly biological sequence alignment editor and analysis program for windows 95/98/NT. Nucleic Acids Symposium Series 41: 95–98. https://doi.org/10.1021/bk-1999-0734.ch008

Harman GE, Lorito M, Lynch JM (2004) Uses of *Trichoderma* spp. to alleviate or remediate soil and water pollution. Advances in Applied Microbiology 56: 313–330. https://doi.org/10.1016/S0065-2164(04)56010-0

Hasan MM, Rahman S, Kim GH, Abdallah E, Oh DH (2012) Antagonistic potentiality of *Trichoderma harzianum* towards seed-borne fungal pathogens of winter wheat cv. Protiva in vitro and in vivo. Journal of Microbiology and Biotechnology 22(5): 585–591. https://doi.org/10.4014/jmb.1107.07063

Huang L, He C, Si C, Shi H, Duan J (2023) Nutritional, Bioactive, and Flavor Components of Giant *Stropharia* (*Stropharia rugoso-annulata*): A review. Journal of Fungi 9(8): 792. https://doi.org/10.3390/jof9080792

Jaklitsch WM (2009) European species of *Hypocrea* Part I. The green-spored species. Studies in Mycology 63: 1–91. https://doi.org/10.3114/sim.2009.63.01

Jaklitsch WM, Voglmayr H (2015) Biodiversity of *Trichoderma* (Hypocreaceae) in southern Europe and Macaronesia. Studies in Mycology 80(1): 1–87. https://doi.org/10.1016/j.simyco.2014.11.001

Jaklitsch WM, Komon M, Kubicek CP, Druzhinina IS (2005) *Hypocrea voglmayrii* sp. nov. from the Austrian Alps represents a new phylogenetic clade in *Hypocrea*/*Trichoderma*. Mycologia 97(6): 1365–1378. https://doi.org/10.1080/15572536.2006.11832743

Jaklitsch WM, Lechat C, Voglmayr H (2014) The rise and fall of *Sarawakus* (Hypocreaceae, Ascomycota). Mycologia 106(1): 133–144. https://doi.org/10.3852/13-117

Jambhulkar PP, Singh B, Raja M, Ismaiel A, Lakshman DK, Tomar M, Sharma P (2024) Genetic diversity and antagonistic properties of *Trichoderma* strains from the crop rhizospheres in southern Rajasthan, India. Scientific Reports 14(1): 8610. https://doi.org/10.1038/s41598-024-58302-5

Jun H, Kieselbach T, Jönsson LJ (2011) Enzyme production by filamentous fungi: Analysis of the secretome of *Trichoderma reesei* grown on unconventional carbon source. Microbial Cell Factories 10(1): 1–10. https://doi.org/10.1186/1475-2859-10-68

Katayama A, Matsumura F (1993) Degradation of organochlorine pesticides, particularly endosulfan, by *Trichoderma harzianum*. Environmental Toxicology and Chemistry 12(6): 1059–1065. https://doi.org/10.1002/etc.5620120612

Katoh K, Rozewicki J, Yamada KD (2019) MAFFT online service: Multiple sequence alignment, interactive sequence choice and visualization. Briefings in Bioinformatics 20(4): 1160–1166. https://doi.org/10.1093/bib/bbx108

Kumar S, Stecher G, Tamura K (2016) MEGA7: Molecular evolutionary genetics analysis version 7.0 for bigger datasets. Molecular Biology and Evolution 33(7): 1870–1874. https://doi.org/10.1093/molbev/msw054

Li QR, Tan P, Jiang YL, Hyde KD, Mckenzie EH, Bahkali AH, Wang Y (2013) A novel *Trichoderma* species isolated from soil in Guizhou, *T. guizhouense*. Mycological Progress 12(2): 167–172. https://doi.org/10.1007/s11557-012-0821-2

Liu YJ, Whelen S, Hall BD (1999) Phylogenetic relationships among ascomycetes: Evidence from an RNA polymerse II subunit. Molecular Biology and Evolution 16(12): 1799–1808. https://doi.org/10.1093/oxfordjournals.molbev.a026092

Liu M, Liu J, Wang WM (2012) Isolation and functional analysis of Thmfs1, the first major facilitator superfamily transporter from the biocontrol fungus *Trichoderma harzianum*. Biotechnology Letters 34(10): 1857–1862. https://doi.org/10.1007/s10529-012-0972-x

Põldmaa K (2011) Tropical species of *Cladobotryum* and *Hypomyces* producing red pigments. Studies in Mycology 68: 1–34. https://doi.org/10.3114/sim.2011.68.01

Poveda J, Hermosa R, Monte E, Nicolás C (2019) *Trichoderma harzianum* favours the access of arbuscular mycorrhizal fungi to non-host Brassicaceae roots and increases plant productivity. Scientific Reports 9(1): 11650. https://doi.org/10.1038/s41598-019-48269-z

Rambaut A (2016) FigTree version 1.4.3 [Online]. https://github.com/rambaut/figtree/releases/tag/v1.4.3 [accessed May 2024]

Ronquist F, Teslenko M, van der Mark P, Ayres DL, Darling A, Höhna S, Larget B, Liu L, Suchard MA, Huelsenbeck JP (2012) MrBayes 3.2: Efficient Bayesian Phylogenetic Inference and Model Choice Across a Large Model Space. Systematic Biology 61(3): 539–542. https://doi.org/10.1093/sysbio/sys029

Stamatakis A (2014) RAxML version 8: A tool for phylogenetic analysis and post-analysis of large phylogenies. Bioinformatics 30(9): 1312–1313. https://doi.org/10.1093/bioinformatics/btu033

Tian FH, Li CT, Li Y (2017) First report of *Penicillium brevicompactum* causing blue mold disease of *Grifola frondosa* in China. Plant Disease 101(8): 1549–1549. https://doi.org/10.1094/PDIS-09-16-1301-PDN

Wang GZ, Luo Y, Li JL, Kadri P, Bian YB, Zhou Y (2019) Characteristics of cob-web disease in fruiting bodies of *Auricularia cornea* and physiological feature and control strategy of the pathogenic fungus *Cladobotryum cubitense*. Mycosystema 38: 341–348. https://doi.org/10.13346/j.mycosystema.180270

Wei GY, Mo WI, Wen JT, Chang LF, Chen YS, Yang Q, Wang Y (2024) A new species and one new record of Sporocadaceae in Guizhou Province, China. Current Research in Environmental & Applied Mycology 14(1): 157–166. [Journal of Fungal Biology]

White TJ, Bruns TD, Lee SB, Taylor JW (1990) Amplification and direct sequencing of fungal ribosomal RNA genes for phylogenetics. PCR protocols: A guide to methods and applications. Academic Press, New York, 315–322. https://doi.org/10.1016/B978-0-12-372180-8.50042-1

Wijayawardene NN, Hyde KD, Dai DQ, Sánchez-García M, Goto BT, Saxena RK, Erdoğdu M, Selçuk F, Rajeshkumar KC, Aptroot A, Błaszkowski J, Boonyuen N, da Silva GA, de Souza FA, Dong W, Ertz D, Haelewaters D, Jones EBG, Karunarathna SC, Kirk PM, Kukwa M, Kumla J, Leontyev DV, Lumbsch HT, Maharachchikumbura SSN, Marguno F, Martínez-Rodríguez P, Mešić A, Monteiro JS, Oehl F, Pawłowska J, Pem D, Pfliegler WP, Phillips AJL, Pošta A, He MQ, Li JX, Raza M, Sruthi OP, Suetrong S, Suwannarach N, Tedersoo L, Thiyagaraja V, Tibpromma S, Tkalčec Z, Tokarev YS, Wanasinghe DN, Wijesundara DSA, Wimalaseana SDMK, Madrid H, Zhang GQ, Gao Y, Sánchez-Castro I, Tang LZ, Stadler M, Yurkov A, Thines M (2022) Outline of Fungi and fungus-like taxa – 2021. Mycosphere 13(1): 53–453. https://doi.org/10.5943/mycosphere/13/1/2

Xie J, Lu S, Tarafder E, Pan Y, Peng K, Zeng X, Tian F (2024) Taxonomy, biological characterization and fungicide sensitivity assays of *Hypomyces cornea* sp. nov. causing cobweb disease on *Auricularia cornea*. Fungal Biology 128(1): 1616–1625. https://doi.org/10.1016/j.funbio.2023.12.007

Yan QX, Huang MX, Sun P, Cheng SX, Zhang Q, Dai H (2020) Steroids, fatty acids and ceramide from the mushroom *Stropharia rugosoannulata* Farlow apud Murrill. Biochemical Systematics and Ecology 88: 103963. https://doi.org/10.1016/j.bse.2019.103963

Zeng XY, Yuan XX, Peng KQ, Pan YT, Tan TJ, Wu N, Tian FH (2022) Taxonomy and control of *Trichoderma hymenopellicola* sp. nov. responsible for the first green mold disease on *Hymenopellis raphanipes*. Frontiers in Microbiology 13: 991987. https://doi.org/10.3389/fmicb.2022.991987

Zeng XY, Tan TJ, Tian FH, Wang Y, Wen TC (2023) OFPT: A one-stop software for fungal phylogeny. Mycosphere 14(1): 1730–1741. https://doi.org/10.5943/mycosphere/14/1/20

Zeng M, Zhao Q, Gentekaki E, Su H (2024) *Pseudoplectania globospora* (Sarcosomataceae, *Pezizales*), a new species from Yunnan, China. Current Research in Environmental & Applied Mycology 14(1): 63–70. [Journal of Fungal Biology]

Zhang QH, Wang W, Li CH, Wen ZQ (2015) Biological characteristics of *Hypomyces aurantius* parasitic on *Hypsizygus marmoreus*. Mycosystema 34: 350–356. https://doi.org/10.13346/j.mycosystema.140248

Zhang GZ, Yang HT, Zhang XJ, Zhou FY, Wu XQ, Xie XY, Zhao XY, Zhou HZ (2022) Five new species of *Trichoderma* from moist soils in China. MycoKeys 87: 133–157. https://doi.org/10.3897/mycokeys.87.76085